1995

Diffusive And Advective-diffusive Transport Through Saturated And Unsaturated Soils

Kazem Badv

DIFFUSIVE AND ADVECTIVE-DIFFUSIVE TRANSPORT THROUGH SATURATED AND UNSATURATED SOILS

by

KAZEM BADV

Faculty of Engineering Science

Department of Civil Engineering

Submitted in partial fulfilment

of the requirements for the degree of

Doctor of Philosophy

Faculty of Graduate Studies

The University of Western Ontario

London, Ontario

November, 1994

ISBN 0-315-99244-1

ABSTRACT

This thesis describes a series of laboratory experiments together with the theoretical analysis of NaCl migration through single and double layer soil systems for a range of physical and chemical characteristics. The soil materials were tested under saturated and unsaturated (gravity drainage) conditions. The small and large scale apparatus were designed so that soil samples could be tested for "diffusive" and "advective-diffusive" migration.

The experiments examining NaCl diffusion through the saturated fine sand and clayey silt were used to obtain the reference diffusion coefficients for the individual types of soil. The fine sand and clayey silt were then used in a combined system to simulate a compacted clayey liner over a natural deposit of nearly saturated fine sand. The migration process involved downward advective-diffusive transport of NaCl from a source solution placed on top of the clay plug through the clay and fine sand and into a receptor solution. Using the contaminant transport model POLLUTE and Cl^- diffusion coefficient in the fine sand and clay determined from diffusion experiments conducted on isolated soils, the transport of Cl^- in the combined soil system was predicted and found to agree well with the experiments indicating the reproducibility of the transport parameters in the combined soil systems.

The diffusion characteristics of the coarse sand and fine gravel were studied by first testing the materials under saturated conditions and determining the reference diffusion coefficients of Cl^- and Na^+. These materials were then tested for unsaturated conditions under gravity drainage with atmospheric pressure being maintained at the bottom of the samples. Relatively slow migration of the ions was observed in the unsaturated portion of the samples. The unsaturated diffusion coefficients were predicted using the reference diffusion coefficients and assuming a linear relationship to exist between the volumetric moisture content and diffusion coefficient of the unsaturated sample. A theoretical analysis was performed using these predicted diffusion coefficients and the observed non-uniform moisture content profiles. The predicted values provided a good fit to the experimental data both in the soil and source solution.

The diffusion coefficients determined from diffusion tests on the isolated clayey

soil and unsaturated fine gravel were used to predict the advective-diffusive migration of the Cl^- and Na^+ ions in a combined soil systems. These tests simulated a hydrogeological situation in a landfill site including a compacted clayey liner over a natural deposit of an unsaturated fine gravel. The predicted profiles fit the experimental data reasonably well, confirming the accuracy of the developed method for estimating the diffusion coefficients and theoretical model used.

Using the large scale advection-diffusion apparatus, laboratory experiments were conducted to simulate a compacted silt or clayey silt liner over an unsaturated secondary leachate collection system. Experiments were conducted under "high", "moderate" and "low" flow rates. Relatively steep and uniform Cl^- concentration profiles were observed in the unsaturated stone layer. This behaviour was accurately modelled by the advection-diffusion theory using POLLUTE and transport parameters obtained from the previous experiments. A small amount of dispersion was inferred from the results of the theoretical modelling in the unsaturated stone layer and the effect of groundwater velocity was found to be significant in migration through the stone, even in the low flow rate system.

In a series of laboratory experiments, the geotextile and granular filter/separators efficiently prevented intrusion of a compacted clayey soil into a pressurized stone layer under high applied pressures. A significant amount of soil was observed to be intruded into the void spaces in the stone layer, when no filter/separator was used between the soil and stone.

ACKNOWLEDGEMENTS

The author would like to express his sincere gratitude and appreciation to his chief advisor, Dr. R.K. Rowe, for his guidance and encouragement during the course of study leading to this thesis.

Sincere thanks are extended to Dr. R.M. Quigley and Dr. K.Y. Lo for their helpful guidance with respect to this thesis.

Special thanks are extended to Mr. G. Lusk and Mr. W. Logan for their technical assistance throughout this study.

The work described in this thesis was supported by grant No. A1007 from the Natural Science and Engineering Research Council of Canada. Special thanks are also extended to the Ministry of Jahad Sazandeghi and Ministry of Science and Higher Education of I.R. Iran for their financial support to the author throughout the period of this study.

Sincere thanks are also extended to the faculty and staff of geotechnical research centre and my fellow graduate students for their encouragement and companionship.

The last but not the least, the author is most grateful to his wife, Nahid and his children Hadi, Maryam and Mohsen for their love, understanding, encouragement and patience throughout the course of study leading to this thesis.

TABLE OF CONTENTS

Page

Page

LIST OF TABLES

LIST OF FIGURES

LIST OF PHOTOS IN CHAPTER 11

LIST OF APPENDICES

CHAPTER 1

INTRODUCTION

1.1 GENERAL

The migration of contaminants through porous media is studied in many branches of science and engineering. Examples are found in hydrogeology and geoenvironmental engineering, including:

1 - salt water intrusion in coastal aquifers

2 - recharge with water of a different quality

3 - secondary recovery techniques of oil reservoirs, where the injected fluid dissolves the oil

4 - the use of tracers, such as dyes, electrolytes and radioactive isotopes, for the determination of the flow velocity and the flow path of the water, in groundwater pollution control

5 - rainwater infiltration through sanitary landfills and waste disposal sites and transfer of contaminants from the waste into the underlying soils and aquifers

6 - transfer of contaminants from rivers into aquifers

7 - accidents with tankers and pipelines

8 - pollution due to septic tanks

9 - pollution due to agricultural practice, such as excessive applications of fertilizers, herbicides and pesticides

10 - radioactive and infiltration of contaminants in industrial areas, in agriculture, e.g.,

11 - movement of fertilizers in the soil

12 - investigations of salt affected soils

14 - movement and accumulation of toxic materials.

The most widely used theory for explaining the transport of contaminants in soil water, is hydrodynamic dispersion theory. In this theory the transport characteristics are described in a macroscopic way, as it is usually done in hydrogeology. This means that the parameters are averaged over volumes or surfaces that are large compared to the dimensions of the pores and solid particles. When the porous matrix is inert and variations in viscosity and density of the solution are negligibly small, the hydrodynamic dispersion theory assumes that the flow of a solute, through a porous media, depends upon the processes of advection and hydrodynamic dispersion. Advection is the movement of the solute along with the macroscopic flow. Hydrodynamic dispersion is solute transfer due to molecular diffusion and mechanical dispersion. Molecular diffusion is the ever-present thermal motion of molecules. Mechanical dispersion is the movement induced by the presence of the solid matrix. It results from the difference in the microscopic and macroscopic water flow velocities, both in magnitude and direction. It has an effect similar to molecular diffusion.

The need to predict the movement of contaminants being transported by the processes mentioned above has led to considerable recent interest in the phenomena associated with mass transport through unsaturated soils. The transport of dissolved chemicals through unsaturated soils has long been a concern of soil physicists and agricultural engineers, particularly with respect to the movement of fertilizers and

pesticides in the upper layers of a soil profile. However, with the increasing awareness of potential environmental damage due to contaminants in the subsurface, this problem has attracted interest from a number of other engineering disciplines. The amalgam of geologists, hydrogeologists and geotechnical engineers which makes up the emerging discipline of geoenvironmental engineering has focused considerable research effort on transport through unsaturated soil profiles, a problem which is encountered in many geoenvironmental applications.

In the case of landfill design, for example, there are those who recommended sitting landfills on a relatively deep unsaturated zone as an alternative to construction of liners (Campbell et al., 1983; Bagchi, 1987), a concept which has gained the editorial backing of the Journal of Ground Water (Heath & Lehr, 1987). The majority of landfill sites in existence today have been located above the water table in the unsaturated zone. Natural attenuation sites rely upon the unsaturated zone to renovate leachate to acceptable levels prior to reaching the groundwater. Sites designed with low permeability liners and leachate collection systems may also depend upon the unsaturated zone to attenuate any leachate that is not removed by the collection system and to act as a back up system to possible engineering failures (Gerhardt, 1984). Before this potentially money saving approach can be implemented, however, it is necessary to be able to predict with some confidence the fate of the dissolved contaminants in the landfill leachate as they travel through this unsaturated barrier. Even in the case of lined landfills, prediction of the fate of possible leakage should be an integral part of any feasibility study prior to construction.

Only recently has the full impact of careless landfilling practices begun to come

to light. Much of the current activity in the field of groundwater pollution is in response to leakage from old storage tanks, industrial facilities and landfill sites. In such situations, as well as cases where there has been a spill of contaminants, accurate prediction of transport through both unsaturated and saturated zones is vital to the design of remediation programs.

The increased attention of geoenvironmental engineers and soil physicists has led to the development of a large variety of numerical models attacking the problem of unsaturated flow and transport. These models are of necessity quite complex, dealing as they do with processes governed by parameters which in many cases vary in time and space in highly non-linear fashions. These mathematical complexities, combined with some shortcomings in our fundamental understanding of unsaturated transport processes, have thus far forestalled our ability to predict the results of these processes with any degree of confidence. It is the thesis of this research that laboratory modelling is a tool which can be of use in the struggle to understand more the phenomena of transport in the unsaturated zone.

Despite the considerable progress which has been made in the field of flow and contaminant transport in unsaturated porous media in the past twenty years, there are still uncertainties with predicting contaminant transport through the unsaturated zone. According to Nielsen et al. (1989): "Transport models remain more or less undependable to predict when, where, and how much of a contaminant released at the soil surface will reach the groundwater ".

Although many of these uncertainties have to do with the problems of applying results of theoretical analysis and laboratory work to the field scale, there are also

deficiencies in our fundamental understanding of the unsaturated flow and transport processes. It is in this area of basis research that laboratory modelling can play a role, both in determining transport parameters for use in numerical models, and more importantly, as a tool for validation of numerical models. Specifically this thesis will focus on contaminant migration through generally unsaturated granular soil located beneath a compacted soil liner.

The specific goals of this research in landfill applications are illustrated using a hypothetical landfill shown in Fig. 1.1. This landfill consists of primary and secondary leachate collection systems (made of coarse stone) and compacted clayey liners (made of clayey silt). These engineered layers are separated by geotextile (or granular) filter/separators. The landfill is assumed to be located in a natural deposit (silt, sand or gravel) with a ground water table below the base of the engineered containment system. Due to the perched condition, clayey liners are expected to remain saturated or nearly saturated. There is likely to be a leachate mound inside the primary drainage layer on top of the primary liner which will create a low gradient across the underlying layers. Due to the low flow through the primary liner combined with regular pumping, the secondary drainage layer is expected to remain unsaturated. Depending on the location of the ground water table and grain size and structure of the natural deposit materials below the landfill, these materials might remain either nearly saturated (due to the matric suction in these materials, such as fine sand or silt) or become unsaturated due to the gravity drainage (e.g., gravel).

As indicated, stone drainage layers should be protected from intrusion of the fine

grained overlying or underlying clayey material, otherwise their effective void space could be potentially reduced and be occupied by liner material. One chapter of this thesis focused on this issue. Two types of filter/separator materials; a nonwoven needle punched geotextile (type TS650) and layered granular material were selected and their separation characteristics were studied using a series laboratory tests. The location of this part of study in the landfill is shown as boxes A and B in Fig. 1.1. The study was extended to the case where there is no filter/separator between the clay and stone, and results were compared with those from the tests with a geotextile or granular filter/separators.

The major part of the research focused on contaminant migration through the engineered layers overlying the natural deposit in the landfill. First the soil materials (e.g., clayey silt, sand and gravel) were tested for their "diffusion" characteristics using NaCl salt as the migrating chemical. The effective diffusion coefficients of the diffusing ions (mainly Cl^-) were determined under gravity drainage conditions (i.e., saturated or unsaturated). The study was then extended to consider advective-diffusive transport through two layer soil systems. A part of the study focused on the transport through the compacted clayey layer overlying either a near saturated fine sand and silt or unsaturated fine gravel. The location of this part of study in the landfill is shown as box D in Fig. 1.1.

The final part of the study focused on advective-diffusive (and may be dispersive) transport through two layer systems including a compacted soil (silt or clay) on top of an unsaturated coarse stone layer. The response of unsaturated stone layer for three flow rates (classified as low, moderate, and high) was studied. This zone of interest is shown

as box C in Fig. 1.1.

The methodology used in this research program was as follows:

(a) Design the appropriate equipment :

. An intrusion test cell was designed so that the proposed materials could be tested under relatively high applied pressures.

. A small scale apparatus was designed to perform both diffusion and advection-diffusion experiments on fine grained and granular materials.

. A large scale apparatus was designed to perform the advection-diffusion tests on compacted soil o. rlying a coarse stone layer.

(b) Select and prepare the soil materials :

Clayey soil and coarse stone from the Halton Waste Management Facility were used for the engineered materials. A commercially available fine Ottawa sand and fine gravel were used to simulate the natural deposit materials. The silt was prepared from a natural deposit.

(c) Develop the test methods :

For the intrusion, diffusion, and advection-diffusion (small and large scale) experiments, test methods were developed and evaluated prior to the actual experiments.

(d) Observe, measure, interpret and finally model the experimental behaviour:

The tests were performed according to the developed procedures and the experimental data obtained was interpreted. Then a theoretical model (program POLLUTE) was used to predict the experimental behaviour for multilayered

system using the key transport parameters (e.g., the effective diffusion coefficients) inferred from the single layer systems.

An overview of the experimental program is shown in Fig. 1.2. In this figure, the numbers in the brackets indicate the number of tests performed.

1.2 THESIS FORMAT

Following a description of the basic concepts concerning flow and contaminant transport and relevant equations and controlling parameters in Chapter 2, the thesis comprises ten additional chapters in which, Chapters 3-8 describe the laboratory diffusion and advection-diffusion experiments conducted on saturated and unsaturated fine grained and granular material using small scale diffusion/advection-diffusion apparatus, and present the findings from these experiments. Chapters 9 and 10 describe the advection-diffusion experiments conducted on compacted silt (with trace clay and some clay) and clayey silt underlain by a layer of unsaturated coarse stone and a simulated aquifer, using a large scale advection-diffusion apparatus, and present the findings from these experiments. Chapter 11 describes the experiments conducted to examine the physical intrusion of a compacted clayey soil into a coarse stone layer. Finally, Chapter 12 summarizes the results and conclusions of this research, and some recommendations for further research are given. The specific focus of each of the chapters is outlined below:

Chapter 3 explains the introductory experiments conducted to examine the different

testing procedures to be adopted in this study. This chapter also describes the methodology of the diffusion and advection-diffusion testing and the apparatus designed and built to suit this methodology.

Chapter 4 presents the results of 6 laboratory diffusion tests conducted on saturated fine sand and clayey silt. In these experiments the diffusion coefficients of Cl^- and Na^+ ions are measured by fitting a theoretical profiles to the observed data using computer program POLLUTE.

Chapter 5 presents the results of three advection-diffusion tests conducted on a compacted clayey soil underlain by a layer of fine sand. The fine sand layer was saturated by wetting or drying mechanisms. The predicted profiles fitted the experimental data using the diffusion coefficients found for clay and fine sand in single soil diffusion tests (Chapter 4). The effect of "hysteresis" on transport behaviour was also studied.

Chapter 6 presents the results of two advection-diffusion tests conducted on a compacted clayey soil underlain by a layer of silt. The silt layer was saturated by wetting or drying mechanisms. The effect of "hysteresis" on transport behaviour was also studied.

Chapter 7 presents the results of eight diffusion tests conducted on saturated and unsaturated coarse sand and fine gravel. A procedure to predict the diffusion coefficient of solute (e.g. Cl^-) in an unsaturated granular material having non-uniform water content was presented.

Chapter 8 presents the results of two advection-diffusion tests conducted on a compacted clayey soil underlain by a layer of unsaturated fine gravel. The methodology adopted in diffusion experiments in Chapter 7 was used to predict the diffusion coefficients of Cl^- and Na^+ in unsaturated fine gravel sublayers and the predictions were compared with the experimental observations.

Chapter 9 presents the results of two advection-diffusion tests conducted on a layer of compacted silt (with trace clay and some clay) underlain by a layer of unsaturated coarse stone and a simulated aquifer. "High and moderate" flow rates were examined in these experiments to observe the transport of contaminant through the test systems with special attention being devoted to the behaviour of unsaturated coarse stone.

Chapter 10 presents the results of two duplicated advection-diffusion tests conducted on a layer of compacted clayey silt underlain by a layer of unsaturated coarse stone and a simulated aquifer. "Low" flow rate was examined in these experiments to observe the transport of contaminant through the test systems with special attention being devoted to the behaviour of unsaturated coarse stone.

Chapter 11 presents the results of seven intrusion tests conducted to examine the potential intrusion of a compacted clayey soil into a pressurized coarse stone layer under high applied vertical pressures. Two different cases when the coarse stone is "separated" or "not separated" from the clayey soil by a filter/separator were examined.

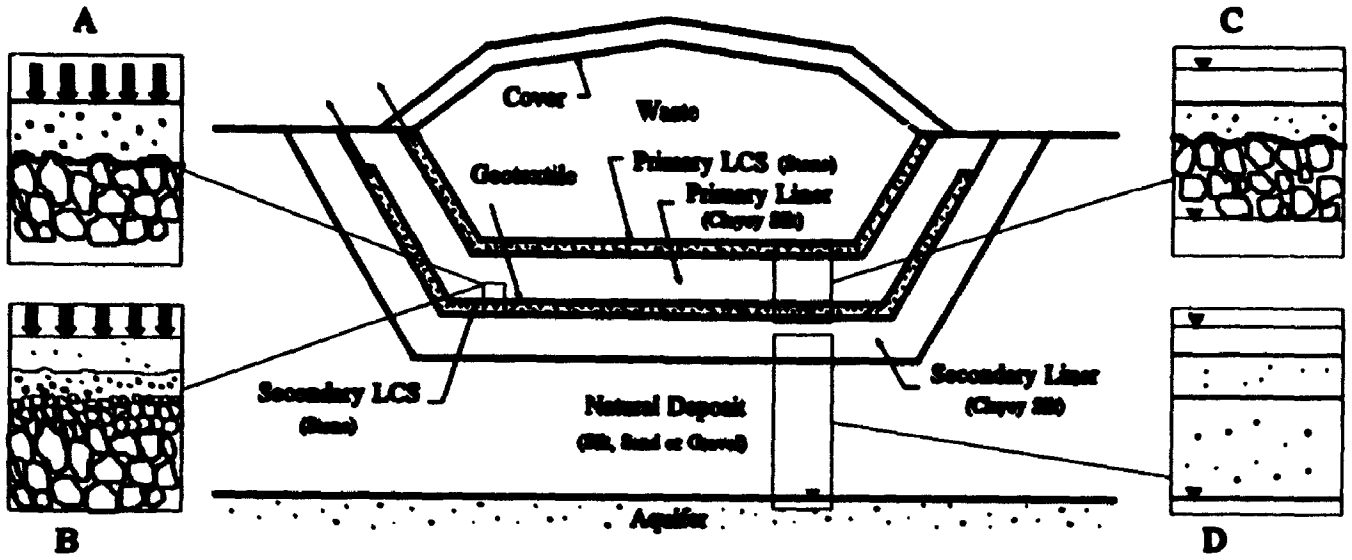

FIG. 1.1 A HYPOTHETICAL LANDFILL WITH SOME RESEARCH AREAS FOCUSED IN THE THESIS :

A & B : INTRUSION TESTING WITH GEOTEXTILE AND GRANULAR FILTER/SEPARATORS

C : ADVECTION-DIFFUSION TESTING ON A COMPACTED SOIL OVERLYING AN UNSATURATED COARSE STONE AND,

D : A COMPACTED CLAYEY SOIL OVERLYING A SATURATED OR UNSATURATED GRANULAR MATERIAL

EXPERIMENTAL PROGRAM

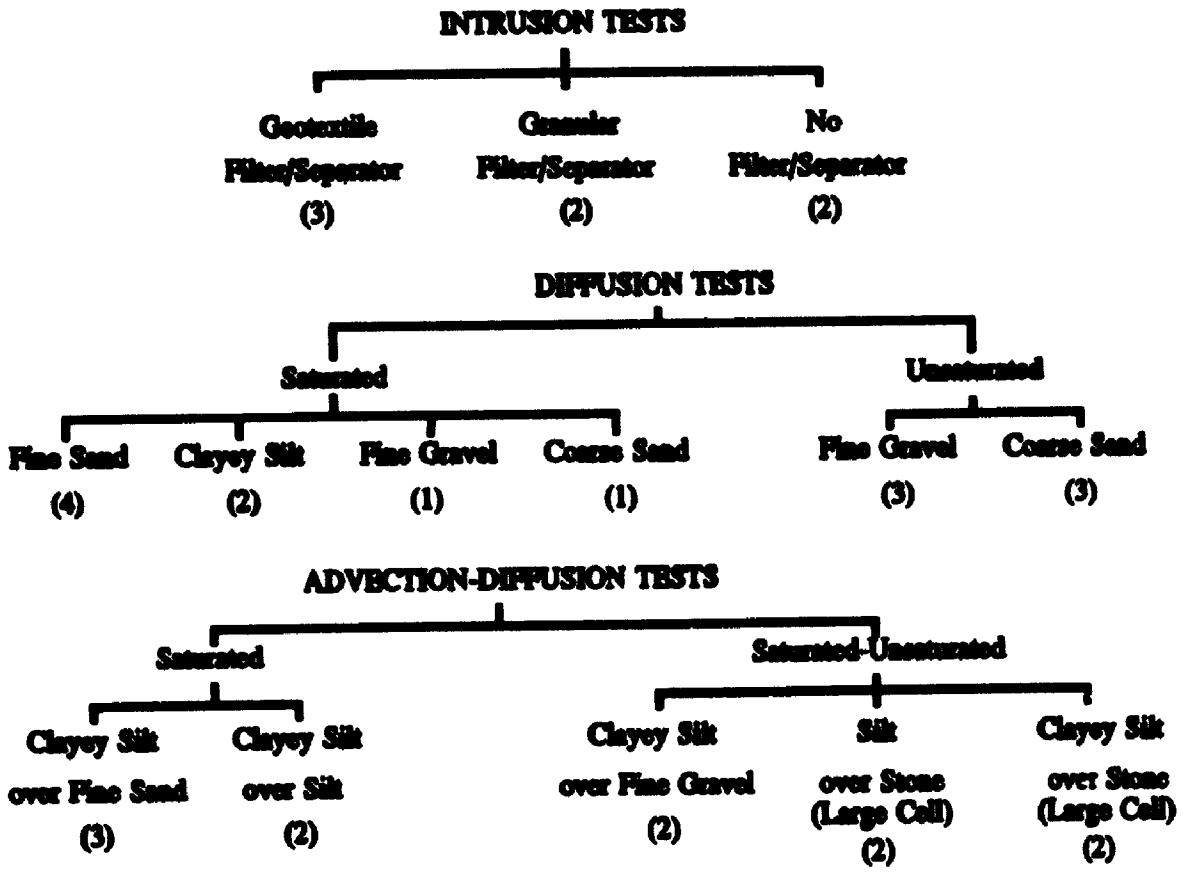

FIG. 1.2 OVERVIEW OF THE EXPERIMENTAL PROGRAM

CHAPTER 2

LITERATURE REVIEW AND THEORETICAL BACKGROUND

2.1 INTRODUCTION

The current research employs laboratory techniques to conduct physical modelling of contaminant transport through one or two-layer soil system under saturated and/or unsaturated conditions. The processes that govern the transport of inorganic chemicals through saturated soils are equally valid for unsaturated soils; however, the nature of the transport parameters may be different. Characterization of these parameters for unsaturated soils is of fundamental importance to the prediction of contaminant migration.

The first part of this literature review focuses on the definition of the basic transport mechanisms for saturated porous media. The second part discusses key issues involving the flow and transport in unsaturated porous media.

2.2 CONTAMINANT MIGRATION THROUGH SATURATED POROUS MEDIA

The evaluation of a design for a waste disposal facility involves making a quantitative prediction of potential impact of the waste on groundwater quality, keeping in mind that under most circumstances involving contaminant movement through a barrier and into an aquifer, the most one can expect to do is to predict trends and a likely range of concentrations at any given point in space and time (Rowe et al., 1994).

When dealing with contaminant transport through saturated soils such as clayey barriers or the matrix of an intact rock, the primary transport mechanisms are "advection" and "diffusion". When dealing with transport through aquifers the key transport mechanisms are advection and dispersion. The following sections (2.2.1-2.2.6) are based on Rowe et al. (1994).

2.2.1 ADVECTIVE TRANSPORT

Advection involves the movement of contaminant with flowing water. The movement of contaminants at a speed corresponding to the groundwater velocity is often referred to as "plug flow". When dealing with contaminants in groundwater, the mass of contaminant transported by advection per unit area per unit time (i.e. the "mass flux" f) is given by:

$$f = n\, v\, c \qquad (2.1a)$$

$$= v_a\, c \qquad (2.1b)$$

where n = effective porosity of the soil

v = the groundwater velocity (seepage velocity)

v_a = Darcy velocity = n v

c = concentration of the contaminant at the point and time of interest

The total mass transported from a contaminant source into a soil to some specific time t, is obtained by integrating the mass flux (Eq. 2.1) with respect to time, t, viz.

$$m_a = A_o \int_0^t nvc\,dt \qquad (2.2)$$

where m_a is the mass of contaminant transported from the source by advection, A_o is the cross-sectional area of the soil through which contaminant is passing, and all other terms are as defined above.

It is obvious that if there was no flow, then there would be no movement of contaminant into the soil by advection.

2.2.2 DIFFUSIVE TRANSPORT

Diffusion involves the movement of contaminant from points of high concentration to points of low chemical concentration. Experimental and field evidence (e.g. Goodall and Quigley, 1977; Rowe et al., 1988; Desaulniers et al., 1981) would suggest that in a saturated porous media, the diffusive mass flux of a non-reactive solute can be approximated by Fick's first law, which in one dimensional form can be written as:

$$f = -D_p \frac{\partial c}{\partial z} = -nD_e \frac{\partial c}{\partial z} \qquad (2.3)$$

where n is the effective porosity of the soil (as previously defined), D_p is the porous media diffusion coefficient, D_e is the effective diffusion coefficient, and $\partial c/\partial z$ is the concentration gradient (i.e. the change in concentration with position). The negative sign arises from the fact that contaminants move from high to low concentrations and hence the gradient $\partial c/\partial z$ will usually be negative. It should be noted that Eq. 2.3 assumes that the driving force behind diffusion of a given species is its concentration gradient. This

assumption, however, is only true for diffusion of neutral species. For charged species, diffusion may be driven in part by electrical forces between the species itself and co-diffusing charged species. Therefore, Eq. 2.3 should theoretically have a second term on the right hand side, to account for the influence of electrical interactions between co-diffusing charged species. For practical purposes, however, this term is not included, and the effect of electrical interactions on the diffusive mass flux is considered to be indirectly accounted for through the magnitude of the diffusion coefficient. The total mass of contaminant m_d transported out of a source by diffusion up to some specific time t is obtained by integrating Eq. 2.3 with respect to time t, to give:

$$m_d = A_o \int_0^t \left(-nD_e \frac{\partial c}{\partial z}\right) dt \qquad (2.4)$$

where all terms are as previously defined.

Under transient conditions, the principal of conservation of mass requires that the change in mass flux of a diffusing solute across an infinitesimal soil element ($\partial f/\partial z$) must equal the time rate of change of concentration within the element, i.e.,

$$\frac{\partial c}{\partial t} = D \frac{\partial^2 c}{\partial z^2} \qquad (2.5)$$

which has the form of Fick's second law. This equation represents the one-dimensional equation for transient diffusion of a non-reactive solute, and will serve as a basis for subsequent theoretical formulation presented herein.

2.2.3 ADVECTIVE-DIFFUSIVE TRANSPORT

When there is a groundwater velocity through the soil, both advective and diffusive transport mechanisms occur simultaneously. For the case of advective-diffusive transport, the mass flux f is given by:

$$f = nvc - nD_e \frac{\partial c}{\partial z} \qquad (2.6)$$

and the total mass m transported from the source up to a specific time t is given by:

$$m = A_o \int_0^t \left(nvc - nD_e \frac{\partial c}{\partial z}\right) dt \qquad (2.7)$$

where the velocity v is positive if it is out of the contaminant source and negative if it is into the landfill and all other terms are as previously defined.

2.2.4 DISPERSION

When concerned with contaminant migration in association with relatively high flows, there is a third transport mechanism to be considered; namely, mechanical dispersion. This process involves mixing that occurs due to local variations in the flow velocity of the groundwater. The dispersion of contaminants also involves a mixing and spreading of the contaminants due to non-homogeneity in aquifers (see Freeze and Cherry, 1979). Because of the shape of the interconnected pore space, the (microscopic) streamlines fluctuate in space with respect to the mean direction of flows. This phenomenon causes the spreading of any initially close group of tracer particles, as flow

continues, they occupy an ever increasing volume of the flow domain. The spreading is in both the longitudinal direction, namely that of the average flow (longitudinal dispersivity), and in the direction transverse to the average flow (transverse dispersivity).

Although this phenomenon is totally different from the diffusion process, for most practical purposes, it can be mathematically modelled in the same way as a composite parameter D called the "coefficient of hydrodynamic dispersion" viz.

$$D = D_e + D_{md} \qquad (2.8)$$

where D_e is the effective (molecular) diffusion coefficient for the contaminant species of interest, and D_{md} is the coefficient of mechanical dispersion.

The mass flux is given by:

$$f = nvc - nD\frac{\partial c}{\partial z} \qquad (2.9)$$

where D is defined by Eqs. 2.8 and 2.10 (discussed below) and all other terms are as previously defined.

When dealing with transport through intact clayey soil, diffusion will usually control the parameter D and dispersion is negligible (see Gillham & cherry, 1982; Rowe, 1987). In aquifers, the opposite tends to be true and dispersion tends to dominate. It is often convenient to model the dispersive process as a linear function of velocity (Bear, 1979; Freeze & Cherry, 1979) viz.

$$D_{md} = \alpha v \qquad (2.10)$$

in which α is the dispersivity and v is the seepage velocity (i.e., $v = v_s/n$).

2.2.5 SORPTION

In the previous sections, various transport mechanisms were discussed. These represent means by which contaminant species in solution move in the groundwater. Equally important, however, are the mechanisms which remove contaminant from solution. These processes may include cation exchange whereby cations such as K^+, Na^+, Pb^{++}, Cd^{++}, Fe^{++}, Cu^{++} etc. replace other cations (e.g. Ca^{++}, Mg^{++}) on the surface of the clay and hence are removed from solution (this is usually accompanied by an increase in the pore fluid concentration of the desorbed cations Ca^{++}, Mg^{++} etc.). Other mechanisms include precipitation of heavy metals (e.g. see Yanful et al., 1988b) and removal of organic matter in the soil.

In the simplest case, the sorption processes can be modelled as being linear and reversible and so the mass of contaminant removed from solution 'S' is proportional to the concentration in solution 'c', viz.

$$S = K_d\, c \qquad (2.11)$$

where S is the mass of solute removed from solution per unit mass of solid, K_d is the partitioning or distribution coefficient, and c is the equilibrium concentration of solute (mass of solute per unit volume of pore fluid). The product ρK_d (where ρ is the dry density of the soil) is a dimensionless measure of the amount of sorption which is likely to occur. A contaminant species is said to be "conservative" if there is no sorption (i.e. $\rho K_d = 0$). A typical example of a conservative contaminant would be the chloride ion (Cl^-). Typical examples of contaminants whose migration and impact may be greatly retarded by sorption processes are the heavy metals Pb^{++}, Cd^{++}, Fe^{++}, Cu^{++}, and, in

the presence of organic in soil, hydrocarbons such as benzene, toluene and halogenated aliphatic compounds such as dichloromethane etc.

2.2.6 RADIOACTIVE AND BIOLOGICAL DECAY

Some elements undergo radioactive decay to lighter elements and many organic compounds undergo biological decay into other simplest compounds. The time it takes for the concentration of the particular species to be reduced to half of the original concentration may be referred to as its half-life.

For substances which undergo first order decay, the rate of reduction of concentration is proportional to the current concentration so that:

$$\frac{\partial c}{\partial t} = -\lambda c \qquad (2.12)$$

where λ = first order decay constant

$= \Gamma_R + \Gamma_B + \Gamma_s$

Γ_R = radioactive decay constant = $\ell n2$/(radioactive half-life)

Γ_B = biological decay constant = $\ell n2$/(biological decay half-life)

Γ_s = dilution that occurs when a volume of fluid is removed (per unit volume of soil per unit time) and is replaced with fresh water as described below

This equation has the solution:

$$c(t) = c_o e^{-\lambda t} \qquad (2.13)$$

where c_o = initial concentration

In the absence of radioactive and biological decay, a decrease in concentration

may also occur if fluid is removed from soil by some mechanism. In this case $\lambda = \Gamma_s$, where Γ_s equals the volume of contaminated fluid removed (per unit volume of soil per unit time) in the region where fluid is being removed from below the landfill. There are a number of possible ways in which this may occur. For example, it may arise if there is a horizontal flow in a soil deposit where the transport of contaminant is predominantly vertical. In this case water entering below the upgradient edge of the overlying landfill will generally bring negligible contaminant into the aquifer beneath the landfill while on the downgradient edge of the landfill contaminant will be removed from beneath the landfill by the flowing water.

2.3 GOVERNING DIFFERENTIAL EQUATIONS FOR SATURATED POROUS MEDIA

As previously noted (e.g. see Eq. 2.9) the mass flux, f, which is transported per unit area per unit time due to advective-diffusive-dispersive transport can be given by:

$$f = nvc - nD\frac{\partial c}{\partial z} \qquad (2.9)$$

thus, by considering conservation of mass within any small region, the change in concentration with time is given by:

$$n\frac{\partial c}{\partial t} = -\frac{\partial f}{\partial z} - \rho\frac{\partial S}{\partial t} - n\lambda c \qquad (2.14a)$$

which indicates that the increase in contaminant concentration within a small volume is equal to the increase in mass due to advective-diffusive transport ($-\partial f/\partial z$, where the

negative sign implies a net increase in mass within the element) minus the decrease in mass due to sorption ($-\partial S/\partial t$) minus the decrease in mass due to first order decay processes ($-n\lambda c$).

Substituting Eq. 2.9 for the flux f and Eq. 2.11 for the sorbed concentration S into Eq. 2.14a then gives:

$$n\frac{\partial c}{\partial t} = (nD\frac{\partial^2 c}{\partial z^2} - nv\frac{\partial c}{\partial z}) - \rho K_d\frac{\partial c}{\partial t} - n\lambda c \qquad (2.14b)$$

where n = effective porosity of the soil

c = concentration at depth z and time t

$D = D_e + D_{md}$ = coefficient of hydrodynamic dispersion

v = seepage or (average linearized) groundwater velocity

ρ = dry density of the soil

K_d = distribution or partitioning coefficient

$v_a = nv$ is the Darcy velocity or discharge velocity

and λ is as defined in Eq. 2.12.

2.4 FLOW AND CONTAMINANT TRANSPORT IN UNSATURATED POROUS MEDIA

Transport parameters such as hydraulic conductivity for advection, diffusion coefficient for molecular diffusion and adsorption coefficient for adsorption-exchange phenomenon are constant for saturated soil. However, in unsaturated soils, there may need to be functional relationships between these parameters and the water content of the soil. In order to predict the contaminant migration through unsaturated soils, these

parameters should be characterized.

The advective-diffusive movement of contaminants through unsaturated soils is somewhat more complicated than for saturated soils. The partial differential equation governing one-dimensional movement is given by:

$$\frac{\partial}{\partial t}(\theta c) = \frac{\partial}{\partial z}(\theta D \frac{\partial c}{\partial z}) - \frac{\partial}{\partial z}(v_a c) - \theta \lambda c \qquad (2.15)$$

where θ is the volumetric water content (=porosity for saturated soil) and λ is a term which takes account of first order biological, chemical and radioactive decay and also mass removed from the source, and all other terms are as previously defined.

It is generally accepted that Eq. 2.15 is valid for unsaturated porous media (Bear and Verruijt, 1987). This equation bears a marked similarity with Eq. 2.14b, however this similarity may be deceptive (Rowe, 1987). For an unsaturated soil, the volumetric water content θ, the coefficient of hydrodynamic dispersion D, and the Darcy velocity may vary both spatially and temporally. The movement of contaminant through unsaturated soils is a very complex phenomenon as demonstrated by a number of laboratory and field studies (e.g. De Smedt, 1981; Gerhardt, 1984 and others).

The simplest case is that in which there is negligible advective transport through unsaturated soils. This situation can only arise when the net infiltration is negligible. Under these circumstances, the migration of contaminant in solution will be very slow since the migration will be purely by diffusion and it has been shown (e.g. Klute & Letey, 1958; Porter et al., 1960 and others) that the effective diffusion coefficient in unsaturated soils may be substantially lower than in saturated soils. This subject will be discussed more in detail later in this chapter.

The validity of the classical hydrodynamic dispersion theory (i.e. Eq. 2.15) was proven by the experiments of Kirda et al. (1973), Bresler and Laufer (1974), Hildebrand and Himmelbau (1977), and Yule and Gardner (1976). However, various investigators have questioned the direct application of Eq. 2.15 for unsaturated soils. Many investigators (e.g. Nielsen and Biggar, 1961; Krupp and Elrick, 1968; Gaudet et al., 1977; De Smedt and Wierenga, 1984) have observed "tailing" in concentration profiles and breakthrough curves. This was taken as an indication that unsaturated porous media contain an immobile water phase, providing a relatively slow diffusive source or sink for the transported solute. Others found that chemical reactions affected solute transport. They show the necessity of reformulating Eq. 2.15 to include the chemical processes. In this regard, anion exclusion has been demonstrated to be important (e.g. Corey et al., 1963; McMahon and Thomas, 1974; Cassel et al., 1975; Bond et al., 1982) and its effects have been theoretically treated by Bresler (1973). Adsorption of solutes was significant in the studies of Biggar and Nielsen (1963), McMahon and Thomas (1974), and Mansell et al. (1977), among others. In each of these studies, even when the appropriate chemical terms were included in the equations, deviations from model predictions were observed.

The equations which describe the movement of a non-interacting solute in a porous media containing mobile and immobile water, were presented by Coats and Smith (1964). The system consists of a classical dispersion convection equation for the mobile zone, coupled with a term, which describes the sidewards movement of solute in and out of the immobile zone. A second equation expresses this solute flux as being proportional to the difference in concentration between the two zones:

$$\theta_m \frac{\partial C_m}{\partial t} + \theta_{im} \frac{\partial C_{im}}{\partial t} = \theta_m D_m \frac{\partial^2 C_m}{\partial z^2} - v_a \frac{\partial C_m}{\partial z} \qquad (2.16a)$$

$$\theta_{im} \frac{\partial C_{im}}{\partial t} = \beta (C_m - C_{im}) \qquad (2.16b)$$

where C_m and C_{im} are the concentrations of the solute in the mobile and immobile zones (mg/L), respectively, θ_m and θ_{im} are the volumetric water contents in these zones (cm^3/cm^3), and β is the mass transfer coefficient of the solute transfer between the two zones (s^{-1}).

De Smedt (1981) has shown that a reasonable fit to his experimental data could also be obtained using Eq. 2.15 and an apparent dispersion coefficient D_{ap} given by:

$$D_{ap} = \frac{\theta_m}{\theta} D_m + \frac{\theta^2_{im} v^2}{\theta \theta_m \beta} \qquad (2.17)$$

An inspection of Eq. 2.17 indicates the difficulties of using this approach in practice since the parameters β, v, θ_m, θ_{im}, θ may be expected to vary both temporally and spatially. Furthermore, the parameter β must be determined by curve fitting laboratory results for a particular situation.

Transport studies that allow evaluation of models based on equations such as 2.15 have been formulated to include anion exclusion in unsaturated soils. Bresler (1973) treated the one dimensional transport of an anionic solute in a vertical column of unsaturated soil exhibiting anion exclusion. For conditions of uniform water content, steady water flux, and constant hydrodynamic dispersion, he showed that the anion concentration in the pore water is described by:

The solution to Eq. 2.18 for a flux-type boundary condition and a semi-infinite

$$(\theta-\theta_{ex})\frac{\partial c}{\partial t}=D\frac{\partial^2 c}{\partial z^2}-v_e\frac{\partial c}{\partial z} \qquad (2.18)$$

column is given by Brenner (1962). It can be shown that for the relatively large Peclet numbers resulting from the experimental conditions in this study the solution reduces to:

$$\frac{c-c_i}{c_o-c_i}=1/2\ erfc\left(\frac{(\theta-\theta_{ex})z-v_e t}{2\sqrt{(\theta-\theta_{ex})Dt}}\right) \qquad (2.19)$$

where c is the concentration of a single solute in the bulk pore solution, c_i is the anion concentration of the soil solution in the column before displacement begins, c_o is the anion concentration of the infiltrating solution, θ is the volumetric water content of the soil, θ_{ex} is the excluded volumetric water content, z is the depth, and t is the time.

The analytical methods employed in this study determine total quantities of anionic solute and water per unit volume of porous material, therefore, the observed concentration, c_{obs}, is less than c. This occurs because the water in the exclusion volume, which contains no anion, is included in the water volume used to calculate the anion concentration. The interrelationship of c and c_{obs} is given by:

$$c_{obs}=c[1-(\theta_{ex}/\theta)] \qquad (2.20)$$

Excluded water content, θ_{ex} can be calculated from the observed concentration by rearranging Eq. 2.20 to give (Bond et al., 1982):

$$\theta_{ex}=\theta\ [1-(c_{obs}/c)] \qquad (2.21)$$

It has been shown that for some intact saturated soils with predominantly active clay minerals (e.g. montmorillonite), the effective porosity of the soil can be significantly less than the total porosity (e.g. Thomas and Swoboda, 1970; Appelt et al., 1975) due

to the anion exclusion. The effective porosity with respect to diffusion through saturated (or near saturated) clayey soils of low activity and soils containing mostly illite and/or vermiculite as the dominant clay mineral, is often reasonably estimated based on water content determined according to usual geotechnical practice (Rowe et al., 1988, 1994), i.e., the effective porosity is essentially the same as the total porosity.

For illitic clayey soils and granular material (e.g. sand and gravel) used in this thesis, the effect of anion exclusion and immobile water is considered to be negligible.

2.4.1 FLOW THROUGH UNSATURATED POROUS MEDIA

The modern era of the study of flow through porous media begins with the work of Henry Darcy (1856), who developed his law for flow through porous media while designing fountains for the city of Dijon, France. Although originally formulated as an empirical, one-dimensional equation, it has since been derived in vector form from the Navier-Stokes equation (De Wiest, 1965) with appropriate notice taken of the tensorial nature of K, the proportionality constant.

The next major development in the field came in 1907, with the publication of a research monograph by Edgar Buckingham (1907), a scientist with the U.S. Bureau of Agriculture. In his paper, Buckingham introduced the concepts of capillary potential and capillary conductivity. Having a background in thermodynamics, Buckingham derived a generalized law for movement of soil moisture on the macroscopic scale based on energy considerations. Apparently unaware of Darcy's work, he described his flux law as analogous to Ohm's law for flow of electrical current.

Buckingham's paper laid the theoretical foundation on which Richard (1931) built his equation for flow in unsaturated porous media, which remains the basis for much of the theoretical work in this field. The Richards' equation may be derived from the equation of continuity and Darcy's law, which is assumed to remain valid for unsaturated flow in a modified form in which "hydraulic conductivity is a function of moisture content". The validity of this assumption has subsequently been confirmed experimentally by numerous researchers (e.g., Childs and Collis-George, 1950; Vachaud, 1967; Nimmo et al., 1987).

The general form of the Richards' equation is:

$$\frac{\partial \theta}{\partial t} = \nabla . (K \nabla h) + \frac{\partial K}{\partial z} \qquad (2.22)$$

where z is the vertical position coordinate and the hydraulic conductivity K may be expressed as a function of either the volumetric water content θ or the suction head h.

Like Buckingham's work, Richards' theoretical development of a general equation of unsaturated flow would remain essentially unused for over twenty years, "a raft of mathematical rigour adrift on a sea of engineering empiricism" (Cooke, 1991). The main interest of agricultural engineers and hydrogeologists was not in a general solution to the problem of unsaturated flow, but in a solution to the specific problem of infiltration. In response to the need for a simple infiltration equation, Green and Ampt (1911) introduced a semi-empirical equation, which introduced the concept of a sharply defined "wetting front" moving downward through the soil column in response to both gravity and suction gradients. Because of the ease of acquiring input parameters and the relative accuracy of predictions using the Green and Ampt equation, it "is even today much

appealed to" (Childs, 1967).

Other researchers have introduced completely empirical infiltration equations including Kostiakov (1932), Horton (1940), Holtan (1961) and Ghosh (1980). The Horton and Holtan equations, in particular, continue to be widely used by hydrologists. Although useful for the specific application for which they were developed, the empirical nature of these equations render them unsuitable for general theoretical treatment of unsaturated flow.

Interest in the Richards equation was rekindled when it was presented in the diffusion form by Klute (1952). Assuming that K and h are single valued functions of θ permits introduction of D, the soil water diffusivity, which is also a single-valued function of θ defined as:

$$D(\theta) = K(\theta) \frac{\partial h}{\partial \theta} \qquad (2.23)$$

This definition, combined with a chain rule expansion of (2.22), leads to:

$$\frac{\partial \theta}{\partial t} = \nabla(D\nabla\theta) + \frac{\partial K}{\partial z} \qquad (2.24)$$

For situations where gravity is not important, such as horizontal flow, the last term on the right side may be dropped, and the equation becomes:

$$\frac{\partial \theta}{\partial t} = \nabla(D\nabla\theta) \qquad (2.25)$$

which is analogous to the equation for heat flow, but with the added complication that D, rather than being a constant, is a function of water content.

Recognizing the similarity between this form of the Richards equation and the heat

flow equation, Philip (1954) used the Boltzmann transformation to arrive at a series solution of the one-dimensional form of (2.25), the first two terms of which he proposed be used as a concise infiltration equation:

$$q = \frac{S_o}{\sqrt{t}} + B_1 \qquad (2.26)$$

where q is the infiltration rate, t is the time, and S_o and B_1 are constants. The constant S_o has been termed the "sorptivity", which, according to Philip (1969) "embodies in a single parameter the influence of capillarity on the transient flow processes". The physical meaning of sorptivity and methods of determining it remain a topic of discussion among soil scientists attempting to model infiltration (e.g. Youngs, 1969; Whisler and Bouwer, 1970, Brutsaert, 1976; Chong and Green, 1983; El-Kadi, 1986).

Although useful in a number of applications, analytical solutions are only applicable to highly simplified systems. The widespread availability of computers has reduced the dependence of researchers on analytic and quasi-analytic solutions to the Richards equation, in favour of solution by numerical methods. As well as allowing solution of the Richards equation for "real-world" situations, the use of computers facilitates analysis of increasingly complex problems, such as the coupling of the Richards equation with the equation of advective-dispersive transport, in order to describe contaminant transport through unsaturated soils.

2.4.2 HYDRAULIC CONDUCTIVITY-WATER CONTENT RELATIONSHIP IN UNSATURATED POROUS MEDIA

In a soil stratum, as the saturation decreases, the large pores drain first so that

the flow takes place through the smaller pores. This causes both a reduction in the cross-sectional area available for the flow and an increase in tortuosity of the flow paths. The combined effect causes a rather rapid reduction in the hydraulic conductivity as the moisture content decreases (Bear 1979). As the water films become thinner, curtain phenomena at the solid-water interface come into play, causing a further reduction in hydraulic conductivity. Among such factors we may mention an increase of viscosity of the water in close proximity to the solid surfaces.

Several authors suggest different relationships between the permeability (k), the hydraulic conductivity (K) and saturation S, or the water content θ. Childs and Collis-George (1950) assume:

$$K = \frac{B\theta^3}{M^2} \qquad (2.27)$$

where M is the specific surface area of the soil phase and B is a constant. Irmay (1954) derives a similar relationship assuming that resistance to flow offered by the soil matrix is proportional to the solid-liquid interface area. The hydraulic conductivity K then becomes proportional to the hydraulic radius, i.e. to the volume of voids divided by the wetted area:

$$R = \frac{V_v}{A_s} = \frac{nV_b}{M(1-n)V_b} = \frac{n}{M(1-n)} \qquad (2.28)$$

for a cubic arrangement of spheres of radius d, the specific surface is $M = 6/d$. subscripts v, b, and s denote voids, bulk and solids, respectively. This model leads to:

$$K=K_o\left(\frac{\theta-\theta_r}{n-\theta_r}\right)^3=k_o\left(\frac{S-S_r}{1-S_r}\right)^3; \quad \left(\frac{K}{K_o}\right)^{\frac{1}{3}}=\frac{\theta-\theta_r}{n-\theta_r} \qquad (2.29)$$

where K_o is the hydraulic conductivity at saturation, θ and θ_r are the volumetric water content at unsaturated and at irreducible states, n is the porosity, S is the degree of saturation ($\theta=nS$) and S_r is the irreducible water saturation ($\theta_r = nS_r$), or "residual" degree of saturation.

Corey (1954) suggested an approximate functional relationship between the coefficient of permeability and degree of saturation on the basis of the theory developed by Burdine in 1953. This approximation is written as:

$$K=K_o\left(\frac{S-S_r}{1-S_r}\right)^4 \qquad (2.30)$$

The approximate equation of Corey has considerable utility because the only parameters needed for the solution are the residual degree of saturation and the saturated hydraulic conductivity.

A few years later, Corey (1957) attempted to use the equipment developed for the measurement of oil and gas flow in oil producing sands to study the unsaturated permeability of a soil. In the end, Corey was able to show that the values obtained experimentally compare favourably with the calculated values based on his earlier proposed approximation (Eq. 2.30).

Elzeftawy and Dempsey (1976) and Elzeftawy and Cartwright (1981) conducted two independent studies in predicting saturated and unsaturated permeability for different soil samples. Both groups utilized the commercially available Tempe pressure cell to determine the moisture characteristic and the saturated coefficient of permeability, and

the Green and Corey model to calculate the permeability characteristics, which is written as:

$$K(\theta)_i = \frac{K_o}{K_{oc}} \frac{30T^2nP}{\rho g \eta N^2} \cdot \sum_{j=1}^{m} [(2j+1-2i)h_j^{-2}] \qquad (2.31)$$

where $K(\theta)_i$ = the calculated permeability for a specified water content or suction (cm/min)

K_o/K_{oc} = the matching factor (measured saturated coefficient of permeability / calculated saturated coefficient of permeability)

i = last water content class on the wet end, e.g., i=1 identifies the pore class corresponding to the saturated water content, and $i=m$ identifies the pore class corresponding to the lowest water content

h_j = suction (negative water pressure head) for a given class of water-filled pores (cm of water)

N = total number of pore classes between θ_o and θ_r

θ = volumetric water content (cm^3/cm^3)

θ_r = lowest water content on the experimental $h(\theta)$ curve

T = surface tension of water (Dyn/cm)

n = water saturated porosity, i.e., $n=\theta_s$ (cm^3/cm^3)

η = viscosity of water ($g/cm.S^{-1}$)

g = the gravitational constant (cm/s^2)

ρ = density of water (g/cm^3)

P = a parameter that counts for the interaction of pore classes; taken to be equal to 7 in Elzeftawy and Dempsey's calculations.

By comparing the measured and computed values, Elzeftawy and Dempsey concluded that the Green and Corey model (Eq. 2.31) successfully predicts the permeability characteristics for a wide range of soils and that the proposed Tempe pressure cell method is reliable and can be used to determine the moisture characteristics.

The relationship between the volumetric moisture content (or degree of saturation) and the coefficient of permeability appear to exhibit little hysteresis (Nielson and Biggar, 1961; Topp and Miller, 1966; Corey, 1977; and Hillel, 1982), however, there is hysteresis in the relationship between the coefficient of permeability and matric suction (Fredlund and Rahardjo, 1993).

2.4.3 DIFFUSION COEFFICIENT-WATER CONTENT RELATIONSHIP IN UNSATURATED POROUS MEDIA

Functional relationships for the diffusion of an unsaturated soil have emerged primarily through the soil science literature. It is known that the diffusion coefficient varies with the water content, but the form of the functionals as reported by different researchers seems to differ. Many researchers attribute the decrease in the rate of diffusion as the water content decreases, to the increased tortuosity of the pathway for diffusion. The mobility of ions in water absorbed on soil surfaces has been reported to be very small (Kemper, 1960 and Porter et al., 1960). The presence of discontinuous water filled pores or water films, and the small mobility of ionic species in the thin water films could have serious implications on the adsorption characteristics of an unsaturated soil. The role of water content on the pathway for diffusion and on the adsorption characteristics are essential information that needs to be verified.

The porous system diffusion coefficient, D_p, calculated from Fick's law (Eq. 2.3) might be written:

$$D_p = D_o W_T = \theta D_e \qquad (2.32)$$

in which W_T is a complex "tortuosity factor" having the following components:

$$W_T = \alpha_{sf}\gamma_e (L/L_e)^2 \theta = \tau\theta \qquad (2.33a)$$

$$D_e = \alpha_{sf}\gamma_e (L/L_e)^2 D_o = \tau D_o \qquad (2.33b)$$

where α_{sf} = decreased fluidity factor related to adsorbed double layer water, γ_e = electrostatic interaction factor, $(L/L_e)^2$ = tortuosity factor, θ = volumetric water content (= n, the porosity for a saturated system), and $\tau = \alpha_{sf}\gamma_e(L/L_e)^2$ is the tortuosity factor for the clay.

Carman (1937) introduced the tortuosity as $(L/L_e)^2 < 1$ which is called the tortuosity of the porous medium, in which L is the length of the straight line connecting the two ends of a tortuous tube of length L_e. Estimates on the numerical value of the tortuosity factor $(L/L_e)^2$ are given by several authors. Irmay (1968) mentions the value 0.4 for Carman's tortuosity factor $(L/L_e)^2$. However, if $(L/L_e)^2 = 0.4$, the $L/L_e = \sqrt{0.4} = 0.63$. Carman (1937) mentions the empirical value $L/L_e = 0.71$, which is close to the values mentioned above. Other values mentioned in the literature for L/L_e vary in the range 0.56 to 0.8.

It is noted that in the text such as Bear (1979), the use of the term "tortuosity" relates only to the "geometric" tortuosity $(L/L_e)^2$ and ignores the effects of α_{sf} and γ_e. While this may not be a bad approximation for granular materials, it is not correct to ignore α_{sf} and γ_e for clayey soils.

The term D_o in Eq. (2.32b) represents the species diffusion coefficient if it was

diffusing from a source solution, into a purely aqueous solution without the presence of soil. For neutral species at concentrations up to about 5 mole percent, D_o is dependent on viscosity of the aqueous solution, molar volume of the solute, and temperature, as indicated by empirical expression (Wilke and Chang, 1955):

$$D_o = \frac{5.06 \times 10^{-7} \, T_A}{\eta \, V^{0.6}} \qquad (2.34)$$

where, D_o = diffusion coefficient in aqueous solution (cm^2/s), T_A = absolute temperature °K, η = viscosity of water at temperature T_A (cp), and V = molar volume of the solute at its normal boiling point (cm^3/mole). For a variety of neutral species, values of D_o obtained from the above equation and also experimentally, are given in Hayduk and Laudie (1974), and Reid et al. (1987, p. 610).

It should be noted that Eq. 2.34 is based on experiments conducted at an aqueous phase pressure approximately equal to atmospheric pressure. Assuming a constant temperature, an increase in water pressure would produce an increase in the viscosity of the water (η), which according to Eq. 2.34, would result in a decrease in the aqueous diffusion coefficient. Nevertheless, for the range of water phase pressures examined in this thesis (about 1 - 2 atmospheres), the variation in water viscosity is negligible (e.g., see Benedek and Purcell, 1954). Therefore, for the purpose of this thesis, the aqueous diffusion coefficient and hence, the porous media diffusion coefficient, are considered to be independent of aqueous phase pressure.

In practice, the diffusion coefficient of a species in porous media, is often estimated from Eq. 2.33b using a tortuosity factor back-figured from Cl^- diffusion tests, and an appropriate D_o value. With this approach, however, there are two important

shortcomings. Firstly, one does not know whether the value of τ determined for Cl^- is appropriate for the species of interest. For example, a species having a hydrated radius significantly larger than that of Cl^- might experience more difficulty in diffusing through the smaller pore spaces, and therefore may be better represented by a lower value of τ. Furthermore, for situations where the species of interest is an ion which is diffusing simultaneously with a number of other ions, some of which are diffusing in the opposite direction, the choice of an appropriate D_e becomes more difficult.

An alternative approach for obtaining the diffusion coefficient, is by laboratory diffusion tests on samples of the porous media under consideration. This approach represents the focus of some parts of this thesis.

Dependence of the hydrodynamic dispersion coefficient (in displacement experiments) and diffusion coefficient (in diffusion experiments) on volumetric moisture content of the medium has been observed in the experimental work of Gaudet et al. (1977), Klute and Letey (1960), Wierenga and Van Genuchten (1989), De Smedt et al. (1986), Kemper and Van Schaik (1966), Bresler (1973), Porter et al. (1960), Barraclough and Tinker (1982), Conca and Wright (1990), Rowell et al. (1967), Warncke and Barber (1972), Romkens and Brace (1964), Graham-Bryce (1963) and Lim et al. (1994). For a soil profile with a steady state non-uniform distribution of the water content with depth, the equation governing one-dimensional solute transport is given by De Smedt and Wierenga (1978) as:

$$\theta(z)\frac{\partial c}{\partial t} = \frac{\partial}{\partial z}\left[D(z)\theta(z)\frac{\partial c}{\partial z}\right] - q\frac{\partial c}{\partial z} \qquad (2.35)$$

where the dispersion coefficient (D) and the volumetric moisture content (θ), vary with

depth, while the flow (q) is constant for steady state flow conditions. This equation is in fact similar to Eq. 2.15 except that the effect of sorption, biological, chemical and radioactive decay have not been considered.

Experiments conducted by Klute and Letey (1958) indicated a very rapid decrease of diffusion as the moisture content of the soil was decreased. The results of these experiments were discussed in relation to the path length and moisture content of the medium. It was shown that the decrease of the value of D_e/D_o (defined earlier) as the volumetric moisture content is reduced from saturation, is due to the changing geometry of the water in the pore system. There are two aspects of this geometry that are important. The first of these is the fraction of the cross section of the porous medium that is available for diffusion. This is measured by the volumetric moisture content, θ. The second geometrical factor is the "effective path length" through which diffusion occurs. The effective path length should not be confused with the mean free path. The effective path length is greater than the path length as measured by the macroscopic length of the diffusion system. As the moisture content decreases the effective path length increases. These experiments showed that a large decrease in the effective diffusion coefficient occurs in the range of suction which most of the solution is removed from the sample.

According to Bresler (1973), hydrodynamic dispersion coefficient $D(v,\theta)$ is expressed as :

$$D(v,\theta) = D_e(\theta) + D_{md}(v) \qquad (2.36)$$

in which $D_{md}(v)$ is the mechanical dispersion coefficient which is a function of average interstitial velocity, and $D_e(\theta)$ is as defined earlier. The functional relationship between

D_e and θ according to Kemper and Van Shaik (1966) is of the type:

$$D_e(\theta) = D_o a e^{b\theta} \qquad (2.37)$$

where a and b are empirical constants characterizing the soil. Porter et al. (1960) and Kemper and Van Schaik (1966) show that for practical purposes the diffusion coefficient in a clay-water system is independent of the salt concentration and dependent on the water content only.

Experiments reported by Porter et al. (1960) have focused on chloride diffusion as influenced by moisture content. By taking into account the factors such as tortuosity and others, they expressed the Fick's first law as:

$$\frac{\Delta Q}{\Delta t} = D_o \gamma \left(\frac{L}{L_e}\right)^2 \theta A \frac{\Delta c}{\Delta z} \qquad (2.38)$$

in which:

'Q' is the amount of diffused tracer in g

'D_o' is the diffusion coefficient in free solution (cm^2/s)

'A' is the cross sectional area across which the diffusion takes place (cm^2)

'Δc' is the change in concentration (g/cm^3)

'Δz' is the distance in the direction of the net movement of ions (cm)

'Δt' is the change in time (s)

'θ' is the volumetric moisture content (cm^3/cm^3)

'γ' is the factor which takes into account ionic interaction and the increased viscosity of water in the porous system

'$(L/L_e)^2$' is the factor due to the tortuosity and direction of the paths.

The term $D_o\gamma(L/L_e)^2$ may be called the effective diffusion coefficient (D_e). If this

is done, equation 2.38 for steady state diffusion of anions in porous system may be written as :

$$9\frac{\Delta Q}{\Delta t} = D_o \lambda \theta \frac{\Delta c}{\Delta z} \qquad (2.39)$$

Since steady state diffusion experiment is difficult to set up particularly at high matric suctions, transient diffusion systems can more readily be set up at these matric suctions consequently, Fick's second law:

$$\frac{\partial c}{\partial t} = D_o \theta \frac{\partial^2 c}{\partial z^2} \qquad (2.40)$$

which is developed from the first law and describes the transient state, was used.

Porter et al. conducted different diffusion experiments using Na and Ca saturated silty clay loam and clay and loam samples at various suctions, and concentration of chloride was determined at the end of each test. The effective diffusion coefficient of chloride ($D_e = D_o \gamma (L/L_o)^2$) was divided by the diffusion coefficient for chloride in bulk water at 23 °C ($D_o = 1.85 \times 10^{-9}$ m^2/s) to obtain the transmission factor $\gamma (L/L_o)^2$. Values of the transmission factor are plotted as functions of the volumetric moisture content for Ca saturated systems in Fig. 2.1 and for 12 to 15 % exchangeable Na-saturated systems in Fig. 2.2. In both systems, the transmission factors of all three soils are essentially linear functions of the moisture content. According to Porter et al., at high matric suctions almost all of the reduction in the transmission factor must be due to the 'tortuosity factor' $(L/L_o)^2$. This factor can go as low as 0.04 in some soils.

Fig. 2.3 shows the relationship between the product of $\alpha\gamma (L/L_o)^2$ which is in fact the normalized diffusion coefficient (D_e/D_o), and the volumetric moisture content (θ),

found by Kemper and Van Schaik (1966) in their Na-clay soils. As it can be seen in this figure, the relationship between D_e/D_o and θ is of the non-linear form but can be approximated by a linear relationship over much of the range examined.

2.5 MODELLING THE FINITE MASS OF CONTAMINANT AND AN AQUIFER

In many practical situations, the mass of contaminant within a landfill (in the field) or a source reservoir (in the laboratory, e.g. experiments conducted in this thesis) is limited and mass will be reduced as contaminant is transported into the soil.

The mass of contaminant available for transport into the soil can be represented in terms of the peak concentration c_o and the reference height of leachate H_r or the equivalent height of leachate H_f. In the case of laboratory diffusion tests, the reference height of leachate H_r and the equivalent height of leachate, H_f, are identical and correspond to the actual height of source fluid directly above the soil. In the case of the landfill the difference between H_r and H_f is that H_r includes the mass collected by the leachate collection system while H_f excludes this mass.

Considering conservation of mass within the source solution, one can write (Rowe et al. 1994):

[Mass of Contaminant Within Source at Time t] = [Initial Mass of Contaminant Within Source] - [Mass of Contaminant Transported Into the Soil] - [Mass of Contaminant Lost Due to First Order Decay Processes]

$$m_t = m_{ic} - m_f - m_{dc} \qquad (2.41)$$

Substituting Eq. 2.7 for the mass of contaminant transported into the soil gives

$$m_t = m_{tc} - A_o\int_0^t (nvc - nD\frac{\partial c}{\partial z})\,d\tau - m_{dc} \qquad (2.42)$$

where $m_t = A_o H_r c(t)$ = mass of contaminant in source at time τ

$m_{tc} = A_o H_r c_o$ = initial mass of contaminant in the source

$m_{dc} = A_o H_r \int_0^t \lambda_T c\,d\tau$ = mass lost due to the first order decay processes (see Eq. 2.12)

H_r = reference height of leachate.

Thus, if f_T is the flux entering the surface of the deposit and c_T is the concentration at the surface, then:

$$c_T(t) = c_o - \frac{1}{H_r}\int_0^t f_T(\tau)\,d\tau - \int_0^t \lambda_T c_T(\tau)\,d\tau \qquad (2.43)$$

If $\lambda_T = 0$ and $H_r \to \infty$, Eq. 2.43 leads to the boundary condition $c_T(t) = c_o$.

Equation 2.43 explicitly models the full mass of a given contaminant in the landfill ($m_{tc} = A_o H_r c_o$) and also explicitly models removal of contaminant from the source (e.g. by sampling from the source reservoir in laboratory experiments) in terms of Γ_s (Eq. 2.12).

For two-dimensional problems, an aquifer can be modelled as a bottom boundary condition for a landfill situation. In a simulated laboratory advection-diffusion experiments, the receptor reservoir below the soil, simulates the aquifer. The concentration in the receptor can be described by:

$$c_b(t) = \int_o^t [\frac{f_b(\tau)}{h}]\,d\tau - \frac{q_b}{h}\int_o^t c_b(\tau)\,d\tau \qquad (2.44)$$

where $f_b(\tau)$ is the flux entering the receptor at time τ, h is the thickness of the receptor,

and q_b is the volume of fluid per cross-sectional unit area of the sample per unit time removed from the receptor for chemical analysis during the test.

A solution to Eq. 2.14b which allow consideration of a finite mass of contaminant in the source, a reservoir receptor, and the replacement of sampled reservoir fluid by distilled water (i.e. the boundary condition given by Eqs. 2.43 and 2.44), has been given by Rowe and Booker (1985, 1987, 1994) and has been implemented in the computer program POLLUTE v6 (Rowe and Booker, 1994).

2.6 GRAVITY DRAINAGE AND CAPILLARITY IN UNSATURATED POROUS MEDIA

In ground-water aquifers and petroleum reservoirs, gravity drainage is an important process. This process also occurs in primary and secondary leachate collection and removal systems of the landfills consisting of a granular material such as gravel or stone, where the system drains by gravity upon removal of collected leachate. If liquid, initially saturating the pores of a soil, is allowed to drain from that soil, no such complete drainage as occurs in a simple capillary tube is observed; large quantities of liquid are retained. The quantity of liquid held by the soil immediately after drainage gradually alters; it decreases to a stationary value and the liquid so held finally arranges itself in a stable distribution.

The amount of water remaining in the soil stratum, after the gravity drainage, is called as "field capacity" (Bear, 1979). The intermediate zone extends from the lower edge of the zone containing field capacity to the upper limit of the capillary zone. Within the capillary zone, there is usually a gradual decrease in moisture content with

height above the water table. The upper limit of the capillary zone called as "capillary fringe", has an irregular shape. For practical purposes some average, smooth surface is taken as the capillary fringe, such that below it the soil is practically saturated.

After termination of the gravity drainage, the water available in the pores of the unsaturated soil, has been classified by Zunker (1930) and Rode (1952) as "bound water" and "free water" (Fig. 2.4). Bound water is also classified as "adsorbed water or heavily bound water" and "solvate water or easily bound water". The main force acting on free water is gravity. As in Fig. 2.4, "fine capillary water" may often be qualified as free water. In an unsaturated soil, the main appearance of free water is "capillary water".

Soil Suction

Soil suction is commonly referred to as the free energy state of the soil water (Edlefsen and Anderson, 1943). The free energy of the soil water can be measured in terms of the partial vapour pressure of the soil water (Richards, 1965). The soil suction is commonly called "total suction". It has two components namely, matric and osmotic suction (Aitchison, 1965a). In an equation form, this can be written as follows:

$$\Psi = (u_a - u_w) + \pi \qquad (2.45)$$

where $(u_a - u_w)$ is the matric suction, u_a is the pore-air pressure, u_w is the pore-water pressure and π is the osmotic suction. The decrease in relative humidity due to the presence of dissolved salts in the pore-water is referred to as the osmotic suction, π. The matric suction component is commonly associated with the capillary phenomenon arising from the surface tension of water. The height of water rise and the radius of curvature have direct implications on the water content versus matric suction relationship

in soils (i.e., the soil moisture characteristic curve). This relationship is different for the wetting and drying portions of the curve. At a given matric suction, the soil water content during the wetting and drying processes are different. In addition, the contact angle at an advancing interface during the wetting process is different from that at a receding interface during the drying process (Bear, 1979). The above factors, as well as the presence of entrapped air in the soil, are considered to be the main causes for hysteresis in the soil moisture characteristic curve.

Gravity drainage in layered systems

Gravity drainage and soil moisture retention are the controlling parameters in designing layered systems. One of the key issues relating to the gravity drainage is the negative fluid pressures that may develop in unsaturated coarse grained soils during drainage of layered soil systems such as those used for covers and liners (e.g., covers for mine tailings). Theoretical analysis and numerical modelling of these systems have indicated that this pressure will be the pressure at which an underlying material (e.g., sand) reaches its residual water content (e.g., Nicholson et al., 1989; Akindunni et al., 1991). The hydraulic conductivity of the underlying material at these pressures is so small that "static" nonequilibrium pressures are sustained over long periods of time. Using column drainage tests, Barbour and Yanful (1993) verified the existence of pressures corresponding to that of the residual water content of the draining materials. They explained that as the residual water content of the material is approached, it may be that the water phase becomes increasingly discontinuous, leaving isolated pockets of water. Without any other mechanism of moisture redistribution (such as vapour

migration), these pockets would have "locked in" pressures equal to that pressure in them just before the liquid phase became discontinuous. Consequently, the last pressure measured by the tensiometer correspond to the pressure at which the sand reached the residual water content.

It was demonstrated by Barbour (1990) that the moisture content distribution within a two layer soil system (i.e., fine grained cover overlying a coarse grained material in mine tailings) is not solely a function of the moisture retention characteristics of the material but may also be influenced by the water flux through the system. According to his results, this effect is more pronounced for unsaturated materials subjected to a relatively high flux. This effect may be negligible when the applied flux is low or when the materials are essentially saturated or nearly saturated.

Akindunni et al. (1991) demonstrated that in the case of very coarse underlying materials (e.g., gravel) with low negative pressure values at residual saturation, the resulting interface pressure head could be so small that it could practically be considered to be zero (i.e., atmospheric pressure).

A historical review on the capillary phenomenon and gravity drainage

The process of capillary suction is described by Zunker (1930) in the following way: "Near the water table, the lifting capacity is great in the larger pores, menisci in these pores will, so to speak, hurry forward and the finer pores will be able to keep up only if they can suck water from them. Later, it is the velocity developed in the finer pores that plays the decisive role; as a consequence of their filling up, air will be trapped in the larger pores. The number of air locks will increase more and more since the

velocity difference is increasing too; the lifting force will fail to act in more and more pores and in addition, as a consequence of capillary pressure, air will leave the water. At a certain height, air locks being already in connection with the atmospheric or with air in the top layer are also found; this plane is the border between the 'closed capillary zone' and the zone of 'aeration' (open zone)".

Rode (1952), describes the process in a similar way, emphasizing the fact that with increasing height, hydrostatic pressure with their superficial pressure difference (which is a function of the radius of curvature) will diminish more and more. Ornatsky (1950), noted that the volume of confined air in a "coarser soil" is smaller because of the existence of larger volume of "free water" in the pores which causes that the confined air to escape easily from the porous medium. Zimmerman (1936) attached great importance to sack-shaped capillaries, these can not be filled up by water because their compressed air content exerts resistance to the force driving the water in. Terzaghi (1943), distinguished between three zones as "fully saturated zone", "partly continuous zone penetrated by air columns", and "a zone hydrostatically independent of the phreatic water".

For the purpose of better understanding the ordinary gravity-drainage mechanism, let us consider the experiment conducted by Smith (1961) which is described in the remainder of this subsection as follows:

" Shown in Fig. 2.5, a long column of uniform sand packed in column *A* is joined to column *B* by tube a. Column *B* contains liquid only. The free liquid surface in column *B* is denoted as W_h. This column will serve as a well and *P* as a pump which is used to remove liquid. W_h in actual practice is the water table or phreatic surface.

Suppose the sand column *A* is fully packed to within a 2 cm or more of the top, that all pore are completely filled with water, and that the liquid initially forms a free surface W_s just above the packing. The initial water table W_i in well *B* will occupy a position W_i in such a manner that W_s and W_i are at equal heights above the reference plane *rr'*. When pump *P* is started, water will be removed from column *B* and W_i will fall. In column *A*, the water level W_s will fall until it reaches the top of the sand. There, it will form a capillary meniscus C_i at the top of the sand and in the first layer of grains. W_h drops further down in well *B* until the distance between C_i and W_h becomes a value of h_m, which is the height of the maximum capillary rise meniscus C_m (Smith, Foote, and Busang, 1931).

As well *B* is further pumped and the water table W_h is progressively lowered, the main capillary meniscus C_m will fall but always in such a way as to maintain a height h_m above W_h. However, the sand above C_m is not drained completely of liquid. Isolated water pockets are left behind. They are of two types: pendular water, consisting of rings of liquid wrapped around contact point of two adjacent grains, as in Fig. 2.6A; and funicular water, which is contained in a cluster of grains whose pores are completely filled and bounded by a single closed capillary meniscus as in Fig. 2.6B (Versluys, 1917). The bounding meniscus of each is formed by detachment from the main capillary meniscus C_m (Fig. 2.5) as it passes through the sand column (Smith, 1936). The wetting layer, one molecule or so thick, is supposed to exist over the grain surfaces.

As the well is further pumped the water table W_h (Fig. 2.5) finally reaches the bottom of column *B*. At this point the main capillary meniscus assumes a final position C_f. The bulk liquid separates from the sand along *bb'*, its contact with the sand column.

The part of the sand between the reference plane rr' and the final position of the capillary meniscus remains saturated.

The origin of the maximum capillary rise meniscus under gravity drainage is not difficult to understand. Referring to Fig. 2.7A, the water table W_h is under atmospheric pressure. Initially, the free water surface W_s above the top of sand in column A, shown in Fig. 2.5, is plane and under atmospheric pressure A. As W_h recedes, W_s falls until it reaches the top of the sand, where a complexly curved meniscus C_i begins to form. The meniscus is a multiply connected surface that extends across the column. It is a capillary meniscus and gives rise to a pressure jump Δp as we pass through its surface from point a to point a´, Fig. 2.7C. The pressure beneath the meniscus is negative, and the pressure just under the surface, for example, at a´, is less by an amount Δp than that of the atmospheric pressure A by an amount given by the Laplace capillary equation (Pockless, 1908):

$$\Delta p = T(1/R_1+1/R_2) \qquad (2.46)$$

where T is the surface tension of the liquid and R_1 and R_2 are the principal radii of curvature of the capillary surface. Because this pressure deficiency Δp (Eq. 2.46) characterizes every capillary surface, and (if the meniscus is concave upward as in the sand column under discussion) leaves the liquid just below the meniscus in tension, the meniscus C_i will seek a position in the multiple conical type capillary (Smith, Foote, and Busang, 1931) which will leave a head h_i of water above the water table just sufficient to maintain it at atmospheric pressure A (Fig. 2.7A); otherwise sufficient water would flow into sand to maintain this equilibrium (Drysdale, 1923). As the water table falls in the well (Fig. 2.5), the meniscus C_i will fall in the top layer of grains that contains it

until it reaches the minimum opening, which is located in the diametral plane *D-D´* (Fig. 2.7B) (Smith, 1933). This opening corresponds to the narrowest capillary and corresponds to maximum rise h_m. It will support the maximum column of liquid above the water table. The head h_m of water characterizing this position is the "maximum capillary rise" of the sand. As the water table is further withdrawn the meniscus c_m, that of maximum capillary rise, falls through the sand from one grain layer to the next, always at a height h_m above the water table W_h. The maximum capillary rise meniscus is considered in the statistical sense. Fluctuations in each grain layer depend upon the single pore sizes.

Finally, when W_h reaches the reference line *rr´* (Fig. 2.5), the meniscus C_m is at a height h_m above it. The liquid along the reference line is at atmospheric pressure. No further liquid can be withdrawn from the sand by gravity drainage and a meniscus forms at *bb´*, severing the liquid body in the pores from any bulk liquid in the well, which has been drained by the pump.

Observations of any sand packing, such as shown in Fig. 2.5, being drained under gravity shows that isolated bodies of liquid are left after the capillary meniscus C_m has passed over them. They are either of the 'pendular' or 'funicular' type (Versluys, 1917). Fig. 2.8 shows the formation of a pendular body, which includes an idealized section through a small element of the capillary meniscus and grains lying in the section. The dotted top grain in Figure 2.8A is just behind the section, but its point of contact *O* is in the section. C_m has just passed the dotted grain. The meniscus will ride above the contact point *O* (Smith, 1933, p. 426) since there are no pressure distributions which will cause its rupture. At the top point S_T, it will have a pressure deficiency greater than that

of the meniscus C_m by an amount $\Delta' p = \rho g \Delta h$ where Δh is its height above C_m. If the liquid at S_T recedes too far into the contact zone toward O, with consequent increase in the meniscus curvature above S_T, $\Delta' p$ will be decreased beyond that permitted by h and liquid will flow from C_m to the point S_T to restore the curvature to a value permitted by Δh. Hence the curvature at S_T will be virtually that of C_m. It differs only by an amount permitted by Δh, which is a few grain diameters.

In Fig. 2.8B, the liquid is passing from cell layer which is occupied in Fig. 2.8A, but liquid is still flowing from S_a and S_b to S_T and there is a constant retreat of the parts of the meniscus at S_a and S_b into the liquid body just below S_T. These parts finally meet just below O in the section O-O', and a detachment of a part of the meniscus around O from the main meniscus C_m occurs. The result is a ring of liquid around the point O, completely separated from the main capillary meniscus C_m, as shown in Fig. 2.8C.

Fig. 2.9 shows, similarly, successive stages in the formation of a "funicular" body of liquid. The process may be more clearly described by considering the passage of the meniscus over the contact point of two adjacent grains of a three-grain element in the rhombohedral cell of close hexagonal packing.

At the points S_a and S_b (Fig. 2.9A), which are in the wider part of the pore just below the top grains in contact at O, the menisci curvatures are less than those of the maximum capillary rise meniscus C_m, since the meniscus is falling and presently located in a pore section larger than the minimum pore section of maximum capillary rise. The pressure just under it is therefore greater than just under the maximum rise meniscus and much greater than the pressure at S_T. Hence liquid from S_a and S_b will move inward toward the minimum pore section through O-O' as shown in Fig. 2.8B.

Liquid must accumulate in these positions (pendular and/or funicular) rather than in a uniform layer over the grain surfaces. They are detached from the pore liquid just under the capillary meniscus, C_m, and their bounding meniscus is detached from the main capillary meniscus, C_m as it passes through the sand (Smith, 1936).

Very little water will be found at the top of a long column whereas a large quantity will be found just above the capillary meniscus. It is obvious that in the final state the column, if sufficiently long, may contain pendular bodies in its upper part, funicular bodies just above the main capillary meniscus C_m, and the bulk water of capillary rise just above the water table ".

It is true that thin films of water may be held on a surface of grains, but these are at most of the order of a few hundred angstrom units (10^{-8} cm), and generally much less (Smith, 1961). In sand the water so held is negligible; in fine clays, however, it may be considerable (Smith, 1961). According to Bear (1979), below "field capacity" which is the amount of water remaining in the soil after an extended period of drainage, the soil contains "capillary water" in the form of "continuous films" around the particles, held by surface tension. This water is moved by capillary action and is available for plants.

In diffusion transport studies of a solute through a granular material such as sand or fine gravel, this thin film of water around the grains is thick enough to produce a narrow path through which solute can diffuse. For example, hydrated ionic diameter of chloride is about 0.0007 μm (Horvath, 1985), which compared to the thickness of water films around soil particles is very small so that the chloride ion can diffuse easily through this narrow path.

The maximum capillary rise in a uniform sand has been shown by Smith, Foote, and Busang (1931) to be given by:

$$\frac{T}{\rho g h_c d} = \frac{1}{4}\left[\frac{0.959}{(1-n)^{\frac{2}{3}}} - 1\right] \qquad (2.47)$$

in which T is the surface tension of the liquid, ρ its density, g the acceleration of gravity, h_c the height of maximum capillary rise, d the grain radius, and n is the porosity of the sand.

On a more realistic basis, Zunker (1930), constructed a formula which was valid for soils having a mixed granulometric composition. It is in the form of:

$$h_c = \frac{0.3}{ed} \qquad (2.48)$$

where e is the void ratio of the soil, and d is the effective grain size (d_{10}). According to Zunker's experiments, the actual rise is some 1.7 times the value given by the formula. His explanation of this was the deviating size of the soil pores.

Often relationships such as:

$$h_c = \frac{2.2}{d_H}\left(\frac{1-n}{n}\right)^{\frac{3}{2}} \qquad (2.49)$$

for sand (Maris and Tsui, 1939), is used where h_c is in inches, n is porosity, and d_H (in inches) is the harmonic mean grain diameter.

Another equation introduced by Polubarinova and Kochina (1952, 1962) has the form of:

$$h_c = \frac{0.45}{d_{10}} \frac{1-n}{n} \qquad (2.50)$$

where both d_{10} (effective particle diameter) and h_c are in cm.

From the above given equations, one can reasonably predict the height of the maximum capillary rise in a given porous medium having uniform grain size, by knowing the physical parameters of the porous medium such as porosity (n) or void ratio (e) and effective grain size (d_{10}). A comparison of observed and predicted maximum capillary rise has been made for coarse sand and fine gravel, which will be discussed in Chapter 7.

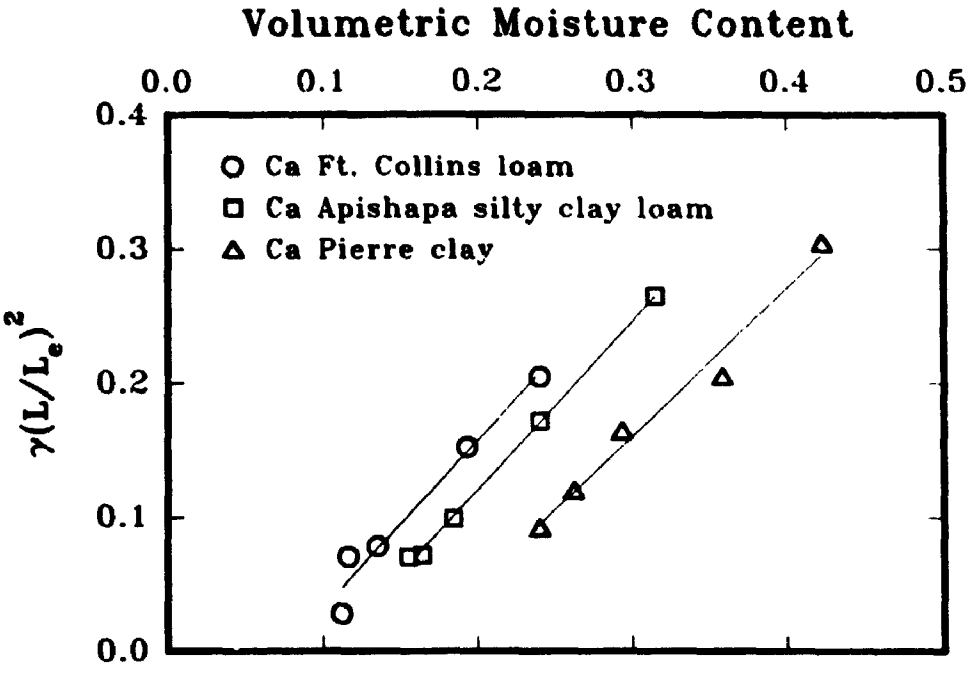

FIG. 2.1 TRANSMISSION FACTORS, $\gamma(L/L_e)^2$, FOR Ca SOIL SYSTEMS AT 1/3, 1, 5, 10 AND 15 ATM. TENSION (MODIFIED AFTER PORTER ET. AL., 1960)

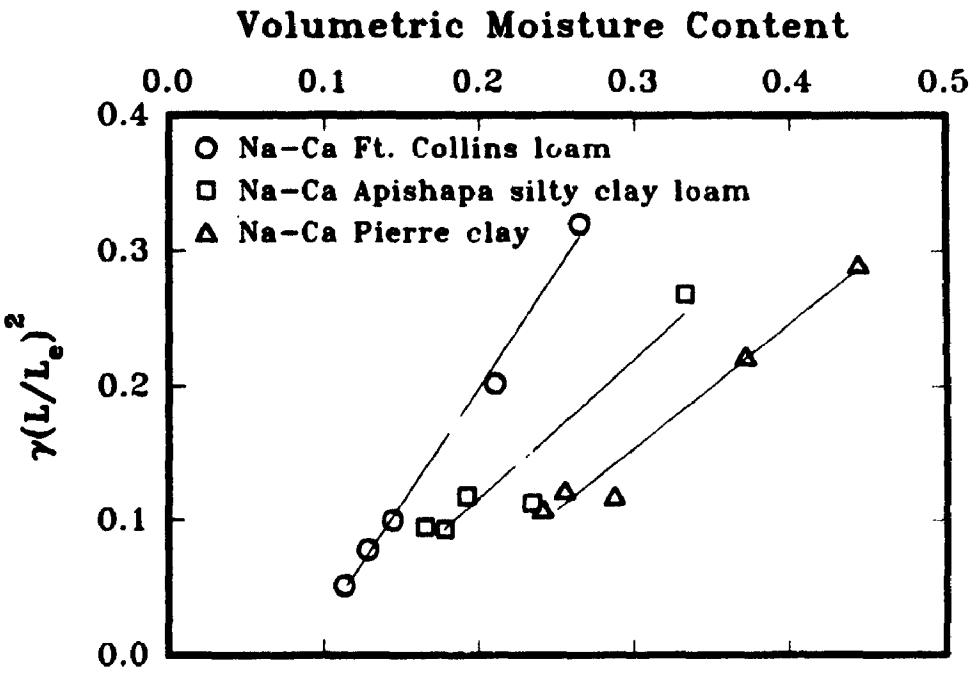

FIG. 2.2 TRANSMISSION FACTORS, $\gamma(L/L_e)^2$, FOR 12 TO 15% EXCHANGEABLE Na^+ SOIL SYSTEMS AT 1/3, 1, 5 10, 15 ATM. TENSION (MODIFIED AFTER PORTER-ET. AL., 1960)

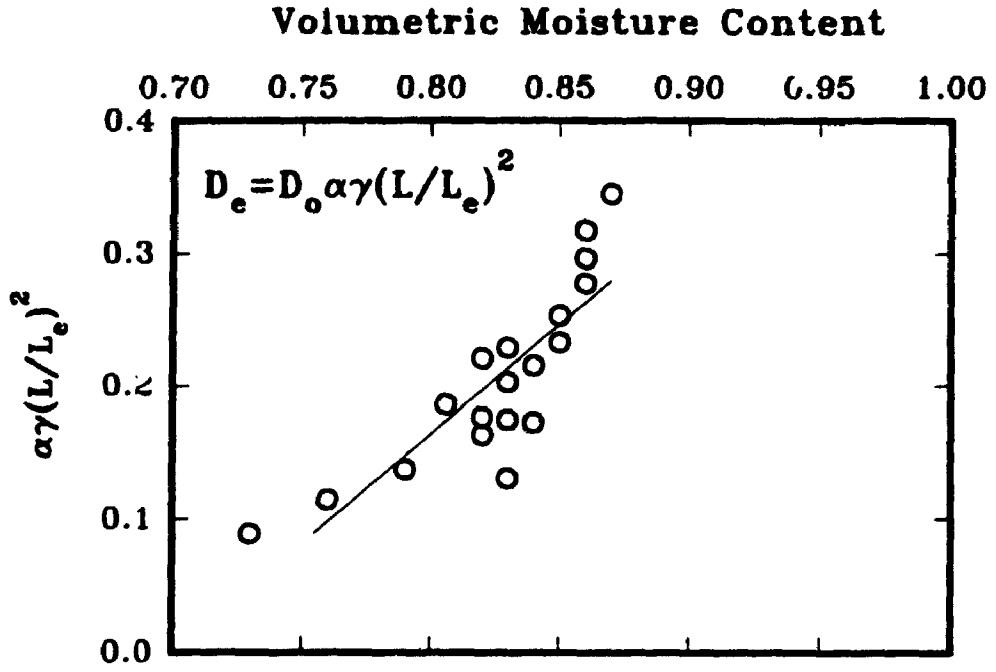

FIG. 2.3 RELATION OF THE PRODUCT OF THE TORTUOSITY (L/L_e^2, DECREASED FLUIDITY α, AND ELECTRICAL INTERACTION γ) FACTORS AND THE VOLUMETRIC MOISTURE CONTENT, θ, IN Na-CLAY PLUGS (MODIFIED FROM KEMPER AND VAN SCHAIK, 1966)

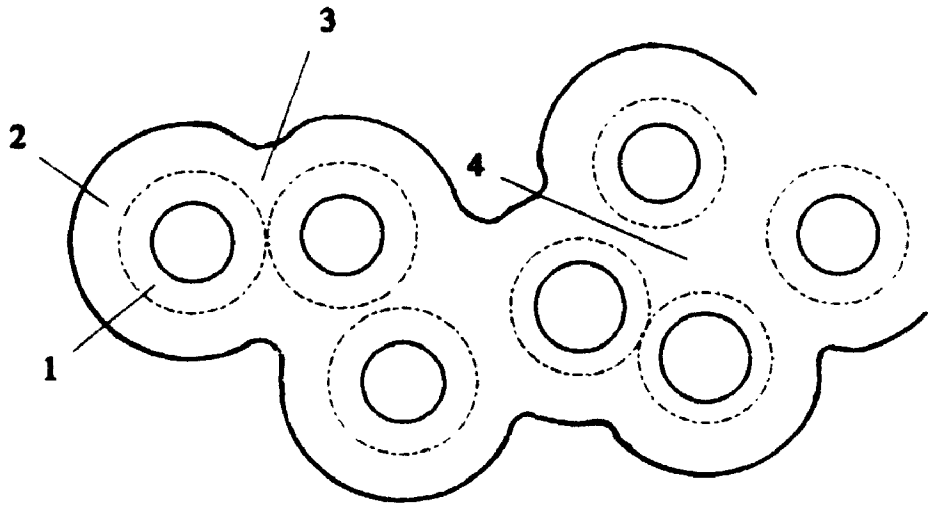

FIG. 2.4 CLASSIFICATION OF SOIL PORE WATER ACCORDING TO ZUNKER (1930) AND RODE (1952):

1: HEAVILY BOUND WATER

2: EASILY BOUND WATER

3: INTERSTITIAL WATER

4: FINE CAPILLARY WATER

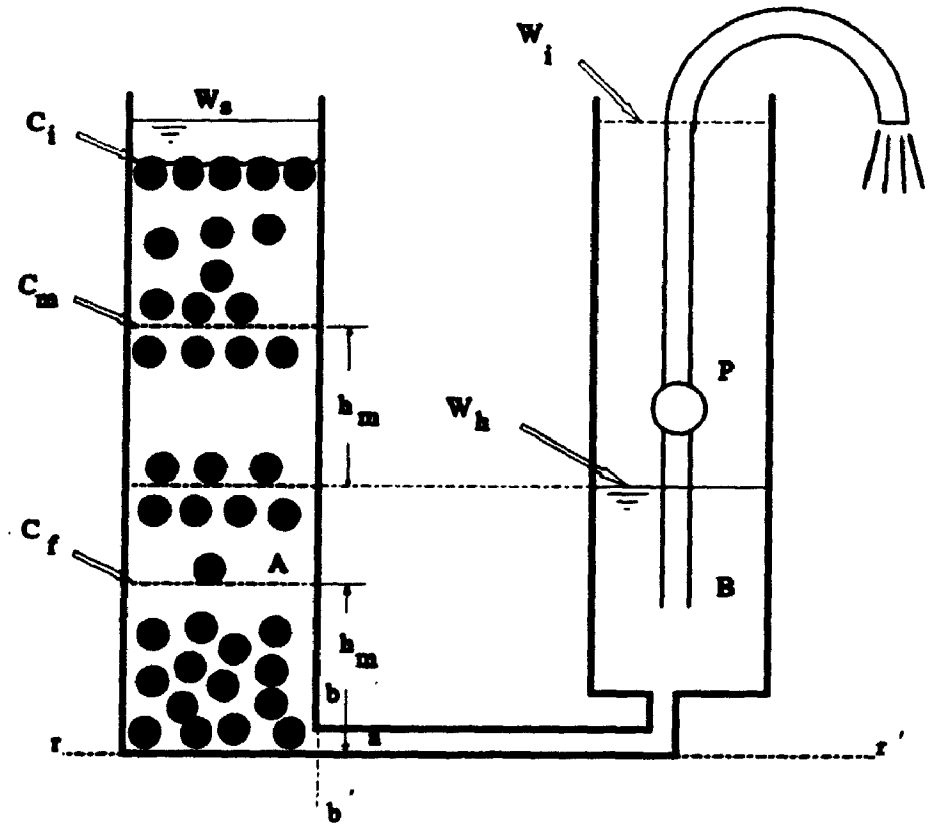

FIG. 2.5 SCHEMATIC DIAGRAM OF APPARATUS USED TO DRAIN A UNIFORM SAND (MODIFIED AFTER SMITH, 1961)

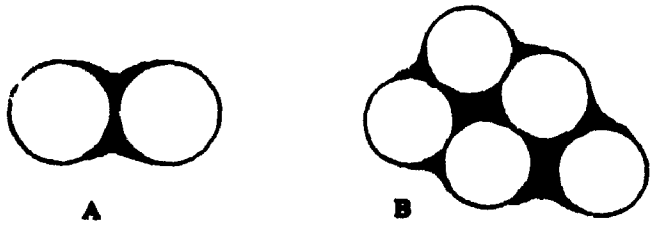

FIG. 2.6 TYPES OF CAPILLARY WATER PRESENT IN AN UNSATURATED SAND : A, PENDULAR WATER; B, FUNICULAR WATER

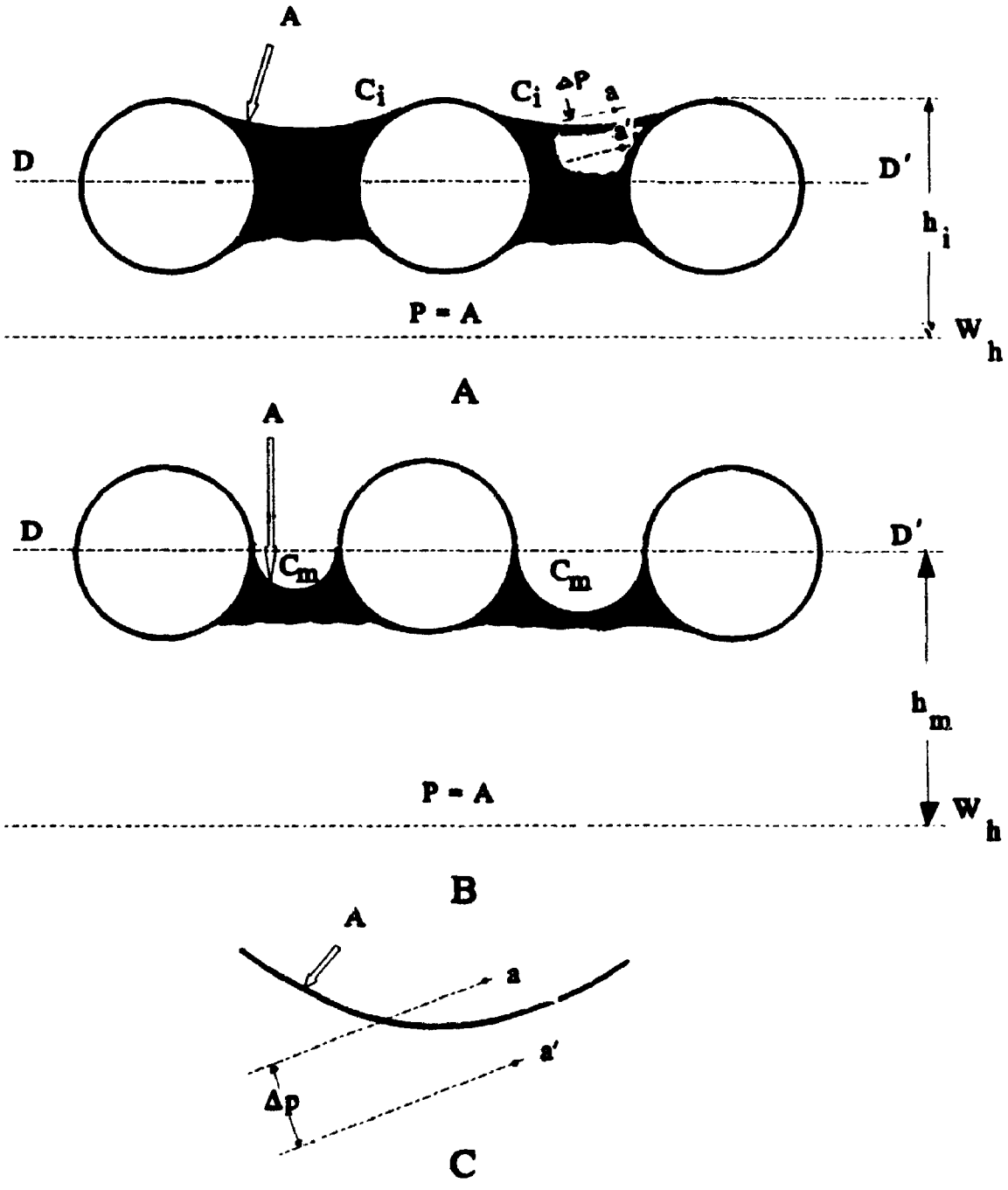

FIG. 2.7 DEVELOPMENT OF MAXIMUM CAPILLARY RISE : A, INITIAL POSITION OF MENISCUS, LOCATED IN THE LARGEST PORE-CROSS SECTION. B, POSITION OF MAXIMUM CAPILLARY RISE, LOCATED IN THE SMALLEST PORE CROSS SECTION. C, PRESSURE DISCONTINUITY, ΔP, JUST ACROSS A CAPILLARY SURFACE (MODIFIED AFTER SMITH, 1961)

techniques of shaking were adopted. Some samples were selected to be shaken by hand, and others were shaken by a heavy duty shaker which shakes the samples by moving in a horizontal direction at 250 rpm for a specified time. The same procedure that was used for fine and medium sand was adopted for fine gravel. The contaminated sample was drained over a #100 sieve and the damp sample was divided into 5 approximately equal sections. Each section was then transferred into stainless steel containers (the sectioning plates used in the diffusion tests) and the wet weight of each sample was recorded. All containers were oven dried and the moisture content was calculated. Samples were numbered from 1 to 5. Samples numbered 1, 2 and 4 were shaken by hand. Samples 3 and 5 were shaken using the heavy duty shaker. The sample characteristics and recovered concentration results are shown in Table 3.2. Recognising that some fluctuation in concentration is normal with this type of measurements using 701A digital pH/mv meter, it is apparent that almost all the chloride mass which had been converted into a solid phase by drying the samples, was recovered during the washing process. Results of samples shaken by hand for 10 minutes, are in good agreement with the results of samples shaken by shaker for 3 hours indicating that shaking by hand for 10 minutes is enough to recover the mass from solid phase. The small fluctuation in the results are most likely due to the normal error in $c_{s,w}$ measurement.

3.3 APPARATUS DESIGN FOR DIFFUSION AND ADVECTION-DIFFUSION TESTING

In the first test series of this experimental program, materials were tested for determination of their diffusion coefficients under a condition of gravity drainage. Since

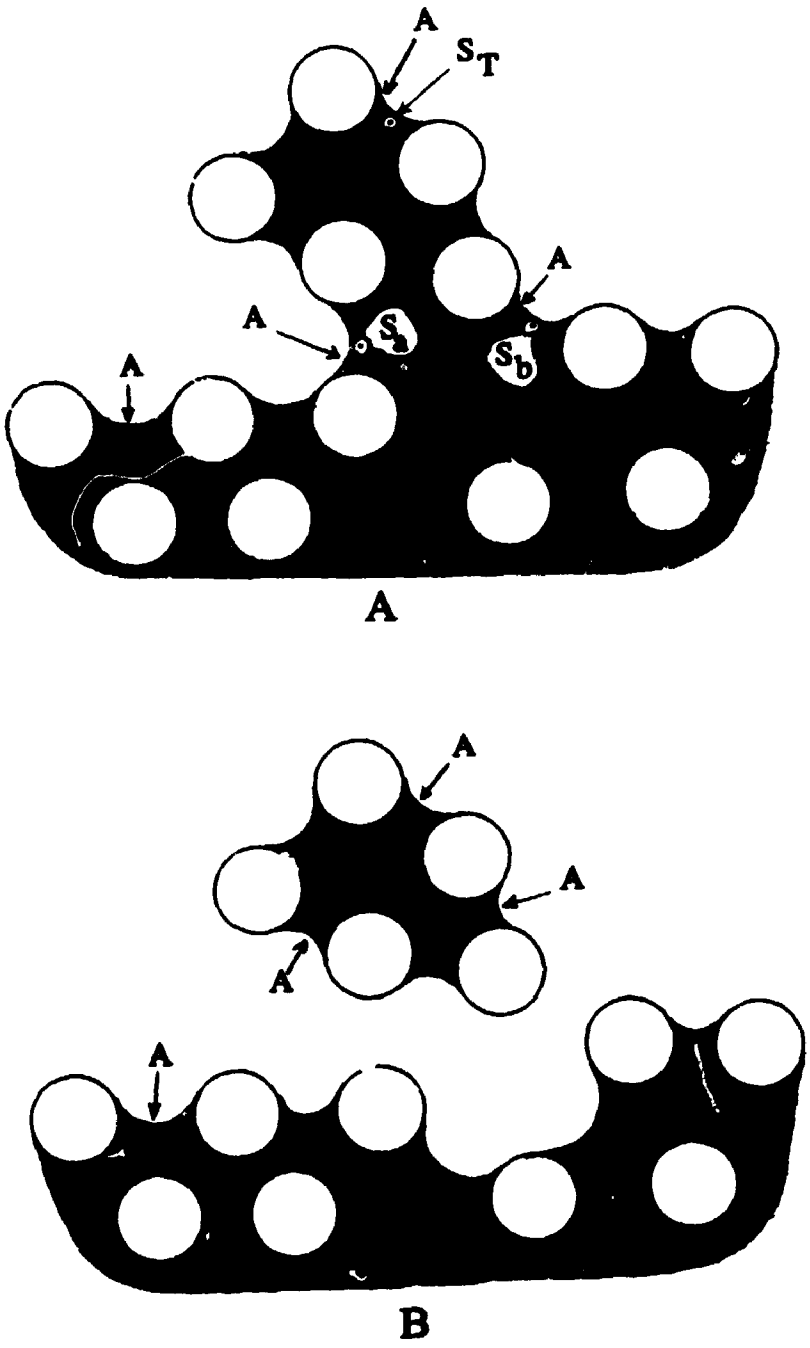

FIG. 2.9 FORMATION OF FUNICULAR BODY BY DETACHMENT FROM MAXIMUM CAPILLARY RISE MENISCUS. A, DETACHMENT OF FUNICULAR BODY BEGINING AT POINTS Sa AND Sb. B, COMPLETED FUNICULAR BODY JUST ABOVE MAXIMUM RISE MENISCUS. (MODIFIED AFTER SMITH, 1961)

CHAPTER 3

PRELIMINARY TESTING AND EQUIPMENT DESIGN FOR PROPOSED EXPERIMENTAL PROGRAM

3.1 INTRODUCTION

In this experimental program, a wide range of soils having different physical and chemical characteristics were tested for a solute (NaCl) migrating under a conditions of gravity drainage. This condition was applied for tested soils by maintaining the atmospheric pressure level at the bottom of the soil and allowing the soil to drain (yield) its pore water. The soils used in this study had different grain sizes as will be shown in relevant chapters. The clayey soil and silt used in the experiments were almost well graded while granular material such as fine and coarse sand, fine gravel, and coarse stone were uniformly graded. Different soils, having different grain sizes, result in different pore sizes and hence different moisture storage capacity in the soil's pores under conditions of gravity drainage. Coarse grained material has a higher hydraulic conductivity than the fine grained material and hence can be drained by gravity under a smaller suction, resulting in a low moisture content in the pores. Due to the higher capillary forces in the pores of fine grained material (clayey silt, silt and fine sand), one can not drain these soils under low suction (used in this experimental program) and hence the pores remain almost saturated after gravity drainage.

To determine the solute concentration profile in the soil at the end of solute migration, the pore water concentration at different depths in the soil was determined.

Because of the wide range of soil type examined it was necessary to use different techniques for the extraction of pore water from the soil. For example, soil squeeze approach was used for clayey soils but this procedure was not applicable for granular soils. At the beginning of this experimental program, an attempt was made to select appropriate techniques for pore water concentration measurement for the different soils tested. This will be described in this chapter.

The experimental program consisted of two types of solute migration testing; "diffusion testing" in which the only mechanism of transport is by diffusion (transport of solute due to concentration gradient in the soil system), and "advection-diffusion testing" in which the mechanism of transport consists of both diffusion and advection (transport of solute by flowing water in the soil system). The equipment was designed to allow examination of both types of test using the one basic apparatus. The equipment design will be described in this chapter.

3.2 TESTING THE APPLICABLE TECHNIQUES FOR SOIL PORE WATER CONCENTRATION MEASUREMENT

3.2.1 PORE WATER EXTRACTION FORM CLAYEY SOIL

For extraction of pore water from clayey soil, pneumatic soil squeezing apparatus was used. This apparatus is designed so that a hydraulic pressure of 25 MPa can be exerted to the clay sample which is installed in a cylinder having a piston on top and a filter paper at the bottom of the soil. Extracted water passes through the filter paper and is collected in a 4 mL glass bottle. For a clayey soil with a moisture content of 13% or

greater a minimum of 60 grams of soil is required to produce at least 3 mL of pore water solution within 5 hours of squeezing. For concentration measurements a minimum of 3 mL pore water is recommended. This method has been successfully used for clayey soils in other research work conducted at the Geotechnical Research Centre of the University of Western Ontario (Barone, 1990).

3.2.2 PORE WATER EXTRACTION FROM SAND

3.2.2.1 EXTRACTION BY MEANS OF CENTRIFUGE

This method was found to be suitable for coarse sand samples having a moisture content of more than 15 %. The procedure involves placing a minimum of 75 grams of clean dry 3 mm diameter glass beads in the bottom of a centrifuge bottle. A 56 mm diameter filter paper is then placed on top of beads and the wet sand sample is placed on the filter paper. The bottle then centrifuged at 2000 rpm for 30 minutes. At the end of centrifuging, the pore water which had collected in the pores between the glass beads at the bottom of the bottle was collected using a 5 mL syringe.

An attempt was made to use this method of extraction of pore fluid from fine sand. Unfortunately, the volume of collected water after centrifuging was insufficient for chemical analysis. Similarly, this method was not applicable for unsaturated coarse sand and fine gravel due to very low volume of fluid that could be collected. Thus, this method was not adopted in this experimental program.

3.2.2.2 EXTRACTION BY MEANS OF SUCTION

This method has been adopted by some researchers to extract pore water from sand and also glass beads (e.g. De Smedth, 1981). In this method, glass beads are placed in a suction cup and vacuum is applied at the bottom of the suction cup to extract the pore water. Due to the lack of experience with this methodology, this method was not adopted in this experimental program.

3.2.3 PORE WATER CONCENTRATION MEASUREMENT USING WASH METHOD

This method (to be described later), was adopted in this experimental program for pore water concentration measurement in silt, sand, gravel and stone and was found to be a successful method of pore water concentration measurement. In fact, this method is the only method suitable for pore water concentration measurement for sand, gravel and stone having a low moisture content.

3.2.3.1 PREVIOUS EXPERIMENTS USING WASH METHOD

This method has been successfully used for determination of pore water concentration of intact Queenston shale (see Barone, 1990). In this method, the rock or soil sample is sliced and the solute pore water concentration profile versus depth is determined by washing oven dried pulverized material from each slice in distilled water. The solute pore water concentration, c, can be calculated from the wash extraction

concentration, c_{sup}, using:

$$c = \frac{c_{sup} v_{sup} \rho_w}{m_s w} \qquad (3.1)$$

where, c = solute pore water concentration (g/L)

c_{sup} = solute concentration in the wash supernatant (g/L)

v_{sup} = volume of supernatant (L)

m_s = mass of solids used in the wash (g)

w = moisture content of the slice which is available to solute (-)

ρ_w = density of water at 22 °C (1000 g/L)

It should be noted that in wash method, it is assumed that the mass of contaminant measured is all available in solution and that the solution volume is accurately represented by the moisture content of the soil.

3.2.3.2 TESTING THE APPLICABILITY OF WASH METHOD FOR SAND AND GRAVEL

The applicability of wash method was examined at the beginning of this study program. Tests were conducted for both fine and medium sand and for fine gravel. The following procedure was adopted in the tests :

1. Original samples were washed to remove any background concentration and then ovendried.
2. A sodium chloride solution was prepared and concentration of chloride in solution was measured using the specific chloride electrode and the multipurpose ion electrometer.

3. A known amount of dry sand was taken and mixed with solution and left to soak in the solution over night.
4. This contaminated sand sample was drained over a sieve # 200 and transferred into 5 containers.
5. The wet samples were weighed and oven dried. The moisture content of each sample was then calculated.
6. Twenty grams (80 grams, for the fine gravel tests) from each dry sample was taken and placed in centrifuge bottles and 200 mL (50 mL, for the fine gravel test) of de-ionized distilled water was added to each bottle.
7. The centrifuge bottles containing sand and water were shaken by hand for 10 minutes and then centrifuged at 2000 rpm for 10 minutes.
8. The solution (wash water) remaining on top of each sand sample was poured into a container and the concentration of the wash water (supernatant), c_{sup}, was determined using chloride electrodes attached to a multi purpose electrometer (701A digital pH/mv meter).
9. Using Equation 3.1, concentration of contaminated sand was then calculated.

The results of the wash tests performed for fine and medium sand are given in Table 3.1. As can be seen from this table, the recovered concentrations are in good agreement with the original concentration, confirming the applicability of wash method for these material.

As noted, during wash test the samples were shaken by hand for 10 minutes. In order to check the efficiency of shaking technique and also applicability of the wash method for gravel, the wash method was also tested for fine gravel. This time, 2

techniques of shaking were adopted. Some samples were selected to be shaken by hand, and others were shaken by a heavy duty shaker which shakes the samples by moving in a horizontal direction at 250 rpm for a specified time. The same procedure that was used for fine and medium sand was adopted for fine gravel. The contaminated sample was drained over a #100 sieve and the damp sample was divided into 5 approximately equal sections. Each section was then transferred into stainless steel containers (the sectioning plates used in the diffusion tests) and the wet weight of each sample was recorded. All containers were oven dried and the moisture content was calculated. Samples were numbered from 1 to 5. Samples numbered 1, 2 and 4 were shaken by hand. Samples 3 and 5 were shaken using the heavy duty shaker. The sample characteristics and recovered concentration results are shown in Table 3.2. Recognising that some fluctuation in concentration is normal with this type of measurements using 701A digital pH/mv meter, it is apparent that almost all the chloride mass which had been converted into a solid phase by drying the samples, was recovered during the washing process. Results of samples shaken by hand for 10 minutes, are in good agreement with the results of samples shaken by shaker for 3 hours indicating that shaking by hand for 10 minutes is enough to recover the mass from solid phase. The small fluctuation in the results are most likely due to the normal error in c_{sup} measurement.

3.3 APPARATUS DESIGN FOR DIFFUSION AND ADVECTION-DIFFUSION TESTING

In the first test series of this experimental program, materials were tested for determination of their diffusion coefficients under a condition of gravity drainage. Since

the objective was to examine purely diffusive transport in these tests, any advective-dispersive transport of solute had to be prevented. Due to the high hydraulic conductivity of the granular materials tested, it is not practical to place the source solution on top of soil sample because of the considerable downward advective flow that would occur under a condition of gravity drainage. Thus the requirement for purely diffusive transport in the granular material (e.g. sand and gravel), requires that the source solution be beneath the soil sample to prevent any leakage (or advective flow) induced by gravity into the soil. Diffusion could occur upward through the soil sample. For these tests it was necessary to separate the soil from the source reservoir by a porous disk. The characteristics of this porous disk will be discussed later.

Diffusion testing requires two types of sampling; soil pore water sampling at the end of the test, to obtain the pore water concentration profile through the soil thickness, and source solution sampling from source reservoir during the test, for determining the variation in source solution concentration with time. Thus, sampling procedures should be taken into account in apparatus design. For the soil pore water concentration determination at the end of the test, it is desirable to section the soil sample in equal thickness and then determine the concentration of each soil section. Since granular materials are more permeable than fine grained materials (e.g. clayey soils), any attempt to push the sample out of the diffusion cell cylinder will disturb the sample and will cause the pore water to be displaced along the sample and result in incorrect and unrepresentative pore water concentrations for each soil depth. For this reason, the samples should be sectioned in place, immediately after the test. This condition requires a segmented type design of diffusion cell cylinder as shown in Fig. 3.1. Plexiglass was

the material of choice since it allows direct visual examination of the sample during the test. At the end of the test, the soil sample was sectioned by slightly separating the adjacent rings from each other and sliding the stainless steel sectioning plates through the ring's interfaces. The segmented rings were sealed at their interfaces to prevent leakage using "o" rings. If the tested materials were fine sand and silt (saturated or unsaturated), breaking the seal at the interface of the two adjacent plexiglass rings during sampling, did not dislocate the pore water. This is because of the strong matric suction in this material which cause the pore water to be held within the sample. In contrast, saturated coarse grained materials such as fine gravel do loose water upon breaking the seal. For these materials, the saturated effective diffusion coefficient can be deduced based on the data obtained from monitoring the variation in source solution concentration with time (will be discussed in Chapter 7). The unsaturated coarse grained materials (e.g., coarse sand and fine gravel) retained their pore water during sampling. Again, this was due to the matric suction in these samples (discussed in Chapter 7). The whole system of rings was fixed together by means of top and bottom stainless steel plates using steel rods (see Fig. 3.1). Sampling from the source reservoir could be done through a septum port installed in the source reservoir. Extracted solution from the source reservoir was replaced with distilled water of the same volume to maintain constant water level inside the soil (this procedure can be directly modelled using the program POLLUTE). The volume of fluid in the source was monitored using an accessory set up consisting of a 2 mL pipette (with 3.5 mm I.D.) and a vertical burette connected to the source reservoir of the diffusion cell by means of plastic tubing (see Fig. 3.2). The burette is filled with distilled water and is used to refill the pipette after sampling. In each sampling, a two

mL of source solution is extracted and the same volume of water is replaced through the pipette. Depending on the condition of the diffusion test (saturated or unsaturated), the level of the horizontal pipette could be adjusted at the top level of the soil sample in saturated condition or at the bottom level of the soil (top surface of the porous disk) in gravity drained unsaturated condition.

During the saturation phase of the "drying" tests and "saturating" tests, the flow of water was upwards from the bottom reservoir towards the top air inlet shown in Fig. 3.1. With an upward hydraulic gradient, there is the possibility of piping during the saturation process for fine grained granular material. To prevent this, a 7.6 cm diameter, number 200 wire mesh and a perforated stainless steel plate (consolidation plate) was placed on top of the sample and pressure was applied to the sample by means of a spring squeezed between the perforated plate and top stainless steel plate (see Figs. 3.3 and 3.4 for details).

The base plexiglass ring was fixed into the reservoir chamber and sealed by means of an "o" ring installed in the chamber. The reservoir chamber had two openings; an inlet and an outlet. Two teflon valves attached to these openings were used to control the flow of fluid in and out of the reservoir during saturation and de-saturation (gravity draining) and flushing the reservoir (to be discussed later) and also sampling from the reservoir. Sampling was done through the septum port in the reservoir chamber using a 2.5 mL capacity syringe with a 5 cm long hypodermic needle. The use of a long needle facilitates sampling of the solution from almost the centre of the reservoir.

In order to maintain a uniform concentration distribution within the source solution throughout the test, a 13 mm long magnetic bar was placed in the source reservoir and

the cell was placed on a magnetic stirrer which operates the magnetic bar during the test (Fig. 3.2).

The apparatus described above was also used for advection-diffusion testing. In these tests (to be explained in coming chapters) two soils were used in any given test with a clayey soil being placed on top of a granular soil (sand or gravel). The source solution was placed on top of the clayey soil in an upper reservoir which consisted of two extra plexiglass rings on top of the clayey soil ring. In these tests the bottom reservoir chamber which was the source reservoir in the diffusion testing acted as a receptor reservoir. The sampling procedure for the receptor reservoir was similar to that used for the diffusion testing. Sampling from the source reservoir was performed by removing the top stainless steel plate, extracting the solution by a syringe, replacing the extracted solution by distilled water having the same volume, and then mixing the solution by hand using a small plastic spoon.

3.3.1 TESTING THE FLUSHING TECHNIQUE FOR THE SOURCE RESERVOIR

Assembling the apparatus, installation, saturation and de-saturation (gravity draining) of the sample, will be explained in later chapters. In the diffusion testing, once the sample was saturated for the saturated condition tests, or drained for the unsaturated condition tests, the water in the source reservoir was replaced (flushed) by the source solution. A schematic of the flushing technique is shown in Fig. 3.5. To flush the reservoir, a tank containing the NaCl solution was connected to the inlet valve of the reservoir chamber by a plastic tubing. The solution level in the tank was then adjusted

to be at the bottom level of the porous disk by means of a variable height support. In order to replace the water in the reservoir with NaCl solution at the desired concentration, it was necessary to assess the volume of solution that needed to be passed through the reservoir in order to completely flush the water from the reservoir. Three flushing tests were performed during which, inlet and outlet valves in the reservoir chamber were opened simultaneously and solution in the tank was allowed to flow into the reservoir and out into a container. One reservoir volume of 251 cm^3 was collected in each container during the test. During flushing, the tank base was adjusted continuously to maintain the solution level in the tank at the bottom level of the porous disk. The magnetic stirrer was functioning throughout the test to mix the solution in the reservoir. After flushing of about 10 times the reservoir volume, flushing stopped and the concentration of each container was determined and plotted against the number of reservoir volumes. The results are shown in Fig. 3.6 and it can be seen that the concentration of the replaced solution in the reservoir becomes equal to the prepared solution concentration in the tank after a flowing of 5 to 6 times the reservoir volume. For each diffusion test a minimum flush volume of 2000 cm^3 (8 reservoir volumes) was used.

3.3.2 TESTING THE EFFECT OF POROUS DISK AND ACCESSORY ATTACHMENTS ON FREE GRAVITY DRAINAGE

In diffusion tests, the soil is supposed to drain by gravity by maintaining atmospheric pressure at the bottom of the soil (i.e. top level of the porous disk). Water drains by opening the outlet valve and draining the water through the pipette which has been

levelled to the bottom of the soil. In order to check whether these attachments (pipette, flexible tubing and outlet valve) and the porous disk cause any significant head loss during free drainage, a simple test was conducted as described below.

The source reservoir and upper rings were filled with water and the pipette was levelled at the top of the porous disk. The outlet valve was then opened to drain the system. At the end of the test it was observed that the water which had been stored above the porous disk, drained completely and the water level was in equilibrium with the level of horizontal pipette. This result indicates that head losses inside the pipette, flexible tubing connecting the pipette to the source reservoir chamber, valve and porous disk, are so small that they do not interfere the process of free gravity drainage.

3.3.3 MINIMIZING THE EFFECT OF EVAPORATION FROM THE SOIL DURING DIFFUSION TESTING

As noted earlier, an air inlet in the top stainless steel plate was kept partially open during the diffusion tests in order to maintain atmospheric pressure at the top of the soil surface. This could result in some evaporation and reduction of the moisture content of the upper section of the soil sample during diffusion test. To reduce the potential for evaporation, two-level evaporation dish filled with distilled water was placed in free space above the soil surface between the consolidation plate and top stainless steel plate as shown in Figs. 3.3 and 3.4. This dish creates a large surface area for evaporation of water inside the dish and maintains 100% relative humidity on top of the soil and hence minimizes the potential for evaporation from the soil.

3.3.4 SELECTION OF THE POROUS DISK

The selection of the porous disk to be used as an interface between the soil and source solution in the bottom reservoir chamber, was based on four considerations. Firstly, the primary task of this disk is to prevent movement of the soil particles into the source reservoir (i.e. separation). Secondly, the disk should be permeable enough to facilitate the saturation and drainage process. Thirdly, the disk should not have any chemical interaction with the solutions used. Finally, the diffusion characteristics of the disk should be such that the disk does not impede diffusion through the soil. Fig. 3.7 shows three potential cases. If the disk has a lower diffusion coefficient than the soil ($D_{disk} < D_{soil}$) this will cause a significant diffusion gradient through the disk and consequently a distorted concentration profile in the soil. Thus the disk should have a diffusion coefficient at least similar to that of the soil. Based on these considerations, a stainless steel disk having a thickness of 0.3075 mm and porosity of 0.53 was selected. A check test was then performed to establish the diffusion coefficient of the Cl^- through the disk.

3.3.4.1 DIFFUSION COEFFICIENT DETERMINATION OF THE STAINLESS STEEL POROUS DISK

A schematic of the test set up is shown in Fig. 3.8. In this test, the source solution was initially poured into the reservoir chamber. The stainless steel disk which had already been saturated by soaking in the source solution for at least 48 hours was placed over the reservoir. Three plexiglass rings were placed on top of the base plexiglass ring

and the top stainless steel ring and top plate were installed and fixed into the base reservoir chamber by means of steel rods. A horizontal pipette was attached and adjusted to be at the bottom level of the disk. The upper reservoir on top of the porous disk was slowly filled with distilled deaerated water using a water tank and a small-diameter tubing connected to the tank. This process of filling was done with a slow flow rate to minimize the mixing of filled water with solution in the source reservoir through the disk. The height of water in the upper reservoir was measured and recorded. Immediately after filling the upper reservoir, the water was stirred by a small plastic spoon and an initial upper reservoir sample was taken. Two initial source solution samples were taken from the source reservoir while the top air inlet was closed. This causes the water in pipette to be replaced with extracted solution instead of replacement with water in the upper reservoir. After sampling, the air inlet was opened. During the test, the source reservoir solution was continuously mixed with magnetic stirrer. For the upper reservoir, mixing was done by hand using a small plastic spoon, for a few minutes before each sampling. After termination of the test, samples were analyzed for chloride concentration and results were plotted as shown in Fig. 3.9. This figure includes the results of two tests (Test 1 and Test 2). As it can be seen in this figure, the lower (source) reservoir concentration decreases with time while the upper reservoir concentration increases. According to the results, after about 4.3 days both reservoir concentrations came into equilibrium. The theoretical curve was fitted to the experimental data points using program POLLUTE. The best fit was obtained using a diffusion coefficient of 8.7×10^{-10} m^2/s. This value was used in diffusion tests as the diffusion coefficient of the stainless steel porous disk. A chloride mass balance

calculations was performed for Test 1 and showed that all the initial mass has been recovered after the test. The detailed calculations are given in Appendix A.

TABLE 3.1 INITIAL AND RECOVERED CHLORIDE CONCENTRATION IN FINE AND MEDIUM SAND USING WASH METHOD

Sand Type	Initial Concn. (mg/L)	m_s (g)	v_{sup} (mL)	w (%)	Recovered Concn. (mg/L)
Fine Sand (Wedron 710)	550	20	200	24	537
Medium Sand (Wedron 460)	550	20	200	24	547

TABLE 3.2 INITIAL AND RECOVERED CHLORIDE CONCENTRATION IN FINE GRAVEL USING WASH METHOD

Sample No.	Initial Concn. (mg/L)	m_s (g)	v_{sup} (mL)	w (%)	Shaking Method	Recovered Concn. (mg/L)
1	1050	86.0	49.8	18.5	hand	1037
2	1050	86.5	49.9	18.2	hand	1086
3	1050	85.8	49.8	18.9	shaker	1052
4	1050	87.1	49.9	17.9	hand	1056
5	1050	85.1	49.9	20.3	shaker	1048

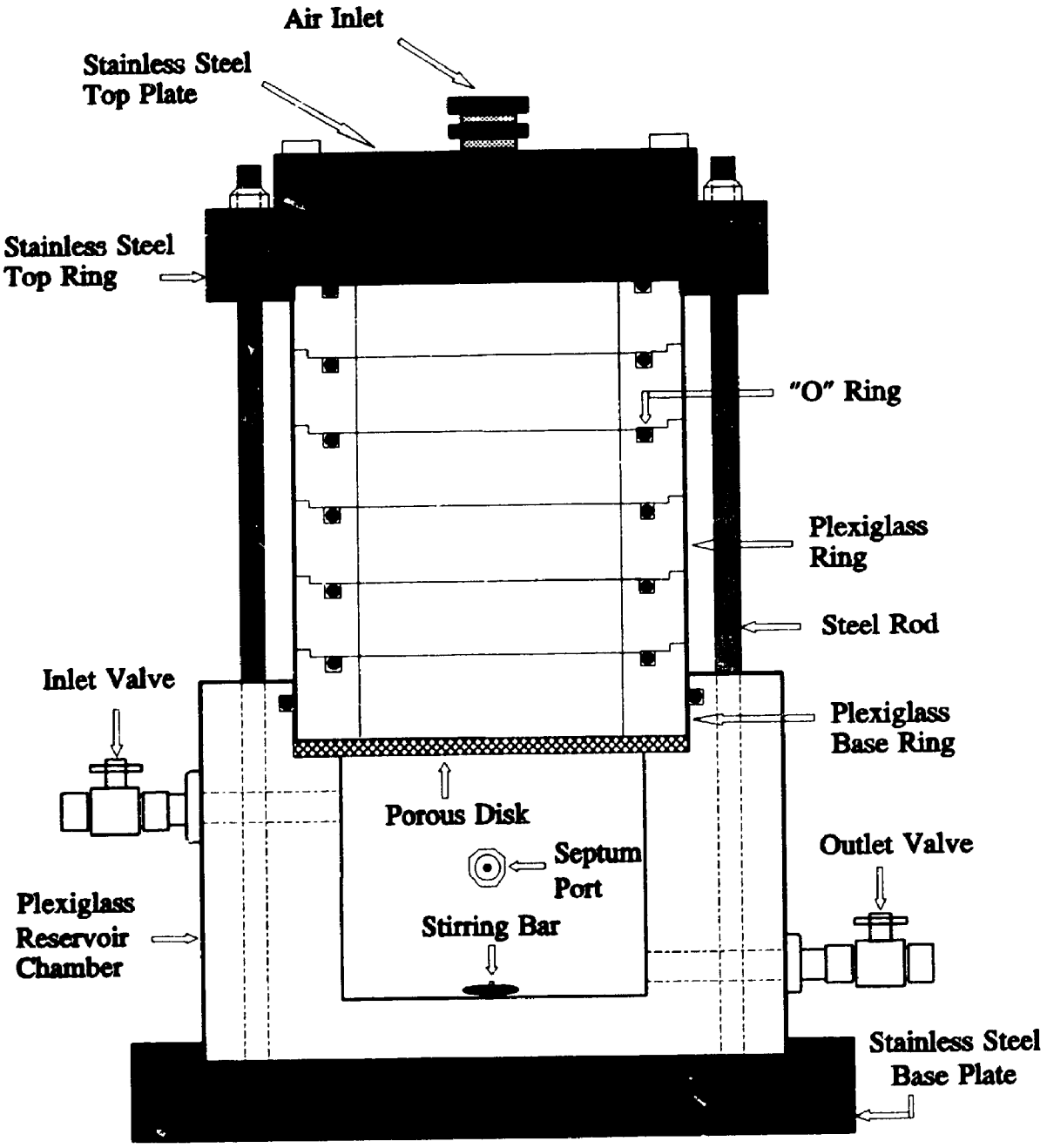

FIG. 3.1 SCHEMATIC OF THE DIFFUSION CELL

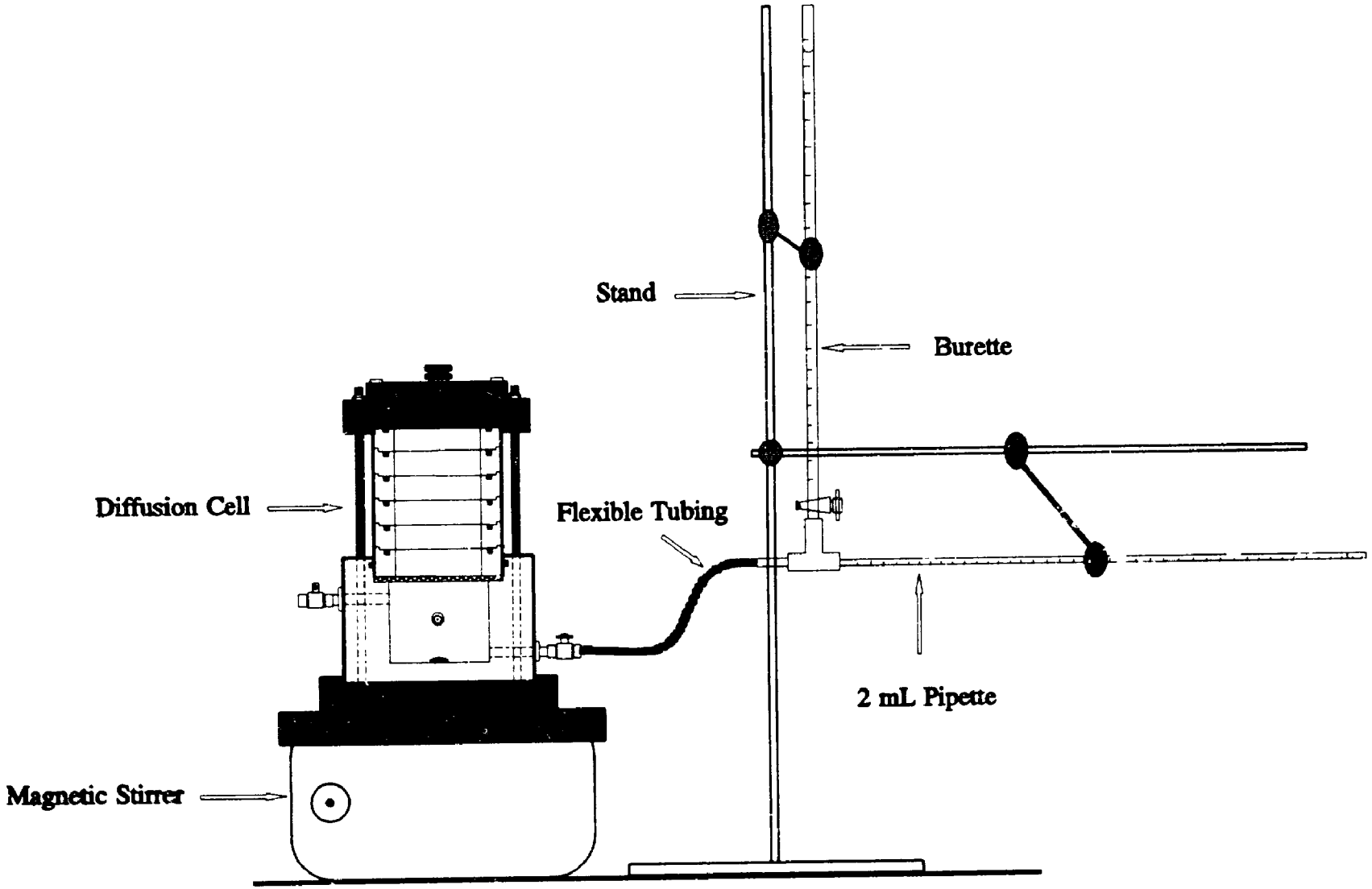

FIG. 3.2 FULL VIEW OF THE DIFFUSION CELL AND ITS ACCESSORIES

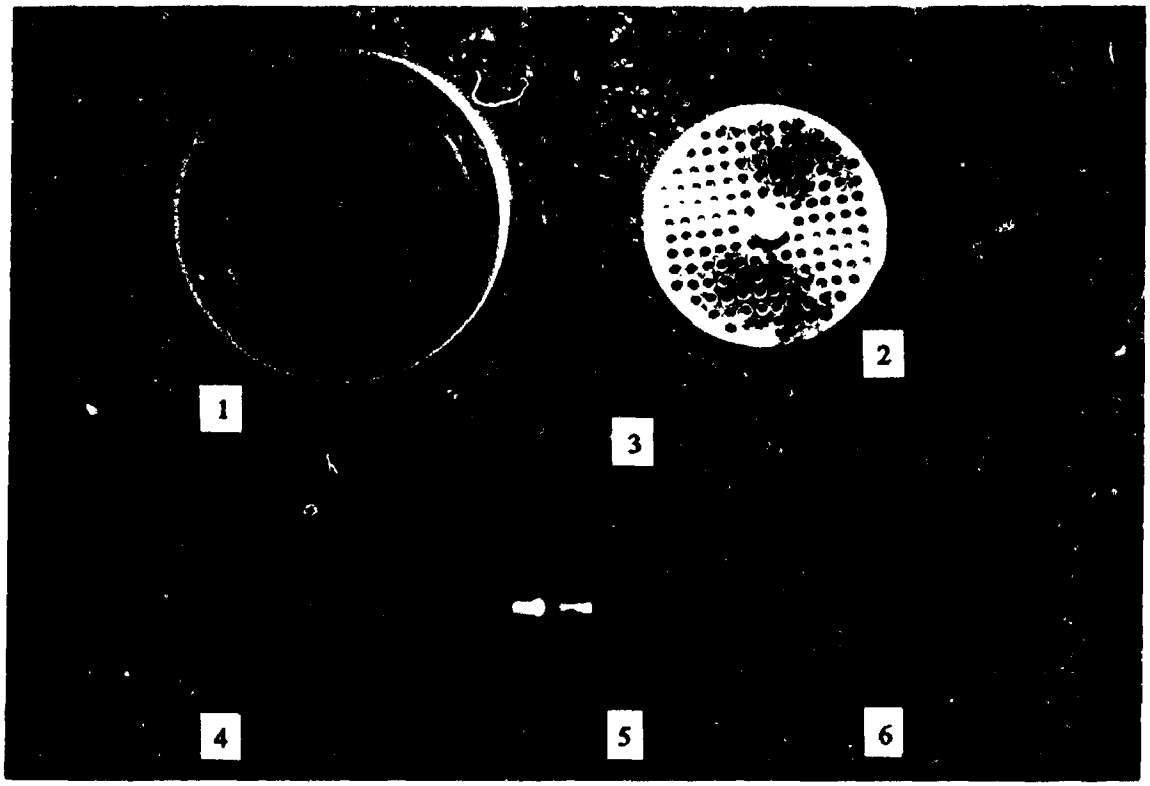

FIG. 3.3 ACCESSORY PARTS USED IN DIFFUSION CELL:
1. PLEXIGLASS RING INCLUDING "O" RING
2. STAINLESS STEEL PERFORATED PLATE (CONSOLIDATION PLATE)
3. SPRING
4. PLAN VIEW OF THE EVAPORATION DISH
5. SIDE VIEW OF THE EVAPORATION DISH
6. #200 WIRE MESH

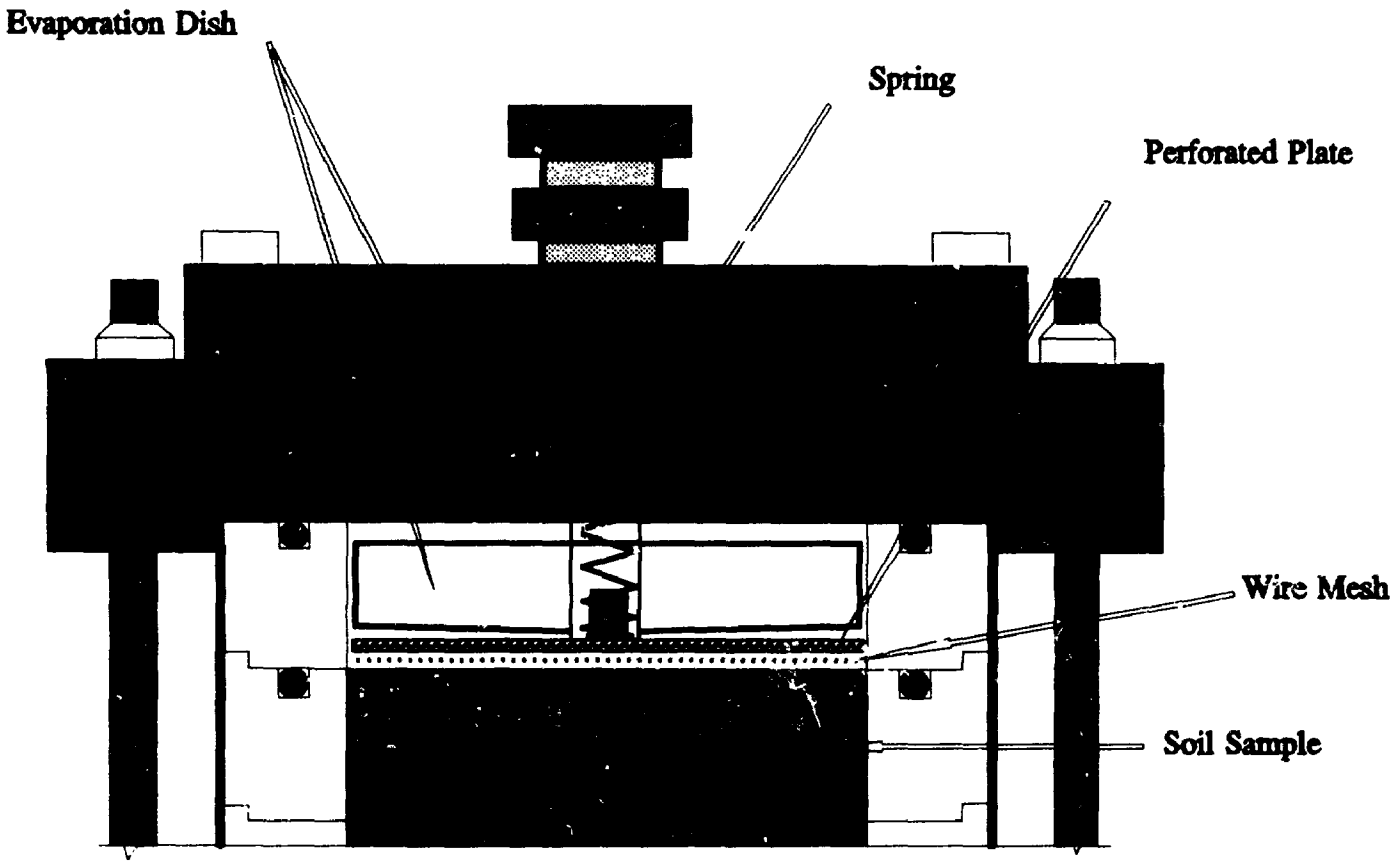

FIG. 3.4 SCHEMATIC OF THE EVAPORATION DISH, SPRING, PERFORATED PLATE AND WIRE MESH IN DIFFUSION TESTING SET UP

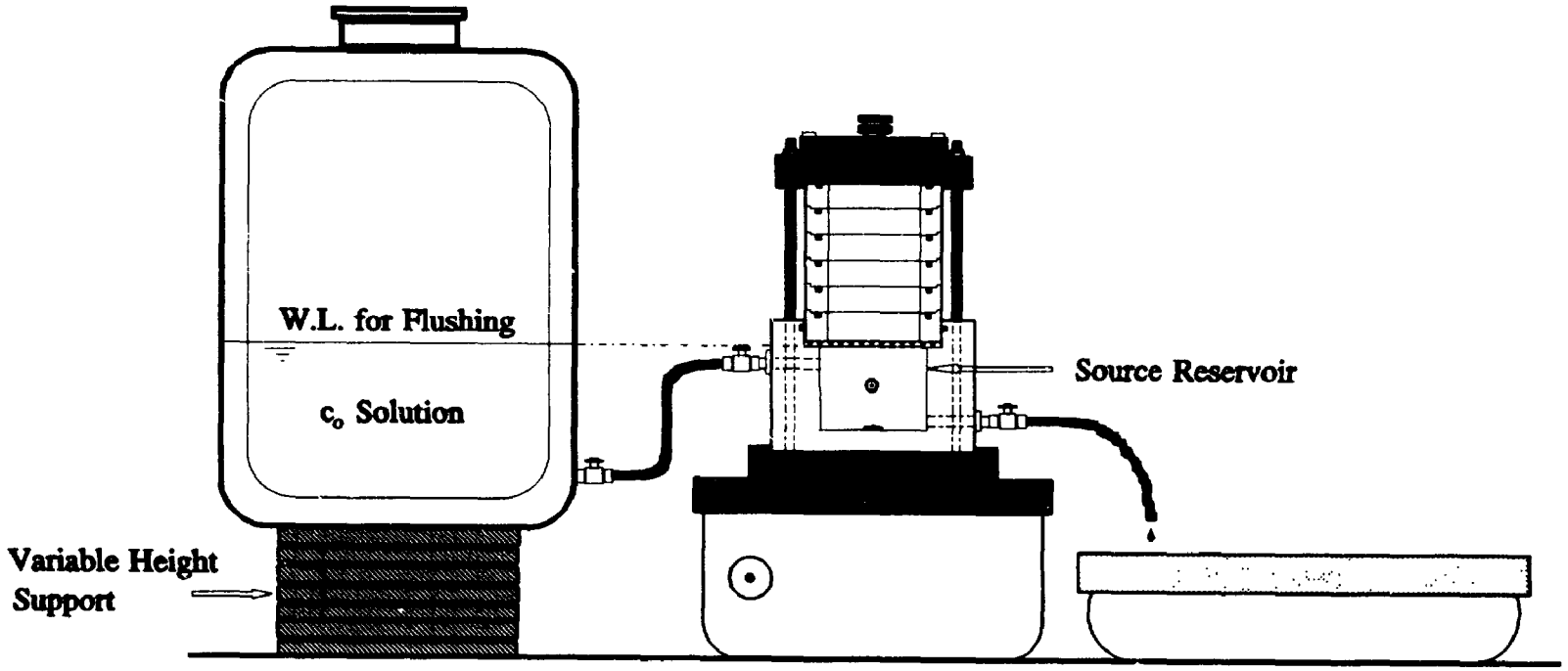

FIG. 3.5 FLUSHING TECHNIQUE FOR SOURCE RESERVOIR USED IN DIFFUSION TESTING

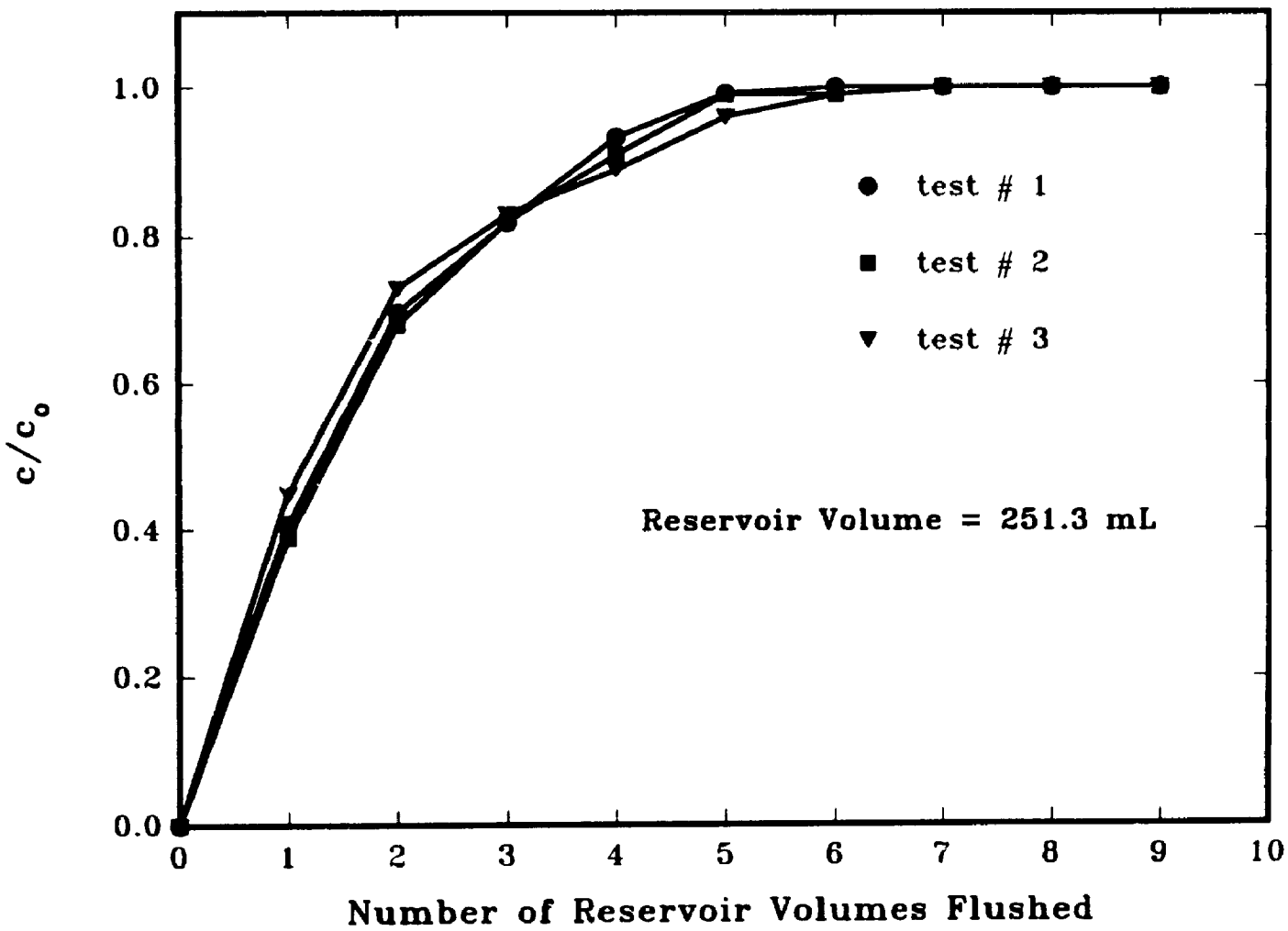

FIG. 3.6 RESULTS OF THE SOURCE RESERVOIR FLUSHING TESTS CONDUCTED ON THE DIFFUSION CELL

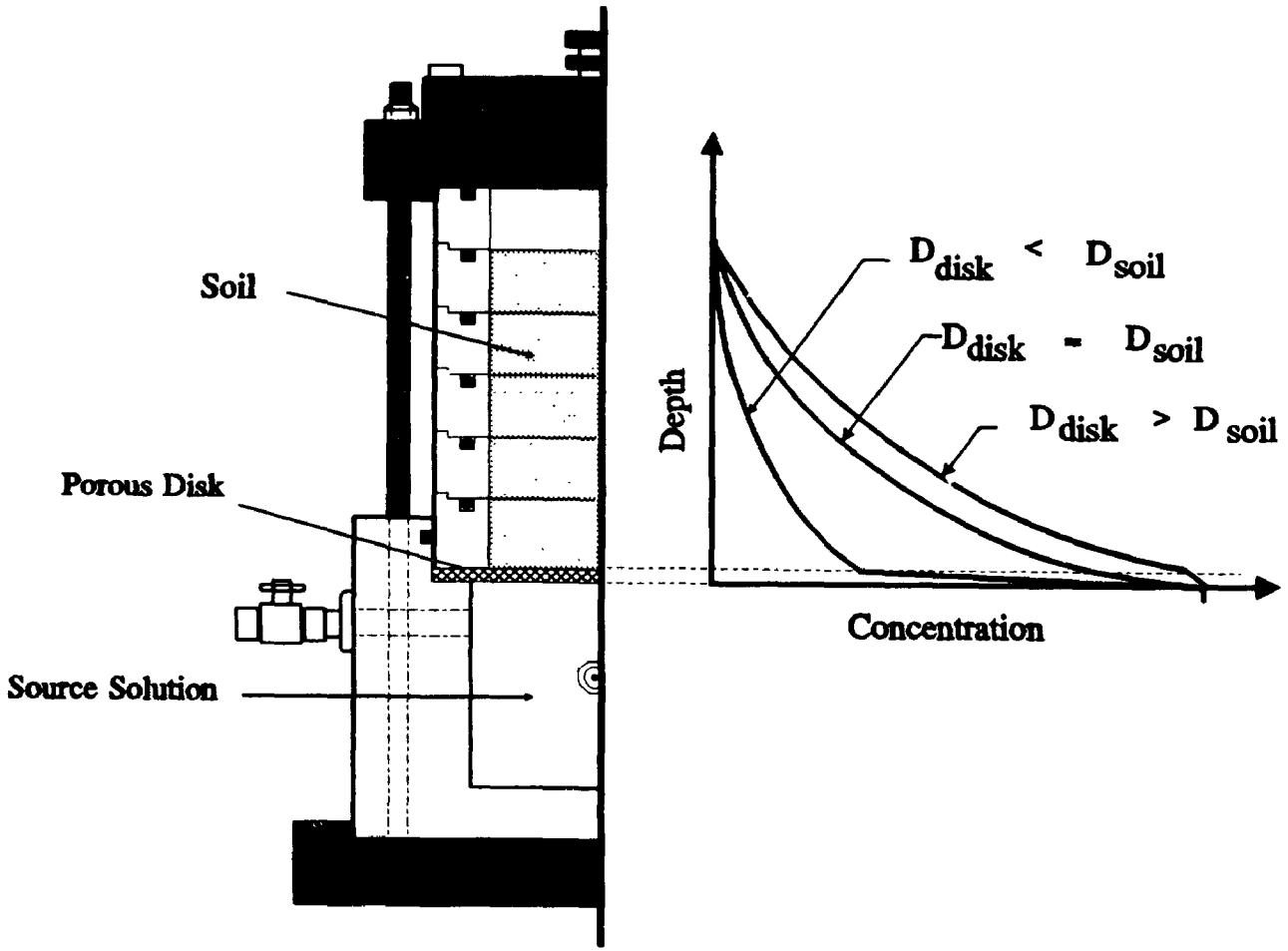

FIG. 3.7 EFFECT OF POROUS DISK DIFFUSION PROPERTIES ON THE SOIL CONCENTRATION PROFILE

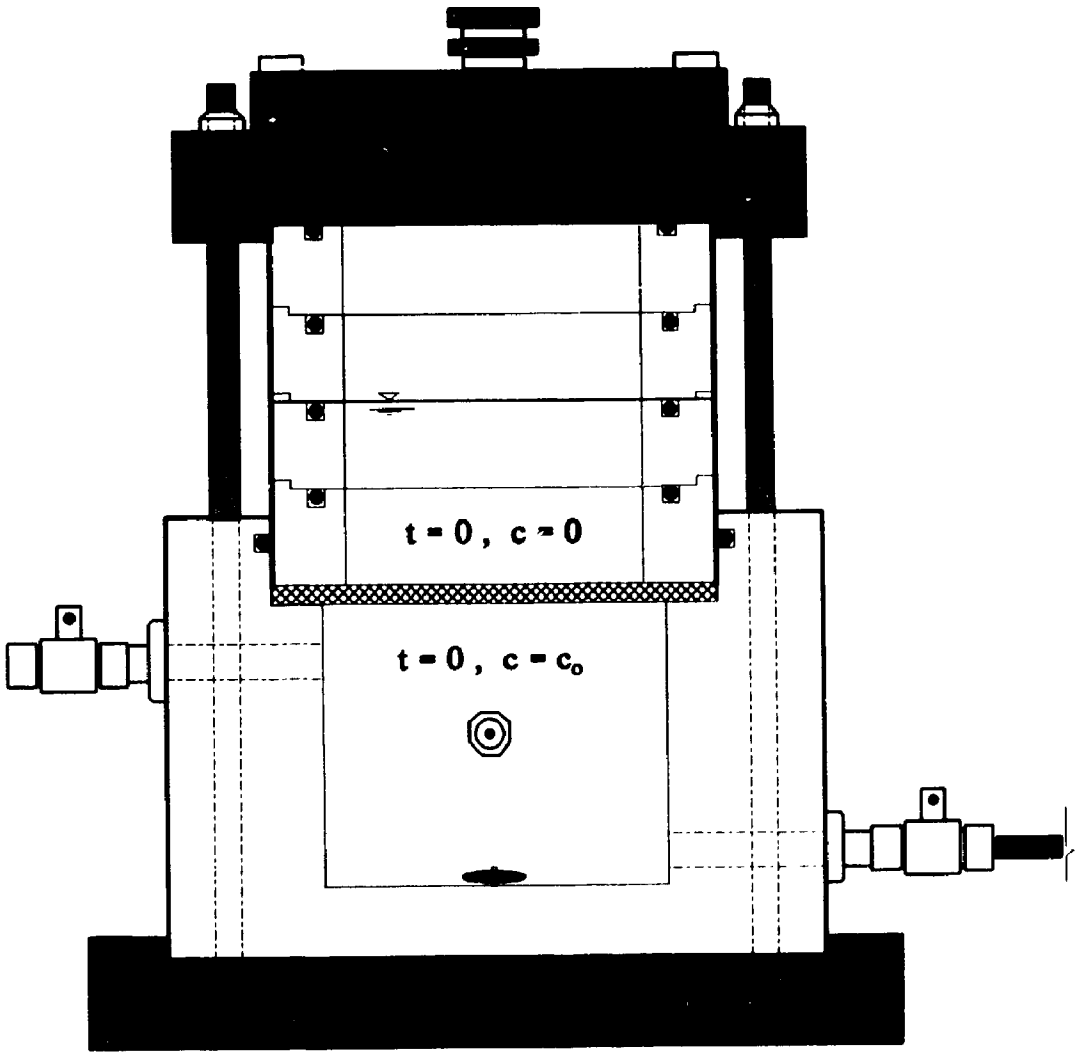

FIG. 3.8 SCHEMATIC OF THE STAINLESS STEEL POROUS DISK DIFFUSION TEST

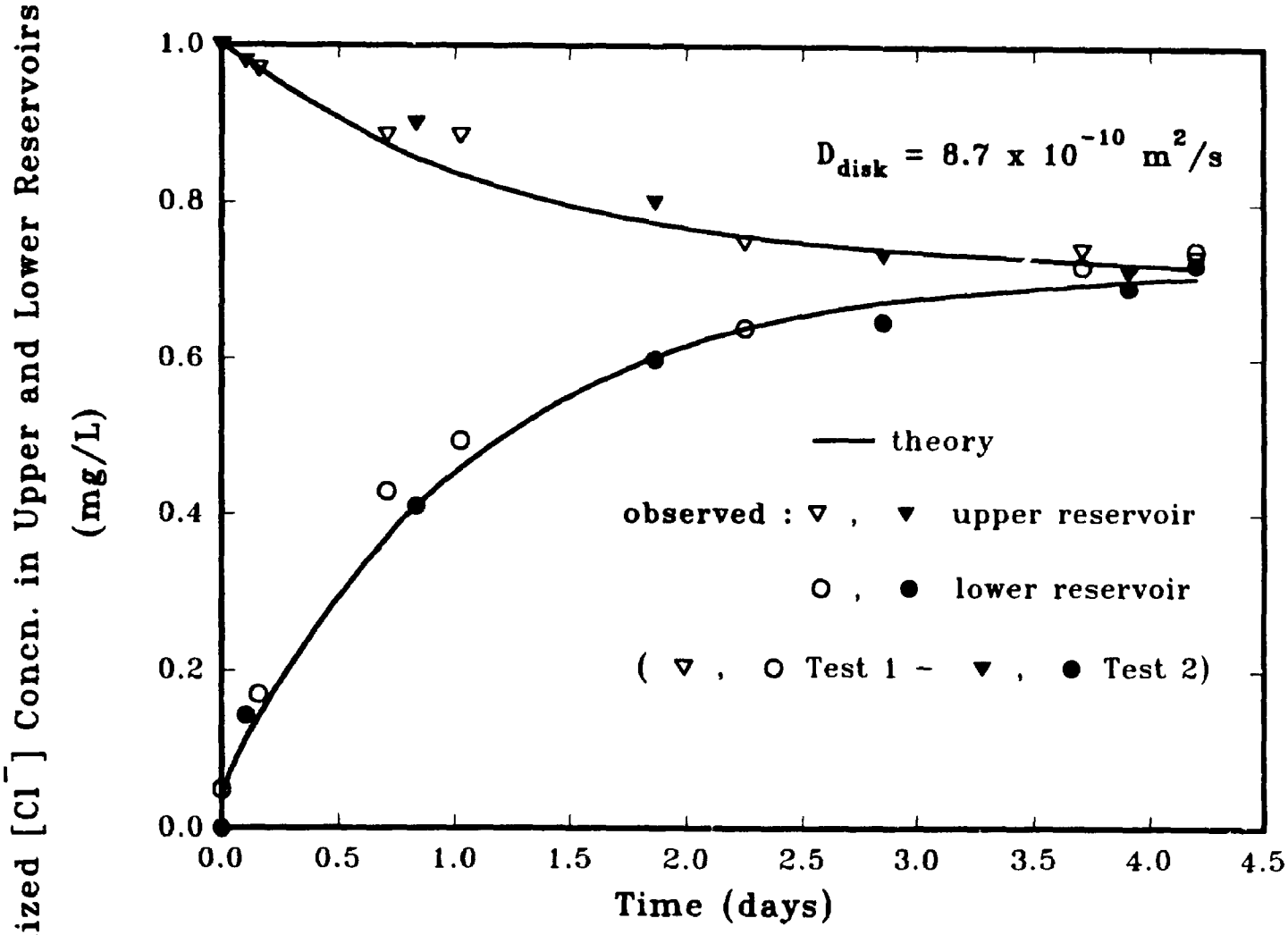

FIG. 3.9 OBSERVED AND THEORETICAL CONCENTRATION PROFILES IN STAINLESS STEEL POROUS DISK DIFFUSION TESTS

CHAPTER 4

DIFFUSION THROUGH FINE SAND AND CLAYEY SILT

4.1 INTRODUCTION

The purpose of this series of experiments was to observe the diffusion behaviour in the fine sand (Wedron 710) and clayey silt, and to determine the diffusion coefficient for (Cl^-) through the sand under a conditions of gravity drainage, and for (Cl^-) and (Na^+) through the clayey silt. Four tests (# D1, D2, D3 & D4) were conducted using the fine sand with test durations of 2.96, 5.27, 8 and 21 days, and two tests (# CD1 and CD2) were conducted using the clayey silt with the test durations of 5.3 and 12.21 days, respectively. The grain size distributions for sand and clayey silt are shown in Fig. 4.1 and some of their physical, chemical and mineralogical characteristics are listed in Tables 4.1 and 4.2. A description of chemical tests used for quantitative mineralogical analysis is given in Appendix B.

4.2 DIFFUSION TESTING ON FINE SAND

4.2.1 INSTALLATION OF THE MATERIAL AND TEST SET UP

Prior to the test, all parts of the diffusion cell shown in Fig. 3.1, were washed with distilled water. The stainless steel porous disk was washed and boiled in distilled

water for removal of any contaminant and then soaked in water for at least 24 hours. To assemble the cell, the base reservoir chamber was placed on the base plate, a magnetic bar was placed in the reservoir and the porous disk was installed. The base and segmented plexiglass rings and the top stainless steel ring were installed and clamped using metal rods and nuts. The cell was packed by pouring washed dry sand into the column in 1.5 to 2.0 cm thicknesses and then tamping the surface of the sand and vibrating the circumference of the cell using a plastic septa until no change in volume occurred. This procedure was repeated until the resulting length of the sand column was 13 cm. An extra plexiglass ring was placed on top of the sand column.

A fine wire mesh (# 200) having the same diameter as the inner diameter of the rings, was placed on top of the sand and a stainless steel perforated plate was placed on the wire mesh. Humidity dishes were filled with water and placed on top of the perforated plate (see Figs. 3.3 and 3.4). The top stainless steel plate was fixed into the stainless steel ring. Fig. 4.2 shows the schematic of the final set up for the tests conducted. The assembled cell was transferred into the sink and a water tank containing distilled deaerated water was placed on top of a spacer to create a certain gradient for water flow through the sample. The plastic tubing on the tank was attached to the inlet valve of the source reservoir chamber and both the tank and inlet valves were opened.

The sample was saturated by allowing distilled de-aired water to flow upward from the reservoir chamber into the sand and out from the air inlet at the top. Out-flowing water drained into the sink. Any air bubbles entrapped in the source reservoir were removed by slightly tilting the cell and opening the outlet valve and flushing the bubbles through the valve. After passing 6 litres of water through the sand, the inlet

valve was closed and the sample was left to soak over night. To ensure complete saturation, the inlet valve was re-opened and flow re-established for a few hours the following day.

The cell was transferred on top of a magnetic stirrer and levelled. The horizontal pipette was attached to the outlet valve by flexible plastic tubing and adjusted to be level with the top surface of the porous disk (bottom surface of the sand) to maintain atmospheric pressure at this level. The outlet valve was opened and the sample was allowed to drain by gravity. The duration of drainage for each test was at least 12 hours.

Observations of the drainage process for all four tests showed that the samples remained saturated after drainage and no water drained from the samples. This is because the capillary rise in the fine sand was greater than the height of the samples tested (Bear, 1972) and the matric suction in the sand pores was in equilibrium with the forces of gravity. After the drainage process, the pipette was detached from the cell and a tank containing sodium chloride solution was connected to the inlet valve. The surface of the solution in the tank was adjusted to be level with the bottom surface of the porous disk by means of spacers. A magnetic stirrer was turned on and both the inlet and outlet valves in the source reservoir chamber were opened simultaneously and reservoir flushed by flowing solution in and out of the reservoir (Fig. 3.5). During flushing, the level of solution in the tank was adjusted continuously to be level with the bottom surface of the disk.

After passing of about 8 reservoir volumes (2000 mL) through the reservoir chamber, both valves were closed simultaneously and the source solution tank was detached from the cell. The pipette, burette and plastic tubing were filled with de-aired

distilled water and cleared of any air bubbles. The pipette was then attached to the outlet valve. A few minutes after flushing and attaching the pipette, two samples from the source reservoir were taken through the septum port as samples for initial source solution concentration measurements. Sampling was done using a 5 cm length hypodermic needle and a syringe and the extracted solution was transferred into 4 mL capacity glass bottles for storage. The extracted solution was replaced with distilled water from the pipette during sampling. After each sampling the outlet valve was closed and the pipette refilled through the burette.

4.2.2 MONITORING, TERMINATION AND EXPERIMENTAL ANALYSIS FOR THE TESTS

Two mL capacity samples for monitoring the source solution concentration with time were taken from source reservoir during the test and stored at room temperature for concentration analysis. Room temperature was recorded once a day and averaged over the total period of the test as representative temperature.

Before termination of each test, two final source reservoir samples were taken. The outlet valve in the source reservoir was closed. The top stainless steel plate, the humidity dishes, metal rods, and stainless steel ring were removed. Using the sectioning plates, the first ring was slightly detached from the lower ring at one end and the sectioning plate was slid through the interface to detach the first ring and the contained sand from the lower rings. The ring was removed from the sectioning plate and cleaned of any sand grains. The plate and sand were weighed and then placed into the oven. The same process was repeated for the remaining rings until the entire column was

sectioned. The dry weight of each sand sample was measured and samples were transferred into plastic containers and stored for concentration measurement. The moisture content of each sample was calculated.

Fig. 4.3 shows moisture content profiles measured at the end of each test. As can be seen, the moisture content profiles are very similar and uniform with depth for all tests. The samples remained essentially saturated (99% - 100% saturation) after gravity drainage (see Table 4.3).

The source reservoir samples were analyzed for chloride concentrations. To bring the concentrations of the samples into the standard solution concentration range, samples were diluted (normally 25 times). The concentration of the diluted samples was determined using a multi purpose electrometer using chloride electrodes. Details regarding the method of analysis are given in Appendix C. To measure the concentration of chloride in the sand, 80 grams of the dried sand samples were washed with 50 mL de-ionized distilled water, the concentration of supernatant was measured and the original pore water concentration of each sample was calculated using equation 3.1. Details regarding of wash method were given in the previous chapter.

The concentrations for chloride in the sand pore water are plotted versus soil depth and source solution concentrations are plotted versus elapsed time in Figs. 4.4 to 4.7 for the Tests D1, D2, D3 and D4. In the concentration versus depth graphs, the right border of the graph corresponds to the initial source concentration for the test and bottom border corresponds to the bottom of the porous disk (interface between the porous disk and source reservoir). In the concentration versus elapsed time graphs, the right border corresponds to the total duration of the test and the top border corresponds to the

initial concentration for the test. To observe the advance of contaminant front in soil profile with elapsed time, the measured and theoretical concentration profiles with soil depth for the Tests # D1, D3, and D4 are plotted on one graph in Fig. 4.8a. Moisture content profiles of these three tests are shown in Fig. 4.8b. Based on theoretical calculations a uniform concentration in the soil would have been established after about 75 days.

4.2.3 THEORETICAL ANALYSIS AND DETERMINATION OF DIFFUSION COEFFICIENT

A theoretical analysis was performed to determine the diffusion coefficient of chloride through the fine sand. The input to the analysis was based on the known soil physical, chemical and geometrical parameters. Program POLLUTE (Rowe and Booker, 1994) was used to find the best theoretical fit to the experimental data points. The only unknown in the input data was the hydrodynamic dispersion coefficient (molecular diffusion coefficient in these experiments) and this was obtained from the analysis which resulted in best fit 'by eye' to the experimental points. Results of these analysis are summarized in Table 4.3 and show that the diffusion coefficient of 9.83×10^{-10} m^2/s could be taken as the average representative value for chloride in the fine sand.

4.2.4 CALCULATION OF THE TORTUOSITY FACTOR FOR FINE SAND

The Cl^- diffusion coefficient determined for the fine sand may be related to the Cl^- diffusion coefficient in aqueous solution (D_o) by the expression,

$$D_e = \tau D_o \qquad (4.1)$$

where τ, ($0 < \tau < 1.0$), is the tortuosity factor for Cl^- in the fine sand examined. Using the above equation, the value of tortuosity is calculated to be 0.531 (averaged for 4 values in Table 4.3). This value was determined using $D_{o(Cl)} = 1.85 \times 10^{-9}$ (m^2/s), which is the aqueous diffusion coefficient for Cl^- when diffusing together with Na^+ at 23°C from a source solution (Scott and Paetzold, 1978). Fig. 4.9 shows the diffusion coefficient values of the different tracers in aqueous solution at various temperatures.

The soil tortuosity factor is an empirical factor which accounts for the fact that the rate of diffusion in a porous medium is slower than that in aqueous solution. This is due to microscopic diffusion pathways around soil grains being much longer and more "tortuous" than the direct pathways in aqueous solution (Freeze and Cherry, 1979). The tortuosity factor is often assumed to be a physical property of the porous media, dependent on fabric and pore structure rather than the nature of the species considered (Rowe, 1987). Hence, it is often back figured from the results of laboratory diffusion experiments for simple non-reactive species such as chloride, and then assumed to be applicable for other species. An example of a typical tortuosity factor, back-figured from Cl^- diffusion tests on a clayey soil, is 0.35 (Rowe et al., 1988), and on glass beads with grain sizes similar to the fine sand tested is 0.54 (De Smedt, 1981). In general, the more compact the porous media (i.e., the smaller the pore size), the lower the tortuosity factor.

4.2.5 MASS BALANCE CALCULATIONS FOR CHLORIDE

Mass balance calculations for chloride recovery were performed for all fine sand diffusion tests showed a recovery of 98-102 % of the original mass, suggesting that there is no significant mass loss and almost all the chloride mass was recovered. These calculations are based on the initial properties of the soil and initial mass available for diffusion and final mass recovered in soil and source reservoir at the end of the test. Table 4.4 summarizes the results of these calculations and a sample of calculations for diffusion tests is shown in Appendix D.

4.2.6 COMPARISON OF THE RESULTS WITH THE RESULTS OF THE PREVIOUS WORK CONDUCTED USING GLASS BEADS

De Smedt (1981) used glass beads as a porous medium for his miscible displacement experiments under saturated and un-saturated water flow conditions. He also conducted saturated diffusion tests with chloride as a tracer. The porous medium consisted of 50% of 1° normal glass beads of type Class IVA Unispheres # 1217, diameter range 88-125 μm and 50% of type # 1420, diameter range 74-105 μm. The resulting porous medium was fairly homogenous because of small range in particle diameter with an average of 100 μm and porosity of 0.37. In the diffusion experiment, the tracer was allowed to penetrate the porous medium for 55.8 days. The resulting data consisted of solute concentration distributions inside the column and are shown in Fig 4.10. The analytical solution for molecular diffusion in a semi-infinite porous medium, in contact with a reservoir, where a constant concentration of the solute is maintained,

is given by:

$$\frac{C}{C_o} = erfc\left(\frac{z}{2\sqrt{D_{diff}t}}\right) \qquad (4.2)$$

This equation was fitted to the data and the calculated diffusion coefficient for chloride was found to be $D_{diff} = 10x10^{-10}$ m^2/s.

The porous medium used in this experiment has similar characteristics to the fine sand used in present study. The average porosity of fine sand is 0.37 which is the same as the porosity of porous medium consisting of glass beads. Taking into account the differences in test set up and test procedure, the obtained diffusion coefficient of $9.83x10^{-10}$ m^2/s for the fine sand is in good agreement with the value of $10x10^{-10}$ m^2/s found for glass beads. The resulting tortuosity factor of 0.531 for the fine sand is also in good agreement with the value of 0.54 calculated for glass beads. In these calculations, the diffusion coefficient of chloride in free water at 23 °C was taken to be $1.85x10^{-9}$ m^2/s (Scott and Paetzold, 1978).

4.3 DIFFUSION TESTING ON CLAYEY SILT

4.3.1 SOIL, DESCRIPTION AND PREPARATION

The clayey soil was an unweathered grey, sandy, clayey silt till with some gravel that was being used to construct a liner for the Halton Waste Management Site in Milton, Ontario. The physical, chemical and mineralogical characteristics of the soil examined are summarized in Table 4.2.

The clayey soil was air dried, pulverized and oversize material was removed by passing soil through a #4 sieve. The soil was mixed with tap water to a water content of 12.9-14.9% (2-4 % wet of optimum water content) and allowed to cure. The water content of the wetted soil was measured and the sample was compacted in a standard Proctor mold. Samples were then extruded from the mold and sectioned into 2 parts about 6 cm thick for testing.

4.3.2 INSTALLATION OF THE MATERIAL AND TEST SET UP

A 6.4 cm long compacted clayey sample was inserted into the 11.5 cm long plexiglass tube by placing a brass cutting ring having slightly larger I.D. than the plexiglass tube, onto the bottom of the ring and pressing down on the clayey sample using the triaxial compression machine, until the entire length of the sample entered the plexiglass ring. The slightly larger I.D. for the cutting ring, ensured a tight seal between the soil and the inside of the cylinder. This, in turn, prevented any seepage along the sides of the sample. Once the soil sample was in place, an impermeable plexiglass plate was placed at the bottom of the tube directly below the soil layer and the contact line between the plate and tube was sealed using vacuum grease. A schematic of the test set up is shown in insert of Fig. 4.11. Background pore water solution was obtained by squeezing the unused sample and was subsequently poured on top of the clayey sample to ensure that any wetting of the sample was by fluid with a background concentration the same as that of the clayey sample at the beginning of the test. The clayey sample was left in contact with this background concentration for about 14 days to eliminate any

matric suction effects prior to placing the sodium chloride solution in contact with the clayey soil. The background solution on top of the sample was the replaced with a sodium chloride solution.

4.3.3 MONITORING, TERMINATION, AND EXPERIMENTAL ANALYSIS

Each day, a 2 mL solution sample was taken from the source reservoir. Room temperature was recorded and averaged for the duration of the tests. After 5.3 days (Test # CD1) and 12.21 days (Test # CD2) the tests were terminated, the source solution was removed, the base plate was detached, and the clayey sample was extruded from the plexiglass tube and sliced into five sub-layers of approximately equal thicknesses. The thickness of each slice was measured and a small sample was taken for water content determination. The porosity, degree of saturation and volumetric moisture content of the soils in each test was found to be 0.288, 96% and 0.276 for Test #CD1 and 0.285, 96.3% and 0.274 for Test #CD2, respectively. The remaining soil was squeezed in a pneumatic pressure device at 25 MPa pressure and the pore water collected to determine the sodium and chloride concentrations. Chloride concentrations in clay squeezed pore water and the source reservoir were measured using chloride electrodes attached to a multipurpose meter. Sodium concentrations were measured using atomic absorption spectrophotometry. The source reservoir chloride concentration data was plotted against elapsed time for each test and are shown in Figs. 4.11a (Test #CD1) and 4.12a (Test #CD2). The chloride concentration data in the soil squeezed pore water was plotted against the soil depth and are shown in Figs. 4.11b (Test #CD1) and 4.12b (Test #CD2).

The corresponding concentration data for sodium is plotted in Figs 4.13 and 4.14. The solid lines in these figures show the results of the best fit theoretical analysis which will be discussed in the next subsection.

4.3.4 THEORETICAL ANALYSIS AND DETERMINATION OF THE DIFFUSION COEFFICIENTS

Mathematical fitting of the measured concentration profiles for both chloride and sodium was performed for each test using program POLLUTE and the geometrical and physical characteristics of the test. The best fit (by eye) to the experimental data is shown in all relevant figures and the corresponding D and K_d values are summarized in Table 4.5. For chloride, the diffusion coefficient of 5.74×10^{-10} m^2/s (Test #CD1) and 5.70×10^{-10} m^2/s (Test #CD2) resulted in the best fit theoretical profile in the tests. For sodium, the two parameters of diffusion and distribution coefficients were adjusted in the modelling until th` pair of values resulting in the best fit profile was obtained. This was taken as the representative values. In Test #CD1 the sodium diffusion coefficient of 5.07×10^{-10} m^2/s and distribution coefficient of 0.15 mL/g resulted in the best fit profile. The corresponding values in Test #CD2 were 5.03×10^{-10} m^2/s and 0.15 mL/g respectively.

4.4 SUMMARY AND CONCLUSIONS

Table 4.3 summarizes the results of the diffusion tests conducted on the fine sand. Calculated values of the degree of saturation of the samples indicates that all tests have

been conducted for essentially saturated conditions. The water content profiles for all tests were almost identical and uniform with depth. The calculated values of the diffusion coefficients for all tests, which were obtained based on the best theoretical fit through the experimental data points (both in soil sample and source reservoir) using program POLLUTE, gave almost identical values for the diffusion coefficient of chloride in the fine sand tested. The values ranged from 9.8×10^{-10} to 9.9×10^{-10} with an average of 9.83×10^{-10} m^2/s. The calculated percent of mass recovery for all tests showed that more than 98 percent of the chloride mass has been recovered. The calculated tortuosity factor for all tests were essentially identical (with the average of 0.531) and are consistent with the published value for glass beads of similar size.

Table 4.5 summarizes the results of the two diffusion tests conducted on compacted clayey silt. The degree of saturation and volumetric moisture content of both samples were essentially the same (96% and 0.275 cm^3/cm^3 respectively) and hence the diffusion coefficient for chloride giving the best fit was essentially the same with the average of 5.72×10^{-10} m^2/s. The diffusion and distribution coefficients used in the analysis for sodium data was also essentially the same with the average of 5.05×10^{-10} m^2/s and 0.15 mL/g respectively.

TABLE 4.1 SOME PHYSICAL, CHEMICAL AND MINERALOGICAL CHARACTERISTICS OF THE FINE SAND (WEDRON 710)

Physical characteristics

Specific gravity G_s = 2.65

Hydraulic conductivity[1] = 8.3×10^{-3} cm/s

Range of the porosity = 0.364-0.37

Range of the moisture content = 19.6-21.3

Dry density = 1.68 g/cm^3

D_{60} = 0.14 mm

D_{10} = 0.08 mm

Chemical and mineralogical characteristics[2]

Cation exchange capacity[3] (C.E.C, meq/100 g soil):

2.4 (AgTh wash), 1.43 (KCl wash)

[Cl^-] background concentration = 5 mg/L

Minerals present (%):

SiO_2	TiO_2	Fe_2O_3	MnO	MgO	CaO	Total
97.87	0.03	0.03	0.01	0.08	0.02	98.04

Undetected minerals: 1.96%

Carbonates:

Percent dolomite = 0.0 (%)

Percent calcite = 0.0 (%)

1 - Constant head method

2 - See Appendix B for description of chemical tests

3 - CEC by combined KCl/Ag thiourea exchange method

TABLE 4.2 SOME PHYSICAL, CHEMICAL AND MINERALOGICAL CHARACTERISTICS OF THE UNWEATHERED CLAYEY TILL

Physical characteristics

Specific gravity = 2.75-2.79

Porosity = 0.29-0.31

Dry density = 1.91-2.02 g/cm^3

Moisture content = 13.22-15.94 %

Liquid limit = 21.7 %

Plastic limit = 15.4 %

Chemical and mineralogical characteristics[1]

Mineral species:

Quartz	23-27 %
Carbonate	17-25 %
Feldspars	7 %
Organic matter	0.2-1.0 %
Clay minerals	45-48 % :
Illite	35-37 %
Verm/smectite	3-8 %
Chlorite	2-8 %

Organic carbon content : 0.1-0.4 %

Cation exchange capacity[2] : 14-18 meq/100 g soil

[Cl^-] background concentration : 95-293 mg/L

[Na^+] background concentration : 70-260 mg/L

1 - See Appendix B for description of chemical tests

2 - CEC by combined KCl/Ag thiourea exchange method

TABLE 4.3 SUMMARY OF THE RESULTS OF THE DIFFUSION TESTS ON FINE SAND (WEDRON 710)

Test #	Time (days)	Sample Height (cm)	Average (n)[1]	Average (S)[2] (%)	Diffusion Coefficient (m^2/s)	Tortuosity Factor (τ)
D1	2.96	13.1	0.371	100	9.9×10^{-10}	0.535
D2	5.27	13.1	0.364	99.3	9.8×10^{-10}	0.530
D3	8.0	13.1	0.366	100	9.8×10^{-10}	0.530
D4	21.0	13.1	0.370	99.0	9.8×10^{-10}	0.530

(1) n = Porosity

(2) S = Degree of saturation

TABLE 4.4 SUMMARY OF THE CHLORIDE MASS BALANCE CALCULATIONS FOR FINE SAND DIFFUSION TESTS # D1, D2, D3 & D4

Test #	Initial Mass (mg)			Final Mass (mg)				Percent Recovery
	in source	in soil	total mass	in source	in soil	mass removed	total mass	(%)
D1	6.90	0.024	6.91	5.90	0.752	0.385	7.05	102
D2	7.03	0.024	7.05	5.30	0.966	0.633	6.90	97.8
D3	7.00	0.024	7.02	5.16	1.222	0.780	7.16	102
D4	7.43	0.024	7.45	4.36	2.090	0.960	7.41	99.5

TABLE 4.5 SUMMARY OF THE RESULTS OF THE DIFFUSION TESTS ON CLAYEY SILT

Test #	Time (days)	Sample Height (cm)	Average (θ)[1] (cm^3/cm^3)	Average (S)[2] (%)	Cl^- Diffusion coefficient (m^2/s)	Na^+ Diffusion coefficient (m^2/s)	Na^+ Distribution coefficient (mL/g)
CD1	5.30	6.42	0.276	96.0	5.74×10^{-10}	5.07×10^{-10}	0.15
CD2	12.21	6.42	0.274	96.3	5.70×10^{-10}	5.03×10^{-10}	0.15

1 θ = Volumetric moisture content (θ=Sn)

2 S = Degree of saturation

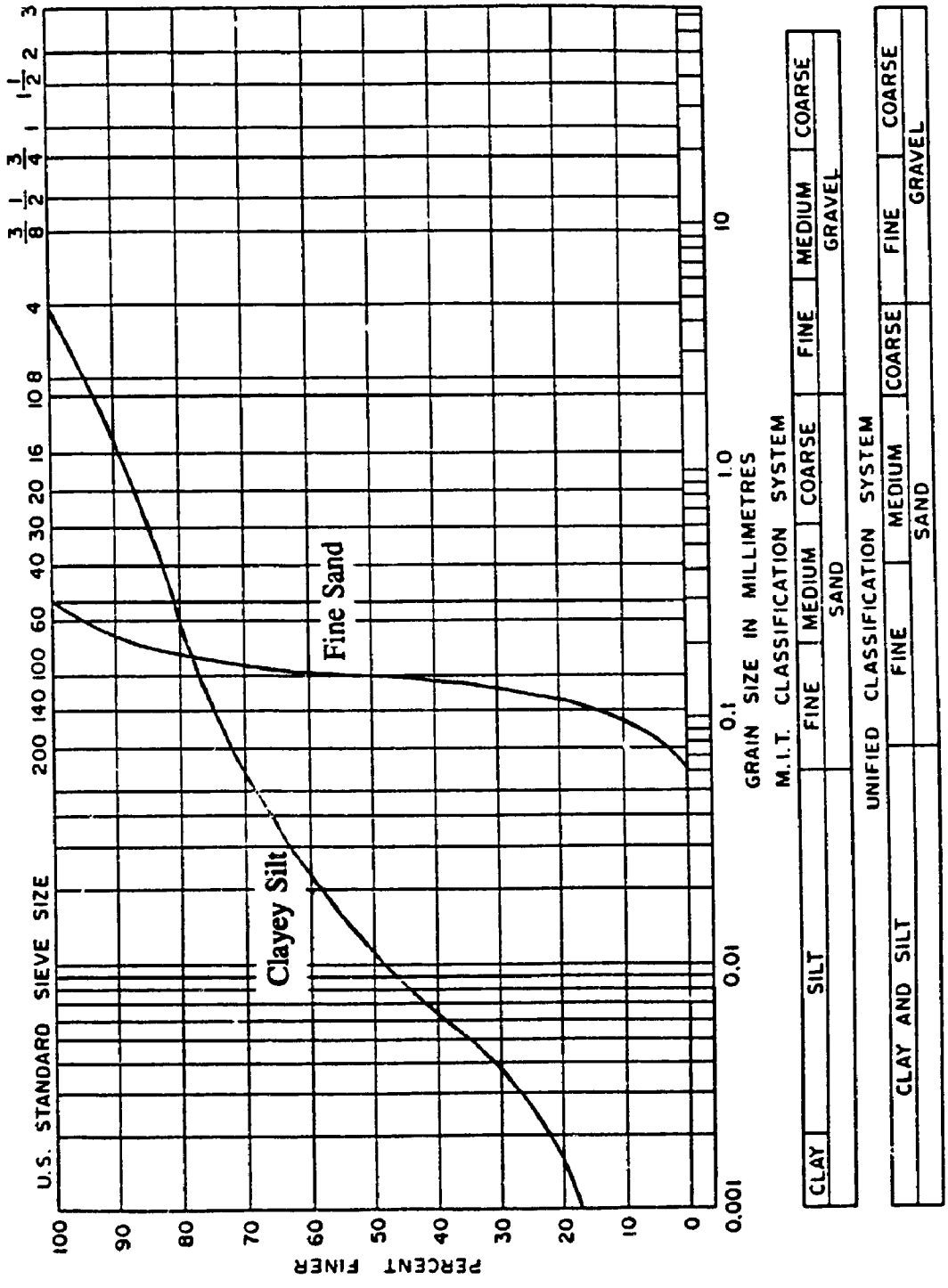

FIG. 4.1 GRAIN SIZE DISTRIBUTIONS OF THE CLAYEY TILL AND FINE SAND (WEDRON 710) USED IN DIFFUSION TESTS

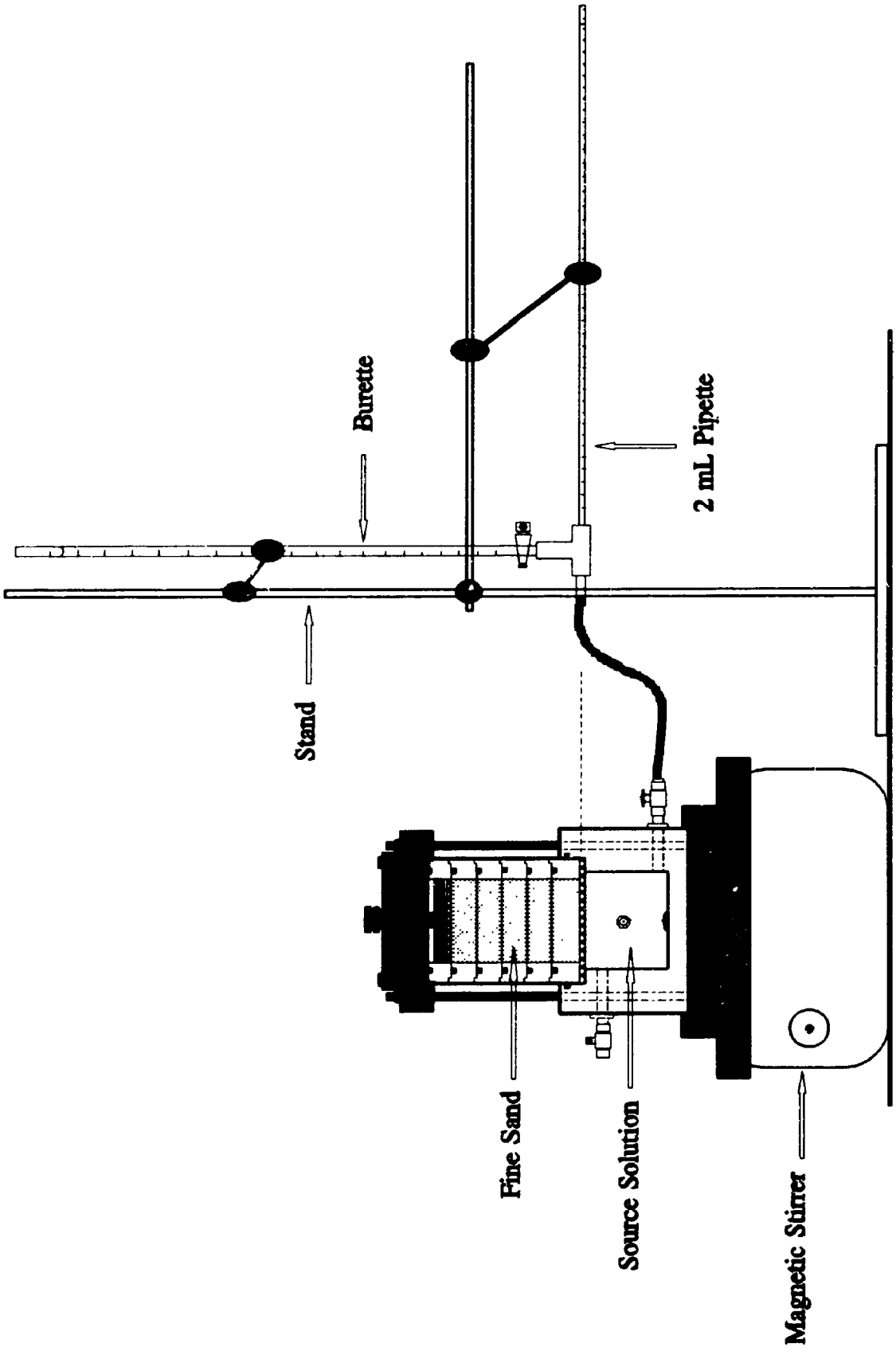

FIG. 4.2 SCHEMATIC OF THE FINE SAND DIFFUSION TESTING SET UP

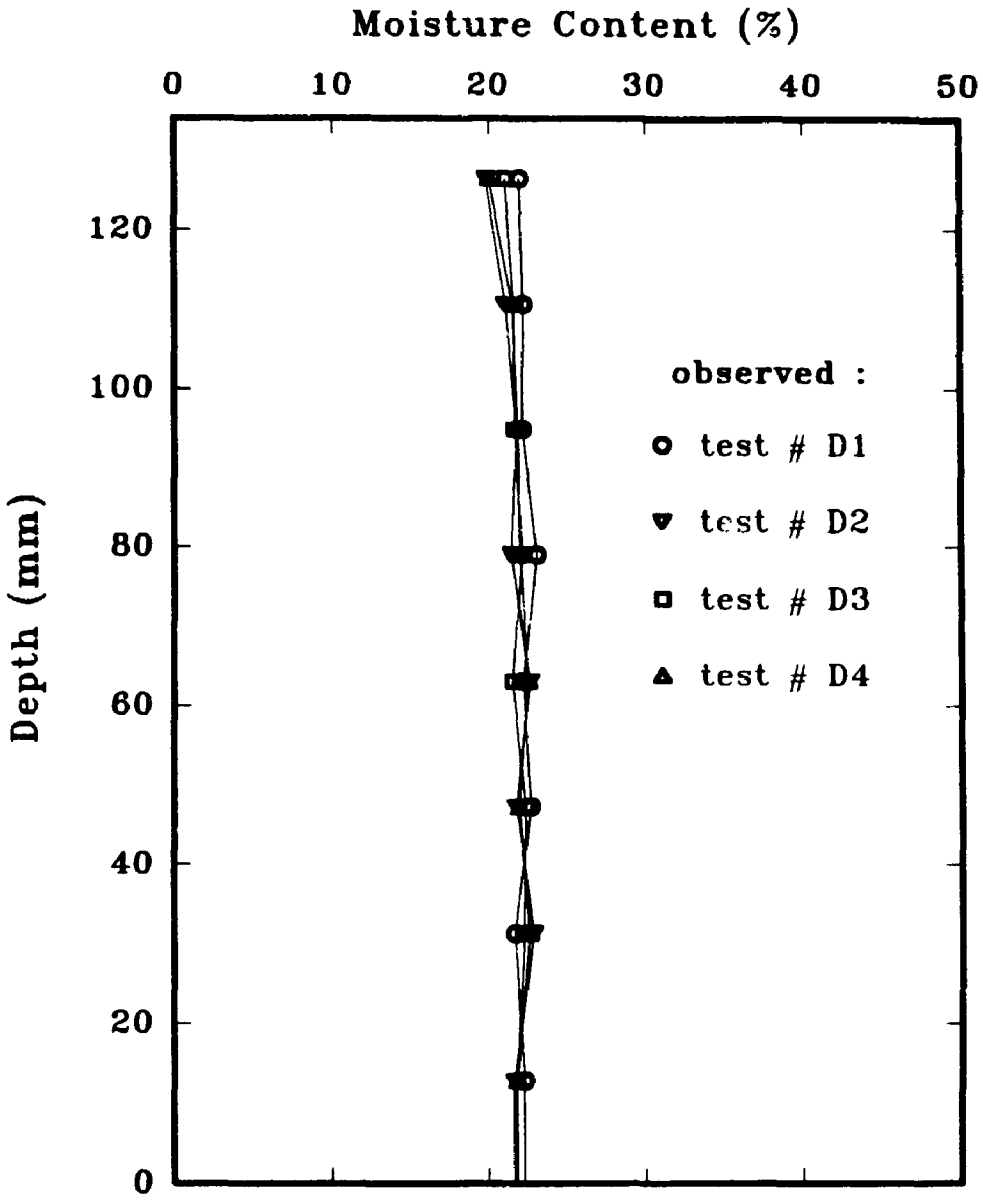

FIG. 4.3 MOISTURE CONTENT PROFILES IN FINE SAND DIFFUSION TESTS

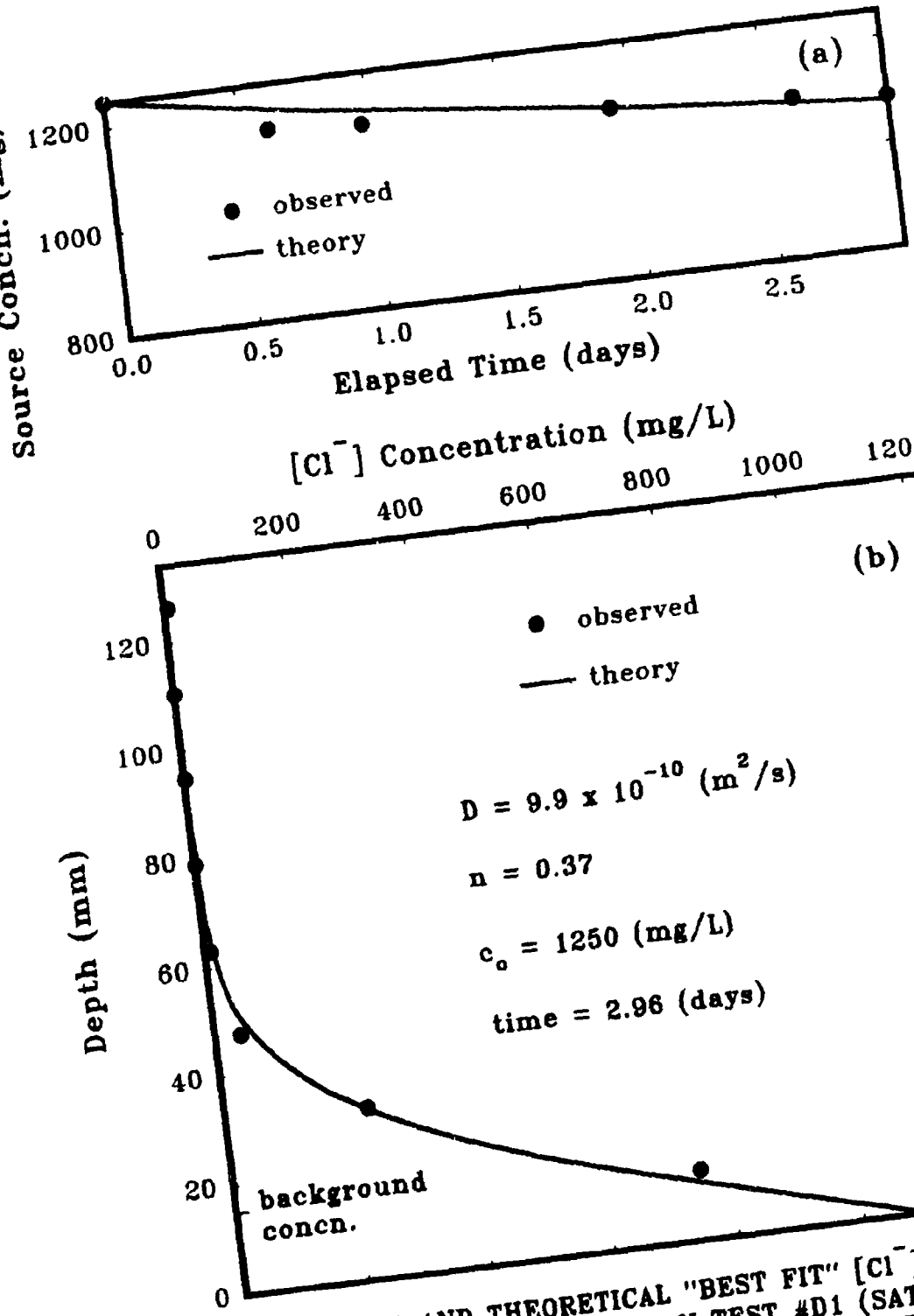

FIG. 4.4 OBSERVED AND THEORETICAL "BEST FIT" $[Cl^-]$ CONCENTRATION IN DIFFUSION TEST #D1 (SATURATED FINE SAND), (a): SOURCE SOLUTION CONCENTRATION VS TIME, (b): PORE-WATER CONCENTRATION VS DEPTH

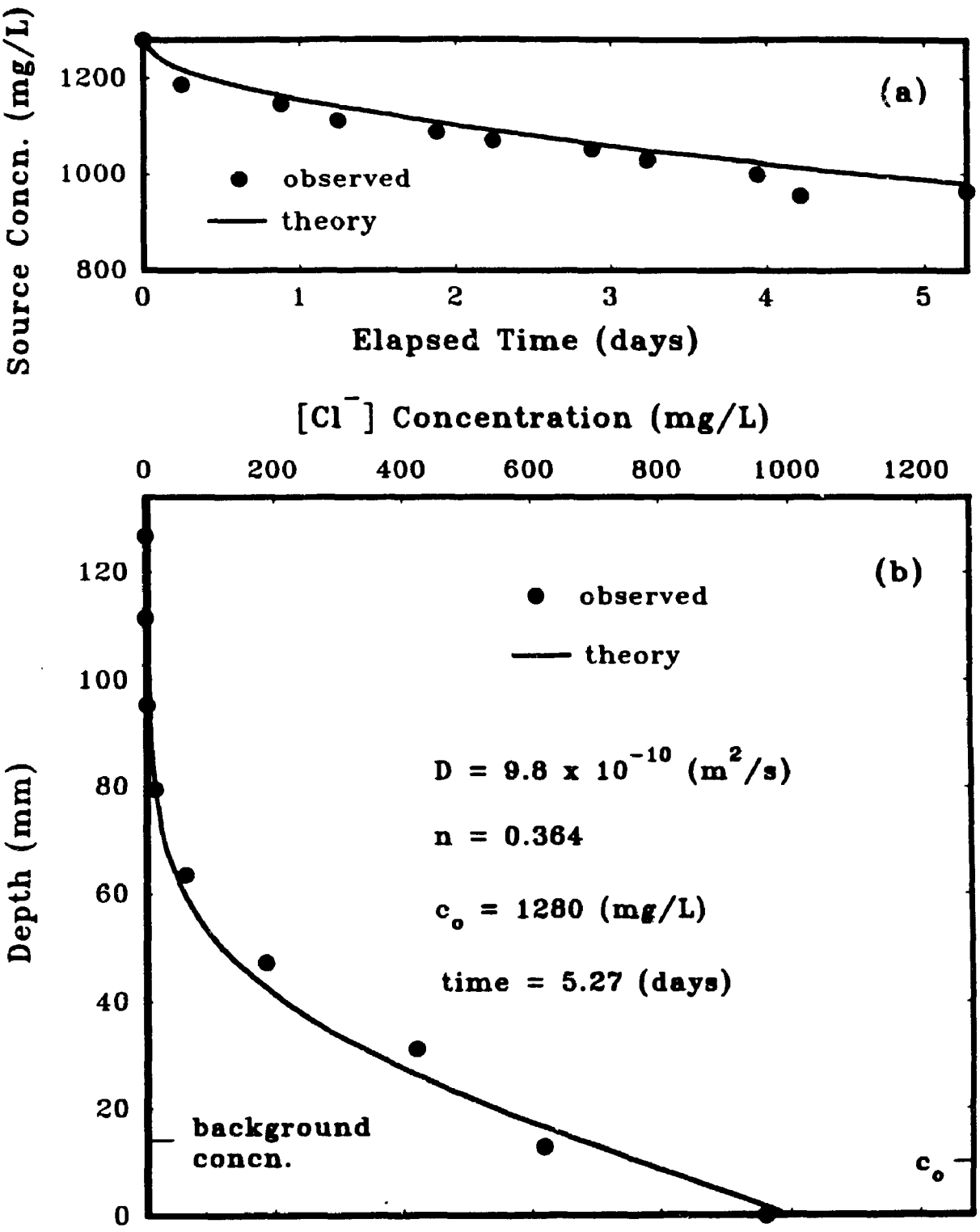

FIG. 4.5 OBSERVED AND THEORETICAL "BEST FIT" [Cl^-] CONCENTRATION IN DIFFUSION TEST #D2 (SATURATED FINE SAND), (a): SOURCE SOLUTION CONCENTRATION VS TIME, (b): PORE-WATER CONCENTRATION VS DEPTH

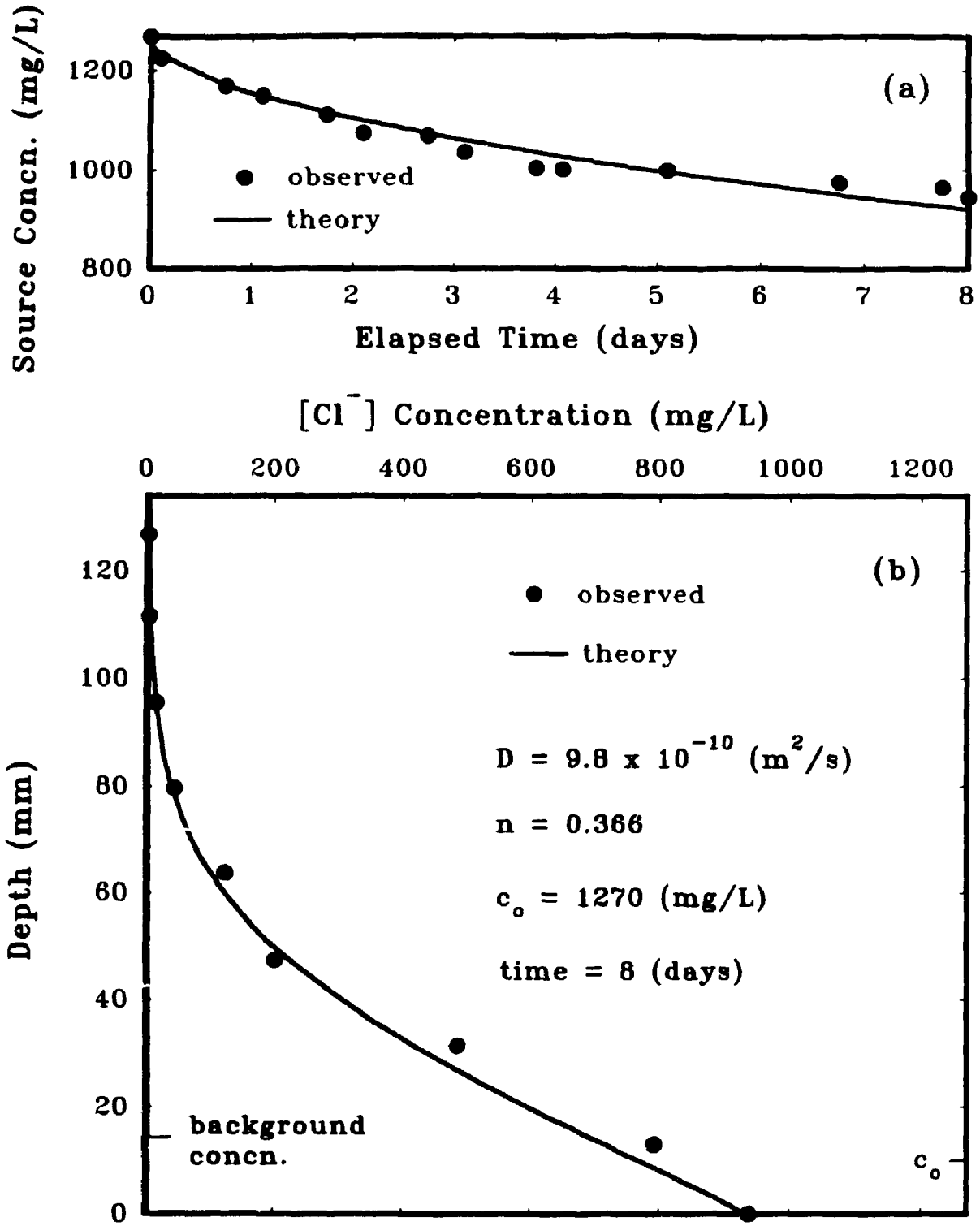

FIG. 4.6 OBSERVED AND THEORETICAL "BEST FIT" [Cl^-] CONCENTRATION IN DIFFUSION TEST #D3 (SATURATED FINE SAND), (a): SOURCE SOLUTION CONCENTRATION VS TIME, (b): PORE-WATER CONCENTRATION VS DEPTH

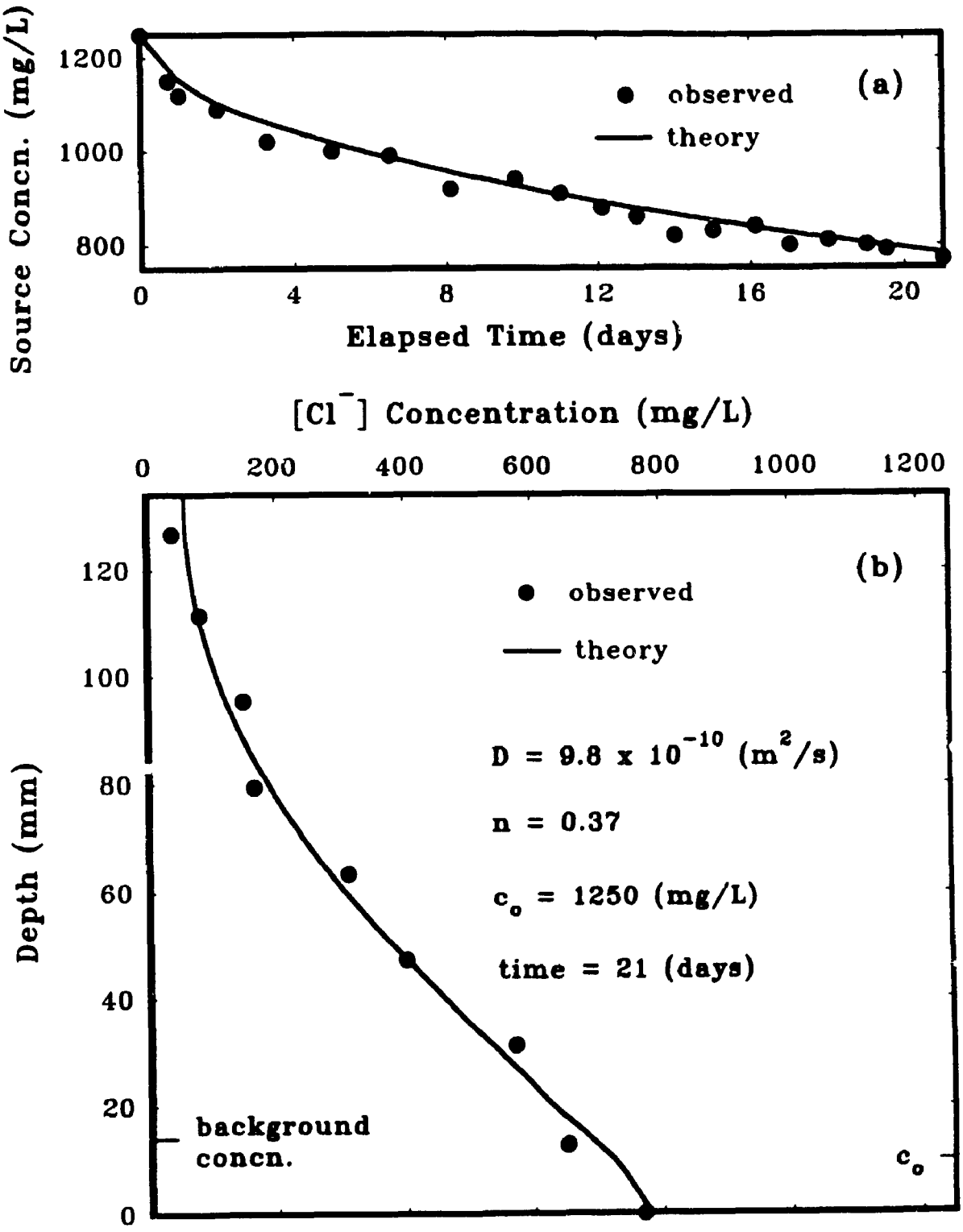

FIG. 4.7 OBSERVED AND THEORETICAL "BEST FIT" [Cl^-] CONCENTRATION IN DIFFUSION TEST #D4 (SATURATED FINE SAND), (a): SOURCE SOLUTION CONCENTRATION VS TIME, (b): PORE-WATER CONCENTRATION VS DEPTH

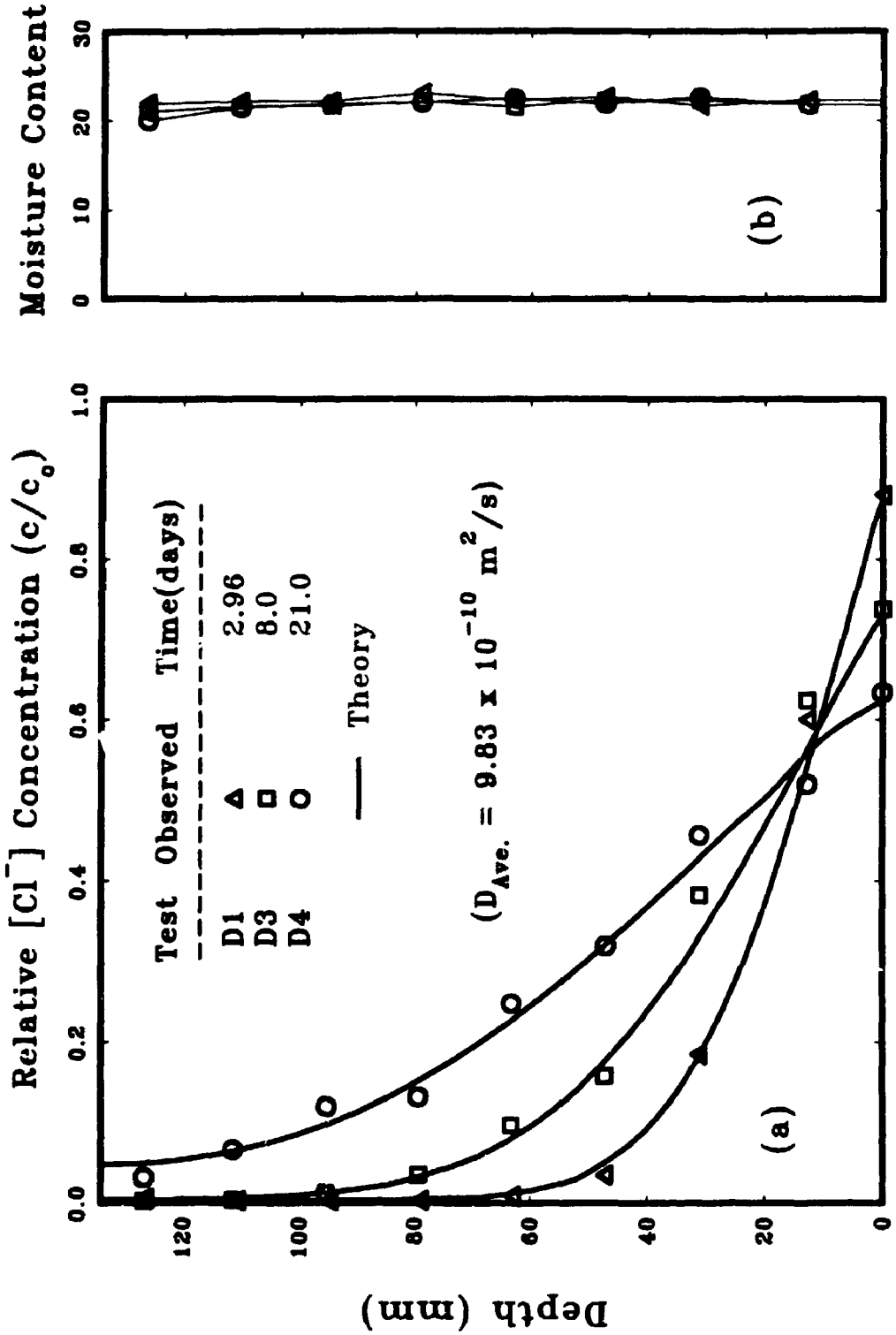

FIG. 4.8 OBSERVED AND BEST FIT THEORETICAL PROFILES OF FINE SAND DIFFUSION TESTS # D1, D3, AND D4, (a) RELATIVE [Cl^-] CONCENTRATION VERSUS SOIL DEPTH, (b) WATER CONTENTS VERSUS SOIL DEPTH

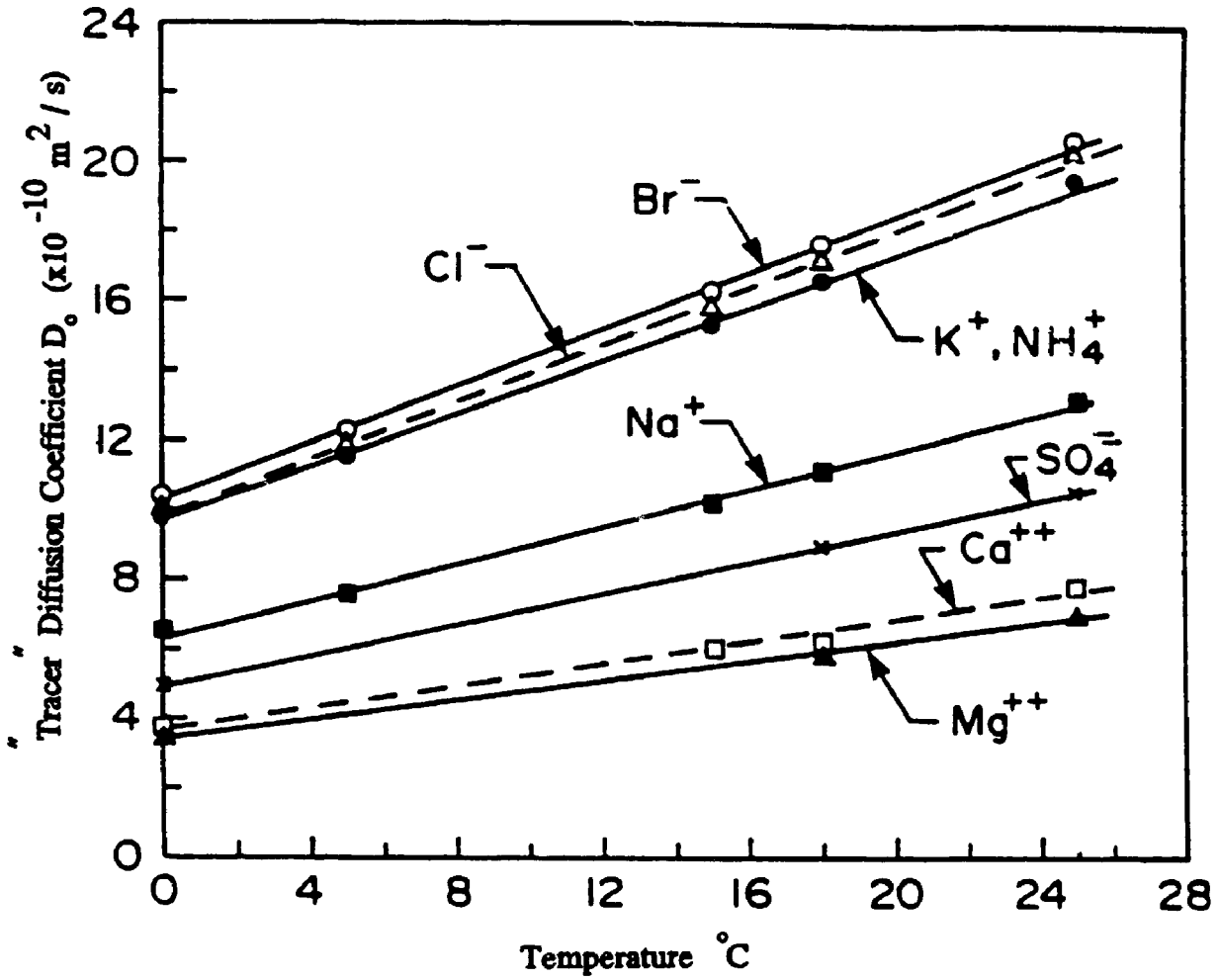

FIG. 4.9 VALUES OF TRACER DIFFUSION COEFFICIENT D_o AT VARIOUS TEMPERATURES

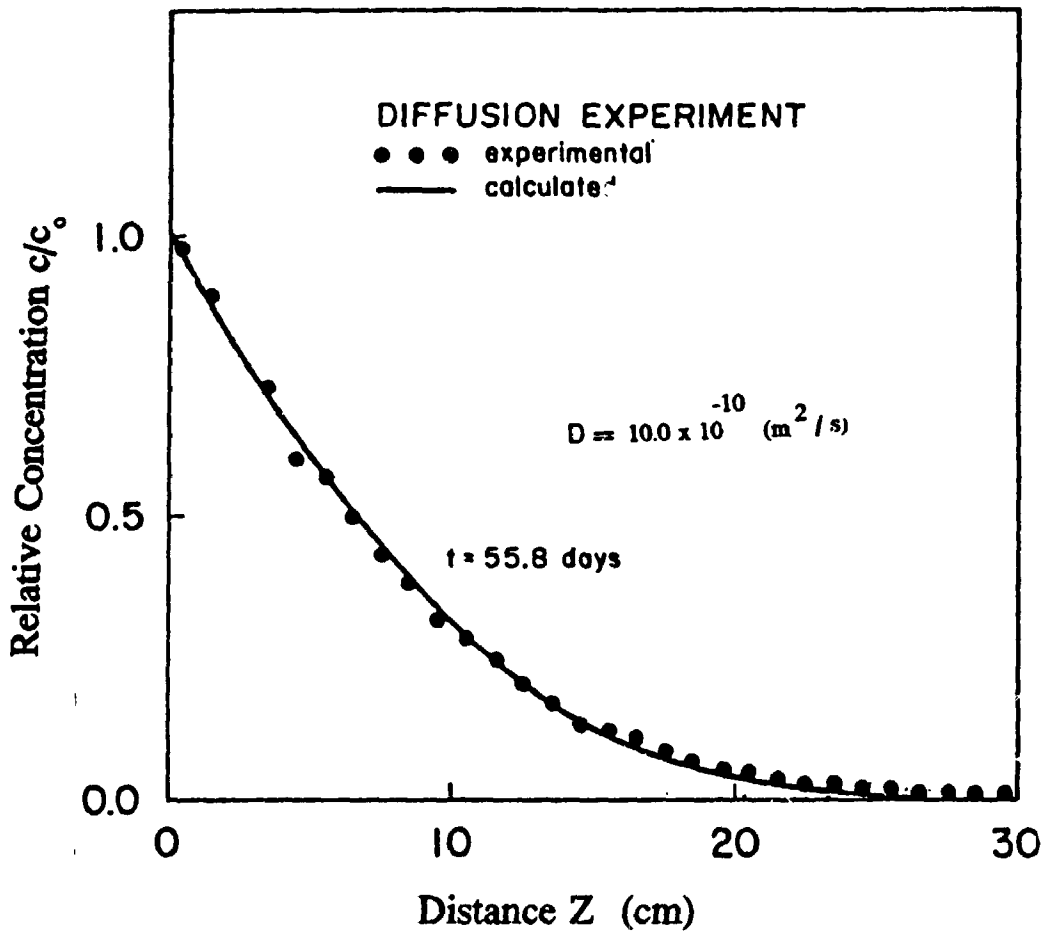

FIG. 4.10 OBSERVED AND CALCULATED CHLORIDE CONCENTRATION DISTRIBUTION OF THE DIFFUSION EXPERIMENT (AFTER DE SMEDT, 1981)

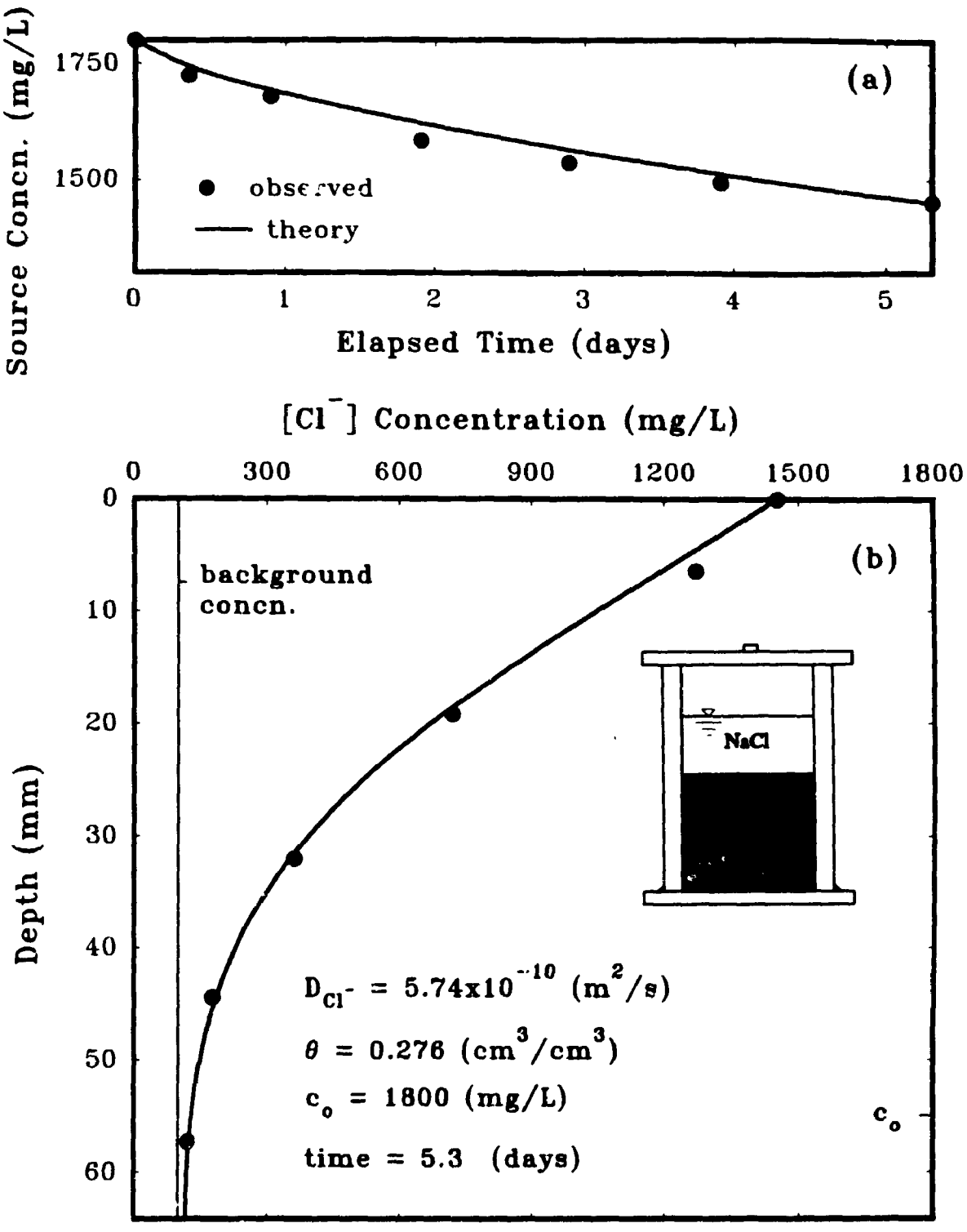

FIG. 4.11 OBSERVED AND THEORETICAL "BEST FIT" [Cl^-] CONCENTRATION IN DIFFUSION TEST # CD1, (COMPACTED CLAYEY SILT), (a): SOURCE SOLUTION CONCENTRATION VS TIME, (b): PORE-WATER CONCENTRATION VS DEPTH

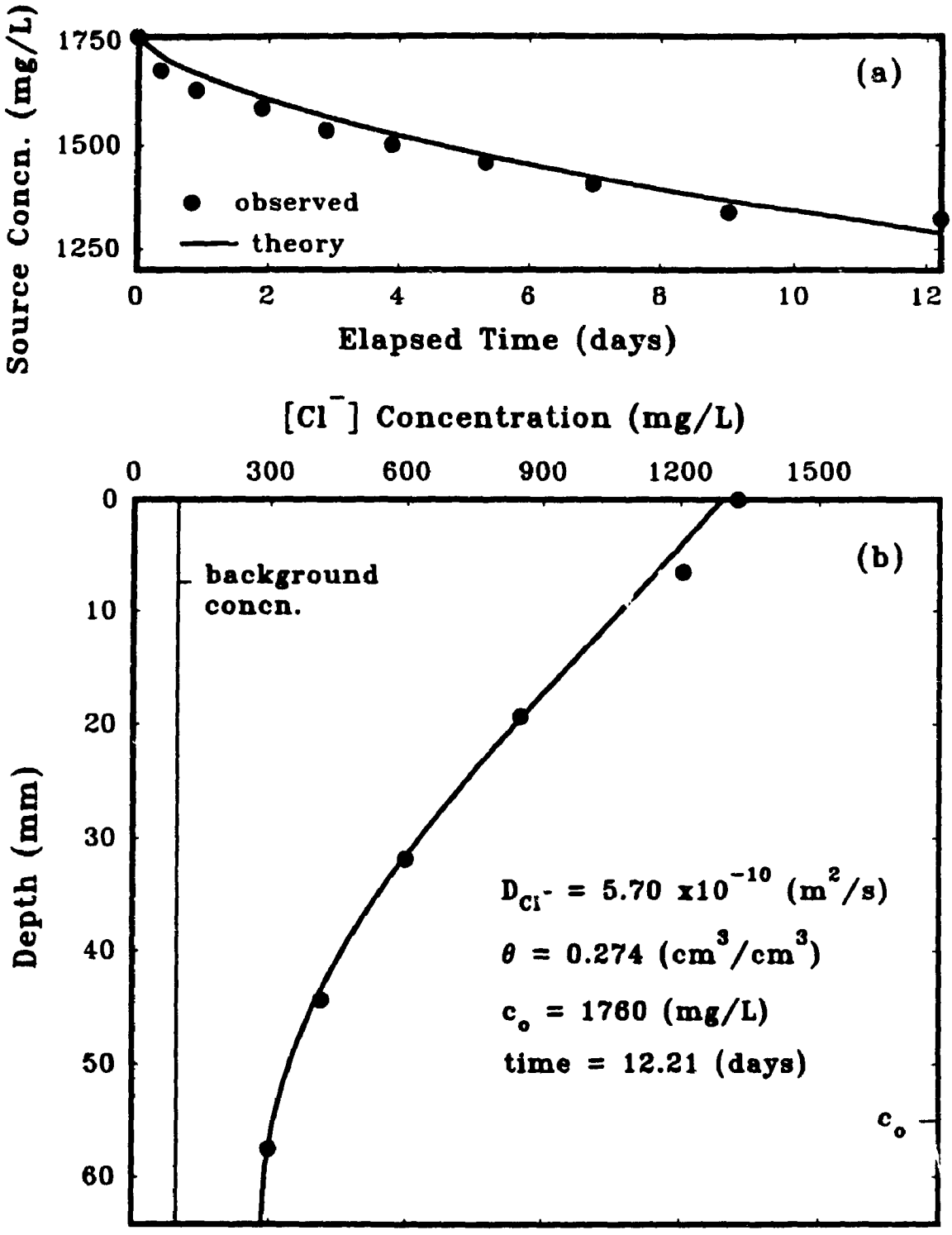

FIG. 4.12 OBSERVED AND THEORETICAL "BEST FIT" [Cl^-] CONCENTRATION IN DIFFUSION TEST # CD2, (COMPACTED CLAYEY SILT), (a): SOURCE SOLUTION CONCENTRATION VS TIME, (b): PORE-WATER CONCENTRATION VS DEPTH

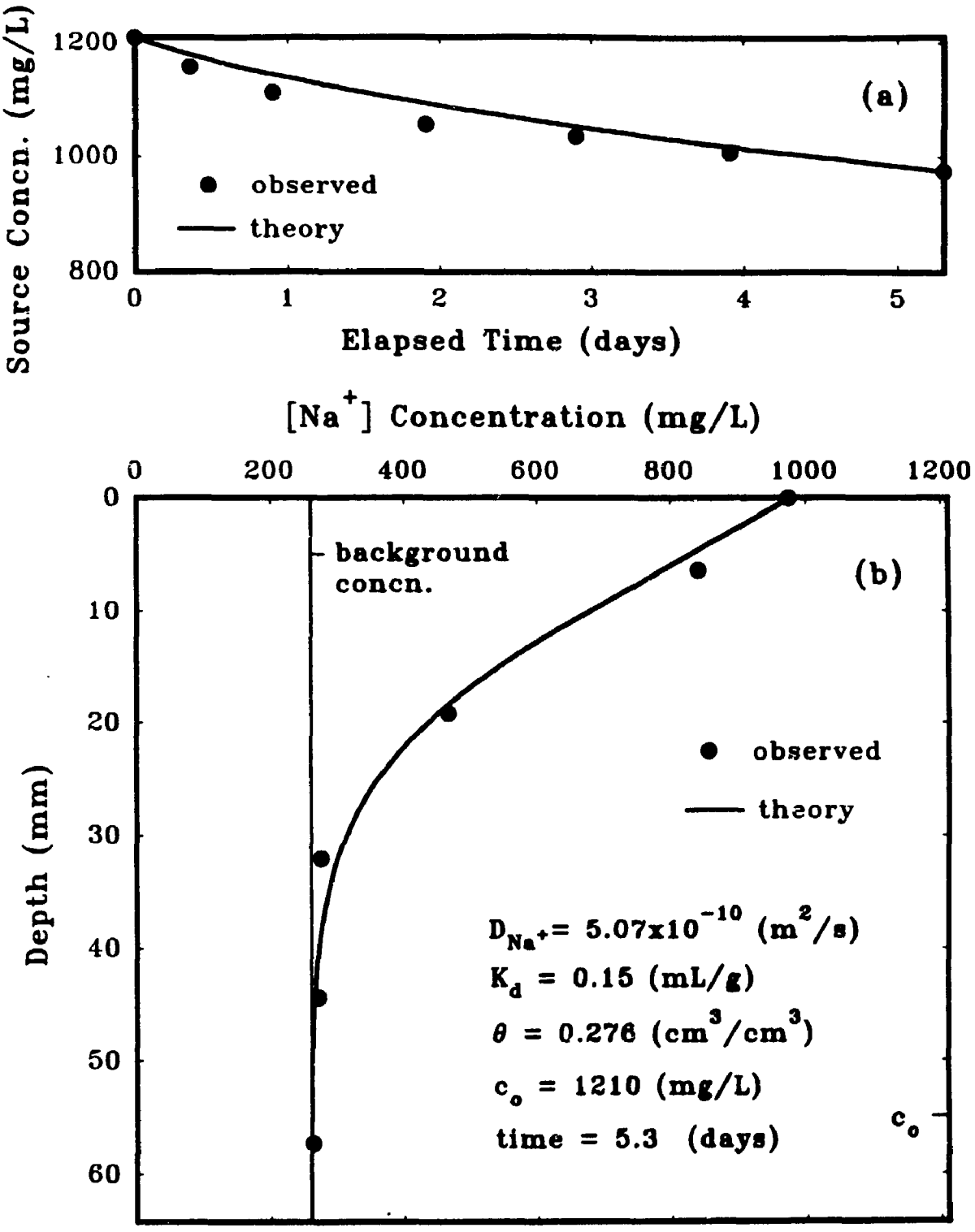

FIG. 4.13 OBSERVED AND THEORETICAL "BEST FIT" [Na^+] CONCENTRATION IN DIFFUSION TEST # CD1, (COMPACTED CLAYEY SILT), (a): SOURCE SOLUTION CONCENTRATION VS TIME, (b): PORE-WATER CONCENTRATION VS DEPTH

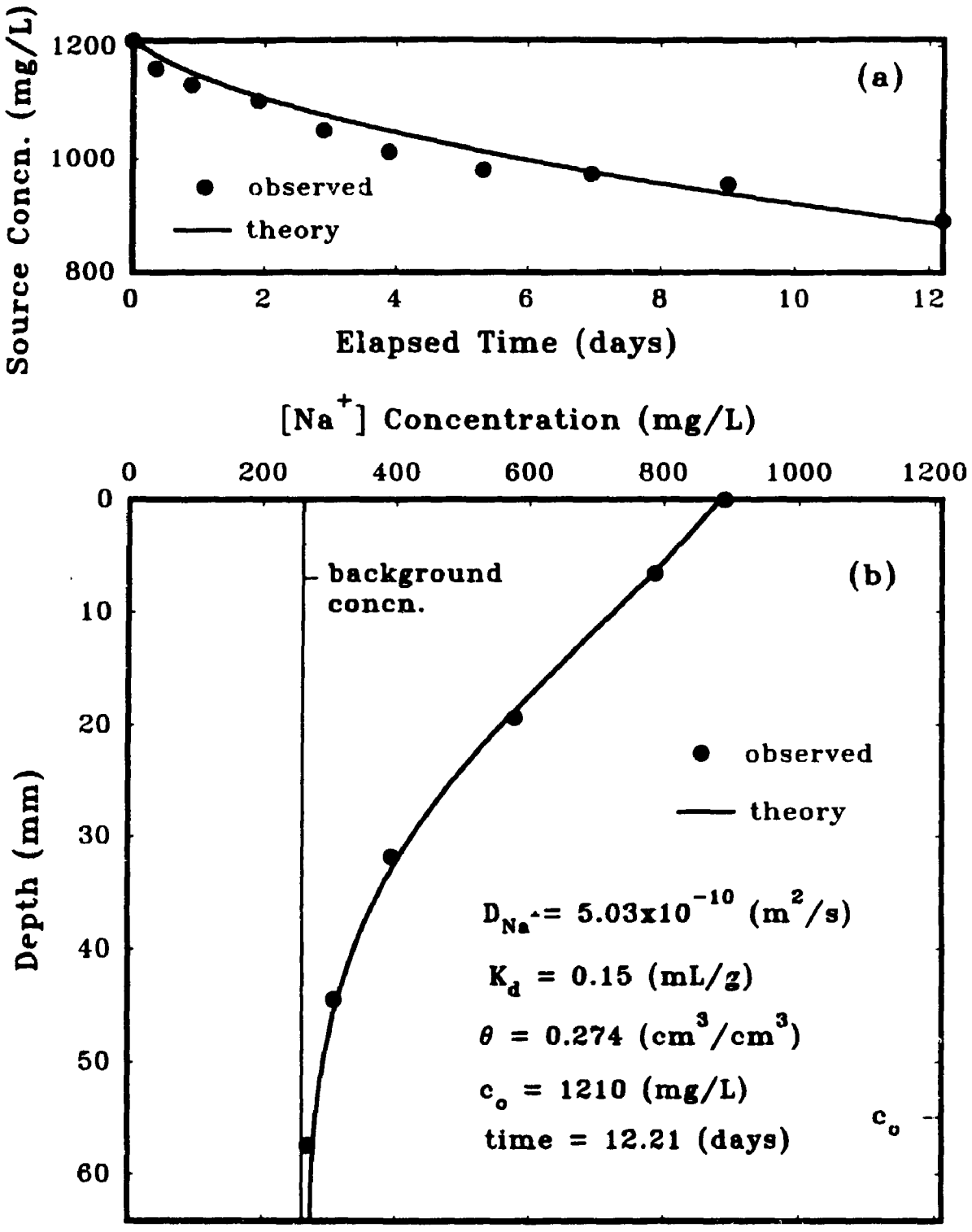

FIG. 4.14 OBSERVED AND THEORETICAL 'BEST FIT" $[Na^+]$ CONCENTRATION IN DIFFUSION TEST # CD2, (COMPACTED CLAYEY SILT), (a): SOURCE SOLUTION CONCENTRATION VS TIME, (b): PORE-WATER CONCENTRATION VS DEPTH

CHAPTER 5

ADVECTION-DIFFUSION TESTS IN A TWO-LAYER SOIL SYSTEM OF CLAYEY SILT OVER FINE SAND

5.1 INTRODUCTION

The majority of reported laboratory studies on contaminant migration through soil, have focused on the transport behaviour of migrating species in a single soil layer, being either fine-grained soil such as clay (e.g. Rowe et al., 1985, 1988; Shackelford and Daniel, 1991) or granular soil such as sand (e.g. De Smedt, 1981). In some practical applications involving waste disposal sites, there is a clayey layer which is underlain by a natural deposit of saturated or nearly saturated granular material such as sand. In order to predict the transport of migrating species through these layers, the diffusion coefficients of migrating ions in each soil layer need to be known. In modelling these systems it is assumed that the migration can be modelled directly (e.g. Rowe & Booker, 1987, 1994) by adopting appropriate layer properties and invoking continuity conditions at the layer boundaries. However the validity of this assumption has not previously been tested using good quality data.

If due to the hydrogeological and design conditions at a landfill site advective flow of contaminants through the landfill (liners) is low (i.e. low Darcy velocity), the major transport mechanism will be by diffusion. This situation is likely to arise when there is a low permeability clay liner and a limited leachate mound (e.g. due to pumping of a drainage layer above the liner).

In Chapter 4, the diffusion coefficient of chloride is determined for both saturated clayey silt and sand. In this part of the laboratory experiments, three tests having identical soil material and test geometry, were conducted, using a 5 cm thick compacted clayey silt on top of a 10 cm fine sand under the gravity drainage condition. In the first two tests, which will be referred to as "drying" Tests # AD1 and AD2, the sand samples were saturated and then allowed to drain by gravity. These tests were duplicated to ensure the reproducibility of the results. The third test, which will be referred to as "wetting" Test # AD3, had similar conditions as Tests AD1 and AD2 except that the sand sample was initially dry and then allowed to wet by capillary action from a water source below the sand sample. The purpose of the third test was to observe the effect of entrapped air in the sand pores on the transport process.

The objective of the experiments described in this chapter was to confirm that diffusion coefficients found in single soil diffusion tests can be used to accurately predict the advective-diffusive migration of the same contaminant in the combined two-layer system.

5.2 MATERIAL PROPERTIES AND PREPARATION

The sand used for the experiments was fine-uniform Ottawa sand (type Wedron 710). The clayey soil was an unweathered grey, sandy, clayey silt till with some gravel that was being used to construct a liner for the Halton Waste Management Site (Rowe et al. 1993). The physical, chemical and mineralogical characteristics of the soils examined are summarized in Tables 4.1 and 4.2 and their grain size distribution are

shown in Fig. 4.1. The clayey soil was air dried, pulverized and oversize material was removed by passing soil through a #4 sieve. The soil was mixed with tap water to a water content of 12.9-14.9% (2-4 % wet of optimum water content), allowed to cure, and compacted in a standard Proctor mold. The samples were then extruded from the mold and sectioned into 2 parts about 6 cm thick for testing.

Sodium chloride solution was used as a tracer solution with attention being devoted to chloride as a conservative species. A finite mass of chloride was provided in the reservoir at the start of each test and the variation in source concentration with time was monitored as sodium and chloride diffused into the soil.

5.3 TEST METHOD

Three compacted clayey samples having about 10 cm diameter and 6 cm thickness were prepared as previously described. The samples were inserted into the plexiglass rings using the method applied for clayey silt diffusion tests described in Chapter 4. An impermeable plexiglass plate was placed at the base of the ring directly below the soil layer and an extra plexiglass ring was placed on top of each clayey sample ring and background solution was applied on top of each clayey sample for about 14 days.

Three identical test cells were assembled using six plexiglass rings as described for the fine sand diffusion tests. Washed dry fine sand was packed in the cells to a height of about 10 cm. Two samples were saturated for 24 hours using the same procedure used in diffusion tests. These tests which were duplicates, will be referred to as the drying Tests # AD1 and AD2. The third sand sample was allowed to wet by

capillary action by connecting a distilled water tank to the outlet valve in the base reservoir chamber and maintaining the water level at the bottom of the sand for about 24 hours to ensure completion of the capillary rise (Fig. 5.1). This test will be referred to as the wetting Test # AD3.

The accessories (horizontal pipette and vertical burette) were attached to the outlet valve of the reservoir chamber in each cell (which acted as the receptor reservoir in these experiments) and were adjusted to be level with the bottom surface of the soil. Samples were allowed to drain by gravity by opening the outlet valve connected to the pipettes. Observations showed that none of the samples yielded any water. This was due to the fact that the height of the capillary rise in fine sand is greater than the height of the samples tested, and the capillary suction in the sand pore spaces did not allow the pore water to drain by gravity.

After installation and wetting of the fine sand samples in each cell as described above, the background solution on top of the clayey samples was removed and clayey samples were placed on top of the sand samples. Care was made to ensure that complete contact was made between the sand and clayey silt. Two extra plexiglass rings (1.6 cm thick each), were placed on top of the clayey sample rings in each cell, to create a space for the source solution reservoir. The stainless steel rings were placed on top of the last plexiglass ring in soil column and clamped to the base stainless steel plates by steel rods. The assembled cells were placed on top of the three magnetic stirrers to operate the stirrer bars inside the lower reservoir chambers. Sodium chloride solution which had already been prepared, was poured on top of the clayey samples in each cell. Two source solution samples were taken from each cell for initial source solution

concentration measurement. The height of the source solution and thickness of the clayey silt and sand samples were measured and recorded. Two samples were also taken from the receptor reservoir for initial concentration measurement (if any). Fig. 5.2 shows the schematic and Fig. 5.3 shows a photographic view of the test set up for advection-diffusion experiments.

The source and receptor reservoirs were stirred to maintain uniform concentration of the solution in the reservoirs. Samples from source and receptor reservoirs were taken regularly during the tests. The 2 mL of fluid removed in each sampling was replaced with the same volume of distilled water and the reservoir was stirred again. During the tests, the solution level inside the source reservoirs in each cell, was monitored and the Darcy velocity through the soil system was calculated based on the observed flow. The infiltrated solution was replaced by the same volume of the distilled water to maintain constant head in the source reservoir throughout the tests.

The expected duration of the tests were estimated based on the preliminary analysis with POLLUTE using the diffusion coefficients obtained from diffusion tests conducted on sand alone and clayey silt alone as described in Chapter 4. In these analysis diffusion is considered to be the dominant mechanism of transport because of existing low Darcy velocity through the soil layers.

The duration of the advection-diffusion tests was 19.94, 19.17 and 51.9 days for Tests # AD1, AD2 and AD3, respectively. Before termination of each test, two final samples from the source and receptor reservoirs were taken. Remaining solution in the source reservoirs was drained and the surface of the clayey samples was cleaned of any remaining solution. Using stainless steel sectioning plates, sand samples were sectioned

in equal thicknesses by slightly lifting the plexiglass rings from one edge and sliding the plate through the interface of the two adjacent rings. Sectioning plates including wet sand were weighed immediately after the sectioning and placed in oven for water content determination.

Using the same method described earlier for clayey silt diffusion tests (Chapter 4), the clayey samples were sliced into four sub-layers of approximately equal thicknesses, samples were squeezed, and pore water was collected to determine the chloride concentration.

5.4 MOISTURE CONTENT PROFILES IN THE SOILS TESTED

Fig. 5.4 shows the moisture content profiles in sand and clayey samples measured at the end of the tests. As can be seen, the water content profiles in the two drying tests were essentially uniform in both the sand and clayey samples. There is a slight non-uniformity in the wetting test profiles both in the sand and clayey samples (Fig. 5.9b) and the water content values in the sand profile were less than in the drying tests. This might be due to the slight differences in the pore structure and porosity of the wetting and drying samples which might arise from the manual packing of the samples in two separate cells. Alternatively, this might also arise from the hysteresis effect in the sand. This effect is well known (Bear, 1972 & 1979) and arises from the presence of entrapped air in wetting process and also difference in contact angles at an advancing and receding interface during the wetting and drying processes. The degree of saturation of the clayey silt and sand sub-layers was calculated and averaged for the entire soil profile as

summarized in Table 5.1. A comparison of the average degree of saturation values in the three sand samples showed 7.6% difference between the drying and wetting samples.

5.5 ESTIMATION OF THE DARCY VELOCITY THROUGH THE SOIL SYSTEM

Estimation of the Darcy velocity in the tests conducted, was based on the measurement of head drop from the source reservoir during the test. A curtain amount of head drop was considered to be due to the evaporation from the surface of the source reservoir during the test. The volume of evaporated water was estimated by measuring the weight of water drops which were accumulated under the top plate during the test. The resulting volume loss due to evaporation was subtracted from the total volume loss in source reservoir. At the early stages of the test, the clayey sample was consolidated and a small amount of water was consumed due to this process. This water is not considered as infiltrating water and hence was subtracted from the volume lost in the source reservoir. This volume of water was calculated using the difference in average values of the moisture contents of the clayey silt before and after the test. After the measurement of the head loss from the source reservoir within early stages of the test, lost volume of solution was replaced with distilled water to maintain constant reference height of solution (H_r) on top of the soil. Based on the volume of water infiltrated into the soil and duration of the infiltration, the flow rate was estimated. Knowing the surface area available for infiltration (total cross section of the cell cylinder), the Darcy velocity through the soil system was calculated. As drying tests had almost identical soils and geometry, measured head drops were almost equal and hence calculated Darcy

velocities for the tests were almost the same having the average value of 5.8×10^{-10} m/s. The calculated Darcy velocity for the wetting test was 4.6×10^{-10} m^2/s. The Darcy velocity in this range results in very low advective flow through the soil system so that the dominant transport mechanism is by diffusion. The effect of advective flow resulting from a Darcy velocity in this range in concentration profiles inside the soil, compared to the effect of diffusion (zero Darcy velocity), was evaluated analytically and will be discussed later in this chapter.

5.6 EXPERIMENTAL FINDING AND TESTS ANALYSIS

Experimental Finding

The chloride concentrations in the sand were measured using the same method as described for the diffusion tests (Chapter 4). These concentrations were plotted against soils depth as shown in Figs. 5.5 and 5.7 for Tests # AD1 and AD2 (drying tests), and in Fig. 5.9 for Test # AD3 (wetting test), along with the theoretical predictions (solid lines) which will be discussed later. The initial soil background concentration is also shown in these figures.

The concentration variations with time in the source reservoir were plotted against elapsed time in Figs. 5.6 and 5.8 for Tests # AD1 and AD2 and in Fig. 5.10 for Test # AD3. The chloride concentration in receptor reservoirs in all tests were very low with almost no significant change for the 19 days duration of the Tests # AD1 and AD2. For Test AD3, which was run for about 52 days, there was a small increase in concentration toward the end of the test (Fig. 5.10). The receptor reservoir concentration at the end

of each test is recorded at the bottom of Figs. 5.5 and 5.7 for Tests AD1 and AD2, and Fig. 5.9 for Test # AD3. The predicted behaviour is also shown by the solid line and will be discussed later.

The duplicate drying tests (# AD1 and AD2) gave essentially identical results with negligible differences which mainly arise from slight differences between the tests. As it is seen in Figs. 5.5 and 5.7, after about 20 days of migration, the concentration gradient in clayey silt is greater than the underlying sand, qualitatively indicating that the migration process in clayey soil is slower than in the fine sand.

Tests Analysis

As discussed in Chapter 2, the effective diffusion coefficient, D_e, varies with the volumetric water content (e.g. Porter et. al., 1960; Kemper and Van Schaik, 1966). Many researchers attribute the decrease in the rate of diffusion as the water content decreases, to the increased tortuosity of the pathway for diffusion.

In this thesis the diffusion coefficient and volumetric water content of the soil obtained from pure diffusion tests conducted on saturated fine sand alone and clayey silt alone (and other soils tested in saturated or nearly saturated condition as will be described in following chapters), were taken as the reference values ($D_{e(ref.)}$ and $\theta_{ref.}$) to predict the diffusion coefficient (D_e) of the same soil having different volumetric water content (θ). The linear relationship of:

$$D_e = D_{e(ref)} \frac{\theta}{\theta_{ref}} \qquad (5.1)$$

was assumed to exist between the above-mentioned parameters. This relationship has

also been adopted in unsaturated coarse sand and fine gravel diffusion experiments conducted in this thesis (will be discussed later) to estimate the unsaturated effective diffusion coefficient of chloride in these soils and proven to reasonably predict the experimental behaviour of the diffusing ion.

Theoretical predictions were made for the advection-diffusion tests for the "duplicated drying tests" # AD1 and AD2 using geometrical and material parameters of each test. For fine sand which was almost saturated (an average value of 97.4% saturation-see Table 5.1), the chloride diffusion coefficient of 9.5×10^{-10} m^2/s predicted using Equation 5.1 and the reference diffusion coefficient of 9.9×10^{-10} m^2/s (Table 4.3) obtained from pure diffusion experiments on sand alone, which was calculated as follows:

$$D_e=(D_{e(ref.)}x\theta)/\theta_{ref.}=(9.9\times10^{-10}\times0.356)/0.371=9.5\times10^{-10}\ m^2/s \text{ (Test \# AD1)}$$

and was used in modelling the advective diffusive transport through the sand in the clayey silt-fine sand system. Similarly, the chloride diffusion coefficients of 6.0×10^{-10} m^2/s (Test #AD1) and 5.8×10^{-10} m^2/s (Test #AD2) for clayey silt predicted using Equation 5.1 and the reference diffusion coefficient of 5.7×10^{-10} m^2/s (Table 4.5) obtained from the pure diffusion test on clayey silt alone (Chapter 4), was used for modelling the advective-diffusive transport through the clayey silt in clayey silt-fine sand system. The obtained predicted diffusion coefficients are listed in Table 5.2 and other input data used in the analysis are shown in Table 5.3. The resulting prediction of variation in concentration with depth and time is shown in Figs. 5.5 to 5.8. It can be seen that the predicted and observed behaviour are in good agreement for both tests. Thus, it may be concluded that the results of the advection-diffusion tests are reproducible with Tests # AD1 and AD2 giving essentially the same results and that the diffusion parameters

obtained from the advection diffusion tests are consistent with those obtained from independent diffusion tests (taking into account the difference in the volumetric water contents of the soils according to Equation 5.1). Also it has been demonstrated that the theory for modelling contaminant transport through layered medium (Rowe and Booker, 1987, 1994) provides a good prediction of the concentration profile based on results from independent diffusion tests.

Due to the slight non-uniformity in the water content profiles in sand and clayey silt layers, in Test #AD3 (wetting test), the theoretical analysis was performed for two different cases. For the first case, the clayey silt and sand layers were divided into 4 and 6 sublayers respectively and then using Equation 5.1 the effective diffusion coefficients of the clayey silt and sand sublayers were predicted using the corresponding volumetric water contents of each soil sublayers and the predicted values were then used in the analysis. The volumetric water contents of the clayey silt sublayers ranged from 0.28 to 0.314 (cm^3/cm^3), so using Equation 5.1 the resulting predicted diffusion coefficients ranged from $5.8x10^{-10}$ m^2/s to $6.5x10^{-10}$ m^2/s (with the average of $6.2x10^{-10}$ m^2/s) for the clayey silt (Table 5.2). The volumetric water contents of sand sublayers ranged from 0.303 to 0.363 (cm^3/cm^3), so using Equation 5.1 the resulting predicted diffusion coefficients ranged from $8.1x10^{-10}$ m^2/s to $9.7x10^{-10}$ m^2/s (with the average of $8.8x10^{-10}$ m^2/s) for the fine sand (Table 5.2). The other input data used in the analysis are shown in Table 5.3. The corresponding predicted theoretical profiles are shown as a solid line in Figs. 5.9 and 5.10 for the soil pore water and source and receptor reservoirs concentration data respectively. The second case used the average volumetric water content and a single diffusion coefficient of $6.2x10^{-10}$ m^2/s and $8.8x10^{-10}$ m^2/s for the

clayey silt and fine sand respectively (Table 5.2) and the resulting predicted profile is shown as the dotted line in Fig. 5.9. As can be seen, there is no significant difference between the two theoretical profiles and both lines fit the observed data reasonably well. Due to the lower average volumetric water content of the sand layer compared to the drying tests (# AD1 and AD2), the predicted profile was obtained using lower diffusion coefficient for sand (8.8×10^{-10} m^2/s) compared to the value used in drying tests (9.5×10^{-10} m^2/s).

The values of the chloride diffusion coefficients obtained for each soil, was divided to the diffusion coefficient of chloride in free solution at 23 °C (1.85×10^{-9} m^2/s) to obtain the normalized diffusion coefficients (D_e/D_o) or tortuosity factor (τ) for each soil. Resulting values are shown in Table 5.2. For drying tests (# AD1 and AD2), the average tortuosity factors of 0.514 and 0.320 was found for fine sand and clayey silt respectively. A slightly lower value of 0.473 for the fine sand and higher value of 0.335 for the clayey silt was found in the wetting Test # AD3.

To examine the sensitivity of the results to Darcy velocity at the range mentioned earlier, a comparison was made with the case when zero advective flow assumed in the analysis. Fig. 5.11 shows the results obtained for the three tests conducted. As can be seen, an assumption of zero Darcy velocity still results in a good fit to the experimental data, suggesting that the advection has negligible effect in these tests and the controlling mechanism is by diffusion.

Another series of sensitivity analysis were performed to examine the effect of different assumed effective volumetric moisture contents, $\theta_{effective}$, of the underlying sand on the predicted profiles. The reduction in θ ($\theta_{effective} < \theta_{measured}$) could arise from

different mechanisms. One is anion exclusion (discussed in Chapter 2). The second is the presence of immobile water during advective flow (Chapter 2). The third is the effect that flux may have in changes of θ during the test such that the value of θ changes between the beginning and the end of the test.

The first series of the analyses assumed that the effective θ ranged from 50% to 95% of the measured value at the end of the test (Table 5.1). All other parameters (including $D_{e(sand)}$) are as listed in Tables 5.2 and 5.3. The results for Tests AD1 and AD3 are shown in Figs. 5.12a (Test AD1) and 5.12b (Test AD3). These results indicate that a 50% reduction in θ resulted in concentration profiles which are far from the observed data. The results for a 10% and 5% reduction are close to the solid lines which assumed $\theta_{effective} = \theta_{measured}$, but still solid lines provide the best fit to the data. Based on these results one could hypothesize that up to 10% uncertainty in θ value (i.e., $\theta_{effective} \geq 0.9\theta_{measured}$), does not have significant effect in predicted profiles and that the assumption of $\theta_{effective} = \theta_{measured}$ appears to be reasonable.

A second series of the analysis used the same θ values as above except that the D_e values for sand were also reduced by the same proportion. This took into account the effect of θ on D_e (as discussed earlier). The results are shown in Figs. 5.12c (Test AD1) and 5.12d (Test AD3) and are similar to those in Figs. 5.12a and 5.12b except that they are slightly shifted to the right due to the change in D_e. The same conclusion can be reached that the effect of 10% uncertainty in the θ and D_e values only has a modest effect on the result but that the original assumption ($\theta_{effective} = \theta_{measured}$) appears to be more reasonable.

The results of the source chloride concentration in Test AD3 were plotted versus the square root of elapsed time. The results are shown in Fig. 5.13. As might be expected, at early times (the 52 days of migration) the chloride concentration varies as a straight line function of the square root of time.

5.7 MASS BALANCE CALCULATIONS FOR CHLORIDE

Mass balance calculations for chloride was performed for three tests conducted and the total chloride mass recovered at the end of each test (both in soil pore water and source and receptor reservoirs), was compared with the total chloride mass available at the beginning of each test. The resulting percent recovery values are very close to 100 % and indicate that almost all chloride mass has been recovered in these tests. A summary of results is shown in Table 5.4 and the calculations performed for Test # AD3 is shown in Appendix E as a sample of mass balance calculations for advection-diffusion tests. In these calculations, the total initial mass comprises the initial mass in source and receptor reservoirs, and initial background mass available in the soil pore water. Final recovered mass in the system comprises the mass remaining in the source and receptor reservoirs and the mass recovered in the soil pore water at the end of the test, plus the mass removed by sampling from source and receptor reservoirs during the test. Percent mass recovery was calculated by dividing the total final mass to the total initial mass.

5.8 SUMMARY AND CONCLUSIONS

Laboratory advection-diffusion experiments were performed to examine the movement of contaminants from a contaminant source through a compacted clayey silt underlain by a layer of fine sand by advective-diffusive transport. Atmospheric pressure was maintained at the bottom of the sand layer in all tests.

In these tests, two samples were initially saturated and then allowed to drain. For these "drying" tests, the soil remained almost saturated after the drainage process. In one test the sample was allowed to wet due to capillary rise from a dry state and the consequent degree of saturation for this test (#AD3) was lower than the drying tests (# AD1 and AD2).

The diffusion coefficients for chloride determined from pure diffusion tests on clayey silt and sand alone, along with the corresponding volumetric water contents of each soil, was taken as the reference values to predict the corresponding diffusion coefficients for clayey silt and sand in advection-diffusion "drying and wetting" tests, assuming a linear relationship to exist between the diffusion coefficient and volumetric water content of the soils. This procedure proved to give good predictions of the concentration profiles in all advection-diffusion tests. The fact that the resulting analytical profiles fit the experimental data quite well, confirms the applicability of the diffusion coefficients obtained from diffusion tests on isolated samples for prediction of the migration through layered system.

Analytical results for the three advection-diffusion tests were compared with the results obtained assuming zero Darcy velocity through the soil layers. It was concluded

that for the tests which involved Darcy velocities similar to that observed in many field situations the velocity was sufficiently small not to significantly affect the transport of contaminants.

A series of sensitivity analysis was performed to examine the assumption that the effective volumetric moisture content was equal to the measured volumetric moisture content. The results showed that up to 10 % uncertainty in this assumption has negligible effect in the predicted profiles and the profiles assuming effective volumetric moisture content being equal to that of measured, provide the best fit to the data.

The analytical prediction to the experimental data obtained from the wetting test was performed using non-uniform volumetric water content and diffusion coefficient values across the soil sub-layers. The results were compared with those obtained using the average volumetric water content and diffusion coefficient in the sand and clayey silt. This comparison showed that a good fit to the experimental data could be obtained using the average values although the first method gave slightly better results. The tortuosity and diffusion coefficient through nearly saturated sand was found to be about 62% greater than through the saturated or nearly saturated clayey silt.

The mass balance calculations for chloride showed that essentially all the initial mass was recovered at the end of the tests and there was no detectable mass loss in the test systems.

TABLE 5.1 VALUES OF THE THICKNESS (H), MOISTURE CONTENT (W), DEGREE OF SATURATION (S), AND VOLUMETRIC MOISTURE CONTENT (θ) OF CLAYEY SILT AND FINE SAND LAYERS IN ADVECTION-DIFFUSION TESTS # AD1, AD2, AND AD3

	Test # AD1				Test # AD2				Test # AD3			
	H^1 (cm)	W^2 (%)	S^3 (%)	θ^4 (cm^3/cm^3)	H^1 (cm)	W^2 (%)	S^3 (%)	θ^4 (cm^3/cm^3)	H^1 (cm)	W^2 (%)	S^3 (%)	θ^4 (cm^3/cm^3)
Clayey-silt[5]	5.00	14.9	99.5	0.288	5.0	14.3	96.0	0.281	1.27	17.9	100	0.314
									1.27	15.8	96.0	0.303
									1.26	15.4	94.0	0.295
									1.30	14.6	89.0	0.280
									Average :	15.94	94.8	0.298
	Porosity = 0.289				Porosity = 0.293				Porosity = 0.314			
Sand[5]	10.0	21.3	97.3	0.356	10.0	21.3	97.5	0.357	1.60	18.0	82.7	0.303
									1.65	18.9	87.0	0.319
									1.65	19.7	90.2	0.330
									1.60	19.4	89.0	0.326
									1.60	19.8	90.8	0.330
									2.00	21.6	99.0	0.363
									Average :	19.57	89.8	0.328
	Porosity = 0.366				Porosity = 0.366				Porosity = 0.365			

(1) Thickness of soil layer(s), (2) Moisture content
(3) Degree of saturation (4) Volumetric moisture content
(5) Listed values for tests # AD1 and AD2 are the average values for the entire soil layer

TABLE 5.2 VALUES OF THE THICKNESS (H), VOLUMETRIC MOISTURE CONTENT (θ), EFFECTIVE DIFFUSION COEFFICIENT (D_e), AND NORMALIZED DIFFUSION COEFFICIENT (D_e/D_o), OF CLAYEY SILT AND FINE SAND LAYERS IN ADVECTION DIFFUSION TESTS # AD1, AD2, AND AD3

	Test # AD1				Test # AD2				Test # AD3			
	H[1]	θ[2]	D_e[3]	D_e/D_o[4]	H[1]	θ[2]	D_e[3]	D_e/D_o[4]	H[1]	θ[2]	D_e[3]	D_e/D_o[4]
Clayey-silt[5]	5.0	0.288	6.0×10^{-10}	0.324	5.0	0.281	5.8×10^{-10}	0.316	1.27	0.314	6.5×10^{-10}	0.353
									1.27	0.303	6.3×10^{-10}	0.340
									1.26	0.295	6.1×10^{-10}	0.331
									1.30	0.280	5.8×10^{-10}	0.315
									Average :	0.298	6.2×10^{-10}	0.335
Sand[5]	10.0	0.356	9.5×10^{-10}	0.514	10.0	0.357	9.5×10^{-10}	0.515	1.60	0.303	8.1×10^{-10}	0.437
									1.65	0.318	8.5×10^{-10}	0.459
									1.65	0.330	8.8×10^{-10}	0.476
									1.60	0.363	9.7×10^{-10}	0.524
									1.60	0.330	8.8×10^{-10}	0.476
									2.00	0.363	9.7×10^{-10}	0.524
									Average :	0.328	8.9×10^{-10}	0.473

1 Thickness of the soil layer(s) (cm)
2 Volumetric moisture content (cm^3/cm^3)
3 Effective diffusion coefficient (m^2/s), $D_e = D_{e(ref.)}(\theta/\theta_{ref.})$ where $D_{e(ref.)}$ and $\theta_{ref.}(=n)$ are the effective diffusion coefficient and volumetric moisture content of the saturated sample
4 Normalized diffusion coefficient or tortuosity $D_e/D_o = \tau$
5 Listed values for tests # AD1 and AD2 are the average values for the entire soil layer

TABLE 5.3 OTHER INPUT DATA USED IN THEORETICAL ANALYSIS OF THE ADVECTION-DIFFUSION TESTS # AD1, AD2, & AD3

	Test #AD1		Test #AD2		Test #AD3	
	Fine sand	Clayey silt	Fine sand	Clayey silt	Fine sand	Clayey silt
Soil thickness (mm)	100	50	99.5	50	101	51
Soil background concn. (mg/L)	5	123	5	123	5	123
Initial source concn. (mg/L)	2050		2140		1660	
Height of source solution (mm)	29.5		29.5		29.0	
Solution collected (q_c) (/area/time, m/s)	4.1×10^{-9}		3.7×10^{-9}		1.7×10^{-9}	
Base outflow velocity (v_b) (m/s)	5.9×10^{-9}		5.3×10^{-9}		2.1×10^{-9}	
Darcy velocity (m/s)	5.8×10^{-10}		5.8×10^{-10}		4.6×10^{-10}	
Duration of the test (days)	19.94		19.17		51.9	

TABLE 5.4 SUMMARY OF THE CHLORIDE MASS BALANCE CALCULATIONS FOR CLAYEY SILT-FINE SAND, ADVECTION-DIFFUSION TESTS # AD1, AD2, & AD3

Test #	Initial Mass (mg)			Final Mass (mg)				Percent Recovery (%)
	in source and receptor	in sand and clay	total mass	in source and receptor	in sand and clay	mass removed	total mass	
AD1	6.07	0.196	6.27	3.49	1.65	1.16	6.30	100.5
AD2	6.35	0.191	6.54	3.85	1.63	1.09	6.57	100.4
AD3	4.82	0.202	5.01	2.36	1.82	0.83	5.01	100.0

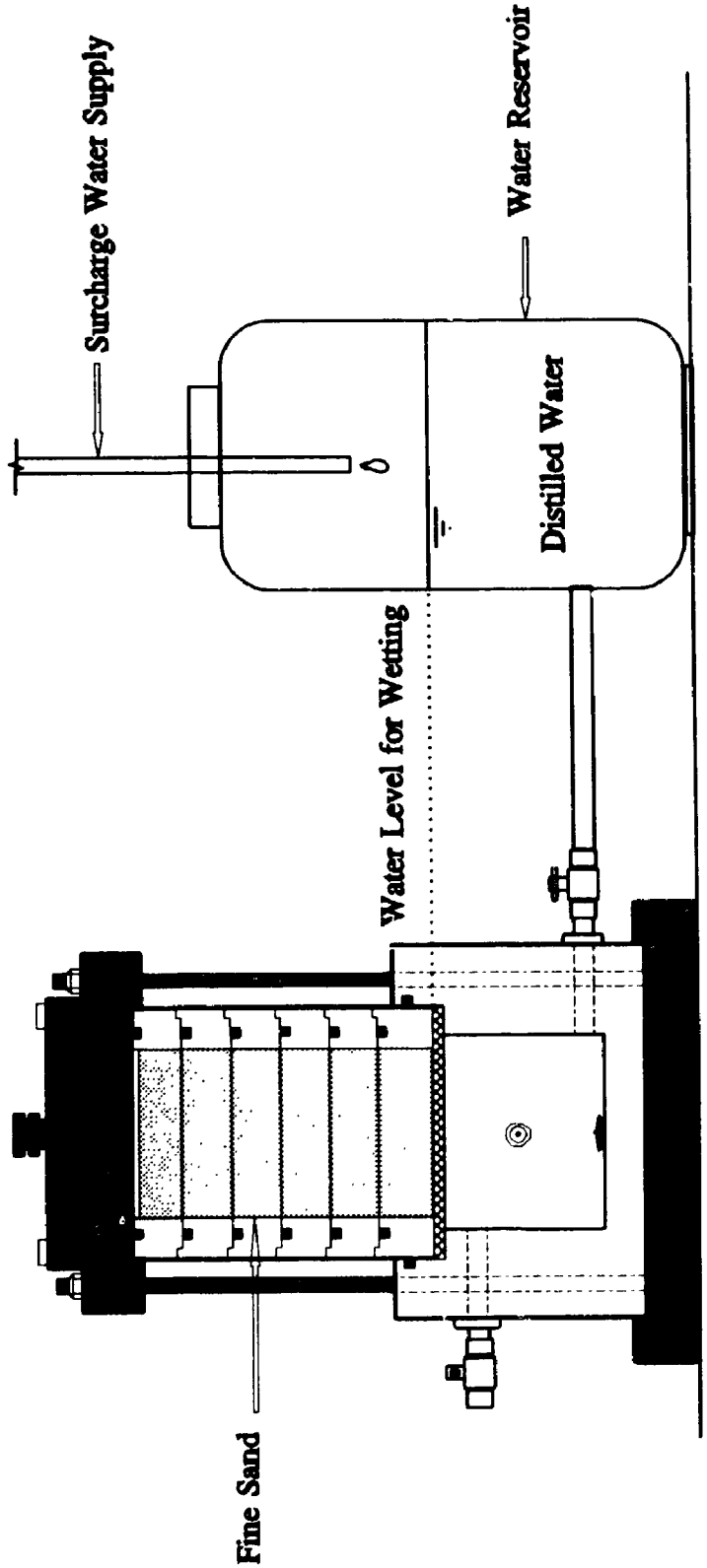

FIG. 5.1 SCHEMATIC OF THE WETTING PROCESS BY CAPILLARY ACTION FOR FINE SAND SAMPLE IN ADVECTION-DIFFUSION TEST # AD3

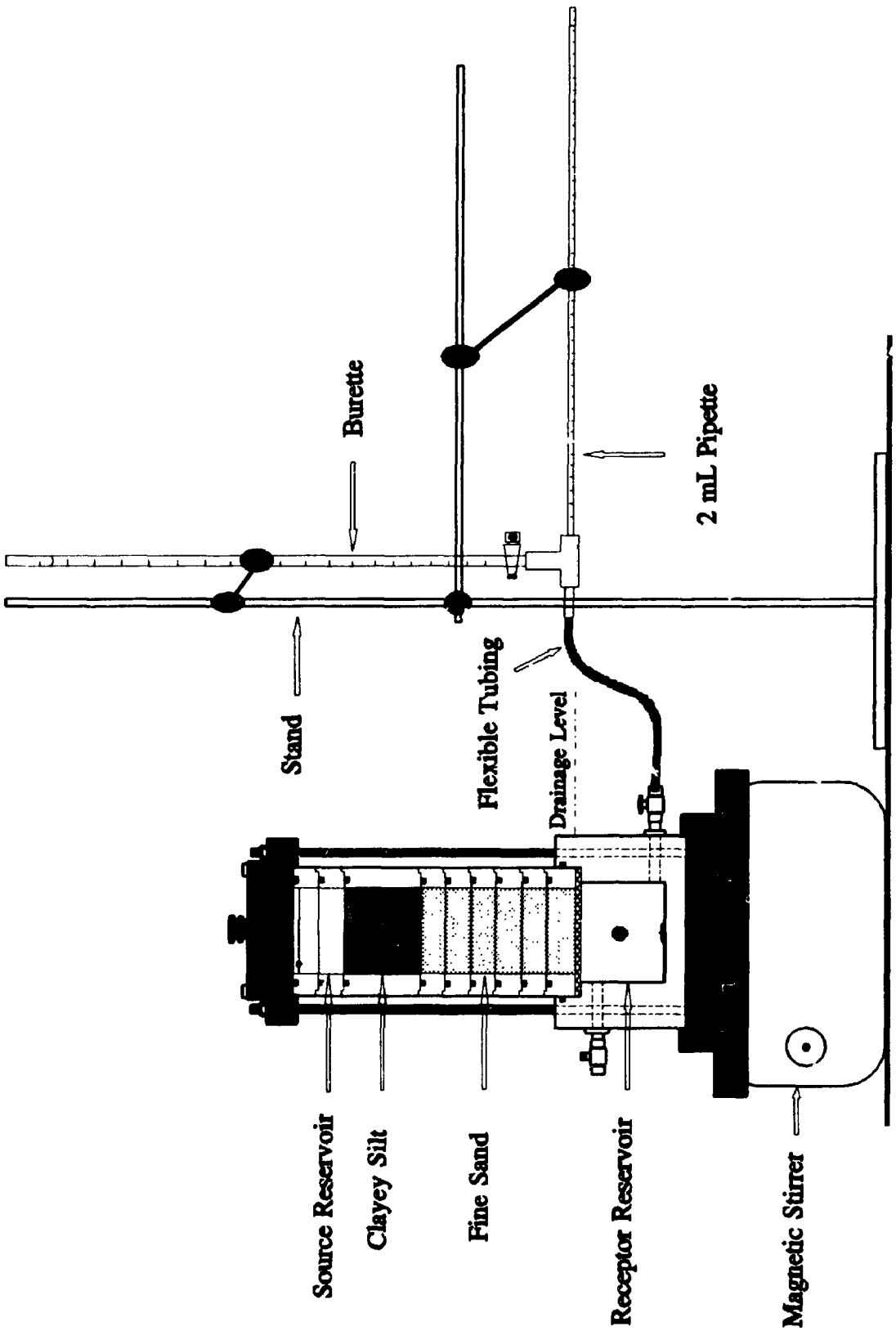

FIG. 5.2 SCHEMATIC OF THE CLAYEY SILT-FINE SAND ADVECTION-DIFFUSION TESTING SET UP

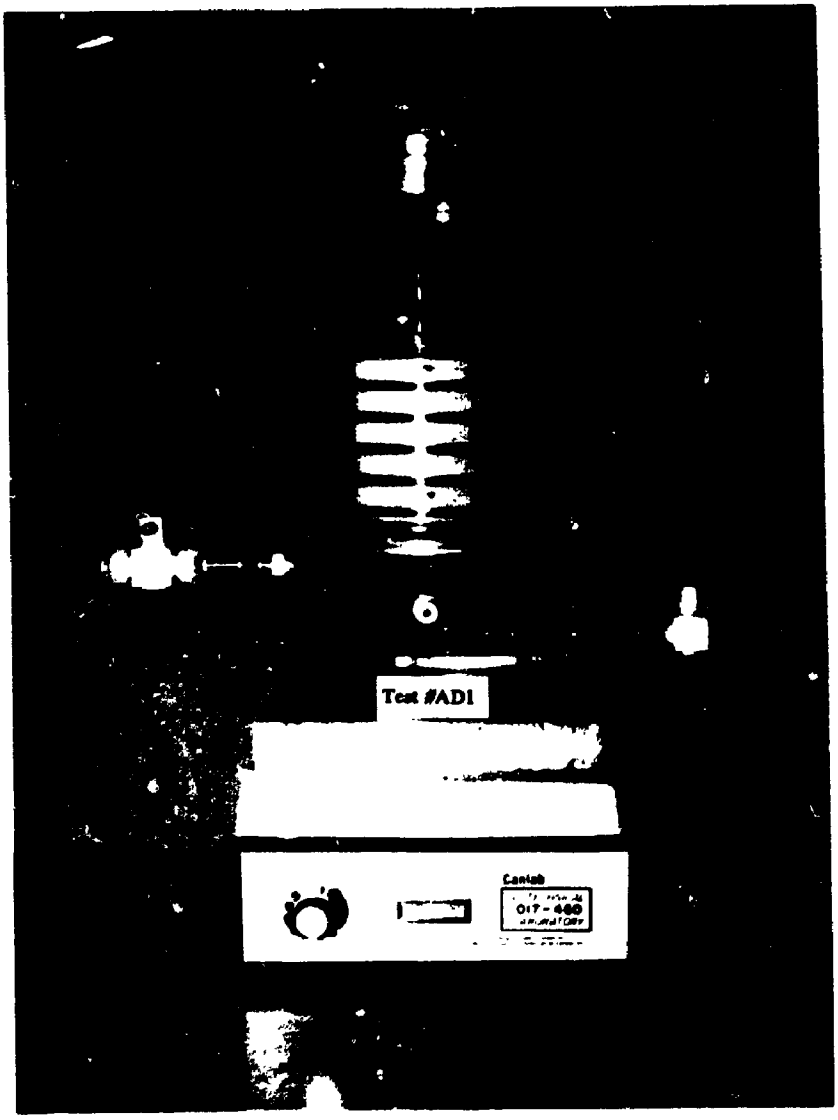

FIG. 5.3 VIEW OF THE ADVECTION-DIFFUSION TEST CONDUCTED ON CLAYEY SILT OVER FINE SAND

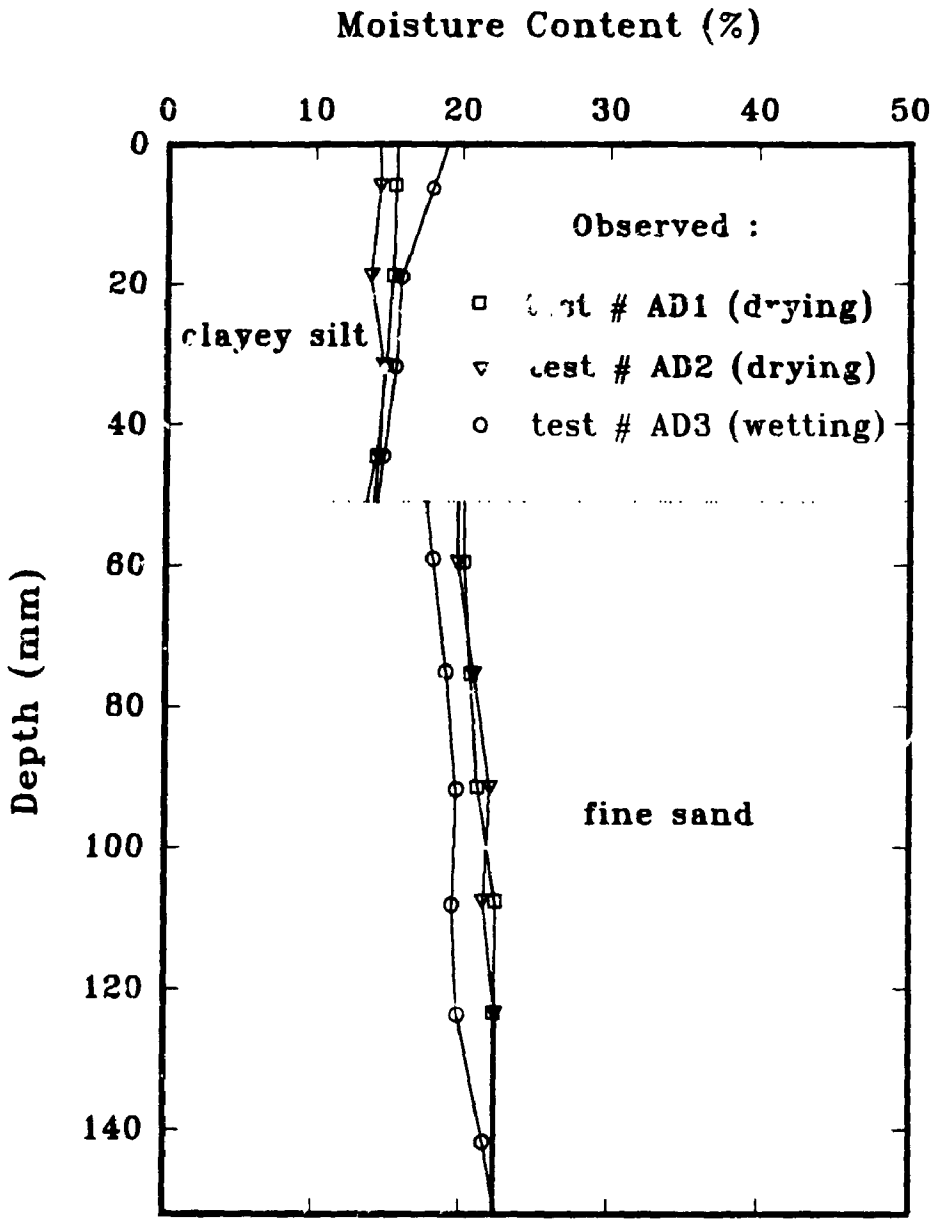

FIG. 5.4 MOISTURE CONTENT PROFILES IN CLAYEY SILT–FINE SAND ADVECTION–DIFFUSION TEST # AD1, AD2 & AD3

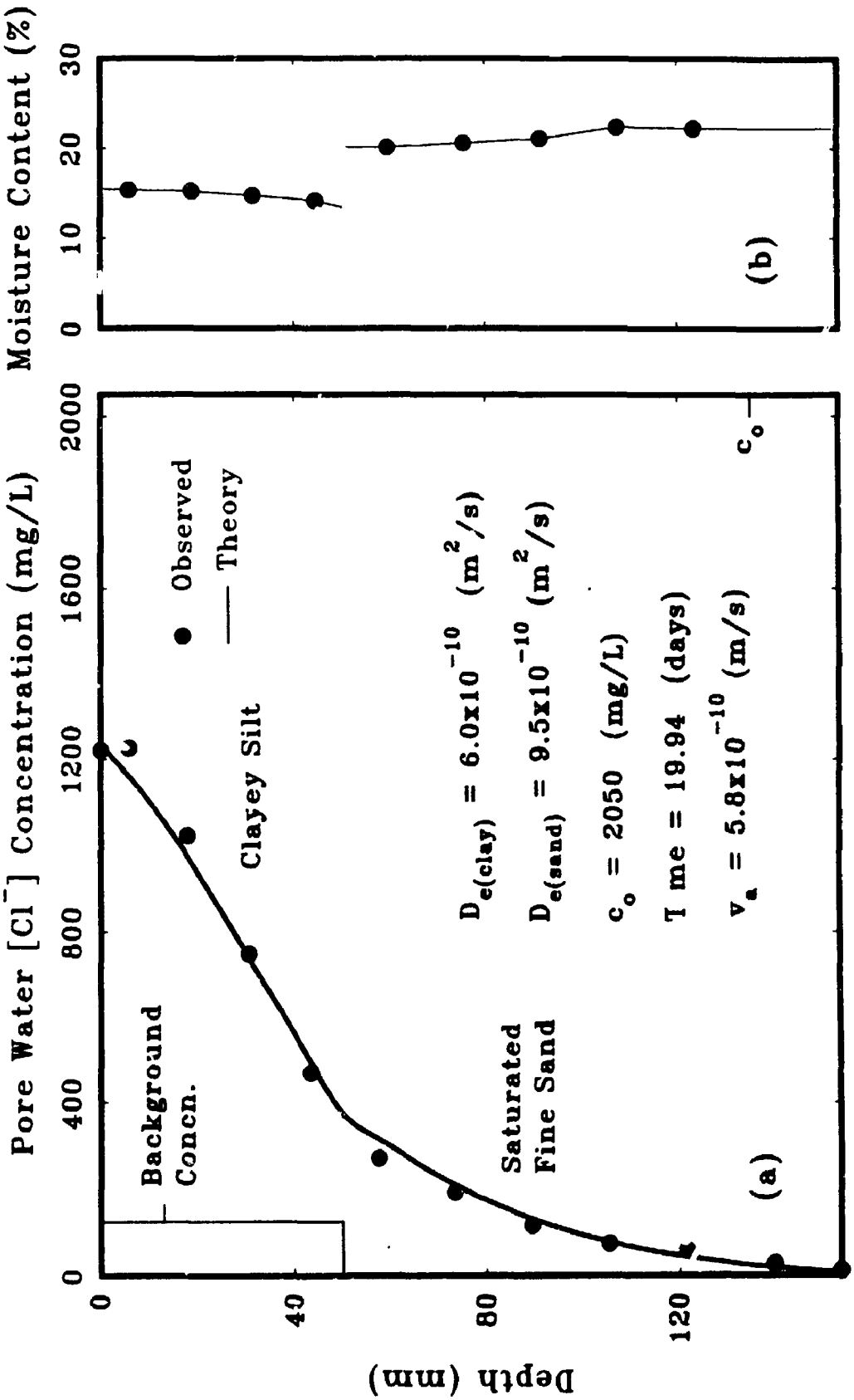

FIG. 5.5 (a) OBSERVED AND PREDICTED CONCENTRATION PROFILES FOR CLAYEY SILT–FINE SAND ADVECTION–DIFFUSION TEST #AD1 (DRYING TEST), (b) OBSERVED WATER CONTENTS VERSUS SOIL DEPTH IN TEST #AD1

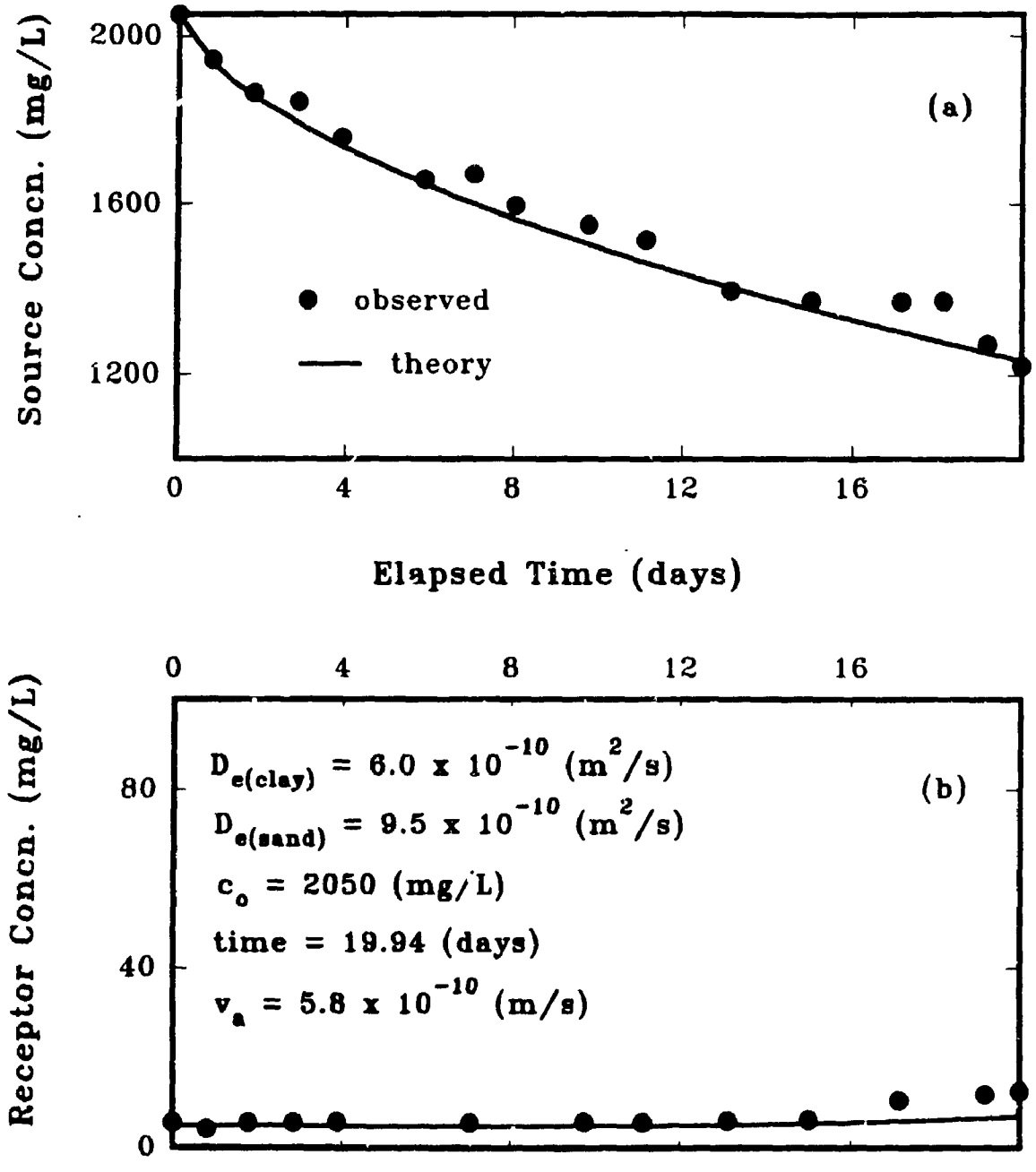

FIG. 5.6 OBSERVED AND THEORETICAL [Cl^-] CONCENTRATIONS VS ELAPSED TIME IN : (a) SOURCE RESERVOIR, AND (b) RECEPTOR RESERVOIR, DURING ADVECTION-DIFFUSION TEST # AD1 (CLAYEY SILT-SATURATED, FINE SAND)

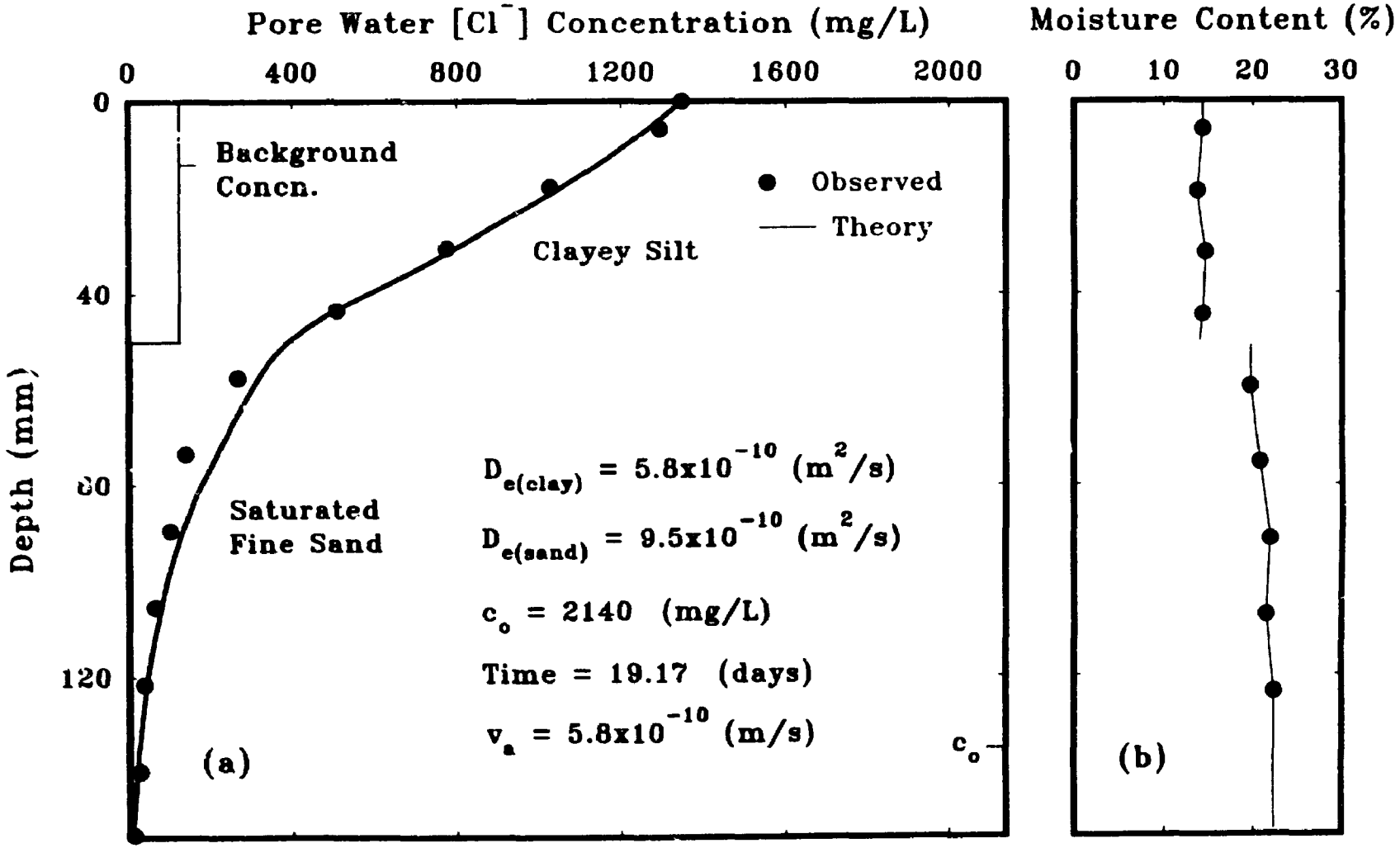

FIG. 5.7 (a) OBSERVED AND PREDICTED CONCENTRATION PROFILES FOR CLAYEY SILT–FINE SAND ADVECTION–DIFFUSION TEST #AD2 (DRYING TEST), (b) OBSERVED MOISTURE CONTENTS VERSUS SOIL DEPTH IN TEST #AD2

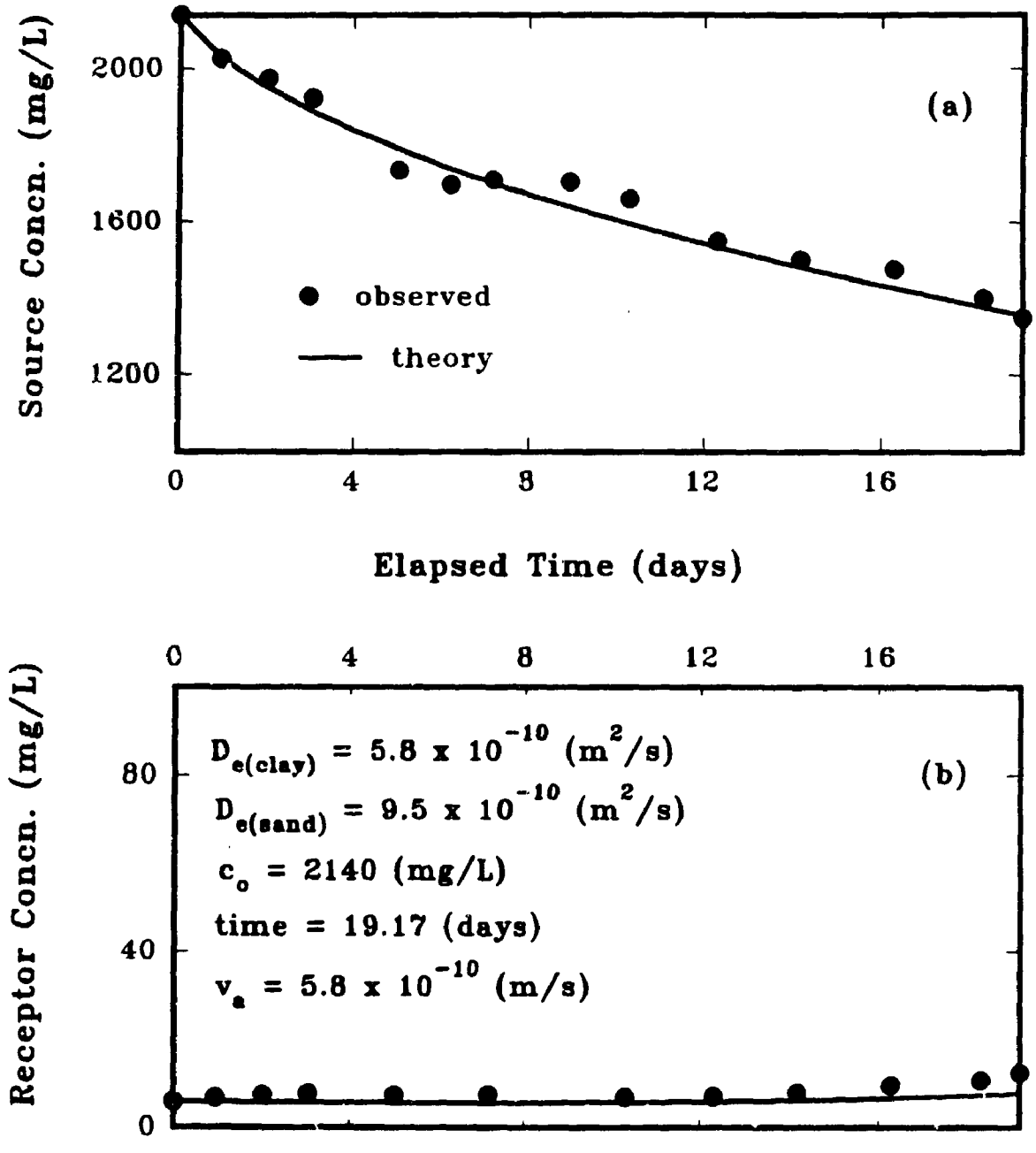

FIG. 5.8 OBSERVED AND THEORETICAL [Cl^-] CONCENTRATIONS VS ELAPSED TIME IN : (a) SOURCE RESERVOIR, AND (b) RECEPTOR RESERVOIR, DURING ADVECTION-DIFFUSION TEST #AD2 (CLAYEY SILT-SATURATED, FINE SAND)

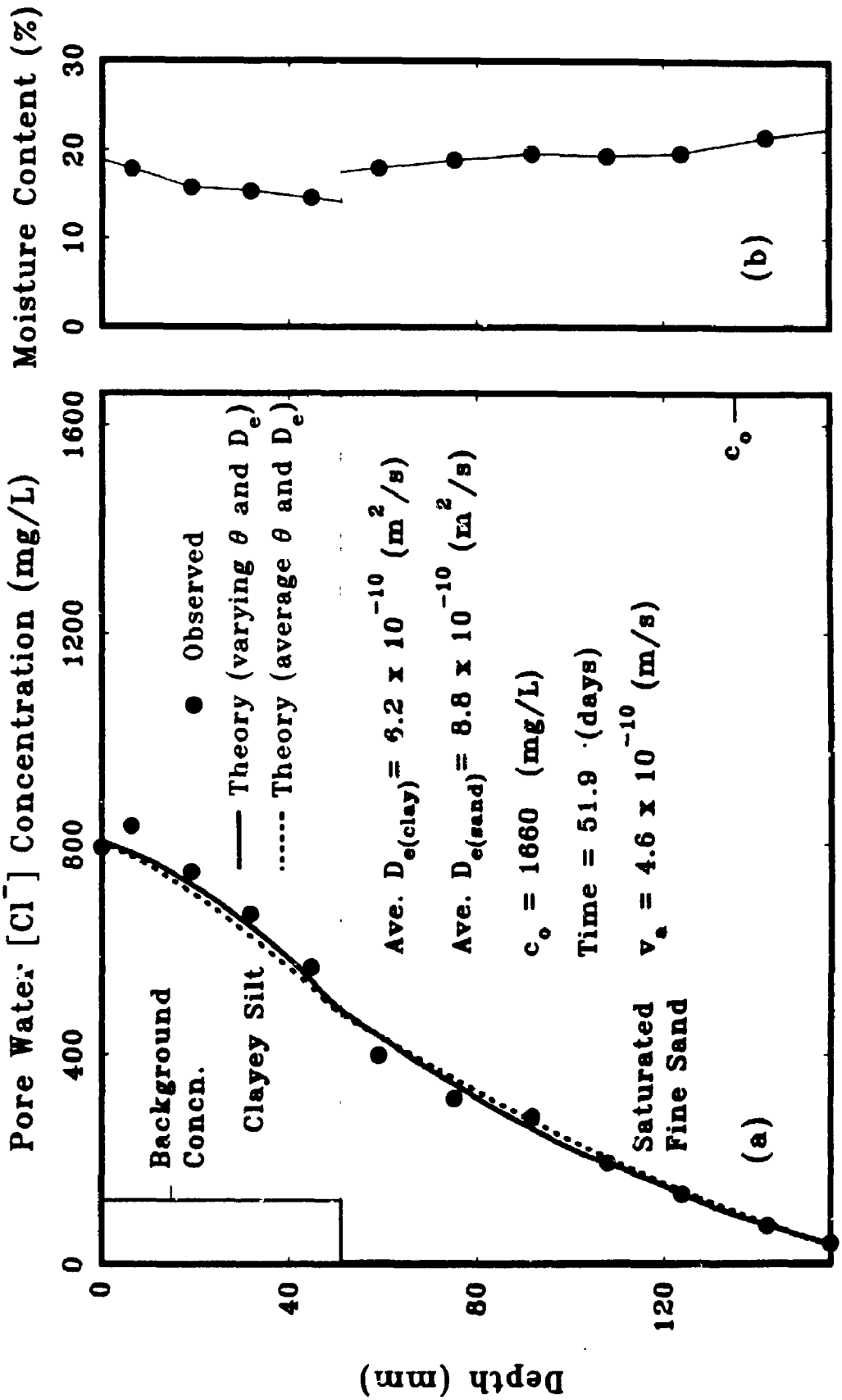

FIG. 5.9 (a) OBSERVED AND PREDICTED CONCENTRATION PROFILES FOR CLAYEY SILT–FINE SAND ADVECTION–DIFFUSION TEST #AD3 (WETTING TEST),
(b) OBSERVED MOISTURE CONTENTS VERSUS SOIL DEPTH IN TEST #AD3

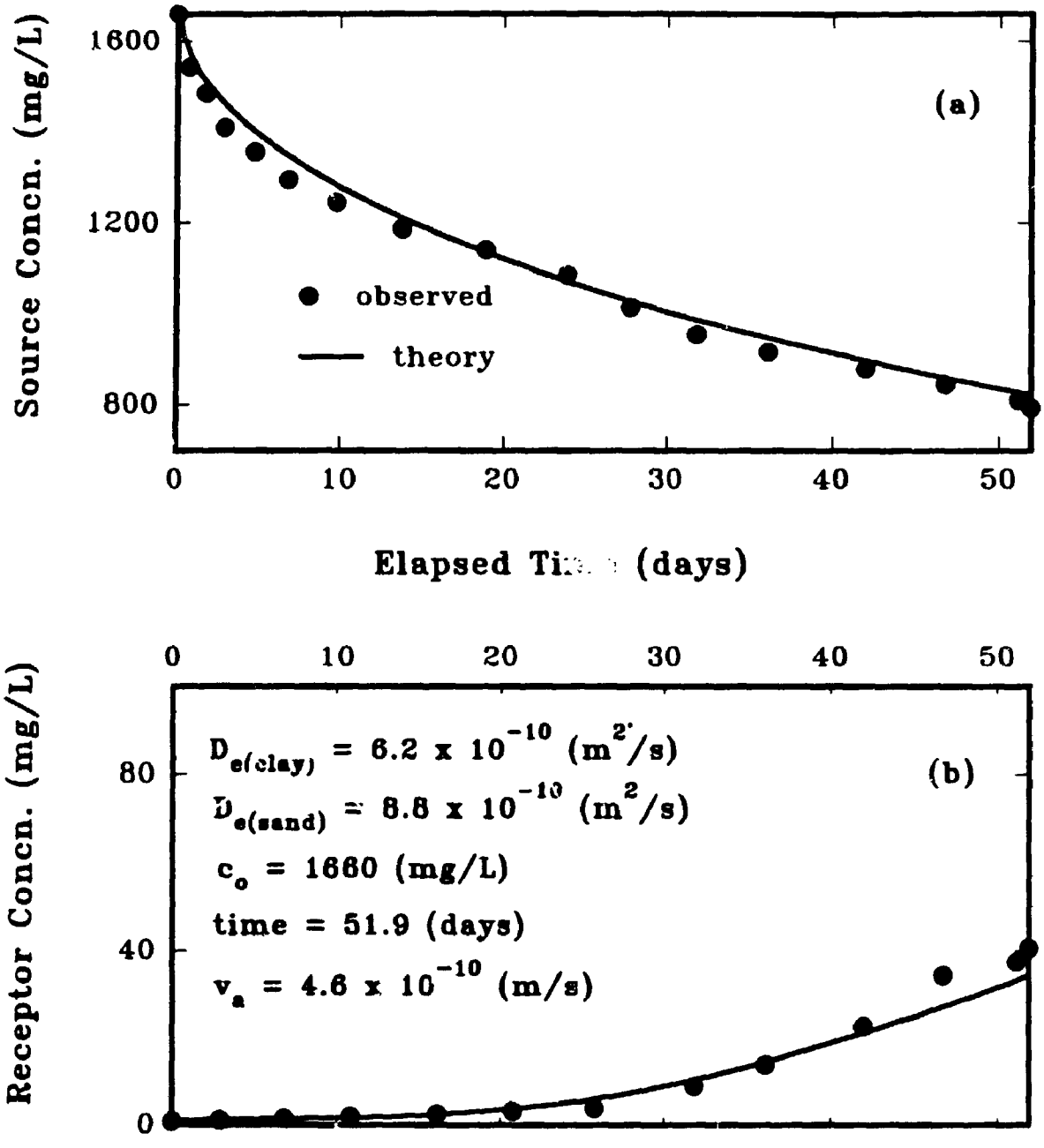

FIG. 5.10 OBSERVED AND THEORETICAL [Cl^-] CONCENTRATIONS VS ELAPSED TIME IN : (a) SOURCE RESERVOIR, AND (b) RECEPTOR RESERVOIR, DURING ADVECTION-DIFFUSION TEST #AD3 (CLAYEY SILT-SATURATED, FINE SAND)

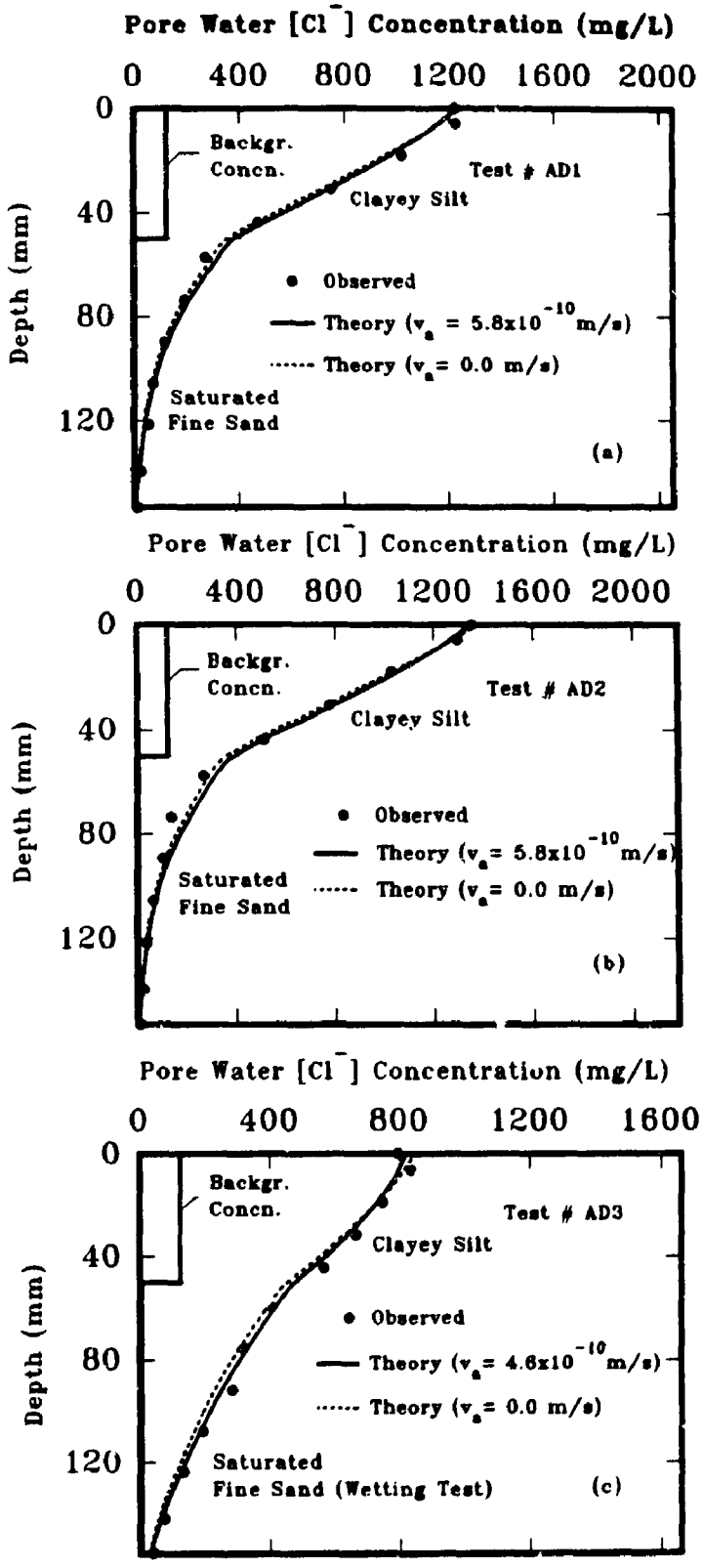

FIG. 5.11 EFFECT OF DARCY VELOCITY ON THEORETICAL CONCENTRATION PROFILES OF ADVECTION-DIFFUSION TESTS (a) TEST #AD1, (b) TEST #AD2, (c) TEST #AD3

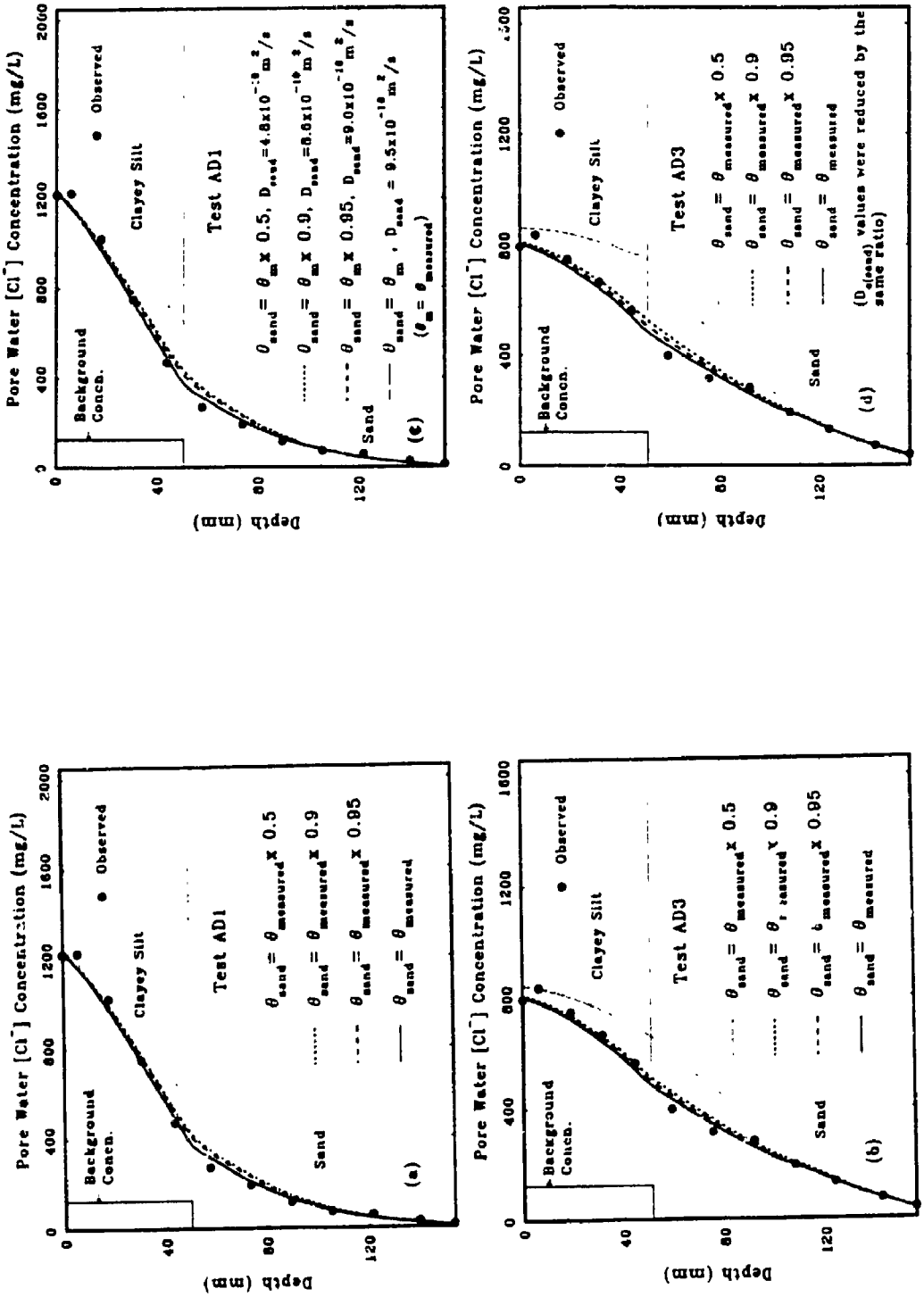

Fig. 5.12 EFFECT OF REDUCED VOLUMETRIC MOISTURE CONTENT (a & b), AND VOLUMETRIC MOISTURE CONTENT AND EFFECTIVE DIFFUSION COEFFICIENT (c & d) OF THE UNDERLYING SAND ON PREDICTED CONCENTRATION PROFILES (TESTS AD1 & AD3)

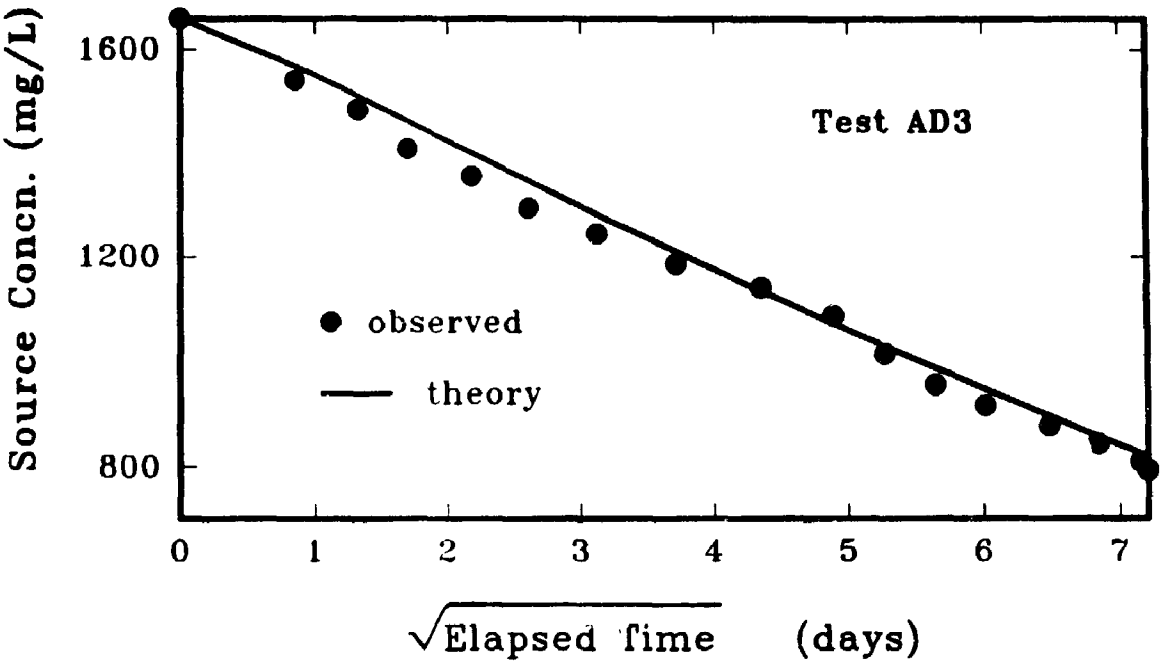

FIG. 5.13 OBSERVED AND THEORETICAL [Cl^-] CONCENTRATIONS VERSUS SQUARE ROOT OF ELAPSED TIME IN SOURCE RESERVOIR OF THE TEST AD3

CHAPTER 6

ADVECTION-DIFFUSION TESTS IN A TWO-LAYER SOIL SYSTEM OF CLAYEY SILT OVER SILT

6.1 INTRODUCTION

This series of the tests was conducted as a continuation of the advection-diffusion experiments on two-layer soil systems having different physical, chemical and mineralogical characteristics. In Chapter 5, experiments were conducted using a compacted clayey silt layer on top of a fine sand layer. In this chapter, the results of two advection-diffusion tests conducted on a compacted clayey silt layer on top of a silt layer are presented. In the first test, which is referred to as "drying" test number AD4, the silt sample was initially saturated and allowed to drain by gravity. In the second test, referred to as "wetting" test number AD5, the silt sample was initially dry and then allowed to saturate by capillary action. The origin, characteristics and preparation of the compacted clayey sample are similar to that used in previous experiments (AD1, AD2 and AD3) as described in Chapter 5. The transport of chloride through these soils and the effect of wetting and drying of the silt on the migration process will be examined in this chapter.

6.2 SOILS, DESCRIPTION AND PREPARATION

The clayey soil used in these experiments was the same as that used in previous

advection-diffusion tests and the chemical and mineralogical characteristics are as listed in Table 4.2. The physical characteristics of the compacted soil differed slightly and the range of the volumetric moisture content (θ) in clayey soil sub-layers at the end of the tests was 0.268-0.299 (cm^3/cm^3) in test AD4 and 0.274-0.297 (cm^3/cm^3) in test AD5. The dry density of the samples was 1.95 g/cm^3 and 1.96 g/cm^3 in tests AD4 and AD5 respectively. The grain size distribution of the soil was as shown in Fig. 4.1. Preparation and compaction methods for clayey soil is similar to that described in section 5.2.

A silty soil was obtained from the Upper Smallman property in London Ontario. The original sample was wet. It was air dried in the lab, pulverized and any oversize material was removed by passing the soil through a #60 sieve (<0.25 mm). The grading curve is shown in Fig. 6.1 and the key physical, chemical and mineralogical characteristics of this soil are listed in Table 6.1.

6.3 INSTALLATION OF THE SOIL MATERIAL AND TEST SET UP

The preparation and installation of the clayey sample was similar to that described in section 5.2. The diffusion cell was assembled as explained in section 4.2 of Chapter 4. The cell column, consisting of 6 plexiglass rings (including the base ring) was packed by pouring the dry silt sample into the column to a height of 10 cm. This filling process consisted of successive placing of silt layers each about 2 cm in high and then tamping the surface of the silt by a plastic septa until silt became stiff. Further vibration was applied to the sample by tamping the circumference of the cell with plastic septa. This

procedure was repeated for all 5 sub-layers until the height of the silt was about 10 cm. The silt surface was then levelled.

For the drying test (AD4), the sample was saturated using the same procedure adopted for fine sand and explained in section 5.3 (Chapter 5). Since the hydraulic conductivity of the silt is expected to be lower than for that of the fine sand, a longer period of time was needed to reach equilibrium, and water was allowed to flow through the sample for about 72 hours. After saturation of the silt sample, a pipette was attached to the outlet valve and adjusted to be level with the top surface of the porous disk (bottom surface of the silt). The outlet valve was opened and the sample was allowed to drain. Due to the higher capillary rise in the silt compared to the height of the sample (10 cm) and equilibrium between the matric suction in the silt and the forces of gravity, sample did not drain. This behaviour was similar to that observed in fine sand.

Installation of the silt sample for the wetting test (AD5) was similar to the drying test and capillary saturation (wetting) of the sample was as described for test number AD3 in Chapter 5 and schematically shown in Fig. 5.1. Monitoring of the water level in the supply tank showed the immediate decrease of the water level (and hence, more water supply into the tank) during first few hours of the saturation process, after which there was no significant change in the water level. To ensure the completion of capillary rise, the wetting period was about 24 hours during which the water level in supply tank was kept constant at the bottom level of the silt.

The clayey plug was carefully installed above the silt so as to ensure complete contact between the clayey soil and silt samples. Any observed soil material around the "o" rings in plexiglass rings was removed and the contact surfaces of the rings were

cleaned of any soil material. Th contact surfaces of the silt and clayey soil were also smooth and level before installation. Once the clayey section was in place, two extra plexiglass rings were placed on top of the clayey section, the stainless steel ring was placed, the steel rods installed, and the cell tightened. The assembled cells were placed on top of the magnetic stirrer to operate the stirrer bars inside the lower reservoirs. Sodium chloride solution of known concentration was poured on top of clayey soil in each cell and starting time of the tests was recorded. The height of the source solution, clayey soil and silt samples were measured and recorded. Two samples from each reservoir (source and receptor) were taken for initial solution concentration measurements. Figs. 6.2a and 6.2b show the schematic and photographic view of the tests conducted.

6.4 MONITORING AND TERMINATION OF THE TESTS

Monitoring of these tests, including sampling of the source and receptor reservoirs, was similar to that described in section 5.3 for clayey silt-fine sand tests. The same procedure which used for termination of the clayey silt-fine sand tests was also used for the clayey silt-silt tests. At the end of each test, the height of the source solution, clayey silt and silt were measured and recorded. After detaching of the clayey silt section from the silt section, the weight of the plexiglass ring and clayey soil was measured and recorded from which the weight of the clayey sample was determined. This value was compared with the weight of the clayey sample before the test. The difference in weight was 6.24 g in test number AD4 and 7.48 g in test number AD5,

indicating an increase in the weight of the samples by the infiltrating solution. This behaviour was consistent with the swelling of the samples that was observed by comparing of the thicknesses of the samples before and after the tests. The moisture content of the clayey sample increased from 13.6 % at the start of the test to an average of 14.8 % (AD4) and 15.2 % (AD5). This swelling and increase in moisture content occurred at the early stages of the test (after application of the source solution on top of the clayey sample) and caused the small increase in degree of saturation of the samples.

The clayey samples were sectioned in 4 sub-layers of approximately equal thicknesses. The silt was sectioned into 6 sub-layers using stainless steel sectioning plates and oven-dried for moisture content determination and chloride concentration measurement using the wash method described in section 3.2.3.

6.5 MOISTURE CONTENT PROFILES IN THE SOILS TESTED

Fig. 6.3 shows the moisture content profiles in silt and clayey silt samples measured at the end of the tests. The degree of saturation and volumetric moisture content of each soil slice (4 slices in clayey silt samples and 6 slices in silt samples) are given in Table 6.2. As shown in Fig. 6.3, the moisture content profiles in clayey sections were almost identical for both tests. The moisture content values in silt samples were different with the wetting test (AD5) having a lower moisture content than the drying test (AD4). This might be partly due to the slight inconsistency in the manual packing of the two silt samples in wetting and drying tests and also partly due to the existence of the entrapped air in the wetting silt which arises from the hysteresis effect

already described for the fine sand in Chapter 5.

6.6 EXPERIMENTAL MEASUREMENTS AND THEORETICAL ANALYSIS

The Darcy velocity for each test was estimated based on the procedure described in section 5.5 for clayey silt-fine sand tests. Both tests had similar Darcy velocities with an average of 2.3×10^{-9} m/s.

The pore water from the clayey samples was obtained by squeezing the samples in pneumatic pressure device at 25 MPa pressure. Because of its dilatancy characteristics, the squeezing procedure was not applicable for silt, so the wash method was used. For each soil sub-layer, 100 g of the silt was washed with 60 mL de-ionized distilled water and the chloride concentration of wash water was determined from which the actual pore water concentration was calculated using Eq. 3.1. The source and receptor reservoir solutions as well as the clayey silt squeezed solutions were diluted 25 times and the concentration of the diluted samples was determined from which the actual concentrations were calculated. The experimental variation in source and receptor reservoir concentrations with time and the experimental variations in soils pore water concentrations with depth were plotted for each test and are shown in Figs. 6.4 to 6.7. The program POLLUTE was used to fit the measured concentration profiles for soil pore water, source and receptor reservoirs and the best fit "by eye" to the experimental data is shown in all relevant figures. For the concentration versus depth figures, the solid lines represent the results of the analysis using varying volumetric moisture content (θ) and effective diffusion coefficients (D_e) in the soil profiles, and the dotted lines represent

the results of the analysis using average θ and D_e values. For the case of using varying volumetric moisture content and effective diffusion coefficient, the values of the effective diffusion coefficient of each soil sub-layer (D_e), was calculated using the volumetric moisture content of each sub-layer, and the reference values of the effective diffusion coefficient ($D_{e(ref.)}$) and volumetric moisture content (θ_{ref}) of the soil having the relationship shown in Eq. 5.1. For the clayey silt samples the reference values listed in Table 4.5 were used. For silt samples the reference values of θ_{ref}=n=0.395 and $D_{e(ref.)}$=9.0x10^{-10} m^2/s were used which resulted in the best fit to the experimental data. Since the variation in volumetric moisture content in the soil profiles was not large, the both methods resulted in a good fit to the experimental data.

A sensitivity analysis was performed to examine the effect of the assumption regarding the effective volumetric moisture content of the underlying silt on the predicted profiles.

The first series of the analyses assumed that the effective θ ranged from 80% to 95% of the measured value at the end of the test (Table 6.2). All other parameters (including $D_{e(silt)}$) are as listed in Tables 6.3a and 6.3b. The results are shown in Fig. 6.8a (Test AD4). These results indicate that a 20% reduction in θ resulted in concentration profiles which are far from the observed data. The results for a 10% and 5% reduction are close to the solid line which assumed $\theta_{effective} = \theta_{measured}$, but still solid line provide the best fit to the data. Based on these results one could hypothesize that up to 10% uncertainty in θ value (i.e., $\theta_{effective} \geq 0.9\theta_{measured}$), does not have significant effect in predicted profiles and that the assumption of $\theta_{effective} = \theta_{measured}$ appears to be reasonable.

A second series of the analysis used the same θ values as above except that the D_e values for silt were also reduced by the same proportion. This took into account the effect of θ on D_e (as discussed earlier). The results are shown in Fig. 6.8b and are similar to those in Fig. 6.8a except that they are slightly shifted to the right due to the change in D_e. The same conclusion can be reached that the effect of 10% uncertainty in the θ and D_e values only has a modest effect on the result but that the original assumption ($\theta_{effective} = \theta_{measured}$) appears to be more reasonable.

6.7 SUMMARY AND CONCLUSIONS

Two advection-diffusion tests were conducted using a compacted clayey silt on top of silt. The experimental set up was similar to that used in clayey silt-fine sand tests, except that silt was used instead of fine sand and the duration of the tests was longer than for clayey silt-fine sand tests. These tests were allowed to run for longer period in order to collect enough data in the receptor reservoir for better observation of the migration process in the entire test system. In order to observe the effect of wetting and drying in the migration process of the NaCl salt solution, two different wetting procedure were adopted for the silt. In test number AD4 the silt was initially saturated by flowing water through the slit for 72 hours which then was allowed to drain by gravity (drying test). In test number AD5, sample was wetted by capillary action from a water reservoir in which the atmospheric pressure level was maintained at the bottom of the soil (wetting test). The moisture content profiles in silt samples showed that the capillary action in wetting test did not saturate the sample.

Theoretical analysis was performed using the clayey silt and silt physical and geometrical characteristics and non-uniform diffusion coefficients for clayey silt and silt. Results of the theoretical analysis using average volumetric moisture content and diffusion coefficients for the soils showed that this method also results in a good fit to the experimental data, suggesting that this method could be applied when the variation in the moisture content throughout the soil profile is not high. The values of the diffusion coefficients for clayey silt (average of $D=5.9\times10^{-10}$ m^2/s = 0.0187 m^2/a) was similar to that obtained in previous experiments, so the only unknown in the analytical calculations was the values of the silt diffusion coefficients which were determined after fitting the best curve to the experimental data. The resulting values of 8.2×10^{-10} and 8.6×10^{-10} was slightly lower than the fine sand diffusion coefficients obtained from previous experiments. Dividing the average diffusion coefficient of chloride for silt in the drying test to the aqueous diffusion coefficient of chloride at 23 °C resulted in the average tortuosity factor of 0.466 for the silt having the average volumetric moisture content of 0.378.

The results of a sensitivity analysis regarding the effect of assumed [illegible] volumetric moisture content of the underlying silt on the predicted profiles (in [illegible]) showed that the original assumption ($\theta_{effective} = \theta_{measured}$) gives the best fit to the experimental data. These results indicated that up to about 10% uncertainty in the θ and D_e values does not have significant effect on the results.

Mass balance calculations were performed for chloride in each test and results showed that 99.8 % and 100 % of the chloride mass has been recovered in the drying and wetting tests respectively.

TABLE 6.1 SOME PHYSICAL, CHEMICAL AND MINERALOGICAL CHARACTERISTICS OF THE UPPER SMALLMAN SILT USED IN ADVECTION-DIFFUSION TESTS # AD4 AND AD5

Physical characteristics

Specific gravity, G_s = 2.67

Porosity = 0.395

Range of the moisture content :

21.2-25.5 % (wetting test), 21.7-25.5 % (drying test)

Dry density = 1.615 g/cm^3

D_{60} = 0.034 mm

D_{10} = 0.0055 mm

Chemical and mineralogical characteristics[1]

Cation exchange capacity[2] (meq/100 g soil):

49.723 (AgTh wash), 8.021 (KCl wash)

Organic carbon content : 0.2 %

[Cl^-] background concentration = 25 mg/L

Minerals present (%):

SiO_2	TiO_2	Al_2O_3	Fe_2O_3	MnO	MgO	CaO	K_2O	P_2O_5	Na_2O	L.O.I	Total
47.02	0.37	7.14	2.17	0.06	5.26	16.39	1.66	0.10	1.38	17.62	99.17

Undetected minerals: 0.83 %

Percent Quartz = 26 %

1 - See Appendix B for description of chemical tests

2 - CEC by combined KCl/Ag thiourea exchange method

TABLE 6.2 VALUES OF THE THICKNESS (H), MOISTURE CONTENT (W), DEGREE OF SATURATION (S), AND VOLUMETRIC MOISTURE CONTENT (θ) OF CLAYEY SILT AND SILT SUB-LAYERS IN ADVECTION-DIFFUSION TESTS # AD4 AND AD5

	Test # AD4 (drying)				Test # AD5 (wetting)			
	H[1] (cm)	W[2] (%)	S[3] (%)	θ[4]	H[1] (cm)	W[2] (%)	S[3] (%)	θ[4]
Clayey silt	1.23	16.82	100	0.299	1.23	17.10	100	0.297
sub-layers	1.23	14.68	96.0	0.287	1.25	15.30	100	0.297
	1.23	14.06	92.0	0.275	1.22	14.60	96.3	0.286
	1.30	13.72	89.6	0.268	1.23	13.90	92.0	0.274
Average values:		14.82	94.4	0.282		15.23	97.1	0.289
Porosity:				0.299				0.297
Silt sub-layers	1.55	21.68	88.6	0.350	1.50	21.20	86.7	0.343
	1.65	22.17	90.7	0.358	1.65	21.20	86.7	0.342
	1.62	23.48	96.0	0.379	1.60	21.40	87.4	0.345
	1.54	24.23	99.1	0.391	1.60	21.50	87.8	0.347
	1.65	25.57	100	0.395	1.60	22.30	91.2	0.360
	2.00	25.50	100	0.395	2.00	25.50	100	0.395
Average values:		23.76	95.7	0.378		22.18	90.0	0.355
Porosity:				0.395				0.395

1 Thickness of soil sub-layer (cm)
2 Moisture content (%)
3 Degree of saturation (%)
4 Volumetric moisture content (cm^3/cm^3)

TABLE 6.3a VALUES OF THE THICKNESS (H), VOLUMETRIC MOISTURE CONTENT (θ), EFFECTIVE DIFFUSION COEFFICIENT (D_e), AND NORMALIZED DIFFUSION COEFFICIENT ($D_e/D_o = \tau$, TORTUOSITY), FOR CLAYEY SILT AND SILT SUB-LAYERS USED IN THEORETICAL ANALYSIS OF THE TESTS # AD4 AND AD5

	Test # AD4 (drying)				Test # AD5 (wetting)			
	H[1] (mm)	θ[2] (cm^3/cm^3)	D_e[3] (m^2/s)	D_e/D_o[4] (-)	H[1] (mm)	θ[2] (cm^3/cm^3)	D_e[3] (m^2/s)	D_e/D_o[4] (-)
Clayey-silt	12.33	0.299	6.2×10^{-10}	0.336	12.33	0.297	6.2×10^{-10}	0.334
	12.33	0.287	6.0×10^{-10}	0.323	12.50	0.297	6.2×10^{-10}	0.334
	12.33	0.275	5.7×10^{-10}	0.309	12.20	0.286	5.9×10^{-10}	0.322
	13.00	0.268	5.6×10^{-10}	0.301	12.30	0.274	5.7×10^{-10}	0.308
Average		0.282	5.9×10^{-10}	0.317		0.289	6.0×10^{-10}	0.325
Silt	15.5	0.350	8.0×10^{-10}	0.432	15.00	0.343	7.8×10^{-10}	0.422
	16.5	0.358	8.2×10^{-10}	0.443	16.50	0.342	7.8×10^{-10}	0.422
	16.15	0.379	8.7×10^{-10}	0.470	16.50	0.345	7.9×10^{-10}	0.427
	15.35	0.391	8.9×10^{-10}	0.481	16.00	0.347	7.9×10^{-10}	0.427
	16.50	0.395	9.0×10^{-10}	0.486	16.00	0.360	8.2×10^{-10}	0.443
	20.00	0.395	9.0×10^{-10}	0.486	20.00	0.395	9.0×10^{-10}	0.486
Average		0.378	8.6×10^{-10}	0.466		0.361	8.2×10^{-10}	0.438

1 - Thickness of the soil sub-layer
2 - Volumetric moisture content
3 - Effective Diffusion coefficient
4 - Normalized diffusion coefficient (tortuosity)

TABLE 6.3b OTHER INPUT DATA USED IN THEORETICAL ANALYSIS OF THE TESTS # AD4 AND AD5

	Test # AD4 (drying)		Test # AD5 (wetting)	
	silt	clayey silt	silt	clayey silt
Soil thickness (cm)	10.0	5.0	10.0	5.0
Soil background Concn. (mg/L)	25	123	25	123
Source concn. (mg/L)	1630		1600	
Height of source solution (Hr) (cm)	3.05		3.05	
Leachate (NaCl) collected (/area/time) (m/s)	1.57×10^{-9}		1.63×10^{-9}	
Base outflow velocity (v_b) (m/s)	2.01×10^{-9}		1.92×10^{-9}	
Darcy velocity (m/s)	2.3×10^{-10}		2.3×10^{-10}	
Duration of the test (days)	58		55.7	

TABLE 6.4 SUMMARY OF THE CHLORIDE MASS BALANCE CALCULATIONS FOR CLAYEY SILT-SILT, ADVECTION-DIFFUSION TESTS # AD4 AND AD5

Test #	Initial Mass (mg)			Final Mass (mg)				Percent Recovery (%)
	in source and receptor	in silt and clay	total mass	in source and receptor	in silt and clay	mass removed	total mass	
AD4	4.98	0.269	5.25	2.58	1.78	0.876	5.24	99.8
AD5	4.89	0.268	5.16	2.59	1.69	0.898	5.18	100.4

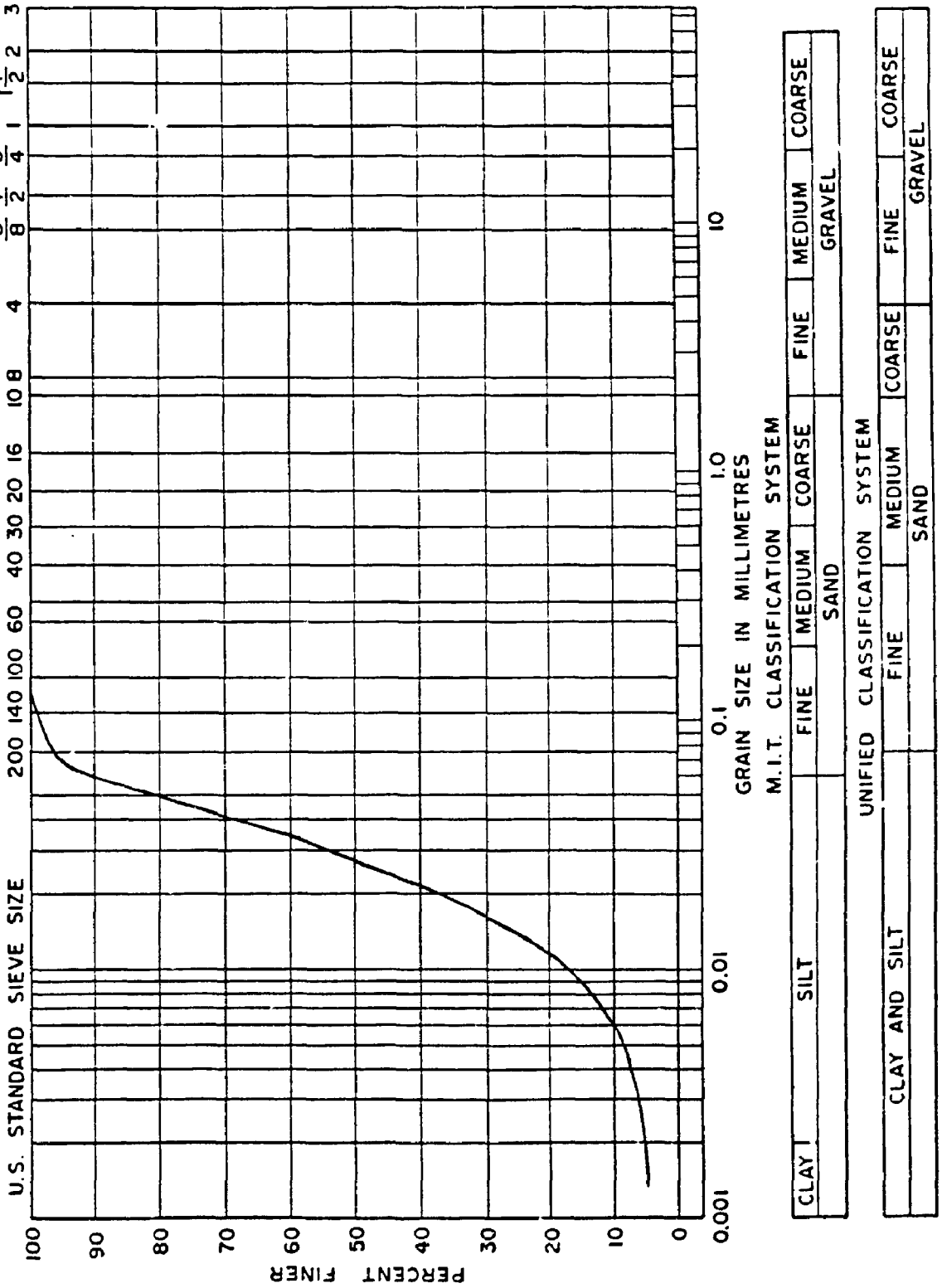

FIG. 6.1 GRAIN SIZE DISTRIBUTION OF THE UPPER SMALLMAN SILT

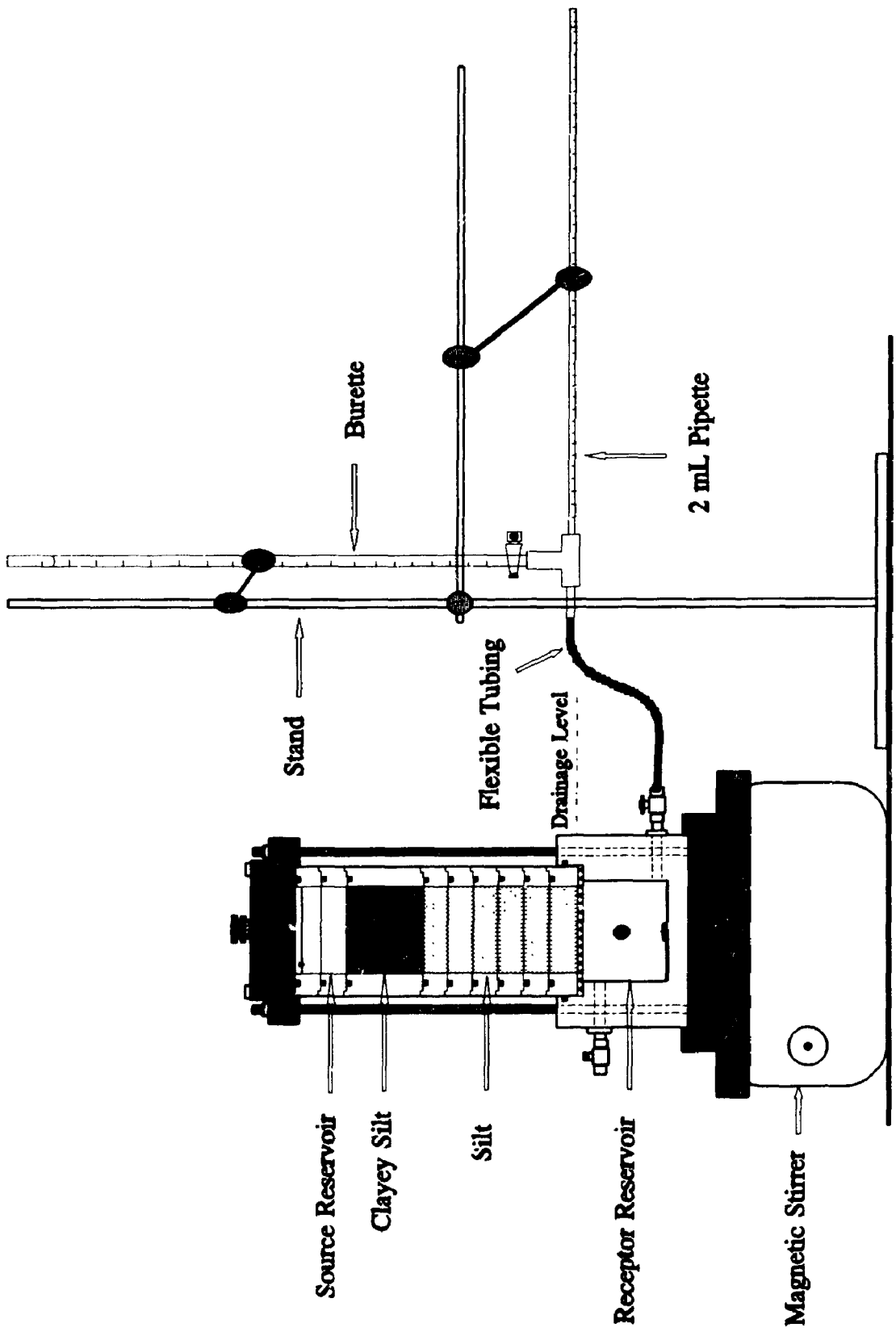

FIG. 6.2a SCHEMATIC OF THE CLAYEY SILT-SILT, ADVECTION-DIFFUSION TESTING SET UP

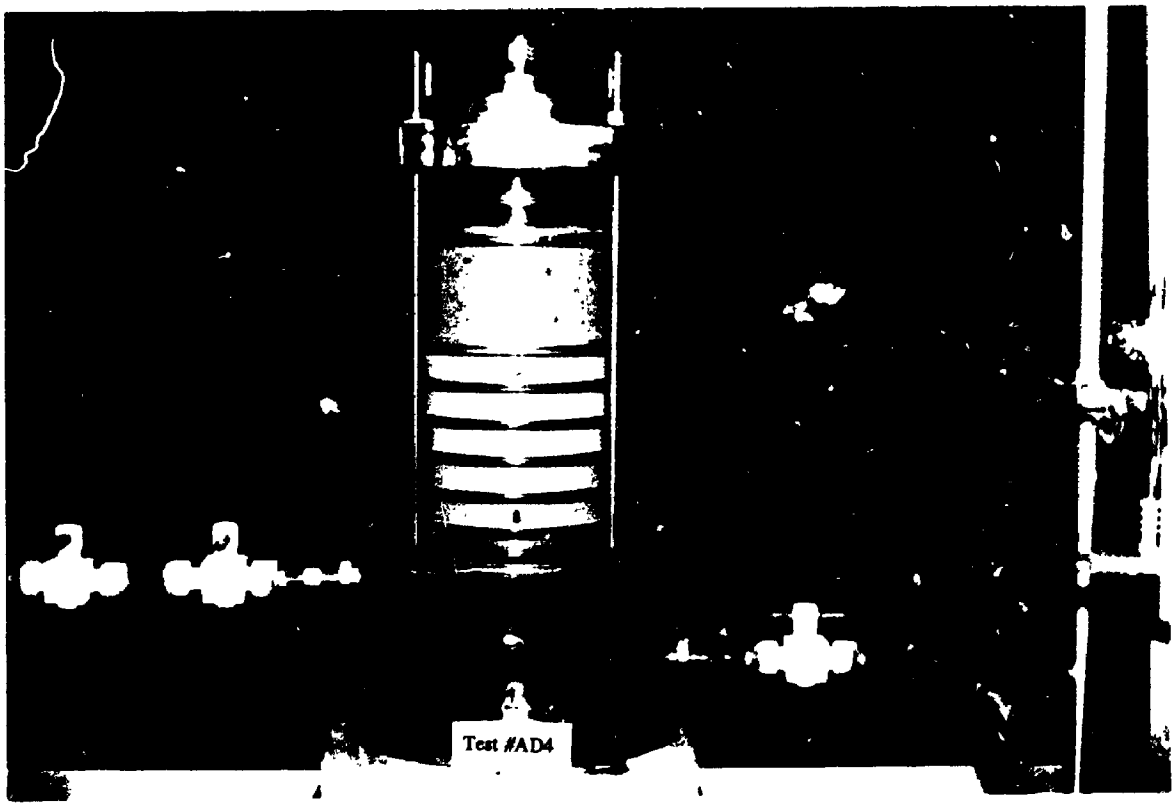

FIG. 6.2b VIEW OF THE ADVECTION-DIFFUSION TEST CONDUCTED ON CLAYEY SILT-SILT SOILS

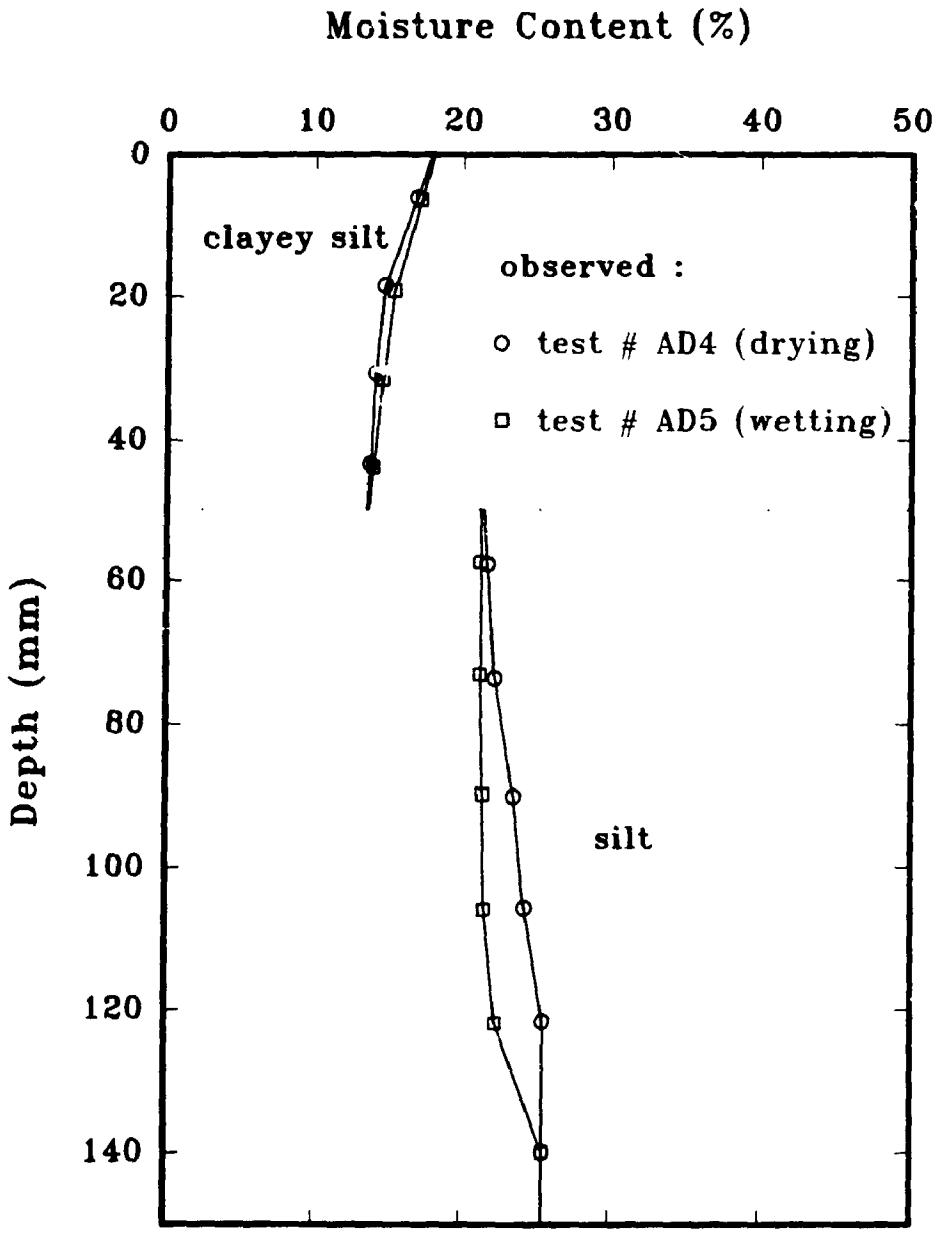

FIG. 6.3 MOISTURE CONTENT PROFILES IN CLAYEY SILT–SILT ADVECTION–DIFFUSION TESTS # AD4 AND AD5

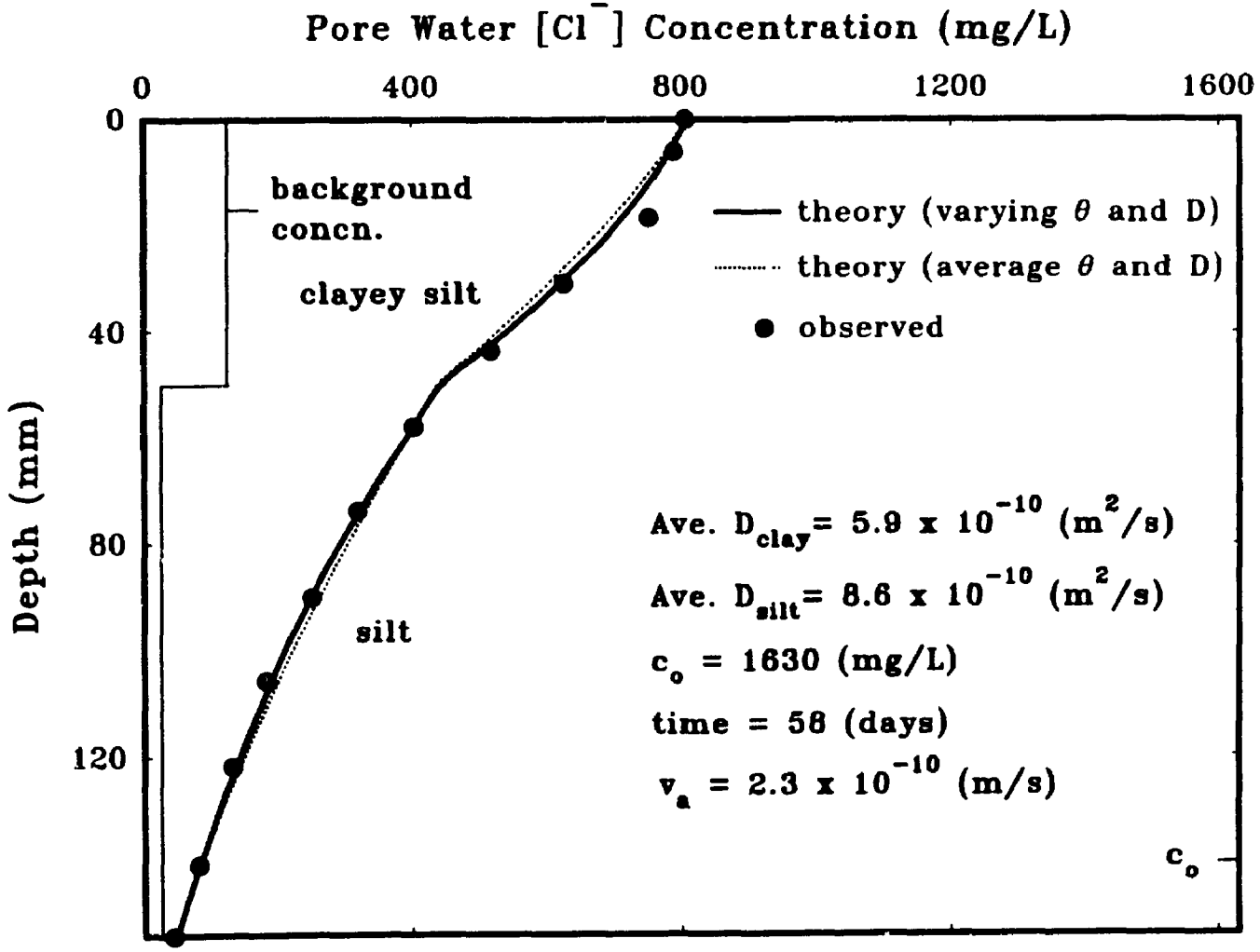

FIG. 6.4 OBSERVED AND THEORETICAL "BEST FIT" [Cl⁻] CONCENTRATION PROFILES IN ADVECTION-DIFFUSION TEST #AD4 (CLAYEY SILT-SATURATED, DRYING SILT)

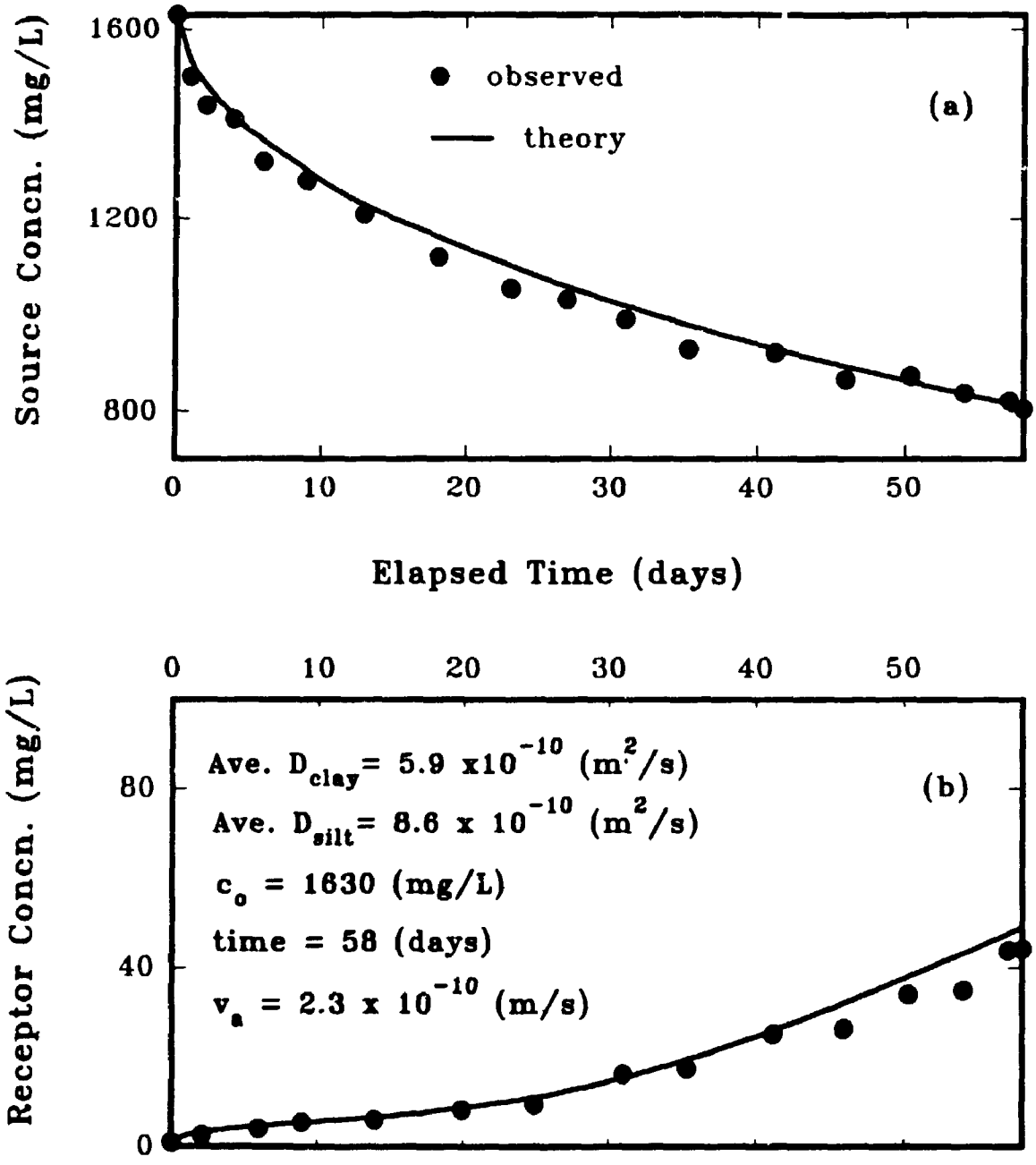

FIG. 6.5 OBSERVED AND THEORETICAL [Cl^-] CONCENTRATIONS VS ELAPSED TIME IN : (a) SOURCE RESERVOIR, AND (b) RECEPTOR RESERVOIR, DURING ADVECTION-DIFFUSION TEST #AD4 (CLAYEY SILT-SATURATED, DRYING SILT)

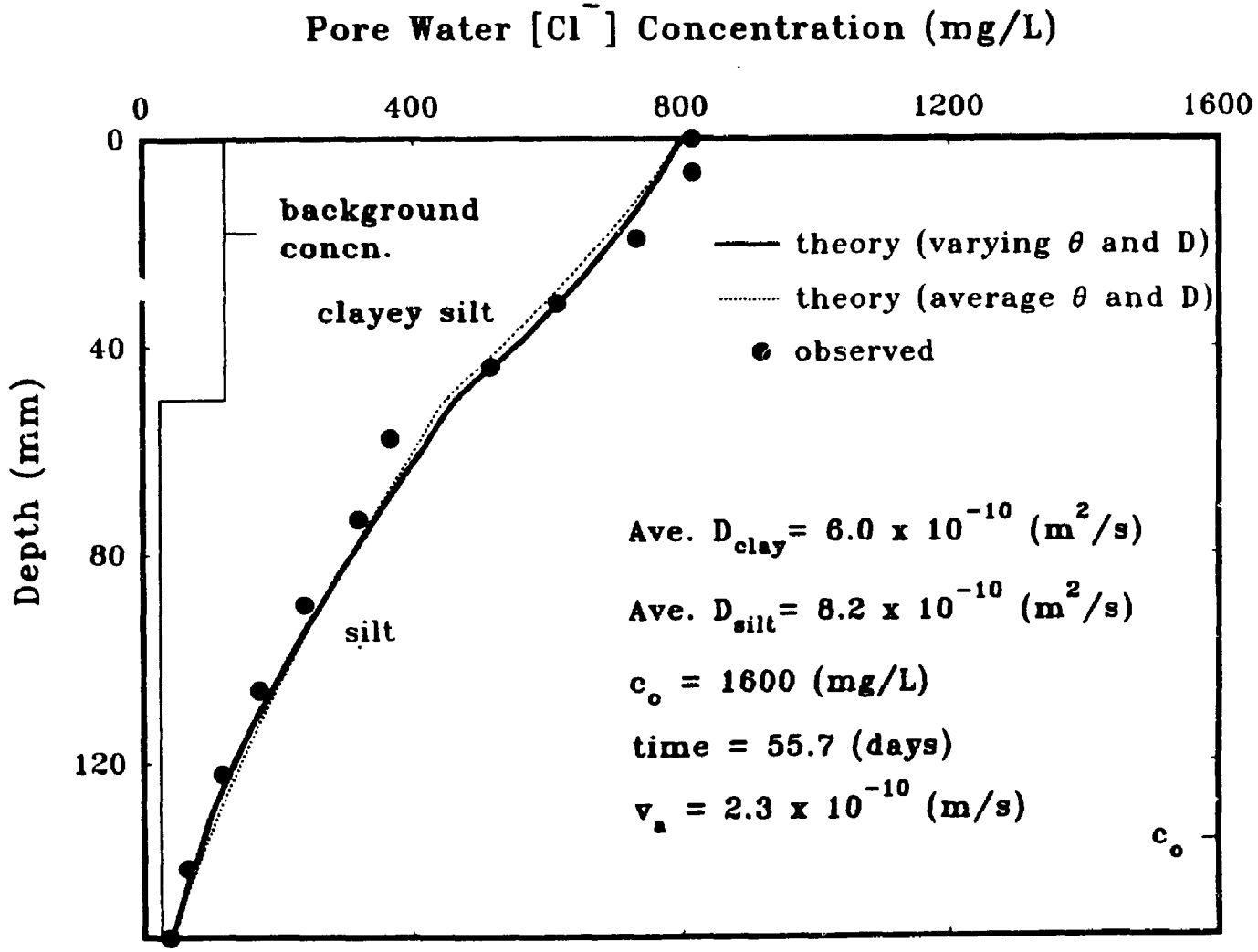

FIG. 6.6 OBSERVED AND THEORETICAL "BEST FIT" [Cl⁻] CONCENTRATION PROFILES IN ADVECTION-DIFFUSION TEST # AD5 (CLAYEY SILT-WETTING SILT)

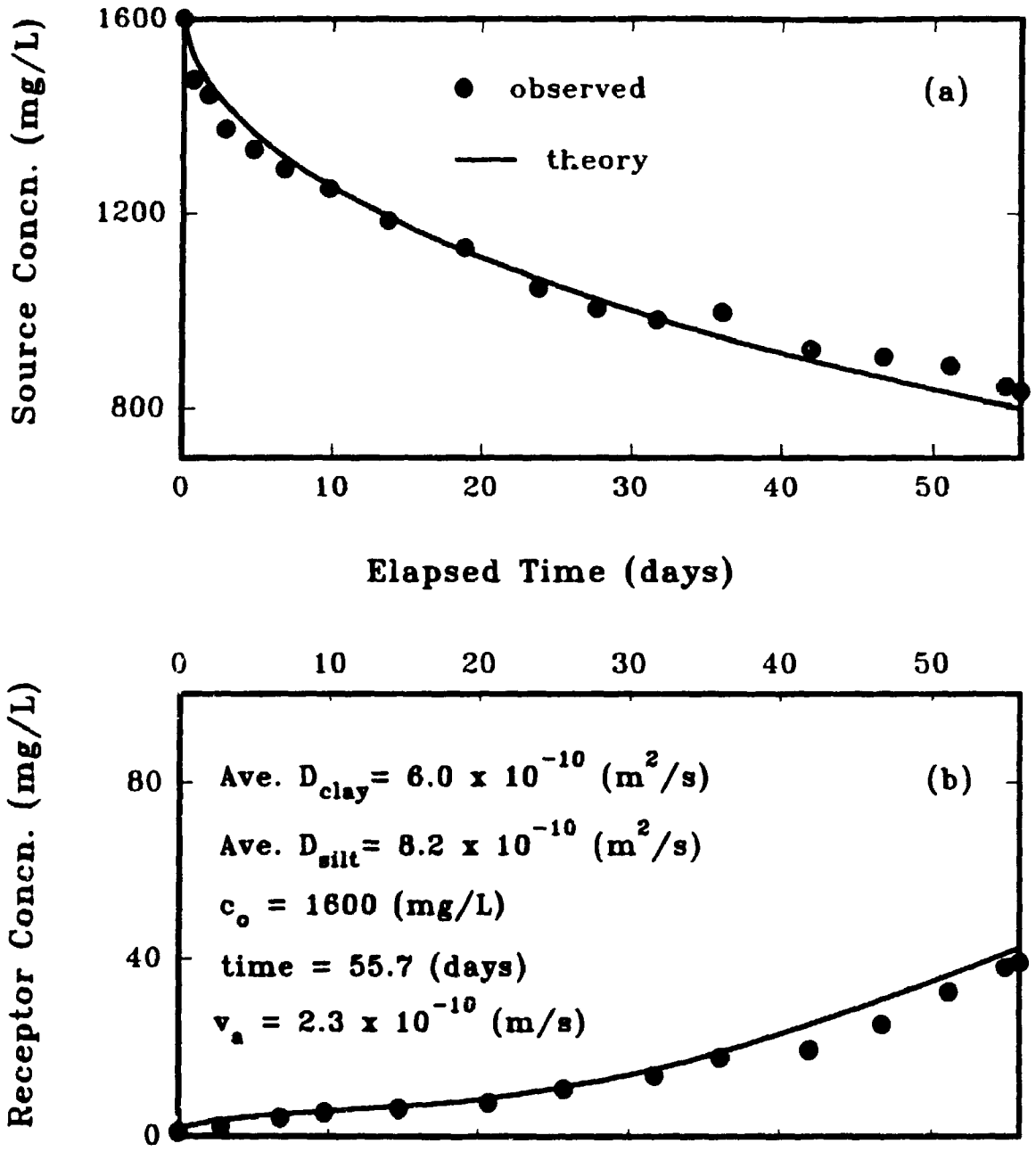

FIG. 6.7 OBSERVED AND THEORETICAL [Cl^-] CONCENTRATIONS VS ELAPSED TIME IN : (a) SOURCE RESERVOIR, AND (b) RECEPTOR RESERVOIR, DURING ADVECTION-DIFFUSION TEST #AD5 (CLAYEY SILT-WETTING SILT)

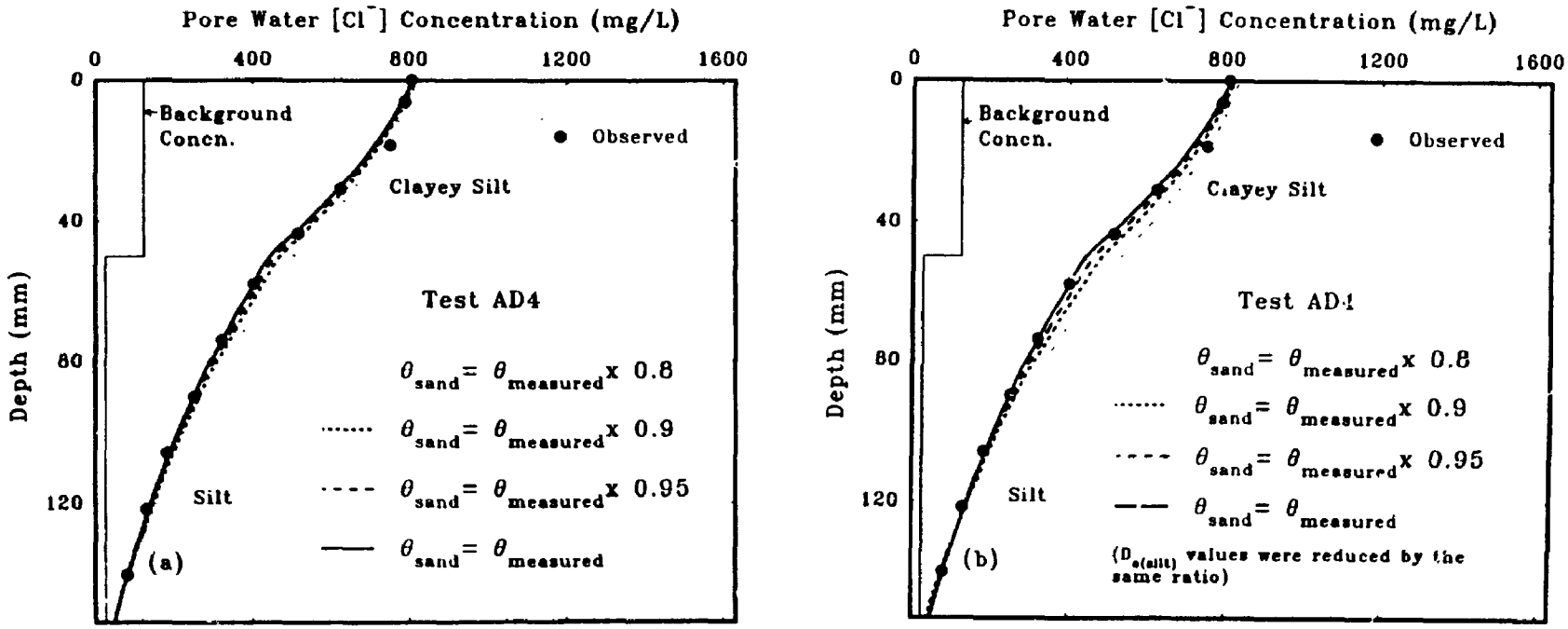

Fig. 6.8 EFFECT OF REDUCED VOLUMETRIC MOISTURE CONTENT (a), AND VOLUMETRIC MOISTURE CONTENT AND EFFECTIVE DIFFUSION COEFFICIENT (b) OF THE UNDERLYING SILT ON CALCULATED CONCENTRATION PROFILES (TEST AD4)

CHAPTER 7

DIFFUSION THROUGH SATURATED AND UNSATURATED COARSE SAND AND FINE GRAVEL

7.1 INTRODUCTION

In previous chapters the diffusive transport of chloride in fine sand and the advective-diffusive transport of chloride in clayey silt-fine sand and clayey silt-silt systems was studied. These tests were conducted under the condition of gravity drainage by maintaining the drainage level (i.e. atmospheric pressure level) at the bottom of the soil. These tests simulated the hydrogeological condition of a liner constructed over a layer of a fine granular material (i.e. fine sand or silt) having the drainage level at the bottom of the system. In these tests, the capillary tensions were such that samples did not drain and the degree of saturation was greater than 90 % in all cases. In these cases, the height of the capillary rise was greater than the height of the samples tested (see Table 7.6). Thus these samples were almost saturated although due to the hysteresis effect, the degree of saturation in drying tests (saturated, gravity drained) was greater than in the wetting tests (capillary saturated).

In Chapter 2, the mechanisms of gravity drainage and contaminant transport in unsaturated porous media was reviewed. The effect of unsaturated porous media on solute transport was described and it was indicated that the natural deposits in the vadose zone or artificially created unsaturated layer or layers of soil attenuate the transport of solute and provide a form of barrier to diffusion. As indicated, there is evidence to

suggest a close relationship between the moisture content (or volumetric moisture content) and the diffusion coefficient or tortuosity of the soil. The lower the moisture content, the lower the tortuosity and hence, the slower migration of solute by diffusion for dissolved contaminants. In the absence of seepage flow, diffusion is the only mechanism of solute transport. The diffusion coefficient will vary both temporally and spatially in a hydrodynamically active region (e.g., Rowe, 1987).

Under low applied values of suction, gravity could not drain the fine granular material such as fine sand or silt; however drainage can be achieved by using coarser granular material such as coarse sand, gravel or stone. These materials will become unsaturated and will have a low water content after drainage. In most of these material, the retained water in the upper parts of the sample is expected to be very close to their residual moisture content.

In this chapter, results of the eight diffusion tests on two types of granular material are presented. The first two tests (# D5a and D5b) were conducted on fine gravel and coarse sand under saturated conditions. Tests # D6, D7, and D8 were conducted using fine gravel but under gravity drainage (unsaturated). Tests # D9, D10, and D11 were conducted using coarse sand, also with gravity drainage (unsaturated).

7.2 TESTED MATERIAL, DESCRIPTION AND PREPARATION

Coarse sand and fine gravel were obtained from the Morie Company Inc. in Hamilton Ontario. These materials were tested for their physical, chemical and mineralogical characteristics and the results are summarized in Tables 7.1 and 7.2. The

grain size distribution of the coarse sand and fine gravel are shown in Fig. 7.1.

Before use, the material was washed with distilled water over a sieve to remove any background concentration and some washed samples were tested for any remaining background concentration.

7.3 DIFFUSION TESTING ON SATURATED FINE GRAVEL AND COARSE SAND

7.3.1 TEST SET UP, MONITORING AND TERMINATION

Two tests, were conducted on fine gravel and coarse sand under saturated conditions, for determination of the chloride and sodium diffusion coefficients using NaCl solution as a tracer. These tests will be referred to as Tests # D5a and D5b. Figs. 7.2 and 7.3 show a schematic and photographic view of the tests set up. Washed, dry material was packed in diffusion cell to a height of 16.3 cm. The packing method consisted of successive placing about 2 cm thick sand/gravel layers, tamping the surface of the sample, and vibrating the circumference of the cell using a plastic septa until no change in volume occurred. This procedure was repeated for all sub-layers until the height of the sample was 16.3 cm. The surface of the sample was then levelled. An extra plexiglass ring on top of the cylinder was kept empty to have a free space for installation of the evaporation dishes. Knowing the height and cross section, the volume of the sample was calculated. The wire mesh, perforated plate, evaporation dish, and spring were placed on top of the sample (Figs. 3.3 and 3.4) and stainless steel plate placed and fixed into the stainless steel ring. A water tank containing distilled de-aired

water was connected to the cell inlet valve in the source reservoir chamber and both tank valve and cell inlet valve were opened and the sample was saturated by flowing water upwards from the reservoir chamber into the sample and out from the air inlet. Any air bubbles entrapped in the source reservoir were removed by slightly tilting the cell and opening the outlet valve and flushing the bubbles through the valve. The saturating time was about 43 hours. The saturated moisture content of the tested material was calculated by measuring the dry weight and saturated weight of the sample in the cell. The dry density of the material was calculated knowing the dry weight of soil in the cell and volume of the material. Knowing the specific gravity, the moisture content, and dry density of the material, the porosity was calculated.

The diffusion cell was placed on top of the magnetic stirrer and the pipette was attached to the outlet valve through the flexible plastic tubing and adjusted to be level with top surface of the sample (Fig. 7.2). In order to flush the reservoir with the source solution, the top air inlet was closed to create suction inside the cell and to maintain the water level at the top of the sample. The flexible tubing was detached from the cell outlet valve and a tank containing the source solution was connected to the inlet valve. Both the inlet and outlet valves were opened and the reservoir water was flushed with the source solution. During flushing, the solution level in the tank was maintained at the bottom surface of the porous disk. The magnetic bar inside the reservoir chamber was functioning during flushing to mix the replaced solution (see Fig. 3.5). Once flushing was terminated, the inlet and outlet valves were closed simultaneously and the solution tank was detached from the cell. The pipette was then reconnected to the outlet valve. The air inlet and outlet valves were opened. Two samples from the source reservoir

were taken through the septum port by opening the outlet valve and replacing the extracted solution by the distilled water inside the pipette. The starting time of the test was recorded.

Monitoring during the test consisted of periodically sampling the source solution from the reservoir and monitoring room temperature. The test durations were 18.9 days and 23 days for fine gravel and coarse sand, after which tests were terminated. In both tests an attempt was made to section the samples using the same procedure applied for previous tests, but because of the highly permeable nature of the samples, they drained some of their pore water during sliding the sectioning plates through the plexiglass rings interfaces. This difficulty was expected for this kind of testing; hence, prediction of the diffusion coefficient of the material was determined based on the source solution concentration versus elapsed time data.

7.3.2 EXPERIMENTAL AND THEORETICAL ANALYSIS

The source reservoir solution samples were analyzed for chloride concentration and the variation in concentrations with time were plotted and shown in Figs. 7.4a (Test #D5a) and 7.5a (Test #D5b) for Cl^- and in Fig. 7.6a for Na^+ (Test #D5a). The theoretical analysis was performed using program POLLUTE and soil physical and geometrical parameters. The best fit "by eye" to the experimental data was obtained using the diffusion coefficient of 10.4×10^{-10} m^2/s for chloride (Figs. 7.4a and 7.5a) and 6.9×10^{-10} m^2/s for Na^+ (Fig. 7.6a, Test #D5a). Figs. 7.4b, 7.5b and 7.6b show the theoretical profiles of the concentration versus soil depth. Table 7.3 summarizes the

results of these tests.

7.4 UNSATURATED DIFFUSION TESTING

Six diffusion tests were conducted on coarse sand and fine gravel; three tests were conducted using fine gravel and these will be referred to as Tests # D6, D7, and D8, and three tests were conducted using coarse sand and will be referred to as Tests # D9, D10, and D11. The grain size distribution and characteristics of the material are as previously discussed in section 7.2. The durations of the tests on fine gravel were 6.8, 10.25, and 30 days and the durations of the tests on coarse sand were 15, 29, and 50 days respectively.

Procedure for installation, saturation and de-saturation (gravity drainage) of the material in all tests were similar and is explained in the following section. Monitoring and termination for the tests was also similar and is explained in another section.

7.4.1 INSTALLATION OF THE MATERIAL, SATURATION AND DE-SATURATION (GRAVITY DRAINAGE)

Washed, dry material was packed in the diffusion cell to the height of 16.3 cm (except Test #D6 with the height of 13.1 cm). The packing and saturation procedure were the same as described in section 7.3.1. The saturation time was about 24 hours for all tests. Due to the highly permeable nature of the material, this period of time is expected to be long enough so that the samples become fully saturated. The diffusion cell was placed on top of the magnetic stirrer and levelled. The pipette was attached to

the outlet valve through the flexible plastic tubing and adjusted to be level with the bottom surface of the material. The outlet valve was opened and sample drained by gravity. The sample was left to drain for at least 24 hours to ensure complete drainage. Observations showed that both granular materials yielded a considerable amount of water at the early stage of the drainage process. After completion of the drainage, the outlet valve was closed and the pipette was detached from the cell. A tank containing NaCl solution was attached to the cell through the inlet valve. Using spacers the level of solution in the tank was adjusted to be level with the porous disk. The air inlet valve was closed and both the outlet and inlet valves were opened simultaneously and the reservoir was flushed with NaCl solution. After completion of the flushing process, both valves were closed, the air inlet was opened and starting time of the test was recorded. The pipette was attached to the cell and two samples were taken from the source reservoir. Fig. 7.7 shows the schematic of the assembled diffusion cell.

7.4.2 MONITORING AND TERMINATION OF THE TESTS

In the tests with fine gravel, it was observed that about 2 cm from the lower part of the sample was completely saturated. This level is considered as the approximate level of the capillary fringe in the sample. The level of saturation decreases significantly as one moves a few millimeters above the saturation level and the remaining portions of the sample had a low moisture content. On the inner surface of the cell in contact with the material grains, many isolated water pockets were observed throughout the test. In the coarse sand tests the capillary fringe was about 5.2 cm above the base of the sample

and the remaining portions of the sample had very low moisture content. No significant change in the capillary fringe level was observed during the tests. The outlet valve was open during the tests to maintain atmospheric pressure at the base of the sample. The source reservoir was sampled periodically during the tests and temperature was recorded.

Prior to the termination of each test, final samples were taken from the source reservoir. The sample was sectioned from top to bottom using sectioning plates, weighed, and then dried in the oven. The sectioning process was performed as quickly as possible to avoid drying of the samples due to evaporation.

7.4.3 MOISTURE CONTENT PROFILES IN THE TESTED MATERIAL

The moisture content of each gravel sub-layer was determined after oven drying the samples at the end of the tests. The results are plotted versus soil depths and shown in Figs 7.8 and 7.9a, for fine gravel and coarse sand tests respectively. As it is shown in these figures, the resulting profiles are non-uniform with depth and are quite different from those described in Chapters 4, 5 and 6 where moisture content profiles observed in fine sand and silt were almost uniform with depth. The observed capillary saturation levels in both material are consistent with the measured saturation levels shown in these figures. Above the capillary fringe, the moisture content drops rapidly to a low moisture content and then decreases gradually towards the top of the sample. Tables 7.4 and 7.5 summarize the observed and calculated values of the moisture content, the degree of saturation and the volumetric moisture content of the fine gravel and coarse sand sub-layers for the six diffusion tests.

The soil moisture characteristic curves for the coarse sand and fine gravel were obtained by plotting the volumetric moisture content values versus pressure head taken to be numerically equal to the height of the sample above the atmospheric pressure level at equilibrium (i.e., drainage level at the bottom of the sample as proposed by Day and Luthin, 1956). These curves are shown in Fig. 7.9b.

As previously noted, observations showed that the height of the maximum capillary rise in both material was less than the height of the samples; hence, both samples drained to the level of capillary fringe, leaving the upper parts unsaturated. For the purpose of the comparison of the observed maximum capillary rise with the theoretical values cited in the literature, an attempt was made to calculate the height of the capillary rise for coarse sand and fine gravel samples tested in this part of the experiments and also fine sand and silt samples tested previously, using Equations 2.47 (Smith et al., 1931) and 2.48 (Zunker, 1930). Results are shown in Table 7.6 along with the observed values. As it is seen, calculated values for coarse sand and fine gravel are very close to the observed values of 2.0 cm and 5.2 cm respectively.

7.4.4 EXPERIMENTAL AND THEORETICAL ANALYSIS

Source reservoir samples were analyzed for Cl^- and Na^+ concentrations and results are plotted versus elapsed time in Figs 7.10-7.17 (Figs 7.13 and 7.16 represent the results for Na^+ in Tests # D8 and D10). 80 g ovendried samples were washed with 50 mL de-ionized distilled water and concentration of wash water was measured, from which concentration in pore water was calculated and results are plotted against soil

depth in Figs 7.10-7.17.

Because of the non-uniform volumetric moisture content of the material sub-layers, they are each treated as independent layers in the theoretical analysis. The effective diffusion coefficient for each layer (D_e) was estimated by linear interpolation using volumetric moisture content of each soil sub-layer (θ), porosity ($n=\theta_{sat.}=0.381$), and saturated diffusion coefficient of fine gravel ($D_{e(sat.)}=10.4\times10^{-10}$ m^2/s for Cl^- and 6.9×10^{-10} m^2/s for Na^+) obtained in section 7.3. The relationship between these parameters was shown in Eq. 5.1 and had the form : $D_e = D_{e(sat.)}(\theta/\theta_{sat.})$. Based on the results of the saturated fine gravel and coarse sand diffusion tests (#D5a and D5b), the saturated diffusion coefficient ($D_{e(sat.)}$) of 10.4×10^{-10} m^2/s was used in the analysis for both materials. The resulting theoretical profiles fit the observed data very well as shown in Figs 7.10-7.17, indicating that this is a reasonable method for dealing with diffusion in unsaturated soils having a non-uniform moisture content. All relevant figures for chloride in fine gravel tests (# D6, D7 and D8) and in coarse sand tests (# D9, D10 and D11) were plotted in a normalized form and shown in Figs. 7.18 (fine gravel tests) and 7.19 (coarse sand tests). In these figures the concentration values were normalized by dividing by the initial source concentrations in each test. A review of the literature on the dependence of the ionic diffusion on the moisture content of the porous medium, was presented in Chapter 2.

From the concentration versus depth profiles given in Figs 7.10 to 7.17 it can be seen that the tracer has diffused quickly in capillary saturated zone and very slowly in the upper unsaturated zone where the moisture content and concentration is very low. This behaviour is manifested by a sharp decrease in the slope of the concentration profile

near the capillary fringe.

Tables 7.7a and 7.7b summarize the values of thickness (H), volumetric moisture content (θ), effective diffusion coefficient of Cl^- (D_e), and normalized diffusion coefficient or tortuosity of Cl^- (D_e/D_o *or* τ), in fine gravel and coarse sand sub-layers respectively. Table 7.7c shows the remaining input data used in theoretical analysis. The corresponding values for Na^+ ion in Tests # D8 and D10 are shown in Table 7.8.

7.4.4.1 SENSITIVITY ANALYSIS FOR TWO SELECTED TESTS (# D8 AND D10)

Theoretical analyses were performed for two selected tests (# D8 and D10) to study the effect of different key parameters such as the level of saturation of the material, diffusion coefficient, etc., on the theoretical diffusion profiles. Two tests were selected because they were both run for essentially the same period of time (29-30 days) and a comparison of the results show the effect of the grain size of the two materials.

Effect of the level of saturation

In order to compare the effect of saturation, a theoretical analysis was performed on Tests # D8 and D10 assuming complete saturation of the soil profiles using the diffusion coefficient of chloride in saturated fine gravel and coarse sand and their porosity. The results are plotted in Fig. 7.20 along with the observed and fitted theoretical profiles for these tests. It can be seen that the saturated diffusion profiles are completely different from those which fit the observed data. If the position of the contaminant front in the soil profile at the end of the test, is considered to be the point

of intersection of the concentration profiles with the soil background concentration profile, it can be seen that in case of Test #D8 (unsaturated fine gravel), this point is almost at the level of 100 mm from the bottom of the sample, and in case of Test #D10 (unsaturated coarse sand), it is at the level of 132 mm from the bottom of the sample, while theoretical profiles of saturated coarse sand and fine gravel show that the contaminant front will reach the top of the soil in even a shorter diffusion time.

This comparison clearly shows that, the diffusion rate of chloride ion in the unsaturated part of the soil profile has become much slower than when the soil is completely saturated.

Effect of the constant diffusion coefficient

In order to check the sensitivity of the analysis to the diffusion coefficient of the material sub-layers, another analysis was performed for Tests # D8 and D10 using the diffusion coefficient of saturated gravel (10.4×10^{-10} m^2/s) for all layers. The results are shown in Fig. 7.21 along with the observed data and fitted theoretical profiles using varying diffusion coefficients. As Fig. 7.21 shows, the profiles obtained by varying the volumetric moisture content but assuming a constant diffusion coefficient do not fit the observed data indicating that the diffusion coefficient of tracer should change with the volumetric moisture content of the medium.

Effect of the averaging volumetric moisture content and diffusion coefficient values in the entire soil profile

This analysis was performed to compare the best fit theoretical diffusion profiles for Tests # D8 and D10, with the theoretical diffusion profiles obtained using the

volumetric moisture contents and diffusion coefficients averaged for the entire soil profile. The results are shown in Fig. 7.22 and it can be seen that the resulting profiles do not fit the observed data, indicating that this method is not applicable in the soils having a highly non-uniform moisture content.

Effect of the averaging volumetric moisture content and diffusion coefficient values in 3 zones of: saturated, transition, and unsaturated, in the soil profile

This analysis was performed to compare the fitted theoretical diffusion profiles in Tests # D8 and D10, with the theoretical diffusion profiles obtained using average volumetric moisture contents and diffusion coefficients in 3 zones in the soil profile. These zones include (1) the saturated zone in which the moisture content is almost uniform, (2) the transition zone connecting the saturated zone to the unsaturated zone which has highly non-uniform moisture content (also unsaturated), and (3) the unsaturated zone which moisture content is almost uniform (see Figs. 7.8 and 7.9a). The resulting profiles are shown by dashed lines in Fig. 7.23. In Test # D10, the best fit profile was obtained using four sub-layers in the analysis in which the parameters averaged in saturated and unsaturated zones and two independent layers were used in transition zone which parameters were not averaged (see insert in Fig. 7.23a). In Test # D8, best fit profile was obtained by using three layers in which parameters were averaged in all three zones (see insert in Fig. 7.23b). As shown in Fig. 7.23, this method resulted in a good fit to the observed data indicating that this method can also be adopted for the soils having a highly non-uniform moisture content.

Effect of the replacement of the unsaturated coarse sand and fine gravel with a saturated-compacted clay

This analysis was performed to compare the fitted theoretical profiles in Tests # D8 and D10 with the theoretical diffusion profile in a clay layer having the same thickness. The typical values used for porosity of clay and diffusion coefficient of chloride to simulate the clay layer was 0.28 and 5.8×10^{-10} m^2/s, respectively. The results are shown in Fig. 7.24. The position of contaminant front which is considered to be the plane of intersection of the diffusion profile with the soil background concentration profile, was compared for clay and unsaturated gravel. As seen in Fig. 7.24, the contaminant front has reached the top of the clay (100% of the soil depth), while in coarse sand it is almost at the level of 135 mm (81% of the soil depth), and in fine gravel at the level of 103 mm (62% of the soil depth). Hence, it is concluded that the movement of chloride ion in the clay is faster than in the unsaturated gravel, and because of the higher level of saturation of the coarse sand compared to the fine gravel, the diffusion process in the coarse sand is faster compared to the fine gravel.

In support to these analysis, another analysis was performed on a 1-m thick clay layer of the same type and the time of migration was considered to be 1 year with the initial source concentration of 2000 mg/L. The results were compared with the results of the analysis on 1 m thick unsaturated coarse sand and also 1 m thick unsaturated fine gravel, using the observed data in Tests # D8 and D10. The results are shown in Fig. 7.25. In this figure, the contaminant front in the clay layer is at the level of 629 mm (63% of the soil depth), while in coarse sand, it is at the level of 318 mm (31.8% of the soil depth), and in fine gravel, at the level of 276 mm (27.6% of the soil depth). These results indicate that unsaturated coarse grained material such as coarse sand and fine

gravel, are capable of being as a good diffusion barrier relative to saturated-compacted clay.

Effect of the number of sub-sublayers in POLLUTE analysis

The effect of the number of sub-sublayers in POLLUTE analysis was examined using the data from Test #D10. The original analysis used 9 sublayers for coarse sand (see Table 7.8) which was equal to the number of slices obtained at the end of the test. In this analysis, 2 sub-sublayers was used for each slice (a total of 18 sub-sublayers). The resulting theoretical profile was shown as the solid line in Fig. 7.15. In order to examine the effect of the number of sub-sublayers in the calculations, the number of sub-sublayers in each sublayer was increased to 10 per slice (a total of 90 sub-sublayers). The resulting profile is shown as the short dashed line in Fig. 7.15. A comparison of these 2 profiles (solid line and short dashed line) show that for the range of the number of sub-sublayers examined, the results are not sensitive to the number of sub-sublayers.

7.5 NORMALIZED DIFFUSION COEFFICIENT (D_e/D_o)-VOLUMETRIC MOISTURE CONTENT (θ) RELATIONSHIP IN CONDUCTED DIFFUSION TESTS

As indicated in section 7.4.4, the diffusion coefficient of granular material sub-layers were estimated assuming a linear relationship between the unsaturated effective diffusion coefficient and the volumetric moisture content (Eq. 5.1). The saturated diffusion coefficient and porosity of the fine gravel and coarse sand which were determined in the saturated diffusion tests, were taken as the reference values for these

calculations. The resulting theoretical profiles provided a reasonable fit to the experimental data, indicating that this procedure may be adopted to estimate the unsaturated diffusion coefficient of chloride in granular material sub-layers. A brief review on previous work (Chapter 2) also supports the concept of linear proportionality between the tortuosity factor and volumetric moisture content of some soils.

The effective diffusion coefficients (D_e) calculated using this method were divided by the diffusion coefficient of chloride in free solution (D_o) at 23 °C (1.85×10^{-9} m^2/s) and the resulting normalized diffusion coefficient values (D_e/D_o, or tortuosity factors) were plotted against the volumetric moisture content values in each test as shown in Figs. 7.26 and 7.27 for coarse sand and fine gravel respectively. The straight line passing through the data points in Figs. 7.26 and 7.27 can be represented by the following equation:

$$D_e/D_o \approx 1.48\,\theta \qquad (7.1)$$

These plots also show that the tortuosity factor drops very fast in the region where volumetric moisture content of the medium drops from its higher value (saturated or near saturated) to very low values (unsaturated), after which there is very small change in the tortuosity factors. This behaviour is also shown in Figs 2.1 and 2.2 of Porter et al. (1960). The change in transmission factors (tortuosity factors or D_e/D_o values) at lower range of volumetric moisture content values, in all tested soils, is smaller than the range of the higher values of the volumetric moisture content.

The lines shown in Figs. 7.26 and 7.27 pass through the origin. This implies that even when the samples were at their residual moisture contents, the diffusion paths in the unsaturated portion of the coarse sand and fine gravel samples were still connected and Cl^- and Na^+ ions could diffuse through these narrow paths. It hypothesized that this is

because there was pore water at the contact points of the grains and also along the surface of the grains (as a thin film of water) such that the Cl^- and Na^+ ions with the hydrated ionic radiuses of 0.0007 μm and 0.001 μm could both diffuse through it (an approximate thickness of the water film along the surface of the unsaturated gravel reported by Conca and Wright (1990) was about 1-50 μm which is larger compared to the hydrated ionic radius of Cl^- and Na^+).

Considering the data presented for unsaturated coarse sand, in Figs. 7.9a and 7.9b show that coarse sand had reached its residual moisture content at about 90 mm depth from the bottom of the sample (i.e., water level). If the diffusion paths were discontinuous from this depth upward when the sample was at its residual moisture content, there would not be any observed Cl^- concentration in this part of the sample. But according to Fig. 7.17, Cl^- ion has been able to diffuse up a distance of about 130 mm from the bottom of the sample during 50 days of diffusion. This indicated that the diffusion paths were continuous in this part of the coarse sand sample. Because of the shorter period of testing (about 30 days) in fine gravel, it is difficult to verify this effect although the experimental data in Fig. 7.13 shows that the Cl^- has been able to diffuse to up a distance of about 70 mm above the zero pressure elevation even though the sample had reached its residual moisture content at about 50 mm above the zero pressure elevation (Fig. 7.8).

7.6 MASS BALANCE CALCULATIONS

Mass balance calculations were performed to determine the percent recovery of

chloride for each diffusion test. The results given in Table 7.9 show that recovery was 98 percent of their original mass or better, suggesting that there is no significant mass loss and almost all the chloride mass was recovered. A sample of calculation is given in Appendix D.

7.7 SUMMARY AND CONCLUSIONS

In this part of the experimental program, the diffusion characteristics of two different granular materials were examined under gravity drainage conditions. During the drainage process, samples yielded a great amount of water, leaving a significant portion of the soil profile unsaturated. The retained water included the capillary fringe water in the lower portion of the soil where the sample was saturated or nearly saturated, and water remaining above the capillary fringe in the form of isolated water pockets interconnected by a thin film of water around the grains, making the diffusion pathways very tortuous. The observed maximum capillary rise was different in the two soils due to the difference in the effective grain size of the material. The observed rise was consistent with the values calculated by two different theoretical methods suggested in the literature.

The observed concentration profiles in six diffusion tests showed that the tracer has diffused much slower in the unsaturated zone compared to the capillary saturated zone. This behaviour was manifested by a sharp decrease in the slope of the concentration profile just above the capillary fringe. The observed and theoretical soil concentration profiles for the two types of material were compared with the theoretical

concentration profiles of the same material assuming that the material is saturated. The resulting theoretical profiles were completely different from the profiles of unsaturated material, indicating the effect of saturation on diffusion transport.

Because of the non-uniformity in the volumetric moisture content of the coarse sand and fine gravel sub-layers, the theoretical analysis was conducted using a non-uniform diffusion coefficient for the material sub-layers. Estimation of these coefficients was based on the assumption of linear proportionality between the volumetric moisture content and the effective diffusion coefficient of each layer. The known saturated diffusion coefficient and porosity of the tested material were used as the basis of estimating the diffusion coefficient of other sub-layers using their volumetric moisture content values. A good fit to the experimental data was obtained using this method. The resulting diffusion coefficients were divided by the diffusion coefficient of chloride in free solution at 23 °C to obtain the normalized diffusion coefficient (D_e/D_o, or tortuosity) values. These values were then plotted against the corresponding volumetric moisture content values (θ). These plots also showed that significant reduction in D_e/D_o occurs when moisture content of the sample changes from saturation to very low values in the unsaturated zone, indicating that the diffusion paths have become significantly tortuous.

Mass balance calculations were performed for all tests and results showed that more than 98 percent of the chloride mass has been recovered at the end of the tests, indicating that there has been no significant mass loss from the test systems.

TABLE 7.1 SOME PHYSICAL, CHEMICAL AND MINERALOGICAL CHARACTERISTICS OF THE COARSE SAND

Physical characteristics

Specific gravity, G_s = 2.60

Hydraulic conductivity[1] = 0.7 cm/s

Porosity = 0.38

Dry density = 1.61

D_{60} = 1.6 mm

D_{10} = 0.91 mm

Chemical and mineralogical characteristics[2]

Cation exchange capacity[3] (C.E.C, meq/100 g soil) :

0.781 (KCl wash), 1.14 (AgTh wash)

[Cl^-] background concentration = 10.0 mg/L

Minerals present (%) :

SiO_2	TiO_2	Fe_2O_3	MgO	CaO	K_2O	Total
97.81	0.02	0.07	0.05	0.03	0.02	98.0

Undetected minerals: 2.0%

Carbonates :

Percent Dolomite = 0.2 (%)

Percent Calcite = 0.0 (%)

1 - Constant head hydraulic conductivity test

2 - See Appendix B for description of chemical tests

3 - CEC by combined KCl/Ag thiourea exchange method

TABLE 7.2 SOME PHYSICAL, CHEMICAL AND MINERALOGICAL CHARACTERISTICS OF FINE GRAVEL

Physical characteristics

Specific gravity, G_s = 2.60

Hydraulic conductivity[1] = 1.5 cm/s

Porosity = 0.38

Dry density = 1.62

D_{60} = 2.5 mm

D_{10} = 1.8 mm

Chemical and mineralogical characteristics[2]

Cation exchange capacity[3] (C.E.C, meq/100 g soil) :

0.61 (KCl wash), 1.13 (AgTh wash)

[Cl^-] background concentration = 10.5 mg/L

Minerals present (%) .

SiO_2	TiO_2	Fe_2O_3	MgO	P_2O_5	Total
98.16	0.02	0.03	0.06	0.01	98.28

Undetected minerals: 1.72%

Carbonates :

Percent Dolomite = 0.2 (%)

Percent Calcite = 0.0 (%)

1 - Constant head hydraulic conductivity test

2 - See Appendix B for description of chemical tests

3 - CEC by combined KCl/Ag thiourea exchange method

TABLE 7.3 SUMMARY OF THE RESULTS OF THE DIFFUSION TESTS CONDUCTED ON SATURATED FINE GRAVEL (#D5a) AND COARSE SAND (#D5b)

Test #	Time (days)	Sample Height (cm)	Porosity	Cl^- Initial Concn. (mg/L)	Na^+ Initial Concn. (mg/L)	Cl^- Diffusion Coefficient (m^2/s)	Na^+ Diffusion Coefficient (m^2/s)
D5a	18.9	16.3	0.381	1720	1100	10.4×10^{-10}	6.9×10^{-10}
D5b	23.0	16.3	0.380	1850	--	10.4×10^{-10}	--

TABLE 7.4 VALUES OF THE THICKNESS (H), MOISTURE CONTENT (W), DEGREE OF SATURATION (S), AND VOLUMETRIC MOISTURE CONTENT (θ) OF FINE GRAVEL SUB-LAYERS IN DIFFUSION TESTS # D6, D7, AND D8

Test # D6				Test # D7				Test # D8			
H[1] (cm)	W[2] (%)	S[3] (%)	θ[4]	H[1] (cm)	W[2] (%)	S[3] (%)	θ[4]	H[1] (cm)	W[2] (%)	S[3] (%)	θ[4]
1.48	1.53	6.45	0.025	1.48	1.45	6.10	0.023	1.50	1.51	6.40	0.025
1.58	1.59	6.70	0.026	1.59	1.61	6.80	0.026	1.60	1.56	6.59	0.026
1.63	1.81	7.70	0.029	1.60	1.71	7.22	0.028	1.60	1.65	6.99	0.027
1.58	2.09	8.80	0.034	1.59	1.82	7.69	0.029	1.60	2.10	8.88	0.035
1.63	2.69	11.4	0.043	1.60	1.91	8.08	0.031	1.60	2.05	8.67	0.034
1.62	3.60	15.2	0.058	1.60	2.07	8.74	0.033	1.60	2.08	8.80	0.034
1.58	11.76	49.7	0.189	1.60	2.54	10.76	0.041	1.65	2.30	9.73	0.038
2.00	23.67	100	0.381	1.60	3.32	14.05	0.054	1.65	2.86	12.1	0.047
				1.60	11.54	48.96	0.187	1.55	4.92	20.8	0.080
				1.95	23.67	100.0	0.381	1.95	23.67	100.0	0.381

1 Thickness of fine gravel sub-layers (cm)
2 Moisture content (%)
3 Degree of saturation (%)
4 Volumetric moisture content (cm^3/cm^3)

TABLE 7.5 VALUES OF THE THICKNESS (H), MOISTURE CONTENT (W), DEGREE OF SATURATION (S), AND VOLUMETRIC MOISTURE CONTENT (θ) OF COARSE SAND SUB-LAYERS IN DIFFUSION TESTS # D9, D10, AND D11

Test # D9				Test # D10				Test # D11			
H^1 (cm)	W^2 (%)	S^3 (%)	θ^4	H^1 (cm)	W^2 (%)	S^3 (%)	θ^4	H^1 (cm)	W^2 (%)	S^3 (%)	θ^4
1.50	1.71	7.20	0.028	1.50	1.96	8.30	0.032	1.50	2.13	8.99	0.034
1.60	1.79	7.58	0.029	1.60	1.89	8.00	0.030	1.60	1.85	7.83	0.030
1.60	2.03	8.58	0.033	1.60	1.98	8.40	0.032	1.60	2.02	8.53	0.033
1.60	2.50	10.6	0.040	1.60	2.37	9.90	0.038	1.60	2.44	10.3	0.039
1.65	3.52	14.9	0.057	1.65	2.83	12.0	0.046	1.60	3.11	13.2	0.050
1.50	5.57	23.5	0.089	1.65	4.50	19.0	0.072	1.60	4.89	20.6	0.079
1.65	15.8	66.8	0.254	1.60	13.7	58.0	0.221	1.60	13.9	58.6	0.223
1.65	23.4	98.8	0.377	1.60	23.3	98.3	0.375	1.65	23.4	99.0	0.377
15.5	23.7	100.0	0.381	15.5	23.7	100.0	0.381	1.60	23.7	100.0	0.381
1.95	23.7	100.0	0.381	1.95	23.7	100.0	0.381	1.95	23.7	100.0	0.381

1 Thickness of fine gravel sub-layers (cm)
2 Moisture content (%)
3 Degree of saturation (%)
4 Volumetric moisture content (cm^3/cm^3)

TABLE 7.6 OBSERVED AND CALCULATED MAXIMUM CAPILLARY RISE IN THE SILT, FINE SAND, COARSE SAND AND FINE GRAVEL

Material	Observed (cm)	Calculated (Smith et al., 1931) (cm)	Calculated (Zunker, 1930) (cm)
Silt (Upper Smallman)	NA	79.4	83.5
Fine sand (Wedron 710)	NA	61	63.9
Coarse sand (Morie Co. Inc.)	5.2	5.1	5.4
Fine gravel (Morie Co. Inc.)	2.0	2.6	2.7

TABLE 7.7a VALUES OF THE THICKNESS (H), VOLUMETRIC MOISTURE CONTENT (θ), [Cl^-] EFFECTIVE DIFFUSION COEFFICIENT (D_e), AND [Cl^-] NORMALIZED DIFFUSION COEFFICIENT (D_e/D_o), IN THE FINE GRAVEL SUB-LAYERS OF THE DIFFUSION TESTS # D6, D7, AND D8

Test # D6				Test # D7				Test # D8			
H[1]	θ[2]	D_e[3]	D_e/D_o[4]	H[1]	θ[2]	D_e[3]	D_e/D_o[4]	H[1]	θ[2]	D_e[3]	D_e/D_o[4]
1.48	0.025	6.7×10^{-11}	0.036	1.48	0.023	6.4×10^{-11}	0.034	1.50	0.025	7.0×10^{-11}	0.038
1.58	0.026	7.0×10^{-11}	0.038	1.59	0.026	7.1x10	0.038	1.60	0.026	7.1×10^{-11}	0.038
1.63	0.029	8.0×10^{-11}	0.043	1.59	0.028	7.5×10^{-11}	0.041	1.60	0.027	7.4×10^{-11}	0.040
1.58	0.032	9.3×10^{-11}	0.050	1.59	0.029	8.1×10^{-11}	0.044	1.60	0.035	9.4×10^{-11}	0.050
1.63	0.043	1.2×10^{-10}	0.064	1.59	0.031	8.5×10^{-11}	0.046	1.60	0.034	9.3×10^{-11}	0.051
1.62	0.058	1.6×10^{-10}	0.086	1.59	0.033	9.1×10^{-11}	0.049	1.60	0.034	9.3×10^{-11}	0.051
1.58	0.189	5.2×10^{-10}	0.280	1.59	0.041	1.1×10^{-10}	0.061	1.65	0.038	1.0×10^{-10}	0.056
2.00	0.381	10.4×10^{-10}	0.563	1.59	0.054	1.5×10^{-10}	0.079	1.65	0.047	1.3×10^{-10}	0.069
				1.60	0.187	5.1×10^{-10}	0.275	1.55	0.080	2.2×10^{-10}	0.118
				2.00	0.381	10.4×10^{-10}	0.563	1.95	0.381	10.4×10^{-10}	0.563

1 Thickness of the fine gravel sub-layer (cm)
2 Volumetric moisture content (cm^3/cm^3)
3 Effective diffusion coefficient (m^2/s), $D_e = D_{e(sat.)}(\theta/\theta_{sat.})$ where $D_{e(sat.)}$ and $\theta_{sat.}(=n)$ are the effective diffusion coefficient and volumetric moisture content of the saturated sample ($D_{e(sat.)} = 10.4\times10^{-10}$ m^2/s; $\theta_{sat.} = n = 0.381$)
4 Normalized diffusion coefficient or tortuosity $D_e/D_o = \tau = \tau_{sat.}(\theta/\theta_{sat.})$

TABLE 7.7b VALUES OF THE THICKNESS (H), VOLUMETRIC MOISTURE CONTENT (θ), [Cl^-] EFFECTIVE DIFFUSION COEFFICIENT (ω_e), AND [Cl^-] NORMALIZED DIFFUSION COEFFICIENT (D_e/D_o) OF THE COARSE SAND SUB-LAYERS IN THE DIFFUSION TESTS # D9, D10, AND D11

Test # D9				Test # D10				Test # D11			
H[1]	θ[2]	D_e[3]	D_e/D_o[4]	H[1]	θ[2]	D_e[3]	D_e/D_o[4]	H[1]	θ[2]	D_e[3]	D_e/D_o[4]
1.50	0.028	7.5×10^{-11}	0.041	1.50	0.032	8.7×10^{-11}	0.047	1.50	0.034	9.4×10^{-11}	0.051
1.50	0.029	7.8×10^{-11}	0.043	1.60	0.030	8.3×10^{-11}	0.045	1.60	0.030	8.1×10^{-11}	0.044
1.60	0.033	8.9×10^{-11}	0.048	1.60	0.032	8.7×10^{-11}	0.047	1.60	0.033	8.9×10^{-11}	0.048
1.60	0.040	1.1×10^{-10}	0.059	1.60	0.038	1.0×10^{-10}	0.056	1.60	0.039	9.3×10^{-11}	0.050
1.65	0.057	1.6×10^{-10}	0.084	1.65	0.046	1.3×10^{-10}	0.068	1.60	0.050	9.5×10^{-11}	0.051
1.55	0.090	2.4×10^{-10}	0.131	1.65	0.072	2.0×10^{-10}	0.106	1.60	0.079	1.4×10^{-10}	0.075
1.65	0.254	6.9×10^{-10}	0.375	1.60	0.221	6.0×10^{-10}	0.325	1.60	0.223	5.8×10^{-10}	0.313
1.65	0.377	10.3×10^{-10}	0.557	1.60	0.375	10.2×10^{-10}	0.554	1.65	0.377	9.8×10^{-10}	0.532
3.50	0.381	10.4×10^{-10}	0.563	3.50	0.381	10.4×10^{-10}	0.563	3.55	0.381	10.4×10^{-10}	0.563

1 Thickness of the coarse sand sub-layer (cm)
2 Volumetric moisture content (cm^3/cm^3)
3 Effective diffusion coefficient (m^2/s), $D_e = D_{e(sat.)}(\theta/\theta_{sat.})$ where $D_{e(sat.)}$ and $\theta_{sat.}(=n)$ are the effective diffusion coefficient and volumetric moisture content of the saturated sample ($D_{e(sat.)} = 10.4\times10^{-10}$ m^2/s; $\theta_{sat.} = n = 0.381$)
4 Normalized diffusion coefficient or tortuosity $D_e/D_o = \tau = \tau_{sat.}(\theta/\theta_{sat.})$

TABLE 7.7c OTHER INPUT DATA USED IN THEORETICAL ANALYSIS OF THE DIFFUSION TESTS # D6, D7, D8, D9, D10, AND D11

	Test # D6	Test # D7	Test # D8	Test # D9	Test # D10	Test # D11
Soil type	Fine gravel	Fine gravel	Fine gravel	Coarse sand	Coarse sand	Coarse sand
Soil thickness (cm)	13.0	16.3	16.3	16.3	16.3	16.3
Soil Cl^- backgr. concn. (mg/L)	10.5	10.5	10.5	10.0	10.0	10.0
Soil Na^+ backgr. concn. (mg/L)	-	-	6	-	6	-
Source Cl^- concn. (mg/L)	1330	1170	1040	950	950	840
Source Na^+ concn. (mg/L)	-	-	680	-	600	-
Base outflow velocity (v_b, cm/s)	1.2×10^{-6}	1.2×10^{-6}	5.5×10^{-7}	5.7×10^{-7}	5.1×10^{-7}	4.4×10^{-7}
Duration of the test (days)	6.79	10.25	29.95	15.07	29.0	49.98

TABLE 7.8 VALUES OF THE THICKNESS (H), VOLUMETRIC MOISTURE CONTENT (θ), EFFECTIVE DIFFUSION COEFFICIENT OF Na^+ (D_e), AND NORMALIZED DIFFUSION COEFFICIENT OF Na^+ (D_e/D_o), IN THE FINE GRAVEL AND COARSE SAND SUB-LAYERS OF THE DIFFUSION TESTS # D8 AND D10

Test # D8				Test # D10			
H^1	θ^1	D_e^3	D_e/D_o^4	H^1	θ^2	D_e^3	D_e/D_o^4
1.50	0.025	4.5×10^{-11}	0.036	1.50	0.032	3.7×10^{-11}	0.030
1.60	0.026	4.6×10^{-11}	0.037	1.60	0.030	5.4×10^{-11}	0.044
1.60	0.027	4.9×10^{-11}	0.040	1.60	0.032	5.7×10^{-11}	0.046
1.60	0.035	6.2×10^{-11}	0.050	1.60	0.038	6.9×10^{-11}	0.056
1.60	0.034	6.0×10^{-11}	0.048	1.65	0.046	8.2×10^{-11}	0.066
1.60	0.034	6.1×10^{-11}	0.049	1.65	0.072	1.3×10^{-10}	0.105
1.65	0.038	6.8×10^{-11}	0.055	1.60	0.221	3.9×10^{-10}	0.319
1.65	0.047	8.4×10^{-11}	0.068	1.60	0.375	6.7×10^{-10}	0.540
1.55	0.080	1.4×10^{-10}	0.116	3.50	0.381	6.9×10^{-10}	0.556
1.95	0.381	6.9×10^{-10}	0.556				

1 Thickness of the soil sub-layer (cm)
2 Volumetric moisture content (cm^3/cm^3)
3 Effective diffusion coefficient (m^2/s)
4 Normalized diffusion coefficient or tortuosity

TABLE 7.9 SUMMARY OF THE CHLORIDE MASS BALANCE CALCULATIONS IN COARSE SAND AND FINE GRAVEL DIFFUSION TESTS

Test #	Initial Mass (mg)			Final Mass (mg)				Percent Recovery (%)
	in source	in soil	total mass	in source	in soil	mass removed	total mass	
D6	7.55	0.017	7.57	5.87	1.20	0.558	7.63	100.8
D7	6.60	0.013	6.61	4.83	0.98	0.709	6.52	98.6
D8	5.85	0.013	5.86	4.21	0.73	0.898	5.84	99.6
D9	5.37	0.030	5.40	3.68	1.23	0.402	5.31	98.4
D10	5.38	0.027	5.41	3.21	1.41	0.682	5.30	98.1
D11	4.73	0.029	4.76	2.69	1.18	0.867	4.73	99.5

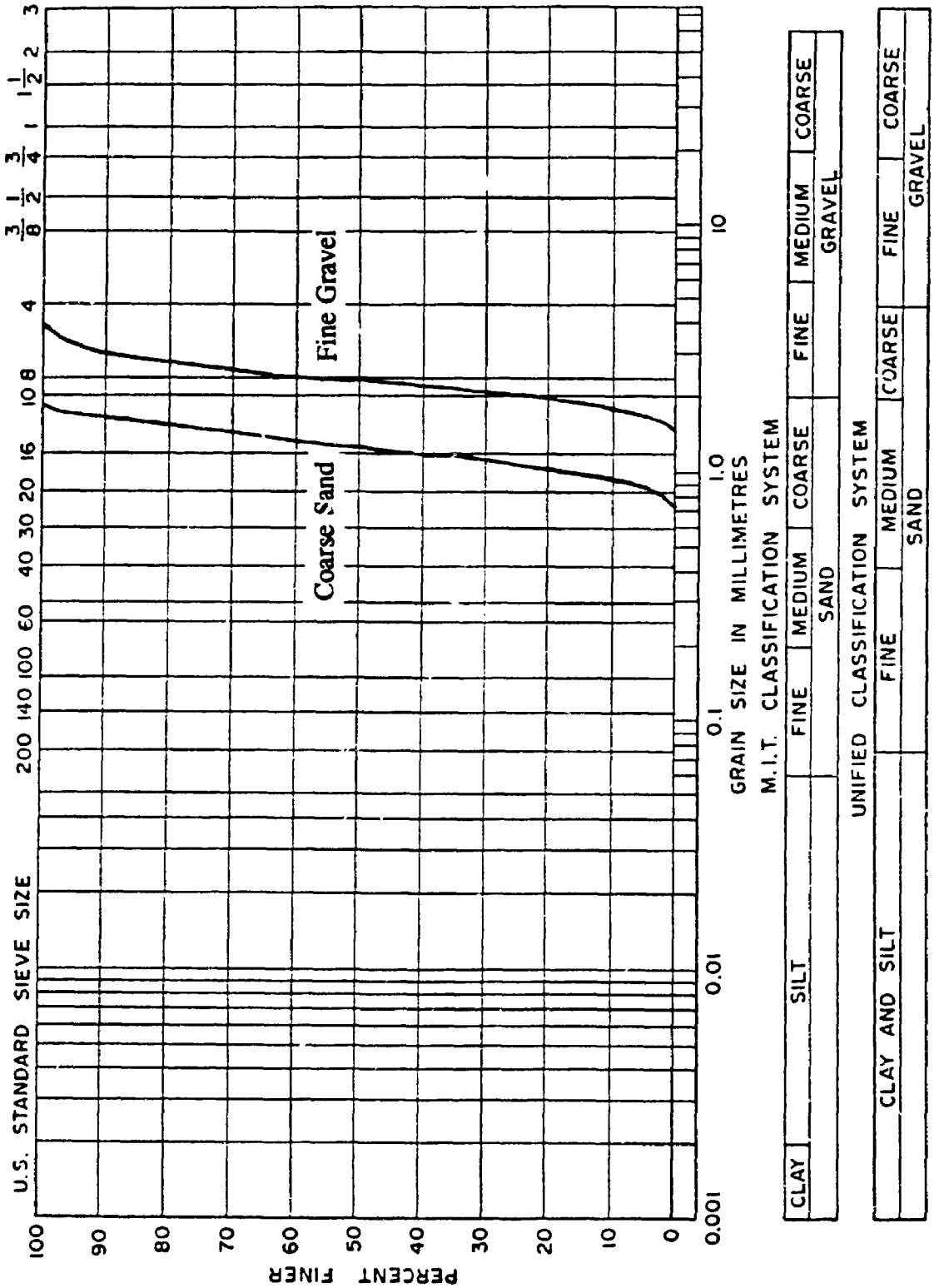

FIG. 7.1 GRAIN SIZE DISTRIBUTIONS OF THE COARSE SAND AND FINE GRAVEL

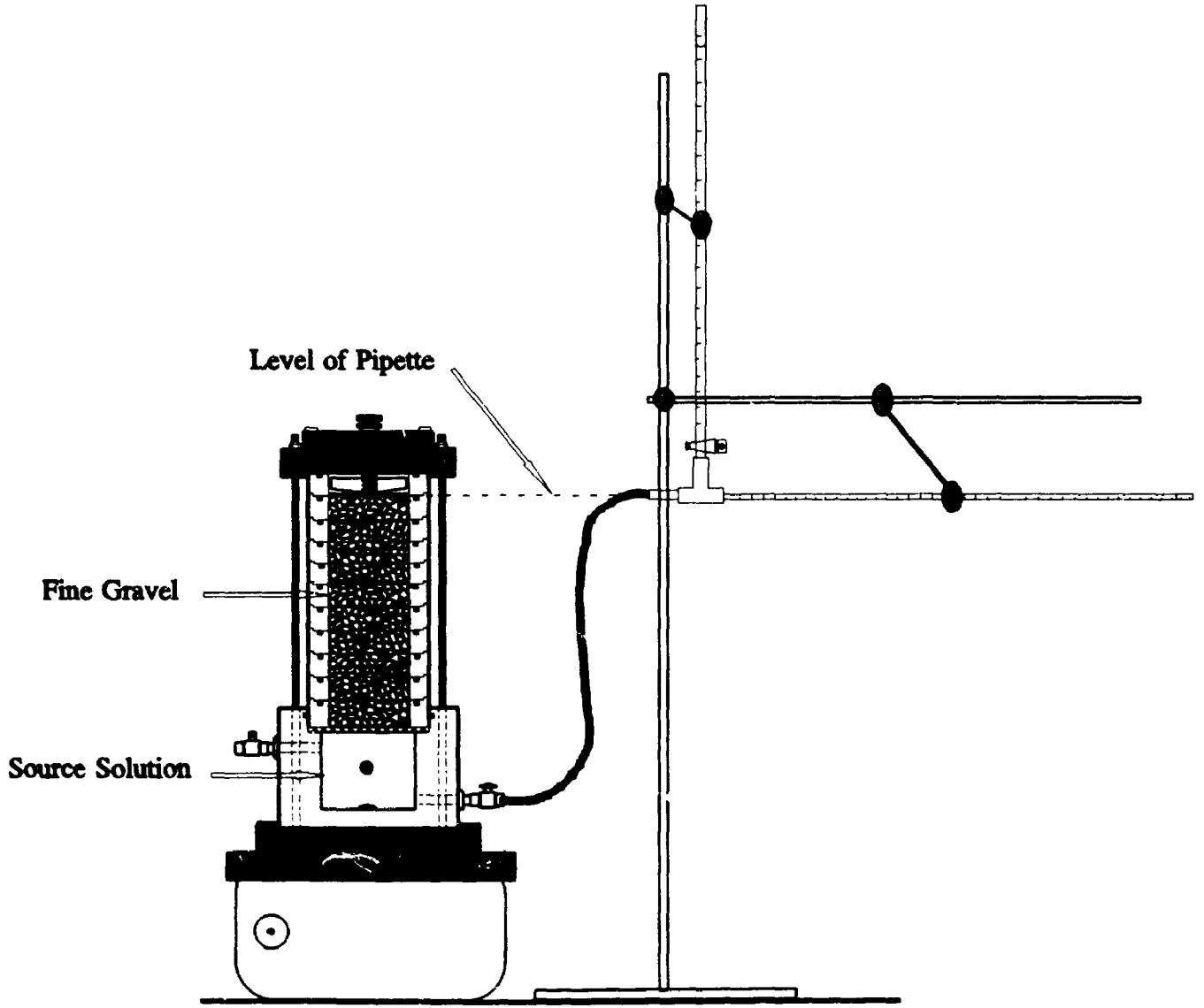

FIG. 7.2 SCHEMATIC OF THE SATURATED FINE GRAVEL AND COARSE SAND DIFFUSION TESTS

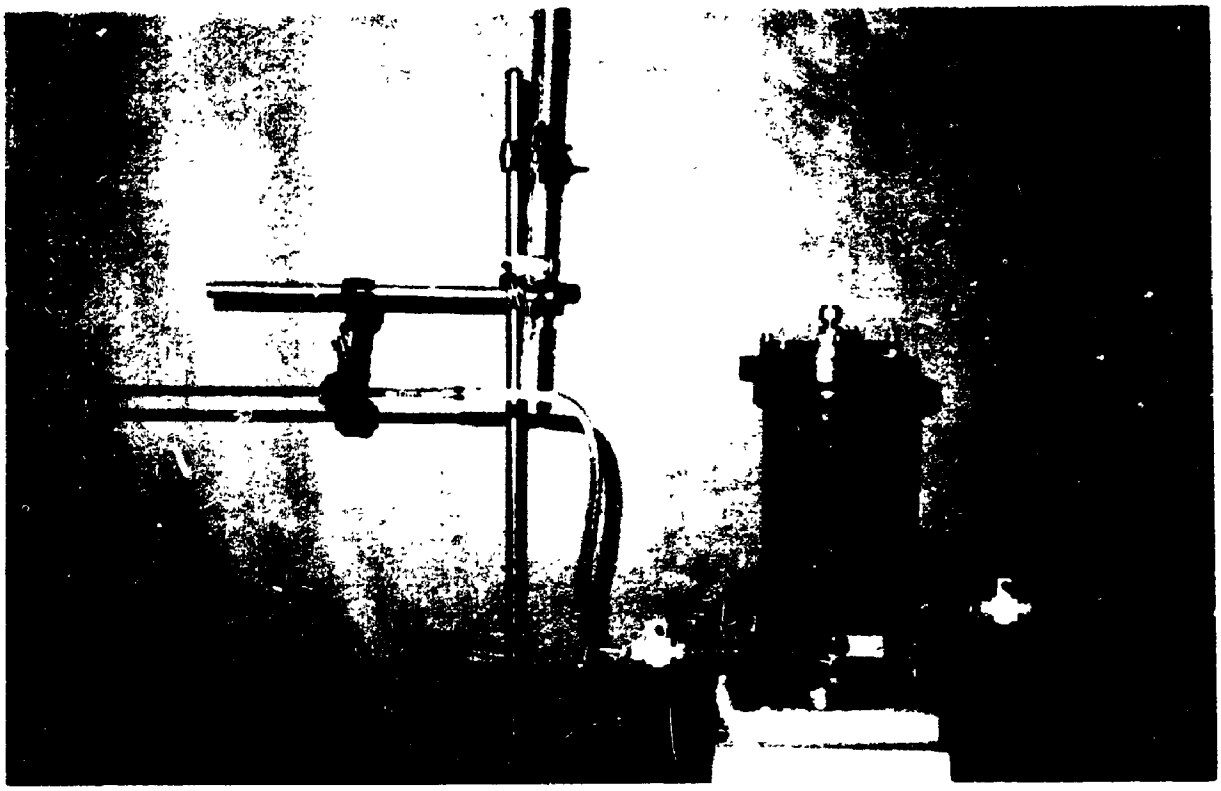

FIG. 7.3 VIEW OF THE DIFFUSION TESTING ON SATURATED FINE-GRAVEL/COARSE SAND

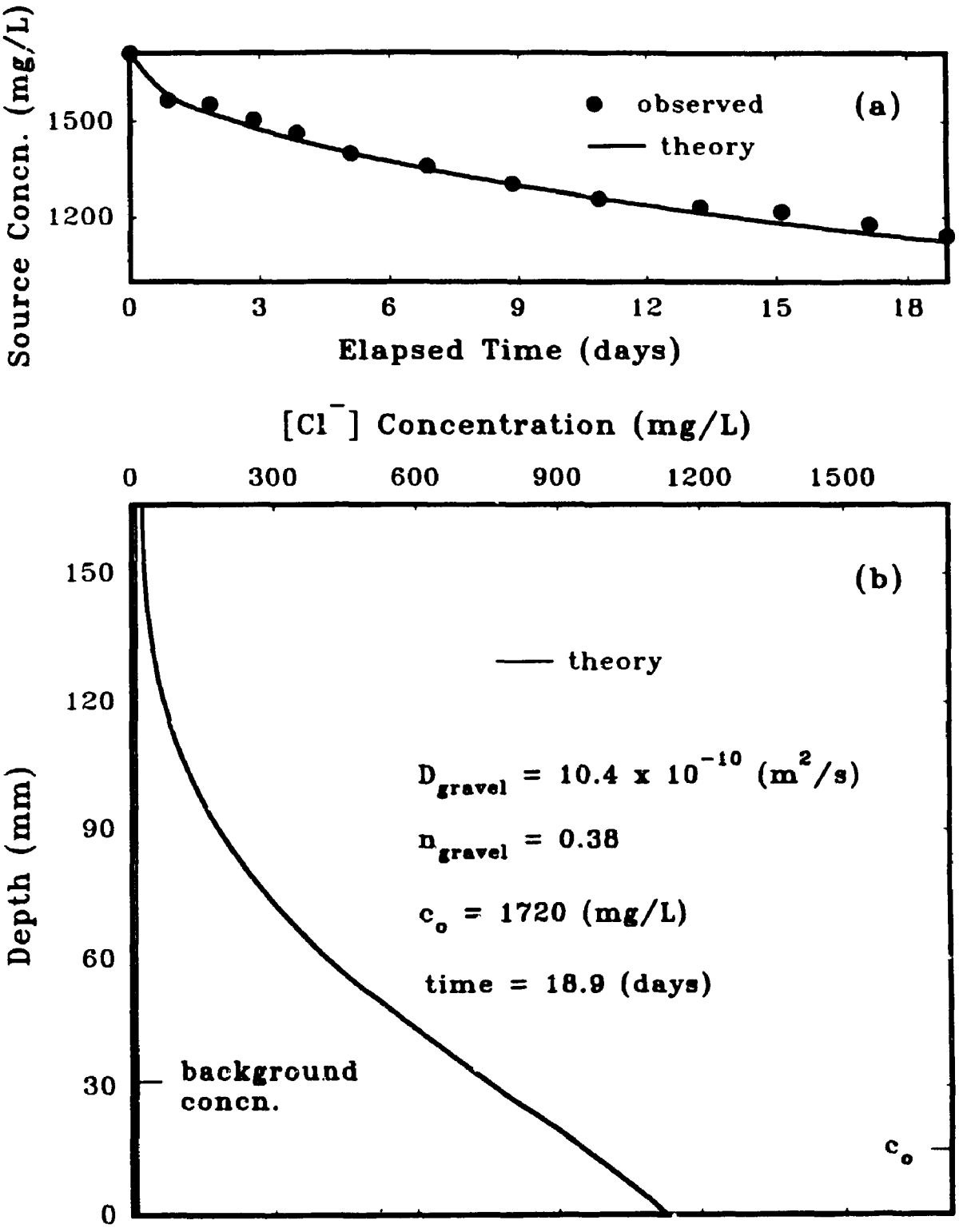

FIG. 7.4 OBSERVED AND THEORETICAL "BEST FIT" $[Cl^-]$ CONCENTRATION IN DIFFUSION TEST #D5a (SATURATED FINE GRAVEL), (a): SOURCE SOLUTION CONCENTRATION VS TIME, (b): PORE-WATER CONCENTRATION VS DEPTH (THEORETICAL)

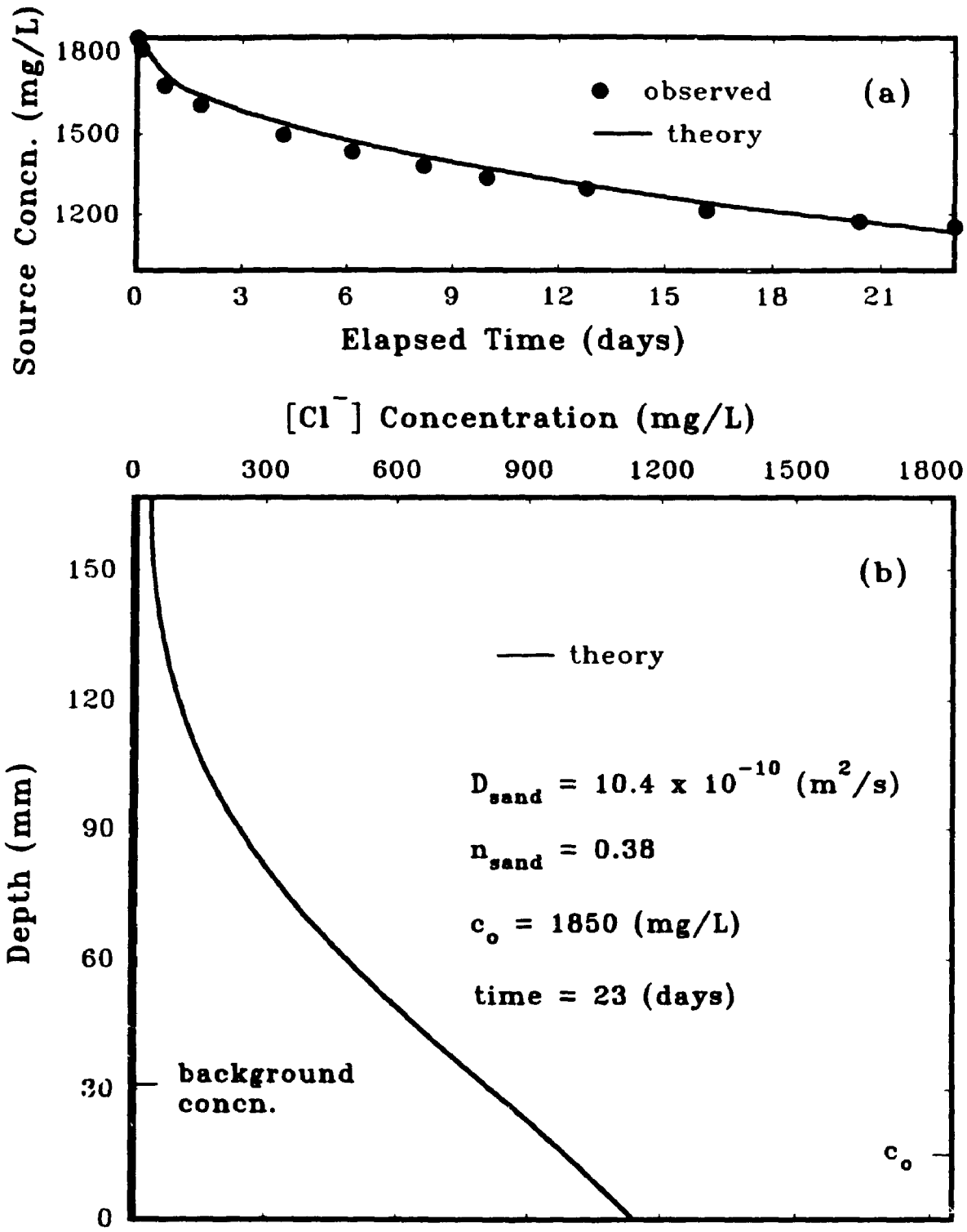

FIG. 7.5 OBSERVED AND THEORETICAL "BEST FIT" [Cl^-] CONCENTRATION IN DIFFUSION TEST #D5b (SATURATED COARSE SAND), (a): SOURCE SOLUTION CONCENTRATION VS TIME, (b): PORE-WATER CONCENTRATION VS DEPTH (THEORETICAL)

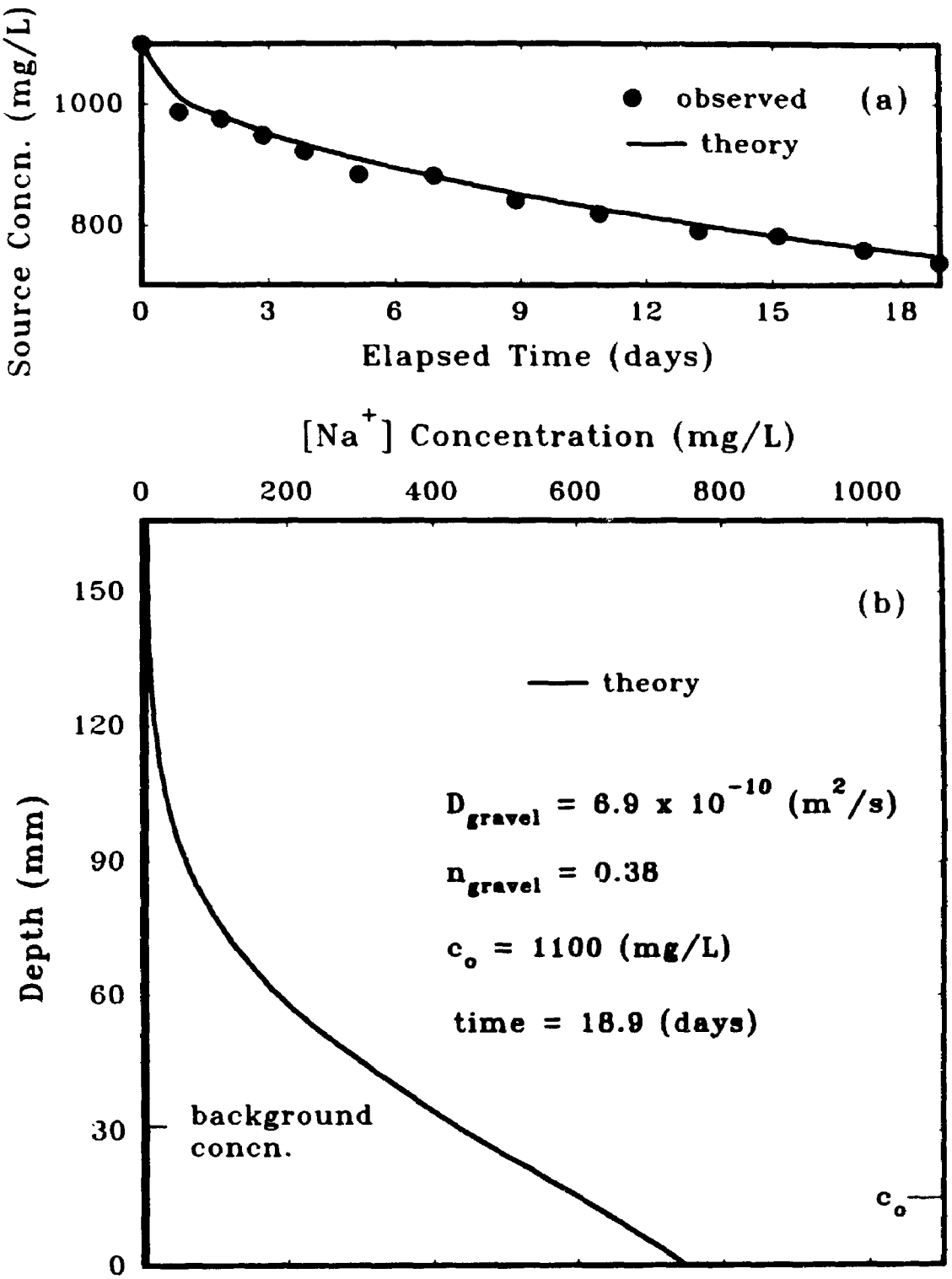

FIG. 7.6 OBSERVED AND THEORETICAL "BEST FIT" $[Na^+]$ CONCENTRATION IN DIFFUSION TEST #D5a (SATURATED FINE GRAVEL), (a): SOURCE SOLUTION CONCENTRATION VS TIME, (b): PORE-WATER CONCENTRATION VS DEPTH (THEORETICAL)

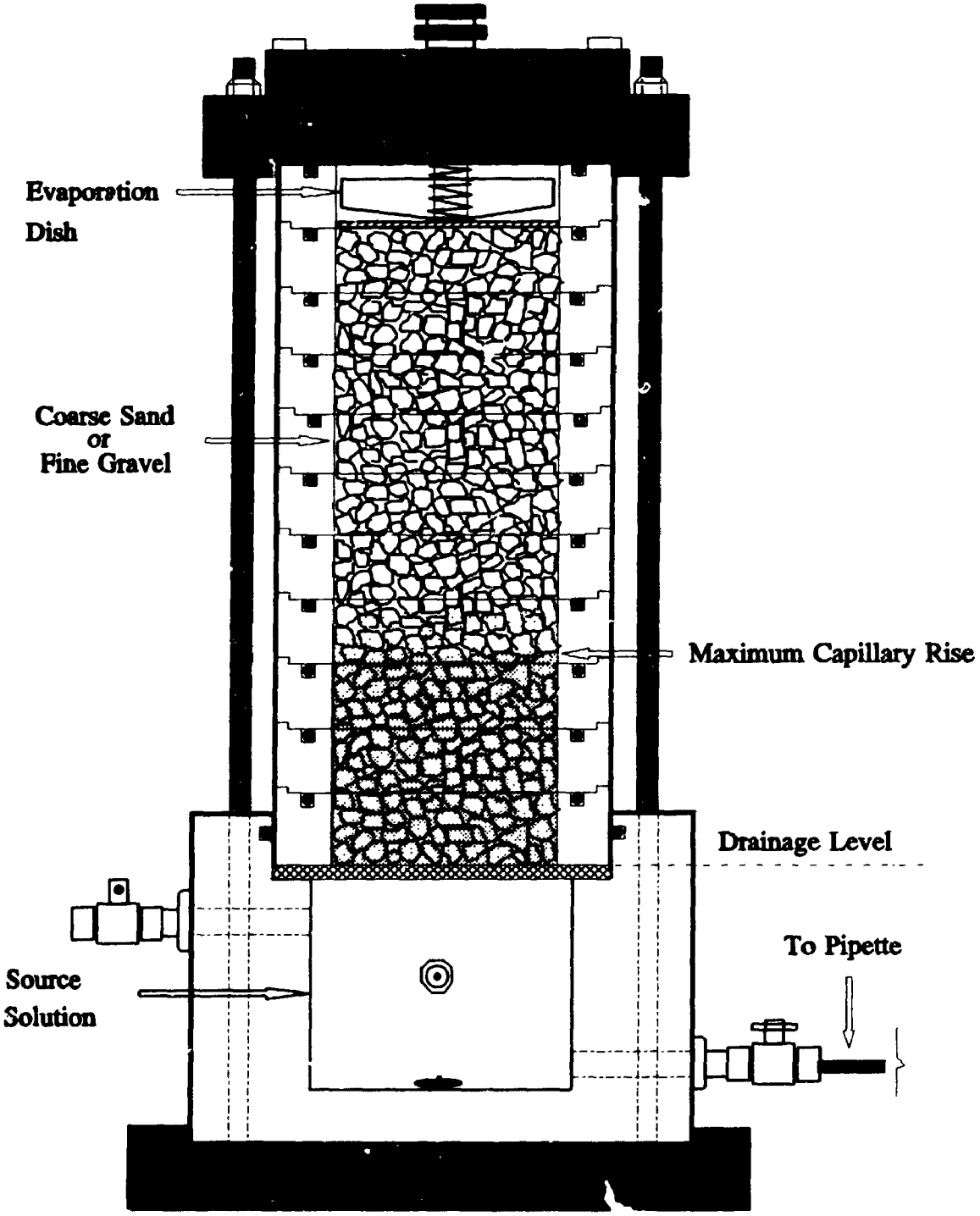

FIG. 7.7 SCHEMATIC OF THE UNSATURATED COARSE SAND AND FINE GRAVEL DIFFUSION TESTS SET UP

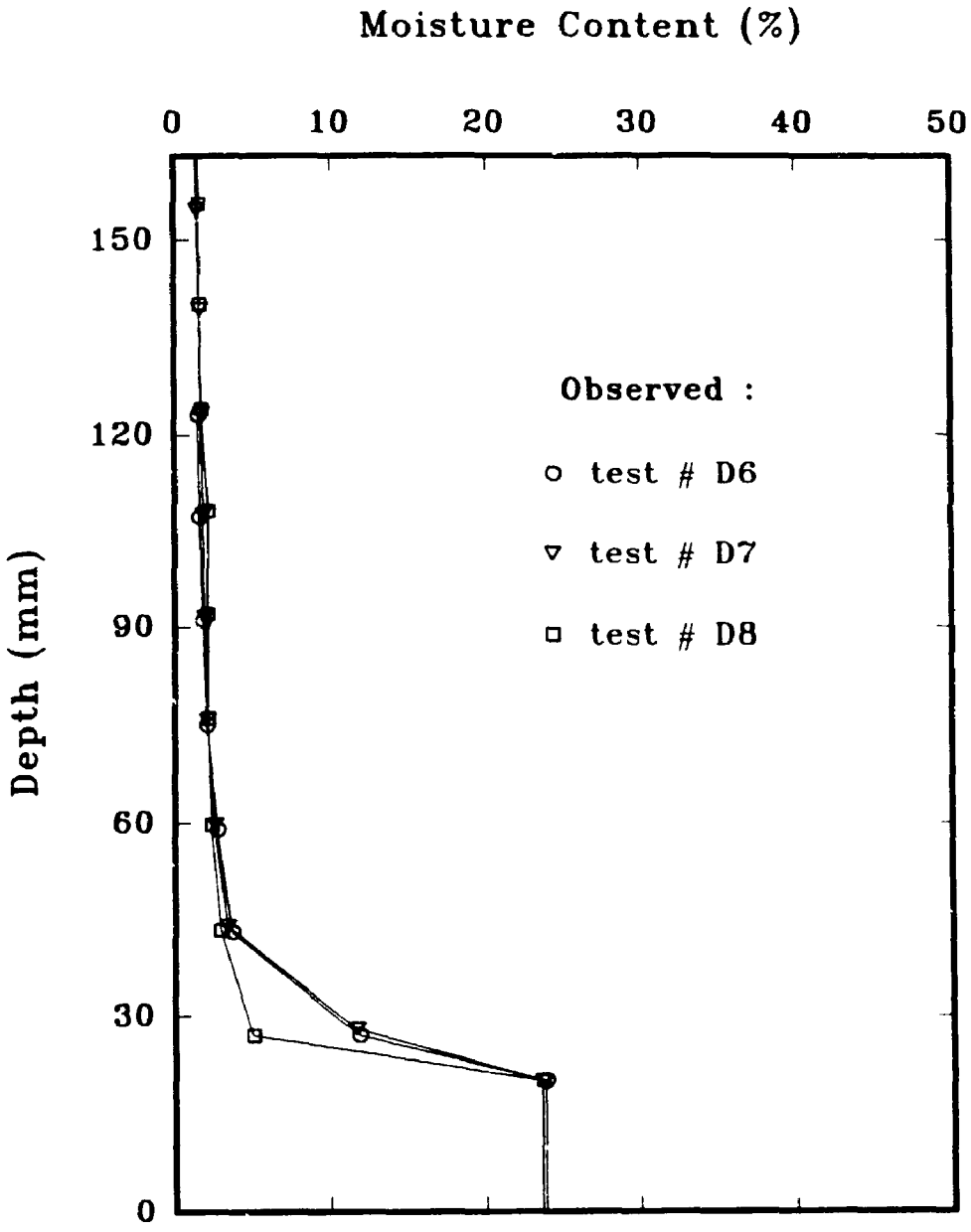

FIG. 7.8 MOISTURE CONTENT PROFILES IN FINE GRAVEL DIFFUSION TESTS

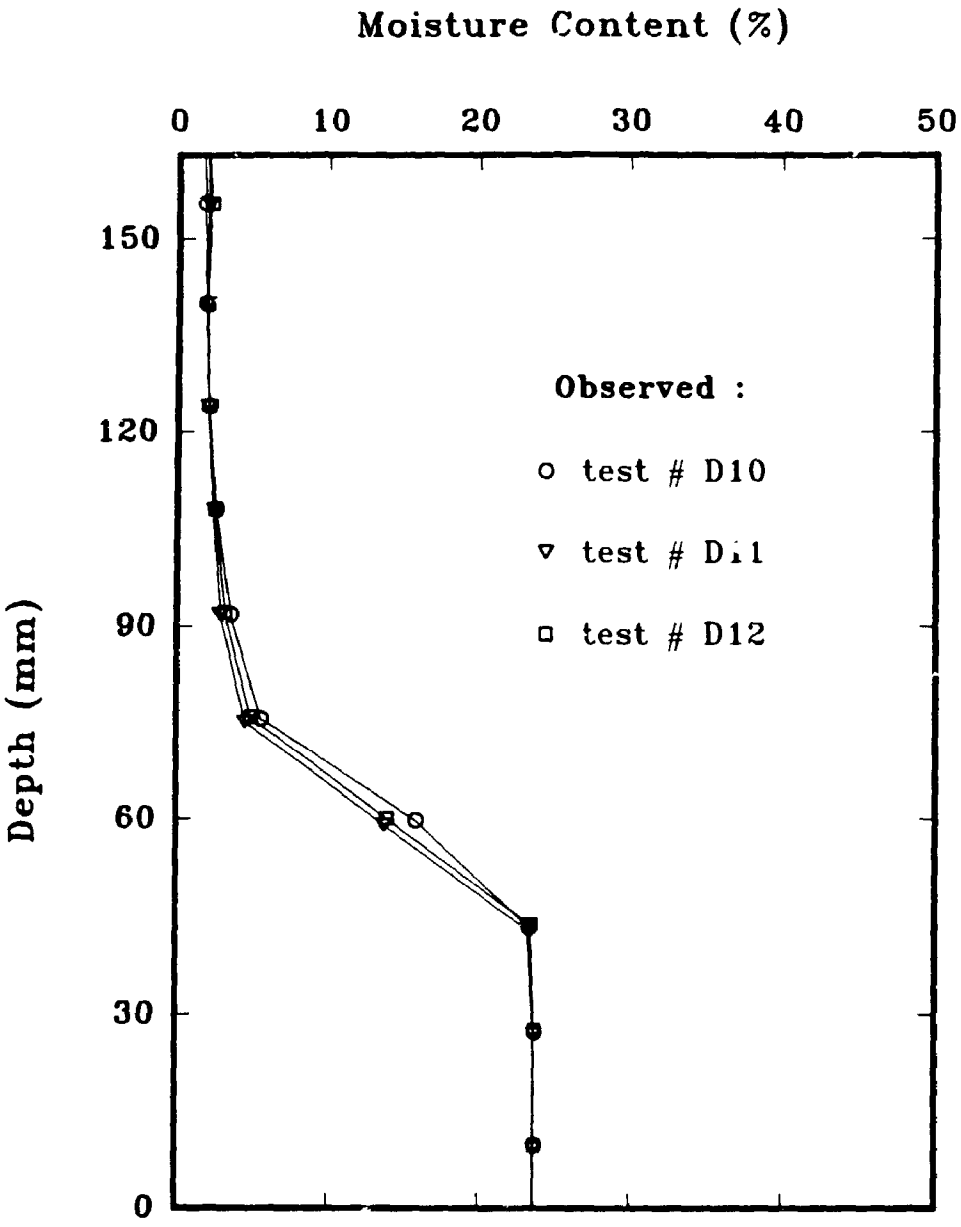

FIG. 7.9a MOISTURE CONTENT PROFILES IN COARSE SAND DIFFUSION TESTS

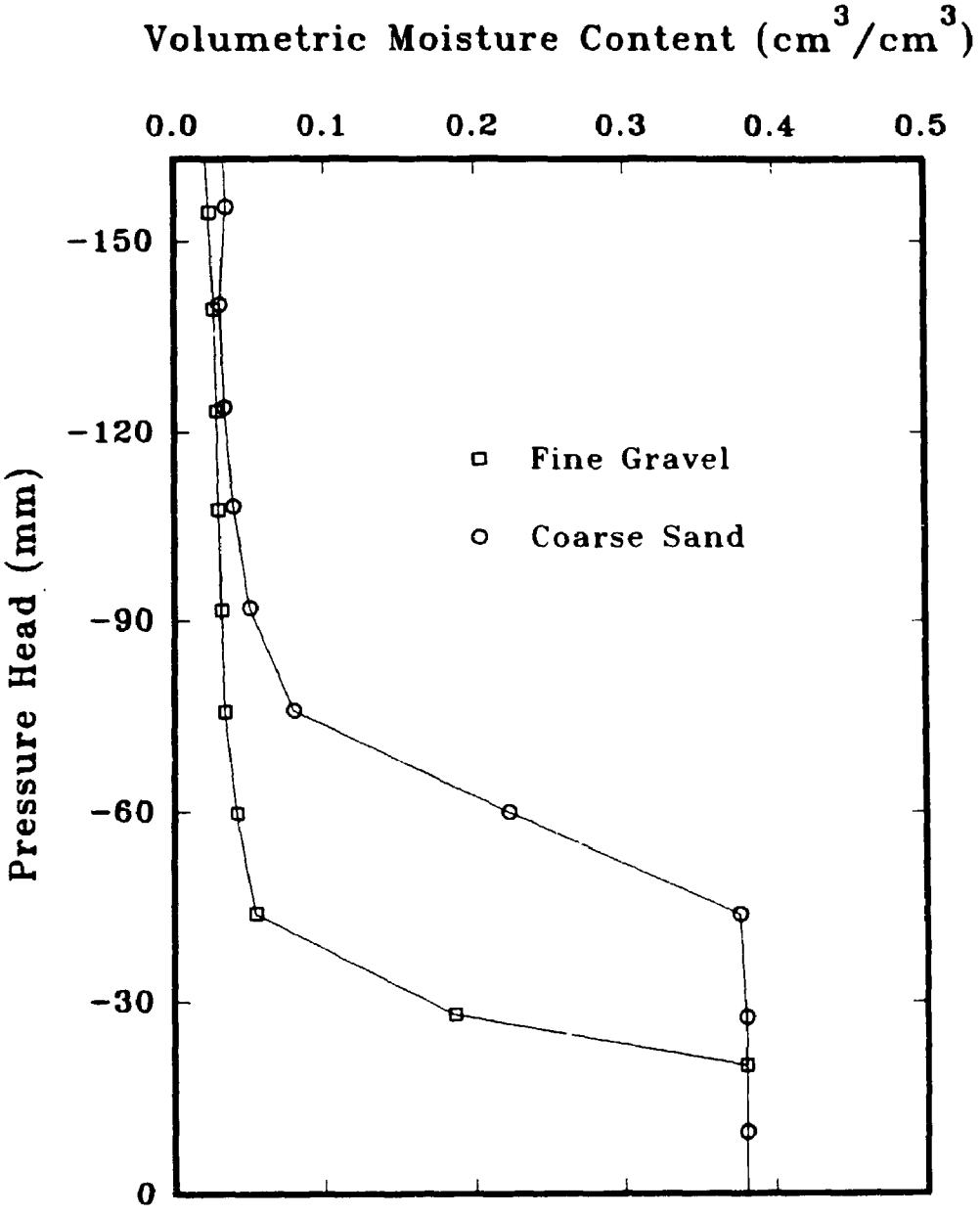

FIG. 7.9b SOIL MOISTURE CHARACTERISTIC CURVES FOR COARSE SAND AND FINE GRAVEL

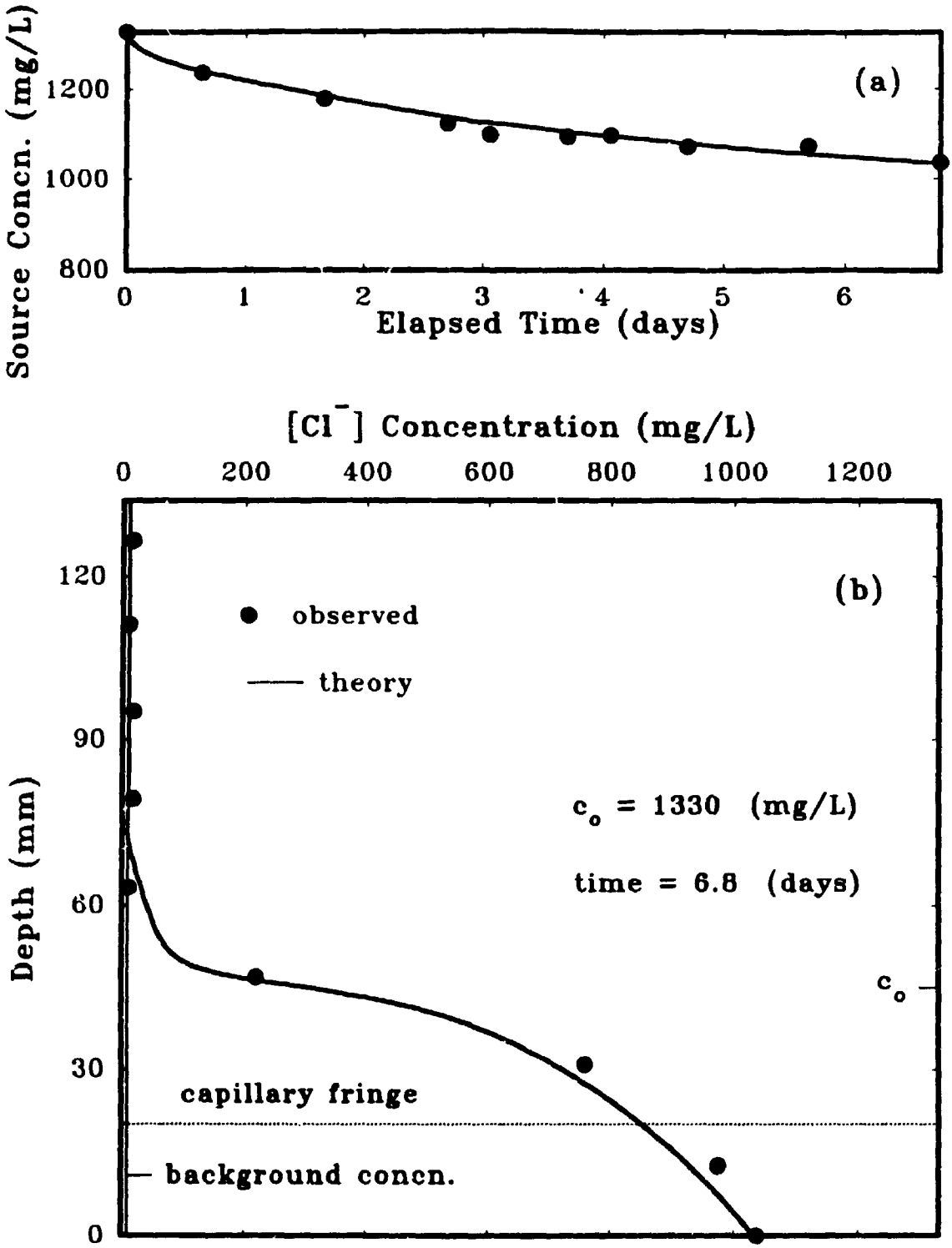

FIG. 7.10 OBSERVED AND THEORETICAL "BEST FIT" [Cl^-] CONCENTRATION IN DIFFUSION TEST #D6, (UNSATURATED FINE GRAVEL), (a): SOURCE SOLUTION CONCENTRATION VS TIME, (b): PORE-WATER CONCENTRATION VS DEPTH

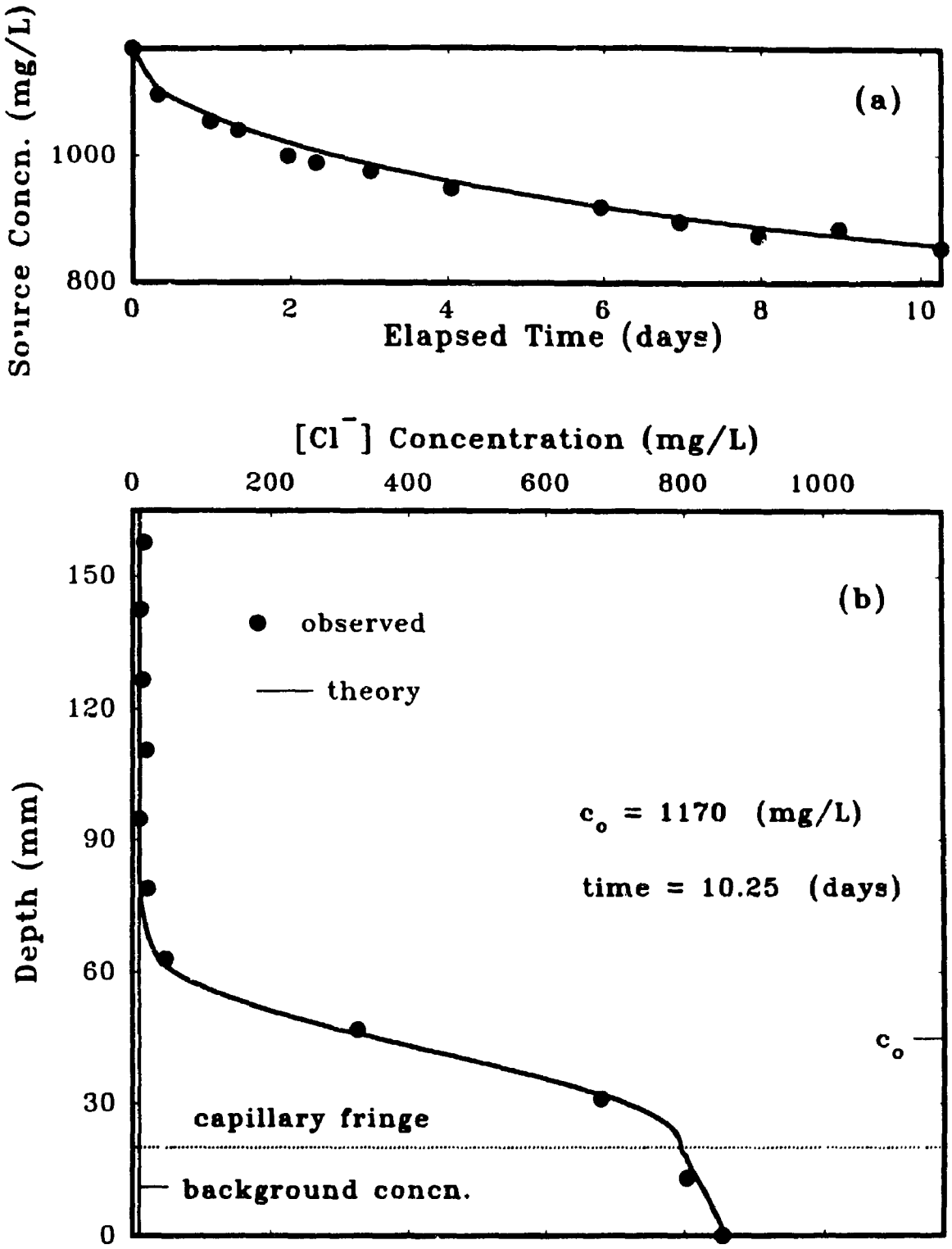

FIG. 7.11 OBSERVED AND THEORETICAL "BEST FIT" [Cl^-] CONCENTRATION IN DIFFUSION TEST #D7, (UNSATURATED FINE GRAVEL), (a): SOURCE SOLUTION CONCENTRATION VS TIME, (b): PORE-WATER CONCENTRATION VS DEPTH

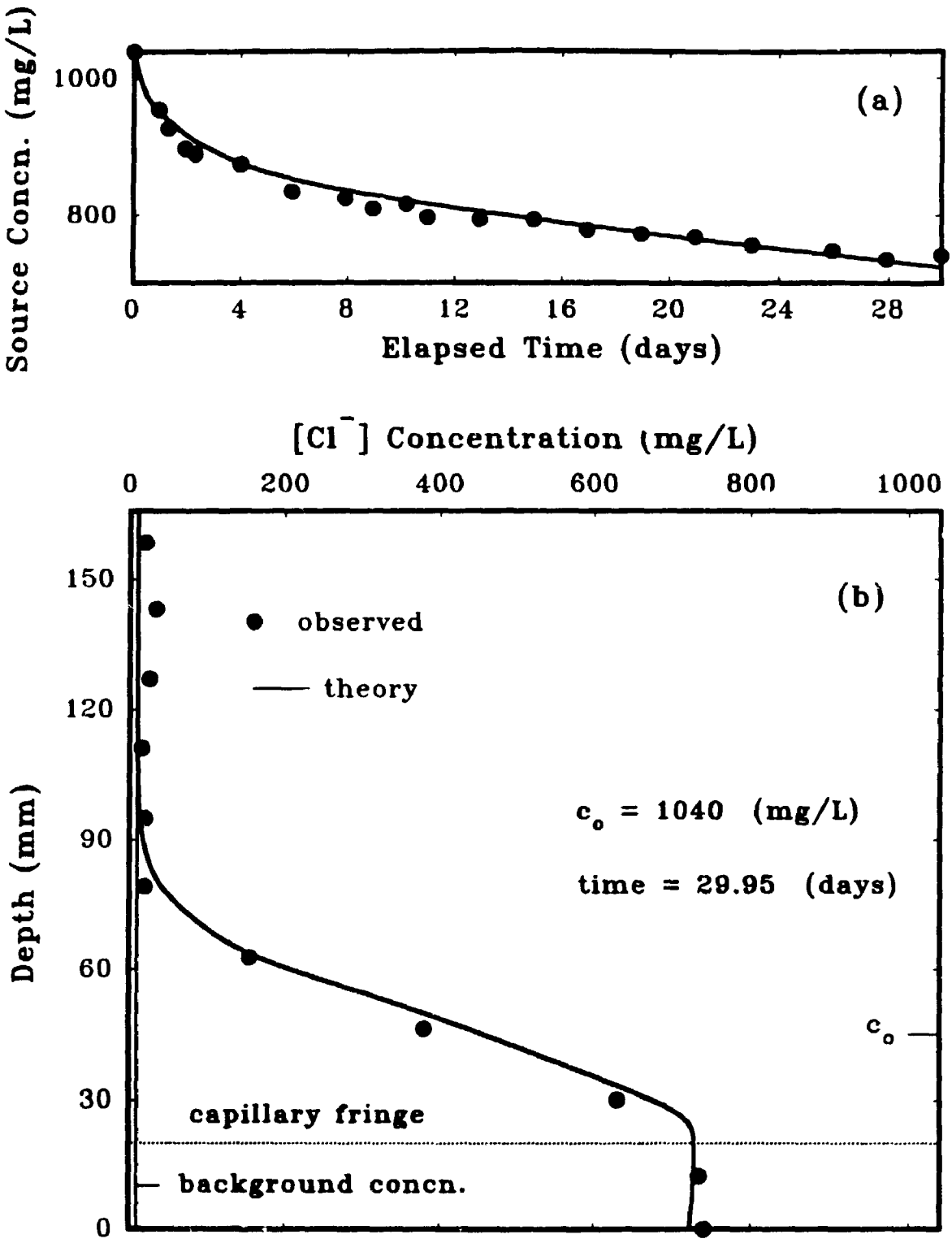

FIG. 7.12 OBSERVED AND THEORETICAL "BEST FIT" [Cl^-] CONCENTRATION IN DIFFUSION TEST #D8, UNSATURATED FINE GRAVEL), (a): SOURCE SOLUTION CONCENTRATION VS TIME, (b): PORE-WATER CONCENTRATION VS DEPTH

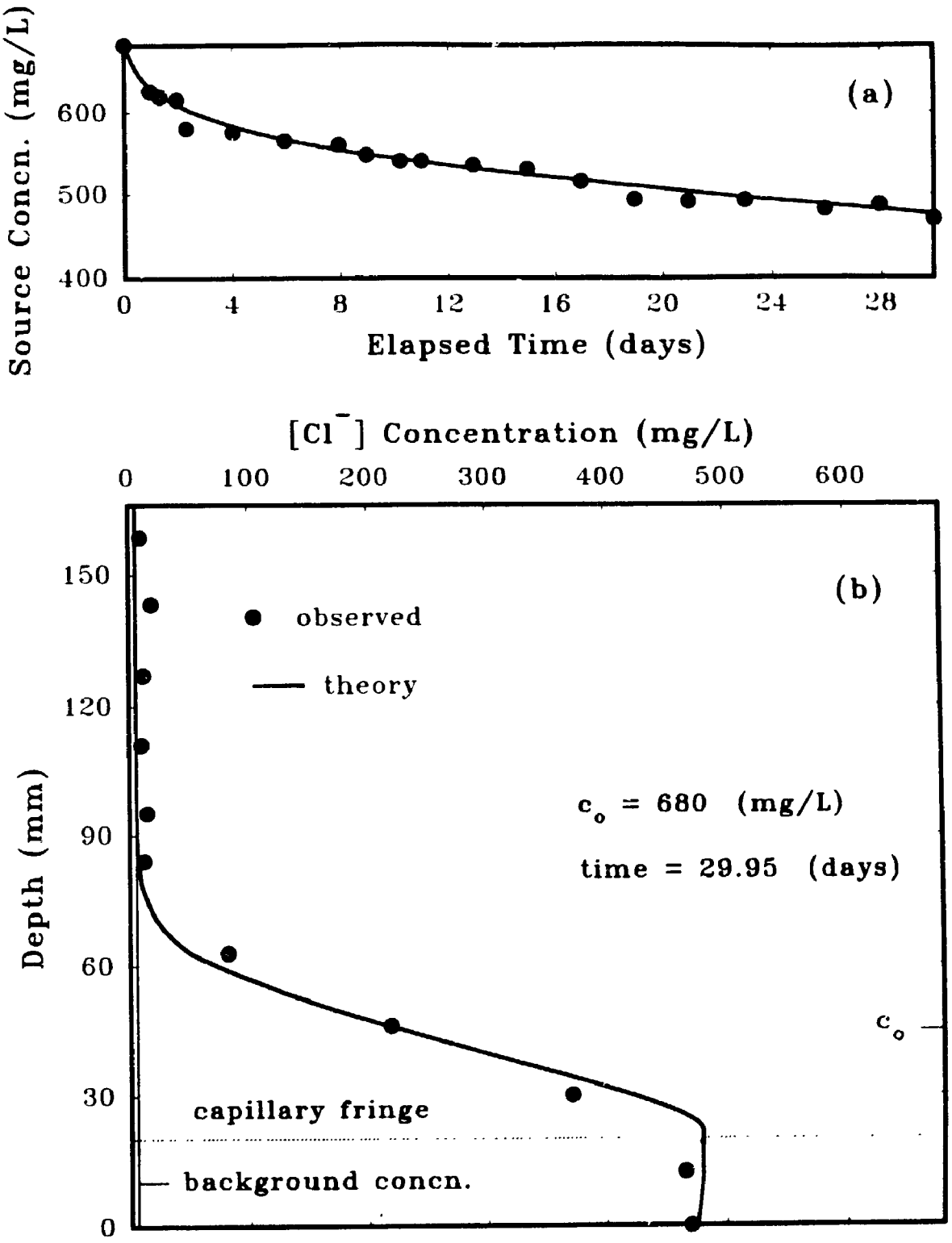

FIG. 7.13 OBSERVED AND THEORETICAL "BEST FIT" [Na^+] CONCENTRATION IN DIFFUSION TEST #D8, UNSATURATED FINE GRAVEL), (a): SOURCE SOLUTION CONCENTRATION VS TIME, (b): PORE-WATER CONCENTRATION VS DEPTH

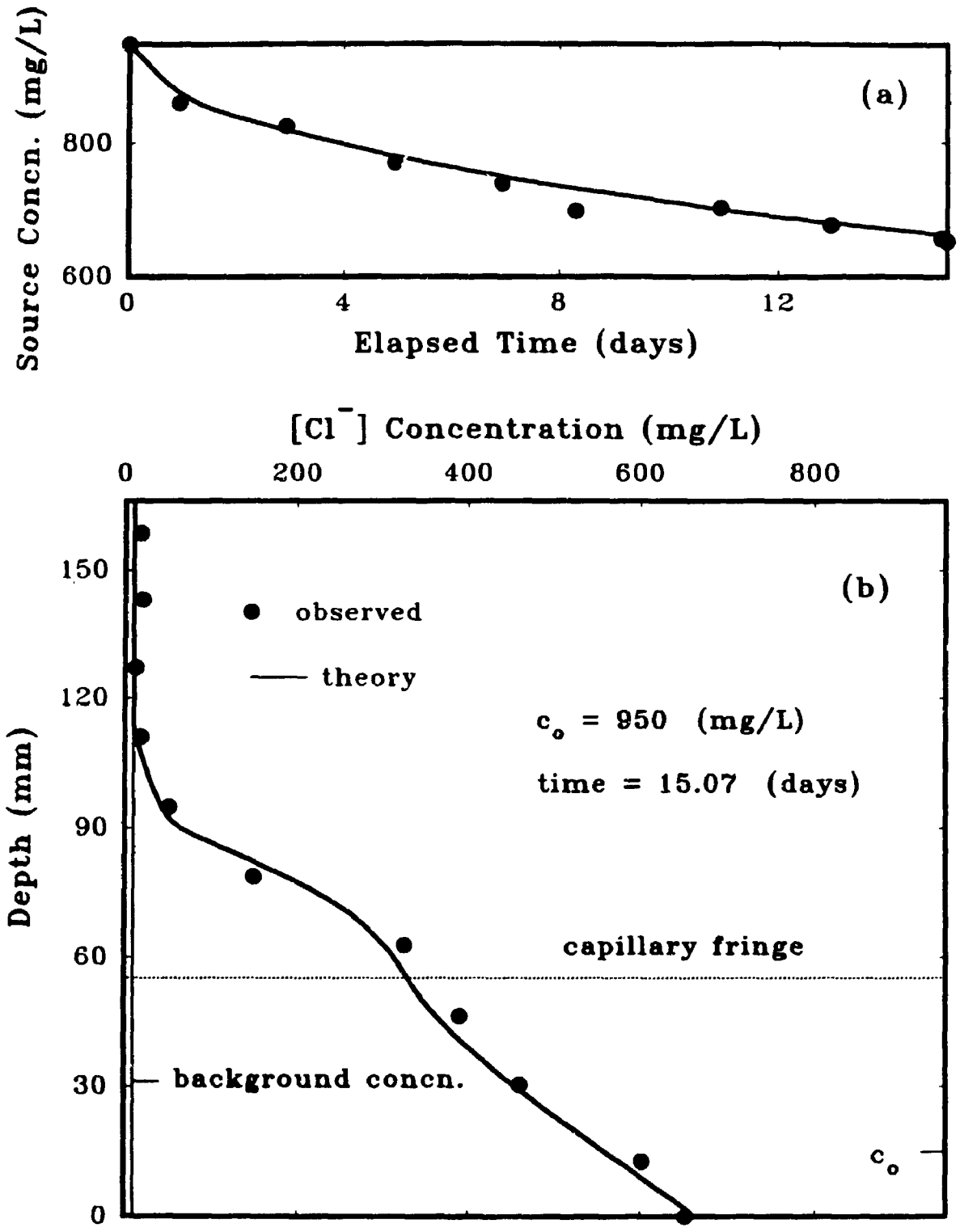

FIG. 7.14 OBSERVED AND THEORETICAL "BEST FIT" [Cl^-] CONCENTRATION IN DIFFUSION TEST #D9, (UNSATURATED COARSE SAND), (a): SOURCE SOLUTION CONCENTRATION VS TIME, (b): PORE-WATER CONCENTRATION VS DEPTH

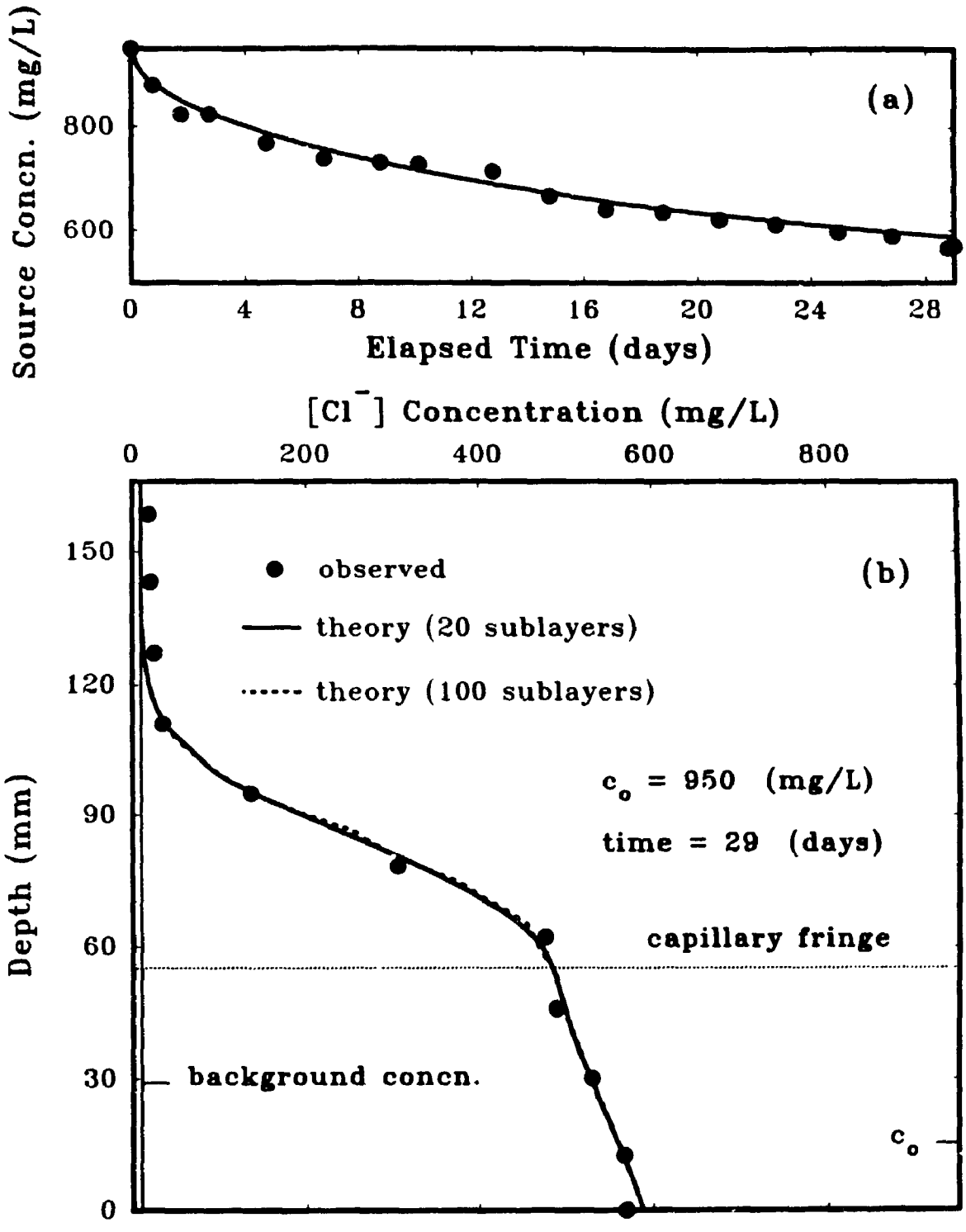

FIG. 7.15 OBSERVED AND THEORETICAL "BEST FIT" [Cl^-] CONCENTRATION IN DIFFUSION TEST #D10, (UNSATURATED COARSE SAND), (a): SOURCE SOLUTION CONCENTRATION VS TIME, (b): PORE-WATER CONCENTRATION VS DEPTH

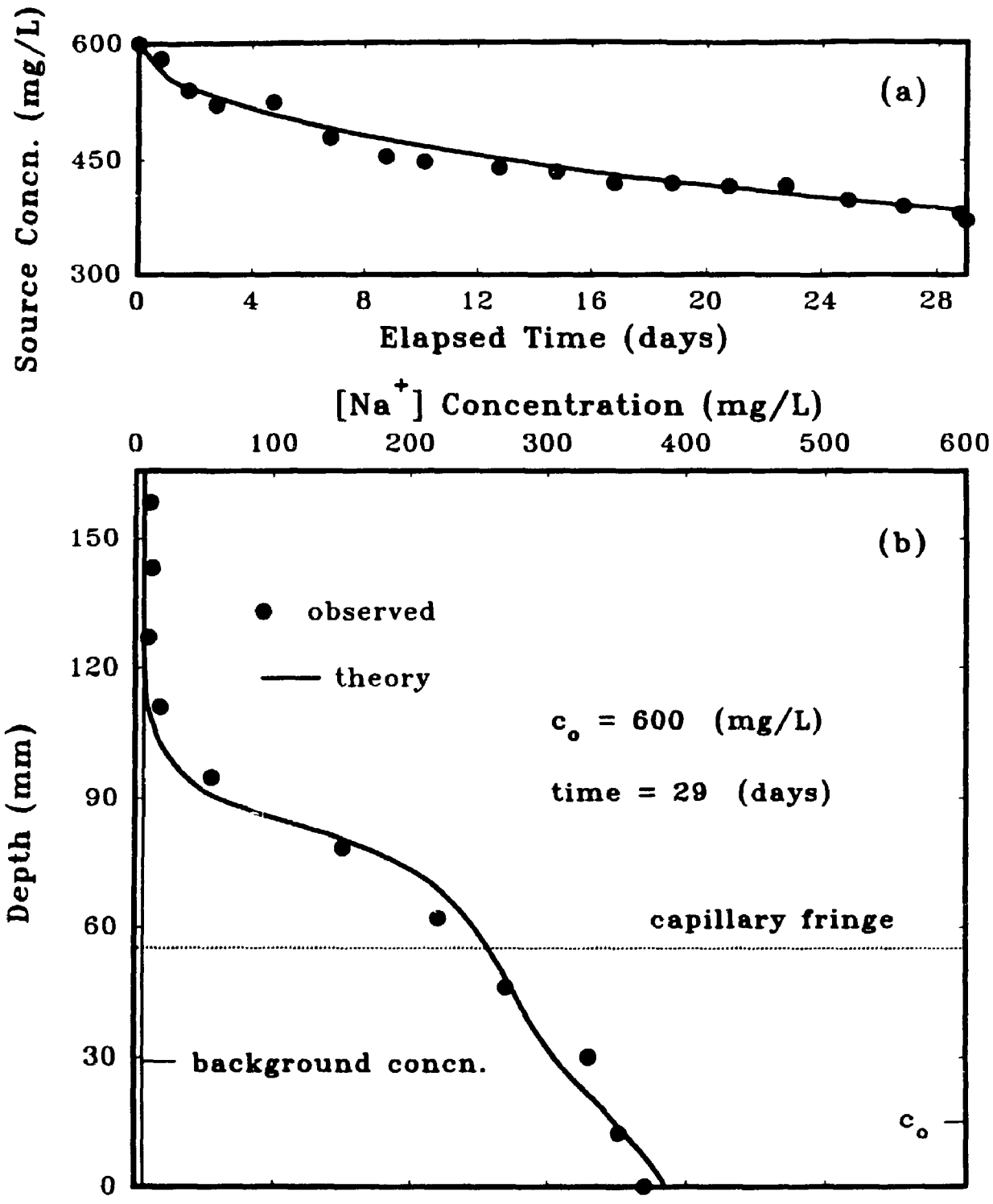

FIG. 7.16 OBSERVED AND THEORETICAL "BEST FIT" $[Na^+]$ CONCENTRATION IN DIFFUSION TEST #D10, (UNSATURATED COARSE SAND), (a): SOURCE SOLUTION CONCENTRATION VS TIME, (b): PORE-WATER CONCENTRATION VS SOIL DEPTH

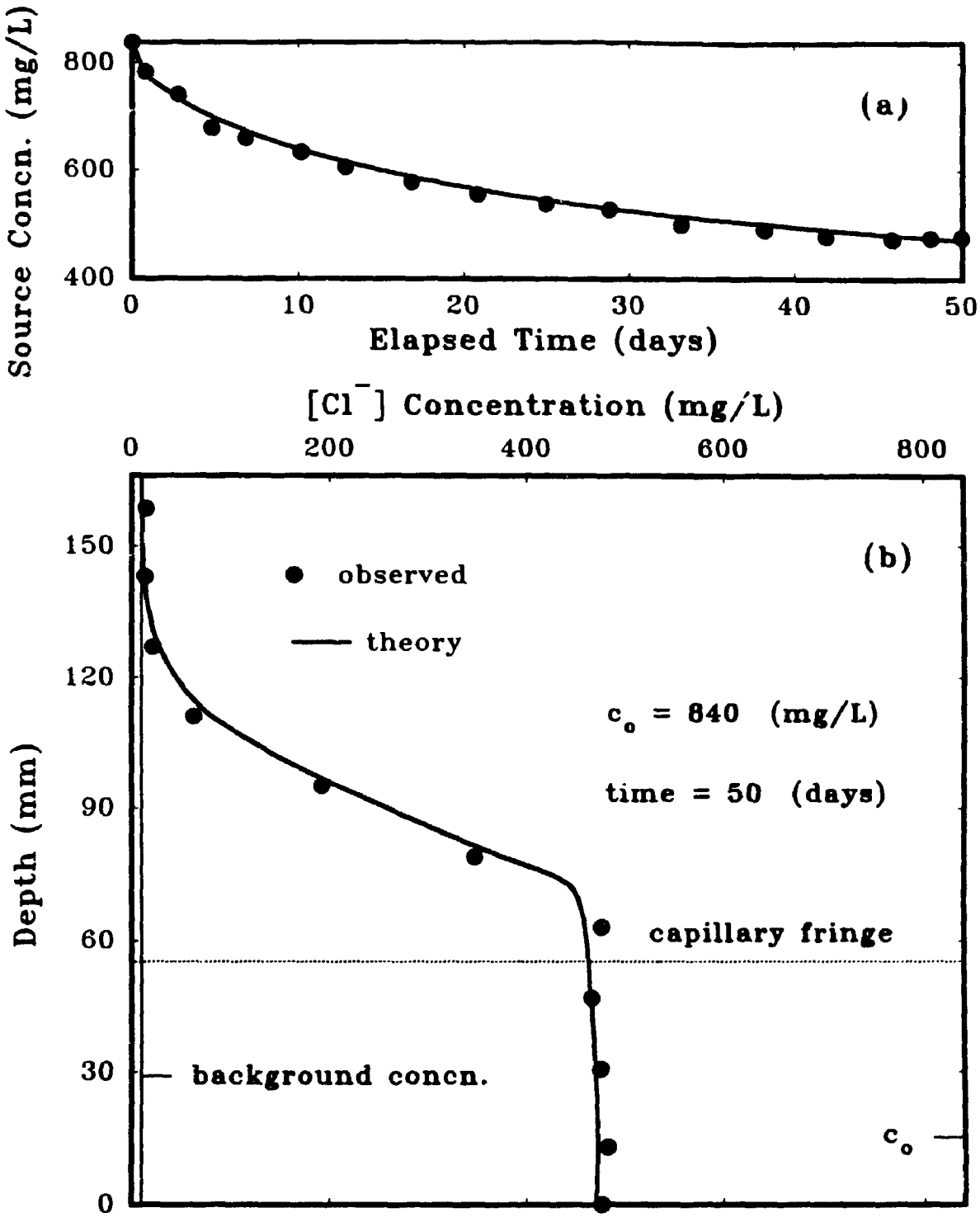

FIG. 7.17 OBSERVED AND THEORETICAL "BEST FIT" [Cl^-] CONCENTRATION IN DIFFUSION TEST #D11, (UNSATURATED COARSE SAND), (a): SOURCE SOLUTION CONCENTRATION VS TIME, (b): PORE-WATER CONCENTRATION VS DEPTH

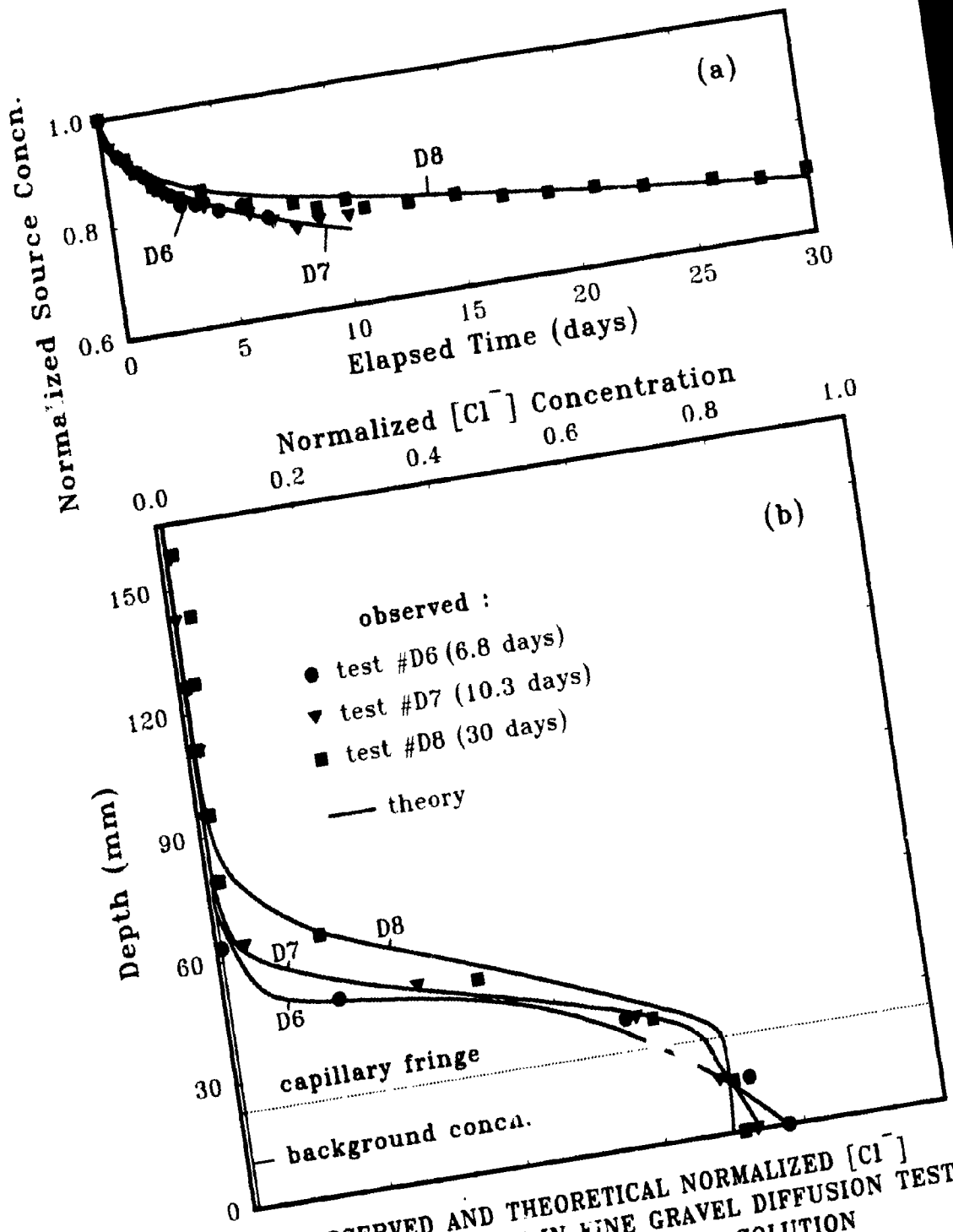

FIG. 7.18 OBSERVED AND THEORETICAL NORMALIZED [Cl^-] CONCENTRATIONS IN FINE GRAVEL DIFFUSION TESTS (# D6, D7 AND D8), (a): SOURCE SOLUTION CONCENTRATION VS TIME, (b): PORE-WATER CONCENTRATION VS DEPTH

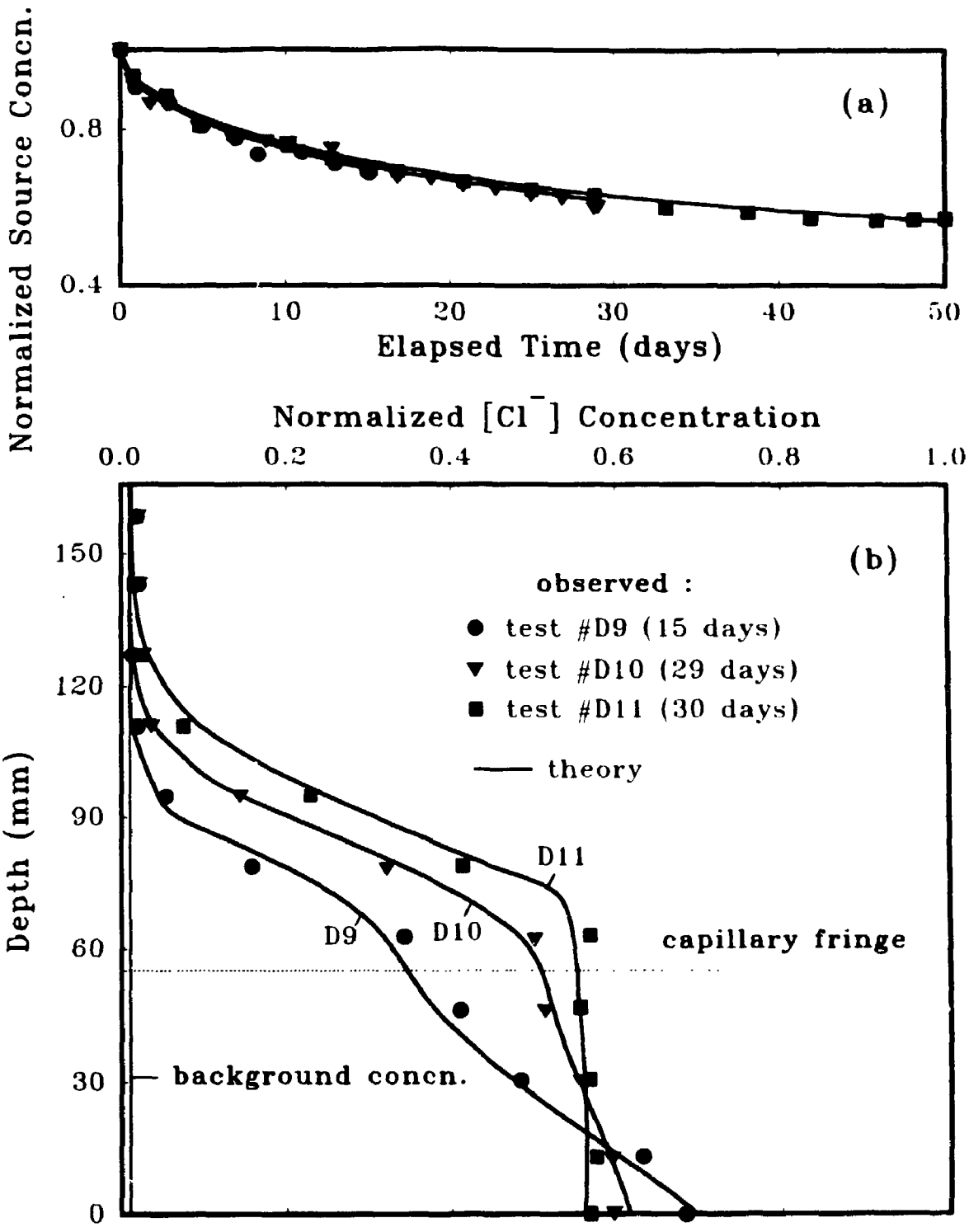

FIG. 7.19 OBSERVED AND THEORETICAL NORMALIZED [Cl^-] CONCENTRATIONS IN COARSE SAND DIFFUSION TESTS (# D9, D10 AND D11), (a): SOURCE SOLUTION CONCENTRATION VS TIME, (b): PORE-WATER CONCENTRATION VS DEPTH

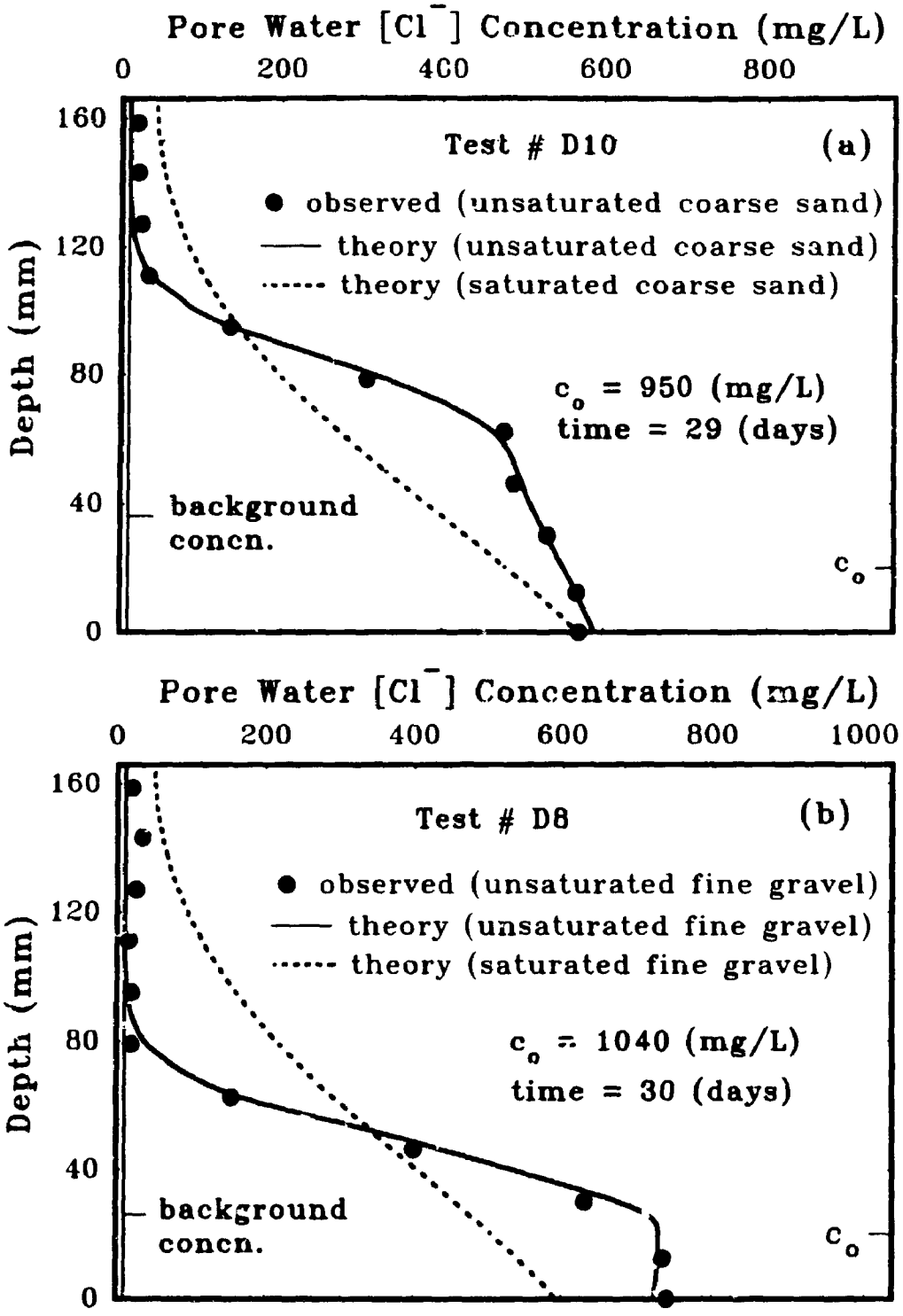

FIG. 7.20 EFFECT OF THE LEVEL OF SATURATION OF THE MATERIAL ON THEORETICAL DIFFUSION PROFILES OF:
(a) TEST #D10, COARSE SAND
(b) TEST #D8, FINE GRAVEL

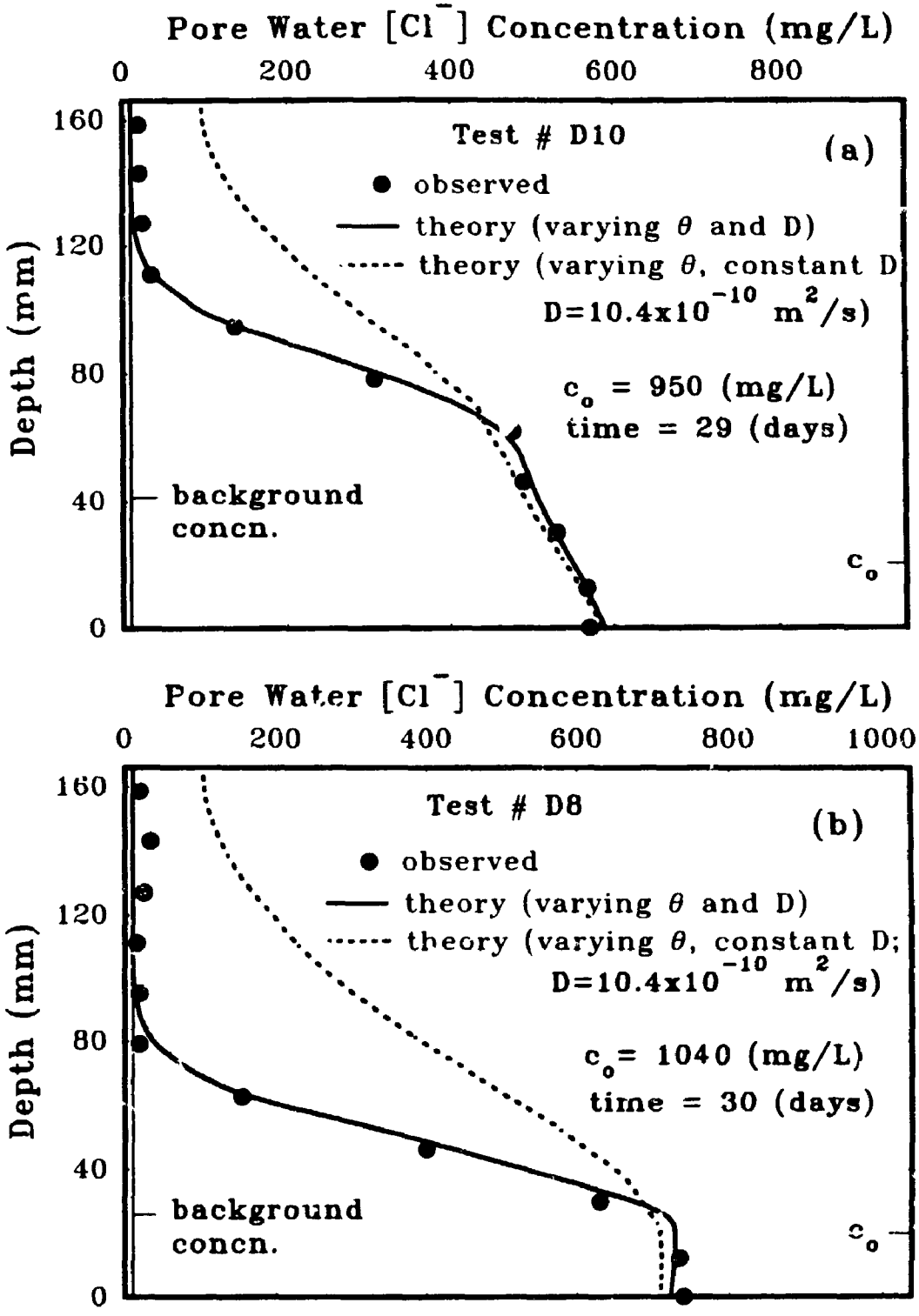

FIG. 7.21 EFFECT OF THE CONSTANT DIFFUSION COEFFICIENT OF THE MATERIAL ON THEORETICAL DIFFUSION PROFILES C' : (a) TEST # D10 (COARSE SAND), AND (b) TEST #D8 (FINE GRAVEL)

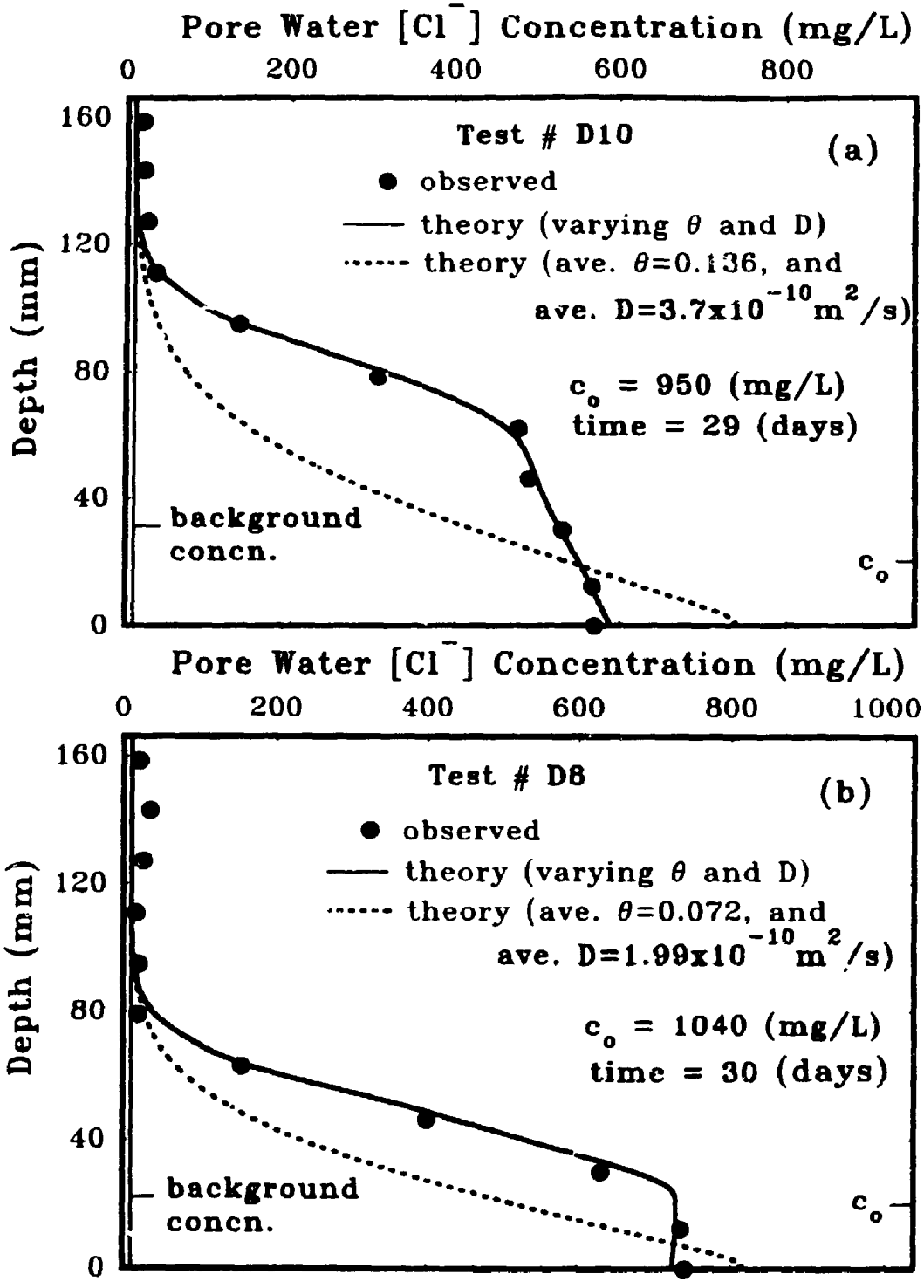

FIG. 7.22 EFFECT OF THE AVERAGE VOLUMETRIC WATER CONTENT AND DIFFUSION COEFFICIENT OF THE MATERIAL ON THEORETICAL DIFFUSION PROFILES OF: (a) TEST #D10 (COARSE SAND) AND (b) TESTS #D8 (FINE GRAVEL)

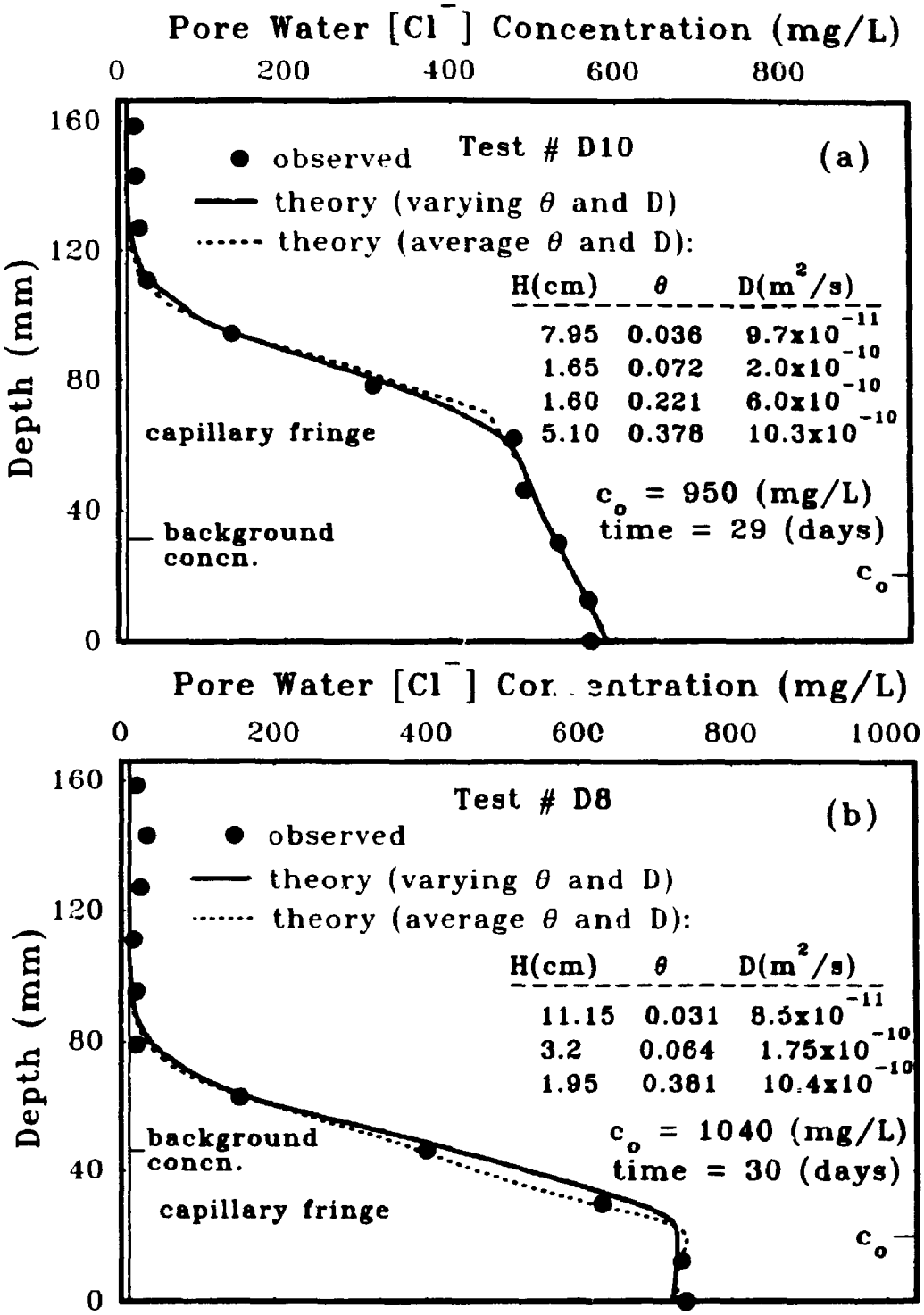

FIG. 7.23 EFFECT OF THE AVERAGING OF THE VOLUMETRIC WATER CONTENT AND DIFFUSION COEFFICIENT OF THE MATERIAL IN 4 SUBLAYERS, ON THEORETICAL DIFFUSION PROFILES OF: (a) TEST #D10 (COARSE SAND) AND (b) TEST #D8 (FINE GRAVEL)

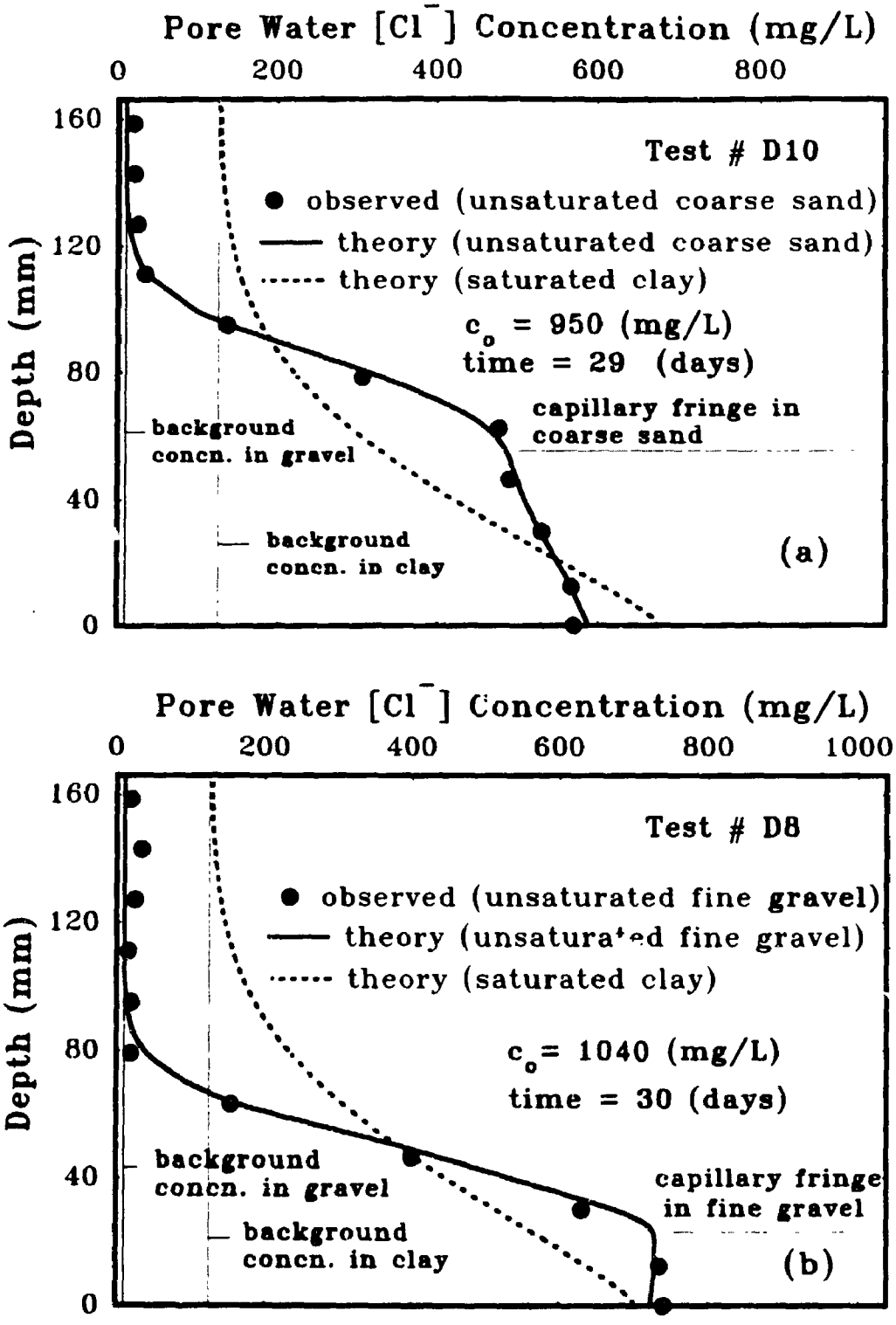

FIG. 7.24 COMPARISON OF THE RESULTS OF THE TESTS # D8 AND D10 WITH THEORETICAL DIFFUSION PROFILE OF A CLAY LAYER HAVING THE SAME THICKNESS, (a) TEST #D10, AND (b) TEST #D8

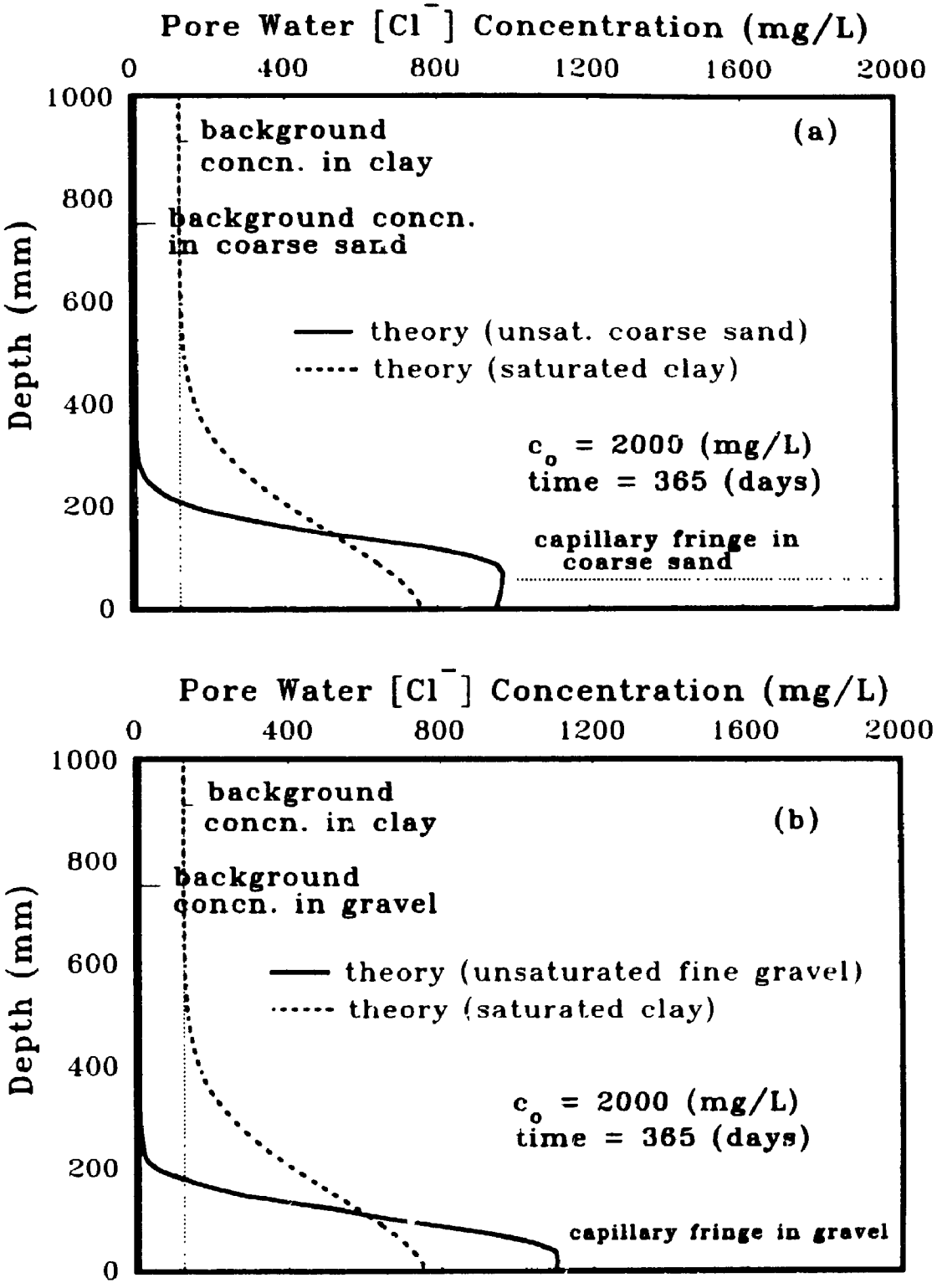

FIG. 7.25 COMPARISON OF THE THEORETICAL DIFFUSION PROFILES IN 1 M THICK UNSATURATED COARSE-SAND (a), AND FINE GRAVEL (b), WITH THE SAME PROFILE IN 1 M THICK SATURATED CLAY

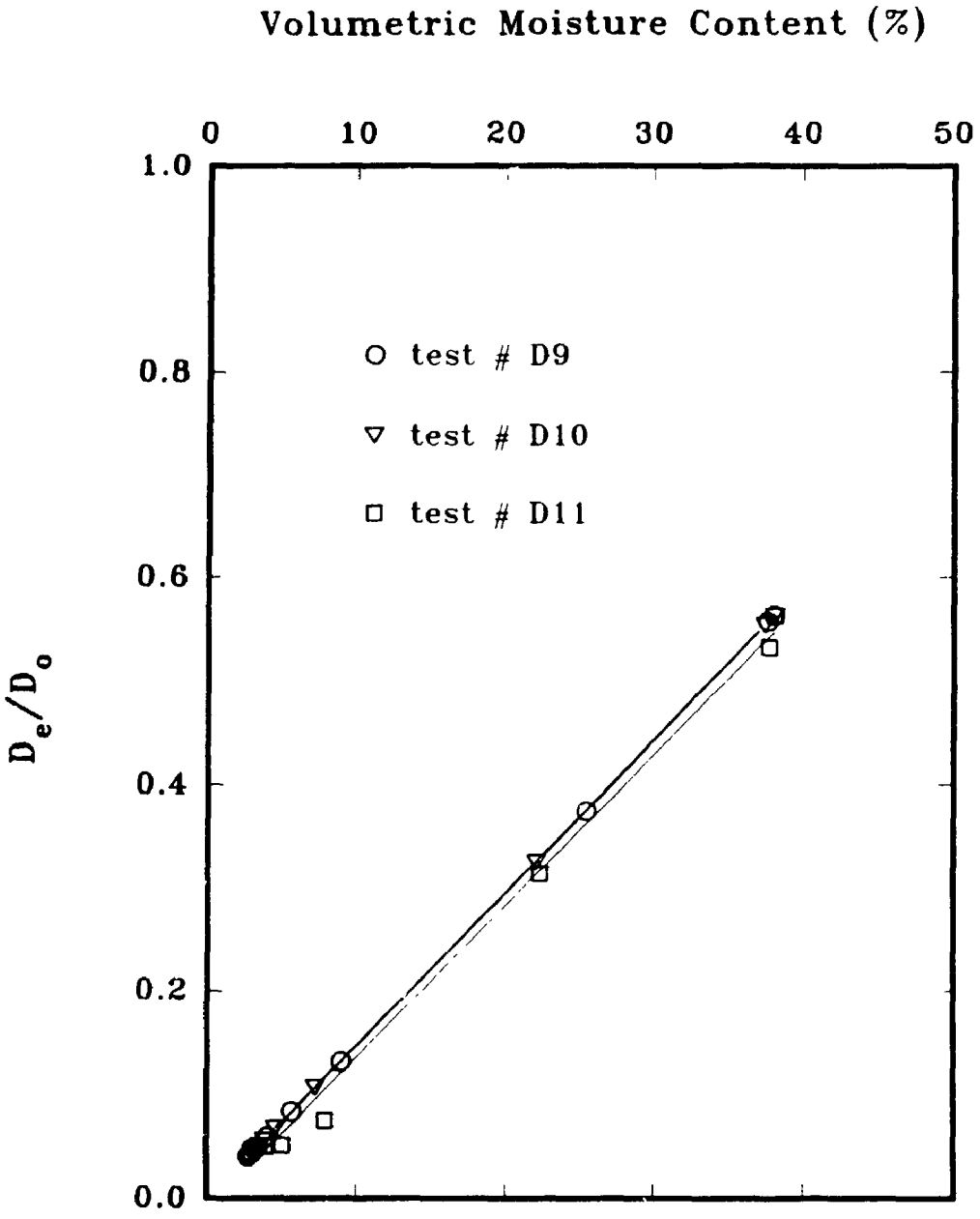

FIG. 7.26 FUNCTIONAL RELATIONSHIP BETWEEN NORMALIZED DIFFUSION COEFFICIENT (D/D_e) AND VOLUMETRIC MOISTURE CONTENT IN COARSE SAND DIFFUSION TESTS

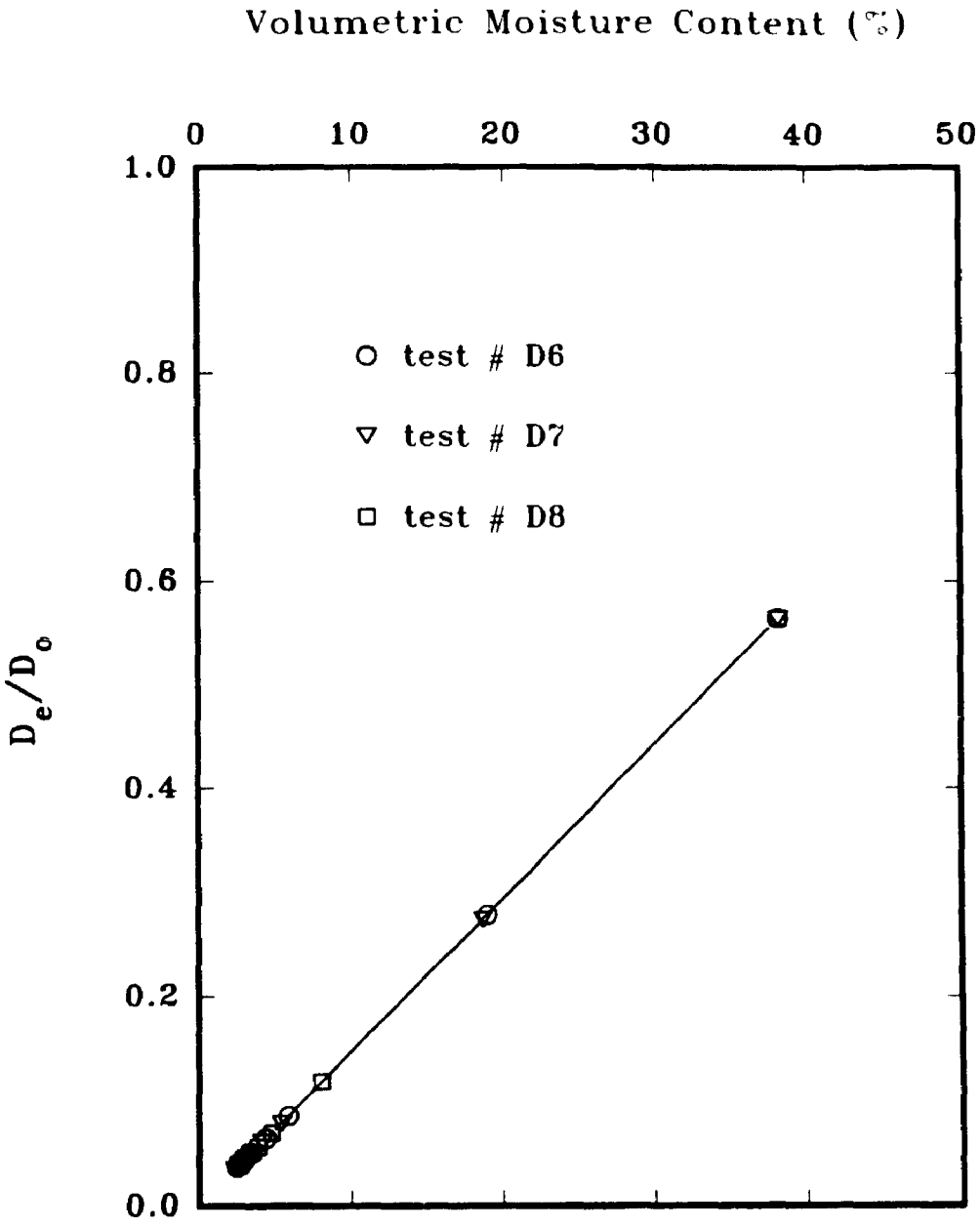

FIG. 7.27 FUNCTIONAL RELATIONSHIP BETWEEN NORMALIZED DIFFUSION COEFFICIENT (D_e/D_o) AND VOLUMETRIC MOISTURE CONTENT IN FINE GRAVEL DIFFUSION TESTS

CHAPTER 8

ADVECTION-DIFFUSION TESTING IN A TWO-LAYER SOIL SYSTEM OF CLAYEY SILT OVER FINE GRAVEL

8.1 INTRODUCTION

In this chapter, the advective-diffusive transport of chloride and sodium through a two layer soil system of clayey silt underlain by unsaturated fine gravel is examined. The clayey silt had the same characteristics as described in previous chapters and was almost saturated. The fine gravel was initially saturated and then allowed to drain under gravity. The method used was the same as that used in diffusion testing of fine gravel which was described in the previous chapter. Using these materials, two advection-diffusion tests were conducted with the test durations of 63 and 80 days. These tests will be referred to as Tests # AD6 and AD7. The configuration and geometry were the same for both tests and were similar to the advection-diffusion tests described in Chapters 5 and 6.

8.2 MATERIAL, INSTALLATION AND TEST SET UP

The clayey silt sample was obtained from the Halton Waste Management Site in Milton, Ontario. Some physical, chemical and mineralogical properties of this soil were given in Table 4.2 and Fig. 4.1 shows its typical grain size distribution. This grain size distribution was obtained after removal of oversize material by passing air-dried,

pulverized soil through a # 4 sieve. The fine gravel is the same material as used in the diffusion tests described in Chapter 7 (see Table 7.2 and Fig. 7.1).

Tap water was added to the air dried clayey soil to obtain the desired moisture content which was typically 2 to 4 percent wet of the optimum moisture content of the soil. The wet sample was compacted in a standard Proctor mold which then extruded and cut into 2 equal thicknesses, each approximately 6 cm height. The compacted samples were placed into the plexiglass rings by placing a brass cutting shoe, having slightly larger I.D. than the plexiglass ring, onto the bottom of the ring and pressing down on a clayey sample using the triaxial compression machine until about 5 cm of the soil entered the plexiglass ring.

The diffusion cell with base plexiglass ring and six extra rings was assembled. The washed, dry gravel was packed in the cell to a height of 10 cm. The packing method consisted of successive filling of gravel layers in about 2 cm thicknesses and tamping the surface of the gravel and vibrating the circumference of the cell by a plastic septa until no change in volume occurred. This procedure was repeated for all gravel layers until the thickness of the gravel was 10 cm. The assembled cell was transferred into a sink and was saturated using the same procedure as described in the previous chapter. The diffusion cell was placed on the magnetic stirrer and the pipette was attached to the outlet valve of the cell and adjusted to be level with the bottom surface of the gravel. The outlet valve was opened and the sample drained through the pipette. Observations showed that the sample yielded a great amount of water during the first few minutes of drainage. The drainage process continued overnight to ensure the completion of the drainage process.

The stainless steel ring on top of the cell was removed and the clayey soil section was placed on top of the unsaturated gravel taking care to ensure a good contact between the clayey soil and gravel. Two extra plexiglass rings were placed on top of the clayey soil section. The stainless steel ring and metal rods were placed and the cell was tightened. A NaCl solution was poured on top of the clayey soil to the height of approximately 3 cm and two samples were taken for initial source solution concentration measurement. One sample was also taken from the receptor reservoir for the measurement of any background concentration.

Two identical tests were conducted using the procedure explained above. Figs. 8.1 and 8.2 show the schematic and photographic view of the conducted tests set up.

8.3 MONITORING AND TERMINATION OF THE TESTS

Samples from the source and receptor reservoirs were taken periodically during the tests. The approximate level of the capillary rise at the beginning of the tests was 2 cm. Observations showed that the thickness of the saturated fine gravel at the bottom of the sample was about 3 cm at the end of both tests. This was due to the accumulation of the infiltrated water at the bottom of the fine gravel during the test. According to the observations, the infiltrated volume did not drain from the cell due to the end meniscus effect in the pipette attached to the cell. The volume of accumulated water was calculated for Tests AD6 and AD7 by subtracting the measured total volume of water in fine gravel at the end of the tests form the average volume of water in the same sublayers in diffusion Tests D6 and D7, measured at the end of these tests. The resulting values

were 26 cm^3 and 34.7 cm^3 in Tests AD6 and AD7 respectively. These values were compared with the infiltrated volumes of 24.7 cm^3 and 35.8 cm^3 in each test (measured by monitoring the water level drop in the source reservoirs). The resulting values agree well indicating that the infiltrated volume has been used in storage in the fine gravel and was responsible for increase in volumetric moisture content of the fine gravel sublayers during the tests. This increase in volumetric moisture content with time, was taken into account in theoretical analysis with POLLUTE and will be discussed later.

Prior to the termination of each test, final samples were taken from the source and receptor reservoirs. The height of the clayey silt and fine gravel samples was measured and compared with the initial values. The remaining solution in the source reservoir was drained and the surface of the clayey soil was cleaned of any remaining solution. The clayey soil was removed. Using stainless steel sectioning plates, the gravel was sliced ring by ring by slightly lifting the ring from one edge and sliding the plate through the interface. Sectioning plates including wet gravel were weighted immediately and placed in oven for moisture content determination. The clayey soil sample was sectioned into 4 sub-layers of approximately equal thicknesses using a wire trimmer. Samples from each slice were taken for moisture content determination and for pore water squeezing to obtain pore water for chemical analysis.

8.4 MOISTURE CONTENT PROFILES IN THE TESTED SOILS

Fig. 8.3 shows the moisture content profiles observed at the end of the tests. The moisture content in clayey silt samples are similar and almost uniform with depth. The

saturation level in the gravel layer in both tests was higher than that observed in diffusion tests discussed in Chapter 7. Test #AD7 with the longer test duration, showed slightly higher moisture content above the capillary fringe than the Test #AD6. This was due to the longer time of the test compared to Test #AD6 which caused more infiltrated water to be accumulated at the bottom of the fine gravel sample.

Values of the thickness, moisture content, degree of saturation and volumetric moisture content for clayey silt and fine gravel sub-layers are listed in Table 8.1.

8.5 EXPERIMENTAL AND THEORETICAL ANALYSIS

The clayey silt samples were squeezed in pneumatic squeeze apparatus to obtain pore water solution. Concentration determination in the unsaturated gravel samples was assessed using the wash method described in previous chapters. 80 g of fine gravel from each slice was washed with 50 mL of de-ionized distilled water and the concentration of wash water was analyzed for both Na^+ and Cl^-. The concentration of Na^+ in the clayey soil squeeze water and gravel wash water was determined with atomic absorption spectrophotometry using a Na^+ lamp. Dilution of the clayey soil squeeze water by the order of 1000 and dilution of gravel wash water by the order of ranging from 10 to 100 was required to bring the concentration of samples into the standard solutions concentration range. The Cl^- concentration of the soil samples and also source and receptor reservoirs samples was determined using the same method described in previous chapters.

Theoretical analyses were performed using program POLLUTE. The best fit 'by

eye' to the experimental data was obtained using variable diffusion coefficients for the clayey soil and gravel layers, depending on the volumetric moisture content of each soil sub-layers. The assessment of the effective diffusion coefficient values was based on the linear interpolation method explained in previous chapter. Tables 8.2a, 8.2b, and 8.2c show the data used in the analysis. The resulting theoretical profiles along with the observed data for chloride are shown in Figs. 8.4 to 8.7. As can be seen, the theoretical profiles fit the experimental data well, indicating that the adopted method for estimating the diffusion coefficients is also applicable in the analysis of advection-diffusion tests. The dotted line in Fig. 8.4 represents the result of the analysis when the volumetric moisture content of the fine gravel changed with time (Test AD6). This analysis considered six, sequentially increasing, volumetric moisture contents and effective diffusion coefficients in fine gravel sublayers as the test progressed. The initial values of the volumetric moisture content was assumed to be equal to that observed in diffusion test D7 (6 bottom sublayers, as listed in Table 7.7a), and the final values are those measured at the end of the test and listed in Table 8.2a. As evident from Fig. 8.4, the dotted line almost overlaps the solid line which was obtained assuming constant values of volumetric moisture content with time for fine gravel sublayers. This indicates that the change in volumetric moisture content does not have significant effect on the predicted results.

Theoretical analysis for Na^+ data was also performed and the results are presented in Figs. 8.8 and 8.9. The best fit to the experimental data was obtained using diffusion and distribution coefficients shown in Table 8.2b. The remaining input data are listed in Table 8.2c. The Na^+ diffusion coefficients for gravel sub-layers were predicted based

on linear interpolation of the obtained values from pure diffusion tests (described in Chapter 7) and the volumetric moisture content of each gravel sublayer in current tests.

The use of the term 'diffusion coefficient' instead of 'hydrodynamic dispersion coefficient' in these analysis is due to the negligible effect of the dispersion in the conducted tests compared to the effect of diffusion as will be discussed in next section. Hence, the assessment of the normalized diffusion coefficient values (i.e. tortuosity factors) for gravel layer was made by dividing the diffusion coefficient values to the diffusion coefficient of chloride in free solution at 23 °C. Fig. 8.10 shows the functional relationship between the normalized diffusion coefficient and volumetric moisture content values adopted for the gravel sub-layers in both tests.

Both experimental and theoretical profiles show that the concentration of chloride drops significantly when it is migrating through the unsaturated zone of the gravel layer. As can be seen in Fig. 8.3, the moisture content of the gravel, 3 cm or more above the capillary saturated zone is very low. This part of gravel layer contains very tortuous paths for sodium and chloride migration which arise from the lower moisture content of the gravel.

8.5.1 EFFECT OF THE DISPERSION IN CONDUCTED TESTS

As noted earlier, the effect of dispersion is considered be negligible in these experiments. This is due to the small Darcy velocities associated with these tests (the average of the two tests was 5.2×10^{-10} m/s or 0.016 m/a). Perkins and Johnston (1963) demonstrated the relative importance of the diffusion and dispersion in unconsolidated

granular porous media. According to their results, for the range of dimensionless parameter $ud_p/D_o < 0.02$ (u is the average interstitial velocity, d_p is the average diameter of the particles, and D_o is the molecular diffusion coefficient of solute in free solution), diffusion controls the transport of solute over the mechanism of dispersion. The calculated value of ud_p/D_o for the fine gravel in the conducted tests is 0.0018 which is much smaller than the limit value of 0.02. Based on the work by Perkins and Johnston, Rowe (1987) demonstrated that for typical problems, mechanical dispersion is likely to be small or negligible for Darcy velocities less than 0.1 m/a (3.1×10^{-9} m/s) and that mechanical dispersion is likely to be dominant for Darcy velocities greater than 10 m/a (3.1×10^{-7} m/s). Between 0.1 and 10 m/a diffusion and/or dispersion may be important depending on the details of the particular case. According to James and Robin (1986), as the porous medium is desaturated, the larger pores empty first, thereby narrowing the range of pore sizes available to flow. In the absence of immobile water in unsaturated soils, this produces a smaller range of velocities than are found in saturated soils at comparable average flow rates. As the range of velocities become smaller, dispersion would tend to decrease. This is not the case for unsaturated soils having immobile water phase in the pore space. According to De Smedt et al. (1986), existence of a mobile water phase, with more or less uniform pore water velocities in combination with an immobile water phase, with zero pore water velocities, results in an increased dispersion of solutes under unsaturated conditions.

8.5.2 SOME SENSITIVITY ANALYSIS ON CONDUCTED TESTS

Effect of the level of saturation of the gravel

To illustrate the effectiveness of the unsaturated zone in these experiments as a barrier for migration, a theoretical analysis was performed for Test #AD6 assuming that the gravel is fully saturated. The result of the analysis is shown in Fig. 8.11. As can be seen, theoretical profile has changed significantly and the chloride ion moves faster when gravel layer is fully saturated. This effect is manifested by a calculated lower concentration of chloride in source reservoir and its higher concentration in receptor reservoir compared to the case when gravel is unsaturated. When gravel becomes saturated, migration paths become much less tortuous compared to the case when gravel is unsaturated. Comparison of the tortuosity factor of the saturated gravel (0.56) with tortuosity factors in the unsaturated gravel (Table 8.2a) shows that the tortuosity factor of gravel drops from 0.56 when it is saturated to as low as 0.06 in upper parts of the gravel which is unsaturated.

Effect of replacement of unsaturated gravel layer with a clay layer

In order to compare the effectiveness of unsaturated gravel layer as a barrier for solute migration, with a saturated-compacted clay layer, another analysis was performed assuming clay layer for the entire soil profile (unsaturated gravel was replaced with a compacted clay). The results are shown in Fig. 8.12. The contaminant moves faster through the 15 cm thick clay layer than through the 15 cm thick clay-unsaturated gravel layers, although the Darcy velocity through the whole clay layer (3.5×10^{-10} m/s) is

smaller than for the case of clayey silt-unsaturated gravel layers (4.6×10^{-10} m/s), indicating that the full compacted clay layer is not as effective as clayey silt over unsaturated gravel in terms of being as a barrier for contaminant migration under condition when diffusion is the dominant transport mechanism. This effect is clear if the concentrations in the source and receptor reservoirs in both analysis are compared. This can be seen in Fig. 8.12, where for the full clay layer, the concentration in the source reservoir is less and the concentration in the receptor reservoir is more than for the case of using clayey silt-unsaturated fine gravel layer.

The same analysis was performed for Na^+ and the results are plotted in Fig. 8.13. Although there are more exchange sites available for Na^+ when a 15 cm thick clay layer is used instead of 5 cm clayey silt and 10 cm unsaturated gravel, and although the Darcy velocity was reduced for the case with more clay, still migration process is faster through 15 cm thick clay compared to the clayey silt-fine gravel layer. Table 8.3 summarizes the values of flux available in the soil and in the base (receptor) at the end of the tests for both cases analyzed. As can be seen, the flux into the base and also the concentration in the base is higher when 15 cm clay layer was used instead of clayey silt-fine gravel layer of the same thickness. These results reveal that even for cations such as sodium which could be absorbed in the clay particles, unsaturated gravel is more effective than clay as a barrier.

Effect of the Darcy velocity

The effect of the Darcy velocity on the theoretical concentration profiles was studied by neglecting the Darcy flux through the layers ($v_s = 0.0$), and the results were

compared with the best fit theoretical profiles observed when a Darcy velocity was used in the calculations. As shown in Fig. 8.14, the theoretical profiles assuming zero Darcy velocity, no longer fit the observed data indicating that the results are sensitive to the Darcy velocity. This effect is more pronounced in the unsaturated zone of the gravel layer than in the saturated clayey silt layer. This is due to the fact that the flow paths available for contaminant flux in the unsaturated zone are limited and comprise only a small portion of the total cross-section of the pores. This causes the contaminant to move much faster (by the process of advection) in the unsaturated zone compared to the saturated zone in which total cross section of the pores are used for water flow. For a better understanding of the effect of the Darcy velocity in the unsaturated media compared to saturated media, refer to Fig. 5.11. As discussed in Chapter 5, neglecting the Darcy velocity in the analysis of Tests # AD1, AD2, and AD3 which were conducted on saturated clayey silt-fine sand materials, still resulted in a good fit to the experimental data indicating that the results are not sensitive to the Darcy velocity at this level of saturation.

Effect of effective volumetric moisture content of the gravel

Another series of sensitivity analysis were performed to examine the effect of different assumed effective volumetric moisture contents, $\theta_{effective}$, of the underlying gravel on the predicted profiles. The first series of the analyses assumed that the effective θ ranged from 50% to 95% of the measured value at the end of the test (Table 8.1). All other parameters (including $D_{e(gravel)}$) are as listed in Tables 8.2a and 8.2c. The results for Test AD6 are shown in Fig. 8.15a. These results indicate that a 50% reduction in

θ resulted in concentration profiles which are far from the observed data. The results for a 20 %, 10% and 5% reduction are close to the solid line which assumed $\theta_{effective} = \theta_{measured}$, but still solid line provide the best fit to the data. Based on these results one could hypothesize that up to 10% uncertainty in θ value (i.e., $\theta_{effective} \geq 0.9\theta_{measured}$), does not have significant effect in predicted profiles and that the assumption of $\theta_{effective} = \theta_{measured}$ appears to be reasonable.

A second series of the analysis used the same θ values as above except that the D_e values for gravel were also reduced by the same proportion. This took into account the effect of θ on D_e (as discussed earlier). The results are shown in Fig. 8.15b and are similar to those in Fig. 8.15a except that they are slightly shifted to the right due to the change in D_e. The same conclusion can be reached that the effect of 10% uncertainty in the θ and D_e only has a modest effect on the result but that the original assumption ($\theta_{effective} = \theta_{measured}$) appears to be more reasonable.

8.5.3 EVALUATION OF THE EFFECT OF FLUX ON VOLUMETRIC MOISTURE CONTENT OF THE UNSATURATED FINE GRAVEL

In some practical situations involving 2 layer soil systems, water flux across the layers might change the moisture contents within the unsaturated layers compared to those postulated on the basis of static conditions. Barbour (1990) demonstrated this effect on a 2 layer soil system consisting of a silt cover overlying a sand tailings. He used a simple design approach originally proposed by Kisch (1959). In this approach Darcy's law was assumed to be valid for both saturated and unsaturated flow; however, the permeability is taken as a function of the volumetric water content or pressure head.

Darcy's law may be written as:

$$q = -k\, dh/dz \qquad (8.1)$$

where q is the unit vertical discharge ($m^3/(s.m^2)$), k is the permeability (m/s), h is the hydraulic head (m), and z is vertical distance increasing upwards (m).

The hydraulic head is equal to elevation head, z, plus pressure head, p, such that:

$$h = z + p \qquad (8.2)$$

where p is equal to fluid pressure divided by the unit weight of water. For steady state flow, 8.1 and 8.2 can be combined to give the following equation:

$$dz = -dp/(q/k + 1) \qquad (8.3)$$

To calculate a vertical pressure profile for a known flux, q, a small pressure increment, dp, is selected. The permeability associated with that pressure interval is known, so the change in vertical coordinate to reach the new pressure $p + dp$ can be calculated. By starting at a known pressure and elevation, for example at the water table, the profile of pressure with elevation may be calculated in an incremental manner.

Using the above method, the effect of flux in Tests AD6 and AD7 was evaluated. According to the results, overlying clay was almost saturated and hence the effect of applied flux was considered to be negligible in this layer. Since the volumetric moisture content of the fine gravel in these tests changed due to the storage, this evaluation was done on the basis of the pressure head versus volumetric moisture content data of the fine gravel obtained in the diffusion Test D7 (Fig. 8.16a). Permeability versus pressure head profile for this gravel was obtained using a computer program KCAL (Lam, 1984) using volumetric moisture content versus pressure head data and also the saturated permeability of the fine gravel (1.5 cm/s). Equation 2.31 proposed by Green and Corey (1971) and

Elzeftawy and Cartwright (1981) (Chapter 2), has been implemented in this program. The resulting profile is shown in Fig. 8.16b. According to this figure the minimum permeability associated with the minimum volumetric moisture content of the fine gravel (residual volumetric moisture content = 0.023 cm^3/cm^3) is about 0.0017 cm/s. The average flow rate observed in Tests AD6 and AD7 was $q = 5.2 \times 10^{-8}$ cm/s; taking the minimum value of 0.0017 cm/s for k, the resulting value of q/k will be a very small value of 3.06×10^{-5} which has no effect in denominator of the equation 8.3. This leads to the conclusion that $dz = -dp$ and hence, there will be no change in volumetric moisture content due to the applied flux. According to these results, the pressure head in entire unsaturated fine gravel will be hydrostatic. This seems unrealistic. According to the literature (e.g., Barbour and Yanful 1993), during drainage, the maximum negative pressure head that would develop in the coarse grained material underlying a fine grained material would be that associated with the residual water content. The pressure head associated with the residual water content of the fine gravel is about -4 cm which is quite low compared to that usually observed in finer material such as sand or silt. Due to a relatively open pore space in this material and very low residual water content which exists only in contact points of the adjacent grains and as a thin layer of water films around the grains, it is hypothesized that the air channels in this part of the profile are connected and hence the air pressure is likely to be close, or equal, to atmospheric pressure.

8.6 MASS BALANCE CALCULATIONS FOR CHLORIDE AND SODIUM

Mass balance calculations were performed for chloride and sodium and percent of mass recovery was calculated for each ion. The method of calculation used for chloride is the same as that used for the previously described advection-diffusion tests.

The adsorbed concentration of sodium was determined for clayey silt samples by a single wash of 10 g of wet soil with 100 mL of 0.01 molar silver thiourea solution (pH=7). The wash extraction was performed at a temperature of 22 °C, using a 250 mL polyethylene centrifuge tube. Upon agitation in a wrist action shaker for about 24 hours, the mixer was centrifuged at 10,000 rpm for 10 minutes and sodium supernatant concentrations measured by atomic absorption spectrophotometry.

Tables 8.4 and 8.5 summarize the results of the mass balance calculations for chloride and sodium respectively. According to the results, at the end of the tests, 98 and 99 percent or more the chloride and sodium mass were recovered, respectively.

8.7 SUMMARY AND CONCLUSIONS

The tests described in this chapter, were conducted as a continuation of a series of laboratory advection-diffusion experiments consisting of a two layer soil system having different characteristics. The difference in tests set up compared to the previous tests was that the second layer beneath the compacted clayey silt layer, was a coarser granular soil (gravel) and it was unsaturated.

De-saturation for gravel layer was obtained by gravity draining the material after

complete saturation. After placement of the clayey soil on top of the gravel and application of the source solution, migration started. After 63 and 80 days of migration, tests were terminated and samples were sliced and concentration in soil profiles was determined. The results showed that the migration in the unsaturated zone of the gravel layer was very slow and the concentration in this zone had dropped to a very low values when it is migrating downwards through the soil profile. As explained in previous chapters, when the soil is unsaturated, migration paths become very tortuous causing that the migration process to be much slower due to the longer path to be travelled by tracer. Theoretical prediction of the concentration profiles which were based on the parameters from the pure diffusive tests gave good agreement with the observed behaviour.

Two theoretical sensitivity analysis were performed first by replacing the unsaturated gravel with a saturated gravel layer, and then by a compacted clay layer. The results showed that the clayey silt over unsaturated gravel provided a better barrier for both anions such as Cl^- and cations such as Na^+, than an equivalent thickness of compacted clay layer for diffusive dominated migration.

The sensitivity of the analysis to the Darcy velocity at the observed range, was studied by neglecting the Darcy flux (v_a=0). The results showed that the Darcy velocity plays important role in migration and theoretical profiles no longer fit the observed data when it is neglected. This was in contrast with the finding in Chapter 5 when soils were almost saturated and the analysis was not sensitive to the Darcy velocity. This is due to the fact that at low levels of saturation in the soil, the flow paths become much narrower and hence water and contaminant moves faster in a zone where flow is limited to a small portion of the soil pore cross-section.

The results of a sensitivity analysis regarding the effect of assumed effective volumetric moisture content of the underlying gravel on predicted profiles (Test AD6) showed that the original assumption ($\theta_{effective} = \theta_{measured}$) gives the best fit to the experimental data. These results indicated that up to about 10% uncertainty in the θ and D_e values does not have significant effect on the results.

The effect of flux on the volumetric moisture content of the fine gravel layer was evaluated. The results showed that for the range of the permeability of the unsaturated fine gravel and applied flux, the volumetric moisture content of the fine gravel during the flux would be equal to that measured at the end of the test when flux was stopped and soil was sampled.

Mass balance calculations for Cl^- and Na^+ showed that there is no significant mass loss in the tests and almost all mass was recovered at the end of the tests.

TABLE 8.1 VALUES OF THE THICKNESS (H), MOISTURE CONTENT (W), DEGREE OF SATURATION (S), AND VOLUMETRIC MOISTURE CONTENT (θ) OF THE CLAY AND FINE GRAVEL SUB-LAYERS IN THE ADVECTION-DIFFUSION TESTS # AD6 AND AD7

	Test # AD6				Test # AD7			
	H^1 (cm)	W^2 (%)	S^3 (%)	θ^4	H^1 (cm)	W^2 (%)	S^3 (%)	θ^4
Clay sub-layers	1.22	16.31	100	0.304	1.25	16.40	100	0.305
	1.20	15.70	100	0.304	1.21	15.67	100	0.305
	1.25	14.73	94.3	0.286	1.22	15 38	97.8	0.298
	1.22	15.50	99.0	0.300	1.22	14.95	95.0	0.290
Porosity:				0.304				0.305
Fine gravel	1.65	2.41	10.2	0.039	1.65	2.82	11.9	0.045
	1.60	2.71	11.4	0.044	1.65	2.94	12.4	0.047
	1.60	3.41	14.4	0.055	1.60	4.22	17.8	0.068
	1.60	9.02	38.1	0.145	1.60	15.28	64.6	0.246
	1.60	22.13	93.6	0.357	1.60	22.64	95.7	0.365
	1.95	23.67	100	0.381	1.95	23.67	100	0.381
Porosity:				0.381				0.381

1 Thickness of soil sub-layer (cm)
2 Moisture content (%)
3 Degree of satur :tion (%)
4 Volumetric moisture content (cm^3/cm^3)

TABLE 8.2a VALUES OF THE THICKNESS (H), VOLUMETRIC MOISTURE CONTENT (θ), CHLORIDE EFFECTIVE DIFFUSION COEFFICIENT ($D_{e(Cl^-)}$), AND NORMALIZED DIFFUSION COEFFICIENTS (D_e/D_o, OR TORTUOSITY), FOR CLAYEY SILT AND FINE GRAVEL SUB-LAYERS USED IN THEORETICAL ANALYSIS OF THE TESTS # AD6 AND AD7

	Test # AD6				Test # AD7			
	H[1] (cm)	θ[2] (cm^3/cm^3)	$D_{e(Cl^-)}$[3] (m^2/s)	D_e/D_o[4] (-)	H[1] (cm)	θ[2] (cm^3/cm^3)	$D_{e(Cl^-)}$[3] (m^2/s)	D_e/D_o[4] (-)
Clayey-silt	1.22	0.304	6.3×10^{-10}	0.303	1.25	0.305	6.3×10^{-10}	0.308
	1.20	0.304	6.3×10^{-10}	0.303	1.21	0.305	6.3×10^{-10}	0.308
	1.25	0.287	6.0×10^{-10}	0.286	1.22	0.298	6.2×10^{-10}	0.297
	1.22	0.300	6.2×10^{-10}	0.303	1.22	0.290	6.0×10^{-10}	0.292
Fine-gravel	1.65	0.039	1.1×10^{-10}	0.059	1.65	0.045	1.2×10^{-10}	0.065
	1.60	0.044	1.2×10^{-10}	0.065	1.60	0.047	1.3×10^{-10}	0.070
	1.60	0.055	1.5×10^{-10}	0.081	1.60	0.068	1.9×10^{-10}	0.103
	1.60	0.145	4.0×10^{-10}	0.216	1.60	0.246	6.7×10^{-10}	0.362
	1.60	0.357	9.8×10^{-10}	0.530	1.60	0.365	10.0×10^{-10}	0.539
	1.95	0.381	10.4×10^{-10}	0.562	1.95	0.381	10.4×10^{-10}	0.562

1 - Thickness of the soil sub-layer (cm)
2 - Volumetric moisture content (cm^3/cm^3)
3 - Effective diffusion coefficient (m^2/s), $D_e = D_{e(sat.)}(\theta/\theta_{sat.})$, where $D_{e(sat.)}$ and $\theta_{sat.}(=n)$ are the effective diffusion coefficient and volumetric moisture content of the saturated sample.
4 - Normalized diffusion coefficient or tortuosity, $D_e/D_o = \tau = \tau_{sat.}(\theta/\theta_{sat.})$

TABLE 8.2b VALUES OF THE VOLUMETRIC MOISTURE CONTENT (θ), SODIUM DIFFUSION COEFFICIENT (D_{Na}^{+}), AND DISTRIBUTION COEFFICIENT (K_d) FOR THE CLAYEY SILT AND FINE GRAVEL SUB-LAYERS USED IN THEORETICAL ANALYSIS OF THE TESTS # AD6 & AD7

	Test # AD6			Test # AD7		
	θ^2 (cm^3/cm^3)	D_{Na}^3 (m^2/s)	K_d^3 (mL/g)	θ^2 (cm^3/cm^3)	D_{Na}^3 (m^2/s)	k_d^3 (mL/g)
Clayey silt	0.304	$5.6x10^{-10}$	0.15	0.305	$5.6x10^{-10}$	0.15
	0.304	$5.6x10^{-10}$	0.15	0.305	$5.6x10^{-10}$	0.15
	0.287	$5.3x10^{-10}$	0.15	0.298	$5.5x10^{-10}$	0.15
	0.300	$5.5x10^{-10}$	0.15	0.290	$5.3x10^{-10}$	0.15
Fine gravel	0.039	$7.0x10^{-11}$	0	0.045	$8.1x10^{-11}$	0
	0.044	$7.8x10^{-11}$	0	0.047	$8.5x10^{-11}$	0
	0.055	$9.9x10^{-11}$	0	0.068	$1.2x10^{-10}$	0
	0.145	$2.6x10^{-10}$	0	0.246	$4.4x10^{-10}$	0
	0.357	$6.4x10^{-10}$	0	0.365	$6.6x10^{-10}$	0
	0.381	$6.9x10^{-10}$	0	0.381	$6.9x10^{-10}$	0

1 Volumetric moisture content
2 Diffusion coefficient of sodium
3 distribution coefficient

TABLE 8.2c OTHER INPUT DATA USED IN THEORETICAL ANALYSIS OF THE TESTS # AD6 & AD7

	Test # AD6		Test # AD7	
	clayey silt	fine gravel	clayey silt	fine gravel
Soil thickness (cm)	4.89	10.0	4.90	10.0
Soil Cl^- background Concn. (mg/L)	125	10.5	125	10.5
Soil Na^+ background Concn. (mg/L)	78	6	78	6
Source Cl^- concn. (mg/L)	1870		1870	
Source Na^+ concn. (mg/L)	1170		1160	
Height of source solution (Hr) (cm)	2.90		2.87	
Leachate (NaCl) collected (q_c) (m/s)	2.17×10^{-9}		1.92×10^{-9}	
Base outflow velocity (v_b) (m/s)	1.70×10^{-9}		1.74×10^{-9}	
Darcy velocity (m/s)	4.6×10^{-10}		5.8×10^{-10}	
Duration of the test (days)	63		80	

TABLE 8.3 VALUES OF THE FLUX INTO SOIL AND INTO BASE, AND CONCENTRATION IN THE BASE FOR Na^+, OBTAINED FROM THEORETICAL ANALYSIS OF THE TESTS # AD6 & AD7, (a): ASSUMING 15 cm THICK CLAY LAYER, (b): 5 cm CLAY AND 10 cm UNSATURATED GRAVEL LAYER

	Test #AD6	Test #AD7
a) 15 cm clay layer		
Flux into soil	1257.2	1320.0
Flux into base	152.3	187.2
Concn. in base	32.2	37.0
b) 5 cm clay, 10 cm unsaturated gravel		
Flux into soil	1198.3	1221.5
Flux into base	10.0	33.5
Concn. in base	6.3	10.6

TABLE 8.4 SUMMARY OF THE CHLORIDE MASS BALANCE CALCULATIONS FOR CLAYEY SILT-FINE GRAVEL, ADVECTION-DIFFUSION TESTS # AD6 AND AD7

Test #	Initial Mass (mg)			Final Mass (mg)				Percent Recovery (%)
	in source and receptor	in gravel and clay	total mass	in source and receptor	in gravel and clay	mass removed	total mass	
AD6	5.33	0.193	5.52	2.16	1.64	1.65	5.45	98.7
AD7	5.59	0.181	5.77	2.30	1.60	1.84	5.74	99.5

TABLE 8.5 SUMMARY OF THE SODIUM MASS BALANCE CALCULATIONS FOR CLAYEY SILT-FINE GRAVEL, ADVECTION-DIFFUSION TESTS # AD6 AND AD7

Test #	Initial Mass (mg)				Final Mass (mg)					Percent Recovery
	in source and receptor	in soils pore water	adsorbed mass	total mass	in source and receptor	in soils pore water	adsorbed mass	mass removed	total mass	(%)
AD6	3.42	0.122	2.86	6.40	1.33	0.84	3.16	1.01	6.34	99.03
AD7	3.23	0.121	2.88	6.35	1.23	0.84	3.17	1.09	6.33	99.70

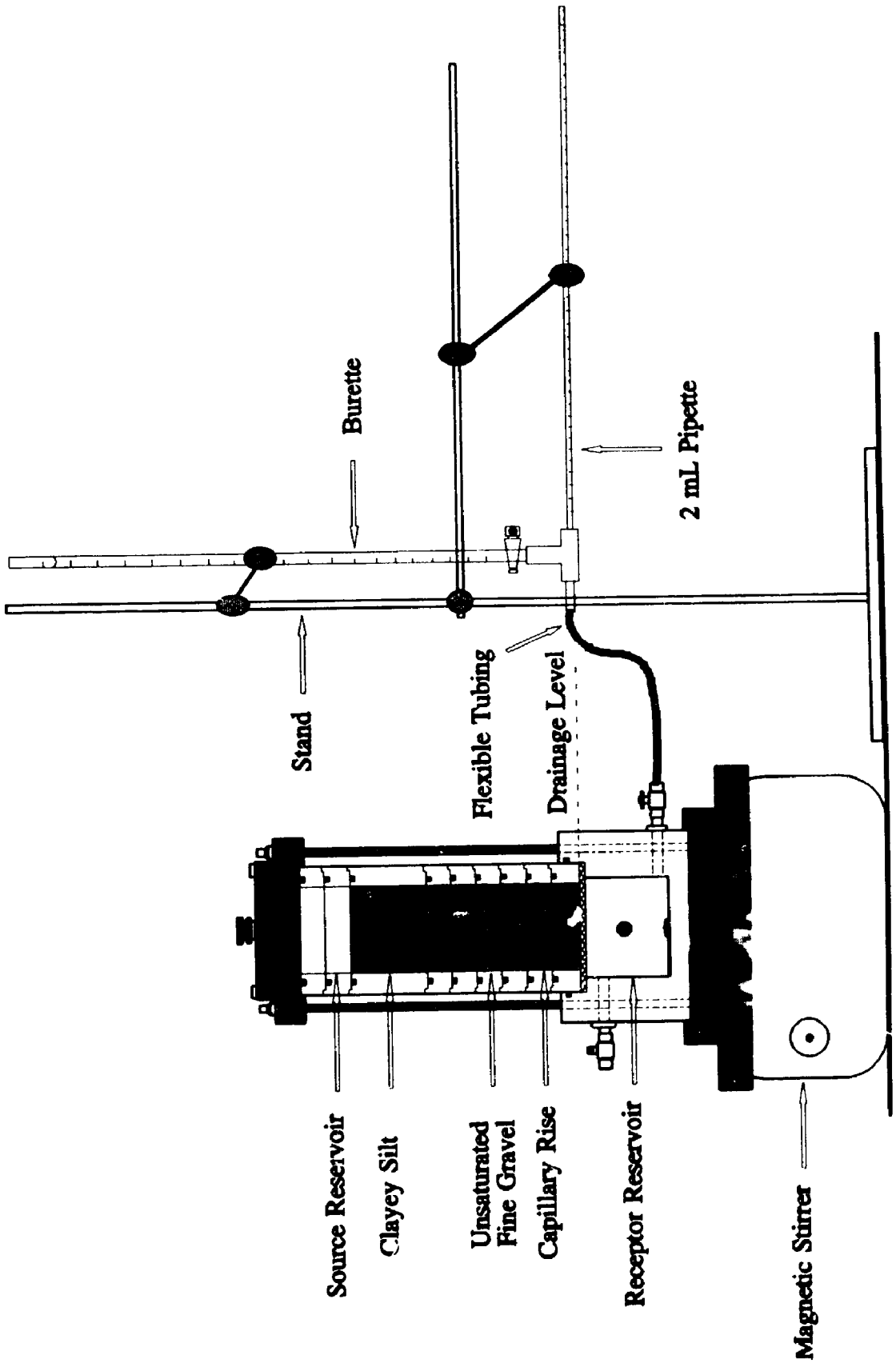

FIG. 8.1 SCHEMATIC OF THE CLAYEY SILT-UNSATURATED FINE GRAVEL ADVECTION-DIFFUSION TESTS SET UP

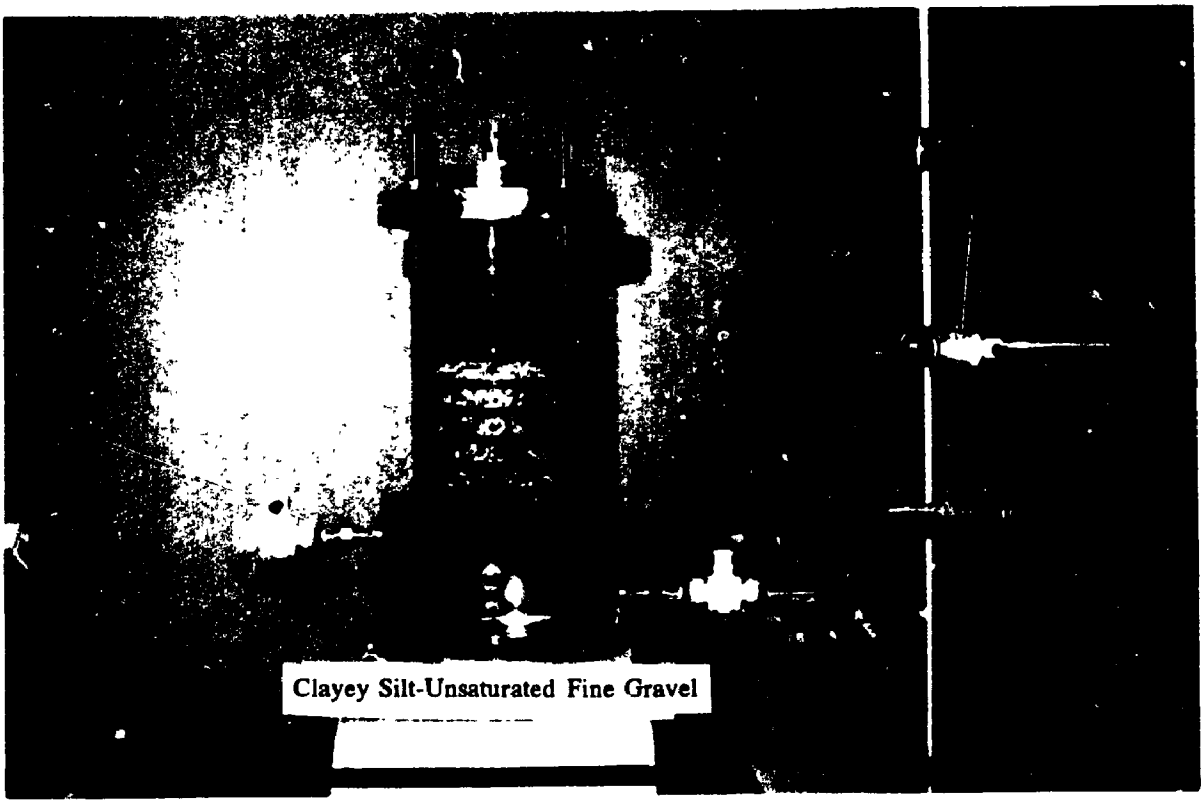

FIG. 8.2 VIEW OF THE ADVECTION-DIFFUSION TEST ON CLAYEY SILT-UNSATURATED FINE GRAVEL

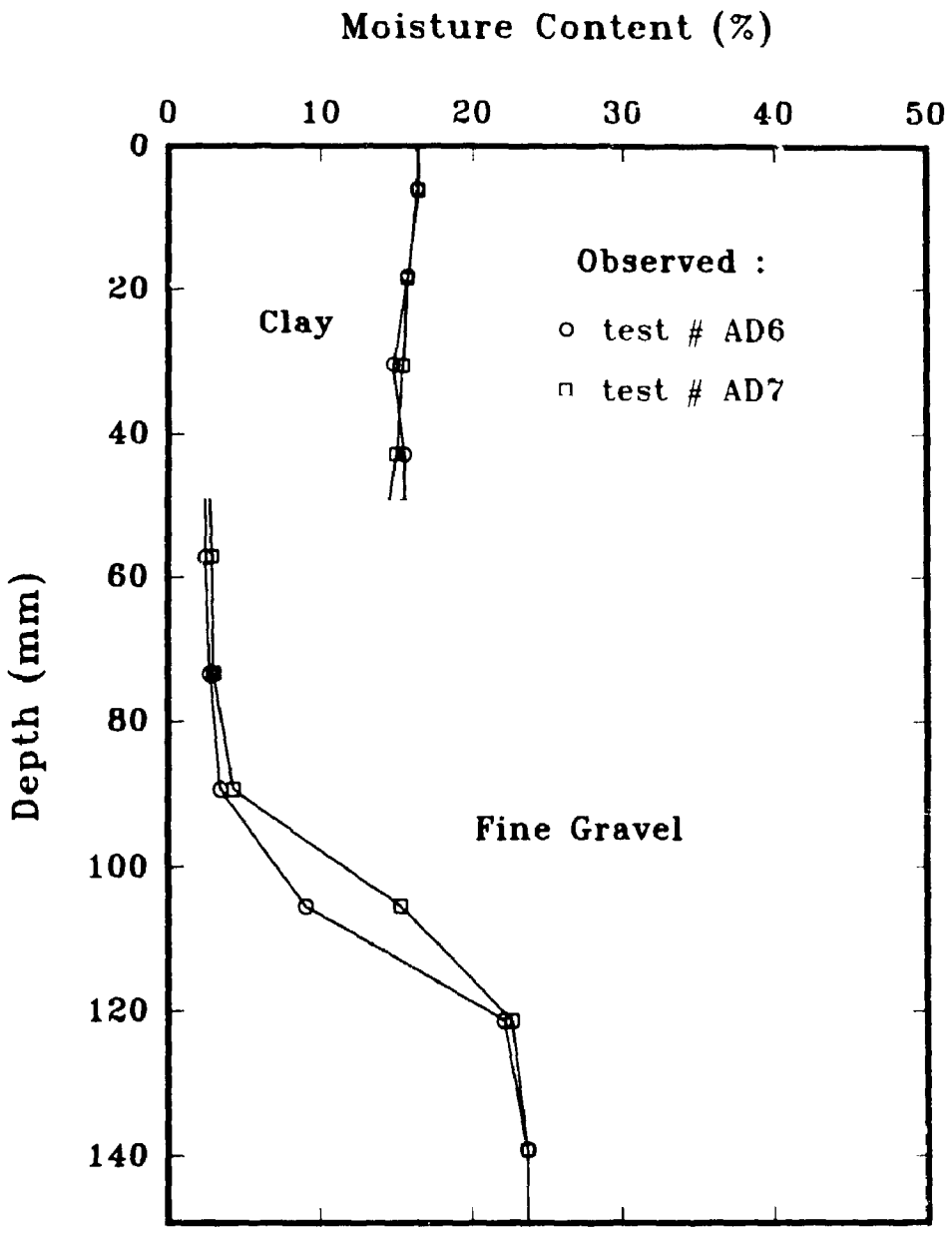

FIG. 8.3 MOISTURE CONTENT PROFILES IN CLAYEY SILT-FINE GRAVEL ADVECTION-DIFFUSION TESTS # AD6 AND AD7

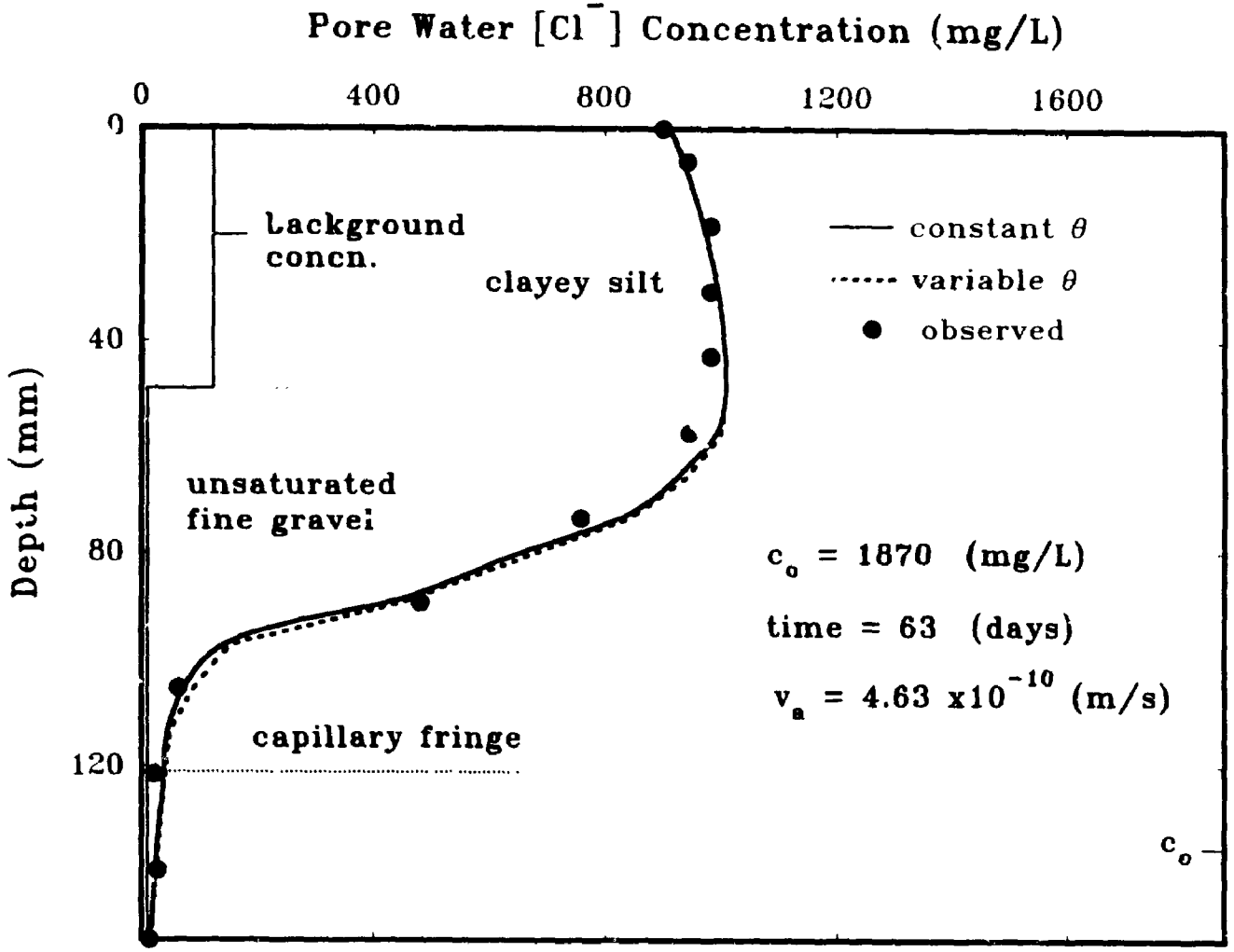

FIG. 8.4 OBSERVED AND THEORETICAL "BEST FIT" [Cl⁻] CONCENTRATION PROFILES IN ADVECTION-DIFFUSION TEST #AD6 (CLAYEY SILT-UNSATURATED FINE GRAVEL)

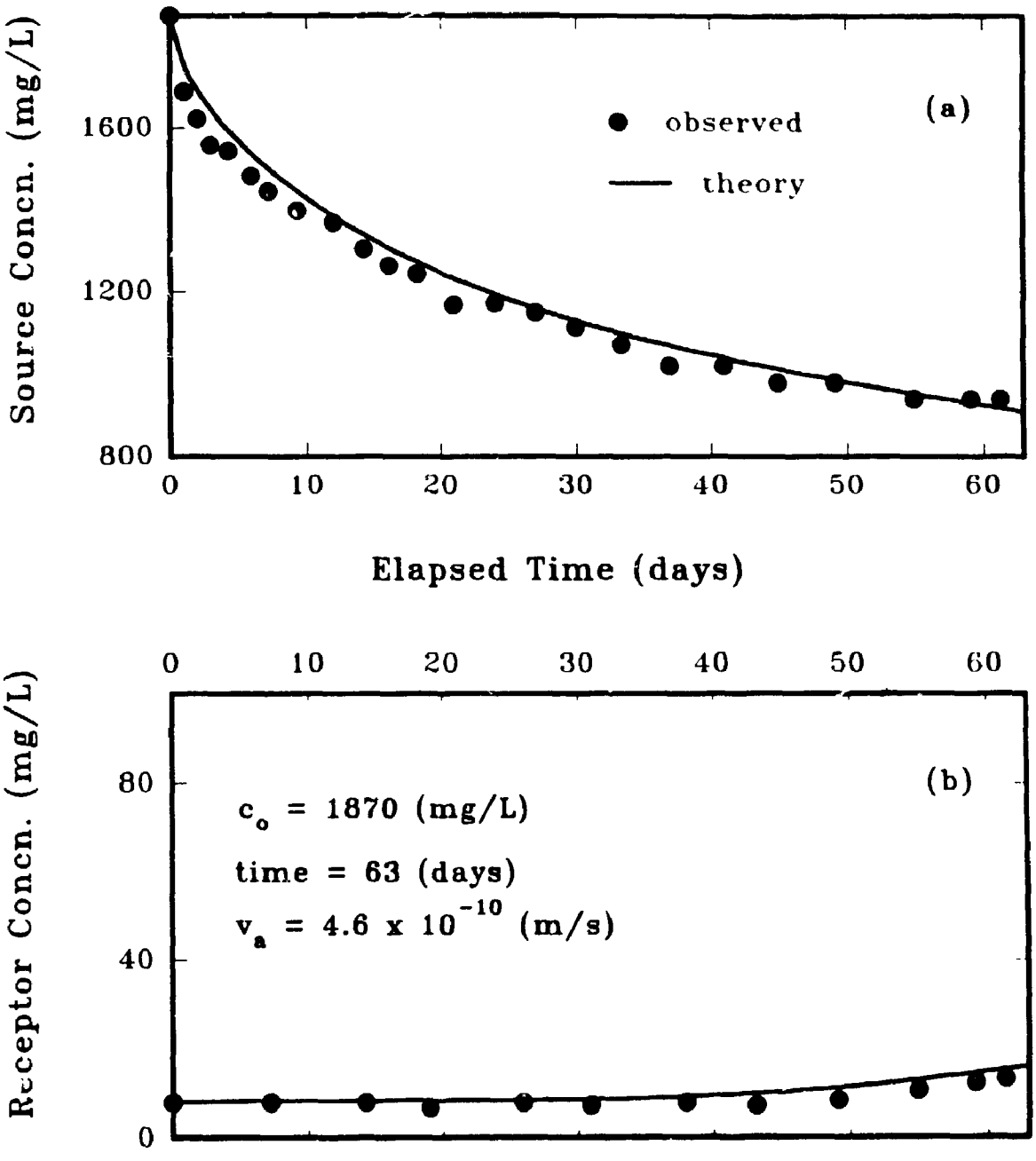

FIG. 8.5 OBSERVED AND THEORETICAL [Cl^-] CONCENTRATIONS VS ELAPSED TIME IN : (a) SOURCE RESERVOIR, AND (b) RECEPTOR RESERVOIR, DURING ADVECTION-DIFFUSION TEST #AD6 (CLAY-UNSATURATED, FINE GRAVEL)

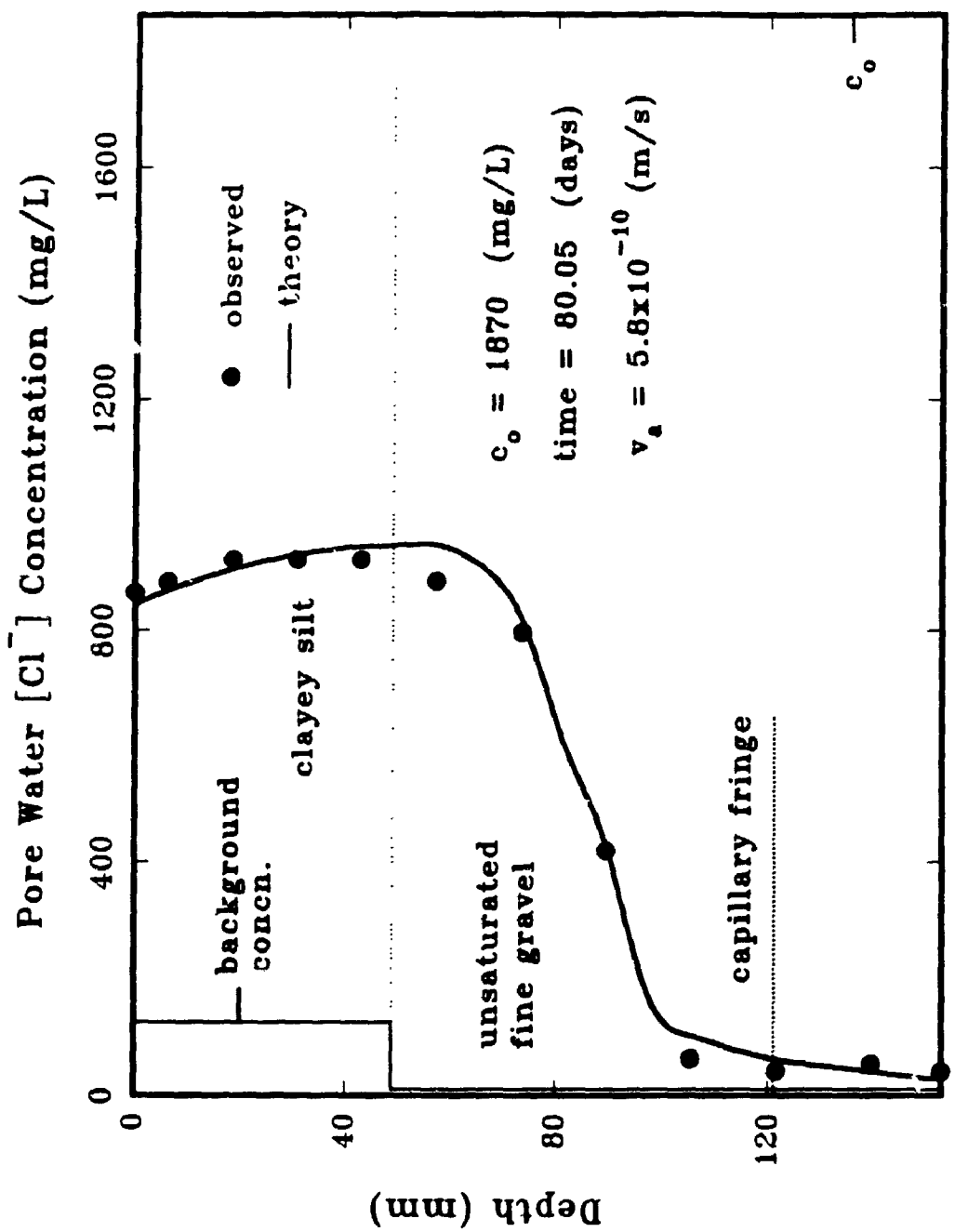

FIG. 8.6 OBSERVED AND THEORETICAL "BEST FIT" [Cl^-] CONCENTRATION PROFILES IN ADVECTION-DIFFUSION TEST #AD7 (CLAYEY SILT-UNSATURATED FINE GRAVEL)

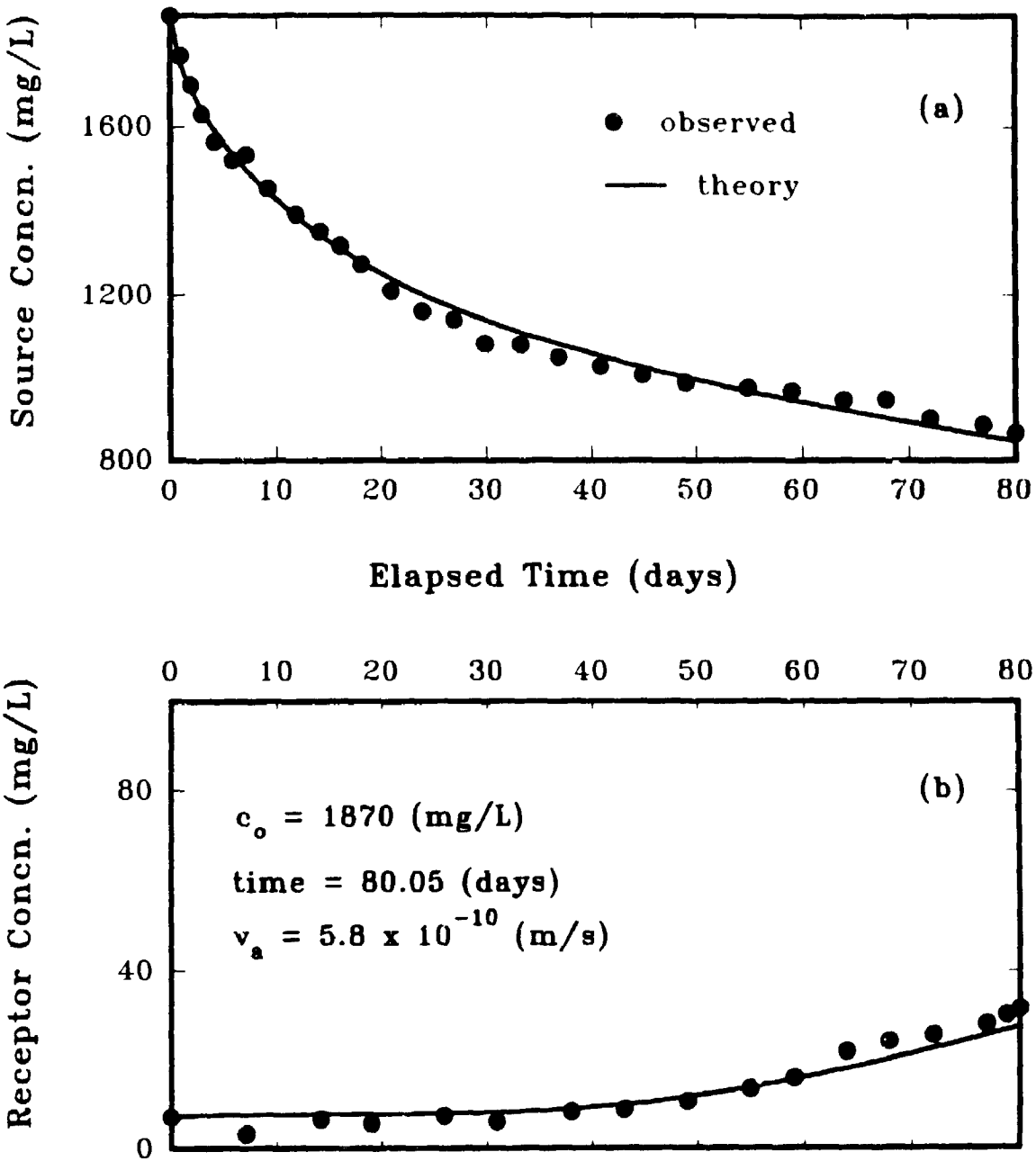

FIG. 8.7 OBSERVED AND THEORETICAL [Cl^-] CONCENTRATIONS VS ELAPSED TIME IN : (a) SOURCE RESERVOIR, AND (b) RECEPTOR RESERVOIR, DURING ADVECTION-DIFFUSION TEST #AD7 (CLAYEY SILT-UNSATURATED FINE GRAVEL)

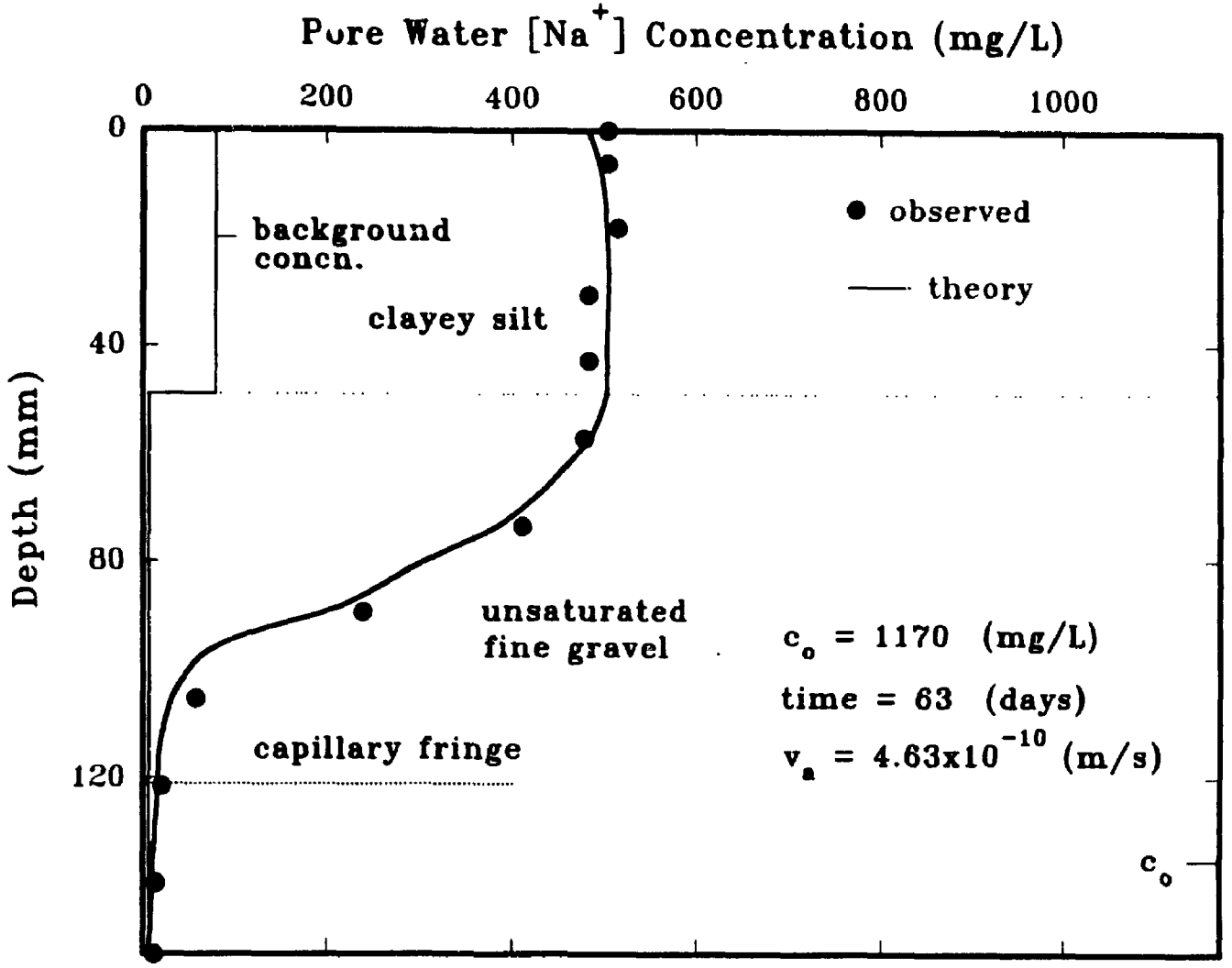

FIG. 8.8 OBSERVED AND THEORETICAL "BEST FIT" [Na^+] CONCENTRATION PROFILES IN ADVECTION-DIFFUSION TEST #AD6 (CLAYEY SILT-UNSATURATED FINE GRAVEL)

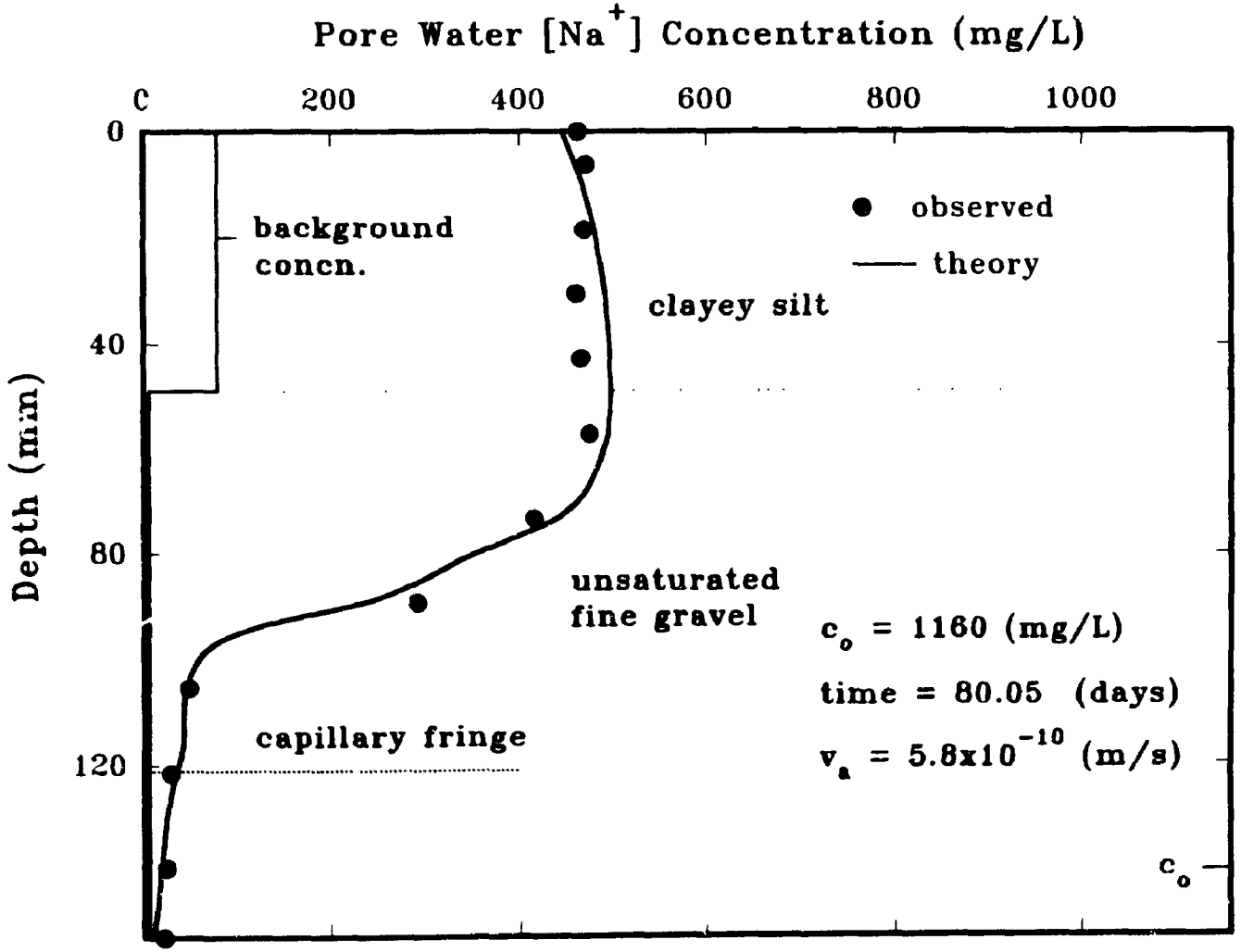

FIG. 8.9 OBSERVED AND THEORETICAL "BEST FIT" [Na^+] CONCENTRATION PROFILES IN ADVECTION-DIFFUSION TEST #AD7 (CLAYEY SILT-UNSATURATED FINE GRAVEL)

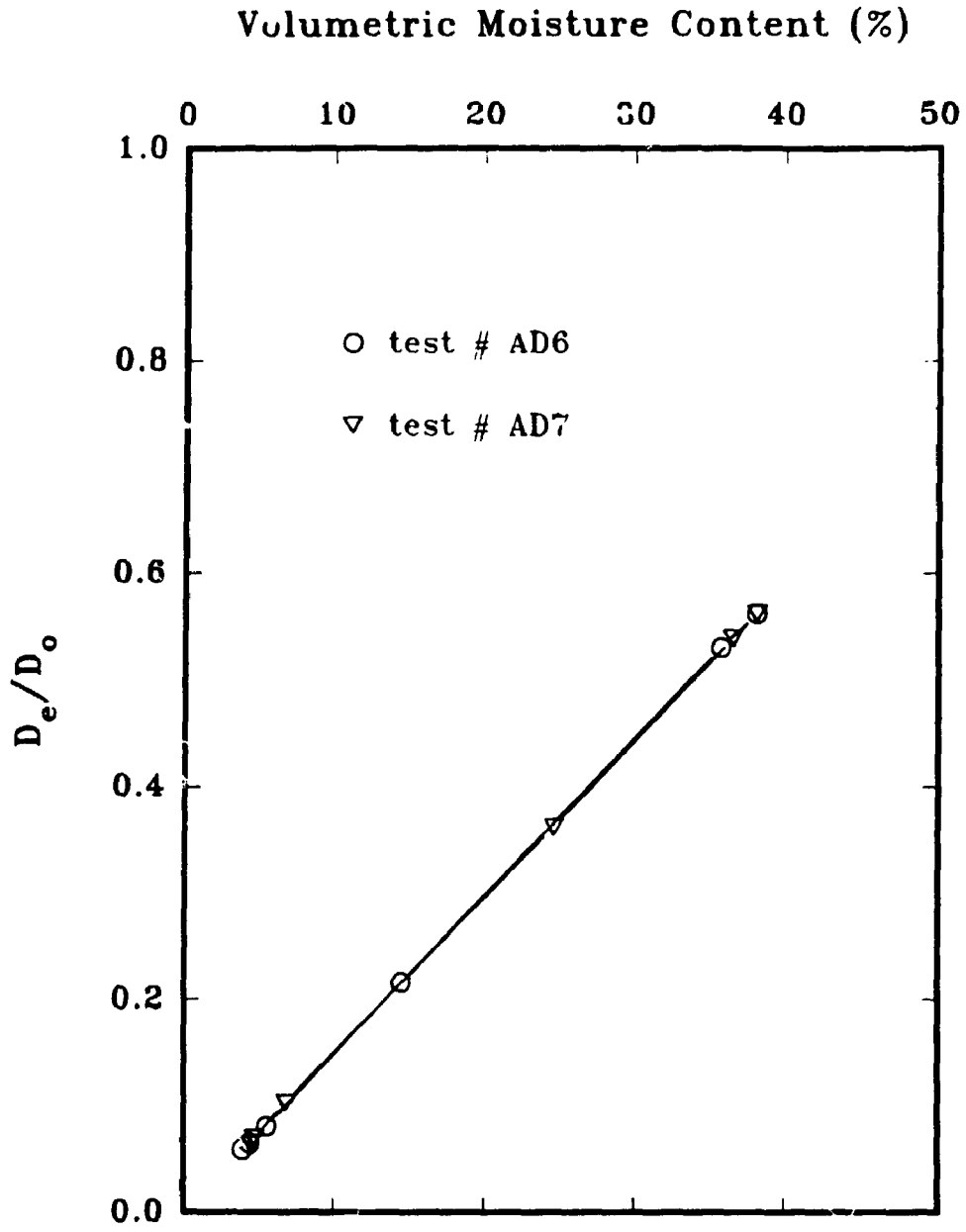

FIG. 8.10 FUNCTIONAL RELATIONSHIP BETWEEN NORMALIZED DIFFUSION COEFFICIENT (D_e/D_o) AND VOLUMETRIC MOISTURE CONTENT IN FINE GRAVEL SUBLAYERS OF ADVECTION DIFFUSION TESTS # AD6 AND AD7

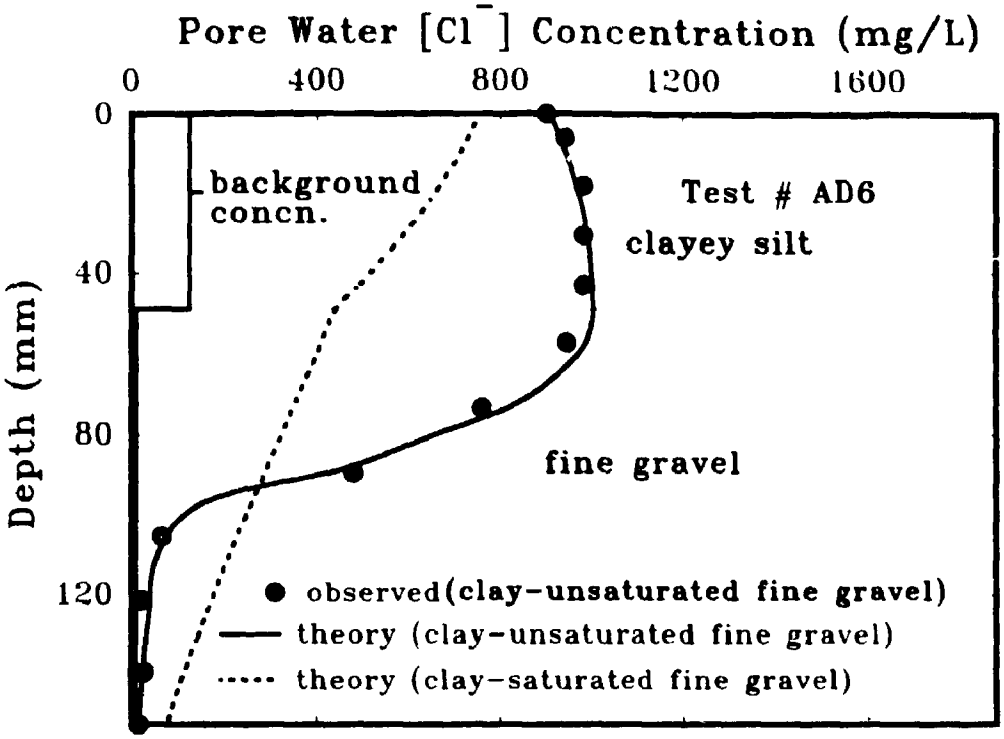

FIG. 8.11 COMPARISON OF THE RESULTS OF TEST #AD6 WITH THE RESULTS OF A THEORETICAL ANALYSIS ASSUMING FINE GRAVEL LAYER IS SATURATED

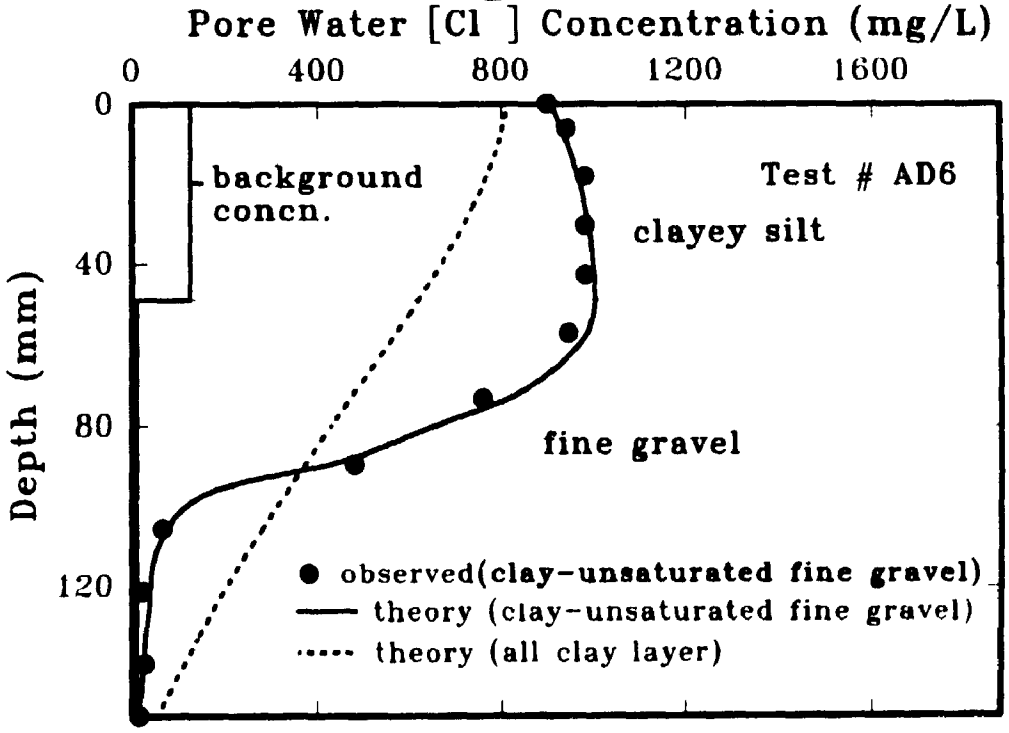

FIG. 8.12 COMPARISON OF THE RESULTS OF TEST #AD6 WITH THE RESULTS OF A THEORETICAL ANALYSIS ASSUMING UNSATURATED FINE GRAVEL LAYER IS REPLACED WITH A CLAY LAYER

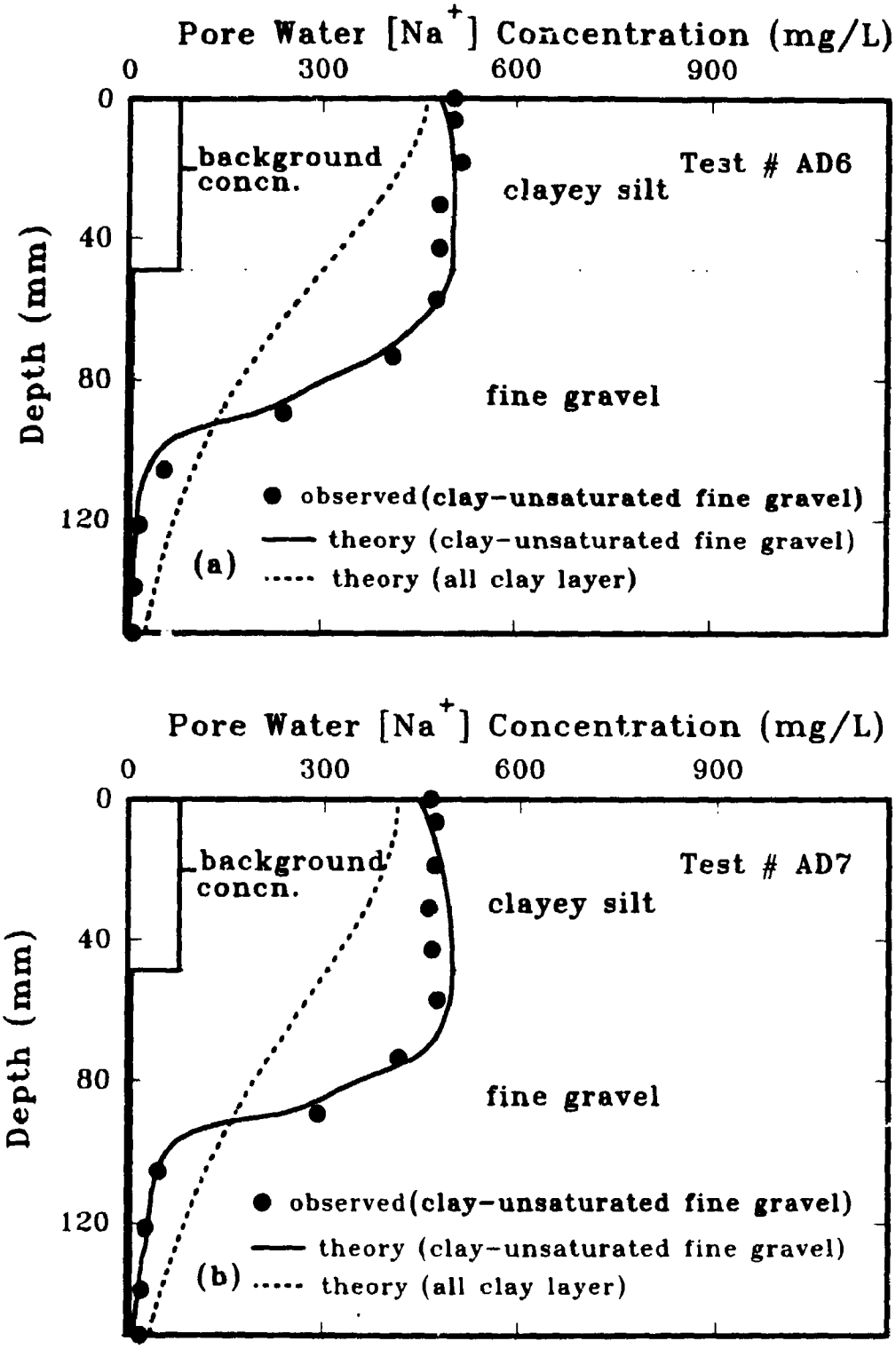

FIG. 8.13 COMPARISON OF THE RESULTS OF (a): TEST #AD6 AND (b): TEST #AD7 (FOR Na^+), WITH THE RESULTS OF A THEORETICAL ANALYSIS ASSUMING UNSATURATED FINE-GRAVEL LAYER IS REPLACED WITH A CLAY LAYER

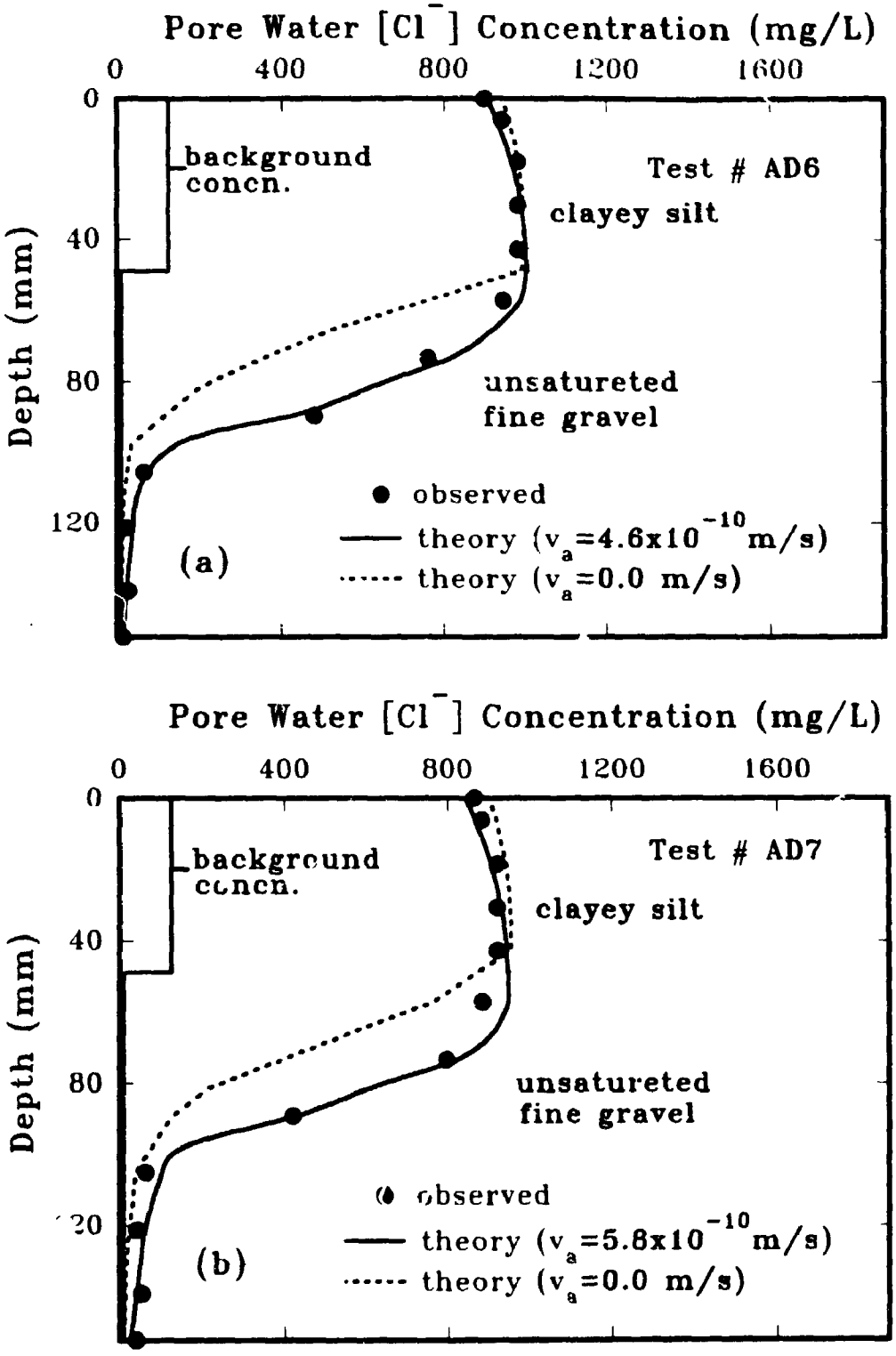

FIG. 8.14 EFFECT OF THE DARCY VELOCITY ON THE THEORETICAL CONCENTRATION PROFILES IN ADVECTION-DIFFUSION TESTS (a) #AD6, AND (b) #AD7

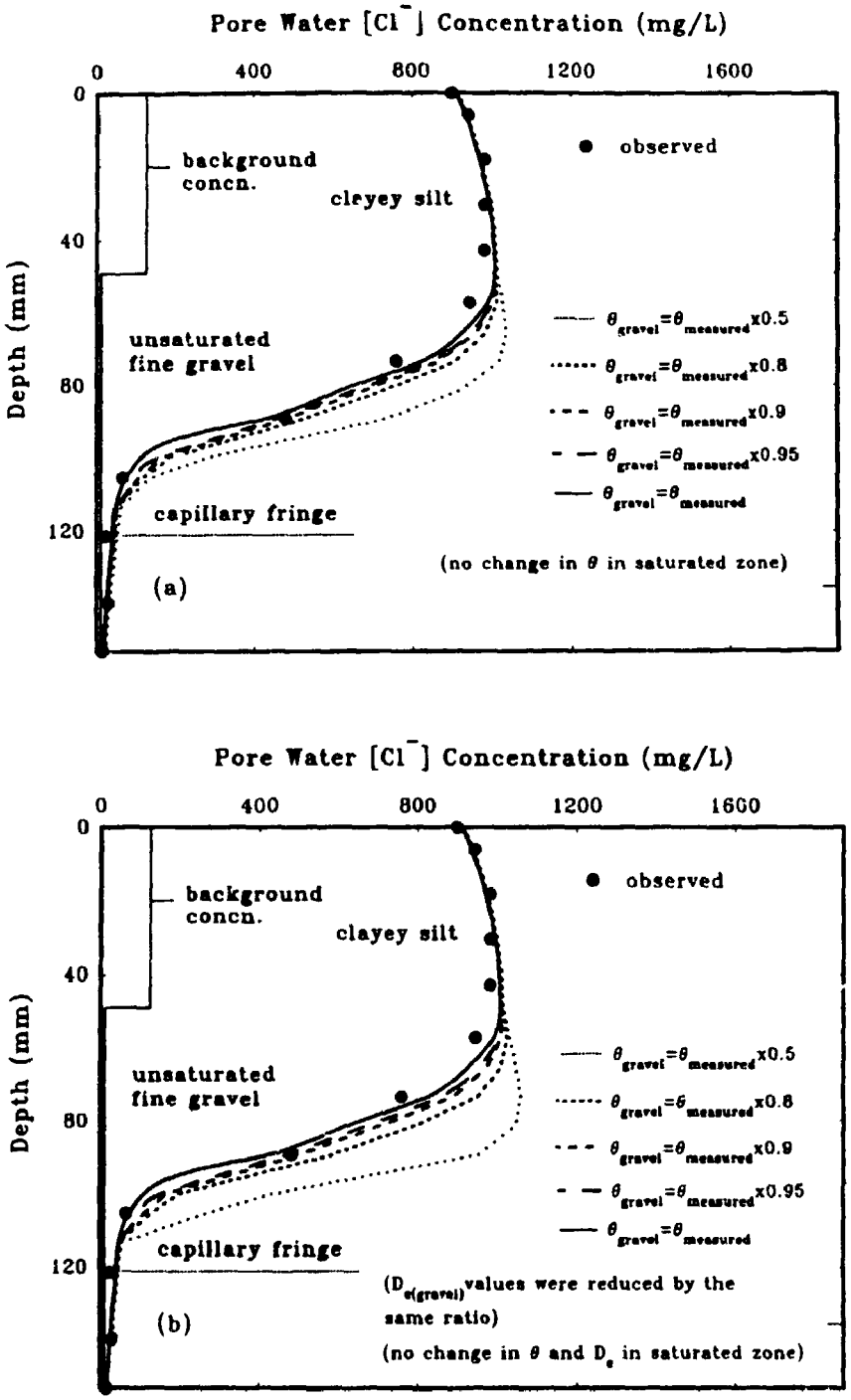

FIG. 8.15 EFFECT OF REDUCED VOLUMETRIC MOISTURE CONTENT (a), AND VOLUMETRIC MOISTURE CONTENT AND EFFECTIVE DIFFUSION COEFFICIENT (b) OF THE UNDERLYING UNSATURATED FINE GRAVEL ON CALCULATED CONCENTRATION PROFILES (TEST AD6)

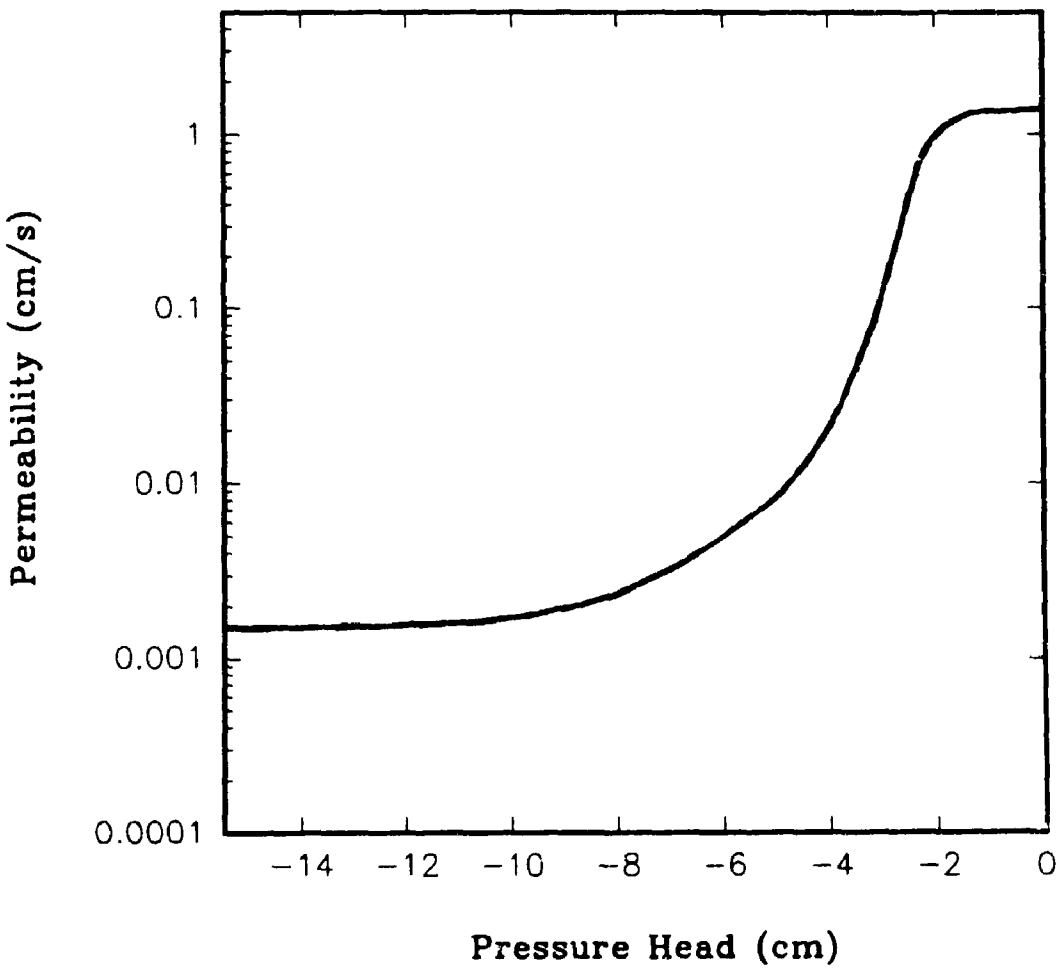

FIG. 8.16 PERMEABILITYY VERSUS PRESSURE HEAD IN UNSATURATED FINE GRAVEL

CHAPTER 9

ADVECTION-DIFFUSION TESTING IN A TWO-LAYER SILT-UNSATURATED CLEAR STONE SYSTEM, UNDER "HIGH" AND "MODERATE" ADVECTIVE FLOW

9.1 INTRODUCTION

This part of the research program comprises the laboratory and theoretical study of contaminant migration through a two-layer system of silt (with trace clay, trace sand and some clay, trace sand) or clayey silt soils underlain by unsaturated clear stone for the case of relatively "high", "moderate" and "low" flow rates. A large scale apparatus was designed and built for this kind of laboratory testing. A total of four tests were performed, two were used for advection diffusion testing on two-layer system of clayey silt soil over clear stone, under "low" flow rate which will be discussed in Chapter 10. One apparatus was used for the "high" and "moderate" flow rate testing discussed in this chapter.

The configuration of the tests described in this chapter comprises a 12 cm thick compacted silt (with trace clay, trace sand and some clay, trace sand) on top of 38 cm thick layer of clear dolomitic stone with a typical diameter of 3.8 cm (1.5 inch). The source solution was poured on top of the silt layer, and effluent samples were collected from a receptor reservoir underneath the stone layer. The compacted silt layer was almost saturated compared to the clear stone layer which was unsaturated with a very low volumetric moisture content. This layer simulates a secor. ary leachate collection system

of a landfill overlain by a permeable or moderately permeable silt liner.

The general geometry of the tests is similar to the small scale advection-diffusion tests conducted on two-layer soil system of clayey silt-unsaturated fine gravel materials (Chapter 8).

As demonstrated in Chapter 8, coarse-grained unsaturated material could be considered as a good diffusion barrier as long as the material remains unsaturated and the hydrogeological and engineering conditions result in negligible or low advective flow through the soil stratigraphy. The results of the field study by Gerhardt (1984) indicated that leachate migration through the unsaturated gravel layer below a landfill site, was quite low compared to that through the surrounding sand layers. However this was not well quantified. The objective of this chapter is to examine the behaviour of a barrier underlain by an unsaturated stone layer under condition of "high" and "moderate" flow rate through the barrier and underlying stone.

Two tests were conducted in this part of the study; the first test which will be referred to as Test #AD8, was conducted with a relatively high permeability ($\sim 4.6 \times 10^{-8}$ m/s) silt with a trace of clay and sand material, on top of the unsaturated stone layer and had a test duration of 14.74 days. The Darcy velocity through the barrier and stone in this test was 8.1×10^{-8} m/s (i.e. 2.6 m/a) and is "high" compared to what one would reasonably expect in a landfill situation. Thus it represents an upper bound on the effect of contaminant migration through a barrier system such as being examined here. The second test which will be referred to as Test #AD9, had the same geometric configuration as Test #AD8 but a lower permeability (2.03×10^{-9} m/s) silt with some clay and a trace of sand, was used and the test duration was 160 days. The Darcy velocity

in this test was 3.9×10^{-9} m/s (0.12 m/a). This is at the upper end of the likely rate of advective movement through a barrier system such as being considered here, but is not unrealistic. It is therefore denoted as the "moderate" flow case.

9.2 APPARATUS DESIGN

Fig. 9.1 shows the schematic of the apparatus used in this part of the study program. This apparatus was made of plexiglass sheets to allow the direct view of the soil and stone samples and also source and receptor reservoir solutions inside the apparatus. It was built of 3 major square cross-sectional chambers (35.6 cm x 35.6 cm) and a top plexiglass plate, which were clamped together by a series of steel bolts and nuts installed in circular openings around the plexiglass clamping flanges glued to the top and bottom of the chambers. The base chamber which served as a receptor reservoir had a 11.5 cm inside height and was sealed at its bottom by a square plexiglass sheet. Fitted to the base chamber were inlet and outlet P.V.C valves, an overflow steel pipe connected to the outlet valve (shown in Fig. 9.2), a septum port, and a small drainage port at the base. The inlet and outlet valves were used for filling and draining the cell. The small drainage port installed at the base plate was used to drain solution in the chamber which could not be drained by the outlet valve. A flexible plastic tubing connected to this port facilitated the drainage process and was also used as a stand pipe for monitoring the receptor reservoir solution level during the test (shown in Fig. 9.3). The septum port, located on the front face of the chamber, was used for receptor solution sampling. A shoulder along the top of the inside wall of the base chamber supported a perforated

stainless steel plate. This plate supported the clear stone. An 'O' ring groove was cut into the top surface of the flange located at the top of the base chamber. This 'O' ring sealed the joint along the flanges. Mixing of the receptor solution was accomplished by a magnetic stirrer placed beneath the base chamber with a 5 cm length magnetic bar inside the chamber.

On top of the receptor reservoir chamber, the intermediate chamber with 38 cm height was located, which was filled with clear stone. This chamber had the same inner and outer cross-sectional area as the receptor chamber. A small 3 mm diameter opening on the top right corner in the front face of the chamber, which was partially covered by cloth, served as an air inlet (vent) to maintain atmospheric pressure inside the chamber and to release any excess pressure which might be built up during installation of the material or during the test (Fig. 9.1). The silt soil sample which was compacted on top of the stone, was separated from the stone by a geotextile. A shoulder along the top of the inside wall of the intermediate chamber supported the geotextile. A series of 1 cm width tapes, 3.8 cm apart and parallel to each other, were stacked to the front and back faces of the chamber and were used as a guide lines during sectioning the stones at the end of the test shown in Figs. 9.3 and 9.4.

The upper chamber, 30 cm in height, on top of the intermediate chamber, was used for installation of the soil, with the thickness of about 12 cm and also application of the source solution (about 12 cm in height) on top of the soil. Two parallel lines 12 cm apart on all faces of the chamber were drawn and used as a guide lines during installation of the soil and application of the source solution. A septum port in front face of the chamber at the level of 29 cm above the interface of the intermediate and upper

chambers, was used for source solution sampling.

The top plexiglass plate (47 cm x 47 cm) included a teflon shaft with 3 teflon paddles for mixing the source solution. The teflon shaft was connected to a clock motor to rotate the shaft in a slow continuous speed. The length of the teflon shaft was designed so that when the top plate is in place, all teflon paddles will be immersed in source reservoir.

9.3 MATERIALS, DESCRIPTION AND PREPARATION

Silt with trace clay, trace sand and silt with some clay, trace sand

The silt sample used for these experiments was prepared in the lab, by mixing the air-dried silt soil (Fig. 6.1), passed through the #60 sieve, with the air-dried clayey soil (Fig. 4.1), passed through sieve #40. The silt soil was obtained from the Upper Smallman property in London Ontario. About 26 kg and 18 kg air-dried silt sample were prepared for Tests # AD8 and AD9 respectively, by pulverizing the original soil and passing it through a #60 sieve. Some physical chemical and mineralogical characteristics of the Upper Smallman silt was shown in Table 6.1 (Chapter 6). The clayey soil was obtained from Halton Waste Management Site in Milton Ontario. Some physical, chemical, and mineralogical characteristics of the clayey soil were shown in Table 4.2 (Chapter 4). The Halton soil was air-dried, pulverized, and oversize material was removed by passing soil through a #4 sieve. Material passed from a #4 sieve was pulverized again and oversize material was removed by passing soil through sieve #40. About 6.5 kg and 14.5 kg of clayey soil was prepared using above method for Tests #

AD8 and AD9, respectively. In order to obtain soils with two different hydraulic conductivities, prepared silt (passing #60 sieve) and clayey soils (passing the #40 sieve) were mixed in different percentages for the two tests. To achieve the desired grain size distribution in the combined soil, for Test #AD8 the relative percentages of silt and clayey sample were 80% and 20%, and for Test #AD9, 55% and 45% respectively. The resulting grain size distributions of the prepared soils are shown in Fig. 9.5. According to the Canadian Foundation Engineering Manual, the soils prepared for Tests # AD8 and AD9 could be described as "silt, trace clay, trace sand" and "silt, some clay, trace sand" respectively. In the remainder of this chapter, these soils will be referred to as "silt".

The Atterberg limit tests were performed on prepared soils to measure the liquid and plastic limits. Soil prepared for Test #AD8 with ~ 10 percent clay content (Fig. 9.5) had a liquid limit of 17.9% but due to a low clay content, the plastic limit test was not applicable on the sample tested. Soil prepared for Test #AD9 with about 17% clay content (Fig. 9.5) had liquid and plastic limits of 19.3% and 15.2% respectively (PI = 4.1%). Using these values and index chart, the soil falls into the CL-ML soils region (dashed area in the chart) for soils having relatively low liquid limit and plasticity index.

Prior to the Test #AD8, a series of compaction tests were performed on prepared soil using the Harward Miniature compaction apparatus, to measure the optimum moisture content of the soil. The resulting moisture content-dry density plot is shown in Fig. 9.6. The optimum moisture content of 12.5% with the maximum dry density of 1.83 g/cm^3 was obtained from this figure. Two variable head hydraulic conductivity tests were conducted on 2 samples using the Harward Miniature compaction apparatus and the average hydraulic conductivity of 1.7×10^{-8} m/s was obtained at an average water content

of 15%. A soil having a hydraulic conductivity in this range is expected to result in a high Darcy velocity through the soil-stone layers, under the test hydraulic gradient of about 2 (more accurate values of hydraulic conductivity, Darcy velocity and hydraulic gradient were obtained during the tests which will be discussed later). A higher percentage of the clayey soil was used for Test #AD9 than for Test #AD8, so as to give a lower hydraulic conductivity of the soil in Test #AD9.

The mixed dry soil was spread in shallow trays and wetted with tap water using a spray until the desired moisture content (13-14 %) was reached. The wet soil was divided into 3 equal parts and each part was used to compact one lift.

Clear stone

The stone used for the tests was 38 mm (1.5 inch) diameter dolomitic stone obtained from Steetley quarries near Hamilton Ontario. This material was the same as that being used in leachate collection system of the Halton Waste Management site in Milton Ontario. The grain size distribution of the stone is shown in Fig. 9.5 and Table 9.1 shows some of its physical, chemical and mineralogical characteristics. The original stones obtained from the quarry contained a cohesive material coated on to the surface of the stones. The preliminary testing (to be explained soon) showed that the stones contain a significant Cl^- background concentration which was detected after washing the stones. To cleanup the stones from their original background concentration, successive wash tests were conducted using three 4.5 L capacity plastic containers which were filled with stones. After placement, the weight of the dry stones in each container was measured and recorded. Each container was filled with distilled water and the weight

of water was measured and recorded. The containers then were placed on a heavy duty shaker and were shaken for 45 minutes in 250 rpm (Fig. 9.7). At the end of the first wash, 2 wash water (supernatant) samples were taken from each container, the remaining wash water in each container was drained and samples were washed with distilled water to make sure that stones had been cleaned of wash water. The containers were then filled with fresh distilled water, weighed, and the weight of added water was recorded. The second wash was performed on samples for another 45 minutes after which 2 wash water samples were collected from each container. This procedure was repeated 2 more times and wash water samples were collected at the end of each process. 24 wash water samples were collected at the end of the wash test and these were analyzed for chloride.

In order to back figure the background concentrations from the measured supernatant concentrations, the moisture content of the samples available for chloride should be estimated. The maximum moisture content which stone particles could sustain, is mostly from a film of water that remains on the surface of the particles after the samples have been immersed in water and then drained. In order to estimate this value, samples of the dry stone were placed in 3 containers and the weight of the dry stones was measured. The containers were then filled with water until all stones were soaked in water. Samples remained in water for 3 weeks after which the stones in each container were picked up one at a time and after giving just sufficient time for water drops to drain from each stone, they were placed in a tray. The weight of the wet stones was measured and trays were placed in the oven. The moisture content of each sample was measured. The measured moisture content values of all 3 samples were very close with the average of 1.6 %. This value was then taken as an estimated value of the original moisture

content of the stone particles in the field and also at the beginning of each wash test. Background concentrations were then calculated using equation 3.1. The calculated values for each wash step were plotted and shown in Fig. 9.8. As can be seen, the stones had a significant original background concentration which was removed after 4 successive wash steps, with 45 minutes shaking in each step. The results of this test showed that about 3 hours of shaking the stone samples with heavy duty shaker is sufficient for clean up the stones from their background concentration.

Using the wash method mentioned above, sufficient stones were washed and prepared for the proposed advection-diffusion tests.

Geotextile

The geotextile used in these experiments was a nonwoven, needle punched geotextile (Polyfelt TS650). Some physical properties of the geotextile are given in Table 9.2. This material was used as a separator between the soil and stone to prevent intrusion of the soil particles into the void spaces of the stone below the soil. A series of laboratory experiments were conducted to study the intrusion of compacted clayey soil through the geotextile and into the stone, to test the effectiveness of this material for being as a separator between the soil and stone. The results of this study will be discussed in Chapter 11.

Two pieces of 38 cm x 38 cm geotextile were washed with distilled water and used in the tests.

9.4 INSTALLATION OF THE MATERIALS AND TEST SET UP

9.4.1 INSTALLATION, SATURATION AND GRAVITY DRAINAGE OF THE CLEAR STONE

A plywood sheet was placed on top of a series of concrete blocks to create a free space for placement of the magnetic stirrer underneath the apparatus (Fig. 9.1). A base chamber (receptor reservoir) was placed on top of the plywood sheet and levelled. A five cm long magnetic bar was placed inside the chamber, the perforated steel plate was installed, the 'O' ring was installed, the intermediate chamber was placed on top of the base chamber and clamped to it by a series of bolts and nuts. Washed stones were randomly placed on top of the perforated plate inside the intermediate chamber. The stones were hand placed in such a manner as to avoid the creation of any large voids inside the stone layer. Further stones were placed in the chamber until the height of the stone layer was about 38 cm and the top surface of the stone layer became level with the level of the geotextile shoulder at the top of the chamber.

A distilled water tank was connected to the inlet valve in the base chamber through a flexible plastic tubing. Valves in the tank and base chamber were opened and the cell was filled with water until the water level reached to the top of the intermediate chamber and all stones were immersed in water. The stone was kept saturated for 2 days, after which outlet valve was opened and cell was drained completely. The cell was refilled with distilled water and then drained to the level of the perforated plate (bottom surface of the stone layer) in order to further clean the stones from any remaining background concentration. Once the water level reached the top surface of the perforated

plate, the outlet valve was closed. The drained water was collected in a container and its volume was measured. The known volume of the drained water and volume of the intermediate chamber (bulk volume of the stones) were used to calculate the porosity of the stone layer. The overflow steel pipe was connected to the outlet valve. The height of the overflow pipe had been designed so that after installation, the spill way level on the horizontal section of the pipe became level with the top surface of the perforated plate (Fig. 9.1). This arrangement facilitated drainage of the excess water which infiltrates through the soil and stone layers and is collected in the base chamber (receptor reservoir). After installation of the overflow pipe, the outlet valve was opened. The geotextile was immersed in distilled water and then placed in its compartment on top of the stones. The upper chamber was placed on top of the intermediate chamber and was fixed to it by bolts and nuts. During this installation, care was taken to ensure that the geotextile remained in its place.

9.4.2 INSTALLATION OF THE SILT AND APPLICATION OF THE SOURCE SOLUTION

The prepared wet soil sample for one lift was placed on top of the geotextile in upper chamber and was evenly spread. Using a Standard Proctor hammer, the first lift was compacted by applying 400 blows per lift to simulate the Standard Proctor compaction method. This was done in 4 stages of 100 blows in each stage. At the end of each stage, material located adjacent to the cell walls, was tamped with a square cross-sectional tamper to ensure complete contact of the soil with cell walls and to avoid sidewall leakage. Using the same procedure, the remaining soil in the 2 other lifts was

compacted. The final surface of the compacted soil was smoothened. The depth of the soil in 12 locations around the cell (4 location in each side) was measured, by reading the distance from the interface of the upper and intermediate chambers (level of the geotextile), to the surface of the soil. The measured average values of the soil thickness in Tests # AD8 and AD9, at the beginning of the tests were 12.03 cm and 12.18 cm, respectively. The distance from the soil surface to the marked line on the circumference of the upper chamber which was in 24 cm distance from the intermediate and upper chambers interface, was measured in 12 locations around the cell and also 5 locations on the surface of the soil. These values were averaged to obtain the value of the source solution height on top of the soil (not yet applied). Using this method, the measured average source solution heights in Tests # AD8 and AD9, were 11.3 cm and 11.81 cm respectively.

Prior to the tests set up, 20 L NaCl solution with the approximate concentration of 2000 mg/L had been prepared and stored in a plastic tank. After compaction of the soil sample and taking measurements, the source solution was poured on top of the soil, by placing the plastic tubing of the tank inside the chamber and opening the valve in the tank until the level of the solution reached the marked level around the upper chamber. The starting time of the test was recorded when the source solution reached the desired level. Two samples were taken from the receptor reservoir for initial concentration measurement. Fig. 9.2 shows the schematic of the assembled apparatus, and Fig. 9.3 shows the photographic view of the test set up.

9.5 MONITORING DURING THE TESTS

Swelling of the silt layers

Visual observations in early stages of the Test #AD8 showed that the silt layer was swelling. Surface heave of the soil layer was monitored once the test started. Measurements showed that after about 17 hours, the surface of the soil heaved about 13 mm from the original level, after which no further swelling was observed. The swelling process in Test #AD9 was somewhat slower than Test #AD8. Comparison of the initial and final thickness of the silt layer in Test #AD9 showed that soil has swelled about 6.2 mm on the average. This value was almost half of the value measured in Test #AD8.

Flow rate measurements, Darcy velocity, and hydraulic conductivity calculations

During the tests, out-flowing water from the base chamber (receptor reservoir) was continuously collected in a container (Figs. 9.2 and 9.3) and the elapsed time and collected volume were recorded. Using a travelling microscope, the water level drop from the original level in the source reservoir, was continuously monitored and recorded with corresponding elapsed time. The infiltrated volume was calculated by multiplying the values of the dropped water level by the surface area of the soil. After measuring the dropped water level, the infiltrated volume of water from the source reservoir was replaced with the same volume of distilled water to re-establish the original water level. This was done by opening the filling port on top of the plexiglass plate (Fig. 9.1) and placing the plastic tubing of the distilled water tank down inside the source reservoir and opening the valve in the tank until the water level reached the desired level. This

process was monitored using the travelling microscope to observe the exact position of the marked source solution level. During the tests, the maximum allowable water drop from the source reservoir was taken to be 5 mm after which infiltrated volume was replaced with distilled water. This fluctuation in the level of the source solution was considered in calculating the existing average hydraulic gradient during the test. The recorded inflow and outflow values with elapsed time were plotted and are shown in Figs. 9.9 and 9.10 for Tests # AD8 and AD9 respectively. Using Figs. 9.9 and 9.10, the average values of the flow rate was found for each test and the Darcy velocity was calculated. Knowing the hydraulic gradient in each test, the hydraulic conductivity of the silt layer was calculated (Table 9.3). As can be seen in Fig. 9.10, there is a larger deviation in the inflow and outflow curves in Test #AD9 compared to Test #AD8 (Fig. 9.9). This is partially due to the slower process of swelling and saturation of the silt layer during the test compared to Test #AD9 which caused some amount of infiltrated water to be used for saturation of the silt layer. Using the initial and final values of the water contents of the silt layer, the volume of water used for saturation, was calculated and deducted from the final infiltrated volume to calculate the representative value of the flow rate and Darcy velocity through the test system. Some smaller amount of water also infiltrated through the soil and into the stone layer but remained stagnant as water particles in contact points of the stones and also on the inner surface of the intermediate chamber, as shown in Fig. 9.4. There was also some evaporation of water from the surface of the upper reservoir as water drops were observed to attach on the inner surface of the top plate.

The hydraulic gradients in these tests were calculated by dividing the sum of the

soil and source solution heights to the soil height. This was based on the assumption of the atmospheric pressure at the base of the soil due to the existence of a vent in front face of the intermediate chamber (Fig. 9.1). The calculated values were 1.76 and 1.94 for Tests # AD8 and AD9 respectively. Knowing the Darcy velocity and hydraulic gradient, the hydraulic conductivity was calculated. Resulting values were 4.60×10^{-8} m/s and 2.03×10^{-9} m/s for Tests # AD8 and AD9 respectively. Table 9.3 summarizes the above mentioned values for the tests conducted.

Source and receptor reservoirs sampling

Samples (4 mL) were taken periodically from the source and receptor reservoirs during the tests. Samples were taken through the septum ports located in front faces of the upper and lower chambers (Fig. 9.1). The extracted volumes were replaced by distilled water by re-injecting the water through the septum ports.

Check analysis during the tests

(a) Test #AD8

Prior to termination of the Test #AD8, a preliminary analysis was performed using program POLLUTE and the available data. The calculated source and receptor reservoir concentrations with elapsed time showed that due to the high Darcy velocity in the test system, the concentration in the source reservoir decreases and that in the receptor reservoir increases at a significant rate so that they approach a similar value after about 16 days of migration. After 10.7 days of migration, 2 samples from the source and receptor reservoirs were analyzed to check the accuracy of the assumed data

used in theoretical analysis. The concentration values obtained were reasonably close to the source and receptor concentration curves obtained from POLLUTE. Based on the results of this analysis, it was decided to terminate the test after 14.7 days of migration.

(b) Test #AD9

Due to the lower hydraulic conductivity of the silt layer in Test #AD9 compared to the Test #AD8, the migration process was somewhat slower. Based on the available geometry and chemical data, a preliminary analysis was performed using program POLLUTE for different test durations. The elapsed time of the test was considered to be when enough experimental data was collected in the receptor reservoir during the test. The results of the analysis were compared with the upper and lower reservoir concentration data obtained by analyzing the samples taken during the test. The results obtained were consistent with the theoretical analysis. Based on these analyses, the test was terminated after about 160 days.

9.6 TERMINATION OF THE TESTS

Sampling from the silt layer

Before the termination of the test, the heights of the source solution and silt layer were measured. Final samples from the source and receptor reservoirs were taken. The top plexiglass plate was opened and the solution in the source reservoir was drained (Fig. 9.11). Using a 5 cm diameter Shelby tube, 5 core samples were taken from the silt layer, in 5 locations; 4 samples from nearby corners and one sample from the centre

(Fig. 9.12). To take the sample, a Shelby tube was located on the desired point and using hand pressure, it was pushed down into the soil. Additional energy was required to push the Shelby tube down to the bottom of the soil. This was achieved using a hydraulic jack and 2 wooden supports attached to the right and left side of the upper chamber (Fig. 9.13). Once contact was made between the Shelby tube and geotextile, the hydraulic jack and wooden supports were removed and the sample was extracted by pulling the Shelby tube out of the soil (Fig. 9.14). During Shelby tube sampling in both Tests AD8 and AD9, it was noted that the upper most 2-3 cm thickness of the soil, was very loose compared to the remaining soil. This can be seen in Figs. 9.15a (Test #AD9) and 9.15b (Test #AD8). This part of the soil was much looser in Test #AD8 compared to Test #AD9. The soil in Shelby tube was extracted in about 2 cm intervals by pushing a steel cylinder having smaller diameter than the inner diameter of the tube, into the other end of the Shelby tube until about 2 cm of the soil was extracted from the tube. The extracted soil was sliced using a wire trimmer (Fig. 9.16) and transferred into a container and weighed. This process was repeated until the entire thickness of the soil was extracted, sliced and weighed. All 5 samples taken by the Shelby tube, were sliced using the above method. Samples were placed into the containers and weighed (Fig. 9.17). In Test #AD8, the collected containers including wet soils were transferred into the oven for their moisture content determination. In Test #AD9 a small moisture content samples were taken from each slice and the remaining samples were wrapped in plastic and saved for their pore water extraction. In Test #AD8, two bulk samples from upper loose and lower stiff parts of the silt layer were taken to measure their moisture contents. In Test #AD9, three samples were taken from upper (loose) and middle and

bottom (stiff) part of the soil. These values were considered as the representative average moisture contents for the entire soil depth to be used in theoretical analysis. The remaining silt in the upper chamber was removed and upper chamber was detached from the intermediate chamber and removed. The geotextile on top of the stones was removed.

Sectioning the clear stone

Immediately after removing the geotextile, sectioning the stone layer was undertaken as fast as possible so as to avoid evaporation of the water on the surface of the stone particles. The left and right half of the stone layer was sectioned into 10 sub-layers of about 3.8 cm thick. Stones were picked up one at a time and transferred into the stainless steel trays (Figs. 9.18 and 9.19). Once the stones of each half sub-layer were placed in the tray, they were weighed using a large digital scale and then placed into the oven for moisture content determination. Sectioning the stones and weighing the trays was done by two people to accelerate sectioning process and avoid any delay which might allow the evaporation of the moisture of the stones. A series of 1 cm width tapes, 3.8 cm apart and parallel to each other which had been installed on front and back faces of the intermediate chamber, were used as the guides for sectioning the stone layer into about 3.8 cm thicknesses (Fig. 9.4).

9.7 MOISTURE CONTENT PROFILES IN SILT AND CLEAR STONE

Figs. 9.20 to 9.23 show the moisture content profiles in the silt and stone layers,

in Tests # AD8 and AD9. Figs. 9.20 and 9.22 represent the moisture content profiles in 3 locations in the silt layer. As it can be seen in each test, the obtained profiles are quite similar but non-uniform with depth. In Test #AD8, the deviation of the observed moisture content profiles from the original profile (dotted line) starts from the bottom of the soil, while in Test #AD9 it starts about the middle of the soil. The moisture content of the soil in its upper part (in both tests), adjacent to the source solution, is higher than its bottom portion which is very close to the original moisture content profile of the sample before the test (dotted line). This behaviour is mostly due to the swelling of the soil and absorbing water during the test. Figs. 9.21 and 9.23 show the moisture content profiles in the clear stone layer, in both tests. As can be seen, the moisture content profiles are quite uniform, with the average of 1.68 % in Test #AD8 and 1.95 % in Test #AD9.

Table 9.4 summarizes the thickness, the average values of the moisture content, the degree of saturation and volumetric moisture content of the silt and clear stone layers in Tests # AD8 and AD9, respectively.

9.8 CONCENTRATION MEASUREMENT IN SILT, STONE, SOURCE AND RECEPTOR RESERVOIRS SAMPLES

Concentration measurement in silt samples

The wash method was used to measure the pore water chloride concentrations in sliced silt samples in Test #AD8. Prior to selection of this method, an attempt was made to obtain pore water from sliced samples using the pneumatic squeeze apparatus used for clayey soils. After about 24 hours of squeezing, these samples did not yield any water,

indicating that this method can not be used to obtain pore water for silt. This behaviour is likely due to the dilatant characteristics of this soil.

From the 30 sliced samples (5 locations on the silt layer) where Shelby tube samples had been obtained, 18 samples from 3 locations (6 samples from each location), were selected for concentration measurements. The sample locations will be referred to as right-front, middle, and left-back. 125 g from each soil slice was washed with 90 mL de-ionized distilled water. This was done by grinding the dry soil and pouring the ground soil and water into the centrifuge bottles. The centrifuge bottles (6 bottles from each location) were then placed on the heavy duty shaker and samples were shaken in 250 rpm for 4 hours. According to previous experiences light duty shakers are not able to properly wash samples and their speed and degree of flexibility to move the centrifuge bottles, are not enough to bring the soil particles completely into suspension in the soil water mixture and consequently, they result in low concentration values for the supernatant. This effect is more critical for washing coarse granular material such as well gravel. The samples were centrifuged in 2000 rpm for 1 hour. Supernatant solutions were then collected and analyzed for chloride concentration. Using equation 3.1, a pore water concentration for each soil slice was then calculated knowing the obtained supernatant concentration.

The squeeze method was examined for the sliced silt samples in Test #AD9 and it was found that samples yielded sufficient pore water. Thus, this method was selected to obtain pore water from 18 sliced samples from 3 locations of right-front, middle, and left-back. The pore water solutions were then analyzed for both Cl^- and Na^+ concentration.

The background concentration of the soil sample was determined using the original wet samples which had been saved from the same material used for the tests.

The Cl^- concentration values from 18 samples in 3 locations of the silt layer (middle, right-front and left-back), were plotted versus the soil depth and are shown in Figs 9.24 (for Test #AD8) and 9.26 (for Test #AD9), along with the stone layer data and predicted theoretical profile which will be discussed later. As it can be seen, in both tests, all soil data points in 3 locations are very consistent and close to each other.

The corresponding Na^+ concentration data in silt layer in Test #AD9 is shown in Fig. 9.28. It can be seen that Na^+ data of all 3 locations in the soil layer are also consistent and fall on a smooth curve.

Concentration measurement in stone

The oven-dried stone samples from the left and right half of the 38 cm thick stone layer which had been sectioned into 10 sub-layers about 3.8 cm thick, and placed in 20 stainless steel trays (Fig. 9.19), were tested for their chloride concentration using the wash method. The weight of the dry stone in each tray was different with an average of 3500 g per tray. All stones in each tray were used in the concentration analysis. The stones in each tray were transferred into a 4.5 litre capacity plastic container and the weight of each container including the dry stone was measured and recorded. Some distilled water was added to the first container so that the stones were partially immersed in water. The weight of the container including stones and water was measured from which the weight of added water was determined. The proportion of the weight of water to the weight of dry stone was calculated. In order to keep the same proportion for the

other 19 containers, the amount of added water to each container was controlled so that the resulting value of the weight of water to the weight of dry stone for all containers was about the same. The plastic containers were placed on the heavy duty shaker and shaken for about 20 hours at 150 rpm (Fig. 9.7). At the end of the shaking, the wash water in each container was transferred into a centrifuge bottle and sample was centrifuged for 15 minutes at 2000 rpm to remove the suspended fines from the solution. The wash water was then analyzed for Cl^- concentration and the pore water concentration was calculated using Equation 3.1. The Cl^- results were plotted versus soil depth as shown in Figs 9.24 and 9.26 for Tests # AD8 and AD9 respectively. The corresponding results for Na^+ in Test #AD9 are shown in Fig. 9.28. As can be seen, there is a greater scatter of the results for the stone than for the soil layer data. This scatter is less in Test #AD9 compared to Test #AD8. This is the first hint that dispersion may be significant at higher velocities. For advective flow through unsaturated coarse porous media (e.g., the coarse stone examined in this chapter) a phenomenon referred to as "preferential flow" or "fingering" may give rise to the scatter of the data. If this happened, preferred flow channels might form inside the medium causing the flow to be greater in some areas than in other adjacent areas. This phenomenon would be expected to give rise to a scatter in the concentration data in stone layer similar to that observed in this test.

Concentration measurement in source and receptor reservoirs samples

The collected solutions from the source and receptor reservoirs were analyzed for their chloride concentration. The resulting values for both tests, were plotted versus elapsed time and are shown in Figs 9.30 and 9.31 along with the best fit theoretical

curves which will be discussed later. As previously discussed, the preliminary theoretical analysis indicated that the rate of decrease and increase of concentrations in the source and receptor reservoirs for Test #AD8 (Fig. 9.30) was very rapid so that after 14.7 days of migration, the concentration difference between the reservoirs dropped from about 2000 mg/L at the beginning of the test, to about 160 mg/L at the end of the test. This was due to the high permeability of the silt layer which resulted in high Darcy velocity (8.1×10^{-6} m/s or 2.5 m/a) through the soil and stone layers.

As can be seen in Fig. 9.31, the rate of decrease in the source concentration and increase in receptor concentration in Test #AD9 was much slower compared to Test #AD8 (Fig. 9.30). For Test #AD9 (Fig. 9.31), the concentration difference between the source and receptor reservoirs at the beginning of the test was 1934 mg/L and after about 160 days of migration this difference had dropped to 838 mg/L. From these results it could be concluded that the decrease in the rate of migration through the unsaturated stone layer is directly related to the decrease of permeability (or Darcy velocity) of the overlying soil.

9.9 THEORETICAL ANALYSIS

Theoretical analysis for the conducted tests was performed using the program POLLUTE and measured data. Table 9.5a shows the average values of the thickness, volumetric moisture content and effective diffusion coefficient of the soil, geotextile, clear stone, and perforated plate, used in the analysis. As can be seen in Table 9.5a, the stiff part of the silt soils in Tests AD8 and AD9 had slightly higher volumetric moisture

content values compared to those typically observed in clayey soils previously tested (e.g. soil used in Chapter 4 for diffusion testing). Hence it was expected that the stiff silt samples in both tests to have slightly higher effective diffusion coefficients. Using Eq. 5.1 and the typical porosity and effective diffusion coefficient of the clayey soil (e.g. see Table 4.5), and the volumetric moisture content of the stiff silt samples, their effective diffusion coefficients were predicted. Using the same method, the corresponding values for loose part of the samples were predicted. The effective diffusion coefficients for unsaturated stone layers in Tests # AD8 and AD9 were predicted using the available data for saturated diffusion coefficient and porosity of the fine gravel obtained in diffusion testing (described earlier in Chapter 7) together with the corresponding volumetric moisture content of the unsaturated stone, using Eq. 5.1. The resulting values are listed in first row of the clear stone section in Table 9.5a. The corresponding effective diffusion coefficients for Na^+ ion in soil and stone layers of the Test #AD9 were predicted using the porosity and Na^+ diffusion coefficient of the clayey silt and fine gravel obtained in Chapters 4 and 7 and the method described above. The remaining input data used in the analysis are summarized in Table 9.5b. The first series of the analysis was performed using the data listed in Tables 9.5a and 9.5b. and the "effective diffusion coefficients" predicted for soil and stone layers. The resulting theoretical concentration versus depth profiles are shown as dotted line in Figs. 9.25 (Test AD8) and 9.27 (Test AD9) for the Cl^- ion, and in Fig 9.29 (Test AD9) for the Na^+ ion. As can be seen in Fig. 9.25 (Test AD8) the theoretical profile fits that observed in silt very well. The prediction is not quite as good in the stone layer where the predicted concentrations are almost uniform throughout the stone while the majority of the stone layer data shows

gradual decrease of the concentration with depth. Both experimental and theoretical concentrations drop at about 3.8 cm above the stone-receptor reservoir interface, with the bottom concentration in the receptor being the lowest value due to the dilution that occurs in the receptor reservoir. In order to get a better prediction to the experimental data in the stone layer of Test #AD8, the value of the "hydrodynamic dispersion coefficient" was increased from that initially used as the effective diffusion coefficient of the unsaturated stone layer. This was done to examine the effect of the "mechanical dispersion" that may have occurred in the unsaturated stone layer due to the applied high flow rate. The range of the values used in the analysis are shown in insert of Fig. 9.25 and the resulting theoretical profiles are shown as medium dashed, solid, and long dashed lines respectively. As can be seen the hydrodynamic dispersion value of 3.6×10^{-7} m^2/s (shown in second row of the stone layer section in Table 9.5a) resulted in a better fit (solid line) than pure diffusion alone. This profile is shown in Fig. 9.24 as the representative theoretical profile through the experimental data in Test #AD8. The scatter of data in the stone may be partly attributed to experimental error but is also likely partly due to statistical variation in stone size, shape and arrangement which would affect mechanical dispersion and also preferential flow (or fingering) at the relatively high velocity examined.

Figs. 9.27 and 9.29 show the results of the analysis using the "effective diffusion coefficient" (dotted line) and three "hydrodynamic dispersion coefficients" (solid, medium dashed and long dashed lines) for unsaturated stone layer for Cl^- and Na^+ ions respectively. These values are shown in insert of Figs. 9.27 and 9.29. As can be seen, the solid lines in both graphs tend to give a better theoretical prediction than the

alternative values examined. The solid lines correspond to hydrodynamic dispersion coefficients of 2.4×10^{-9} m^2/s for Cl^- and 2.0×10^{-9} m^2/s for Na^+ in stone layer. These values are listed in second row of the stone layer section in Table 9.5a for Test #AD9. These profiles are shown in Figs. 9.26 and 9.28 as the representative predicted profiles for Cl^- and Na^+ ions in Test #AD9 respectively.

The dotted line in Fig. 9.26 represents the results of the analysis assuming variable Darcy velocity in the Test #AD9 system. Using the flow rate data in Fig. 9.10, it was assumed that up to 7 days, the Darcy velocity through the silt starts from 4.23×10^{-9} m/s (calculated based on the inflow curve, Fig. 9.10) at the top and decreases linearly to zero at the bottom of the layer which was in contact with the geotextile and remains zero through the underlying layers (i.e. no advection in the stone layer). This assumption was based on the observed outflow data showing that there is no outflow from the system up to about 7 days. On the other hand, due to the higher matric suction in upper part of the silt layer in early stages of the test, the Darcy velocity was assumed to be high (calculated from the inflow curve). Starting at day 8 up to day 10 it was assumed that the Darcy velocity at the bottom of the silt layer increased to 3.73×10^{-9} m/s (calculated according to the outflow curve in Fig. 9.10) and the velocity at the top remained unchanged. Starting at day 11 up to the end of the test (159.8 days), a uniform Darcy velocity of 3.98×10^{-10} m/s, which is the average of the Darcy velocities calculated from inflow (4.23×10^{-9} m/s) and outflow (3.73×10^{-9} m/s) curves, was assumed to exist in the entire system. The results from this second analysis are shown as the dotted line in Fig. 9.26. As can be seen, both the initial analysis assuming a uniform average flow from time zero and the second analysis described above produced essentially the same

results indicating that the first analysis based on the assumption of a constant Darcy velocity of 3.94×10^{-9} m/s through the layers is sufficiently accurate.

The calculated concentration profiles for the source and receptor reservoirs for Test #AD8 are shown in Fig. 9.30. The input data used for the analysis is that used to predict concentration versus depth data shown in Fig. 9.24 and discussed above. As can be seen, these profiles are in good agreement with the experimental data. According to this figure, both experiment and theory indicate that the increase in the receptor reservoir concentration has occurred after about 5 days of migration, after which concentration increased at an almost constant rate. The predicted concentration in the source and receptor were insensitive (to within plotting accuracy) to the range of the coefficient of hydrodynamic dispersion examined in Fig. 9.25.

Fig. 9.31 shows the calculated and observed source and receptor data for Test #AD9. The input data for the analysis is that used to predict concentration versus depth data shown in Fig. 9.26 and discussed earlier. As can be seen, both experiment and prediction are in good agreement. The predicted concentration in the source and receptor were insensitive (for plotting accuracy) to the range of coefficient of hydrodynamic dispersion examined in Fig. 9.27.

As discussed earlier, the results of the theoretical analysis in Tests # AD8 and AD9 suggest that there is some mechanical dispersion in the unsaturated stone layer. Knowing the predicted effective diffusion coefficient and "best fit" hydrodynamic dispersion coefficient values in the stone layer in both tests (first and second rows of the stone layer section in Table 9.5a), and the corresponding Darcy velocities (Table 9.3), the dispersivity values (α) were calculated using equations 2.8 and 2.10 (Chapter 2).

The dispersivity values obtained for the stone layer in Tests AD8 and AD9 are shown at the bottom of Table 9.5a. As can be seen, both values are relatively small compared to those typically cited in the literature for aquifers (e.g. Rowe et al. 1994), and Test #AD8 has greater value than Test #AD9. This is due to the higher seepage rate existed in the Test #AD8 system (v_s = 2.5 m/a) compared to that in Test #AD9 (v_s = 0.12 m/a). It is noted that while the dispersivity for Test #AD8 does have some notable effect on the predicted concentration profile (see Fig. 9.25), the expected dispersivity for Test #AD9 has no effect on the prediction (Fig. 9.27) other than to "round off" the concentration profile near the bottom of the layer.

Some sensitivity analysis

The sensitivity of the calculated profiles for Test #AD9 to the Cl^- hydrodynamic dispersion coefficient, and also volumetric moisture content of the unsaturated stone layer was examined and the results are shown in Fig. 9.32. In the first analysis, a large arbitrary value of 3.2×10^{-6} m^2/s (100 m^2/a) was used as unsaturated stone hydrodynamic dispersion coefficient. The resulting profile is shown as profile #2 (solid line), and as can be seen, there is significant difference between this and the predicted profile (#1), and it shows higher concentration in the receptor reservoir compared to the observed and predicted values. This suggests that for the range of the Darcy velocity examined, the assumption of high dispersion in unsaturated stone layer is on the overconservative side. Profiles # 3 to 7 in Fig. 9.32 (dotted lines) show the results of the analysis assuming that the stone layer is fully saturated (n=0.416). Profile #3 was obtained using the same hydrodynamic dispersion coefficient as used for profile #1 (all other data as shown in

Tables 9.5a and 9.5b). As can be seen, the impact is low when the stone layer is fully saturated and concentration in the receptor reservoir is lower compared to the observed and predicted values (#1). The lower concentrations in soil and stone layers is due to the larger available volume of water in stone pore space (compared to a very low volume in unsaturated case). This large volume results in more dilution of the migrating ion and hence, lower concentration. On the other hand, when the stone is unsaturated, there is a very small volume of water in the pore space so that the concentration reaches a high value in a short period of time. Profiles # 4, 5, 6 and 7 show the results of the analysis assuming different values as hydrodynamic dispersion coefficient for saturated stone layer. These values are listed in insert of Fig. 9.32. As can be seen, the higher the hydrodynamic dispersion coefficient, the higher impact will be in the receptor reservoir, and for the case of large arbitrary value (#7), the concentration in the stone layer become uniform with depth as is the case for unsaturated stone layer (profile #2). The concentration in the receptor for case #7 is close to that observed and predicted for case #1.

Another series of theoretical analysis were performed to examine the sensitivity of the results to the diffusion coefficient and volumetric moisture content of the stone layer when zero Darcy velocity is assumed to exist in the test system (i.e., pure diffusion). The results of these analysis are shown in Fig. 9.33. In this figure, profile #1 shows the result of the analysis when the stone layer is unsaturated (all other data as listed in Tables 9.5a and 9.5b), and profile #2 belongs to the analysis when stone layer is assumed to be saturated (n=0.416, D_e=11.4x10^{-10} m^2/s, and all other data as listed in Tables 9.5a and 9.5b). As can be seen, after 159.8 days of migration both analysis show

negligible concentrations in the receptor reservoirs. In order to see the impact in longer period of time, the analysis was repeated for 3650 days (10 years) and results are shown as profiles #3 and #4. As can be seen, after 10 years of migration, the concentration in receptor reservoir is very low (profile #3) compared to profile #4 which shows concentration of about 460 mg/L in the receptor reservoir.

Another series of sensitivity analysis were performed to examine the effect of different assumed effective volumetric moisture contents, $\theta_{effective}$, of the underlying stone on the calculated profiles. The first series of the analyses assumed that the effective θ ranged from 50% to 90% of the measured value at the end of the test (Table 9.4). All other parameters (including $D_{(stone)}$) are as listed in Tables 9.5a and 9.5b. The results are shown in Figs. 9.34a (Test AD8) and 9.35a (Test AD9). Due to the scatter of the data in the stone layer, interpretation of the results are somewhat difficult. The general conclusion could be that the profiles of 50% reduction in θ_{stone} do not fit the data quite well and hence this amount of reduction is unlikely. The results for a 20% and 10% reduction are close to the solid lines which assumed $\theta_{effective} = \theta_{measured}$. Based on these results one could hypothesize that up to 20% uncertainty in θ value (i.e., $\theta_{effective} \geq 0.8\theta_{measured}$), does not have significant effect in calculated profiles and that the assumption of $\theta_{effective} = \theta_{measured}$ appears to be reasonable.

A second series of the analysis used the same θ_{stone} values as above except that the $D_{(stone)}$ values were also reduced by the same proportion. This took into account the effect of θ on D (as discussed in previous chapters). The results are shown in Figs. 9.34b (Test AD8) and 9.35b (Test AD9) and are similar to those in Figs. 9.34a and 9.35a except that they are slightly shifted to the right due to the change in D. The same

conclusion can be reached that the effect of 20% uncertainty in the θ and D values only has a modest effect on the result but that the original assumption ($\theta_{effective} = \theta_{measured}$) appears to be more reasonable.

From the results of these sensitivity analysis it could be concluded that: (1) the assumption of a large value for hydrodynamic dispersion coefficient of the stone layer might be an overconservative assumption, (2) the unsaturated stone layer could be used as an effective barrier as long as there is zero or negligible advective flow through the system, and (3) 20% uncertainty in the value of θ_{stone} and/or $D_{(stone)}$, did not have a significant effect on the final calculated results however it would appear that $\theta_{effective}$ of the stone could be assumed to be equal to the measured value of θ_{stone}.

9.10 SUMMARY AND CONCLUSIONS

Two large scale advection-diffusion tests were conducted using a compacted silt layer having high (4.6×10^{-8} m/s) and moderate (2×10^{-9} m/s) hydraulic conductivities, underlain by an unsaturated coarse stone layer. Inflow and outflow rates and also concentrations in the source and receptor reservoirs were regularly monitored during the tests. Based on the preliminary theoretical analysis during the tests, expected termination time of the tests were determined after which tests were terminated by draining the source reservoir and slicing the soil and stone layers into smaller sub-layers. Concentrations in sliced sub-layers and also in the source and receptor reservoirs were determined using appropriate methods, from which experimental concentration versus depth and concentration versus time data were obtained for each test. Using the flow

rate data and the measured hydraulic gradient, Darcy velocity and hydraulic conductivity values were calculated for each test. The test conducted with silt layer having 10% clay content (#AD8) showed about 20 times higher hydraulic conductivity compared to the test with 17% clay content (#AD9). A very high migration rate was observed in Test #AD8 having the Darcy velocity of 8.1×10^{-8} m/s (2.5 m/a) so that concentration in the receptor reservoir reached to about 600 mg/L (almost 1/3 of the initial concentration) after only 14.7 days of migration. Somewhat slower migration rate was observed in Test #AD9 ($v_a = 3.9 \times 10^{-9}$ m/s = 0.12 m/a) so that by the end of the test (159.8 days), concentration in receptor reservoir reached about 280 mg/L (about 1/7 of the initial concentration).

A theoretical analysis was performed for Test #AD8 using the observed Darcy velocity and the relevant chemical, physical and geometrical parameters listed in Tables 9.5a and 9.5b. The first series of the analysis was performed using the predicted "effective diffusion coefficients" for unsaturated stone layer in both tests. Resulting profiles fit the observed data in silt layers quite well but predictions were not quite as good in the unsaturated stone layers. The analysis was repeated using higher "hydrodynamic dispersion coefficients" in the unsaturated stone layer to examine the effect of dispersion. Better calculated profiles were obtained for the data in the unsaturated stone layer when the effect of dispersion was taken into account. Dispersivity values in stone layers were calculated for both tests and compared with the range of the values cited in the literature, and it was concluded that the values obtained in both tests are relatively small compared to those reported for aquifer materials. This suggested that for the range of the Darcy velocities examined, the effect of dispersion is low. Furthermore for typical cases where the advective velocity is likely to be of the

order of 0.12 m/a or less, the effect of dispersion can be neglected without any significant loss of accuracy.

Two different theoretical analysis were performed in Test #AD9. In the first analysis it was assumed that the Darcy velocity of 8.1×10^{-8} m/s is constant with time and depth. In second analysis, variable Darcy velocity was assumed with time and depth (see section 9.9). Both methods produced almost the same results with predicted profiles in good agreement with the experimental data (Fig. 9.26).

The technique developed in previous chapters (e.g. Chapters 5 and 7) to predict the unsaturated effective diffusion coefficient of an ion using the saturated diffusion coefficient and porosity of the porous medium and the volumetric moisture content of the unsaturated porous medium (Eq. 5.1), seemed to work well for both silt and stone in the tests conducted. The analysis in Test #AD9 showed that this technique was accurate for both Cl^- and Na^+ ions to predict the relevant effective diffusion coefficients in both silt and stone.

The theoretical sensitivity analysis performed for Test #AD9, showed that for the observed flow rate (v_a = 0.12 m/a), the unsaturated stone layer does not play an effective role as a barrier for contaminants. In this case there is limited pore water available for migration in the stone but the groundwater velocity along the wetted surface of the stone is quite high and hence there is rapid and relatively uniform migration through the stone at the Darcy velocities examined.

Assumption of a high value as a saturated or unsaturated hydrodynamic dispersion coefficient of the stone layer resulted to a concentration profiles which were significantly different from the observed and calculated profiles however the impact in the underlying

receptor was not greatly affected. Analysis showed that this assumption might be an overconservative assumption.

The results of another series of sensitivity analysis which performed using the data obtained from Test #AD9 and assuming zero Darcy velocity through the test system (pure diffusion), showed that unsaturated stone could play an effective role as a "diffusion barrier" compared to the saturated stone. It was concluded from these results that benefit could be made of an unsaturated coarse stone layer in the design of landfills as long as the barrier design results in a very low or negligible advective-dispersive flow through this layer.

The effect of effective volumetric moisture content of the stone layer was examined in a number of sensitivity analysis which showed that the assumption that $\theta_{effective}$ is equal to $\theta_{measured}$ appears reasonable.

TABLE 9.1 SOME PHYSICAL, CHEMICAL, AND MINERALOGICAL CHARACTERISTICS OF THE 38 mm DIAMETER CLEAR STONE

Physical characteristics

Specific gravity, G_s = 2.72

Porosity = 0.415

Dry density = 1.59

D_{60} = 28.0 mm

D_{10} = 21.3 mm

Chemical and mineralogical characteristics[1]

Cation exchange capacity[2] (C.E.C, meq/100 g clay - from powdered stone) :

39.7 (KCl wash), 90.9 (AgTh wash)

[Cl^-] background concentration = 10.0 mg/L

[Na^+] background concentration = 7.0 mg/L

Minerals present (%) :

SiO_2	Fe_2O_3	MnO	MgO	CaO	K_2O	L.O.I	Total
0.43	0.18	0.03	22.78	32.28	0.02	42.82	98.54

Undetected minerals : 1.46 (%)

Carbonates :

Percent Dolomite = 37.2 (%)

Percent Calcite = 66.4 (%)

1 - See Appendix B for description of chemical tests

2 - CEC by combined KCl/Ag thiourea exchange method on powdered stone

TABLE 9.2 ENGINEERING PROPERTIES OF THE POLYFELT TS650 GEOTEXTILE

Property	Polyfelt[1] TS650	Test Method
Mass (g/m^2)	235	ASTM D3776
Thickness[2] (mm)	2.3	ASTM D1777
Grab Tensile[2] (N)	755	ASTM D4632
Mullen Burst[2] (kPa)	179	ASTM D3786
Puncture[2] (N)	375	ASTM D4833
Tear[2] (N)	355	ASTM D4533
Wide Width Tensile[2,4] (kN/m) [%]	14[95%]	ASTM D4595
FOS[3] (μm)	110	CGSB 148.1 Method 10

1 - Manufacturer's stated values.

2 - Minimum roll average value.

3 - Maximum roll average value.

4 - Machine direction. Failure strain shown in brackets.

TABLE 9.3 VALUES OF THE FLOW-RATE, HYDRAULIC GRADIENT, HYDRAULIC CONDUCTIVITY, AND DARCY VELOCITY, THROUGH THE SOIL LAYER IN TESTS # AD8 AND AD9

	Test #AD8	Test #AD9
Flow-rate (m^3/s)	10.2×10^{-9}	5.0×10^{-10}
Hydraulic gradient	1.76	1.94
Hydraulic conductivity (m/s)	4.60×10^{-8}	2.03×10^{-9}
Darcy velocity (m/s)	8.1×10^{-8}	3.94×10^{-9}

TABLE 9.4 AVERAGE VALUES OF THE THICKNESS (H), MOISTURE CONTENT (W), DEGREE OF SATURATION (S), AND VOLUMETRIC MOISTURE CONTENT (θ), FOR THE SILT AND CLEAR STONE LAYERS IN THE ADVECTION-DIFFUSION TESTS # AD8 & AD9

	Test #AD8				Test #AD9			
	H[1] (cm)	W[2] (%)	S[3] (%)	θ[4] (cm^3/cm^3)	H[1] (cm)	W[2] (%)	S[3] (%)	θ[4] (cm^3/cm^3)
Silt :								
Loose	2.87	28.0	100	0.43	2.03	24.22	100	0.40
Stiff	10.77	19.41	89	0.33	4.13	18.04	88	0.33
					6.35	15.21	85	0.30
Clear stone :	38.0	1.65	6.32	0.026	38.0	1.95	7.44	0.031

1 - Thickness of the soil/stone layer
2 - Moisture content
3 - Degree of saturation
4 - Volumetric moisture content

TABLE 9.5a AVERAGE VALUES OF THE LAYER THICKNESS (H), VOLUMETRIC MOISTURE CONTENT (θ), DIFFUSION COEFFICIENT (D_e), AND DISTRIBUTION COEFFICIENT (K_d), FOR THE SOIL, GEOTEXTILE, CLEAR STONE, AND PERFORATED PLATE, USED IN THEORETICAL ANALYSIS OF THE TESTS # AD8 & AD9

	Test #AD8			Test #AD9				
	H (cm)	θ (cm^3/cm^3)	D_{Cl^-} (m^2/s)	H (cm)	θ (cm^3/cm^3)	D_{Cl^-} (m^2/s)	D_{Na^+} (m^2/s)	K_d (mL/g)
Silt :								
Loose	2.87	0.43	8.9×10^{-10}	2.03	0.395	8.2×10^{-10}	7.3×10^{-10}	0.28
Stiff	10.77	0.33	6.9×10^{-10}	4.13	0.328	6.8×10^{-10}	6.0×10^{-10}	0.28
				6.35	0.300	6.2×10^{-10}	5.5×10^{-10}	0.28
Geotextile :	0.15	0.45	9.8×10^{-10}	0.15	0.45	9.8×10^{-10}	8.2×10^{-10}	0.28
Clear-stone :	38.0	0.027	$7.4\times10^{-11*}$ $3.6\times10^{-7**}$	38.0	0.031	$8.5\times10^{-11*}$ $2.4\times10^{-9**}$	$5.5\times10^{-11*}$ $2.0\times10^{-9**}$	0.0
Perforated plate :	0.18	0.6	15.0×10^{-10}	0.18	0.6	15.0×10^{-10}	12.5×10^{-10}	0.0

* - Effective diffusion coefficient (D_e)
** - Hydrodynamic dispersion coefficient, D, ($D = D_e + D_{md}$)

$\alpha_{AD8} = 0.119$ (m) , (α = dispersivity)
$\alpha_{AD9} = 0.018$ (m)

TABLE 9.5b OTHER INPUT DATA USED IN THEORETICAL ANALYSIS OF THE TESTS # AD8 AND AD9

	Test #AD8				Test #AD9			
	Silt	Geotextile	Clear-stone	Per. plate[1]	Silt	Geotextile	Clear-stone	Per. plate[1]
Thickness (cm)	13.64	0.15	38.0	0.18	12.51	0.15	38.0	0.18
Cl^- Background concn. (mg/L)	50	50	10	10	92	92	10	10
Na^+ Background concn. (mg/L)	--	--	--	--	132	132	7	7
Cl^- Source concn. (mg/L)	2010				1930			
Na^+ Source concn. (mg/L)	--				1120			
Darcy velocity (cm/s)	8.1×10^{-6}				3.94×10^{-7}			
Reference height of solution (cm)	10.85				11.72			
Solution collected (/area/time - m/s)	3.7×10^{-9}				6.9×10^{-11}			
Outflow velocity (m/s)	2.51×10^{-7}				1.32×10^{-8}			
Duration of the test (days)	14.74				159.8			

1 - Perforated plate

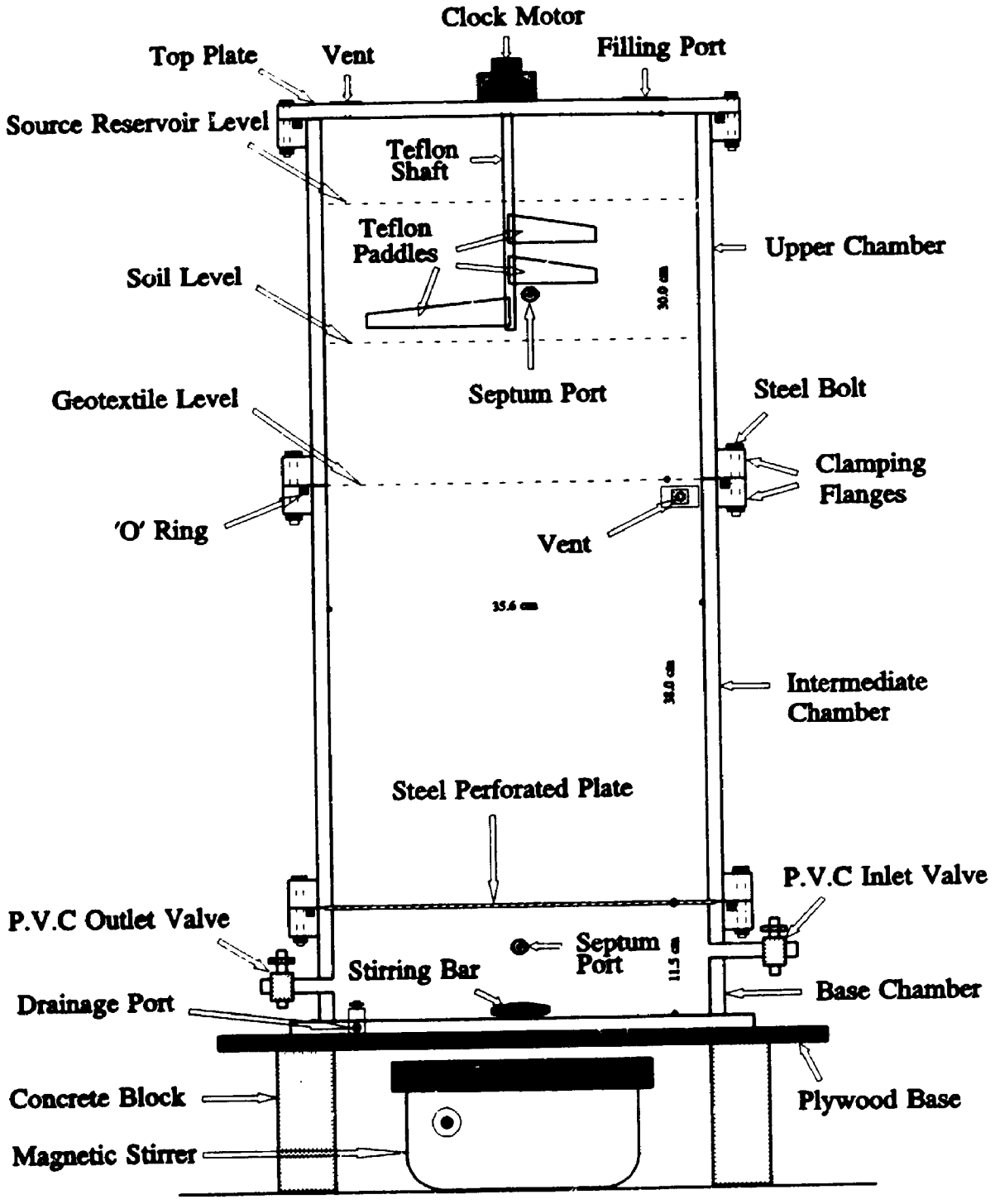

FIG. 9.1 SCHEMATIC OF THE ADVECTION-DIFFUSION APPARATUS USED IN TESTS # AD8 AND AD9

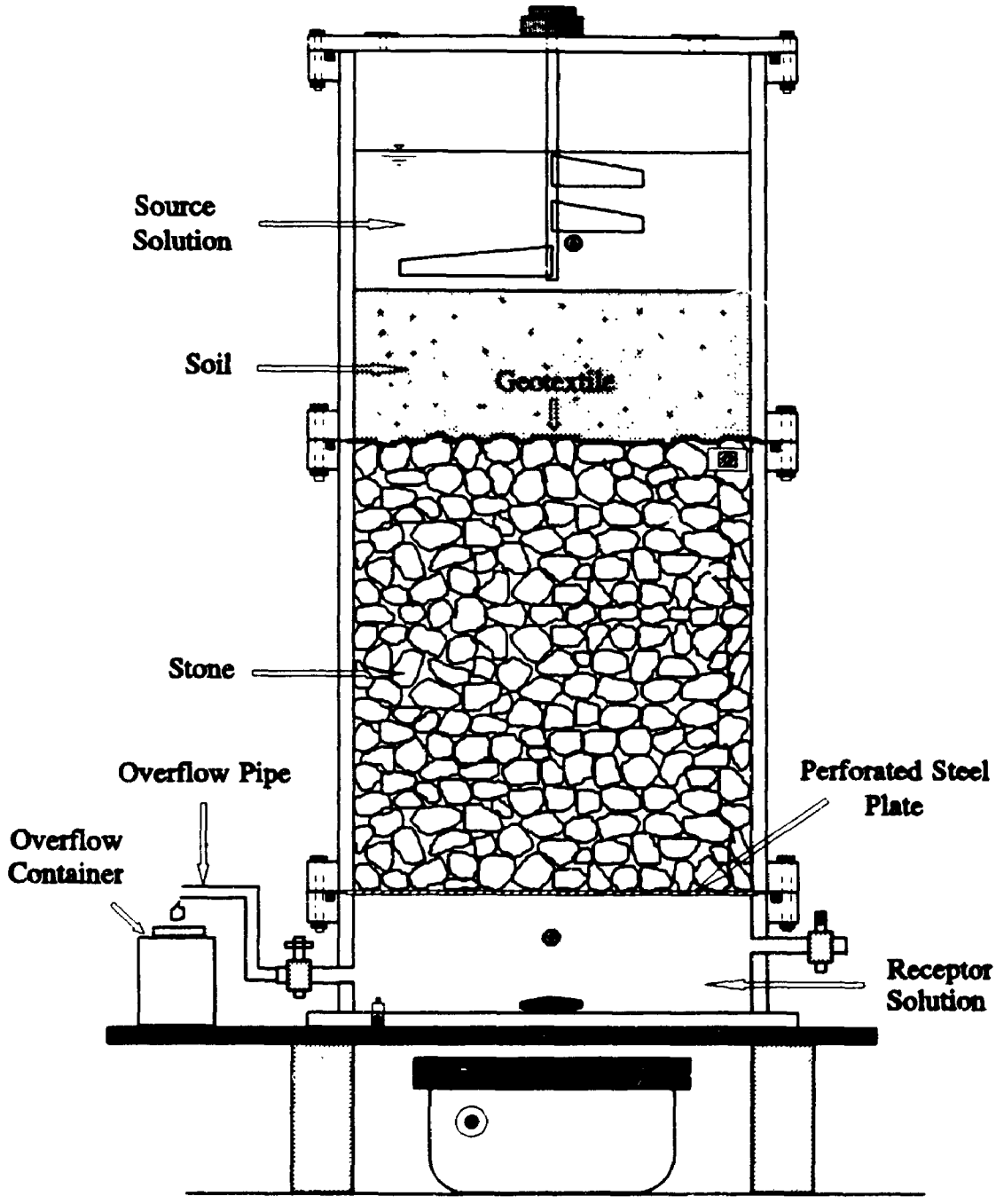

FIG. 9.2 SCHEMATIC OF THE SILT-UNSATURATED CLEAR STONE ADVECTION-DIFFUSION TESTS SET UP

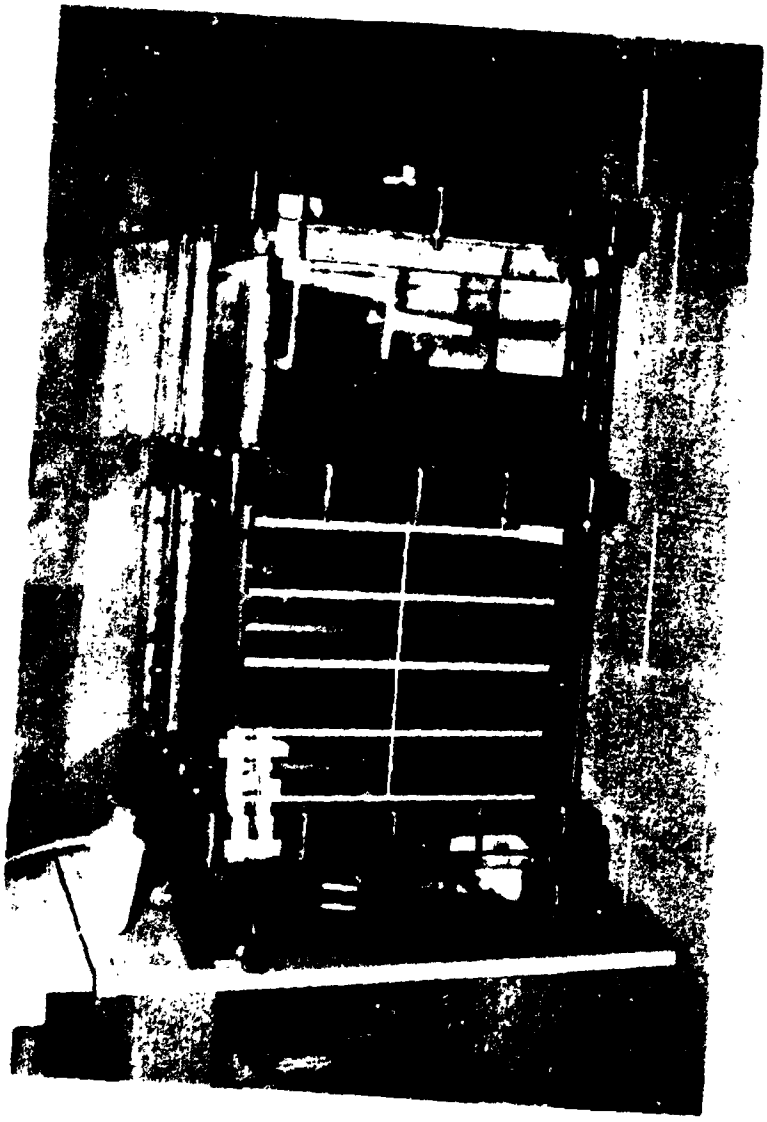

FIG. 9.3 VIEW OF THE ADVECTION-DIFFUSION APPARATUS DURING TEST CONDUCTED ON 2 LAYER SILT-UNSATURATED STONE SYSTEM

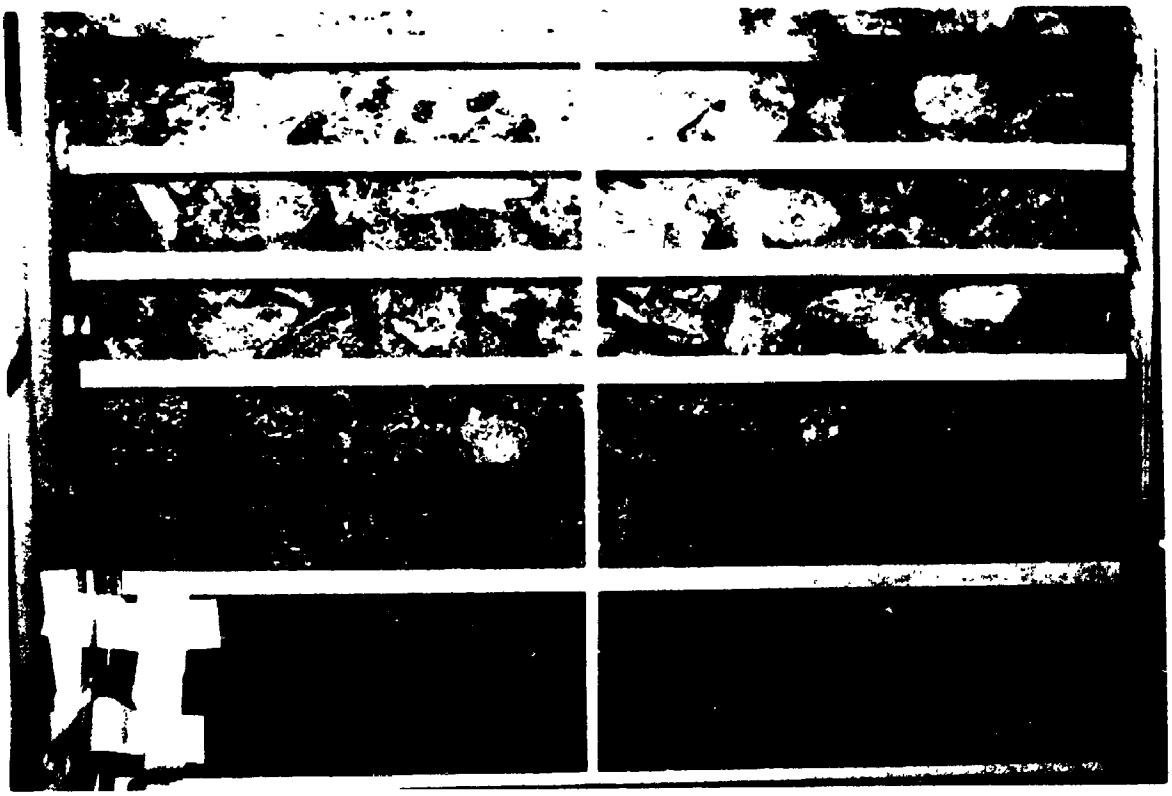

FIG. 9.4 VIEW OF THE INTERMEDIATE CHAMBER SHOWING THE STONES INSTALLED, PARALLEL TAPES STACKED TO THE FRONT FACE AS A GUIDE LINES FOR SECTIONING THE STONES AT THE END OF THE TEST, AND STAGNANT WATER DROPS ON THE INNER SURFACE OF THE CHAMBER OBSERVED DURING THE TEST

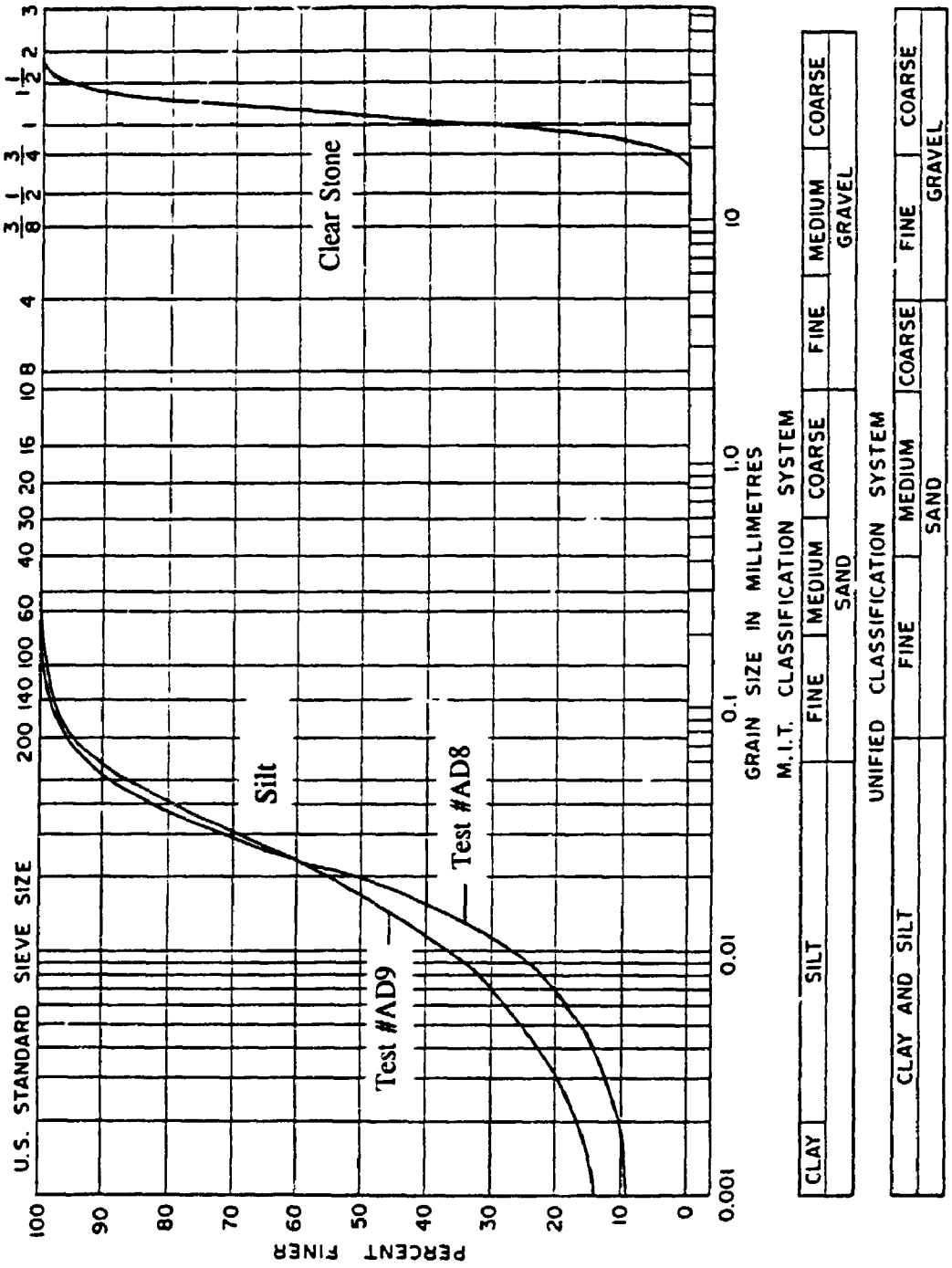

FIG. 9.5 GRAIN SIZE DISTRIBUTIONS OF THE SILT SOILS AND CLEAR STONE USED IN ADVECTION-DIFFUSION TESTS # AD8 AND AD9

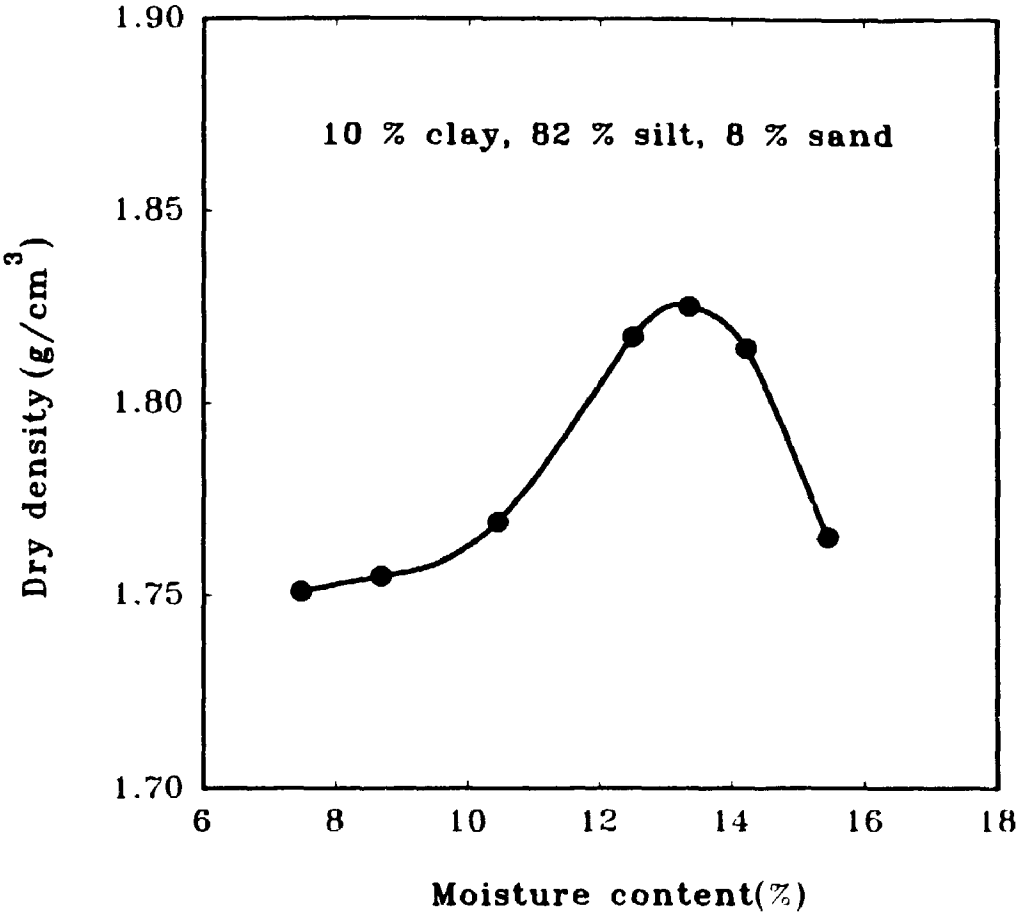

FIG. 9.6 DRY DENSITY–MOISTURE CONTENT RELATIONSHIP IN SILT SOIL USED IN ADVECTION–DIFFUSION TEST #AD8

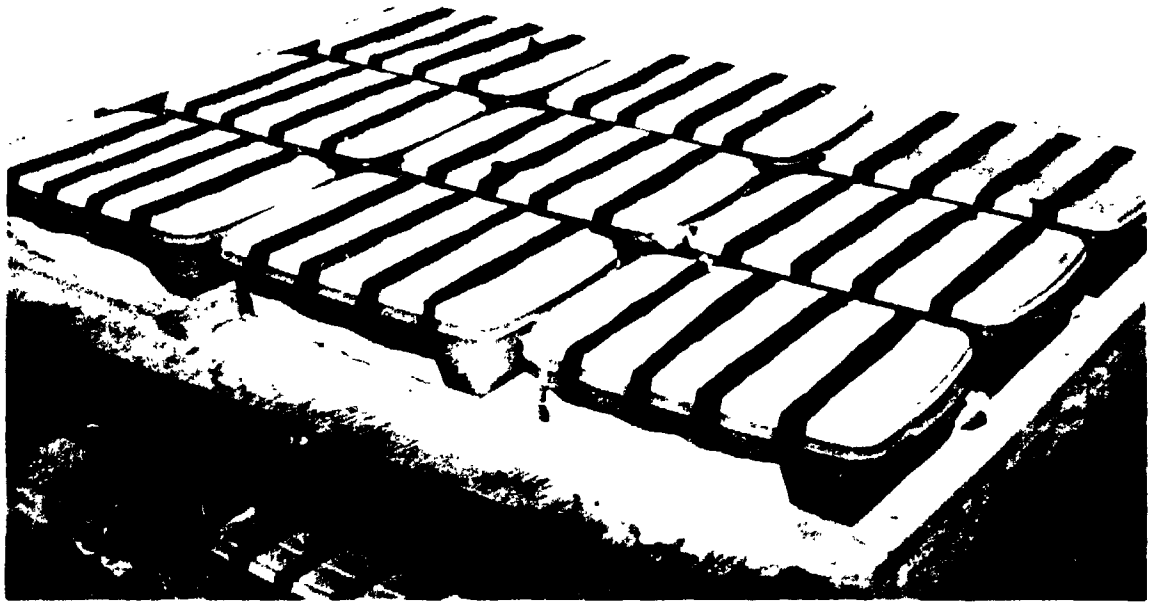

FIG. 9.7 PLASTIC CONTAINERS INCLUDING STONES AND DISTILLED WATER WERE PLACED ON HEAVY DUTY SHAKER TO WASH THE STONES

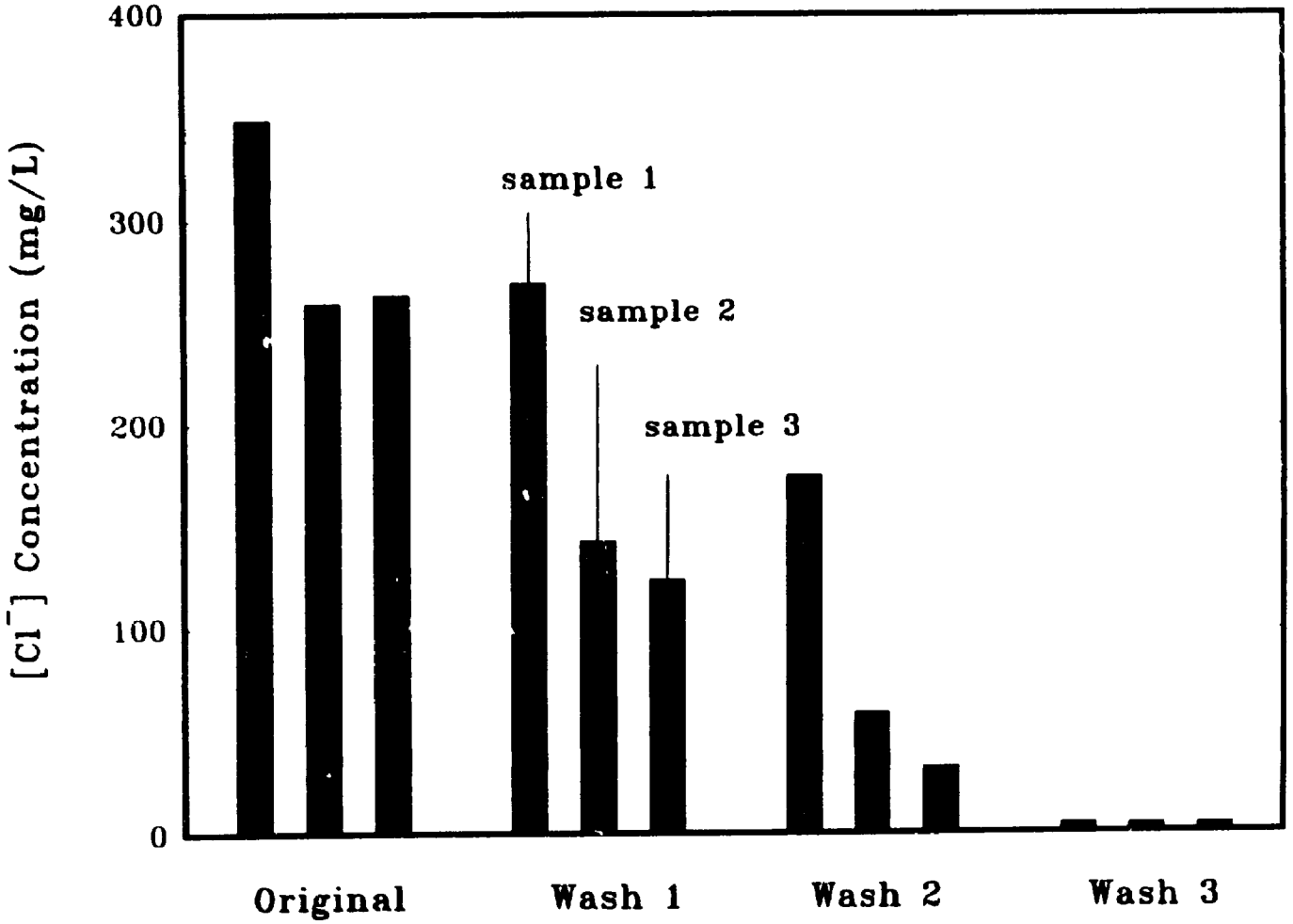

FIG. 9.8 ORIGINAL BACKGROUND CONCENTRATION OF 3 STONE SAMPLES AND CONCENTRATION RECOVERED AT THE END OF 3 WASH STEPS

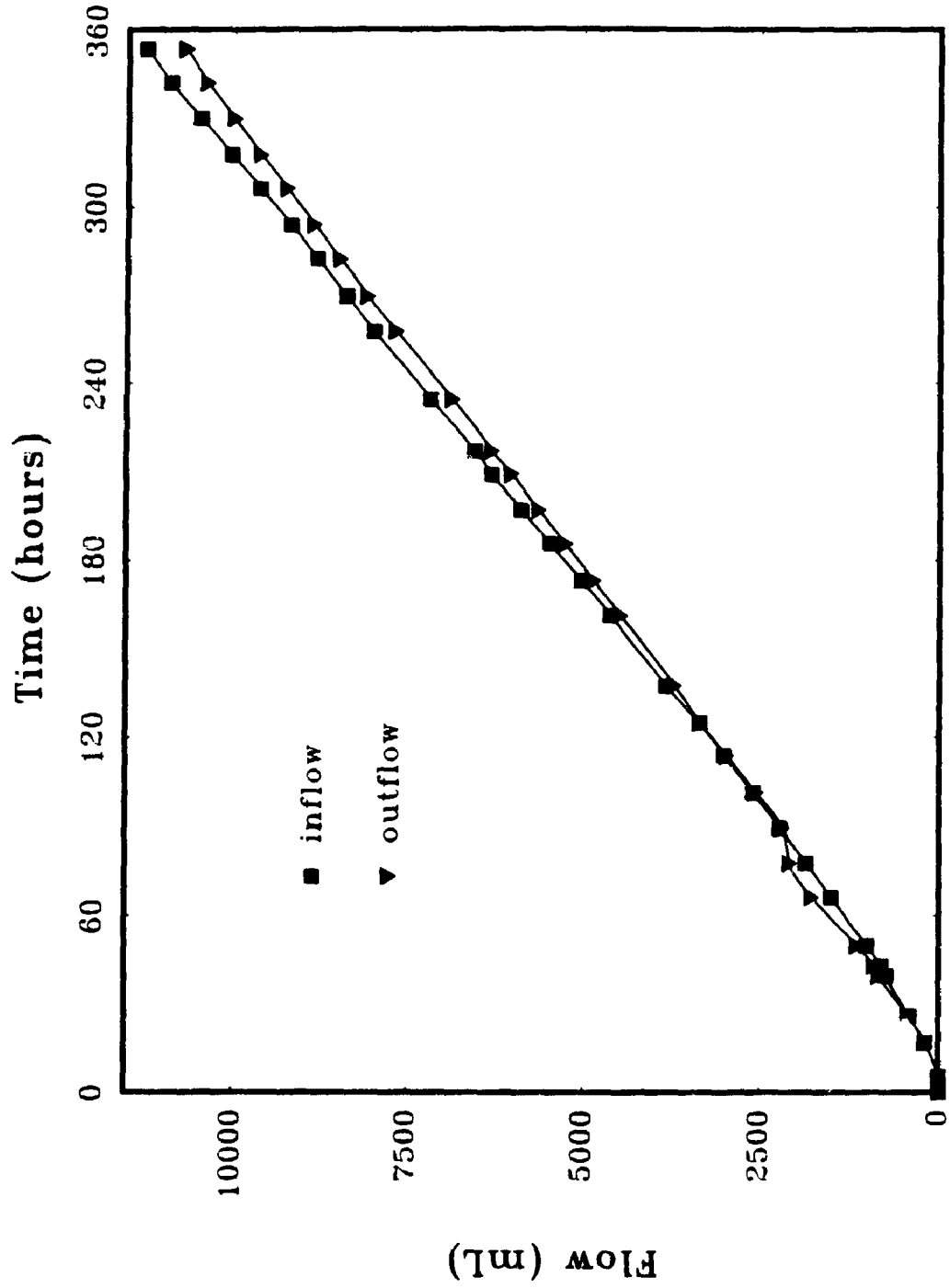

FIG. 9.9 OBSERVED INFLOW AND OUTFLOW RATES VERSUS ELAPSED TIME IN ADVECTION-DIFFUSION TEST #AD8 (SILT-UNSATURATED CLEAR STONE)

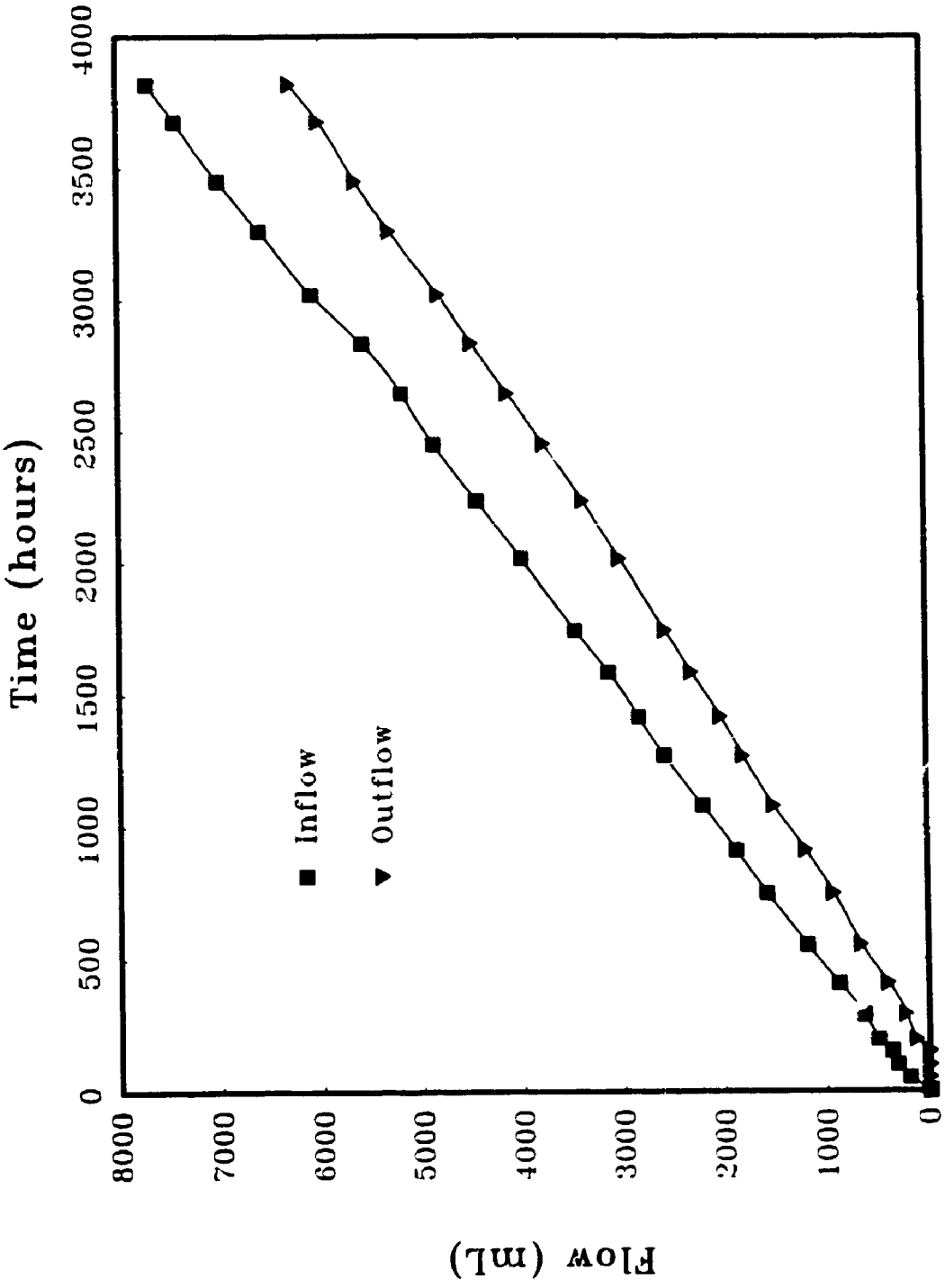

FIG. 9.10 OBSERVED INFLOW AND OUTFLOW RATES VERSUS ELAPSED TIME IN ADVECTION-DIFFUSION TEST #AD9 (SILT-UNSATURATED CLEAR STONE)

FIG. 9.11 TERMINATION OF THE TESTS # AD8 AND AD9 BY DRAINING THE SOURCE RESERVOIR SOLUTION

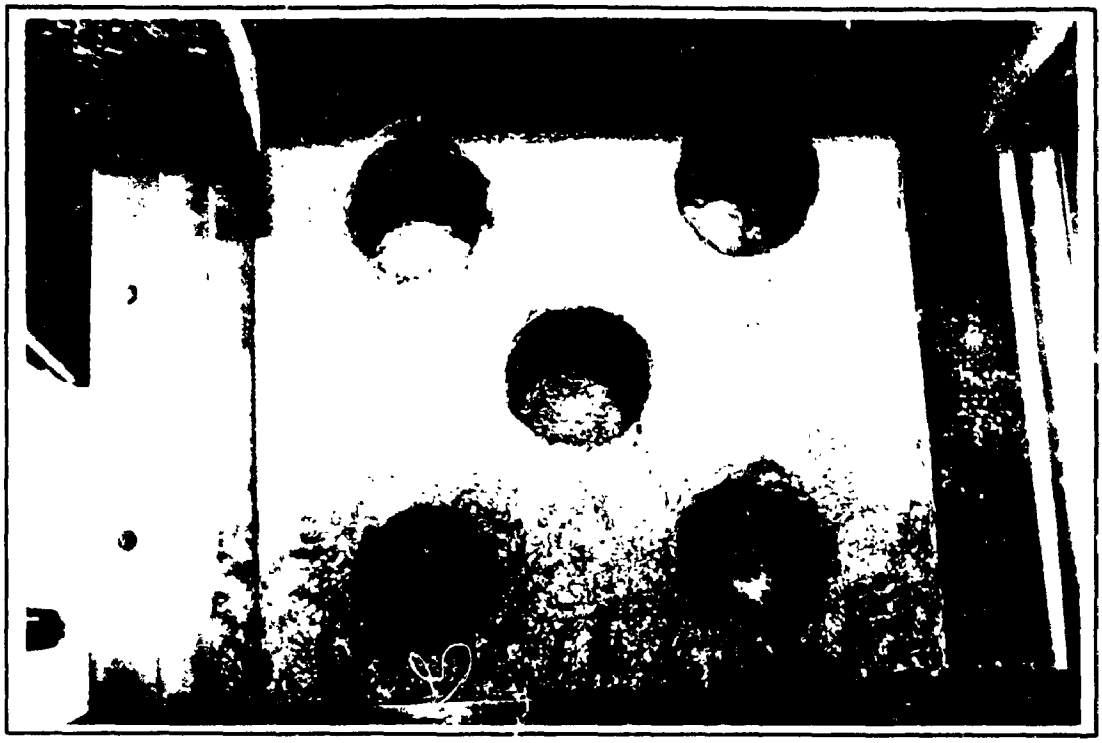

FIG. 9.12 PLAN VIEW OF THE LOCATIONS OF THE SHELBY TUBE SAMPLES TAKEN FROM THE SILT LAYER IN TEST #AD9

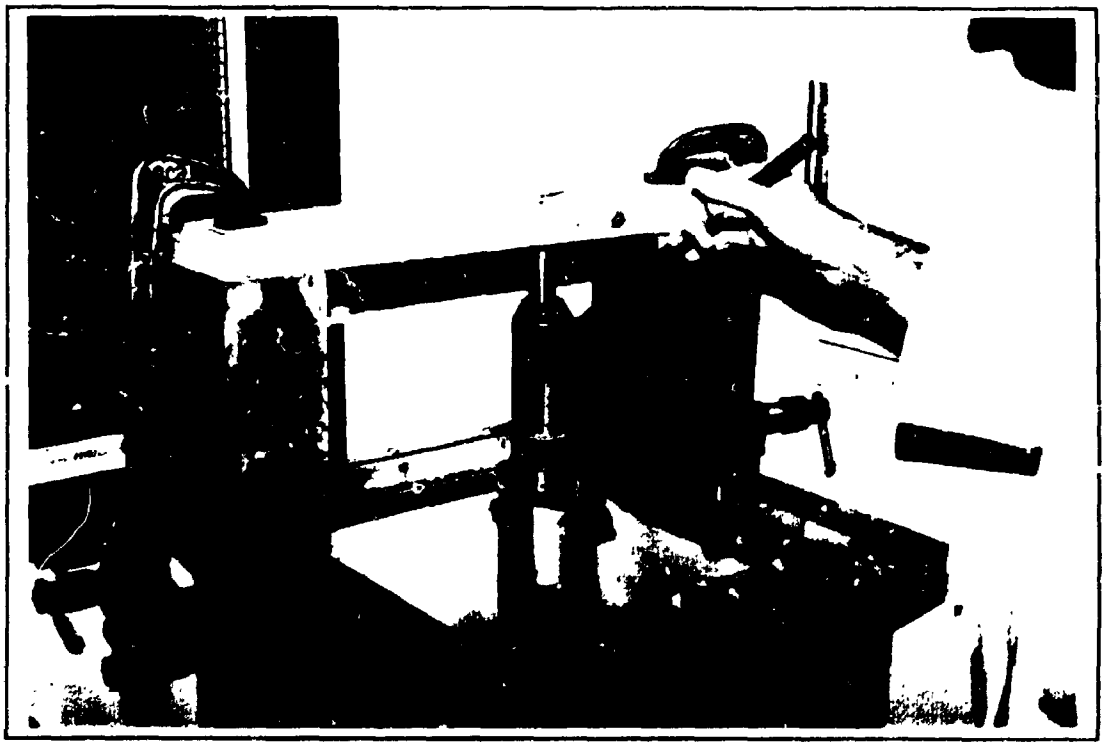

FIG. 9.13 SUPPORTS, HYDRAULIC JACK, AND SHELBY TUBE USED FOR SAMPLING FROM THE SILT LAYER IN TESTS # AD8 AND AD9

FIG. 9.14 SHELBY TUBE WAS PULLED OUT OF THE SOIL AFTER INSERTING THE TUBE INTO THE SOIL BY A HYDRAULIC JACK

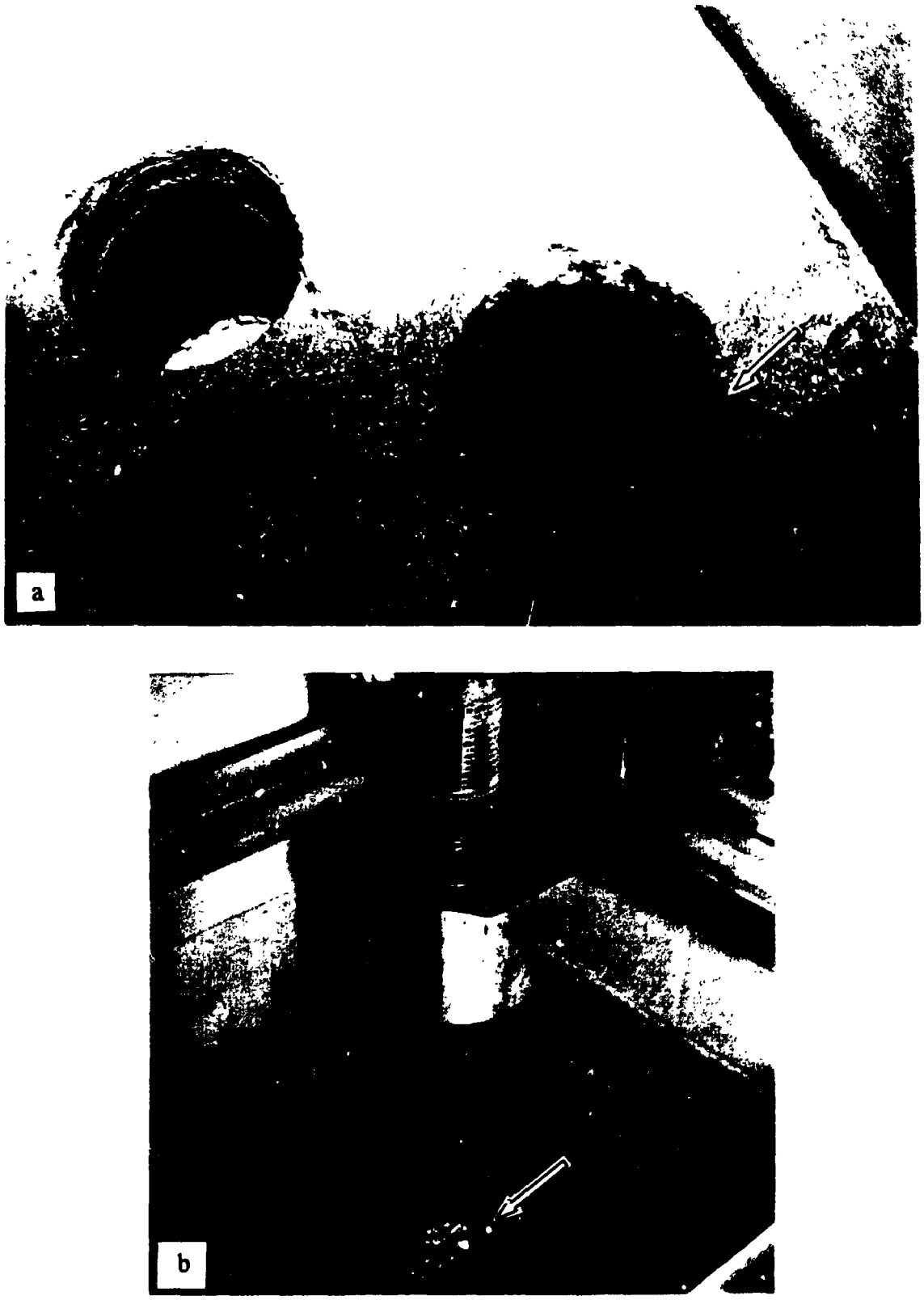

FIG. 9.15 PHOTOS SHOWING THE LOOSE SOIL IN UPPER PARTS OF THE SILT SOIL IN: (a) TEST #AD9, AND (b) TEST #AD8

FIG. 9.16 SOIL SAMPLE WAS PUSHED OUT OF THE SHELBY TUBE AND SLICED IN 2 cm THICKNESSES

FIG. 9.17 SLICED SILT SAMPLES OBTAINED FROM 5 SHELBY TUBE SAMPLES AFTER TERMINATION OF TEST #AD9 (AS OF TEST #AD8)

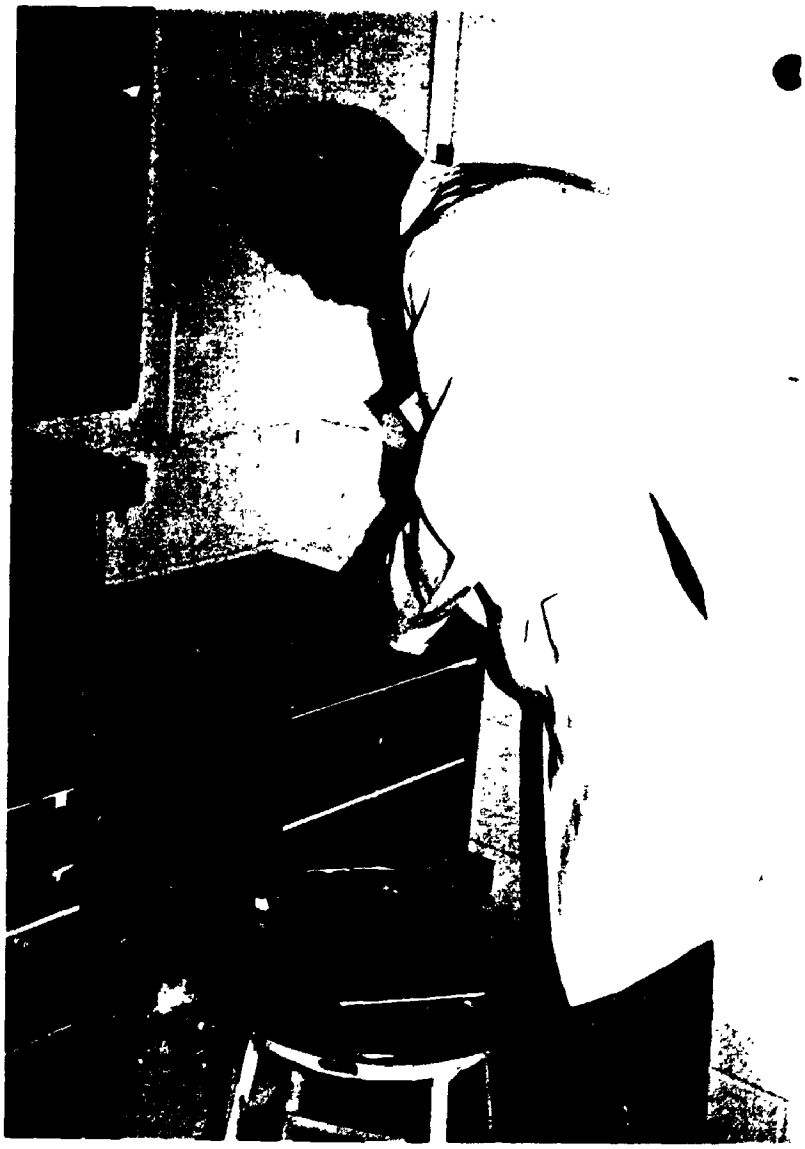

FIG. 9.18 SECTIONING THE STONE LAYER IN 3.8 cm THICKNESSES BY PICKING UP THE STONES AND PLACING EACH HALF OF THE ENTIRE LAYER INTO A STAINLESS STEEL TRAY

FIG. 9.19 COLLECTED STONE SAMPLES AFTER SECTIONING THE STONE LAYER INTO 10 SUBLAYERS (EACH TRAY CONTAINS HALF OF THE STONES FROM EACH SUBLAYER)

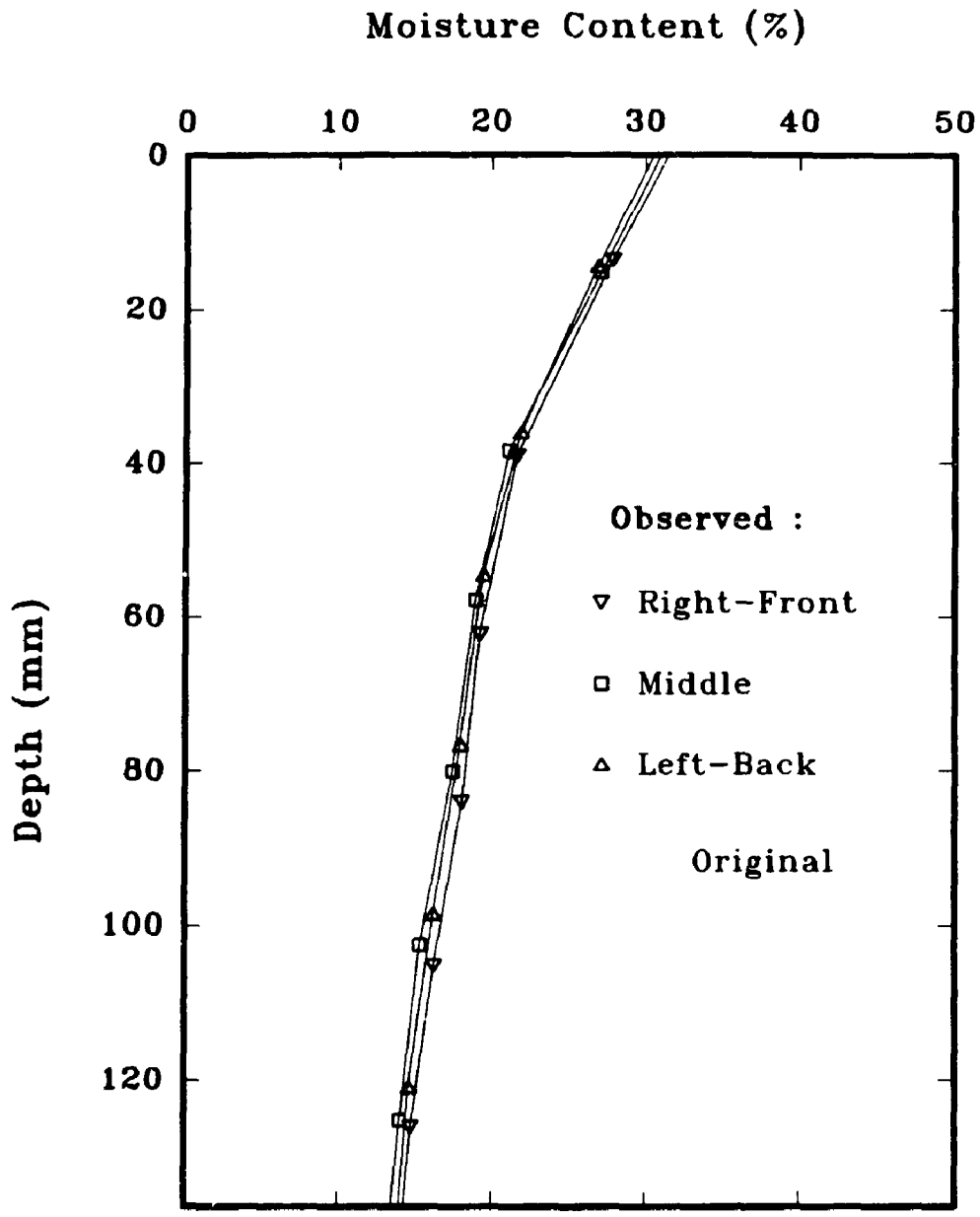

FIG. 9.20 MOISTURE CONTENT PROFILES OF SILT LAYER IN ADVECTION-DIFFUSION TEST #AD8, MEASURED IN THREE LOCATIONS

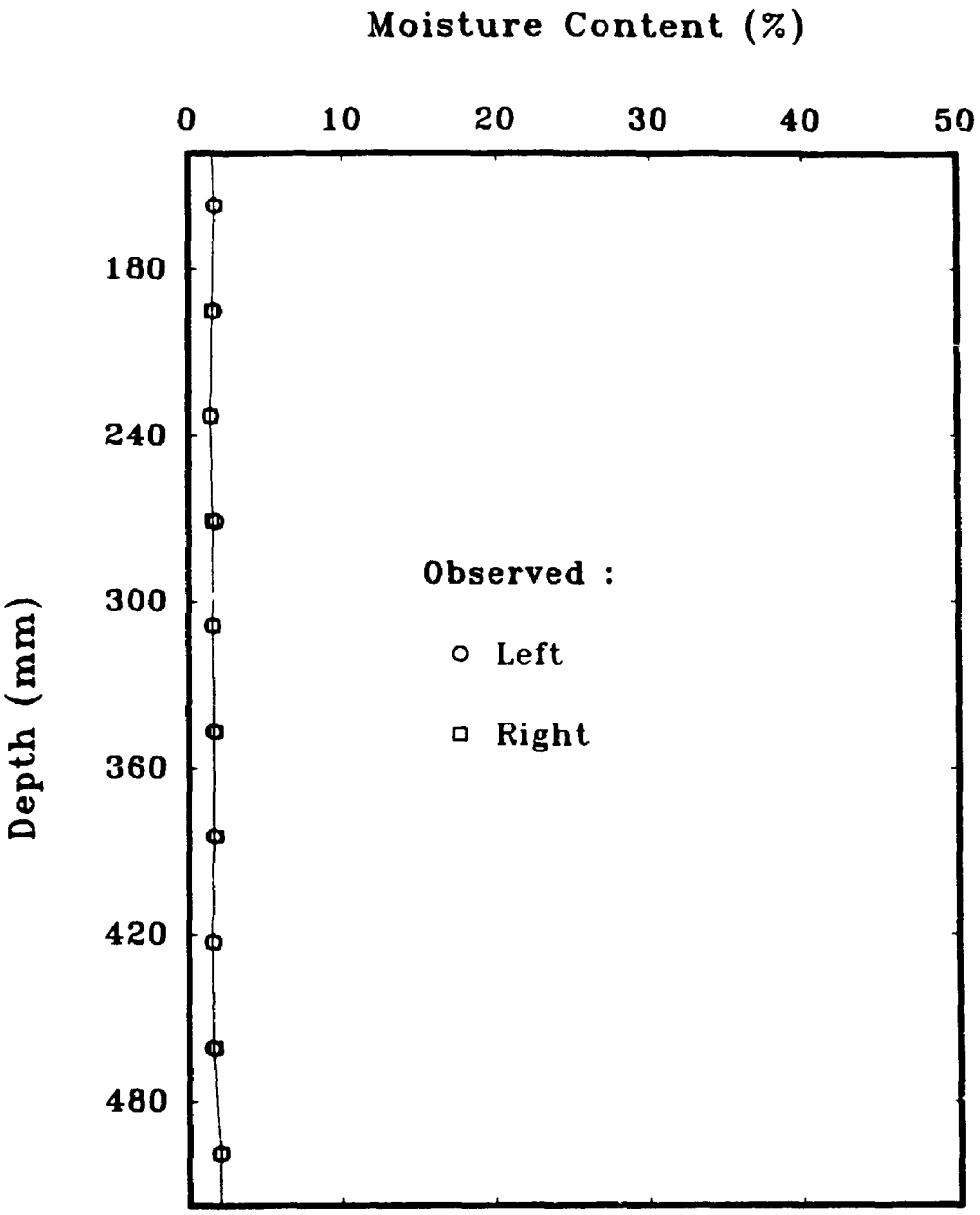

FIG. 9.21 MOISTURE CONTENT PROFILES IN RIGHT AND LEFT SIDE OF THE CLEAR STONE LAYER IN ADVECTION-DIFFUSION TEST # AD8

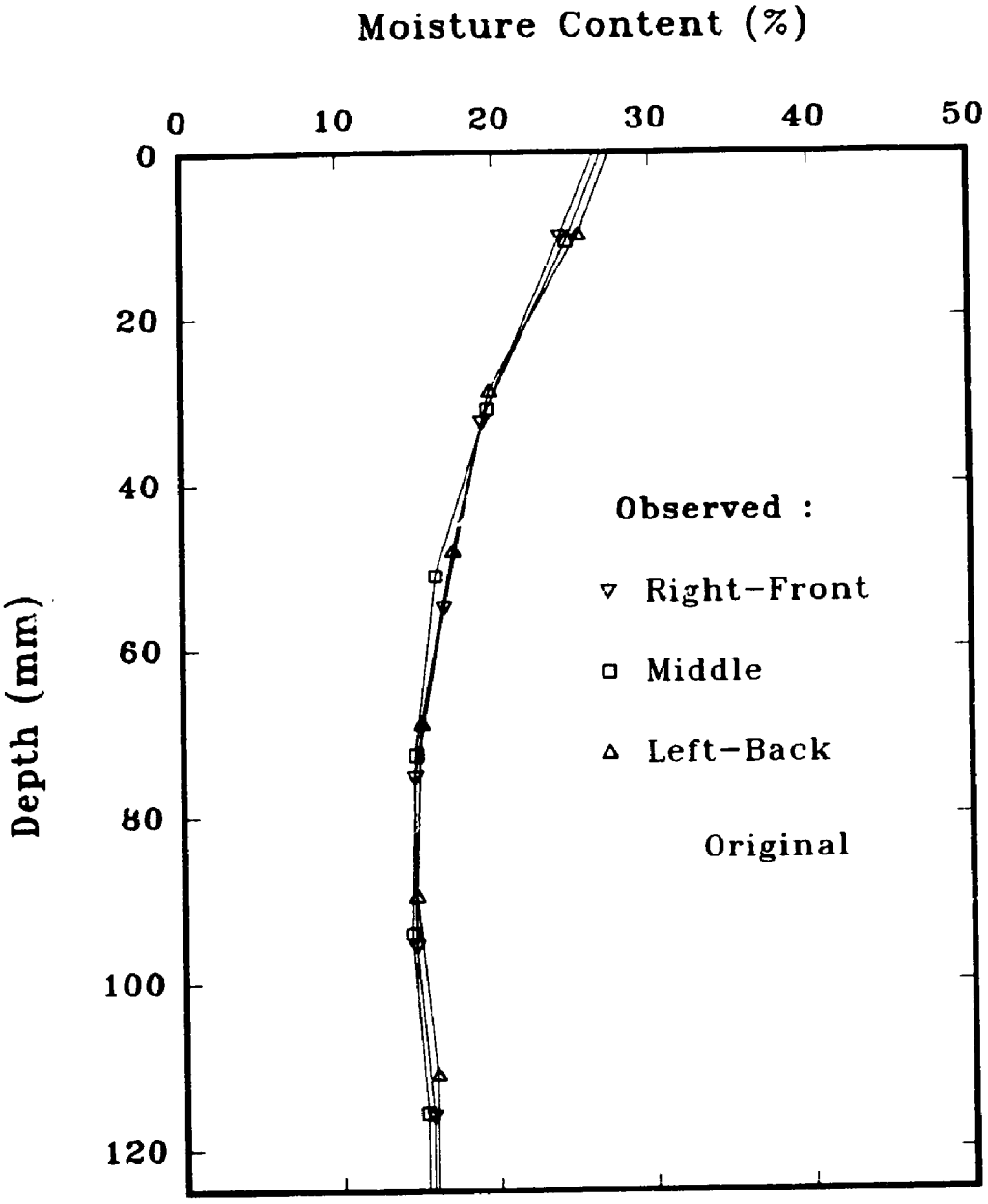

FIG. 9.22 MOISTURE CONTENT PROFILES OF SILT LAYER IN ADVECTION-DIFFUSION TEST #AD9, MEASURED IN THREE LOCATIONS

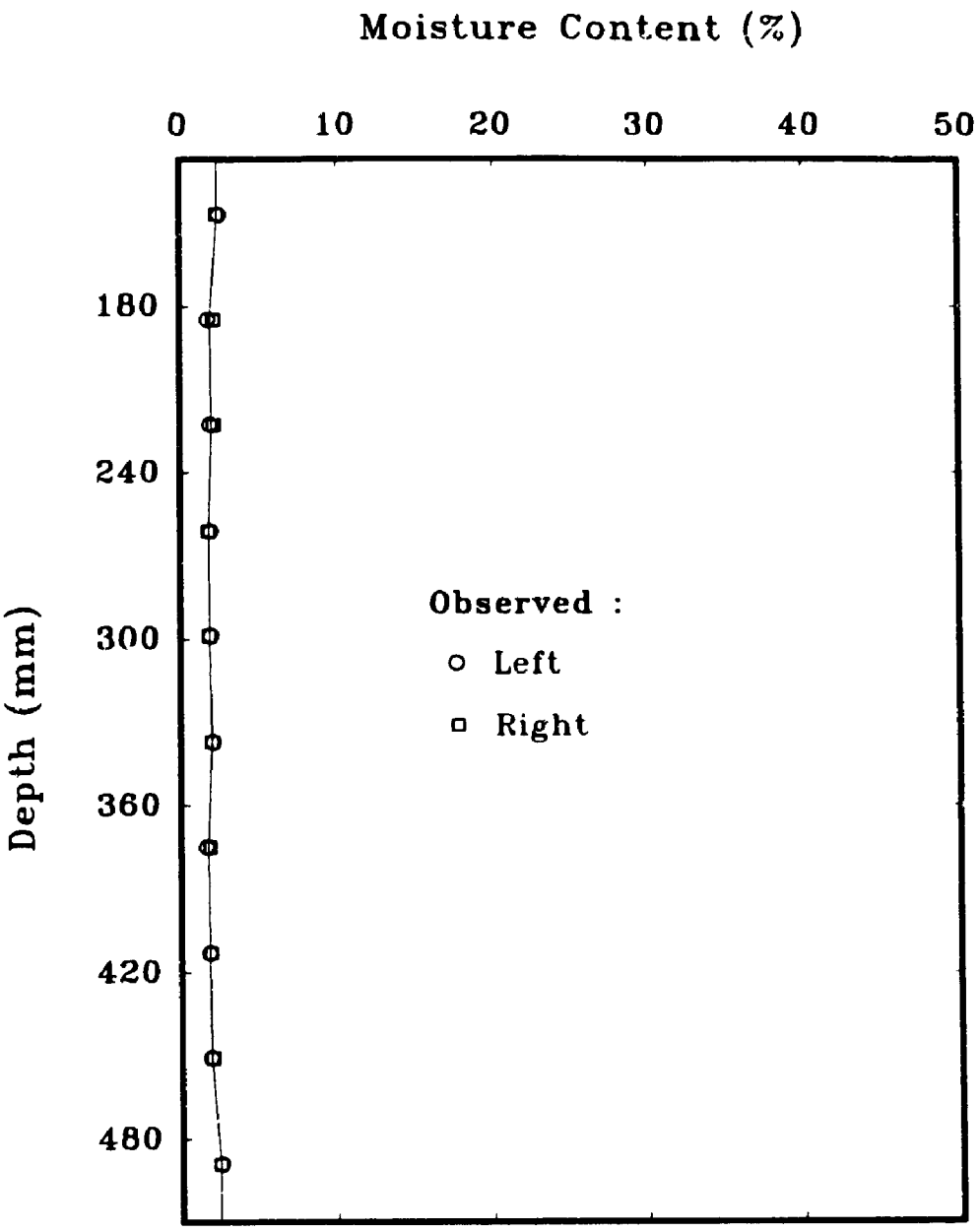

FIG. 9.23 MOISTURE CONTENT PROFILES IN RIGHT AND LEFT SIDE OF THE CLEAR STONE LAYER IN ADVECTION-DIFFUSION TEST #AD9

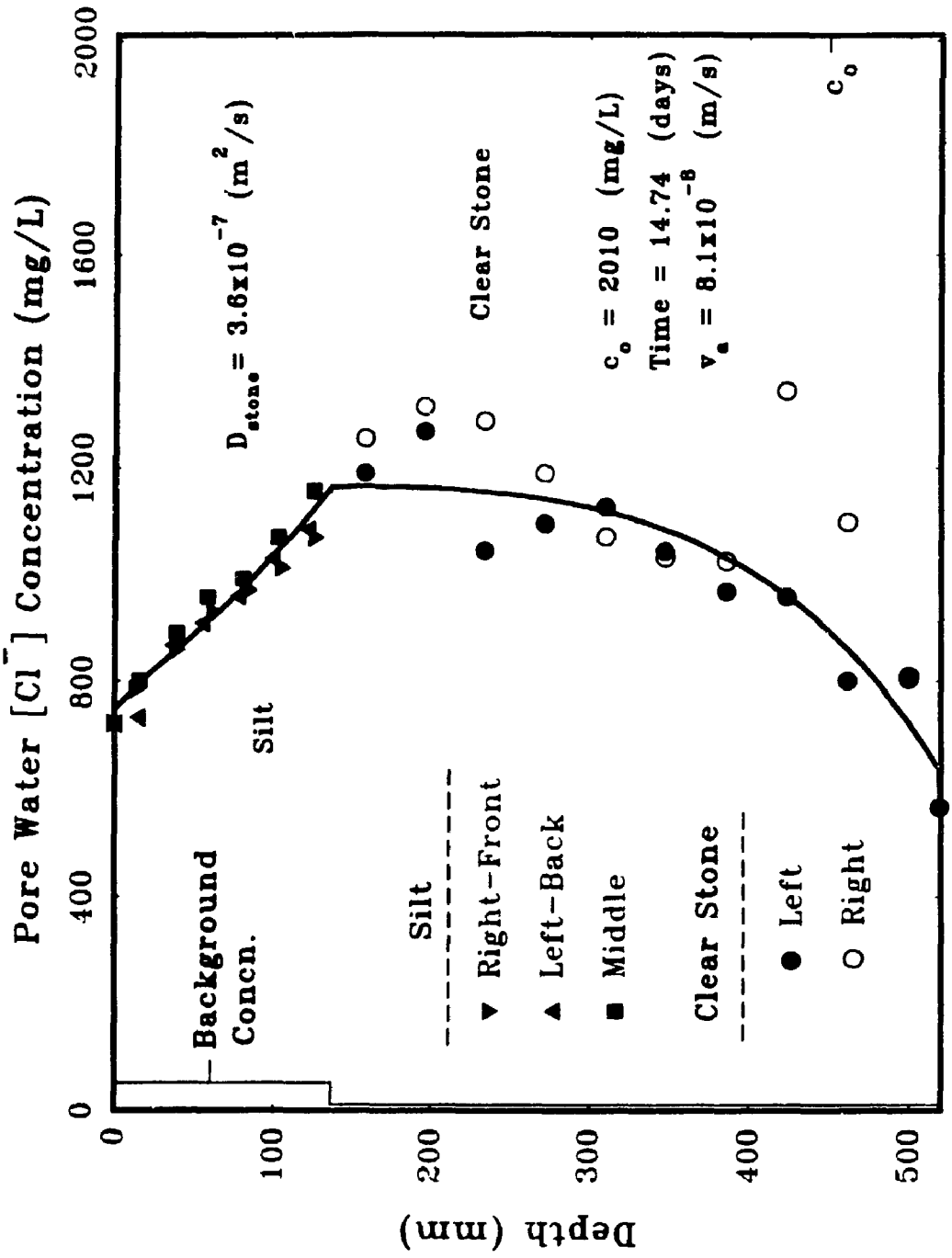

FIG. 9.24 OBSERVED AND CALCULATED [Cl^-] CONCENTRATION PROFILES IN ADVECTION-DIFFUSION TEST #AD8 (SILT-UNSATURATED CLEAR STONE)

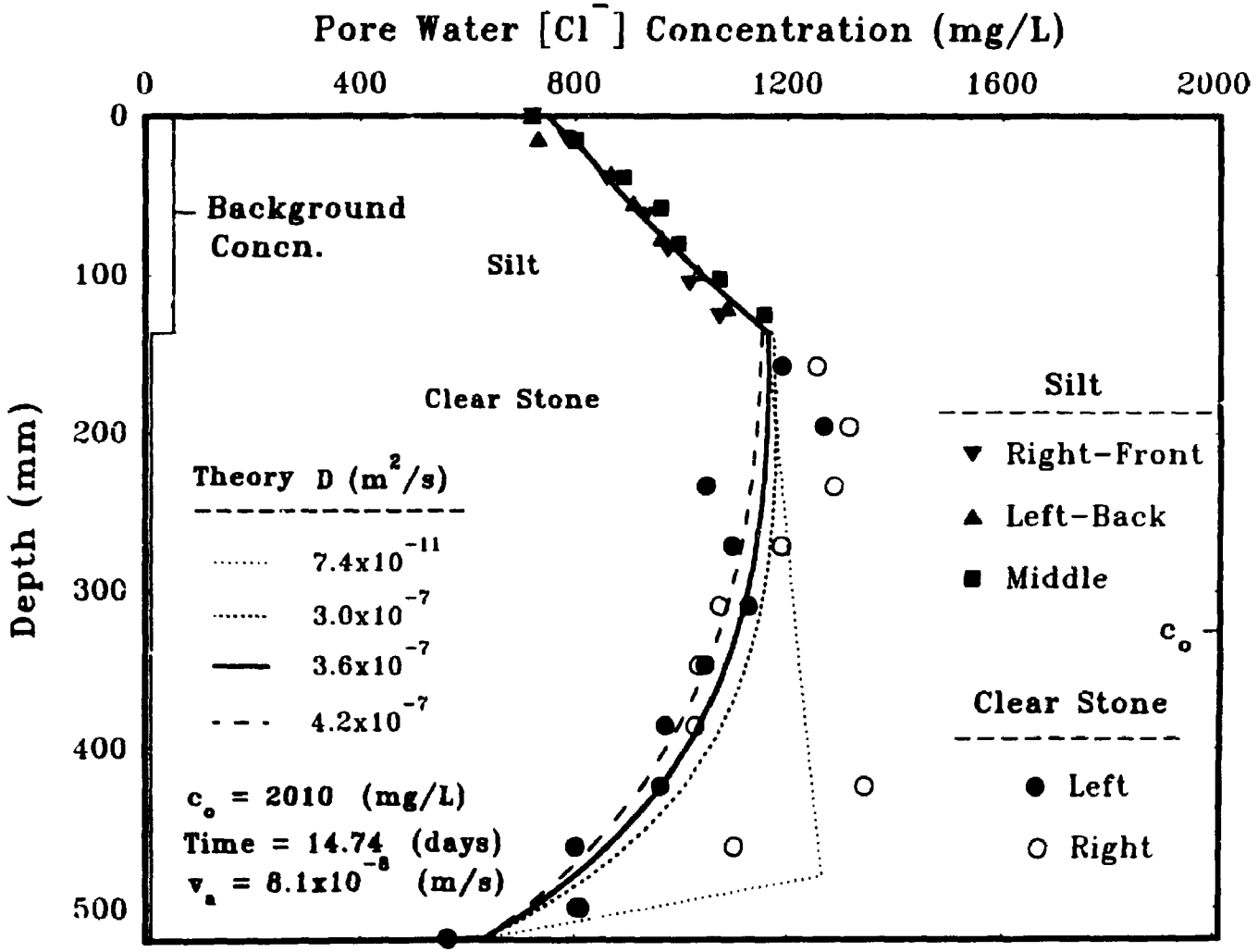

FIG. 9.25 OBSERVED AND CALCULATED [Cl⁻] CONCENTRATION PROFILES IN ADVECTION-DIFFUSION TEST #AD8, USING DIFFERENT HYDRODYNAMIC DISPERSION COEFFICIENT FOR UNSATURATED STONE LAYER

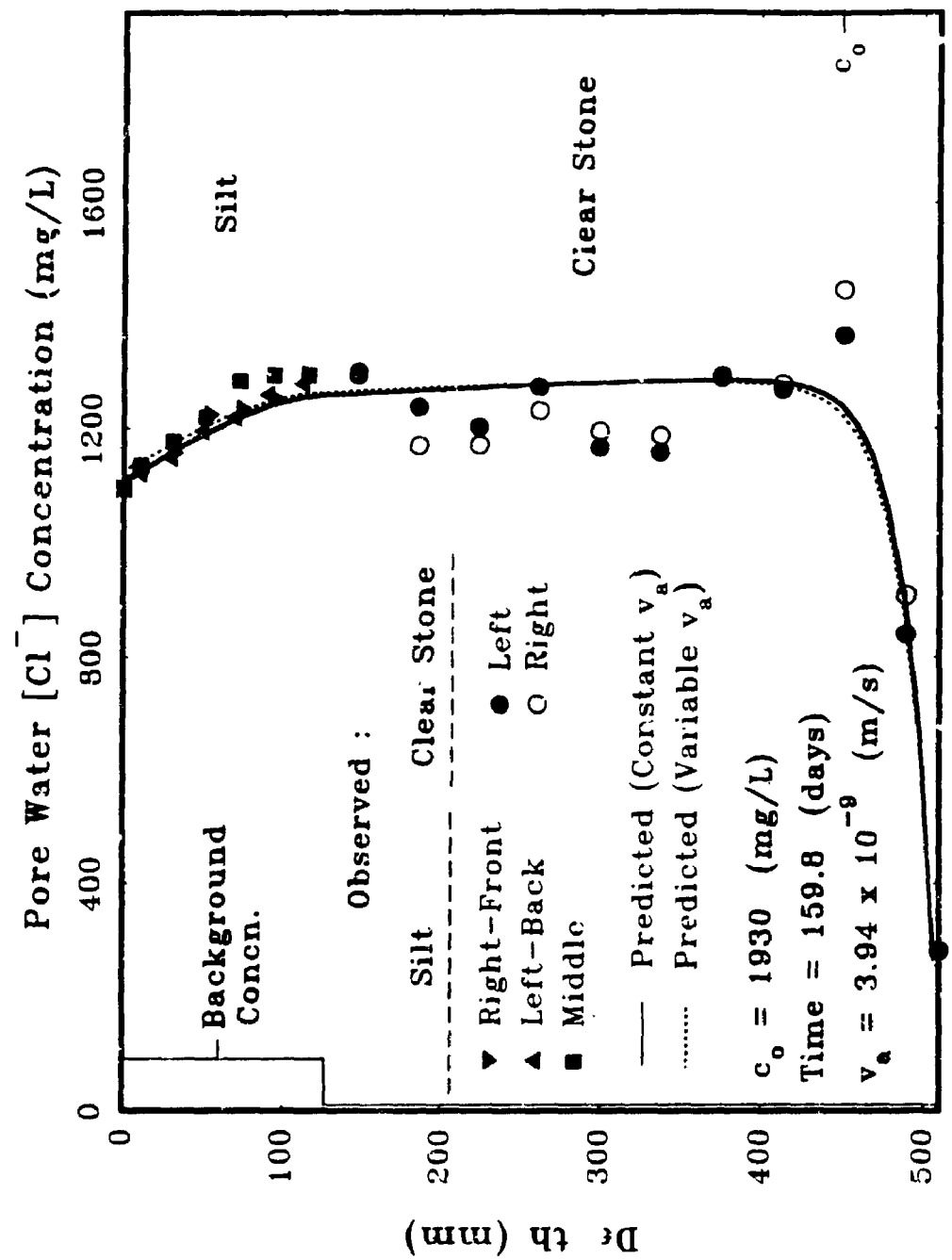

FIG. 9.26 OBSERVED AND CALCULATED [Cl^-] CONCENTRATION PROFILES IN ADVECTION-DIFFUSION TEST #AD9 (SILT-UNSATURATED CLEAR STONE)

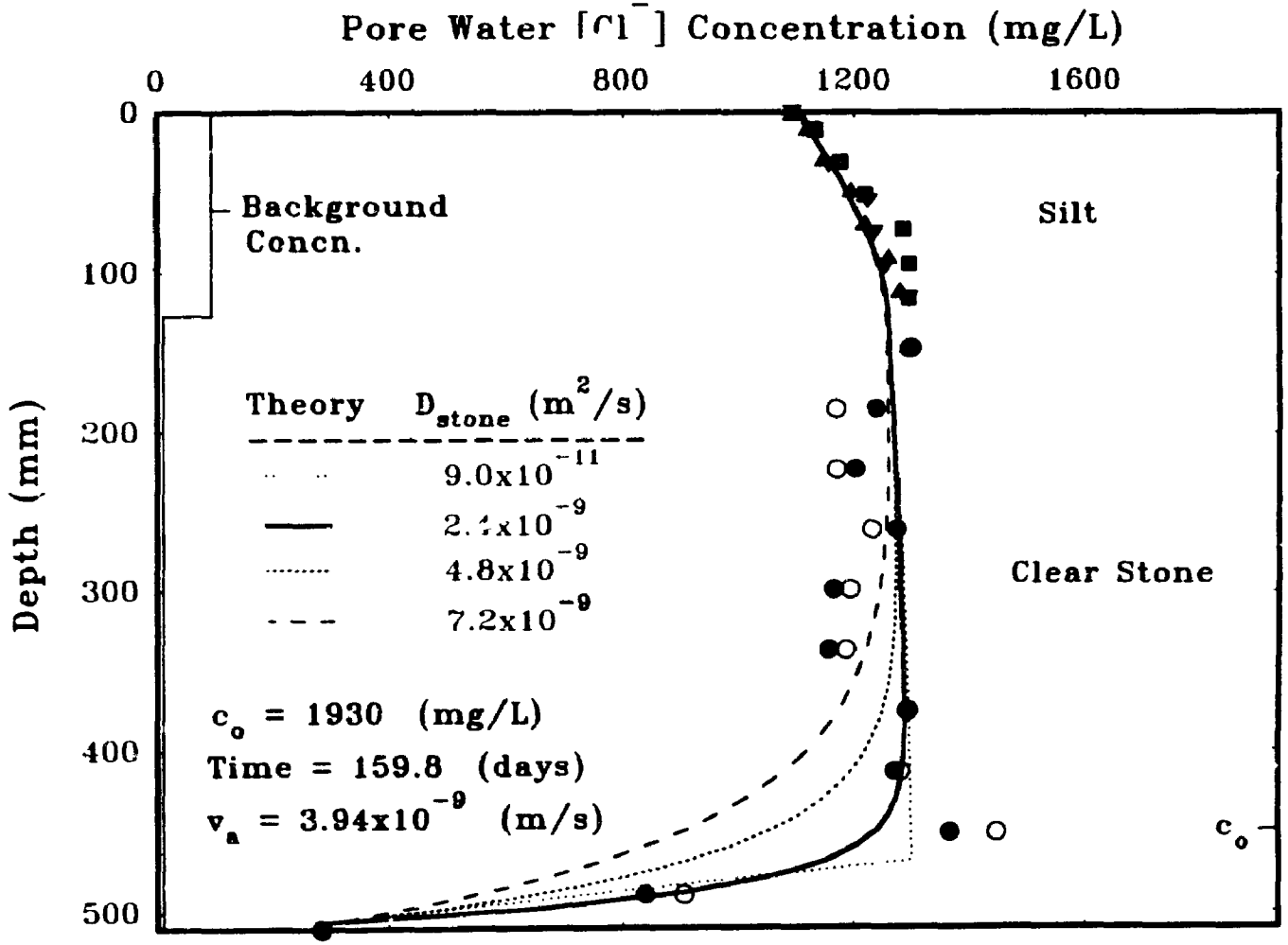

FIG. 9.27 OBSERVED AND CALCULATED [Cl^-] CONCENTRATION PROFILES IN ADVECTION-DIFFUSION TEST #AD9, USING DIFFERENT HYDRODYNMIC DISPERSION COEFFICIENTS FOR UNSATURATED STONE LAYER

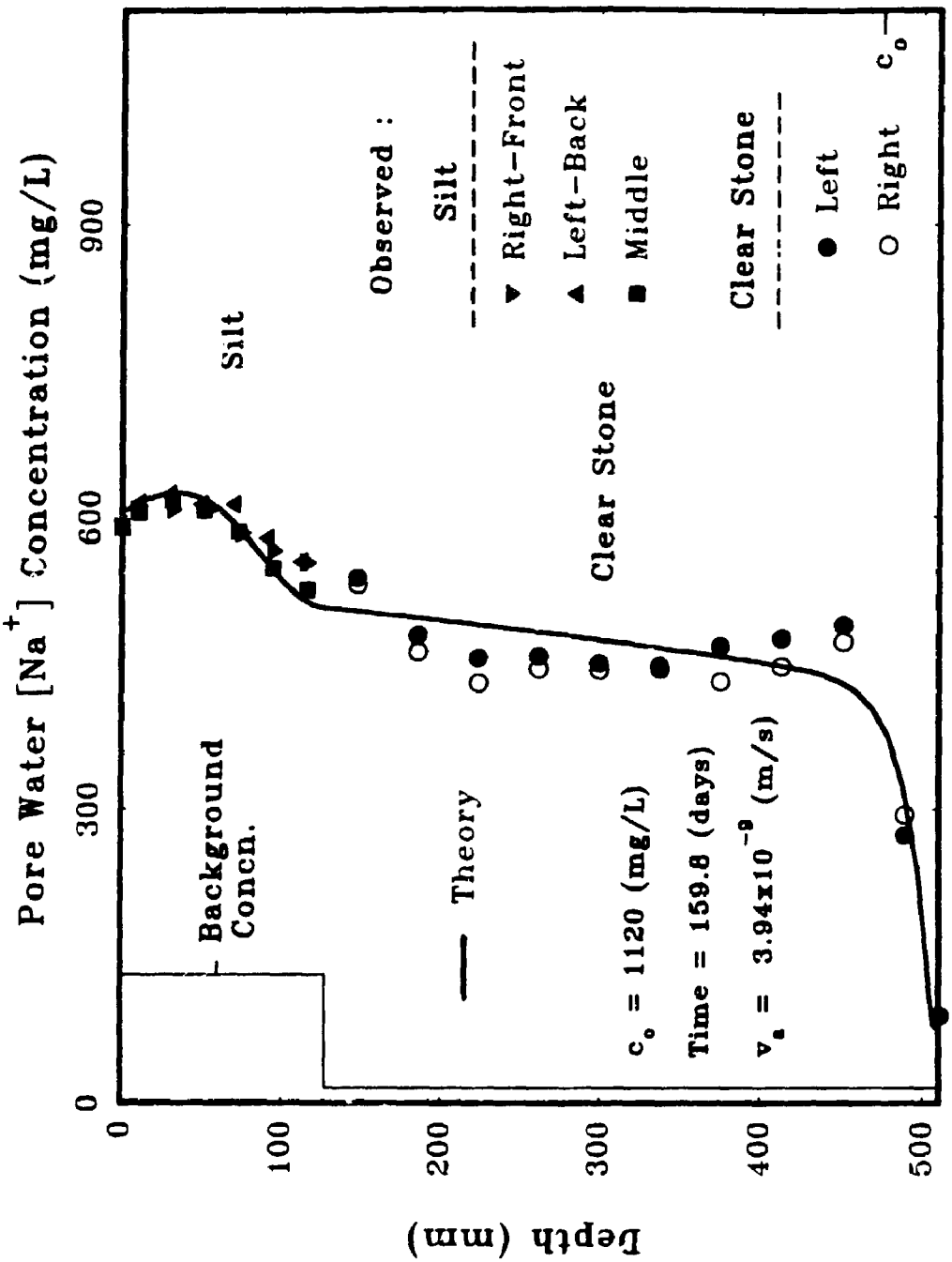

FIG. 9.28 OBSERVED AND CALCULATED [Na^+] CONCENTRATION PROFILES IN ADVECTION-DIFFUSION TEST #AD9 (SILT-UNSATURATED CLEAR STONE)

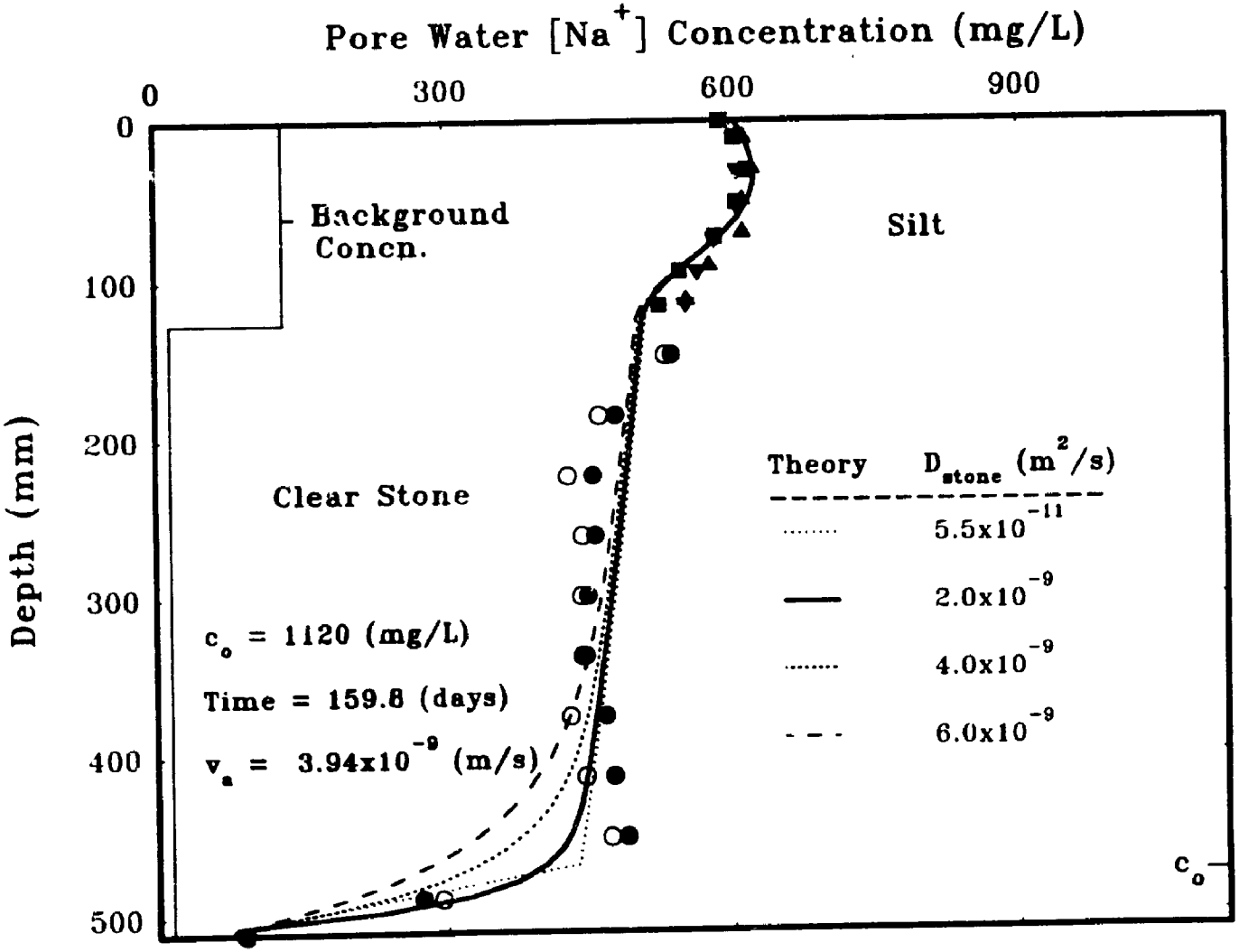

FIG. 9.29 OBSERVED AND CALCULATED [Na^+] CONCENTRATION PROFILES IN ADVECTION-DIFFUSION TEST #AD9, USING DIFFERENT HYDRODYNAMIC DISPERSION COEFFICIENTS FOR UNSATURATED STONE LAYER

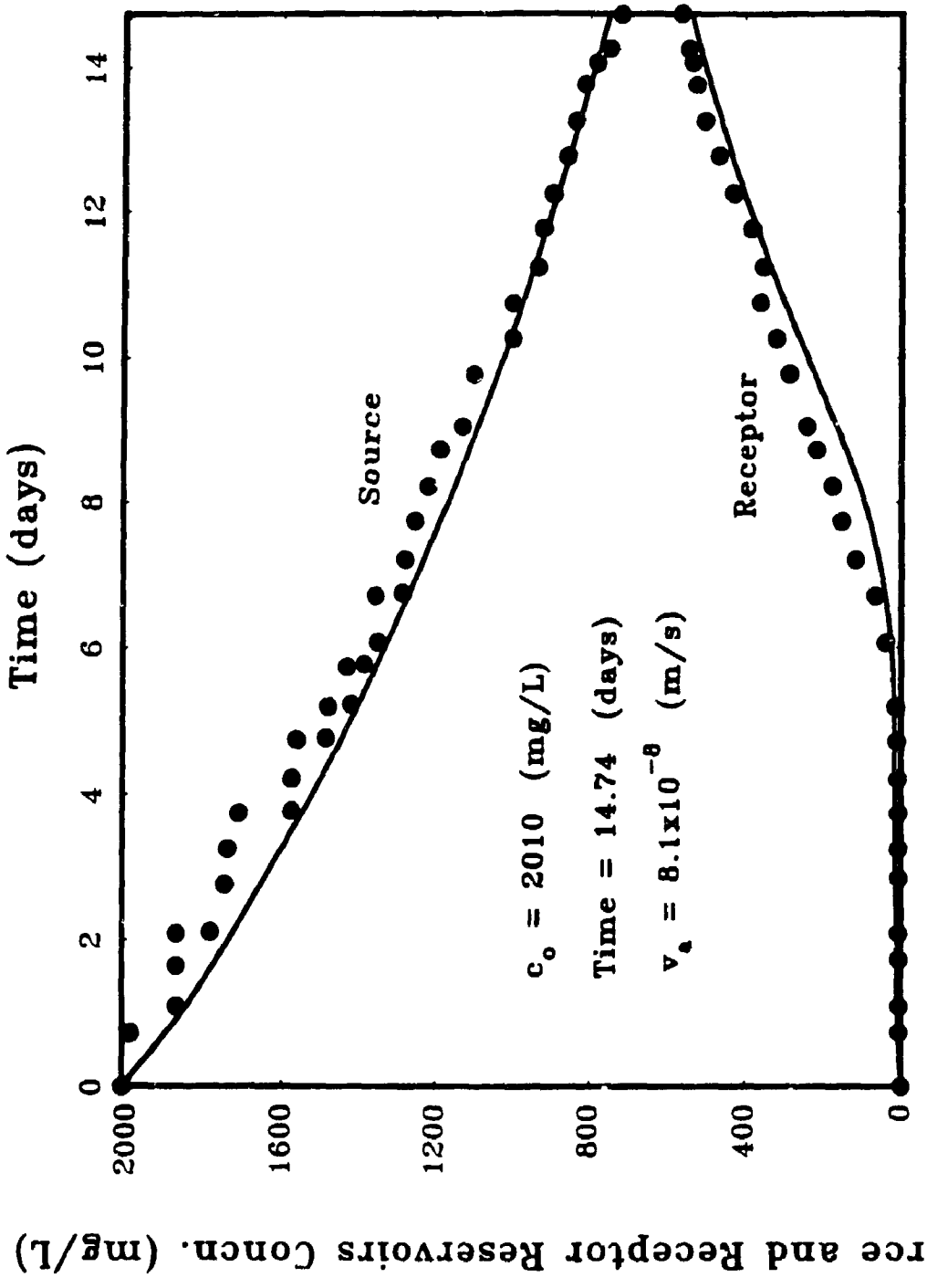

FIG. 9.30 OBSERVED AND THEORETICAL $[Cl^-]$ CONCENTRATIONS VERSUS ELAPSED TIME IN SOURCE AND RECEPTOR RESERVOIRS OF ADVECTION-DIFFUSION TEST #AD8

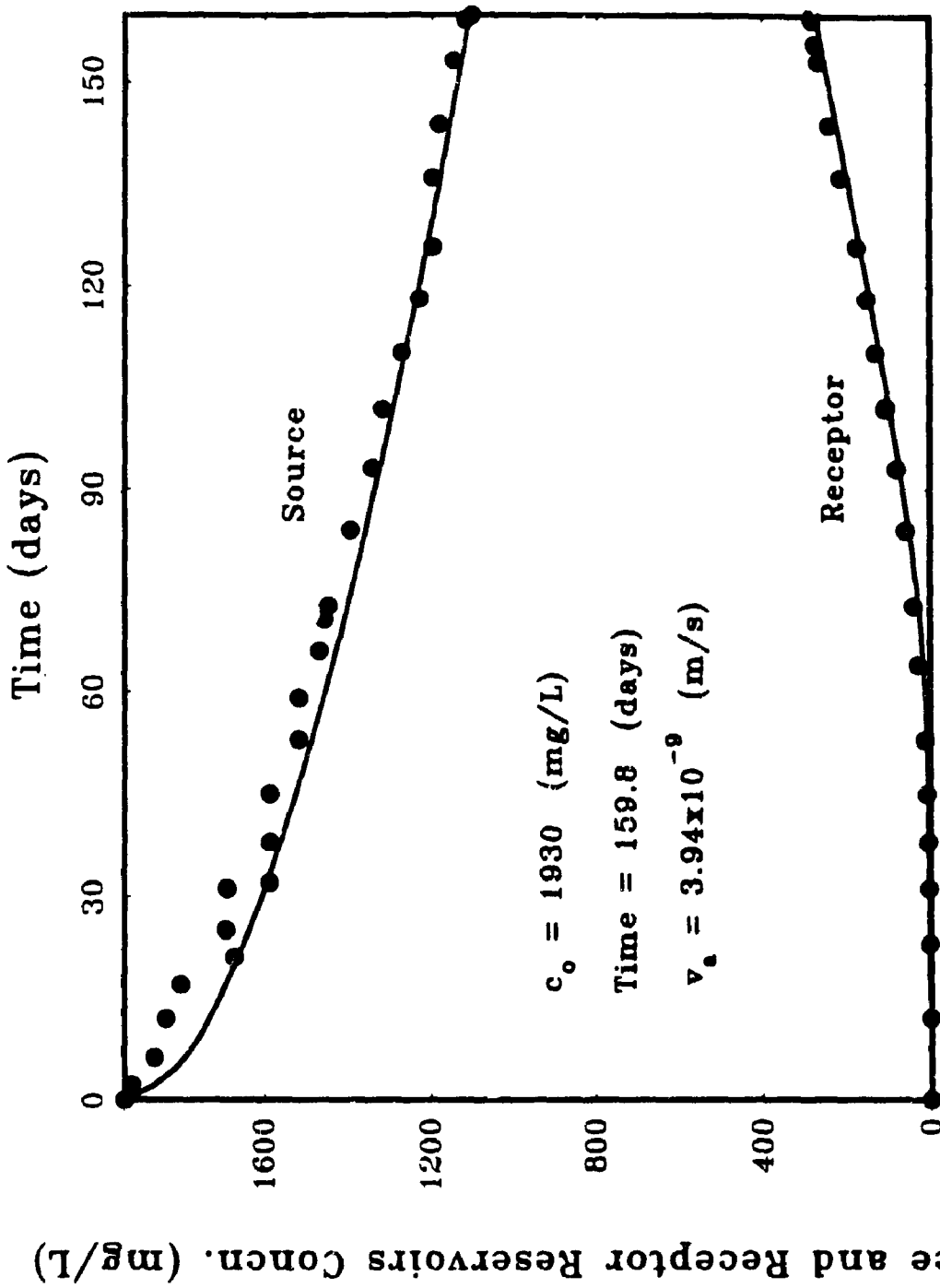

FIG. 9.31 OBSERVED AND THEORETICAL [Cl^-] CONCENTRATIONS VERSUS ELAPSED TIME IN SOURCE AND RECEPTOR RESERVOIRS OF ADVECTION-DIFFUSION TEST #AD9

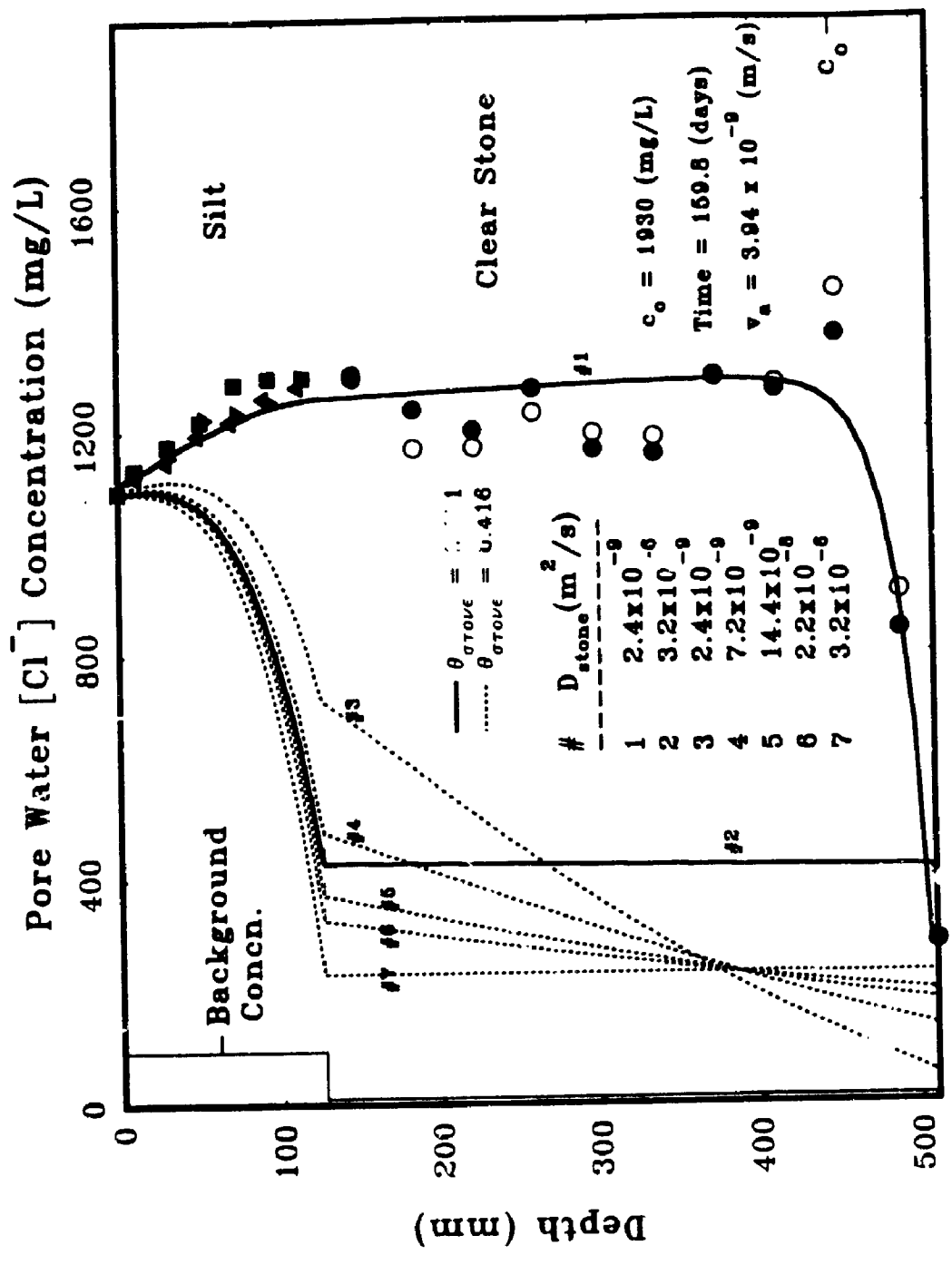

FIG. 9.32 EFFECT OF THE HYDRODYNAMIC DISPERSION COEFFICIENT AND VOLUMETRIC MOISTURE CONTENT OF THE STONE LAYER ON THEORETICAL [Cl^-] CONCENTRATION PROFILES OF THE TEST #AD9

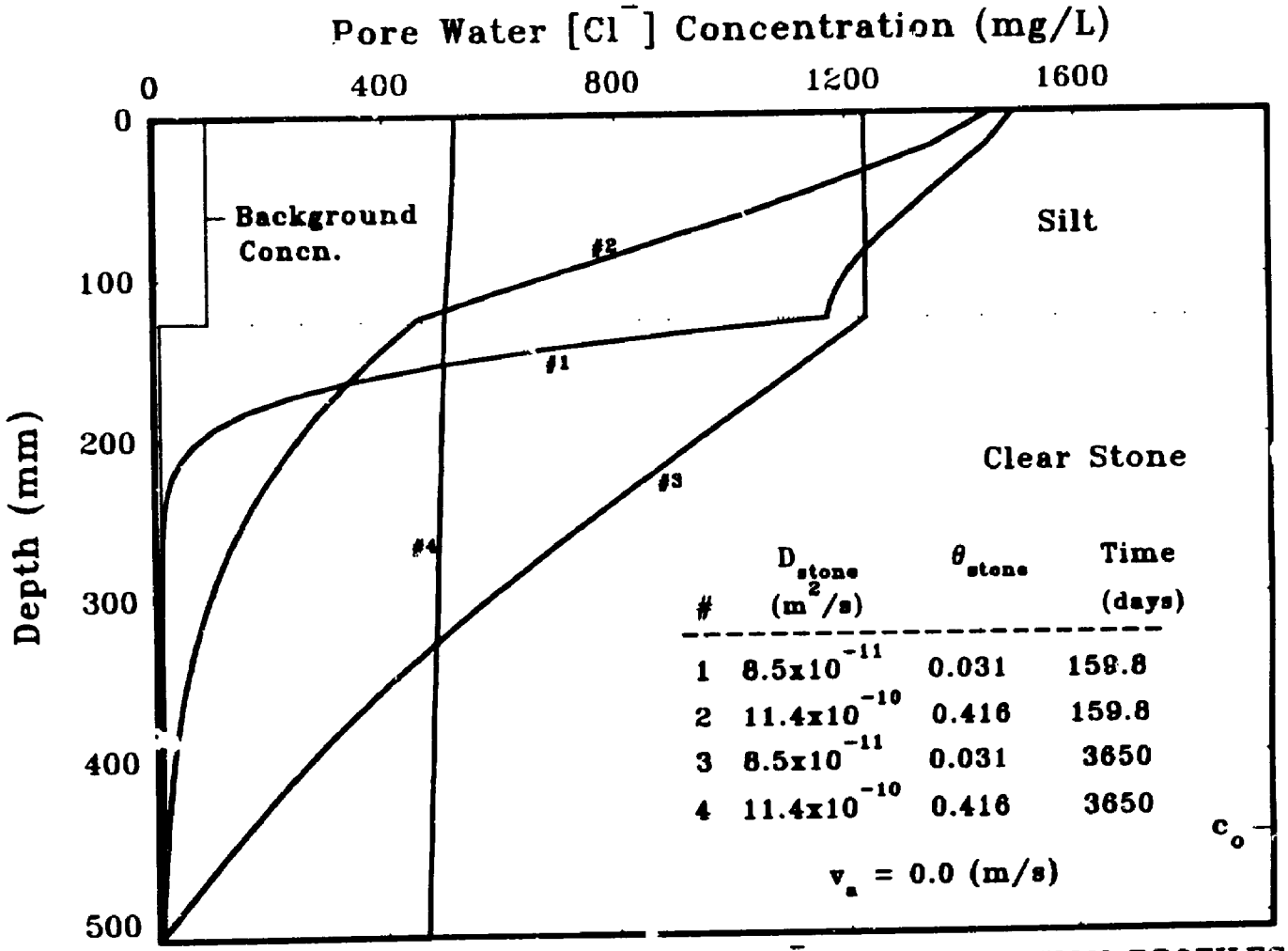

FIG. 9.33 EFFECT OF D_{stone} AND θ_{stone} ON [Cl^-] CONCENTRATION PROFILES OF THE TEST #AD9, ASSUMING PURE DIFFUSION (v_a=0.0) (ANALYSIS PERFORMED FOR 159.8 AND 3650 DAYS)

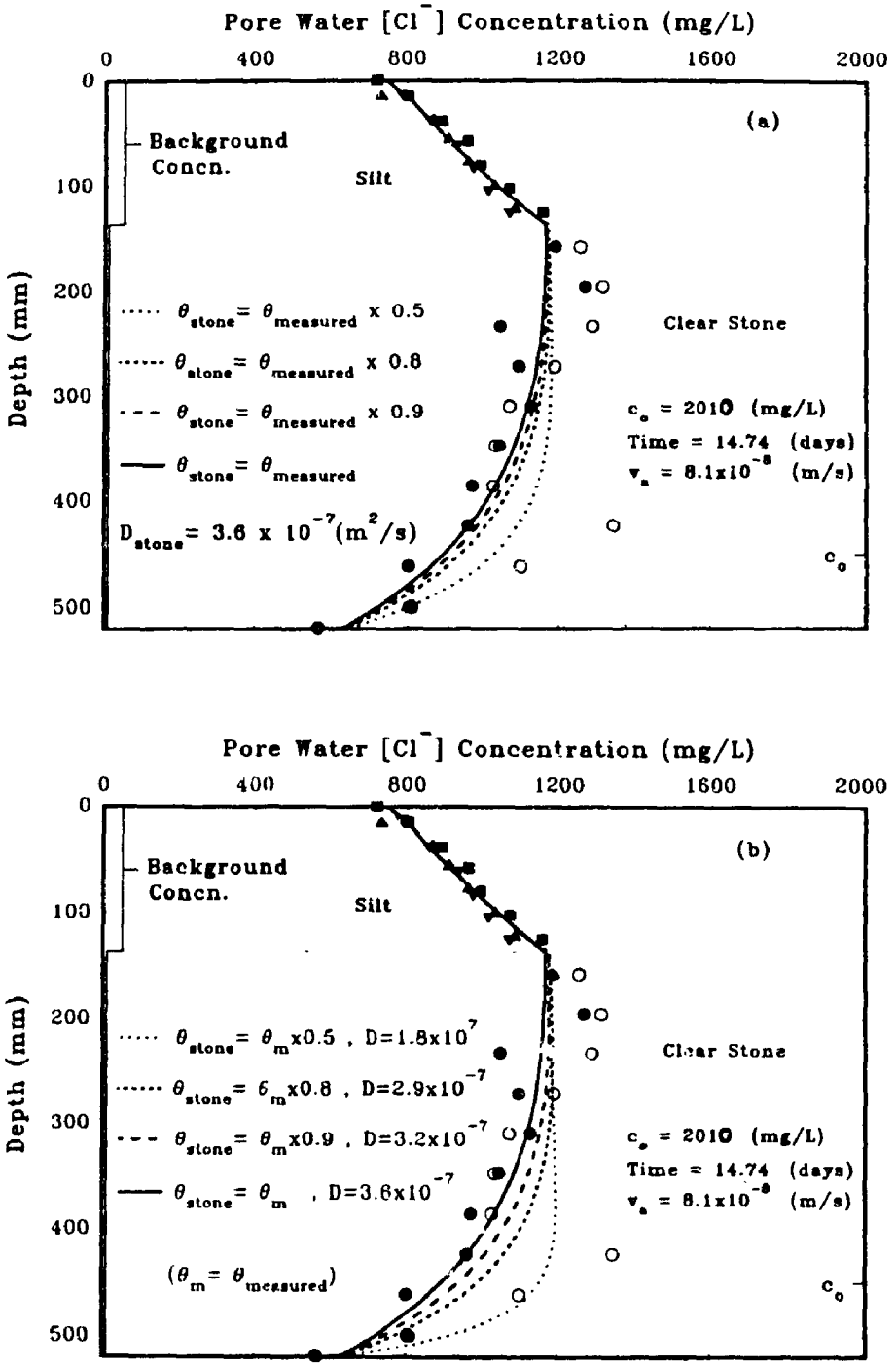

FIG. 9.34 EFFECT OF REDUCED VOLUMETRIC MOISTURE CONTENT (a), AND VOLUMETRIC MOISTURE CONTENT AND EFFECTIVE DIFFUSION COEFFICIENT (b) OF THE UNDERLYING UNSATURATED STONE ON CALCULATED CONCENTRATION PROFILES (TEST AD8)

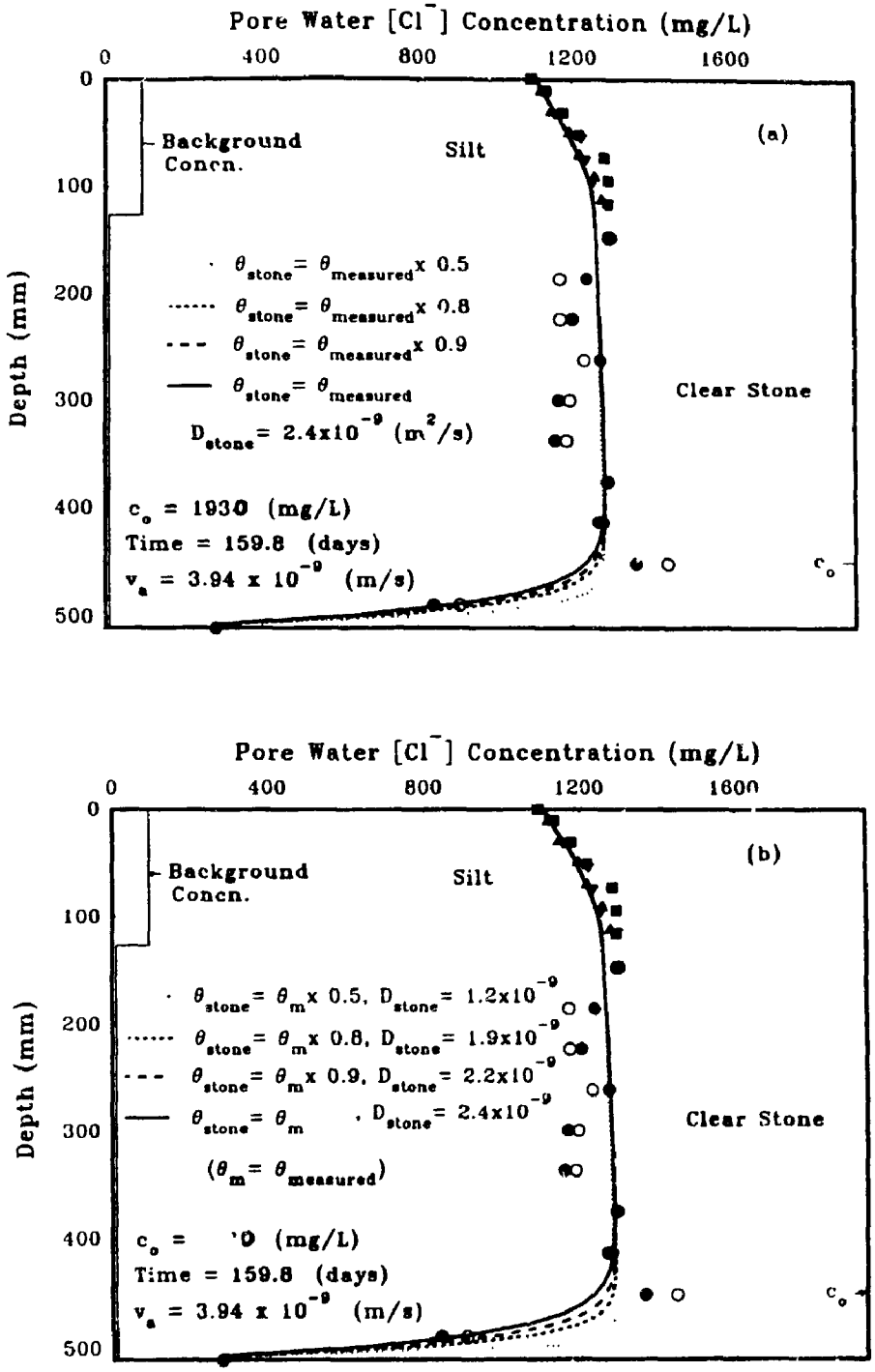

FIG. 9.35 EFFECT OF REDUCED VOLUMETRIC MOISTURE CONTENT (a), AND VOLUMETRIC MOISTURE CONTENT AND EFFECTIVE DIFFUSION COEFFICIENT (b) OF THE UNDERLYING UNSATURATED STONE ON CALCULATED CONCENTRATION PROFILES (TEST AD9)

CHAPTER 10

ADVECTION-DIFFUSION TESTING IN A TWO-LAYER CLAYEY SILT-UNSATURATED CLEAR STONE SYSTEM, UNDER "LOW" ADVECTIVE FLOW

10.1 INTRODUCTION

In this chapter, experimental and theoretical results obtained from two advection-diffusion tests conducted on the two-layer soil system of compacted clayey silt over unsaturated clear stone, are presented. The purpose of these tests was to simulate an engineered situation in a landfill site, comprising a compacted clayey liner underlain by a secondary leachate collection system which was separated from the clayey liner by a geotextile. Many modern landfills consist of multi-layered system of compacted clayey liner and/or geosynthetic liners with coarse grained layer/layers as primary and secondary leachate collection and removal systems. The primary function of a clayey liner is to reduce the migrating of potential contaminants from the landfill through the underlying layers and then into an aquifer by advective-diffusive transport. Chemicals generated in the waste (i.e. leachate) are collected in primary leachate collection system and then removed by regular pumping. There will always be a certain leachate mound at the base of this layer, which creates a low hydraulic gradient across the underlying layers. This low gradient results in a low advective flow through the primary liner and hence, the dominant transport process may be by diffusion.

The secondary leachate collection system is usually constructed from a coarse grained material such as clear stone having the diameter ranging from 2.5 cm to 5.0 cm.

This layer is expected to remain unsaturated. Contaminants migrating through the overlying layers should pass through this unsaturated coarse grained layer which has a very low water content.

For the purpose of better understanding the behaviour of the unsaturated secondary leachate collection system constructed from the coarse clear stone having 3.8 cm (1.5 inch) diameter, overlain by a compacted clayey layer, two laboratory tests were conducted using the large scale advection-diffusion apparatus. Details of the apparatus were described in Chapter 9 and Fig. 9.1 shows a schematic. Both tests had essentially identical characteristics and were duplicated for verification and comparison of the results. The tests configuration consisted of a compacted clayey silt layer with an approximate thickness of 12 to 13 cm, on top of a 38 cm thick unsaturated clear stone which in turn overlays a reservoir. The compacted clayey silt was separated from the stone by a nonwoven, needle punched geotextile. A NaCl salt solution was placed in the source reservoir on top of the clayey layer. These tests will be referred to as Tests # AD10 and AD11. Test #AD10 was terminated after 480 days while Test #AD11 was left for long term monitoring. Thus, for Test #AD11 only the concentrations from the source and receptor reservoirs which were determined using samples collected during the first 480 days of migration, are presented.

10.2 MATERIALS, DESCRIPTION AND PREPARATION

Clayey soil

The clayey soil used in the experiments was the unweathered clayey till obtained

from the Halton Waste Management Site in Milton Ontario. The typical grain size distribution of the soil was shown in Fig. 4.1 and Table 4.2 shows some of its physical, chemical and mineralogical characteristics. Soil was air dried pulverized and oversize material was passed from sieve #4. About 34 kg dry soil was prepared for each test. The sample was placed in shallow trays and wetted by spraying tap water on the surface of the soil and mixing the soil by hand until the desired moisture content (2-4 % wet of optimum) was reached. After each spraying, about 15 minutes were allowed for the soil to absorb water and then the soil was mixed by hand. The soil was poured into plastic bags and moisture content samples were taken from each bag.

Clear stone

The 38 mm diameter clear stone used for this study was the same material used for Tests # AD8 and AD9. The grain size distribution of the stone is shown in Fig. 9.5 and some of its physical, chemical and mineralogical characteristics is shown in Table 9.1. The method of material cleanup from its background concentration was described in Chapter 9. The porosity of the stone was determined by randomly placing it into a cubic container (see Fig. 11.61, Chapter 11) to check the accuracy of the measured porosity after installation in the cell (to be explained later). The procedure consisted of randomly placing the stones in the cubic container of known volume, until container was completely filled with the stones, and placing a rectangular plate on top of the container. Any stone interfering the complete contact of the plate with the container was rearranged or replaced, until surface of the stone was smooth. The weight of the container including dry stone was measured. The container was then filled with water until the water surface

was level with the top surface of the container and all stones were immersed in water (see Fig. 11.62). The weight of the container including the saturated stones was measured and hence the weight of the water added to the container was determined. The porosity of the stone was then calculated by dividing the volume of voids by the total volume of container (bulk volume of the stone).

Geotextile

A description of the geotextile was given in Chapter 9.

10.3 PRELIMINARY TESTING ON ADVECTION-DIFFUSION CELL

Prior to conducting any actual test (i.e. Tests # AD8, AD9 and AD10) with the large scale advection-diffusion apparatus, a preliminary test was conducted using the stone and clayey material having the same geometry as proposed for actual tests. The primary purpose of this test was to gain experience with installation of the material (e.g. placement of the stones, saturation and desaturation, measurement of the porosity of the stone, placement of the geotextile, and compaction of the clayey soil on top of the stone) and then sampling from the clayey soil and stone layers for determination of the moisture content and pore water concentration. The second purpose of this test was to measure the hydraulic conductivity of the clayey soil when it was compacted on top of the stone layer. The hydraulic conductivity tests were performed on the Shelby tube samples obtained from the compacted soil.

A schematic of the advection-diffusion cell was shown in Fig. 9.1 (Chapter 9).

The base chamber of the cell was placed on plywood base and levelled. A stirring bar was placed in the chamber and the steel perforated plate was installed. The intermediate chamber was placed on the base chamber and clamped. The washed-dry stones were randomly placed in the intermediate chamber until it was completely filled with the stones. Using a distilled water tank, the cell was filled with water up to the top of the intermediate chamber, until all stones were immersed in water. The stones were left saturated for about 48 hours after which the outlet valve in the base chamber was opened and stones desaturated by lowering the water table to the bottom surface of the stone layer (top surface of the perforated plate). Drained water was collected in a container and its volume was measured. Knowing the volume of the intermediate chamber, occupied by the stones (bulk volume of the stones), the porosity of the stones was calculated. The porosity obtained was 0.416 which was essentially the same as that obtained using the cubic container (explained earlier). The geotextile was soaked in water and placed on top of the stones. The upper chamber was placed and clamped to the intermediate chamber. The clayey silt sample was placed on the geotextile and compacted on top of the stone (separated by the geotextile), in 3 lifts of approximately 4 cm thicknesses, by applying 400 blows of Standard Proctor hammer to each lift. After compaction of each lift, the sides of the clayey layer in contact with the cell walls, were tamped using a square cross-sectional wooden tamper. This was done to ensure proper contact of the soil with the cell walls and to prevent any leakage through the sides. The final thickness of the clayey silt layer was measured in 12 locations around the upper chamber.

Using a 6.5 cm diameter Shelby tube and a hydraulic jack (as of Fig. 9.13) five

samples were taken from 5 locations on the compacted clayey silt layer. Samples were extruded from the Shelby tube using an extruder. Using parallel guide lines in front and back faces of the intermediate chamber (as of Fig. 9.3), the stone layer was sectioned into 10 sublayers of approximately 3.8 cm thicknesses. Stones were picked up by hand, and placed into 2 stainless steel trays with approximately equal amount of stones in each tray. Trays were immediately weighed and then placed in oven for moisture content determination. The dry weight of the trays was measured and the moisture content of each stone sublayer was calculated. Obtained values were quite uniform with depth with the average of 1.5%.

Two Shelby tube samples obtained from the compacted clayey silt layer, were tested for determination of their hydraulic conductivity using a flexible wall hydraulic conductivity apparatus. Hydraulic conductivity values of 1.6×10^{-10} m/s and 1.8×10^{-10} m/s were obtained from these tests respectively under the effective pressure (σ_z') of 25 kPa. Obtained values were in the desired range for a compacted clayey soil to be used as a clay liner.

10.4 ADVECTION-DIFFUSION TESTS SET UP, MONITORING AND TERMINATION

The same method adopted in preliminary test for installation, saturation, and desaturation of the clear stone and compaction of the clayey soil on top of the stone, were used for installation of the material in the proposed advection-diffusion tests. As of preliminary test, during desaturation of the stone layer, volume of the drained water was measured and the porosity of the stone layer was calculated. The resulting porosity

values were essentially the same as obtained in the preliminary test and the test using a cubic container (described earlier). After compaction of the clayey soil layer using the method explained before, its thickness was measured in 12 locations around the chamber and averaged to obtain the initial thickness of the soil. The distance from the proposed source solution level which was already marked on the cell walls, to the surface of the compacted clayey layer was measured in 17 points. The measured values were averaged to obtain the representative source solution height.

The NaCl solution with approximate Cl^- concentration of 2000 mg/L was poured on top of the clayey soil to the desired level of about 24 cm above the intermediate and upper chambers interface (about 12 cm above the soil surface). The starting time of the test was recorded. A sample was taken from the reservoir for initial source solution concentration measurement. The top plate which was equipped with a clock motor and mixing paddles (Fig. 9.1), was placed on top of the upper chamber and clamped. Two samples from receptor reservoir were taken for initial concentration measurement. A schematic of the test set up is shown in Fig. 9.2, the only significant difference being that due to the expected slower seepage rate, the overflow set up was not installed in the base chamber. Fig. 10.1 shows a view of the Test #AD10 and Fig. 10.2 shows a view of the 3 advection-diffusion tests (#AD9, right - #AD10, left - and #AD11, middle) in progress.

Both tests were started at the same day. Samples (4 mL) were periodically taken from the source and receptor reservoirs during the tests. The compacted clayey silt samples did not show any noticeable swelling and their thickness remained essentially constant throughout the tests. Water levels in source reservoirs were monitored using

a travelling microscope. Compared to the Tests AD8 and AD9 (Chapter 9), the rate of the water level drop was very slow. In order to maintain a relatively constant source solution height in the source reservoir, the infiltrated volume of solution was replaced with the same volume of distilled water. The source reservoirs in both tests were diluted 5 times during 480 days of migration to re-establish the original water level. Prior to each dilution, water level drops from each reservoir were measured using a travelling microscope and samples were taken from source reservoirs before and after each dilution. The volume of water lost (infiltrated) from each reservoir was recorded with elapsed time and results are plotted and shown in Fig. 10.3. As it can be seen, both tests had essentially the same influent curves.

The temperature was recorded throughout the tests. As for Test #AD9, water drops were observed on the inside surfaces of the intermediate chamber where stones had been placed. Water drops were also observed on the bottom surface of the top plate, inside the upper chamber (source reservoir), which was due to some evaporation from source reservoir and accumulation of evaporated water on the bottom surface of the top plate. The amount of these water drops was measured at the end of the test by weighing the wet and dry plate and was subtracted from the total volume of water lost from the source reservoir. Samples from upper and lower reservoirs were periodically analyzed for concentration measurement during the tests. Results indicated that the rate of the concentration decrease in the upper reservoir and increase in the lower reservoir in both tests is substantially slower than that observed in Tests # AD8 and AD9 (Chapter 9), and both tests showed essentially the same behaviour during the tests.

Test #AD10 was terminated after about 480 days of migration. Samples from

source and receptor reservoirs were taken before termination. The heights of the source solution, clayey silt and stone layers were measured. The top plate was opened and source reservoir was drained into a tank (as of Fig. 9.11). Five Shelby tube samples were taken from the clayey layer using the same method described in section 10.3 (Fig. 10.4). In contrast to what observed in Tests # AD8 and AD9 (Chapter 9) in the silt layers, there was no significant difference in the stiffness of the compacted clayey layer in its entire depth. Samples were extruded from the Shelby tube, incased in plastic, waxed, and stored at room temperature. The upper chamber and geotextile were removed and stones were sliced into 10 sublayers using the same method described in section 10.3 and also Chapter 9. Due to the accumulation of the infiltrated water at the bottom of the intermediate chamber, about 3.8 cm thickness (equal to the thickness of the last stone sublayer) from the bottom of the stone layer was saturated. After removing the upper nine stone sublayers on top of the saturated section, 2 pore water samples were taken from the centre of the left and right half of the saturated stone, as a representative pore water samples from this sublayer. The wet and dry weight of the stone samples were measured from which their water content were calculated.

Three Shelby tube samples obtained from right-front, middle, and left-back of the clayey layer were selected for pore water concentration analysis. Each sample was sliced into 6 sublayers and a moisture content samples were taken from each slice. The sliced samples were then squeezed in a pneumatic squeeze apparatus and the pore water was collected for analysis.

10.5 DARCY VELOCITY, HYDRAULIC CONDUCTIVITY, AND MOISTURE CONTENT DETERMINATION

As described earlier, the water level drop from source reservoirs was monitored for both tests during 480 days of migration, from which inflow rates were determined as shown in Fig. 10.3. From this figure the Darcy velocity of 5.5×10^{-10} m/s was obtained for both tests. Knowing the hydraulic gradients of 1.928 and 1.893 for Tests # AD10 and AD11, the hydraulic conductivities of 2.85×10^{-10} m/s and 2.91×10^{-10} m/s respectively were obtained for compacted clayey layers of the tests. Taking into account the difference in the method of hydraulic conductivity measurements, these values were reasonably close to the average value of 1.7×10^{-10} m/s obtained from flexible wall hydraulic conductivity tests (described earlier). Table 10.1 summarizes the values of flow rate, hydraulic gradient, hydraulic conductivity and Darcy velocity through the soil layer in Tests # AD10 and AD11.

The moisture content values of 18 sliced samples from 3 locations of right-front, middle, and left-back in clayey layer of Test #AD10 were plotted versus soil depth and shown in Fig. 10.5. As can be seen, moisture content of the clayey layer had remained almost uniform with depth with no significant change from its initial moisture content (dotted line).

Fig. 10.6 shows the moisture content profiles in left and right half of the stone layer observed at the end of the Test #AD10. The average value of 2.18 % was obtained for the unsaturated part of the stone layer. As described earlier, due to the accumulation of the infiltrated water in the bottom of the intermediate chamber about 3.8 cm from the bottom of the stone layer was saturated. Table 10.2 summarizes the average values of

the thickness, moisture content, degree of saturation, and volumetric moisture content for compacted clayey silt and clear stone layers in Test #AD10. The values shown for Test #AD11 are estimated values equal to the values listed for Test #AD10 except the thickness of the soil and stone layers which are based on real measurements. These values (Test #AD11) were used in theoretical analysis which will be discussed later.

10.6 EXPERIMENTAL AND THEORETICAL ANALYSIS

The source and receptor reservoir samples obtained from Tests # AD10 and AD11 during 480 days of migration, were analyzed for the Cl^- concentration. The results were plotted versus elapsed time and shown in Figs 10.7 and 10.8 for Tests # AD10 and AD11 respectively. As can be seen, the source reservoir data points in both tests do not fall in a smooth curve and there are 5 concentration drops in the curve. These points which were marked as points d1 to d5, represent the times in which both source reservoirs were diluted by adding distilled water to re-establish the initial water levels. As can be seen, after each dilution, there has been a noticeable decrease in the concentration after which a slight increase in the concentration was observed. This is likely due to the diffusion of Cl^- from the soil into the source reservoir due to the concentration drop in the reservoir caused by dilution.

The concentration increase in the receptor reservoirs in both tests was not noticeable until about 300 days of migration, after which concentration increased at a slow rate. After 480 days of migration the concentration difference between the source and receptor reservoirs was 1235 mg/L and 1175 mg/L compared to the initial value of

about 1930 mg/L in Tests # AD10 and AD11 respectively.

The solid lines in Figs 10.7 and 10.8 are the theoretical curves which will be discussed later.

The pore water solutions from sliced clayey samples at 3 locations in the clayey layer for Test #AD10 were analyzed for determination of Cl^- and Na^+ concentration. The ovendried stone samples from right and left half of the 10 stone sublayers were washed with distilled water. The methodology adopted was similar to that used in Tests # AD8 and AD9 (Chapter 9). The concentration of the wash supernatant was analyzed for determination of Cl^- and Na^+ concentration, and pore water concentrations were backfigured using Eq. 3.1. The Cl^- and Na^+ concentrations in the clayey silt and stone layers were plotted against soil depth and shown in Figs. 10 9 and 10.11 respectively. As can be seen in Fig. 10.9, concentrations in the clayey silt sublayers at 3 locations are essentially the same and uniform with depth. The corresponding concentrations in upper 8 stone sublayers were also approximately uniform with depth and close to the concentrations observed in the clayey silt layer. Sublayer 9 which was on top of the lower saturated sublayer (sublayer 10) had the lower concentration compared to the upper sublayers. The lower saturated sublayer had essentially the same concentration observed in the receptor reservoir at the end of the test (data point on lower x axis). As can be seen the scatter in the stone concentration data is smaller than in the Tests # AD8 and AD9 (discussed in Chapter 9). The sodium concentration versus depth data are shown in Fig. 10.11. No significant scatter is observed in stone layer data and concentration values in left half of the layer are in good agreement with the right half. The concentration in the lower saturated sublayer (sublayer 10) is essentially the same as the

lower reservoir concentration observed at the end of the test (data point in the x axis).

A theoretical analysis of the tests was performed using the program POLLUTE and measured data. Table 10.3a shows the average values of the thickness, volumetric moisture content and effective diffusion coefficient of the soil, geotextile, clear stone, and perforated plate, used in the analysis. Using Eq. 5.1 and the typical porosity and effective diffusion coefficient of the clayey soil (e.g. Table 4.5) together with the volumetric moisture content of the tested soil (Table 10.2), its effective diffusion coefficient was predicted. The effective diffusion coefficient for the unsaturated stone layer was predicted using the available data for saturated diffusion coefficient and porosity of the fine gravel obtained in diffusion testing (described earlier in Chapter 9) together with the corresponding volumetric moisture content of the unsaturated stone, using Eq. 5.1. The resulting values are listed in the first row of the clear stone section in Table 10.3a. The corresponding effective diffusion coefficients for Na^+ ion in the soil and stone layers were predicted using the same method described for Cl^-. The remaining input data used in the analysis are summarized in Table 10.3b. As noted earlier, during the duplicated Tests AD10 and AD11 the water levels in the source reservoirs were dropping due to the advective flow into the underlying soil. In order to re-establish the original water levels (i.e. the water levels at the beginning of the tests), distilled water was added to the reservoirs at a number of times (i.e., after 177, 307, 386, 439 and 479 days of migration as shown in Figs. 10.7 & 10.8) which caused dilution of the source concentration. During the time intervals between these dilutions, the water levels in the reservoirs were dropping and consequently the source solution height (H_f) was decreasing

(i.e., $H_f(t_{i-1}) > H_f(t_i)$ in which $H_f(t_{i-1})$ is the solution height at time t_{i-1} ($t_{i-1} < t_i$) and $H_f(t_i)$ is the new solution height at the time t_i after some infiltration). As a result of decrease in H_f, the source concentration was increasing by the proportion of $H_f(t_{i-1})/H_f(t_i)$. The change in solution height (ΔH_f) during the time period Δt ($\Delta t = t_{i-1} - t_i$) could be calculated knowing the Darcy velocity of the test (v_a) (i.e., $\Delta H_f = v_a . \Delta t$) and hence, $H_f(t_i) = H_f(t_{i-1}) - \Delta H_f = H_f(t_{i-1}) - v_a . \Delta t$.

A theoretical analysis of the tests was performed in an incremental manner so as to follow the experimental procedure adopted in the tests. Starting from the known initial source solution concentration and height in the source reservoir and selecting a time interval Δt (say 25 days), the analysis was performed in an incremental manner using the "Variable Properties" option of the program POLLUTE. At the "dilution-times" d_1, d_2, etc the calculated concentration was adjusted knowing the amount of distilled water added and the solution continued using the new (theoretically predicted) source concentration as the starting concentration for the subsequent time interval. The details of this analysis are given in Appendix F.

The resulting calculated variation in source and receptor concentration with time for Test AD10 are shown in Fig. 10.7, and as can be seen the agreement between theory and experiment is good for both source and receptor reservoirs. Using the procedure described above, the first analysis was performed using the data listed in Tables 10.3a and 10.3b and the "effective diffusion coefficients" predicted for soil and stone layers. The resulting theoretical concentration versus depth profile is shown as a dotted line in Figs. 10.10 and 10.12 for Cl^- and Na^+ ions respectively. As can be seen in Fig. 10.10 the theoretical profile fits that observed in the clayey soil very well. The prediction is

not quite as good in the stone layer where the predicted concentrations are almost uniform throughout the unsaturated stone while the experimental data are less than the calculated values. Both experimental and theoretical concentrations drop at about 57 mm above the stone-receptor reservoir interface, with the bottom concentration in the receptor being the lowest value due to the dilution that occurs in the receptor reservoir. In order to get a better prediction to the experimental data of Cl^- in the stone layer, the value of the "hydrodynamic dispersion coefficient" was increased from that initially used as the effective diffusion coefficient of the unsaturated stone layer. This was done to examine the effect of the "mechanical dispersion" that may have occurred in the unsaturated stone layer due to the applied low flow rate. The range of the values used in the analysis are shown in the insert of Fig. 10.10 and the resulting theoretical profiles are shown as solid, medium dashed, and long dashed lines respectively. As can be seen the hydrodynamic dispersion value of 3.0×10^{-10} m^2/s (shown in second row of the stone layer section in Table 10.3a) resulted in a better fit (solid line) than pure diffusion alone. This profile is shown in Fig. 10.9 as the representative theoretical profile through the Cl^- experimental data in Test #AD10.

It may be hypothesized that at very low moisture content there may be a discontinuous fluid zone in the unsaturated zone and hence there would be negligible diffusion. To examine the implications of this hypothesis an analysis was performed for a very low value of diffusion coefficient ($D_{stone} = 1.2 \times 10^{-15}$ m^2/s, as indicated in Fig. 10.10) in the unsaturated stone layer. The results (shown as a dash-dot line in Fig. 10.10), indicate that the elimination of the diffusion in the stone layer does not have any significant effect in the source concentration. It has some effect in the soil concentration

data which was manifested by shifting the concentration profile to the right of the data. Based on these results it might be inferred that there was some diffusion in the unsaturated stone layer which contributed to the other transport mechanisms.

As mentioned in Chapter 9, the scatter of data in the stone may be partly attributed to experimental error but is also likely partly due to statistical variation in stone size, shape and arrangement which would affect mechanical dispersion and diffusion at the relatively low velocity examined, although the effect of dispersion was somewhat smaller than that observed in Test #AD8 and for practical purposes could be neglected (as will be discussed later). The preferential flow (or fingering) in the unsaturated stone layer may also provide an explanation for some (or all) of the scatter in the concentration data in this layer (as discussed in Chapter 9). Finally, it may be hypothesized that there could be formation of water droplets at the underside of the clay and that these droplets will increase in size until their weight overcome the surface tension effects holding them to the clay. At this point the droplets would fall and Cl^- and Na^+ would be dispersed as the droplets contacted stones in their path. This is considered a likely mechanism for much of the apparent dispersion evident in the tests. It is of significance to note that although this mechanism has some impact on the concentration distribution in the stone layer, it has negligible effect on either the source or receptor concentrations (i.e., the concentration of primary interest in a landfill design) for the likely range of the apparent coefficient of hydrodynamic dispersion as demonstrated below.

Fig. 10.12 shows the results of the analysis using two different values as the "effective diffusion coefficient" (dash-dot line and dot line) and three "hydrodynamic

dispersion coefficients" (solid, medium dashed and long dashed lines) for tne unsaturated stone layer for Na^+ ion. These values are shown in the insert of Fig. 10.12. As can be seen, the solid line in this graph tends to give a better theoretical prediction than the alternative values examined. The solid line corresponds to hydrodynamic dispersion coefficient of $2.5x10^{-10}$ m^2/s for Na^+ in unsaturated stone layer. This value is listed in the second row of the stone layer section in Table 10.3a. This profile (solid line) is shown in Fig. 10.11 as the representative predicted profile for Na^+ ion in Test #AD10.

The analysis discussed above which corresponds to the data listed in Tables 10.3a and 10.3b, was perfonned assuming that the lower stone sublayer (sublayer 10 with 3.8 cm thickness) was initially saturated. In order to see the effect of this assumption on the final results, another detailed analysis was performed for the case when this sublayer was gradually saturated during the test. The gradual increase of the thickness of the saturated stone which was regularly monitored by a stand pipe, was taken into account in this analysis. The results of this analysis which included 5 runs, is shown in Fig. 10.9 (for Cl^- ion) as a medium dashed line and results of the first analysis (single run, as discussed above) is shown as a solid line. As can be seen, both curves overlap indicating that the rate of saturation of the bottom stone sublayer has no significant effect in the final results.

Figs 10.9 and 10.11 show that there is generally a good agreement between theory and experiment with better agreement in clayey silt layer section. As can be seen, theory also accurately predicted the concentrations in the upper and lower reservoirs at the end of the test (corresponding experimental data points are shown in the upper and

lower x axis of Figs. 10.9 and 10.11 respectively).

As discussed earlier, the results of the theoretical analysis suggest that there is some mechanical dispersion in the unsaturated stone layer. Knowing the predicted effective diffusion coefficient and "best fit" hydrodynamic dispersion coefficient value in the stone layer (listed in the first and second rows of the stone layer section in Table 10.3a), and the corresponding Darcy velocity (Table 10.1), the dispersivity (α) was calculated to be 0.013 m using Equations 2.8 and 2.9. Compared to the dispersivity value obtained in Test #AD8 (Table 9.5a) for the unsaturated stone layer, this value is quite smaller suggesting that the effect of dispersion in Test #AD10 is negligible.

The relationship between seepage velocity ($v = v_a/\theta$) and dispersivity (α) and also seepage velocity and mechanical dispersion (D_{md}, $D_{md} = D - D_e$) in Tests # AD8, AD9 and AD10, was examined by plotting the first in normal scale and the second in log-log scale as shown in Fig. 10.13. The error bars in these plots represent the range of the values of the mechanical dispersion and dispersivity corresponding to the range of the hydrodynamic dispersion coefficients used in the theoretical analysis (listed in the inserts of Figs. 9.25, 9.27 and 10.10). As can be seen, for the conducted tests the dispersivity is essentially a linear function of the seepage velocity. These relationships are presented by the equations shown in the inserts of Figs. 10.13a and 10.13b (the units for seepage velocity is (m/s), for dispersivity is (m) and for mechanical dispersion is (m^2/s)).

Predictions for Test #AD11 data

As it was indicated earlier, Test #AD11 which was essentially duplicate of the Test #AD10, is being continued for longer term data collection. The source and receptor

reservoir samples from this test were collected during 479 days of migration (almost equal to the duration of the Test #AD10) and analyzed for Cl^- concentrations. The results were shown in Fig. 10.8. A theoretical analysis was performed to predict the concentration profile in source and receptor reservoirs using the incremental procedure described for Test AD10, the available data for this test (shown in Tables 10.3a and 10.3b) and the volumetric moisture content and hydrodynamic dispersion coefficient of the Test AD10. Although the volumetric moisture content values of the clayey silt and stone layers in Test #AD11 have not been measured yet, the close similarity of the materials and test methodology to Test AD10 allows one to estimate the parameters assuming that they are approximately the same as in AD10. The results of the analysis are shown in Fig. 10.8 along with the experimental data. As can be seen, the predicted profiles are in good agreement with the experimental data, showing a good prediction by theory.

Some sensitivity analysis

The sensitivity of the calculated profiles for Test #AD10 to the Cl^- hydrodynamic dispersion coefficient, and also volumetric moisture content of the unsaturated stone layer was examined and the results are shown in Fig. 10.14. In the first analysis, a large arbitrary value of 3.2×10^{-6} m^2/s (100 m^2/a) was used as unsaturated stone hydrodynamic dispersion coefficient. The profile is shown as profile #2 (solid line), and as can be seen, there is significant difference between this and predicted profile (#1), and it shows higher concentration in the receptor reservoir compared to the observed and predicted values. This suggests that for the range of the Darcy velocity examined, the assumption

of high dispersion in the unsaturated stone layer is overconservative. Profiles # 3 to 7 in Fig. 10.14 (medium dashed lines) show the results of the analysis assuming that the stone layer is fully saturated (n=0.416). Profile #3 was obtained using the predicted hydrodynamic dispersion coefficient of 1.1×10^{-9} m^2/s (all other data as shown in Tables 10.3a and 10.3b). As can be seen, for the period of migration examined (480 days) the impact is essentially the same as that observed and predicted for the case of unsaturated stone (Profile #1), but the calculated concentration in the soil and stone layers are smaller compared to that observed and predicted in Test #AD10. The lower concentrations in the soil and stone layers is due to the larger available volume of water in the stone pore space (compared to a limited volume in the unsaturated case). This large volume results in more dilution of the migrating ion and hence, lower concentration. On the other hand, when the stone is unsaturated, there is a very limited volume of water in the pore space so that the concentration reaches a high value in a short period of time. Profiles # 4, 5, 6 and 7 show the results of the analysis assuming different values as hydrodynamic dispersion coefficient for saturated stone layer. These values are listed in the insert of Fig. 10.14. As can be seen, results are insensitive to the values of the hydrodynamic dispersion coefficient greater than 8.0×10^{-7} m^2/s. Comparison of the profiles #3 and #7 shows that the assumption of a high hydrodynamic dispersion coefficient for saturated stone also results in higher impact and hence is overconservative (as was the case for unsaturated stone).

Another series of theoretical analysis was performed to examine the sensitivity of the results to the diffusion coefficient and volumetric moisture content of the stone layer when zero Darcy velocity is assumed to exist in the test system (i.e., pure diffusion).

The results of these analysis are shown in Fig. 10.15. In this figure, profile #1 shows the result of the original analysis (solid line in Fig. 10.9) with the test Darcy velocity of 5.5×10^{-10} m/s. Profile #2 shows the result of the analysis using the predicted effective diffusion coefficient of 9.5×10^{-11} m^2/s for the unsaturated stone layer when the Darcy velocity is assumed to be zero (all other data as listed in Tables 10.3a and 10.3b). Profile #3 belongs to the analysis when the stone layer is assumed to be saturated (n=0.416, D_e=1.1×10^{-9} m^2/s, v_a=0.0, and all other data as listed in Tables 10.3a and 10.3b). As can be seen, after 480 days of migration, analysis using unsaturated stone (Profile #2) shows no impact in the receptor reservoir while analysis using saturated stone (Profile #3) shows some impact. In order to see the impact in longer period of time, analysis was repeated for 3650 days (10 years) and results are shown as profiles #4 and #5 (long dashed lines). As can be seen, after 10 years of migration, the analysis using unsaturated stone still shows no impact (profile #4) while analysis using saturated stone (Profile #5) shows significant impact.

Comparison of the profile #3 in Fig. 10.14 (v_a = 5.5×10^{-10} m^2/s) with the profile #3 in Fig. 10.15 (v_a = 0.0) shows that the effect of the Darcy velocity (at the examined range) on the concentration profiles when the stone layer is saturated, is less than the case when stone layer is unsaturated (compare profiles #1 and #2 in Fig. 10.15). In the case of saturated stone, the impact in the receptor reservoir is essentially the same (Profiles #3 in Figs. 10.14 and 10.15) while in case of unsaturated stone, the examined Darcy velocity resulted in some impact (Profile #1 in Fig. 10.15) compared to the case with zero Darcy velocity which shows no impact (Profile #2 in Fig. 10.15).

For better clarification of the effect of Darcy velocity on the concentration

profiles when stone layer is unsaturated, another series of analysis was performed in which the Darcy velocity was increased from zero to the observed value of 5.5×10^{-10} m/s in 5 equal intervals. Results are shown as profiles #1 to #6 in Fig. 10.16. Data used for these analysis is the same as the original run (Fig. 10.9) except those data listed in the insert of Fig. 10.16. As can be seen, the small range of the Darcy velocity (from zero to 5.5×10^{-10} m/s) has significant effect on the concentration profiles, particularly on the unsaturated stone section of the profile. The effect is also pronounced in the source and receptor reservoirs and the higher Darcy velocity results in lower concentration in the source and higher concentration in the receptor. As mentioned in Chapter 9, the pronounced effect of the Darcy velocity in the unsaturated stone is due to the high groundwater velocity ($v = v_d/\theta$) along the wetted surface of the stone when the system is unsaturated.

Another series of sensitivity analyses were performed to examine the effect of different assumed effective volumetric moisture contents, $\theta_{effective}$, of the underlying stone on the calculated profiles. The first series of the analyses assumed that the effective θ ranged from 50% to 90% of the measured value at the end of the test (Table 10.2). All other parameters (including $D_{(stone)}$) are as listed in Tables 10.3a and 10.3b. The results shown in Fig. 10.17a indicate that all curves corresponding to the θ_{stone} values (dotted lines) less than that measured (solid line) are shifted to the right and are far from the stone data and the solid line corresponding to the $\theta_{effective} = \theta_{measured}$ still provides the best fit to the data. Based on these results one could hypothesize that the assumption of $\theta_{effective} = \theta_{measured}$ appears to be reasonable.

A second series of the analysis used the same θ_{stone} values as above except that the

$D_{(stone)}$ values were also reduced by the same proportion. This took into account the effect of θ on D. The results are shown in Figs. 10.17b. Based on these results it could be concluded that the original assumptions ($\theta_{effective}=\theta_{measured}$ and D_{stone} as listed in Table 10.3a) appears to be more reasonable.

From the results of these sensitivity analyses it could be concluded that:

1. the assumption of a large value for the hydrodynamic dispersion coefficient of the stone layer might be an overconservative assumption.
2. the unsaturated stone layer could be used as an effective barrier as long as there is zero or negligible advective flow through the system.
3. effect of the Darcy velocity in the unsaturated stone layer is more pronounced compared to the saturated stone.
4. for the case of saturated stone, concentration profiles are insensitive to high coefficient of hydrodynamic dispersion values ($8.0x10^{-7}$ m^2/s or greater).
5. the assumption that the effective volumetric moisture content of the unsaturated stone is equal to the total measured value appears to be reasonable.

10.7 SUMMARY AND CONCLUSIONS

Two large scale advection-diffusion tests were conducted using a compacted clayey soil underlain by an unsaturated clear stone layer. These tests simulated the design condition of a landfill consisting of a low permeability compacted clayey liner over an unsaturated secondary leachate collection system and a simulated aquifer. The

tests were duplicated with almost the same geometry and the same source of material to allow verification of the transport process. The source and receptor concentrations and water level in the source reservoirs were regularly monitored and the infiltrated solution from the source reservoir was replaced with the same volume of distilled water to maintain constant source solution level on top of the clayey silt during the tests. Due to the low permeability of the compacted clayey silt layer, the flow rates in both tests were slower than that observed in the "high" and "moderate" flow rate tests of AD8 and AD9 and were in the range of the reported values for a compacted clayey liner. The preliminary analysis of the source and receptor reservoirs solutions in both tests showed that the migration process is substantially slower than that observed in Tests # AD8 and AD9, and receptor reservoirs did not show any significant increase in concentration until about 300 days of migration, after which a very slow increase in the concentration was observed.

One of the duplicated tests (#AD10) was terminated after 480 days of migration and the other was left for longer term monitoring.

Theoretical analysis was performed for both duplicated tests in an incremental manner described earlier. The volumetric moisture content data of the clayey silt and stone layers obtained at terminated Test #AD10 was used in the analysis of the Test #AD11 to predict the source and receptor reservoirs concentration with time. The effective diffusion coefficient of the clayey silt and unsaturated stone layers were predicted using the same method developed in previous chapters. The first series of the analysis was performed using the predicted effective coefficients for both clayey silt and stone. The resulting profiles fit the observed data in clayey silt layer quite well but

predictions were not quite as good in the unsaturated stone layer. A better fit was obtained when the effect of slight dispersion was taken into account by using slightly larger value as the hydrodynamic dispersion coefficient of the unsaturated stone layer. The calculated value of the dispersivity for stone layer showed that the effect of dispersion in Test #AD10 is negligible. Both theory and experiment showed a high and relatively uniform Cl^- concentration in the clayey silt and stone layers of Test #AD10 with a rapid decrease of the concentration in the vicinity of the receptor reservoir with the bottom concentration being the lowest due to the dilution that occurs in the receptor reservoir. Theory also accurately predicted the change in source and receptor reservoir concentrations with time, taking into account some irregularities observed in source reservoirs due to diluting the reservoirs in 5 time intervals during the tests to maintain constant source solution level.

Discussion on the results of 3 large scale advection-diffusion tests

By comparing the results of 3 advection-diffusion tests described in Chapters 9 and 10 which were performed under 3 different flow rates with essentially the same geometrical conditions, the following conclusions could be made:

The Darcy velocity of the test with higher flow rate (#AD8) was 147 times greater than the test including low permeability compacted clayey silt (#AD10) and hence, very rapid migration was observed in the first test so that after only 14.7 days of migration, the concentration in the lower reservoir was 1/3 of the initial source concentration, while in the second test this ratio was only 1/28 after 480 days of migration (33 times longer test period). This reveals the effectiveness of the low

permeability clayey layer on top of a very permeable stone layer as an advection control layer. The same conclusion could be made if the results of the test with moderate flow rate (#AD9) is compared with low flow rate test of AD10. Using a compacted silt with higher clay content than in Test #AD8, gave rise to a much lower Darcy velocity.

The concentration profiles in the unsaturated stone layers for the tests in discussion showed relatively high concentrations in the small volume of the pore water in this layer. This is partially due to a limited pore water available for migration in the stone which becomes highly concentrated in a relatively short period of time and partially due to the high groundwater velocity along the wetted surface of the stone which causes a relatively rapid migration by the process of advection. The results of the theoretical analysis showed that this effect is less pronounced when the stone is saturated.

Verification of the results of the test with low permeability compacted clayey silt (AD10) showed that both advection and diffusion play comparative role in the migration process and the effect of dispersion is negligible. The role of the advection was verified by comparing the results with that using zero Darcy velocity. These results showed the effectiveness of the advection (or Darcy velocity) even in low flow rate system (Test #AD10) having a lower Darcy velocity of 5.5×10^{-10} m/s, and that the advection plays a comparable role as diffusion.

Comparison of the calculated dispersivity values from the three tests showed that the effect of dispersion is very small and had a negligible effect in moderate and low flow rate tests. The results showed that for the range of the flow rates examined, dispersivity (α) is approximately a linear function of the groundwater velocity (v).

TABLE 10.1 VALUES OF THE FLOW-RATE, HYDRAULIC GRADIENT, HYDRAULIC CONDUCTIVITY, AND DARCY VELOCITY, THROUGH THE SOIL LAYER IN TESTS # AD10 & AD11

	Test #AD10	Test #AD11
Flow-rate (m^3/s)	6.95×10^{-11}	6.95×10^{-11}
Hydraulic gradient	1.928	1.893
Hydraulic conductivity (m/s)	2.85×10^{-10}	2.90×10^{-10}
Darcy velocity (m/s)	5.5×10^{-10}	5.5×10^{-10}

TABLE 10.2 AVERAGE VALUES OF THE THICKNESS (H), MOISTURE CONTENT (W), DEGREE OF SATURATION (S), AND VOLUMETRIC MOISTURE CONTENT (θ), FOR THE COMPACTED CLAYEY SILT AND CLEAR STONE LAYERS IN THE ADVECTION-DIFFUSION TESTS # AD10 & AD11

	Test #AD10				Test #AD11			
	H^1 (cm)	W^2 (%)	S^3 (%)	θ^4 (cm^3/cm^3)	H^1 (cm)	W^2 (%)	S^3 (%)	θ^4 (cm^3/cm^3)
Clayey silt :	12.5	15.05	93.3	0.28	12.72*	nd	nd	0.28**
Clear stone :								
Unsaturated	34.2	2.18	8.34	0.035	33.9*	nd	nd	0.035**
Saturated	3.8	26.2	100	0.416	4.1*	nd	nd	0.416**

Porosity = 0.416

1 - Thickness of the soil/stone layer
2 - Moisture content
3 - Degree of saturation
4 - Volumetric moisture content
* - Measured value
** - Estimated value
nd - Not yet determined

TABLE 10.3a AVERAGE VALUES OF THE LAYER THICKNESS (H), VOLUMETRIC MOISTURE CONTENT (θ), EFFECTIVE DIFFUSION COEFFICIENT (D_e), AND DISTRIBUTION COEFFICIENT (K_d), FOR THE SOIL, GEOTEXTILE, CLEAR STONE, AND PERFORATED PLATE, USED IN THEORETICAL ANALYSIS OF THE TESTS # AD10 & AD11

	Test #AD10					Test #AD11		
	H (cm)	θ (cm^3/cm^3)	D_{Cl^-} (m^2/s)	D_{Na^+} (m^2/s)	K_d (mL/g)	H (cm)	θ (cm^3/cm^3)	D_{Cl^-} (m^2/s)
Clayey silt :	12.5	0.28	5.8×10^{-10}	5.1×10^{-10}	0.28	12.72*	0.28**	$5.8\times10^{-10**}$
Geotextile :	0.15	0.45	1.1×10^{-9}	8.2×10^{-10}	0.2	0.15*	0.45**	$1.1\times10^{-9**}$
Clear-stone :								
Unsaturated	34.2	0.035	9.5×10^{-11a} 3.0×10^{-10b}	6.2×10^{-11a} 2.5×10^{-10b}	0.0	34.2*	0.035**	$9.6\times10^{-11**a}$ $3.0\times10^{-10**b}$
Saturated	3.8	0.416	1.1×10^{-9a} 1.1×10^{-9b}	7.4×10^{-10a} 7.4×10^{-10b}	0.0	3.8*	0.416**	$1.1\times10^{-9**a}$ $1.1\times10^{-9**b}$
Perforated plate :	0.18	0.6	1.5×10^{-9}	1.25×10^{-9}	0.0	0.18*	0.6**	$1.5\times10^{-9**}$

* - Measured
** - Estimated
a - Effective diffusion coefficient (D_e)
b - Hydrodynamic dispersion coefficient, D, ($D = D_e + D_{md}$)

$\alpha_{AD10} = 0.0127$ m, (α = dispersivity)

TABLE 10.3b OTHER INPUT DATA USED IN THEORETICAL ANALYSIS OF THE TESTS # AD10 & AD11

	Test #AD10				Test #AD11			
	Clayey-Silt	Geotextile	Clear-Stone	Perforated-Plate	Clayey-Silt	Geotextile	Clear-Stone	Perforated-Plate
Thickness (cm)	12.50	0.15	38.0	0.18	12.72*	0.15*	38.0*	0.18*
Cl^- Background concn. (mg/L)	125	50	10	10	125*	50**	10*	10**
Na^+ Background concn. (mg/L)	100	50	7	7	--	--	--	--
Cl^- Source concn. (mg/L)	1930				1930*			
Na^+ Source concn. (mg/L)	1120				--			
Darcy velocity (m/s)	5.5×10^{-10}				5.5×10^{-10}*			
Initial reference height of solution, H_f (cm)	12.0				12.1*			
Solution collected (/area/time - m/s)	5.9×10^{-11}				5.9×10^{-11}*			
Base outflow velocity (m/s)	1.72×10^{-9}				1.72×10^{-9}*			
Duration of the test (days)	479.74				479.0*			

* - Measured data, ** - Estimated data

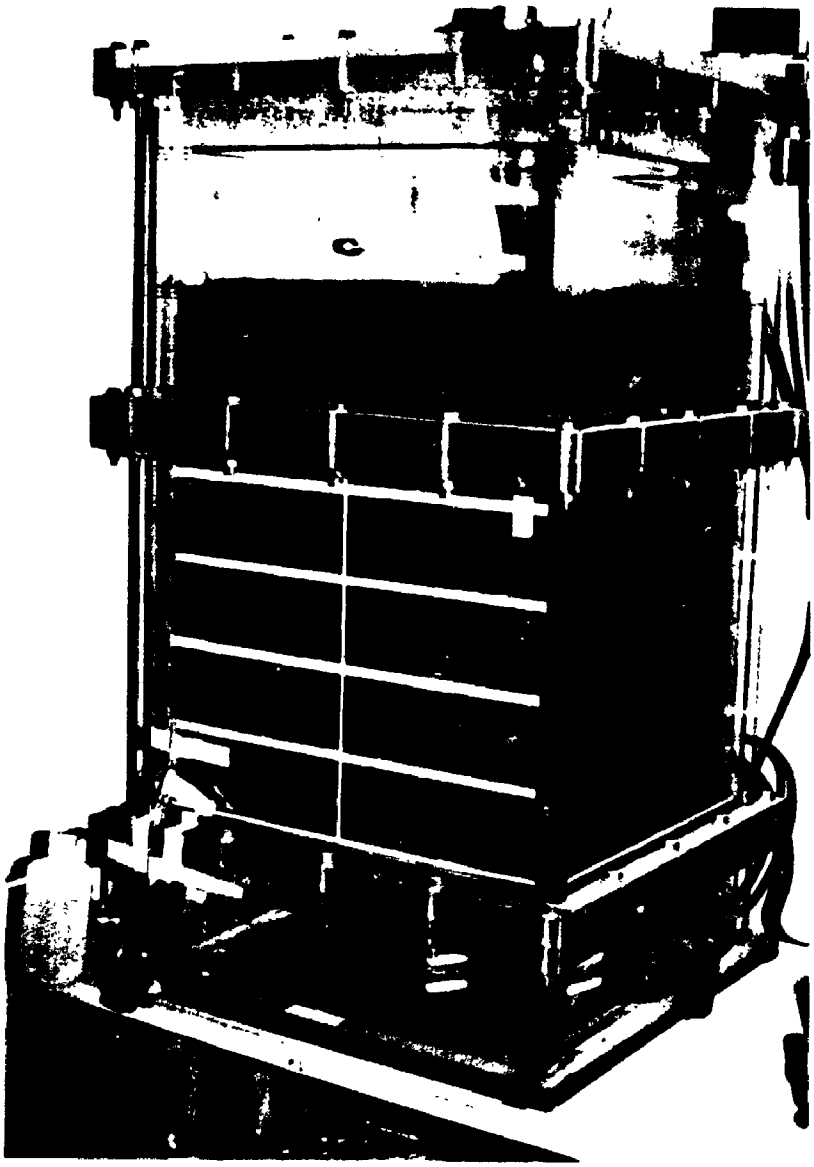

FIG. 10.1 VIEW OF THE LARGE SCALE ADVECTION-DIFFUSION TEST CONDUCTED ON THE COMPACTED CLAYEY SILT OVER UNSATURATED CLEAR STONE

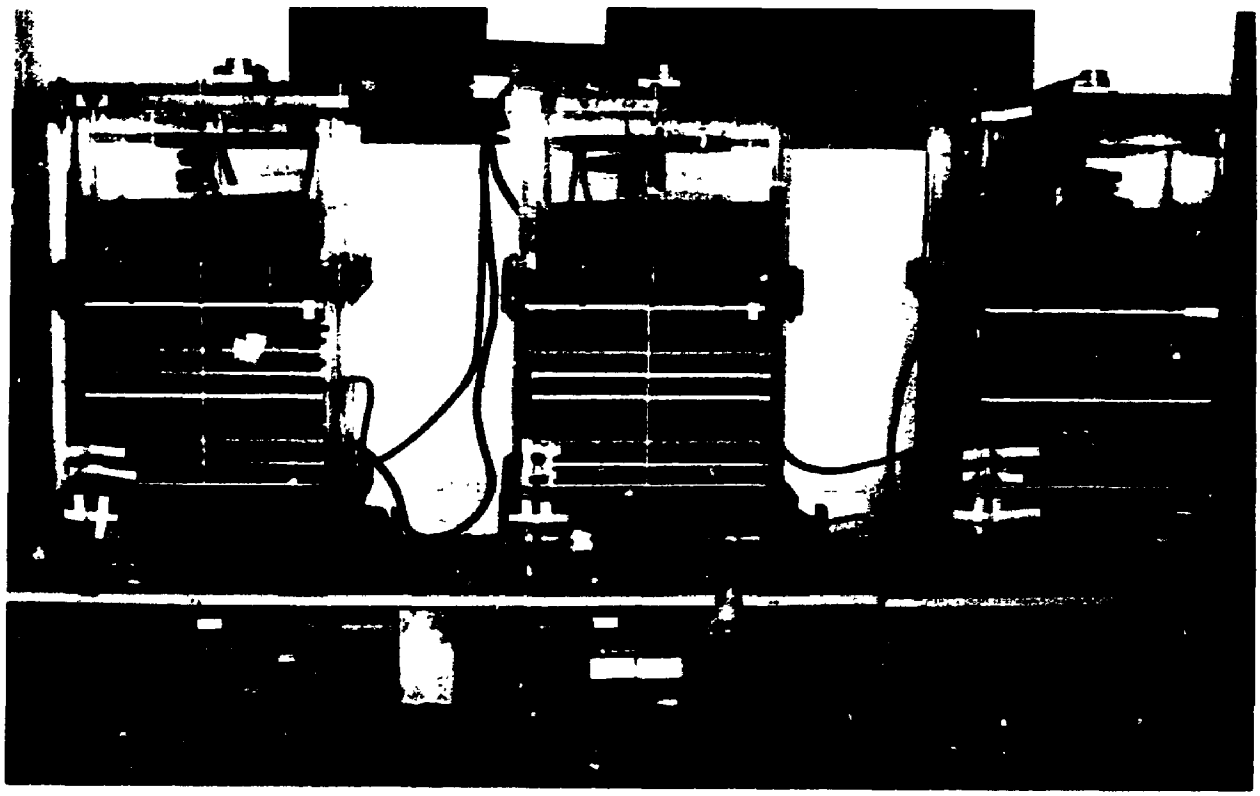

FIG. 10.2 VIEW OF THE THREE LARGE SCALE ADVECTION-DIFFUSION TESTS, RIGHT: TEST #AD9, LEFT: TEST #AD10 & MIDDLE: TEST #AD11

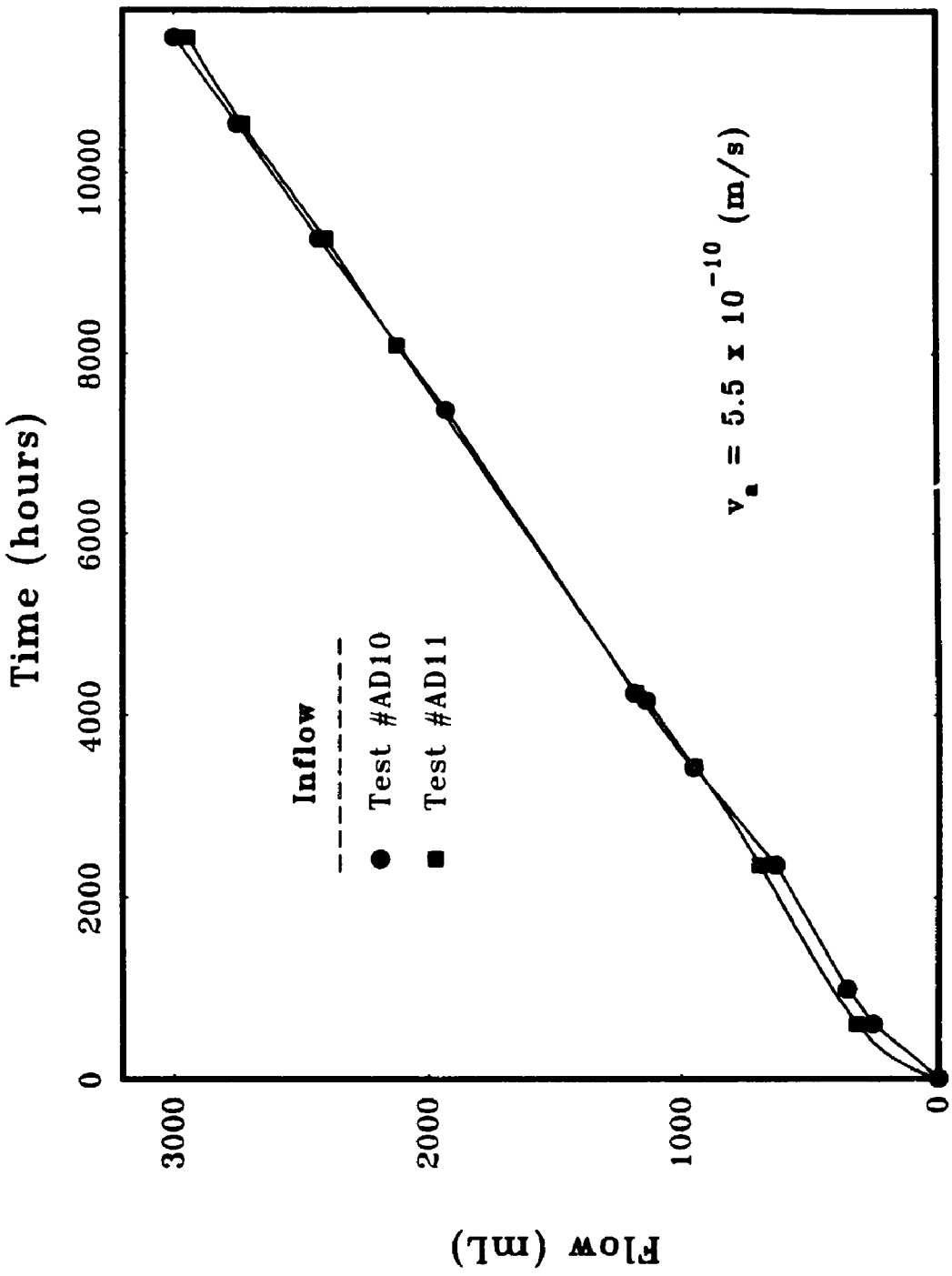

FIG. 10.3 OBSERVED INFLOW RATES VERSUS ELAPSED TIME IN ADVECTION-DIFFUSION TESTS # AD10 & AD11 (CLAYEY SILT-UNSATURATED CLEAR STONE)

FIG. 10.4 PLAN VIEW OF THE LOCATIONS OF THE SHELBY TUBE SAMPLES TAKEN FROM THE COMPACTED CLAYEY SILT LAYER AT THE END OF THE TEST #AD10

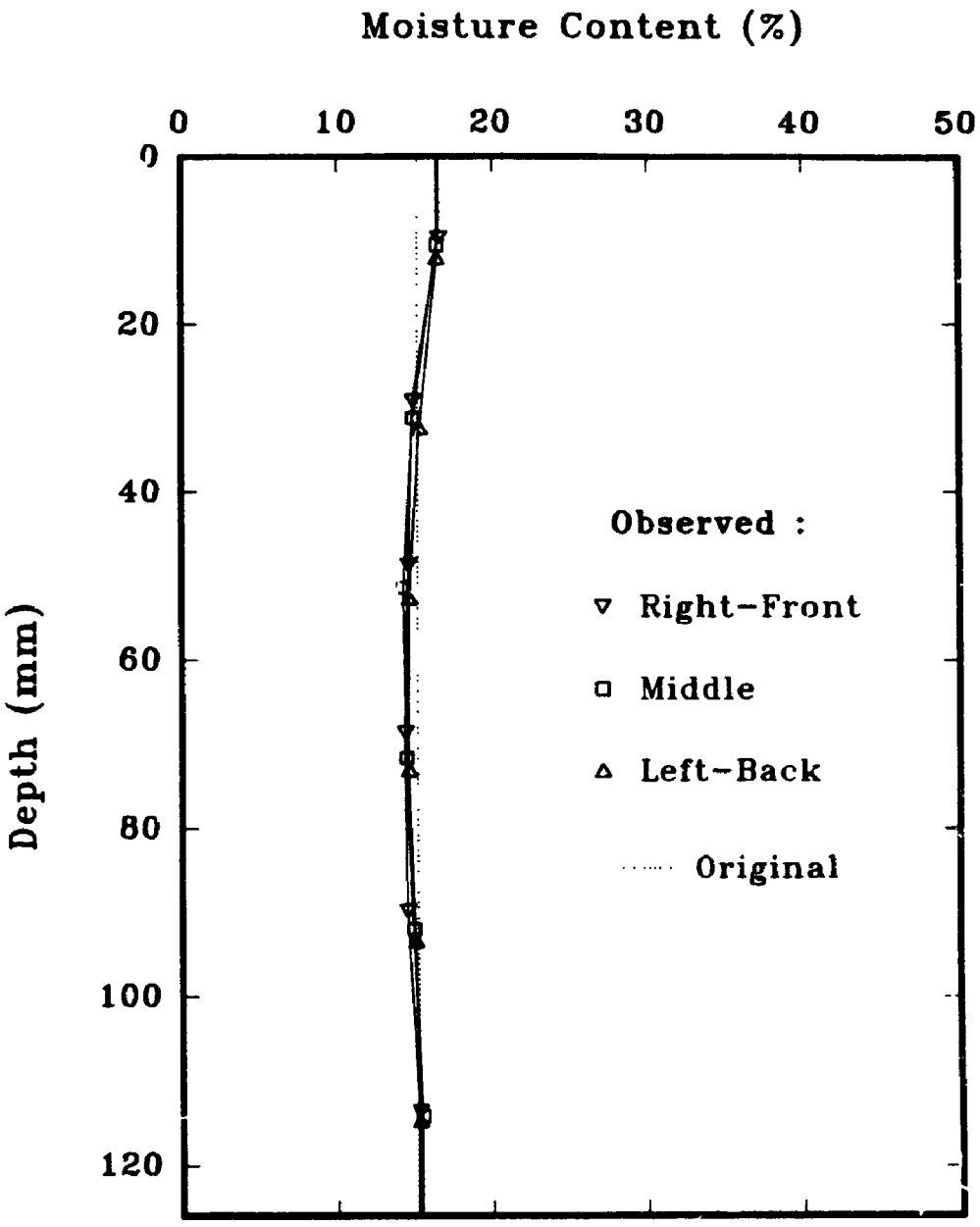

FIG. 10.5 MOISTURE CONTENT PROFILES OF THE COMPACTED CLAYEY SILT LAYER AT THE END OF THE ADVECTION-DIFFUSION TEST #AD10, MEASURED IN 3 LOCATIONS

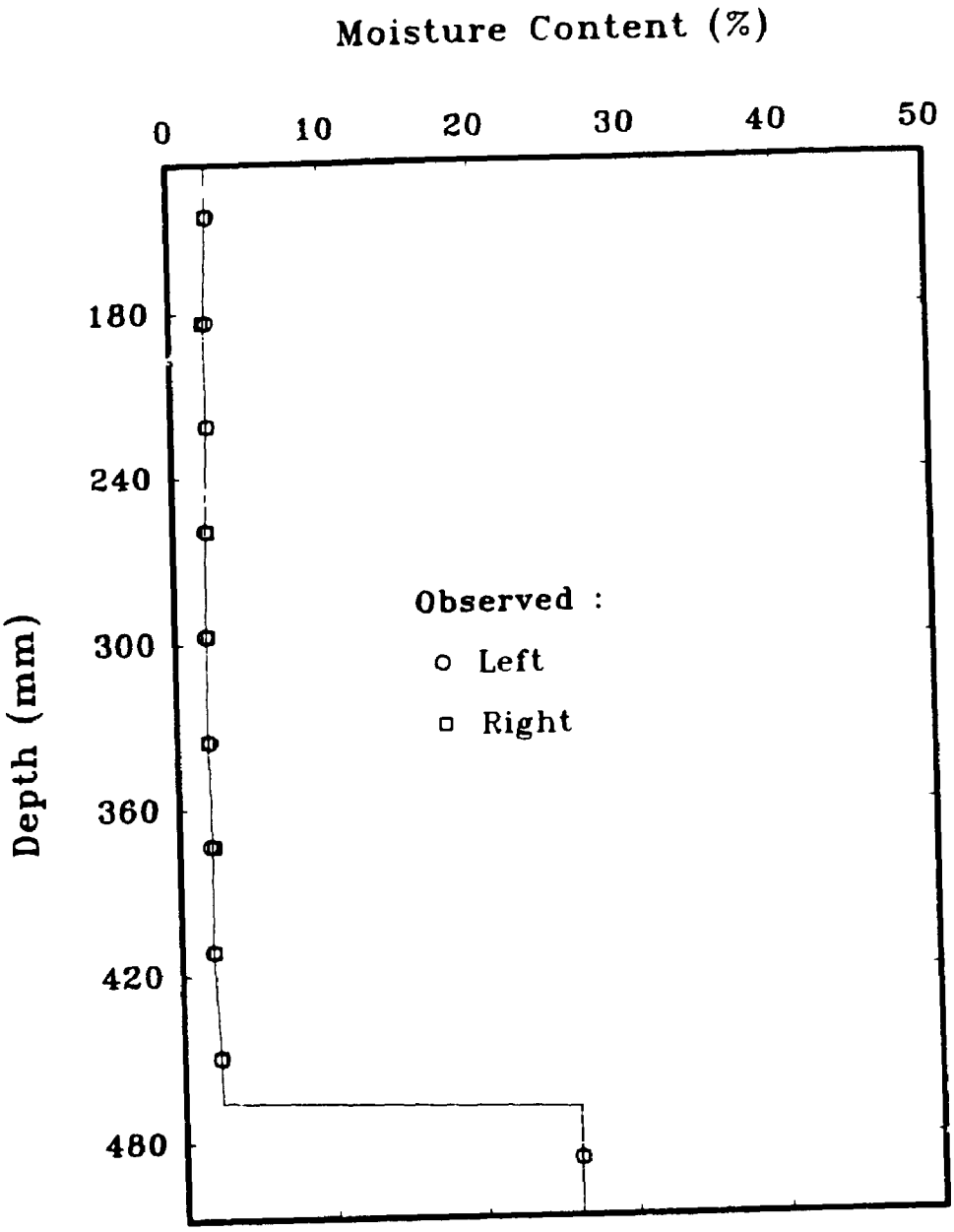

FIG. 10.6 MOISTURE CONTENT PROFILES IN RIGHT AND LEFT SIDE OF THE CLEAR STONE LAYER, MEASURED AT THE END OF THE ADVECTION-DIFFUSION TEST #AD10

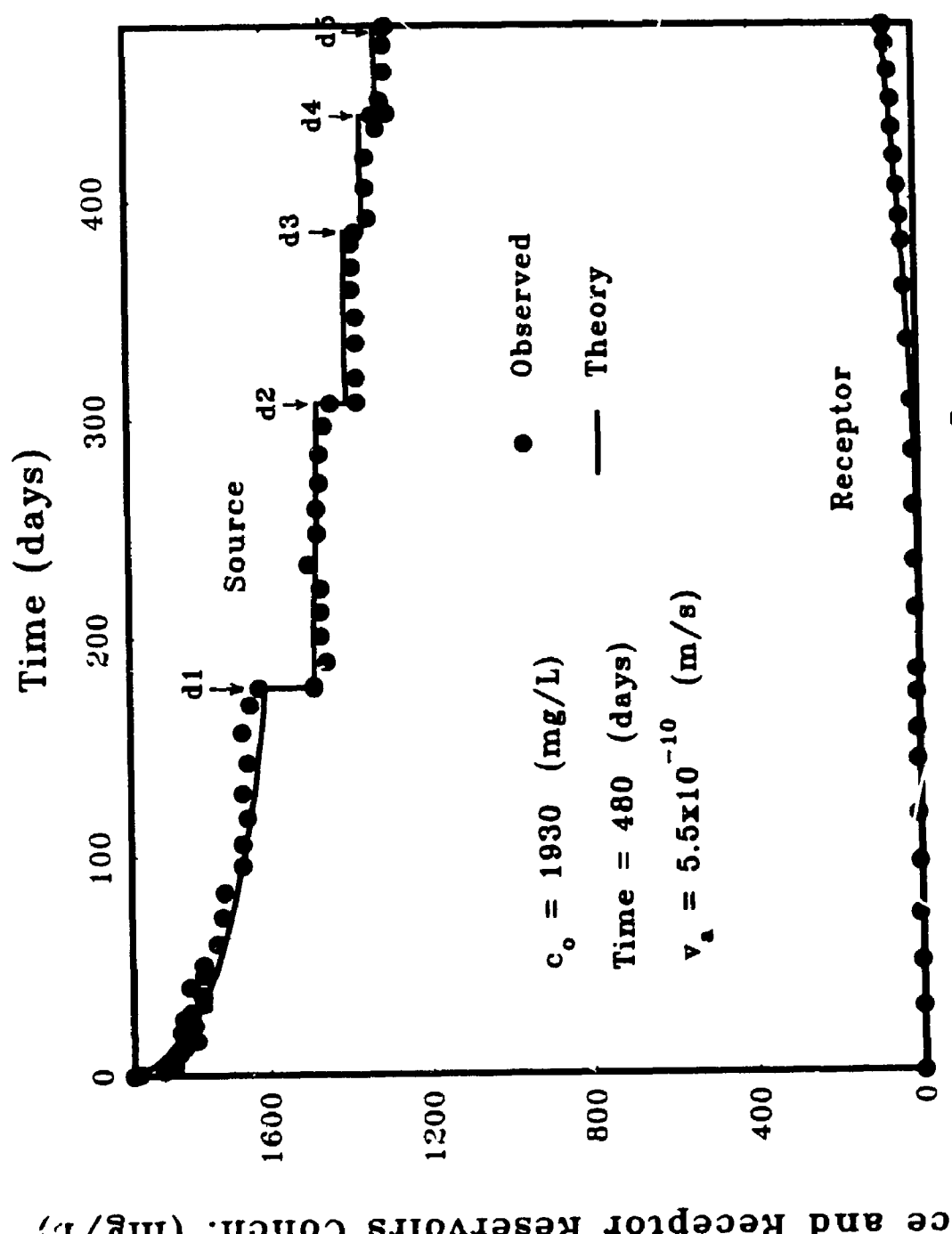

FIG. 10.7 OBSERVED AND CALCULATED $[Cl^-]$ CONCENTRATIONS VERSUS ELAPSED TIME IN SOURCE AND RECEPTOR RESERVOIRS OF ADVECTION-DIFFUSION TEST #AD10

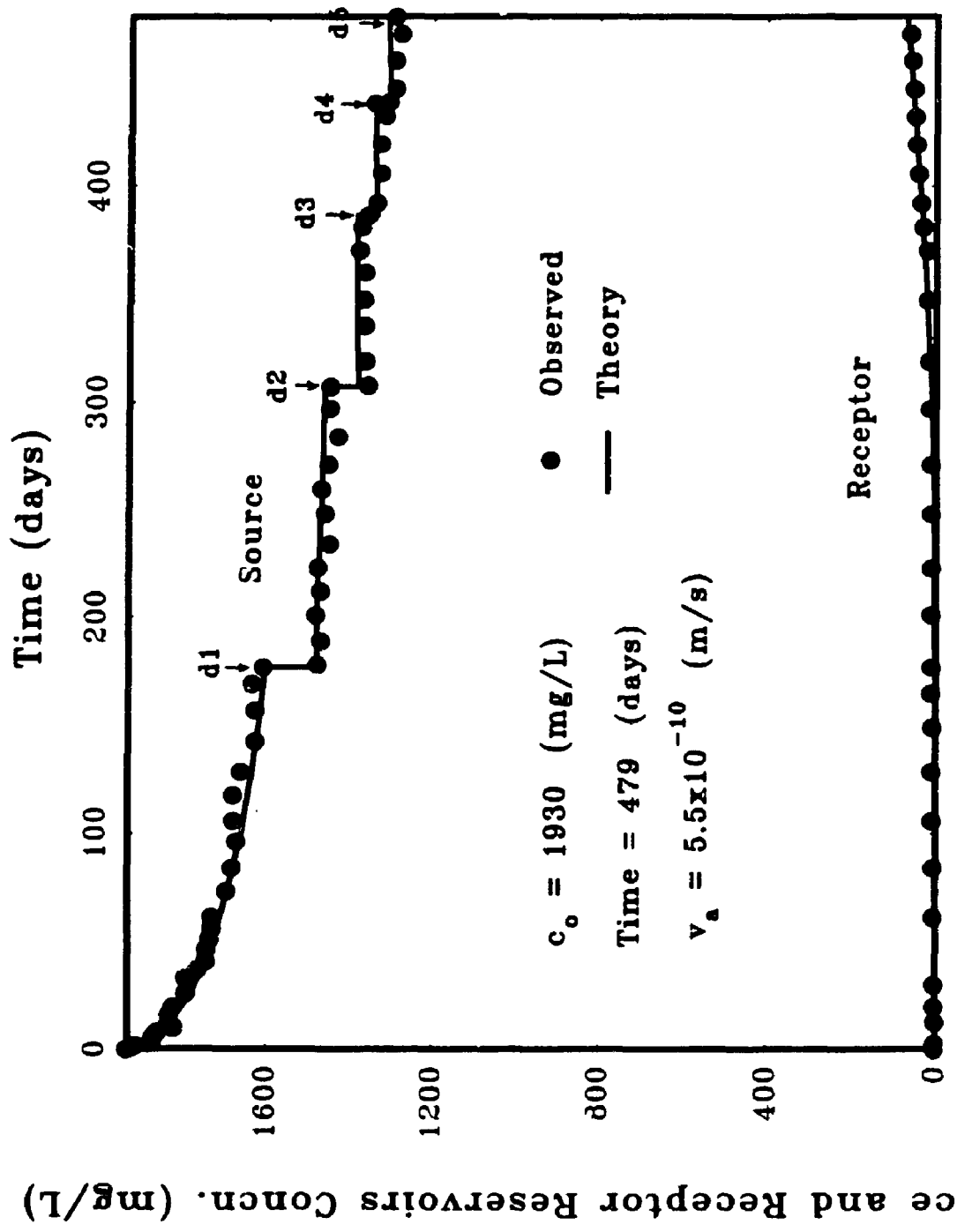

FIG. 10.8 OBSERVED AND CALCULATED [Cl^-] CONCENTRATIONS VERSUS ELAPSED TIME IN SOURCE AND RECEPTOR RESERVOIRS OF ADVECTION-DIFFUSION TEST #AD11

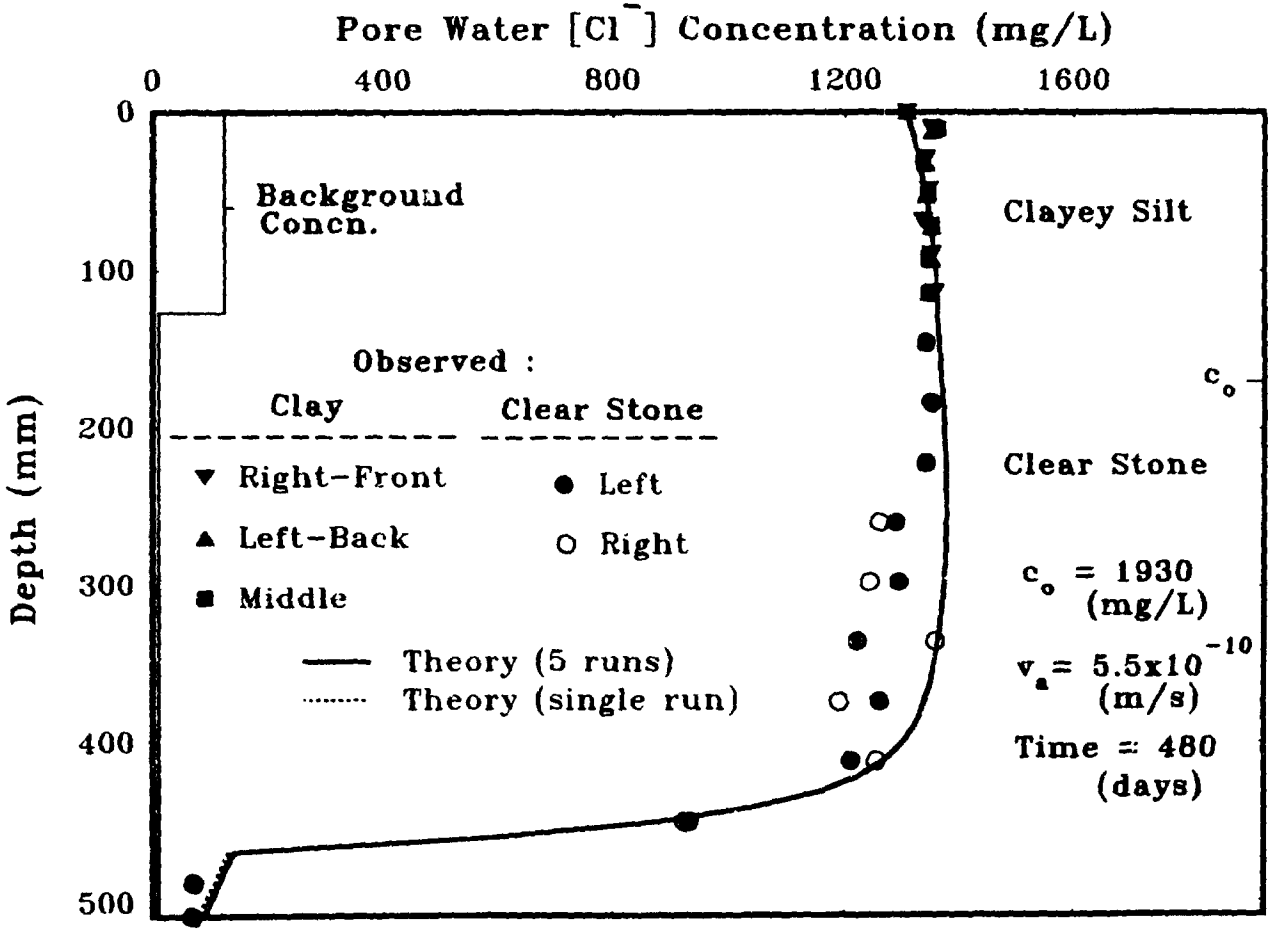

FIG. 10.9 OBSERVED AND CALCULATED [Cl⁻] CONCENTRATION PROFILES IN ADVECTION-DIFFUSION TEST #AD10 (CLAYEY SILT-UNSATURATED CLEAR STONE)

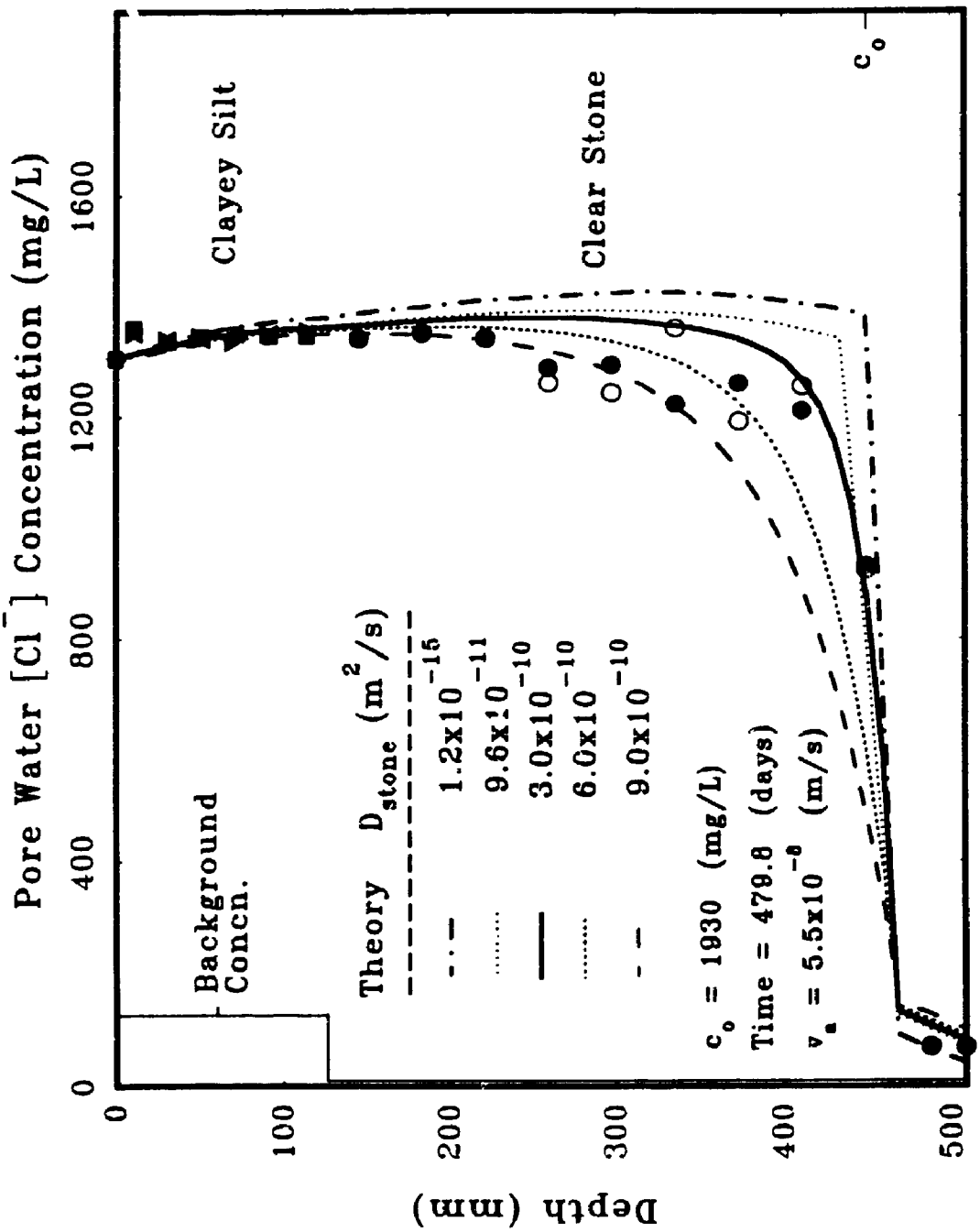

FIG. 10.10 OBSERVED AND CALCULATED [Cl^-] CONCENTRATION PROFILES IN ADVECTION-DIFFUSION TEST #AD10, USING DIFFERENT HYDRODYNAMIC DISPERSION COEFFICIENTS FOR UNSATURATED STONE LAYER

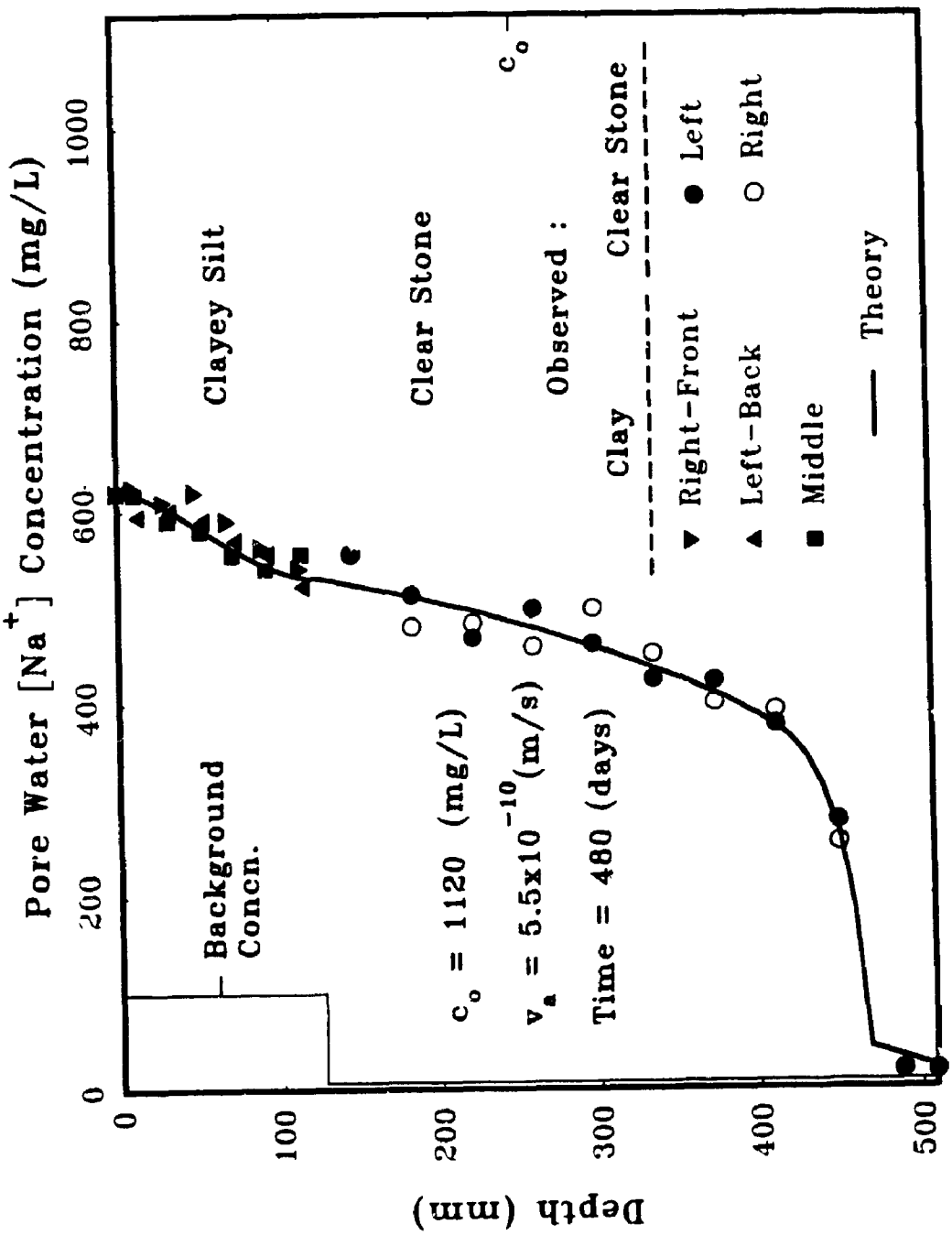

FIG. 10.11 OBSERVED AND CALCULATED [Na^+] CONCENTRATION PROFILES IN ADVECTION-DIFFUSION TEST #AD10 (CLAYEY SILT-UNSATURATED CLEAR STONE)

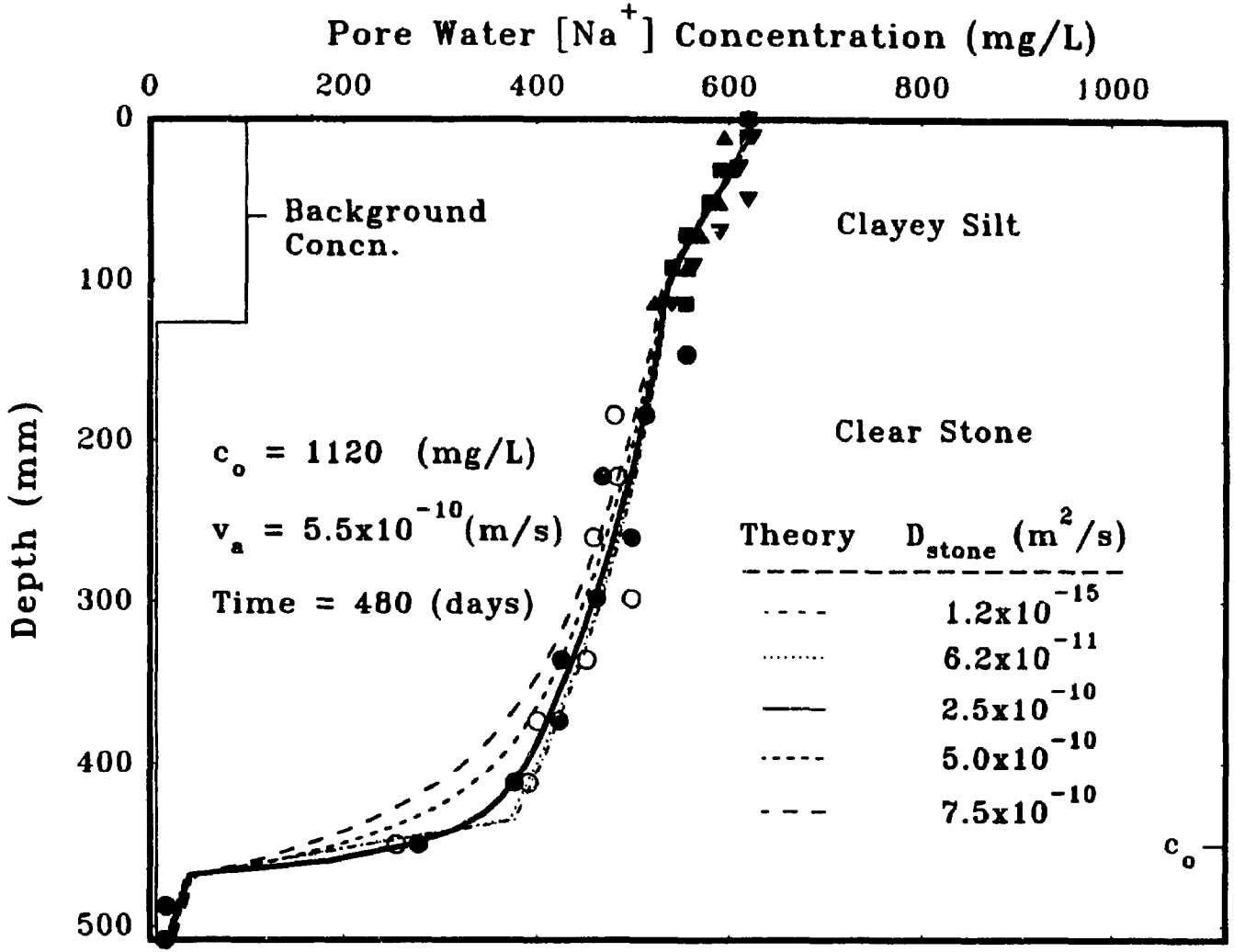

FIG. 10.12 OBSERVED AND CALCULATED [Na^+] CONCENTRATION PROFILES IN ADVECTION-DIFFUSION TEST #AD10, USING DIFFERENT HYDRODYNAMIC DISPERSION COEFFICIENTS FOR UNSATURATED STONE LAYER

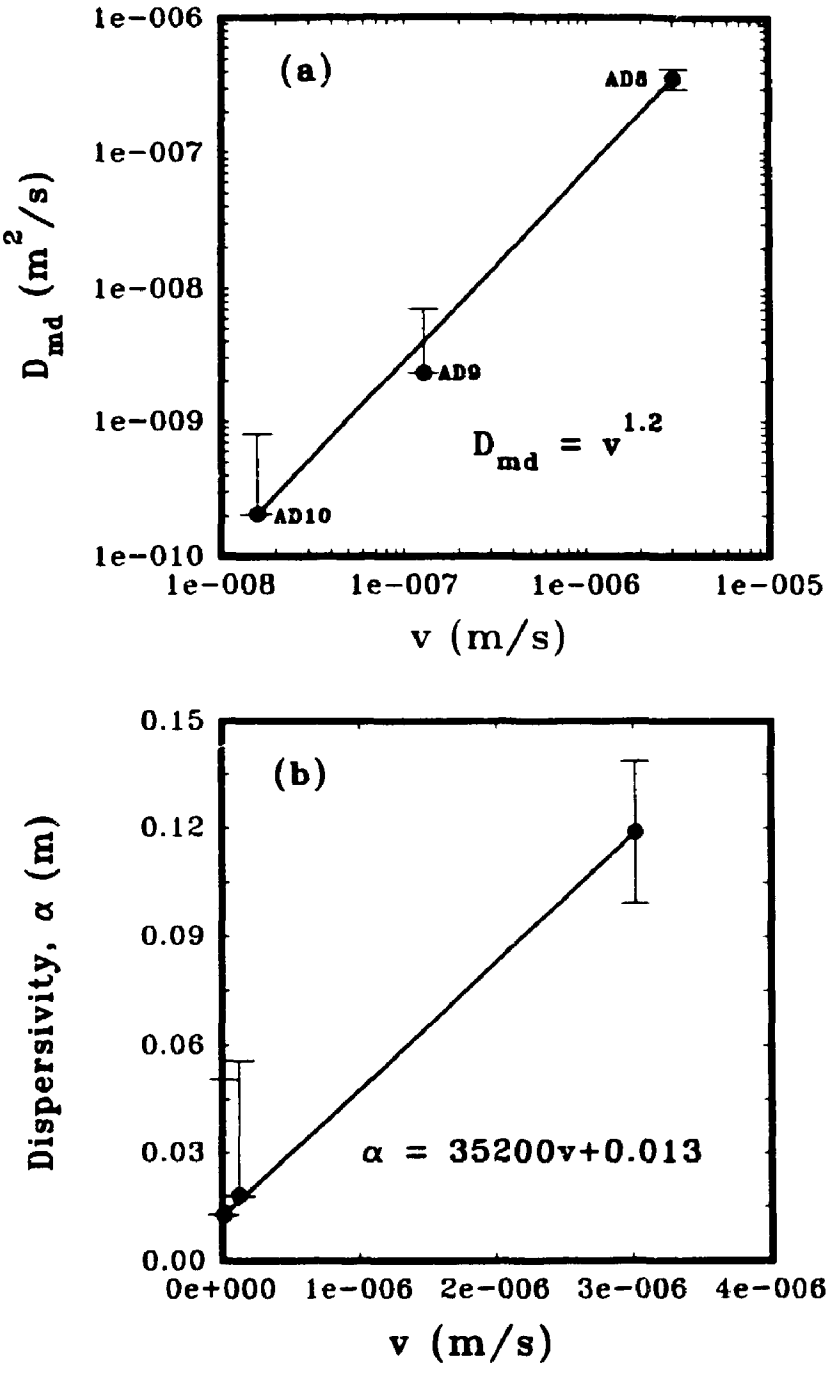

FIG. 10.13 RELATIONSHIP BETWEEN (a) SEEPAGE VELOCITY AND MECHANICAL DISPERSION COEFFICIENT AND (b) SEEPAGE VELOCITY AND DISPERSIVITY, IN TESTS # AD8, AD9 & AD10

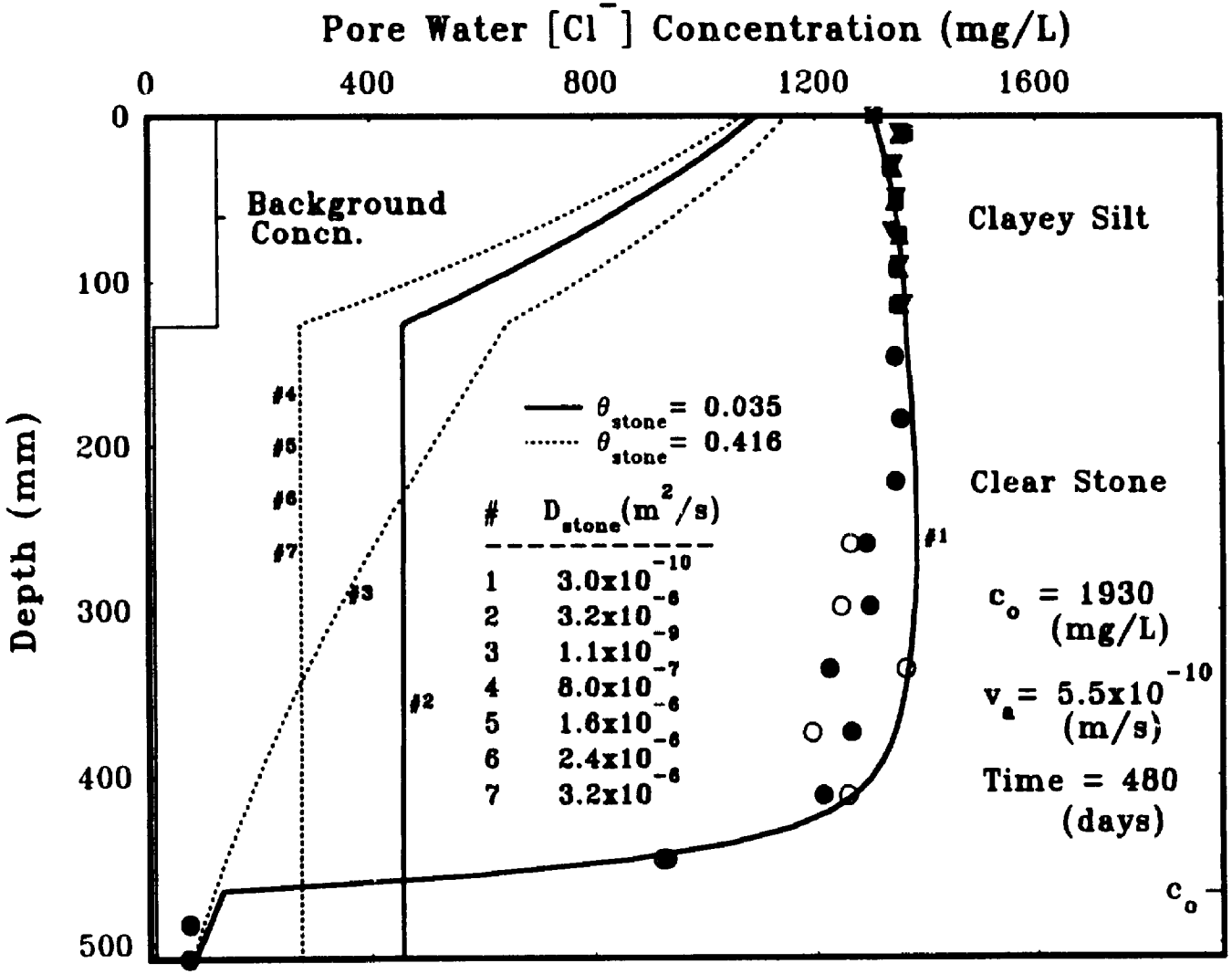

FIG. 10.14 EFFECT OF THE HYDRODYNAMIC DISPERSION COEFFICIENT AND VOLUMETRIC MOISTURE CONTENT OF THE STONE LAYER ON THEORETICAL [Cl^-] CONCENTRATION PROFILES OF THE TEST #AD10

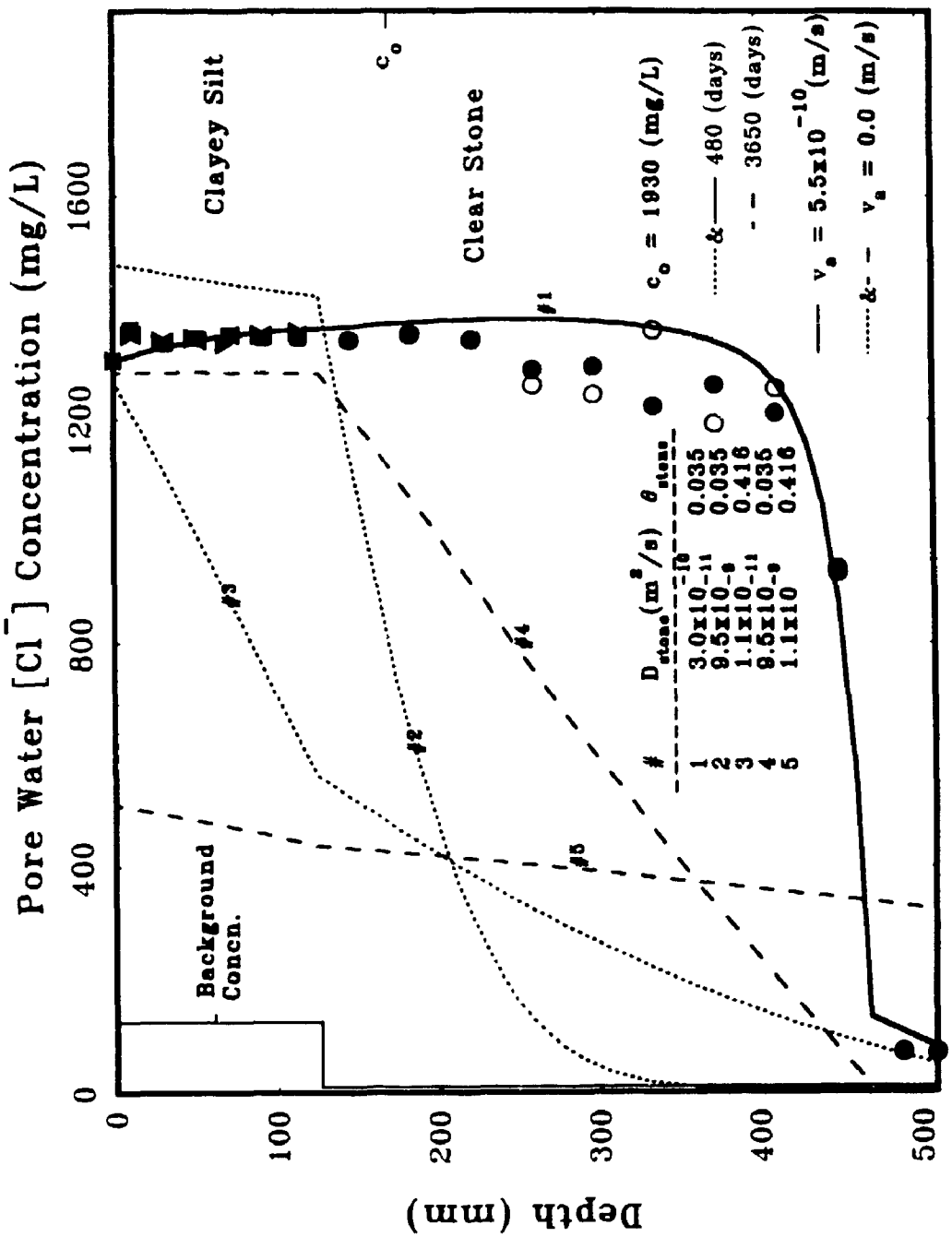

FIG. 10.15 EFFECT OF D_{stone} AND θ_{stone} ON $[Cl^-]$ CONCENTRATION PROFILES OF THE TEST #AD10, ASSUMING PURE DIFFUSION (v_s=0.0) (ANALYSIS PERFORMED FOR 480 AND 3650 DAYS)

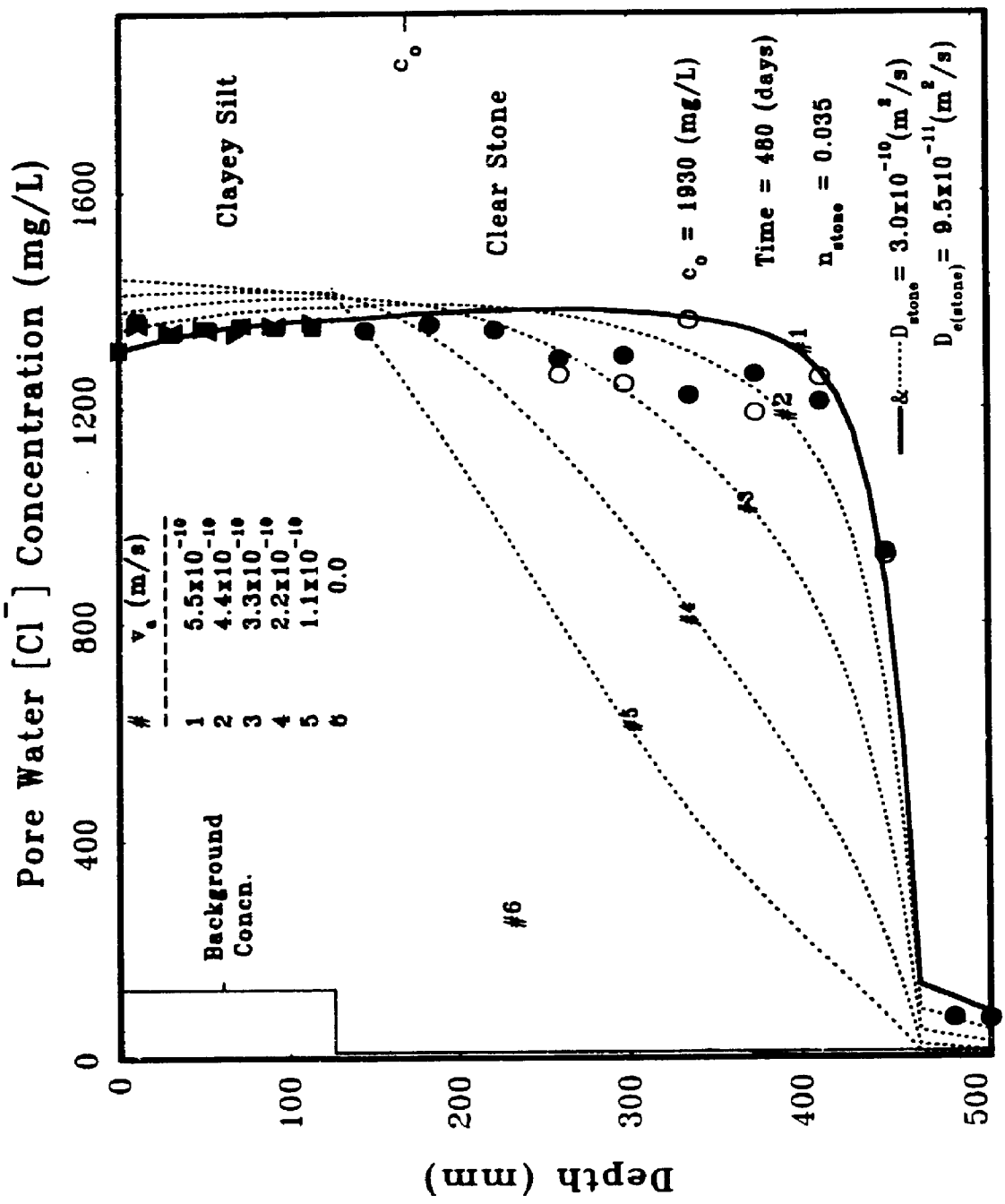

FIG. 10.16 EFFECT OF THE DARCY VELOCITY ON THEORETICAL [Cl^-] CONCENTRATION PROFILES OF THE TEST #AD10

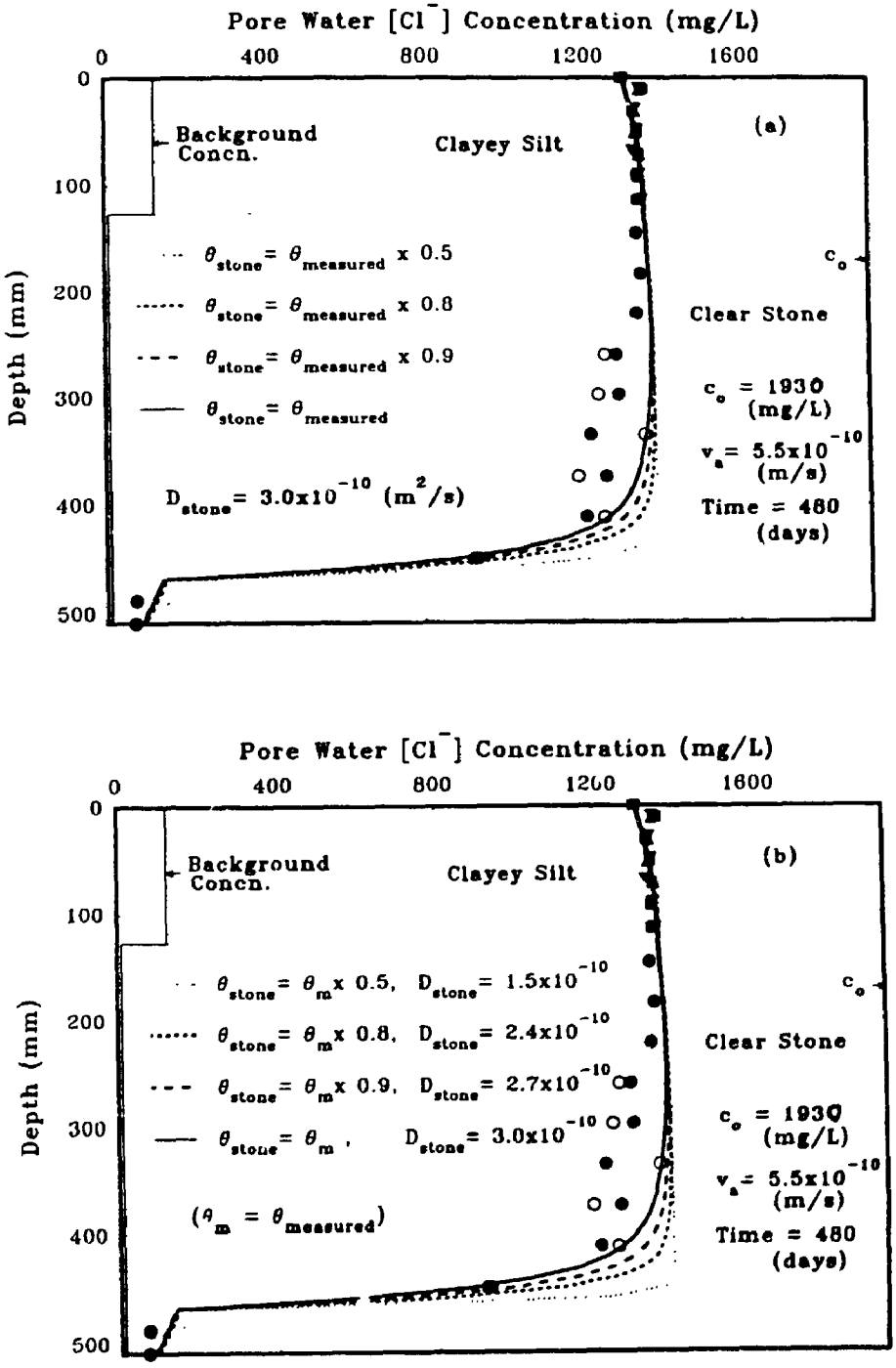

FIG. 10.17 EFFECT OF REDUCED VOLUMETRIC MOISTURE CONTENT (a), & VOLUMETRIC MOISTURE CONTENT AND EFFECTIVE DIFFUSION COEFFICIENT (b) OF THE UNDERLYING UNSATURATED STONE ON CALCULATED CONCENTRATION PROFILES (TEST AD10)

CHAPTER 11

A LABORATORY STUDY OF CLAY INTRUSION INTO A COARSE STONE LAYER UNDER APPLIED PRESSURES

11.1 INTRODUCTION

The Geotechnical Research Centre, University of Western Ontario, was contracted by the Interim Waste Authority Ltd (IWA) to perform a series of tests to examine the potential intrusion of compacted clayey till through (a) geotextile; and (b) graded granular filter/separators and into a layer of coarse stone with a nominal size of 50 mm (e.g. see Fig. 11.1). The geotextile used in this study was essentially the same geotextile as used in advection-diffusion Tests # AD8, AD9, and AD10 as a separator between the soil and stone layers (described in Chapters 9 and 10). Tests were also conducted to examine the potential intrusion of compacted clayey till into the coarse stone layer if there was no filter/separator between the two materials. The coarse stone was saturated and the pore water pressure in the stone was increased to 100 kPa (i.e. equivalent to approximately 10 m of pressure head). The clayey soil was loaded vertically to pressures of up to 600 kPa and the intrusion of the clayey soil into the underlying coarse stone was examined. This chapter describes the tests that were conducted and presents the results.

11.1.1 BACKGROUND - THE HALTON STUDY

The final design studies conducted to gain the Ministry of Energy and

Environment (MOEE) approval for construction of the Halton Waste Management Facility included the construction of a 30 m x 30 m test pad to demonstrate the feasibility of constructing a compacted clayey till liner over a granular layer. The Halton design incorporated a geotextile separator between the liner and the underlying stone. Following construction of the test pad, test pits were excavated through the liner to allow an examination of the liner quality and to allow inspection and sampling of the geotextile separator between the liner and the underlying stone layer (Rowe et al., 1993). The geotextile was examined and tested to assess the effect of construction damage.

Intrusion tests were performed for the "Halton Study" (Rowe et al., 1993). In these tests, the effect of construction damage of the geotextile was directly considered by using actual samples of geotextile which had been exhumed from between the stone and the clay liner in the test pad described above.

11.1.2 IWA STUDY

The procedure adopted in the IWA tests generally follows those previously developed and used in the Halton study.

It is understood that the thickness of waste for one or more of the IWA landfills may exceed the thickness of waste at the Halton landfill. In order to simulate the effect of a greater thickness of waste on potential intrusion, the applied vertical pressure used in the IWA study was substantially increased relative to the Halton study. In addition, the effect of pressurizing the stone layer to simulate 10 m of head in a hydraulic control layer was examined. Thus the primary differences between the tests conducted for this

IWA study and those in the Halton study (Rowe et al., 1993) are:

. the stone was saturated and pressurized to 100 kPa whereas in the previous study, it was unsaturated.

. the applied vertical pressure was up to 600 kPa (compared to a maximum of 300 kPa in the previous study for the smaller Halton landfill).

. a graded granular filter was examined as well as a geotextile (only geotextiles were examined in the previous study).

. the potential intrusion of compacted clayey till into the coarse stone layer was examined in the absence of any filter/separator between the two materials.

The soil used for the simulated compacted clay liner consisted of Halton till (obtained from the Halton Waste Management Site in Milton) and is essentially the same soil ("Unweathered Upper Till") as used in the Halton study and also diffusion and advection-diffusion tests described in previous chapters. To simulate actual construction related defects, the geotextile separator/filter used in this IWA study was material actually taken from the test pad for the Halton study and hence had been subjected to construction damage (Rowe et al., 1993). The stone used was an angular dolomitic limestone with a nominal dimension of 50 mm.

Section 11.2 describes the three tests conducted using a geotextile filter/separator layer between the compacted clayey till and stone layers and presents the results from these tests. Section 11.3 describes the two tests conducted using a graded granular filter/separator layer between the compacted clayey till and stone layers and presents the results from these tests. Section 11.4 describes the 2 tests conducted using compacted clayey till in direct contact with stone and presents the results from these tests. Section

11.5 summarizes the findings and presents the conclusions.

11.2 INTRUSION THROUGH THE TS650 GEOTEXTILE

This section describes the tests conducted to examine potential intrusion of the compacted clayey till through a geotextile filter/separator. Figure 11.1 shows a schematic of the test set up. The geotextile used was Polyfelt TS650 with engineering properties as given in Table 9.2 (Chapter 9). The geotextile had been used to separate the clay liner from a stone layer at the Halton Waste Management test pad (Rowe et al., 1993) and had been subsequently exhumed. Thus the geotextile had experienced some construction damage as a result of this previous use and was used to simulate the effect of construction related defects, as discussed previously.

11.2.1 METHOD

The soil used in the test was air-dried, pulverized (being careful not to break up the pebbles), and oversize material was removed by passing soil through a No. 4 sieve. The grain size distribution of the soil is shown in Fig. 11.2. The soil was then brought to the desired water content (2-4 % wet of optimum, w_{opt} = 10.9 % as determined from the Halton study) and allowed to cure for at least 16 hours. The geotextile sample was cut, washed of fines and observations were made regarding the condition of the sample. Any observed damage to the geotextile was circled with a marker and photographed.

The test cell was inverted, and the load plate brought to the level of the flange

by means of spacers (Photo 11.1). The damp geotextile sample was placed on the load plate and flange, and curled up the inside of the larger cylinder (Photo 11.2). Washed, air dried 50 mm stone having the grain size distribution shown in Fig. 11.2, was randomly placed on the geotextile (Photo 11.3), and additional stone was placed to fill the cylinder (Photo 11.4). Smaller 20 mm river gravel was used to provide a smoother surface in contact with the base plate (Fig. 11.1 & Photo 11.5). The base plate was bolted to the test cell (Photo 11.6).

The test cell was inverted, and the load plate and spacers removed to reveal the exposed geotextile underlain by 50 mm stone (Photo 11.7). If the geotextile had defects, hand pressure was used to observe if these defects were located over a void or on a stone surface. To minimize side shear at the soil-cylinder interface, grease was applied around the inner surface of the smaller cylinder and a piece of plastic was placed between the greased surface and the soil prior to placing the soil. The soil was placed on the geotextile and compacted in a 6 cm thick layer using 100 blows from a 24.5 kN hammer falling 0.3 m to impart standard Proctor energy to the soil (Photo 11.8). In Tests # 1 and 2, the clayey soil was compacted in three lifts giving a total clay thickness of 18 cm. To examine the effect of clayey layer thickness on the results, Test # 3 was conducted using a single 6 cm thick lift of soil. Thus the actual soil thickness was 18 cm in Tests # 1 and 2, and 6 cm in Test # 3. The soil surface was then smoothened by tamping (Photo 11.9) and the load plate was placed onto the soil surface (Photo 11.10). Representative samples of the soil were taken for water content determination.

Tubing from a water reservoir was attached to the inlet valve of test cell. Air outlets on the flange were kept open, the valve opened and the lower cylinder (containing

the stone), was saturated with water (Photos 11.11, 11.12 & 11.13).

The vertical pressures were applied using an MTS mechanism (Photos 11.14 and 11.15). First, a 100 kPa pressure was applied for 2 hours and then the pressure was increased to 200 kPa. To simulate the piezometric head of approximately 10 m in the stone layer, a 100 kPa pressure was applied to the fluid in the stone and regulated using a pressure regulator (Photo 11.16). This cell pressure remained constant during the test.

In Test # 1, the vertical pressure was increased to 500 kPa in 100 kPa increments at 2 hourly intervals and then remained constant during the test. To examine the effect of higher applied pressure, Test # 2 was performed by firstly increasing the vertical pressure to 500 kPa in 100 kPa increments at 2 hourly intervals as in Test # 1 and then, after maintaining this pressure over night, the pressure was increased to 600 kPa the following day and maintained at this value for the rest of the test. The load increment process for Test # 3 was identical to Test # 2.

After the period of about one week for Tests # 1 and 2, and 2 weeks for Test # 3, at the desired vertical load and 100 kPa cell pressure, the applied vertical load and cell pressure were removed (Photo 11.17). The cell was raised by means of a crane at which time water from the larger cylinder was drained into a container through a tube attached to the cell (Photo 11.18). This water was filtered to collect any fines that may have been washed out during drainage process. The load plate was removed, the cell inverted, the base plate opened, and the stones hand excavated and transferred into a tray (Photo 11.19). The stones were then washed over a sieve containing filter paper. The wash water was collected in a container, transferred into trays and oven dried to evaporate the water to allow collection of any fines that may have passed through the filter paper. This

would include fines that had intruded through the geotextile but could also include fines that may have been formed at contact points between the stones. The weight of these fines was measured and recorded. The filter paper containing fines was also oven dried and weight of fines was recorded. The same process was repeated for drainage water and the weight of fines was recorded.

The exposed geotextile was inspected for defects, and defects existing prior to the test were inspected for any changes. Visual observations of the condition of the geotextile were recorded and photographs were taken (Photo 11.20). The geotextile was then removed to expose the soil surface, which was inspected and photographed. The geotextile was washed of fines and the wash water was collected, oven dried, and the weight of fines that had intruded into the geotextile was recorded.

11.2.2 RESULTS

The results obtained for each test are summarized in Table 11.1 and are discussed in the following sub-sections.

11.2.2.1 TEST NUMBER 1

There were 4 defects on the TS650 geotextile sample prior to the test (Photo 11.21) two of which were in contact with clayey soil (the other two were located outside the loaded area defined by the smaller cylinder). The initial holes (in contact with clay) with the dimensions of 2 mm x 3 mm and 1 mm x 1 mm had expanded (during the test)

to almost twice the original size (4 mm x 6 mm and 2 mm x 2 mm) (Photo 11.22) and 4 new small holes were created during the test each having a size of about 1.5 mm x 1.5 mm. As might be expected, these holes were mostly located over the void space between the stones (3 were located over the void space and 1 on the stone). Soil was visible on the stone side of the geotextile where the stone and geotextile had been in contact.

The clayey soil surface was indented but smooth and no voids were apparent on the soil surface (Photo 11.23). The clayey soil and geotextile had been pushed into the upper portion of the voids in the stone, by up to a maximum of 2 cm. When the stone was excavated, the surface of the stones in direct contact with the geotextile were observed to be coated with fine grained material (Photo 11.24). The coating of stone with fines in this test (and in Tests # 2 and 3) was visually similar to that observed on the stone from below the geotextile and compacted clayey till liner in the Halton test pad (Rowe, pres. comm.). The mass of this material and the material recovered in drainage water was found to be 8.7 g. Thus the total mass of the soil that passed through the geotextile was about 0.27 kg/m^2. The total mass of soil recovered from the geotextile was found to be 22.7 g.

11.2.2.2 TEST NUMBER 2

Defects were observed on the TS650 geotextile prior to the test. There were six holes in the geotextile (Photo 11.26) three of which were in contact with soil after installation (holes # 3, 4 & 5 in Photo 11.26). Two of these holes (# 3 & 5) were in contact with the stone surface and one (#4) on the void space between the stones. The

initial holes had the dimensions of 14 mm x 1 mm (#1), 6 mm x 4 mm (#2), 6 mm x 1 mm (#3), 5 mm x 2 mm (#4), 6 mm x 1 mm (#5), and 13 mm x 6 mm (#6). The size of holes # 3, 4, and 5 which were located under the loaded area, changed to approximately 8 mm x 2 mm, 7 mm x 3 mm, and 7 mm x 3 mm and three new holes with the dimensions of 4 mm x 2 mm were created during the test (Photo 11.27). It should be noted that the use of geotextile which had been previously damaged by construction installation gives conservative results because it increases the likelihood of holes being present and forming during the test.

As in Test # 1, when the stone was excavated, the surface of the stones in contact with the geotextile were observed to be coated with fine grained material. The mass of extruded soil was determined by washing the stones, oven drying the wash water and weighing the fines that remained. The weight of fines was found to be 9.2 g. Thus the total mass of the soil that had passed through the geotextile was 0.29 kg/m^2. The total mass of soil intruded into and remaining in the geotextile was found to be 20.5 g.

11.2.2.3 TEST NUMBER 3

There were no defects on the TS650 geotextile prior to this test (Photo 11.28) and no holes were observed at the end of the test (Photo 11.29). Soil was visible on the stone side of the geotextile where the stone and geotextile had been in contact. The soil and geotextile had been pushed into the upper portion of the voids in the stone, by up to maximum of 2 cm.

As was the case for Tests # 1 and 2, when the stone was excavated, the surface

of the stones in contact with the geotextile was observed to be coated with fine grained material. The mass of this material and the material recovered in drainage water was found to be 1.0 g. Thus the total mass of the soil that passed through the geotextile was 0.031 kg/m^2. The total mass of soil recovered from the geotextile was found to be 8.3 g.

11.2.2.4 DISCUSSION

Tests # 1 and 2 were essentially identical except for the 100 kPa higher consolidation pressure used in Test # 2. The soil mass intruded into the stones was the same to all practical purposes and was less than 0.3 kg/m^2. The results from Tests # 1 and 2 are also essentially the same as that obtained for the same type of geotextile and soil source in the Halton study (Rowe et al., 1993) where the intruded mass of 9.6 g (applied pressure was 300 kPa with no water pressure in the underlying stone), is comparable to the values of 8.7 g and 9.2 g in Tests # 1 and 2. The intrusion through the geotextile does not appear to have been affected by the difference in applied vertical pressure (300 kPa, 500 kPa, or 600 kPa) or the water pressure in the stone layer (zero or 100 kPa).

In the Halton study the applied pressure was only maintained for 18 hours where as in the present IWA study the applied stress was maintained at a maximum value of between 130 hours and 183 hours for Tests # 1 and 2 respectively. This order of magnitude difference in the period of loading did not have any measurable effect on the intrusion into the stone layer.

It is concluded that the minor differences in the results from these tests is most likely related to minor difference in the number of defects in the geotextile considering that the compactive effort was similar for these tests. The small movement of soil through the geotextile ($\simeq 0.3$ kg/m^2) is considered to have occurred primarily due to compaction of the soil and not due to the applied pressure. The geotextile (TS650) appears to have performed its separation function well and physical movement of geotextile and soil into the voids at the top of the stone was limited to about 2 cm.

Test # 3 was conducted using only one 6 cm lift of compacted clayey till above the geotextile. In this test the applied pressure was maintained for 336 hours. The mass of soil intruded through the geotextile and into the stone in this case (1 g) was considerably smaller than in Tests # 1 and 2 (8.7-9.2 g) despite the fact that the 600 kPa pressure was sustained for a substantially longer period of time. The physical intrusion of the geotextile and soil into the void space at the top of the stone (2 cm) was essentially the same as in Tests # 1 and 2.

The geotextile used in Test # 3 had no defects and one might hypothesize that the reduced intrusion through the geotextile is due to the absence of defects. However this is considered unlikely in light of results from the Halton study where a test conducted using a geotextile with no holes gave 8 g of soil intruded through the geotextile under less severe loading conditions.

The most likely explanation for the smaller mass of soil intruded through the geotextile in Test # 3 (1 g) is that there was less compaction induced movement of fines through the geotextile due to the fact that only one 6 cm layer was compacted in this test. In contrast, tests conducted with two compacted 6 cm layer in the Halton study gave

intruded mass of 8-9.6 g while Tests # 1 and 2 conducted with three compacted 6 cm layers in the present study, gave intruded mass of 8.7-9.2 g. Thus it would appear that compaction of the second 6 cm layers does result in additional intrusion of mass through the geotextile but that compaction of the third 6 cm layer did not have any significant effect. Consistent with this, the number of compacted layers also influenced the mass of soil in the geotextile, with a mass of 8.3 g being observed for Test # 3 with one 6 cm lift and 20.5-22.7 g being observed for Tests # 1 and 2 with three 6 cm lifts (the amount of soil in the geotextile was not measured in the Halton study).

11.3 INTRUSION THROUGH THE GRANULAR FILTER

11.3.1 FILTER DESIGN

The commonly used granular filter criteria of :

$$D_{15(filter)}/d_{85(soil)} \leq 5 \qquad (11.1)$$

was used in filter design (U.S.B.R., 1974 and J.L. Sherard et al., 1984). Knowing the d_{85} of clayey soil used (about 0.16 mm) and using the above criterion, a filter layer consisting of two sub-layers was designed to act as an interface between clayey soil and 50 mm clear stone. Concrete sand and pea gravel were used to form the first and second sub-layers respectively. Each sub-layer was about 4 cm thick. The grain size distributions of filter material are shown in Fig. 11.3.

11.3.2 METHOD

A total of 2 tests were conducted using the granular filter (Tests # 4 and 5). The test set up, soil and filter materials, and pressures applied were the same for both tests except that the duration of the test for Test # 4 was almost 1 week while for Test # 5 the duration was almost 2 weeks. The clayey soil was from the same source as that used in Tests # 1, 2, and 3.

Concrete sand was washed over sieve # 200 to remove any clay size material. The original pea gravel grains had some fine cohesive material attached on the surface of the grains. To remove this material, the pea gravel was placed in plastic containers, water was added, the containers were shaken using a shaker, and then the material was washed over a # 20 sieve several times to ensure that any remaining fines were removed.

The cell was inverted and the load plate was brought to the level of flange using spacers (Photo 11.1). The first layer of washed dry 50 mm stone was randomly placed (Photo 11.30) and further stone then placed to fill the cylinder (Photo 11.31). Smaller 20 mm river gravel was used to fill the voids and provide a smoother surface at the top of the cylinder (Photo 11.32). The base plate was bolted to the larger cylinder (as in Photo 11.6). The test cell was inverted and the spacers and load plate was removed to reveal the top stone layer which would be in contact with the second filter layer of pea gravel (Photo 11.33). Pea gravel was placed on top of the stone and compacted by vibrating the cell and also tamping the surface of the material. Material was added until the desired thickness of about 4 cm was achieved. The surface of the pea gravel layer was levelled (Photo 11.34).

The washed, wet concrete sand was placed on top of the pea gravel and compacted. During compaction, water was sprayed on the surface of the sand to aid compaction. Sand was added until the desired thickness of about 4 cm was achieved. The final surface of the sand was then levelled (Photo 11.35).

Clayey soil at a moisture content of 14.1-14.4 % (i.e. 3.2-3.5 % wet of optimum moisture content, w_{opt}=10.9 %) was placed on the wet sand filter layer and compacted in two lifts of about 6.5 cm per lift using 100 blows from a 24.5 kN hammer falling 0.3 m. The actual soil thickness was about 12.9 cm. The soil surface was then smoothened by tamping (Photo 11.36) and load plate placed on to the soil surface (as in Photo 11.10). Representative samples of the soil were taken for water content determination.

The test cell was filled with water to saturate the stone and filter layers (as described for Tests # 1, 2, and 3). The vertical pressures were applied using the MTS load/displacement mechanism. The method of application of the vertical loads and cell pressure and their magnitude were the same as previously described for Test # 2. A schematic of the test set up is shown in Fig. 11.4.

After application of the 600 kPa vertical pressure and 100 kPa cell pressure for about one week in Test # 4 and about 2 weeks in Test # 5, the vertical load was slowly decreased to 200 kPa, and the 100 kPa cell pressure released. The cell outlet valve was opened to release any remaining pressure inside the cell and the water was drained into a container. The remaining 200 kPa vertical pressure was released and the 4 air outlet holes on the flange were opened. The cell was drained as already described for Test #1.

The load plate was removed and the surface of the clayey soil was covered with plastic. The base plate was loosened to drain any water remaining in the cell (Photo

11.37). The drained water was collected. The cell was inverted and the base plate opened and removed. The stones were hand excavated and transferred into a tray (as in Photo 11.19). After removal of all stones, the bottom of second filter layer (pea gravel) was exposed and photographed (Photo 11.38). The pea gravel layer was hand excavated and placed into a separate tray. The surface of the first filter layer (concrete sand) was exposed and photographed (Photo 11.39). The sand layer was hand excavated and placed into a tray. The surface of the clayey soil was exposed, photographed (Photo 11.40) and covered with plastic.

The stones were washed over sieve # 200 (Photo 11.41). The wash water was collected in a container and then transferred into trays and placed in an oven to evaporate the water. Subsequently, the weight of remaining fines was measured and recorded. The collected filter material (pea gravel and concrete sand) was washed over sieve # 200 into a separate container and the weight of fines intruded into the filter layer was measured and recorded.

11.3.3 RESULTS

The results obtained for each test are summarized in Table 11.2 and are discussed in the following paragraphs.

11.3.3.1 TEST NUMBER 4

The upper surface of most of the 50 mm stones had a brown colour as a result

of fines adhering to the surface of the stones during the test. The bottom surface of the pea gravel layer was bumpy and the gravel had penetrated into the voids of the 50 mm stones to a maximum depth of 3 cm (Photo 11.38). There were no concrete sand grains visible in the lower portion of the pea gravel layer. During removal of the pea gravel, some concrete sand grains were observed at approximately 2.5 cm distance from the level of flange (level A in Fig. 11.4) which had been penetrated into the pea gravel layer. There was more penetration of concrete sand into the top 1 cm of the pea gravel layer and the interface of the two filter layers consisted of a mix of pea gravel and concrete sand (Photo 11.39). The distance from the exposed surface of the concrete sand to the level of flange (level A in Fig. 11.4) was about 3.8 cm. The typical thickness of the non-mixed pea gravel and sand layers was about 3.8 cm.

The clayey soil surface was not visible due to penetration of the clayey soil into the sand (and vice versa) forming a thin (about 2 mm) layer consisting of a mix of concrete sand and clay. The distance from this surface to the level of flange was about 7.6 cm. The bottom of the clayey soil layer had been pushed down about 0.4 cm due to the applied load. The bottom surface of the clayey soil was almost flat without any bumps.

The total mass of fines measured in the stone layer was 5.5 g. Thus the total mass of soil that had passed through the filter layers and intruded into the stones was 0.17 kg/m^2. The total mass of soil that had intruded into and remained within the filter layers was 8.8 g (i.e. 0.275 kg/m^2).

11.3.3.2 TEST NUMBER 5

As was the case with Test # 4, during hand excavation of stones it was noticed that the upper surface of most of the stones had a brown colour. The bottom surface of the pea gravel layer was bumpy and had intruded into the voids of the top stone layer to a maximum of 2.6 cm. There were no concrete sand grains visible in the lower portion of the pea gravel layer. There was some penetration of concrete sand into the top 1.1 cm of the pea gravel layer and the interface of the two filter layers consisted of a mix of pea gravel and concrete sand as discussed for Test # 4. The distance from the exposed surface of the concrete sand to the level of flange (level A in Fig. 11.4) was about 3.7 cm. The thickness of the non-mixed pea gravel and sand layers was about 3.8 cm and 3.7 cm respectively. The distance from the exposed surface of the clayey soil to the level of flange was about 7.6 cm. This surface was almost flat without any significant indentation. The bottom of clayey soil layer had been pushed down about 0.4 cm due to the applied load.

The total mass of fines measured in the stone was 4.8 g. Thus the total mass of soil that had passed through the filter layers and intruded into the stones was 0.15 kg/m^2. The total mass of soil intruded into and remaining in filter layer was 8.6 g or 0.268 kg/m^2.

11.3.3.3 DISCUSSION

These two tests were essentially duplicates. The total soil mass passing through

the filters and into the stone layer ranged from 4.8 to 5.5 g (0.15-0.17 kg/m^2). This is slightly smaller than that obtained using the geotextile filter (8.7-9.2 g or 0.27-0.29 kg/m^2) in Tests # 1 and 2. However the granular filter intruded 2.6-3.0 cm into the void space of the upper stone compared to about 2 cm for the geotextile filters. Thus in terms of the total loss of void space under an applied pressure of 600 kPa, the two types of filter/separator (i.e. geotextile and granular) appeared to be very similar.

11.4 INTRUSION OF THE COMPACTED CLAYEY SOIL INTO THE 50 mm COARSE STONE WHEN THERE WAS NO FILTER/SEPARATOR

This section describes the intrusion tests conducted to examine potential intrusion of the compacted clayey till into the 50 mm coarse stone layer for the situation where the clayey layer is separated from the stone layer by a geotextile during compaction and consolidation of the clayey layer but where the geotextile is then removed. Thus the movement of the compacted and consolidated clayey till into the stone layer due to applied vertical load and water pressure is studied when there is no filter/separator between the two materials at this stage of the loading process. Fig. 11.5 shows a schematic of the test set up. The clayey till and stone materials were from the same source as previous tests.

11.4.1 METHOD

A total of 2 tests were conducted (Tests # 6 and 7). The materials used and test set up were identical for both tests except for a differences in the sequence of applying

the vertical load and cell pressure as will be discussed below.

The clayey soil with the water content of 14.5 % (i.e. 3.6 % wet of optimum, w_{opt}=10.9 %) was prepared as described for previous tests.

The test cell was inverted and the load plate was brought to the level of flange using spacers (as in Photo 11.1). The geotextile sample was cut, washed of fines, and placed on the load plate (as in Photo 11.2). The stone was installed in the test cell, base plate placed and bolted to the larger cylinder (as in Photos 11.3, 11.4, 11.5, 11.6, and 11.7). The test cell was inverted and clayey soil was placed on a geotextile separator layer that was used to minimize intrusion of the clayey layer into the stone layer during compaction and initial consolidation. The clayey soil was compacted in 1 lift of about 6 cm thickness. Representative samples of the soil were taken for water content determination.

The test cell was placed below the MTS load/displacement mechanism (as in Photo 11.15). In Test # 6, 100 kPa vertical pressure was applied initially for 1.5 hours to allow consolidation of the clayey soil and then released. The reported average value of the coefficient of consolidation for the clayey till used in this study is 7.88 m^2/a (Rowe, 1992). Using this value, the time required for 90% consolidation of the 6 cm thick clayey sample under 100 kPa vertical pressure is about 1 hour. In Test # 7, after application of 100 kPa pressure for 2.5 hours, the load was increased to 200 kPa and then 300 kPa in 2 hourly intervals. After 65 hours at 300 kPa, the load was released. After consolidation of the clayey till and subsequent pressure release, the test cell was removed from the MTS mechanism. The spacers were placed on top of the load plate (on top of the clayey soil) so that the surface of the top spacer became level with the top

of the smaller cylinder and were fixed to the smaller cylinder using tapes (Photo 11.42). This was done to prevent the compacted clayey soil and load plate from moving when the test cell was inverted. After inversion, the base plate was opened, the stones were removed and the geotextile was exposed (Photo 11.43) and removed (Photo 11.44). The distance from the highest point on the clayey soil bumpy surface to the flange was measured and recorded. In both tests this distance was about 1.7 cm. A layer of stones was then placed on the clayey soil surface (Photo 11.45). An attempt was made to use almost the same size stones on the bumpy surface of the clayey soil as there were present prior to excavation of the stones and removal of the geotextile. Additional stones were placed to fill the cylinder (as in Photo 11.4). Smaller 20 mm river gravel was used to provide a smoother surface in contact with the base plate (as shown in Fig. 11.1 and Photo 11.5). The base plate was attached and bolted to the larger cylinder (as in Photo 11.6) and test cell was placed below the MTS load/displacement mechanism.

The following paragraphs describe the test procedure following the removal of the geotextile separator/filter layer and re-assembly of the apparatus as described above.

In Test # 6, the vertical pressure was applied again and gradually increased to 200 kPa in a few minutes. Tubing from a water reservoir was attached to the inlet valve at the bigger cylinder and the lower cylinder (containing the stone), was saturated with water. The 100 kPa pressure was applied to the fluid in the stone and regulated using a pressure regulator (as in Photo 11.16). This pressure was applied to simulate approximately 10 m of pressure head in the stone layer. The vertical pressure was increased to 500 kPa in 100 kPa increments at 2 hourly intervals and then held constant overnight. The following day, the vertical pressure was increased to 600 kPa and held

constant for about 13 days after which test was terminated. During the test, pressure and displacement readings were taken using digital readout equipment connected to the MTS load/displacement mechanism.

In Test # 7, 100 kPa vertical pressure was re-applied for about 22 hours before being increased to 500 kPa in 100 kPa increments at approximately 24 hourly intervals. The following day, the lower cylinder (containing the stone), was saturated with water and a 100 kPa pressure was applied to the fluid in the stone and regulated using a pressure regulator (Photo 11.16). After application of the 100 kPa cell pressure, the vertical pressure was increased to 600 kPa. Both cell and vertical pressures were held constant for almost 13 days after which test was terminated. During the test, pressure and displacement reading were taken using digital readout equipment connected to the MTS lead/displacement mechanism.

The vertical and cell pressure application scheme adopted in Test # 7 was different from that in Test # 6 both before and after removal of the geotextile, although the final pressures were the same. This difference was introduced to identify whether there was any significant effect of the loading sequence on the amount of intruded soil. As will become apparent later, there was no significant effect.

After the period of about 13 days at 600 kPa vertical load and 100 kPa cell pressure both Tests #6 and #7 were terminated by first reducing the vertical pressure to 200 kPa, then reducing the 100 kPa cell pressure to zero and then reducing the applied vertical stress to zero. The spacers were placed on top of the load plate (on top of the clayey soil) so that the surface of the top spacer became level with top of the smaller cylinder (Photo 11.46). The test cell was lifted by means of a crane and the cell water

was drained into a container (Photo 11.47).

The base plate was partially opened and remaining water in the cell was drained into a tray (as in Photo 11.37). The test cell was inverted, the base plate was opened, and the stones hand excavated and transferred into a tray (Photo 11.48). The surface of the clayey soil was exposed (Photo 11.49) and the distance from the highest point of the bumpy clayey soil surface to the surface of the flange was measured and compared with the value measured after removal of the geotextile (Photo 11.44). To estimate the total intrusion of the soil into the stone due to the applied vertical pressure, the loose clayey soil attached to the stone surfaces was removed and placed in a tray (Photo 11.50). The weight of the tray including wet soil was measured, the soil was then oven dried and the weight of the dry soil was measured and recorded. The water content of the soil intruded into the stone pore spaces was determined. The stones were washed of fines (as in Photo 11.41). The wash water was collected, transferred into trays, oven dried to evaporate the water and the weight of the dry fines was measured and recorded. The same process was repeated for drained cell water and the weight of dry fines was measured and recorded. The empty test cell was also washed into a container (Photo 11.51), the wash water was oven dried and amount of dry fines was weighed and recorded. The water content samples from the stiff clayey soil (not intruded) were taken.

11.4.2 RESULTS

The results obtained for Tests # 6 and 7 are summarized in Table 11.3 and are discussed in the following sub-sections.

11.4.2.1 TEST NUMBER 6

When the base plate was opened, the surface of the plate was observed to be covered by loose, very soft soil (Photo 11.52). This indicates that the soil has been intruded into the stone void spaces and had moved a distance of about 20 cm to reach the base plate. This had **not** been observed for the tests with a geotextile or granular filter. On the surface of the exposed bottom layer of the stone, loose soil material was visibly occupying some of the void space (Photo 11.53). When the stones were hand excavated, it was observed that some voids have been partially or completely filled by the intruded loose soil material (Photos 11.54 and 11.55). When stones were further hand excavated, it was observed that almost all the void space of the first layer of stones (i.e., those in initial contact with the clayey layer) was occupied by the intruded soil material (Photo 11.56). This material was very soft. In comparison, the adjacent soil which had not intruded into the stone was stiff.

After removal of all stones the exposed soil surface was bumpy with a distance from the highest point of the exposed clayey soil surface to the surface of the flange of about 4.0 cm compared with the distance of 1.7 cm measured at the exposed clayey soil surface after removal of the geotextile (Photo 11.44). This very soft soil was considered to be part of the intruded soil so it was removed and its dry weight was measured.

Total dry weight of the intruded soil was calculated by adding (1) the dry weight of the fines recovered from the drainage cell water, (2) the dry weight of the fines recovered from the water used to wash the stones, (3) the dry weight of the soil detached from the stone surfaces during excavation of the stones, and (4) the dry weight of the

very soft soil which was intruded into the void spaces in the first stone layer in contact with the soil. Resulting value was 1600 g. Thus the total mass of the soil intruded into the stone void space was 50 kg/m^2.

To observe the load/displacement behaviour of the compacted clayey soil during the tests, readings of the load and displacement were taken using digital readout equipment connected to the MTS load/displacement mechanism. These readings are plotted for Tests # 6 and 7 on Fig. 11.6 and 11.7. Fig. 11.6 shows the load/displacement/time plots of the tests for the period of time during which soil was consolidated and the geotextile was in the cell. Due to the short period of consolidation (1.5 hours) in Test # 6, the corresponding curves which are shown as solid lines in Fig. 11.6, are hardly visible. Fig. 11.7 shows the load/displacement/time plots of the tests after removal of the geotextile and re-application of the loads until the end of the tests.

11.4.2.2 TEST NUMBER 7

After opening the base plate, the surface of the plate was observed to be partially covered by loose, very soft soil as observed in Test # 6 (as in Photo 11.52). On the surface of the exposed bottom layer of the stone, clayey soil was visible (Photo 11.57). When the stones were hand excavated, it was observed that some of the void space in the stone layer had been filled with the intruded soil (Photo 11.58). Most of the void space inside the first layer of stones (i.e. those that were in initial contact with the clayey layer), was occupied by the intruded soil material (Photo 11.59). The condition of the exposed soil surface after removal of all stones was almost the same as was observed in

Test # 6 (Photo 11.60). The distance of the highest point in clayey soil surface from the flange was about 3.5 cm compared with about 1.7 cm observed after removal of the geotextile (as in Photo 11.44).

Total dry weight of the intruded soil was measured as already described for Test # 6 and was found to be 1630 g. Thus the total mass of the soil intruded into the stone void space was 50.9 kg/m^2.

11.4.2.3 ESTIMATION OF THE THICKNESS OF THE STONE WITH VOID SPACE EQUIVALENT TO THE VOLUME OF THE INTRUDED SOIL

The porosity of the stone mass was measured using a cubic container having the dimensions of 30.55 cm. The dry stones were randomly placed in the container until it was completely filled with the stones. The smaller 20 mm river gravel was used to provide a smoother surface at the top of the container (Photo 11.61). The weight of the container, including dry stones, was measured. The container was completely filled with de-aired water until all stones and gravel at the top of the container were immersed in water (Photo 11.62). The weight of the container including saturated stones was measured and the weight of the water used to completely fill the container was determined and from this, the volume of void space in the stone was determined and hence the porosity of the stone was calculated to be 0.449.

In each test, knowing (1) the water content, (2) the dry weight and (3) the specific gravity of the intruded mass and (4) the porosity of the crushed stone, the void space occupied by the intruded soil mass was calculated. These calculations, given in Appendix G, indicate that if one was to adopt the worst case assumption that the clayey

soil was only occupying the void space directly beneath the small cylinder that contained the clayey soil, then the equivalent thickness of the stone whose void space was occupied by the clayey soil was 6.6 cm and 6.9 cm for Tests # 6 and 7 respectively.

11.4.3 DISCUSSION

Tests # 6 and 7 were duplicates except for the sequence of load application. As can be seen from Table 11.3 and Figure 11.7, the final soil displacement and mass of soil intruded was essentially independent of the load sequence and only depended on the final vertical load and water pressure in the stone. However, the change in sequence between Tests # 6 and 7 did reveal the very important role played by water pressure in these tests. From the displacement/time plot for Test # 7 (Fig. 11.7) it can be seen that the majority of the displacement occurred after the cell was saturated and the 100 kPa cell pressure was applied. Thus it would appear that the movement was in large part related to softening of the clayey soil in direct contact with the stone when the pore water in stone was pressurized to 100 kPa. However, after the initial movement occurred, the system quickly stabilized (see Fig. 11.7) and there was no significant additional movement after this.

An equivalent stone thickness of about 7 cm had been filled by intruded clayey soil in these tests.

11.5 SUMMARY AND CONCLUSIONS

A total of 7 intrusion tests were performed in this study. Potential intrusion of compacted clayey till through the Polyfelt TS650 geotextile and into the coarse stone was examined in Tests # 1, 2, and 3. In these tests, the geotextile efficiently minimized the intrusion of the soil mass into the stone void space and the actual quantity of fines which passed through the geotextile was insignificant with respect to the occupancy of void space in the stone. It is considered that most of the fines passed through the geotextile due to compaction during installation of the clayey soil in the test cell and not due to the applied vertical pressure and water pressure. The movement of fines through the geotextile and into the stones in Tests # 1 and 2 was visually similar to that observed due to compaction at the Halton test pad. The movement of fines through the geotextile in Test #3 was much smaller than in Tests #1 and #2 and this is attributed to the lower amount of compactive effort used in Test #3 relative to Tests #1 and #2. Intrusion of clayey soil into the stone was limited to the upper 2 cm of the stone layer and was effectively controlled by the geotextile. The length of time the test was conducted did not appear to influence the results.

In Tests # 4 and 5, the granular filter/separator between the clayey soil and stone worked well and amount of intruded fines was also insignificant with respect to occupancy of void space in the stone. The intrusion of the granular filter into the stone was limited to the upper 2.6-3 cm of the stone.

In Tests # 6 and 7, a geotextile was used as a separator between the clayey layer and stone layer during compaction and consolidation. However the geotextile was then

removed and the compacted clayey till layer was brought into direct contact with the stone layer (no filter/separator was used in the final loading phase of the test), and essentially the same load and water pressure was applied as in previous tests. At the end of these tests, a significant amount of soil was observed to be intruded into the void spaces in the stone layer. The voids in the upper 3.5-4.0 cm of the stone were almost completely filled with clayey soil. Conservatively considering the total intruded mass to be localized directly below the clayey plug, the void space occupied by the clayey soil was equivalent to that of a thickness of about 7 cm of stone. Although there was significant intrusion of clayey soil into the stone when there was no filter/separator between clayey soil and stone at the time the vertical load and pore pressure were applied, even with the worst case interpretation of the data, most of the void space in the stone remained open. Results showed that the pre-consolidation of the clayey soil sample by pressures of between 100 and 300 kPa prior to the removal of the geotextile and re-application of the loads, had negligible effect on the results. The change in the load application scheme in Test # 7 compared to Test # 6, also had negligible effect on the final test results, but did indicate that most of the intrusion occurred after pressurizing of the stone layer and hence appears to have resulted from softening of the clayey soil in direct contact with the stone. Shortly after the initial movement occurred, the system stabilized and there was no significant subsequent movement observed in these tests.

TABLE 11.1 SUMMARY OF RESULTS OF THE INTRUSION TESTING PROGRAM USING TS650 GEOTEXTILE

Test No.	No. of Defects Before Test	No. of Defects After Test	Consolidation* Pressure σ_v (kPa)	Initial Soil Water Content (%)	Final Soil Water Content (%)	Soil Mass Intruded into Stones (g)	Soil Mass Intruded into Stones (kg/m^2)
1	4	8	500	15.0	13.02	8.7	0.271
2	6	9	600	14.9	13.06	9.2	0.287
3	0	0	600	14.3	12.60	1.0	0.031

* A water pressure of 100 kPa was maintained in the stone for all tests.

TABLE 11.2 SUMMARY OF RESULTS OF THE INTRUSION TESTING PROGRAM USING GRANULAR FILTER (BOTH TESTS WERE CONDUCTED AT AN APPLIED VERTICAL PRESSURE OF 600 kPa AND WATER PRESSURE OF 100 kPa IN THE STONE LAYER)

Test No.	First Filter Layer	Second Filter Layer	Soil Initial Water Content (%)	Soil Final Water Content (%)	Soil Mass Intruded into Stones (g)	(kg/m^2)
4	concrete sand	pea gravel	14.44	13.14	5.5	0.172
5	concrete sand	pea gravel	14.07	13.68	4.8	0.150

TABLE 11.3 SUMMARY OF RESULTS OF THE INTRUSION TESTING PROGRAM WITHOUT FILTER/SEPARATOR (BOTH TESTS WERE CONDUCTED AT A FINAL APPLIED VERTICAL PRESSURE OF 600 kPa AND WATER PRESSURE OF 100 kPa IN THE STONE LAYER)

Test No.	Initial Soil Water Content (%)	Final Soil Water Content (%)	Soil Mass Intruded into Stones	
			(g)	(kg/m^2)
6	14.50	14.64	1600	50.0
7	14.50	14.56	1630	50.9

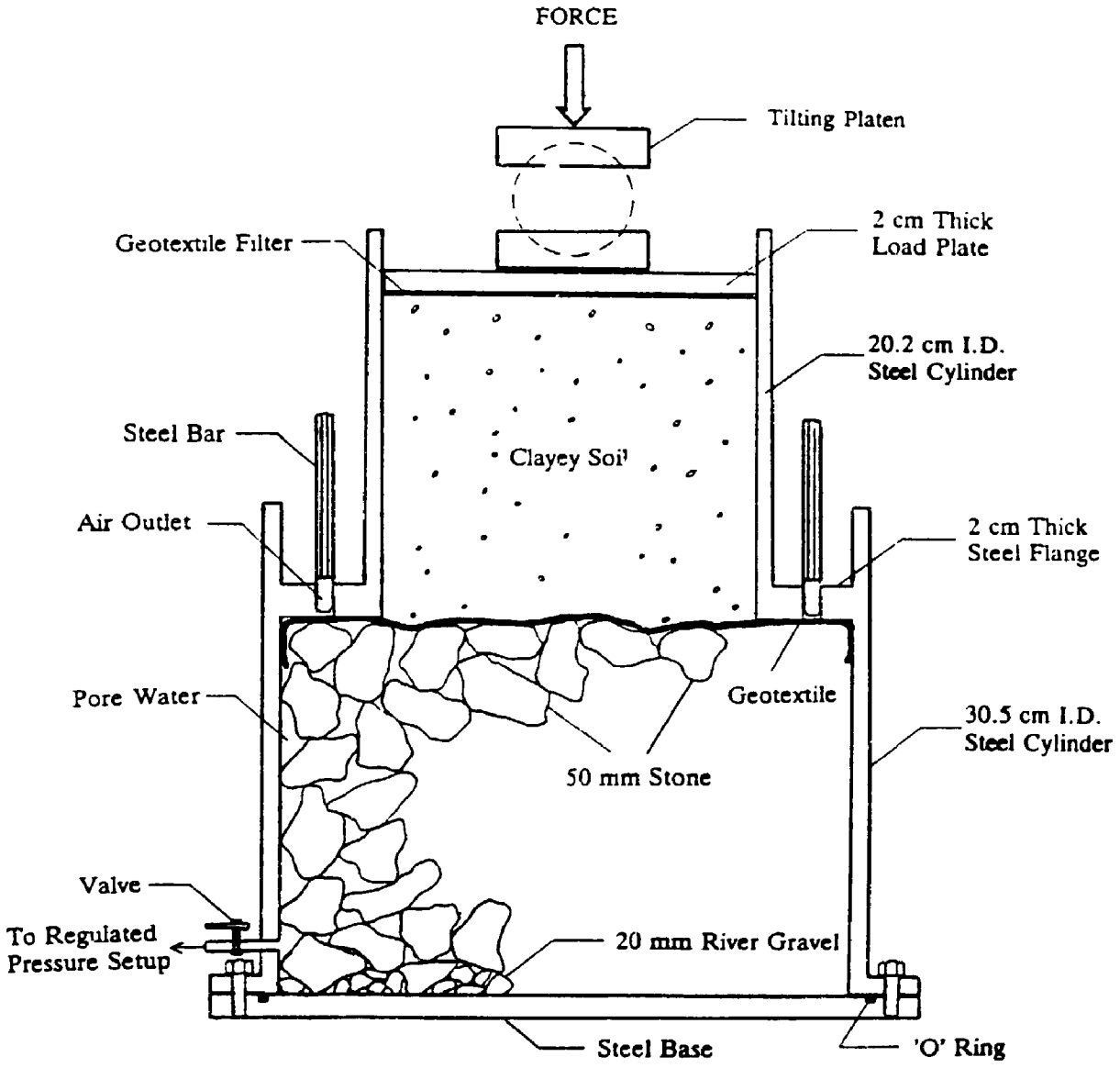

FIG. 11.1 SCHEMATIC OF THE GEOTEXTILE INTRUSION TEST CELL

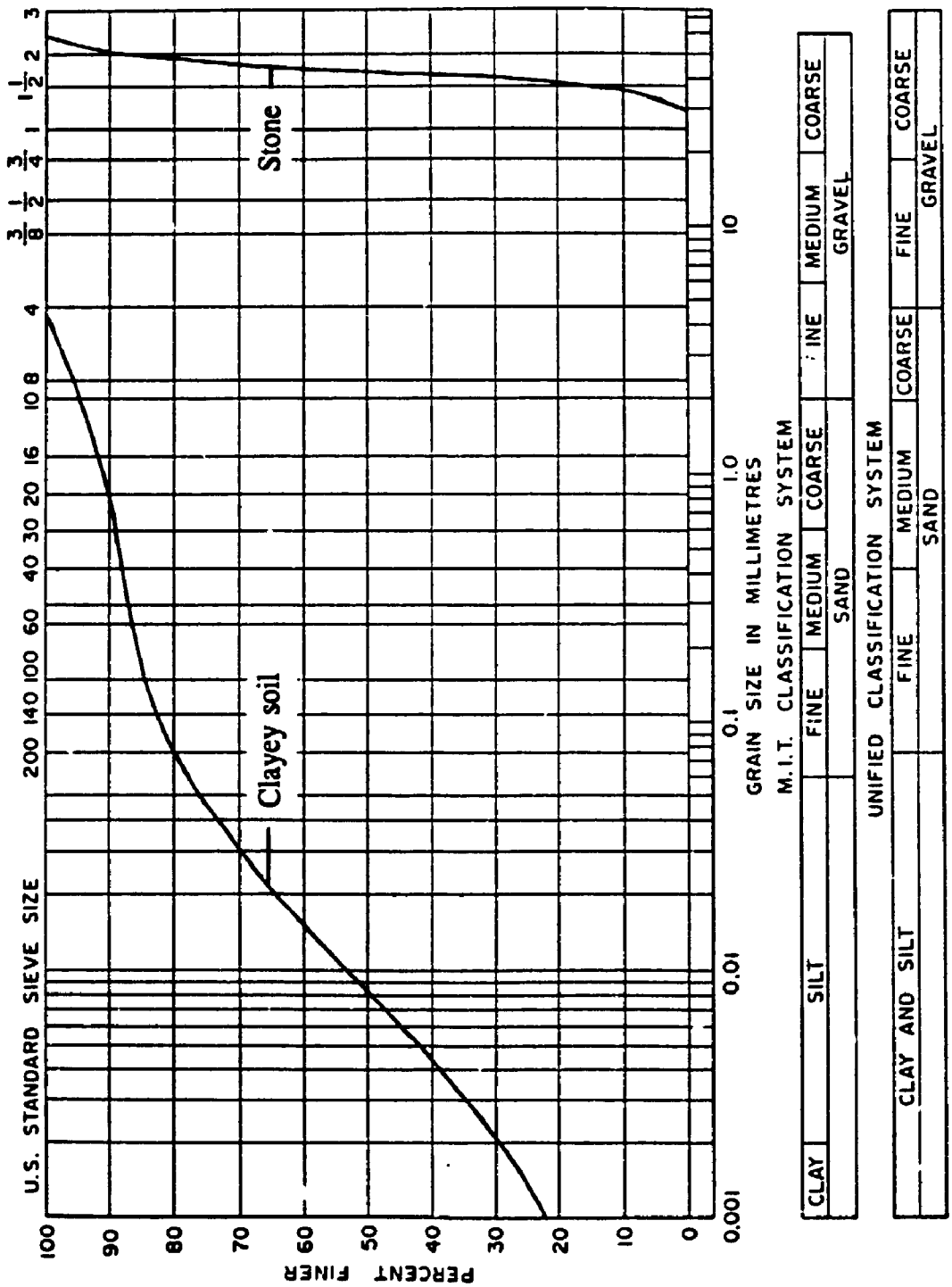

FIG. 11.2 GRAIN SIZE DISTRIBUTION OF THE CLAYEY SOIL AND COARSE STONE USED IN THE INTRUSION TESTS

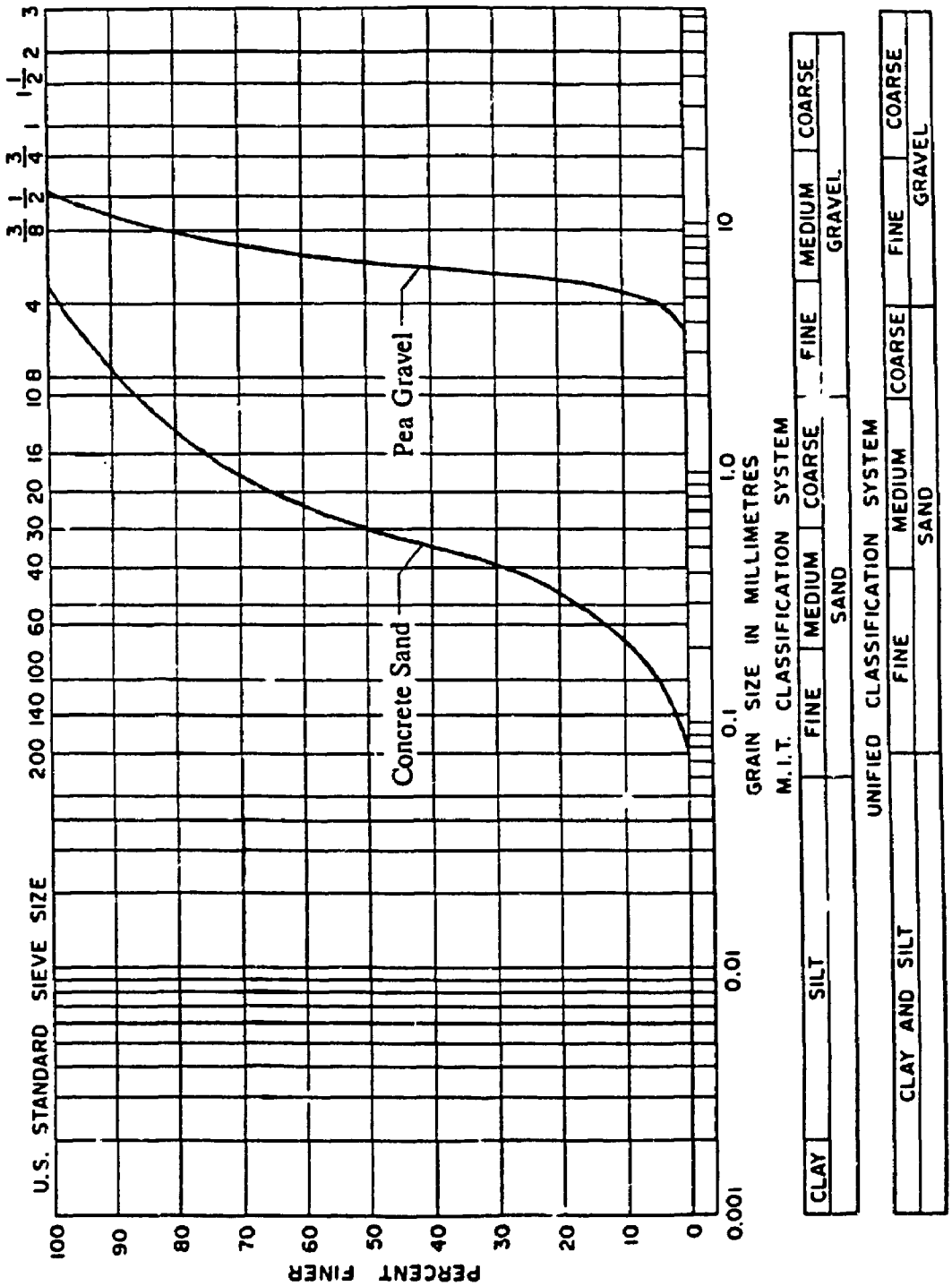

FIG. 11.3 GRAIN SIZE DISTRIBUTION OF THE CONCRETE SAND AND PEA GRAVEL USED AS FILTER MATERIAL IN THE INTRUSION TESTS #4 AND #5

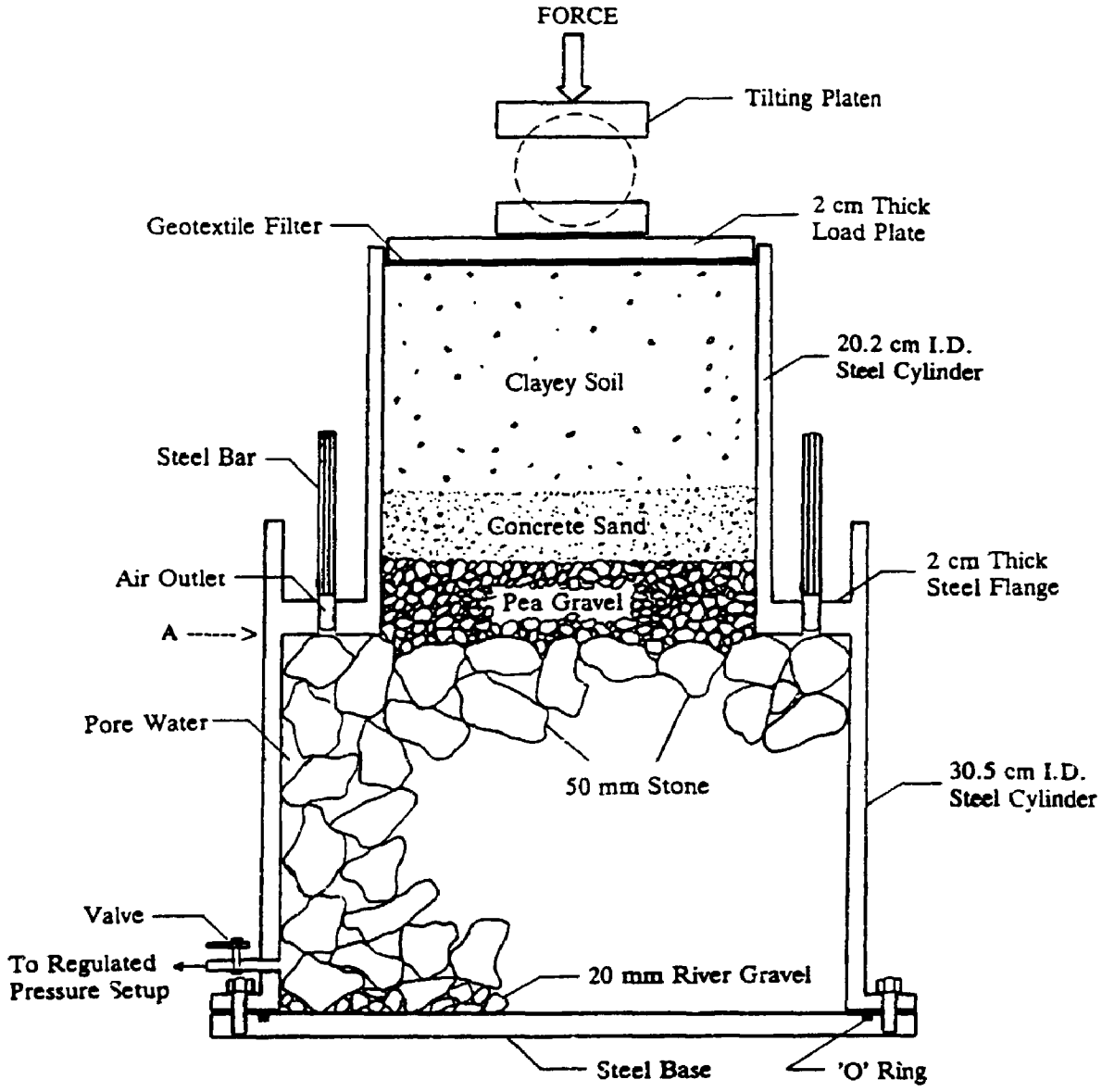

FIG. 11.4 SCHEMATIC OF THE GRANULAR FILTER INTRUSION TEST CELL

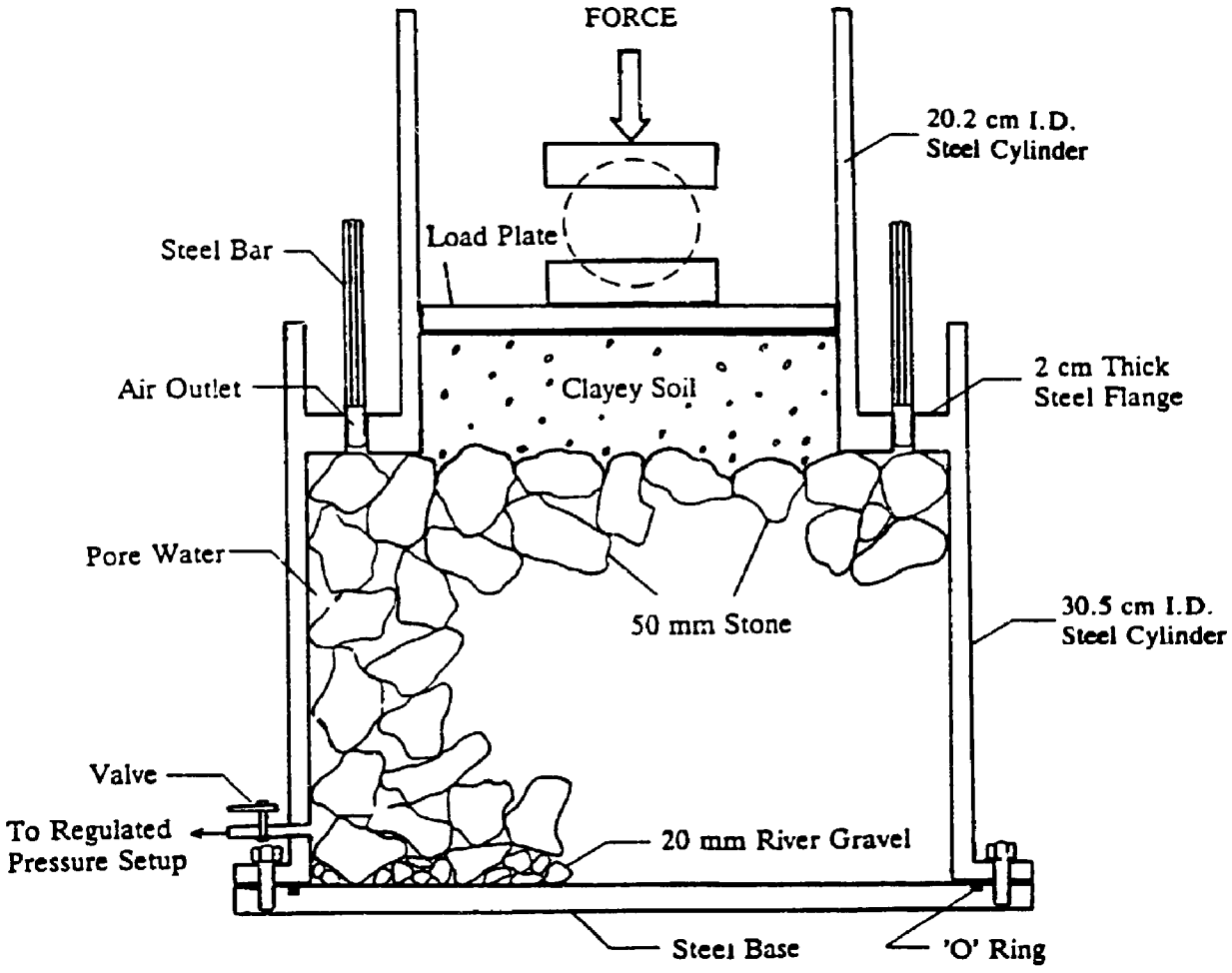

FIG. 11.5 SCHEMATIC OF THE TEST CELL IN INTRUSION TESTS #6 AND #7 WITH NO FILTER/SEPARATOR BETWEEN SOIL AND STONE

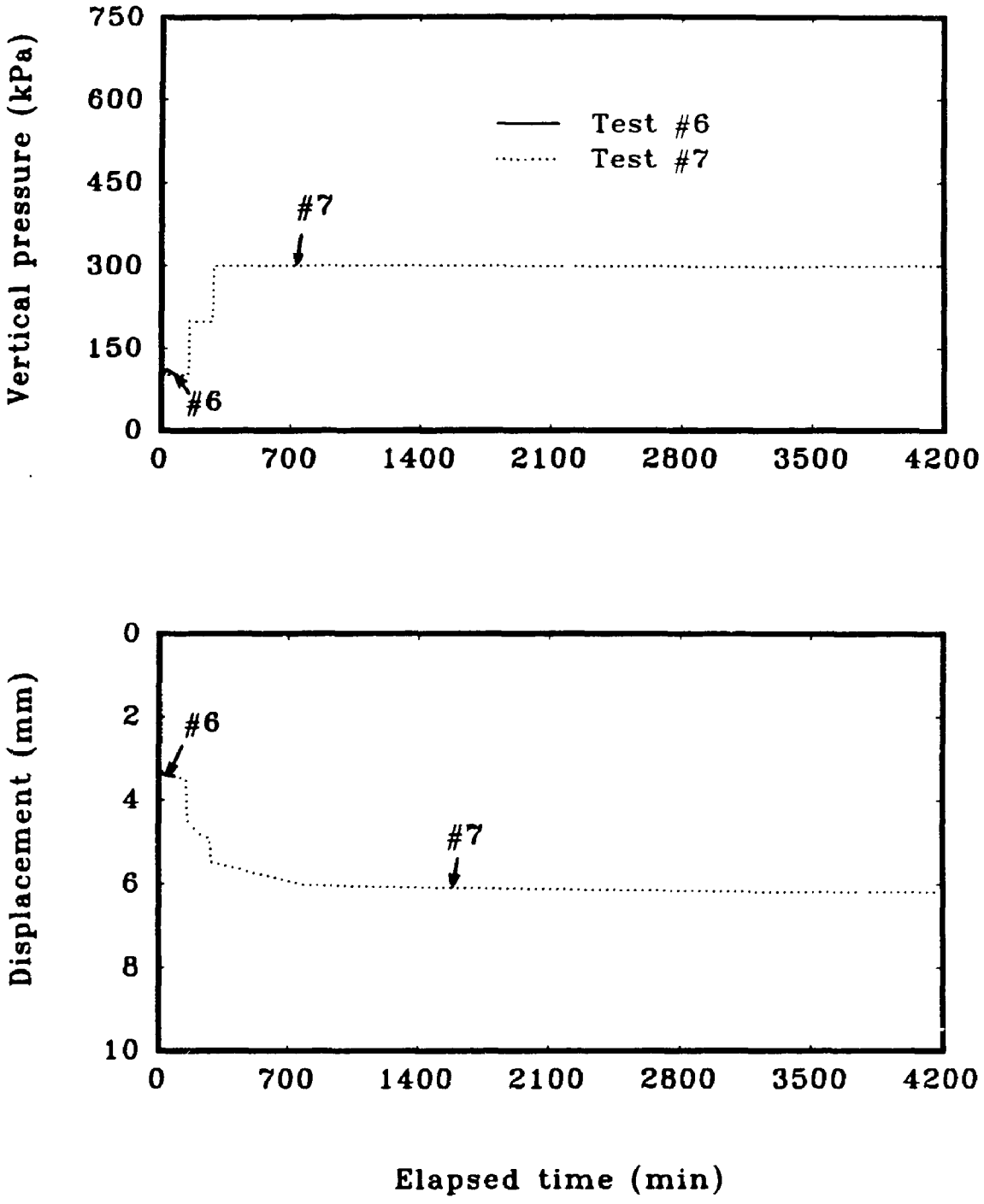

FIG. 11.6 LOAD/DISPLACEMENT/TIME BEHAVIOUR OF THE INTRUSION TESTS #6 AND #7 BEFORE REMOVAL OF THE GEOTEXTILE

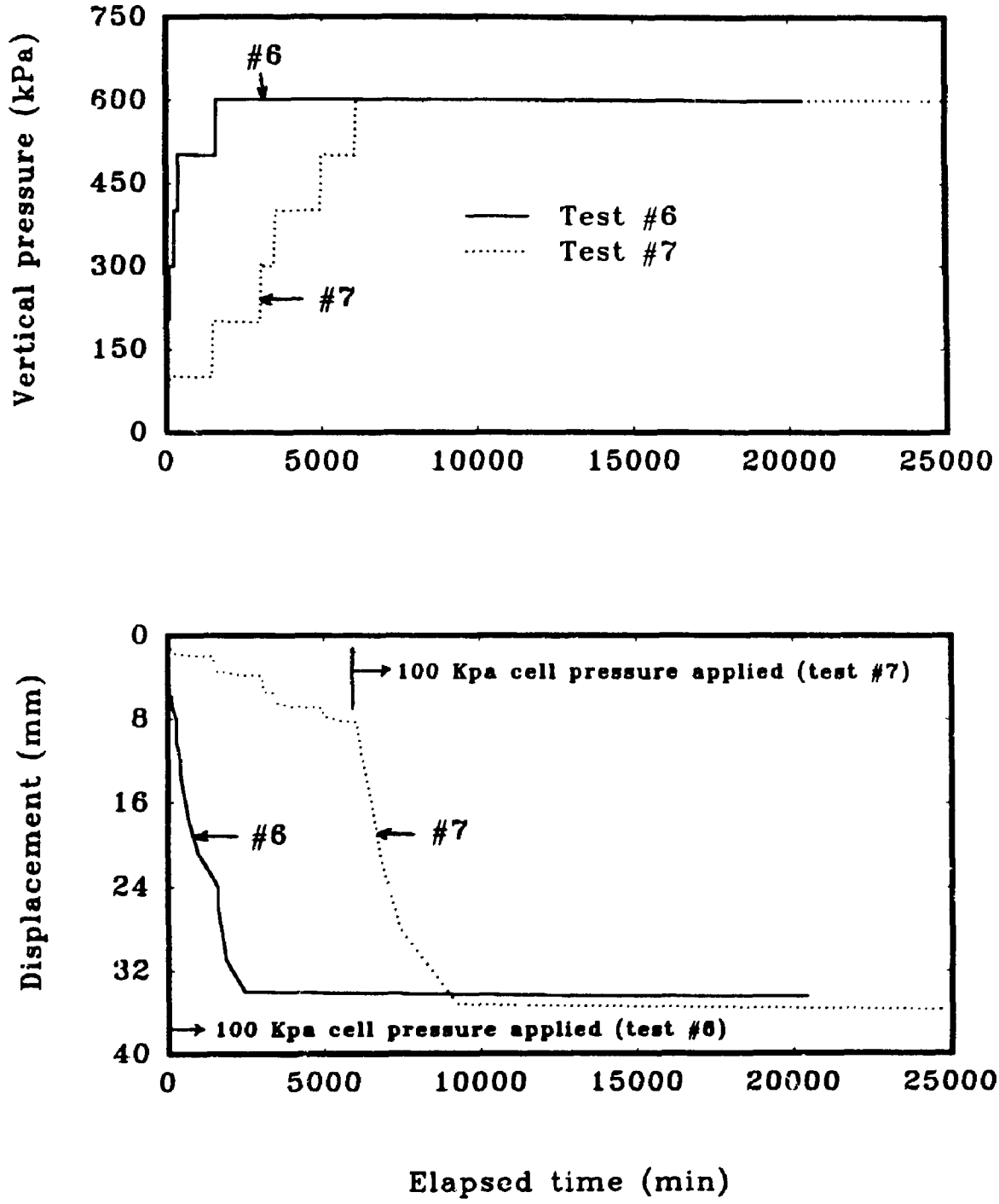

FIG. 11.7 LOAD/DISPLACEMENT/TIME BEHAVIOUR OF THE INTRUSION TESTS #6 AND #7 AFTER REMOVAL OF THE GEOTEXTILE

PHOTO 11.1 LOAD PLATE BROUGHT TO LEVEL OF FLANGE BY MEANS OF SPACERS (ALL INTRUSION TESTS)

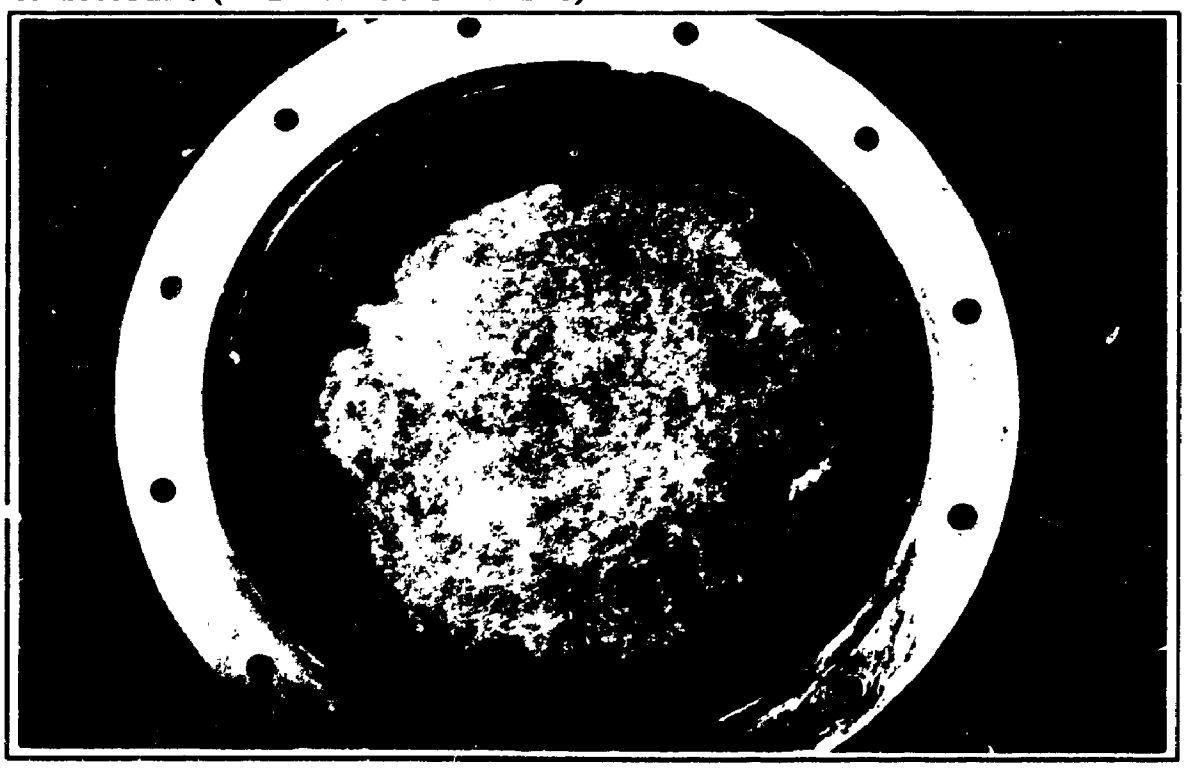

PHOTO 11.2 GEOTEXTILE SPECIMEN PLACED ON LOAD PLATE AND FLANGE WITH EDGES CURLED UP THE INSIDE OF CYLINDER (TESTS #1, #2, AND #3)

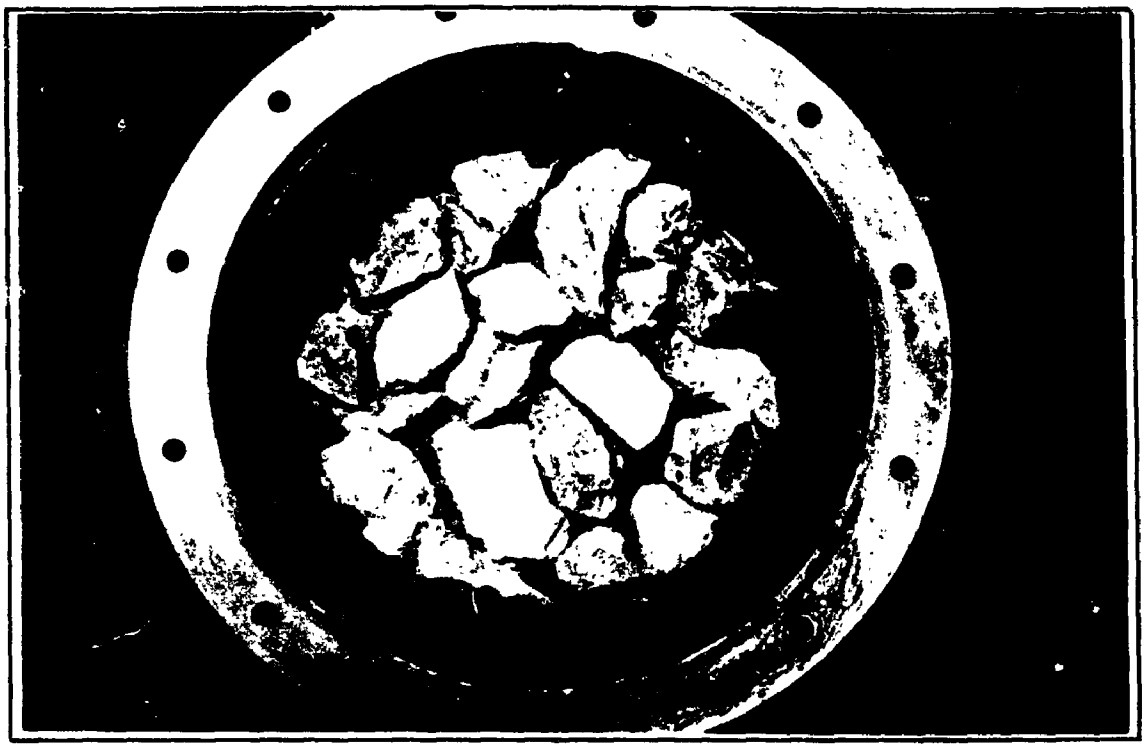

PHOTO 11.3 50 mm STONE PLACED ON GEOTEXTILE SPECIMEN (TESTS #1, #2, AND #3)

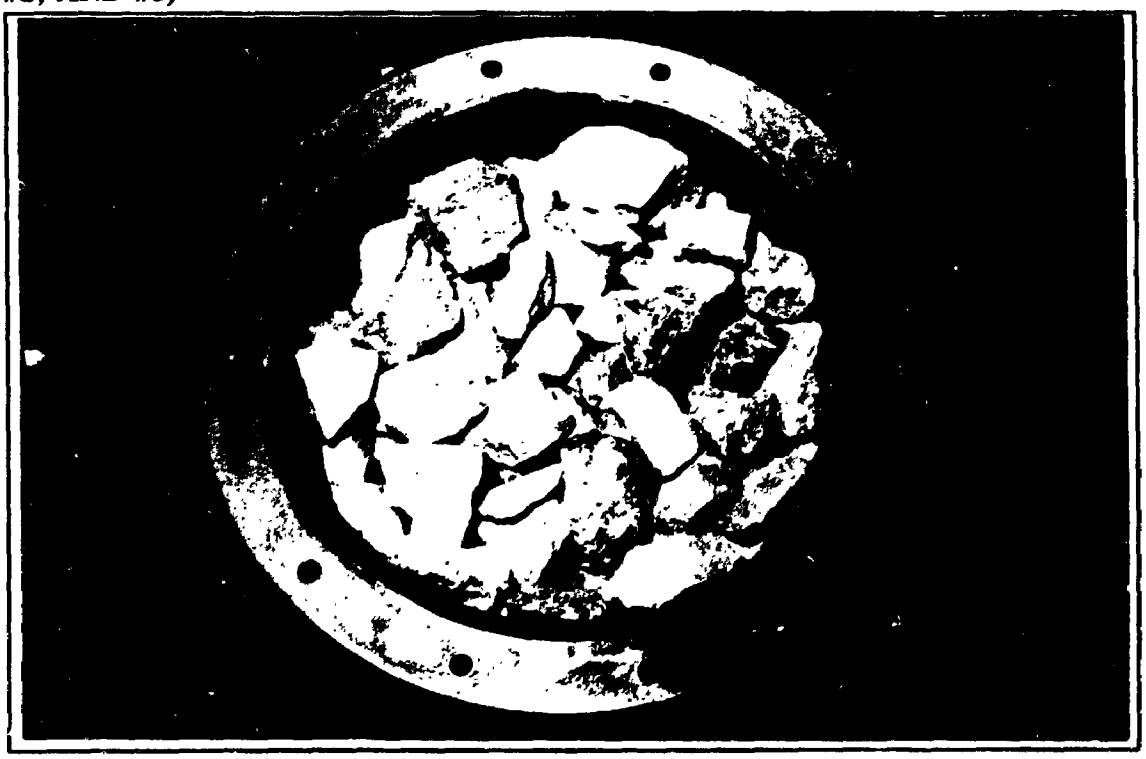

PHOTO 11.4 ADDITIONAL 50 mm STONE PLACED TO FILL CYLINDER (TESTS #1, #2, AND #3)

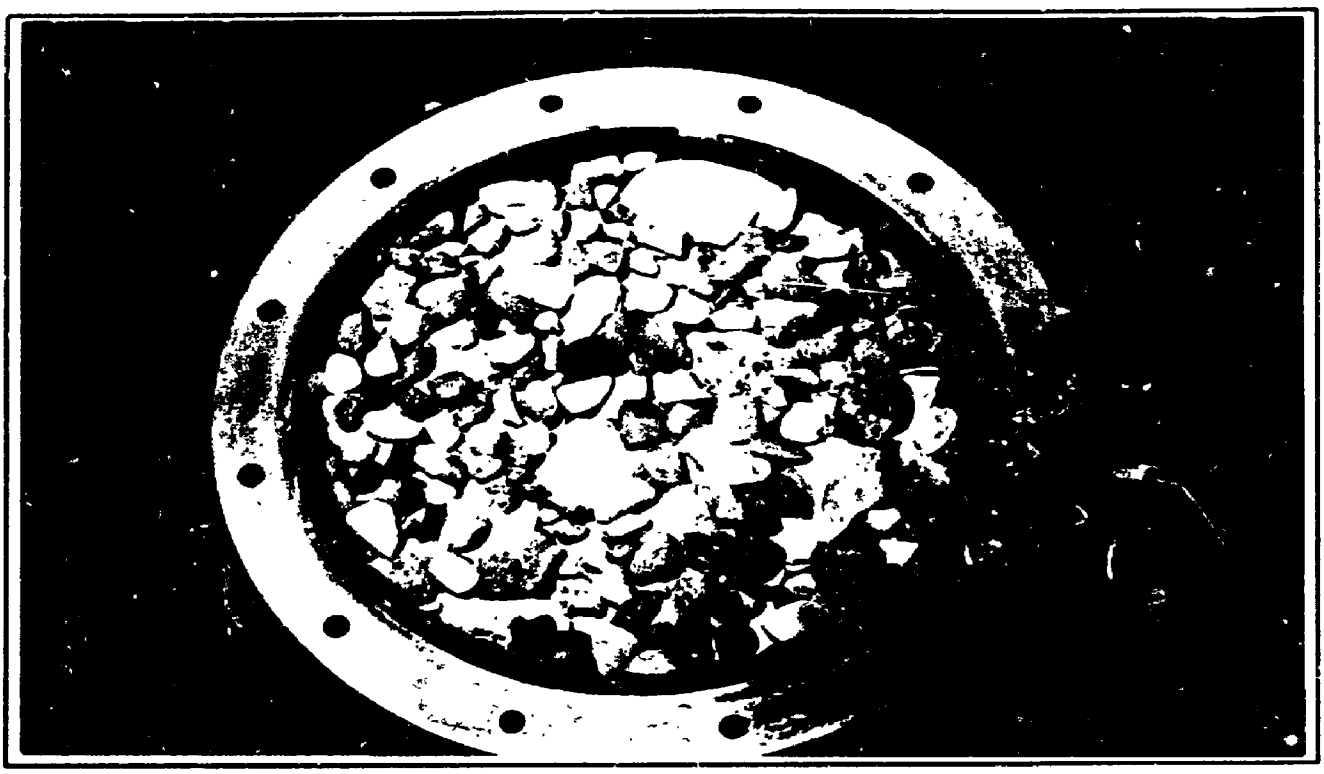

PHOTO 11.5 RIVER GRAVEL (20 mm) PLACED OVER 50 mm STONE TO PROVIDE SMOOTH SURFACE FOR BASE PLATE

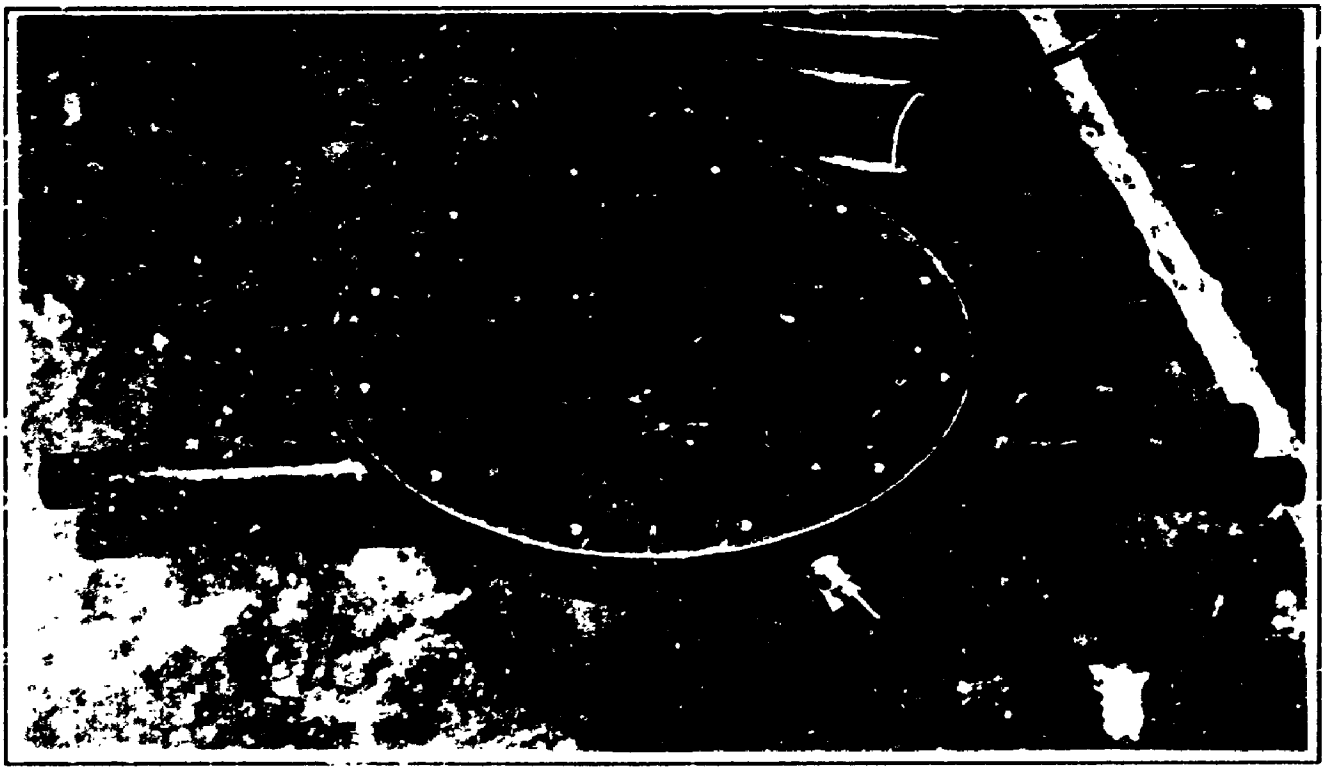

PHOTO 11.6 BASE PLATE PLACED AND BOLTED (ALL TESTS)

PHOTO 11.7 TEST CELL INVERTED TO REVEAL GEOTEXTILE SPECIMEN UNDERLAIN BY 50 mm STONE (TESTS #1, #2, AND #3)

PHOTO 11.8 GREASE AND PLASTIC APPLIED AROUND THE INNER SURFACE OF THE SMALL CYLINDER AND SOIL COMPACTED ON THE GEOTEXTILE

PHOTO 11.9 SOIL COMPACTED ON THE GEOTEXTILE AND FINAL SOIL SURFACE TAMPED TO PROVIDE SMOOTH SURFACE FOR LOAD PLATE

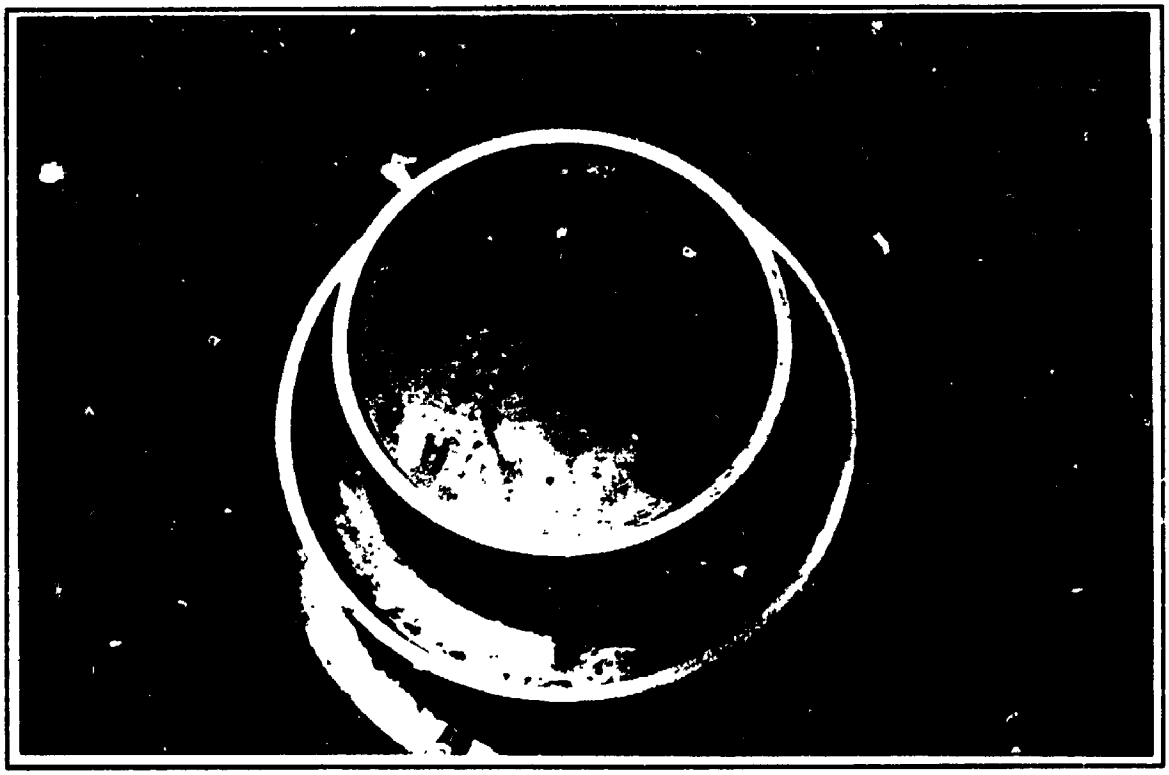

PHOTO 11.10 GEOTEXTILE FILTER AND LOAD PLATE PLACED ON THE SOIL

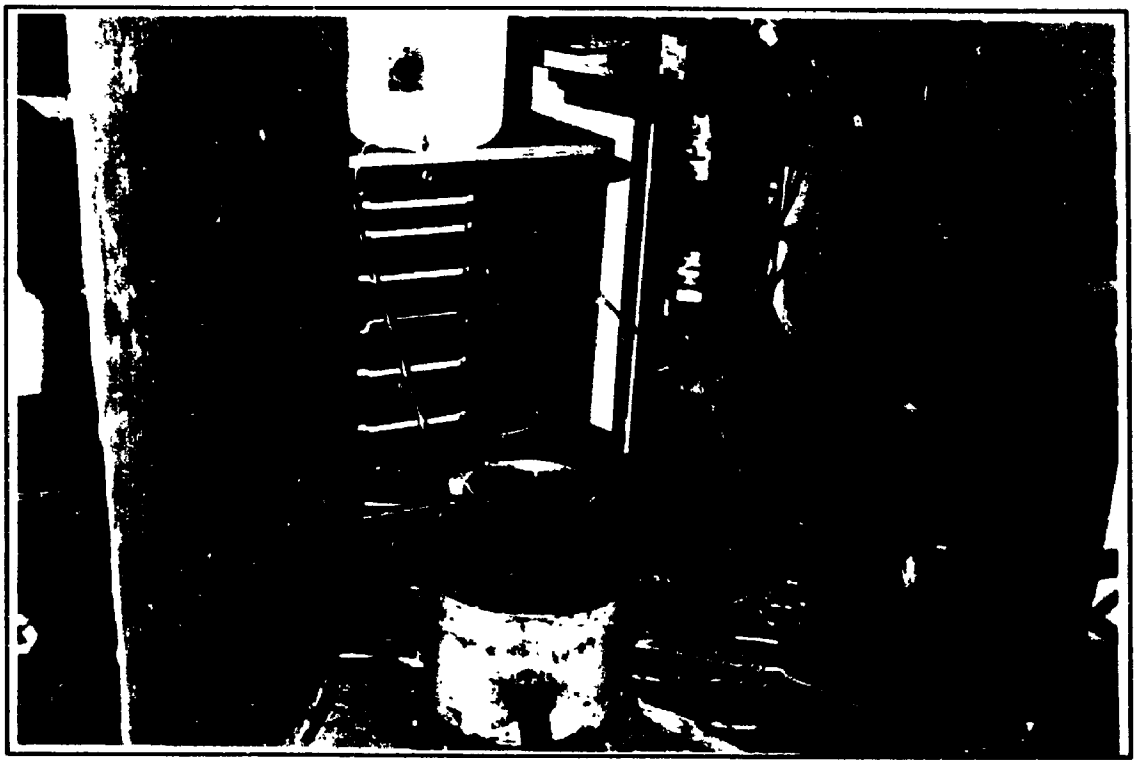

PHOTO 11.11 WATER SUPPLY TUBING ATTACHED TO THE CELL BOTTOM VALVE AND STONES INSIDE THE CELL WERE SATURATED

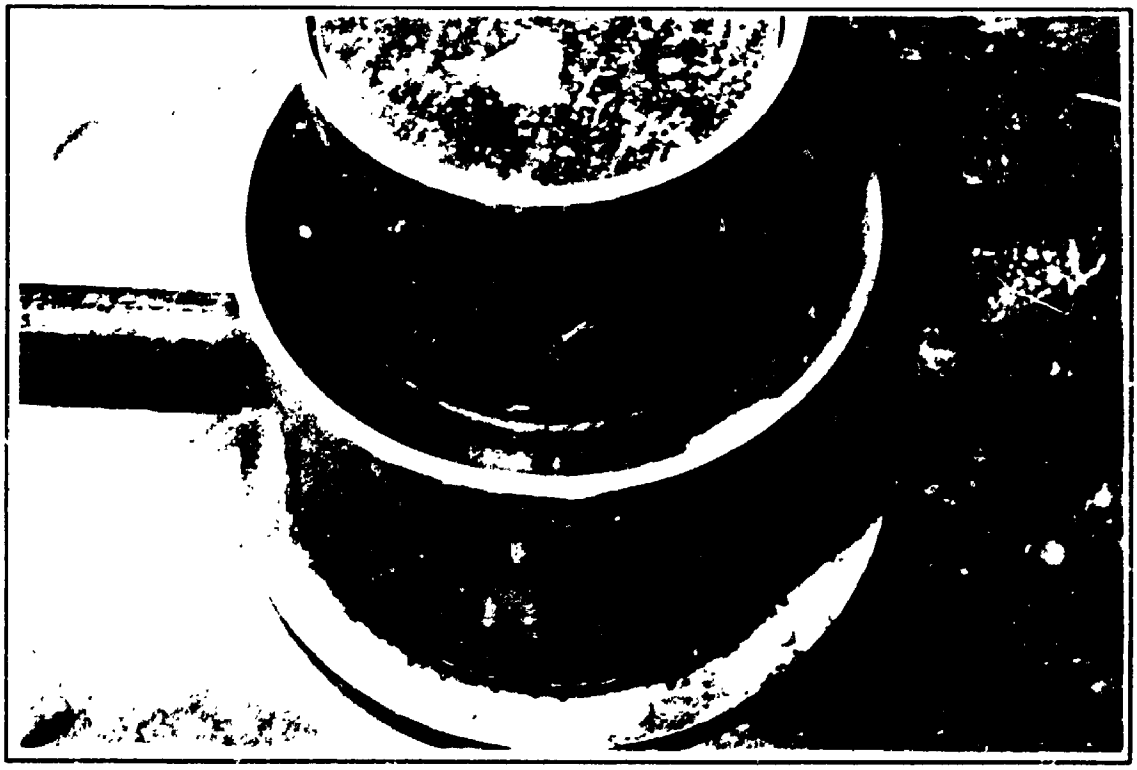

PHOTO 11.12 OUTFLOWING WATER DURING SATURATION (ALL INTRUSION TESTS)

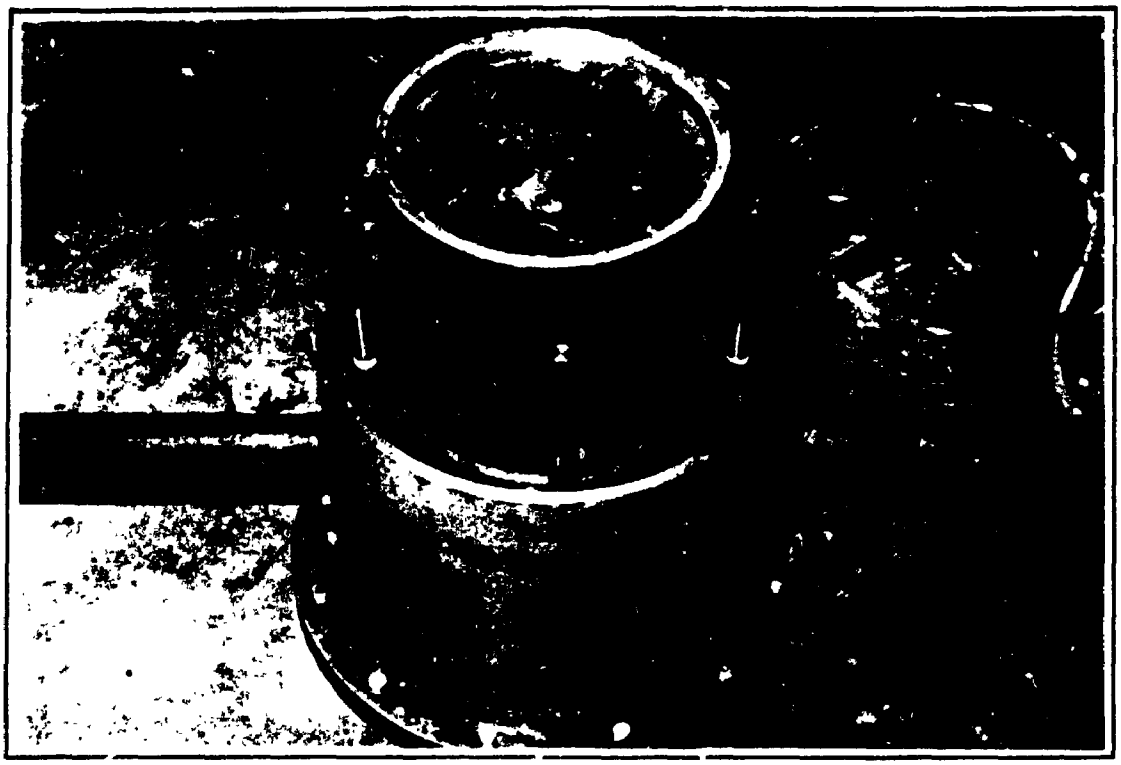

PHOTO 11.13 AFTER SATURATION, THE AIR ESCAPE HOLES WERE CLOSED BY MEANS OF METAL BARS (ALL INTRUSION TESTS)

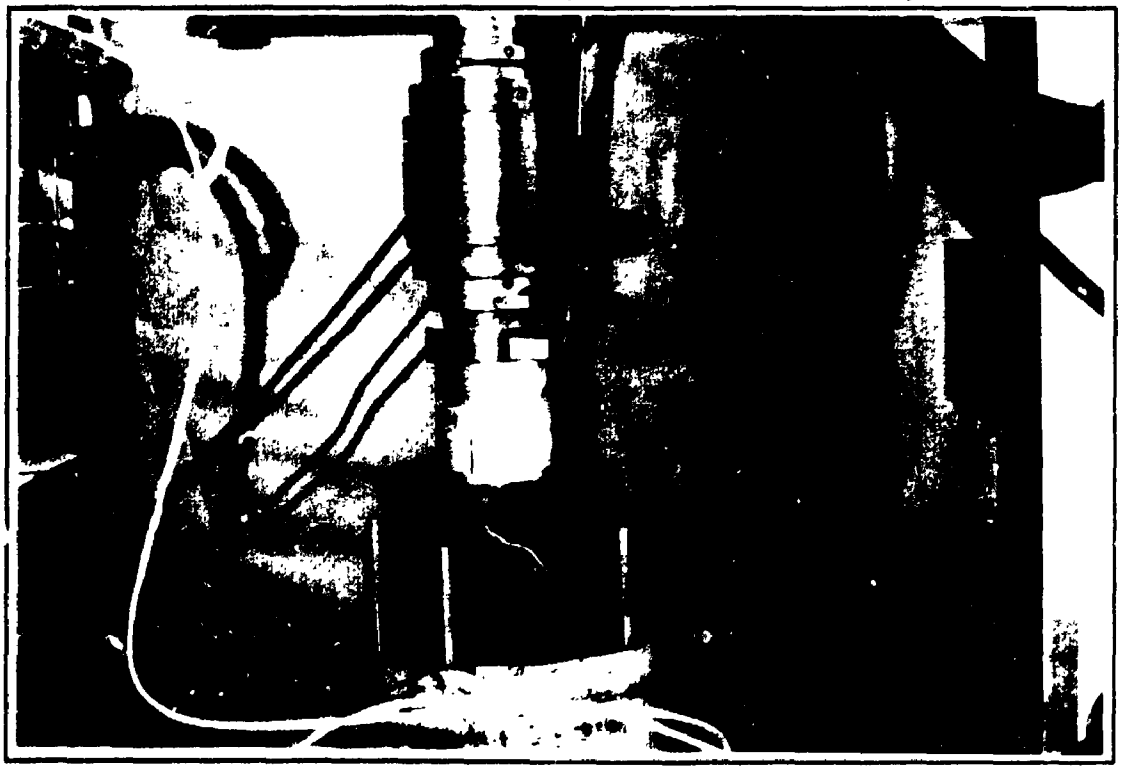

PHOTO 11.14 LOADS APPLIED USING A MTS LOAD/DISPLACEMENT MECHANISM AND TILTING PLATEN (ALL INTRUSION TESTS)

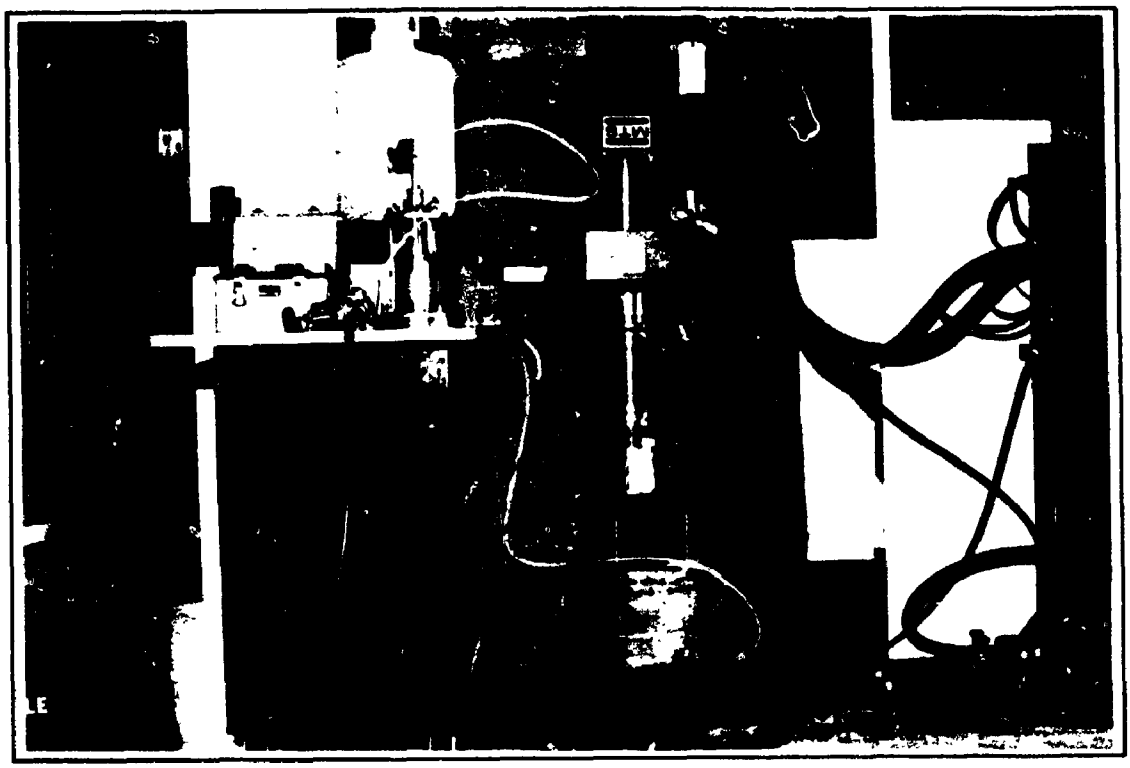

PHOTO 11.15 FULL VIEW OF THE INTRUSION TEST IN PROGRESS

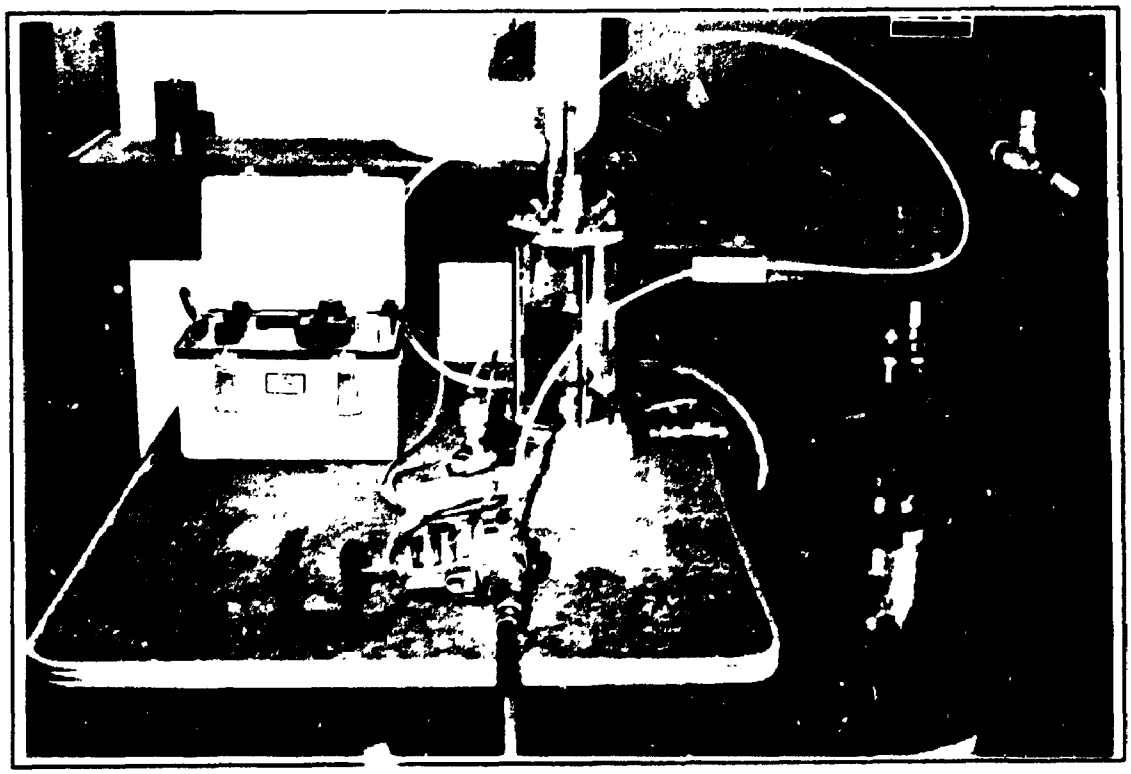

PHOTO 11.16 CELL PRESSURE SET UP CONSISTING OF THE STRAIN-INDICATOR, PRESSURE REGULATOR AND WATER RESERVOIR

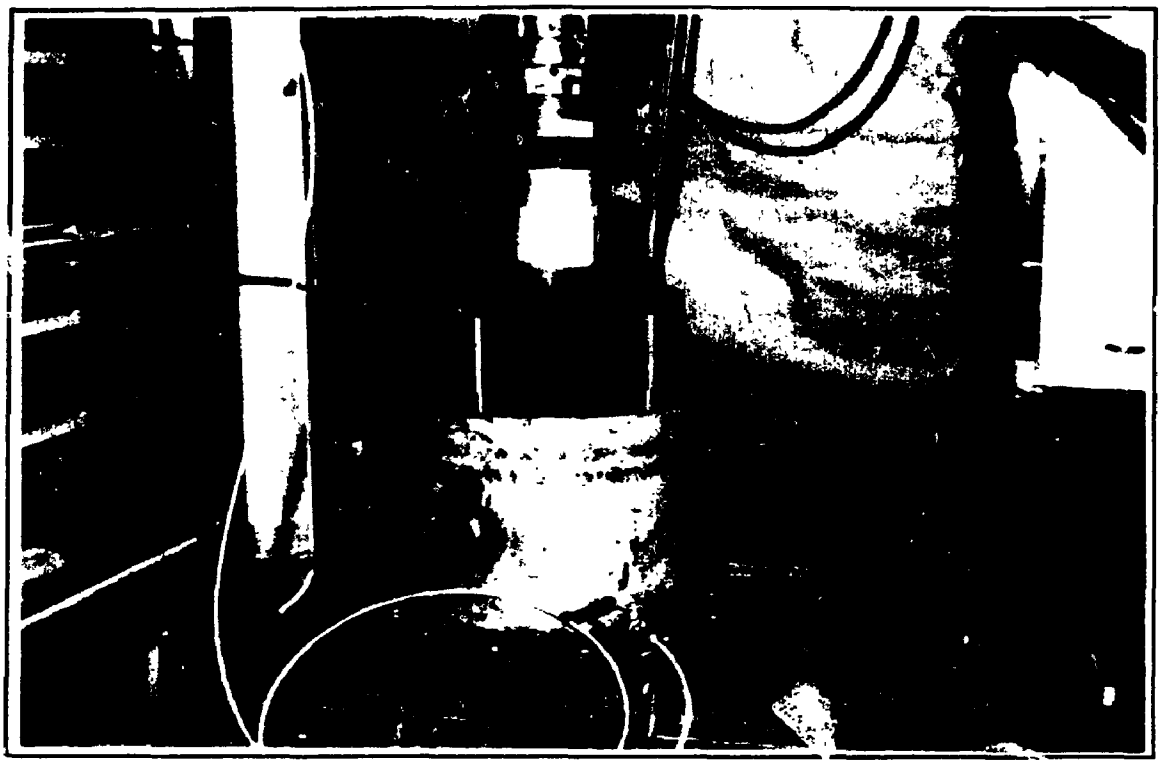

PHOTO 11.17 REMOVAL OF THE LOAD AFTER TERMINATION OF THE TEST

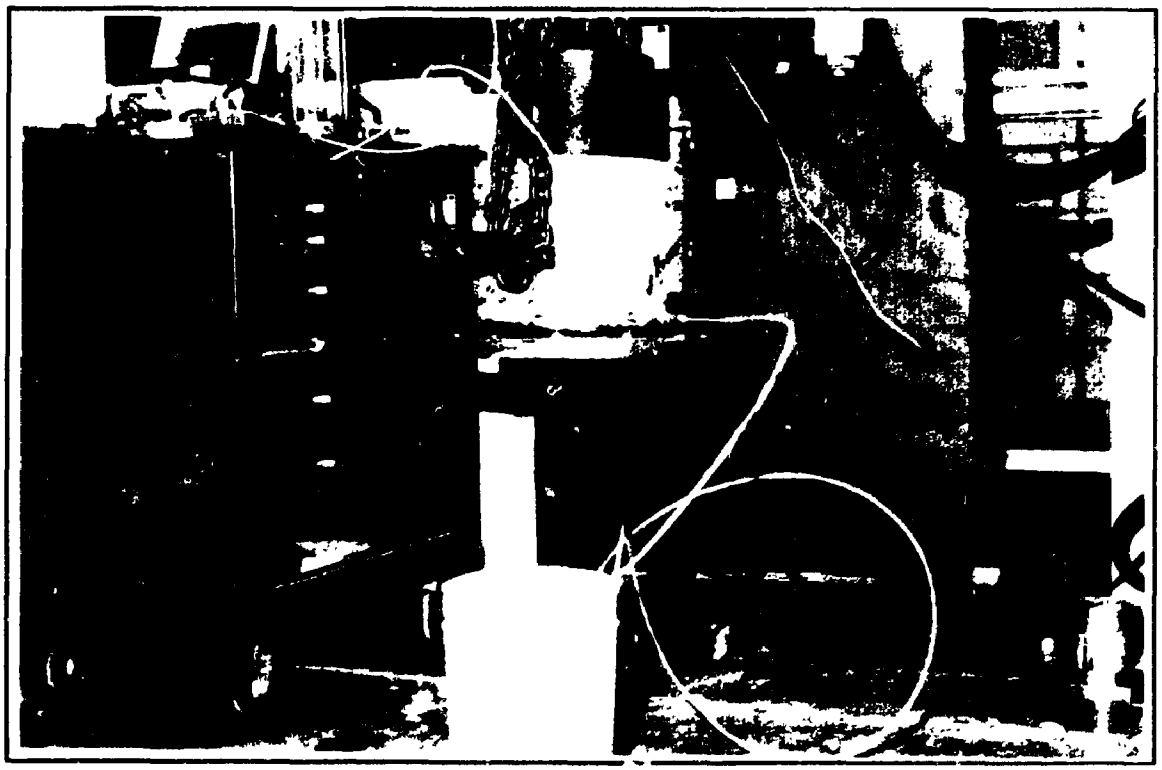

PHOTO 11.18 TEST CELL WAS LIFTED BY MEANS OF A CRANE AND CELL WATER WAS DRAINED INTO A CONTAINER

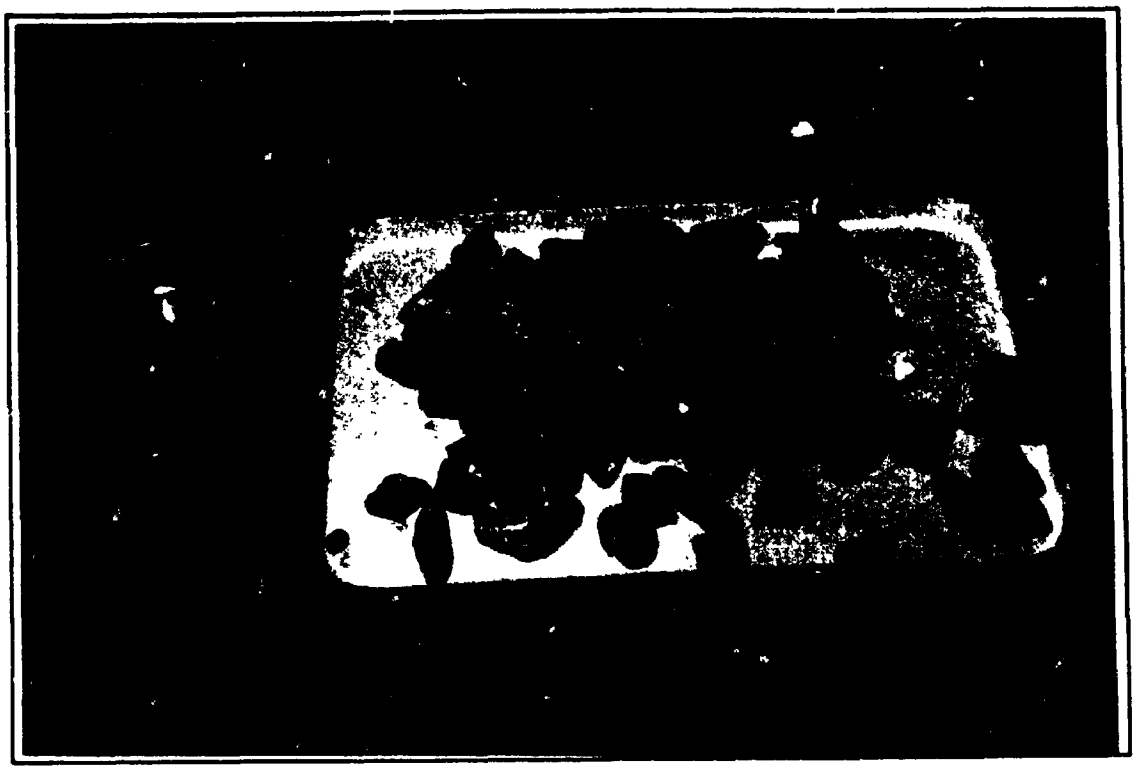

PHOTO 11.19 STONES WERE HAND EXCAVATED AND TRANSFERRED INTO A TRAY

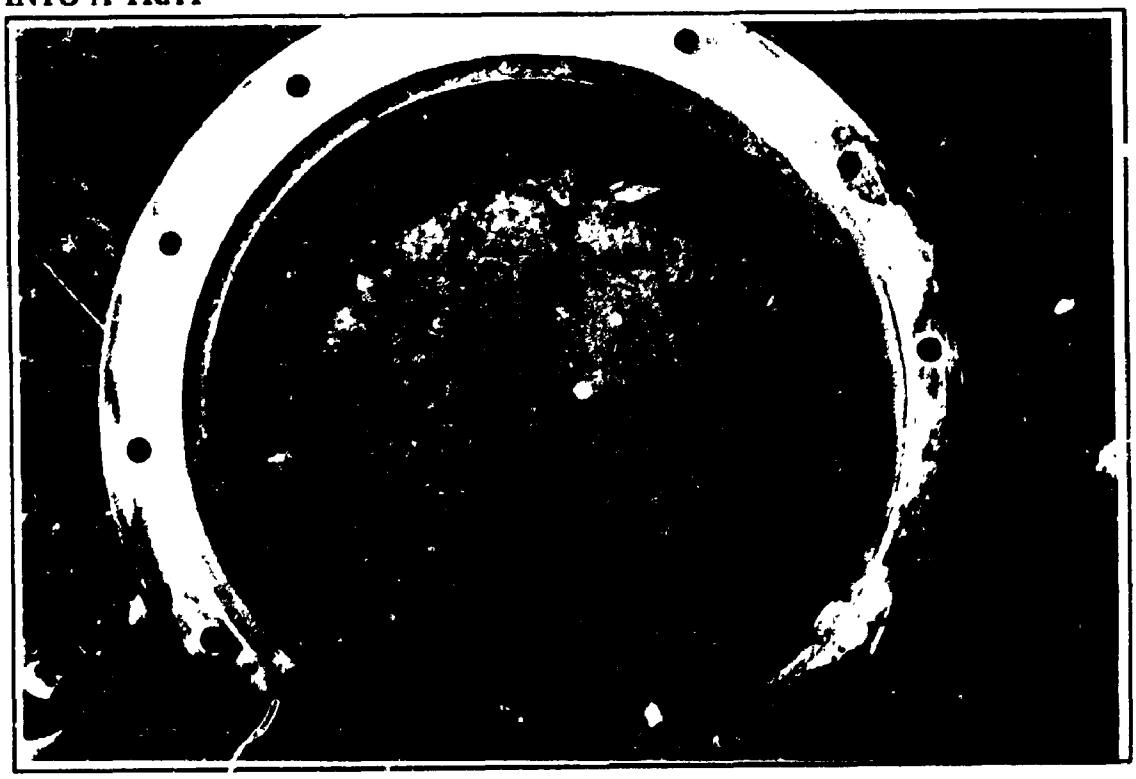

PHOTO 11.20 EXPOSED GEOTEXTILE AFTER THE REMOVAL OF THE STONES

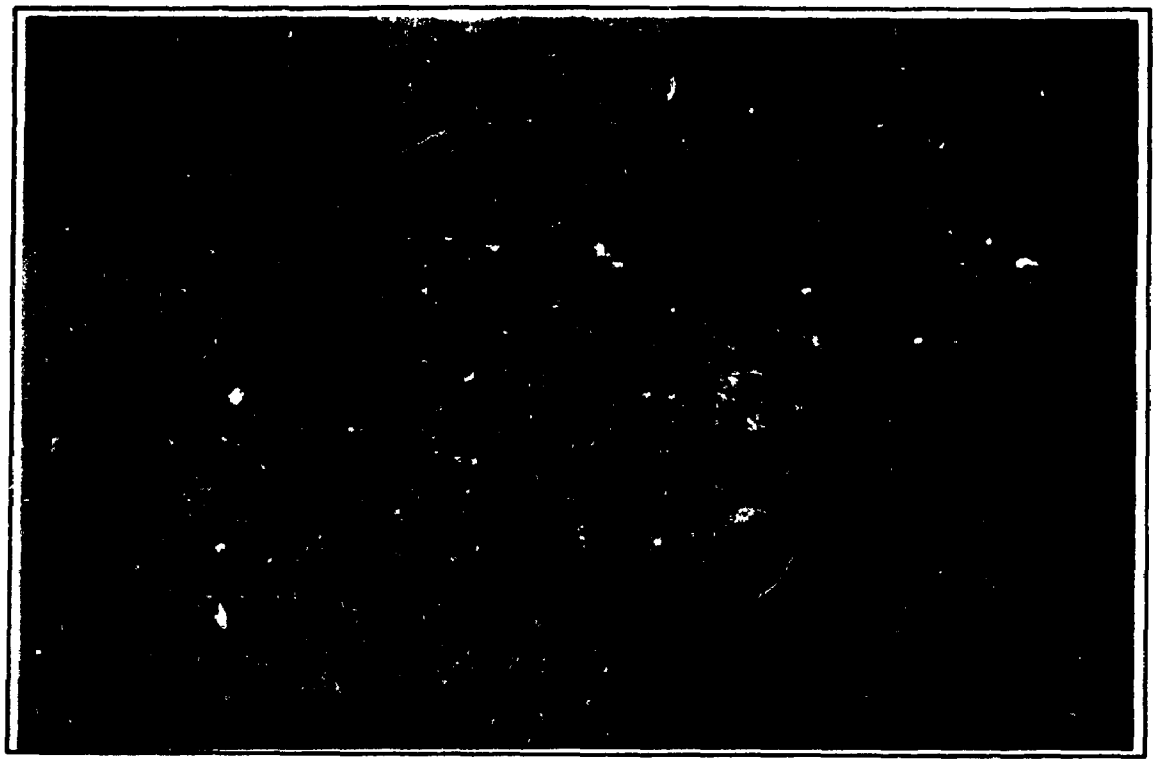

PHOTO 11.21 TS650 GEOTEXTILE PRIOR TO THE TEST WITH DEFECTS MARKED

PHOTO 11.22 EXPANDED HOLES IN GEOTEXTILE AFTER COMPLETION OF TEST #1

PHOTO 11.23 CLAYEY SOIL SURFACE OF TEST #1 AFTER COMPLETION OF THE TEST

PHOTO 11.24 STONES COATED WITH CLAYEY SOIL AFTER COMPLETION OF THE TEST #1

PHOTO 11.25 SOIL SAMPLING AFTER COMPLETION OF TEST #1

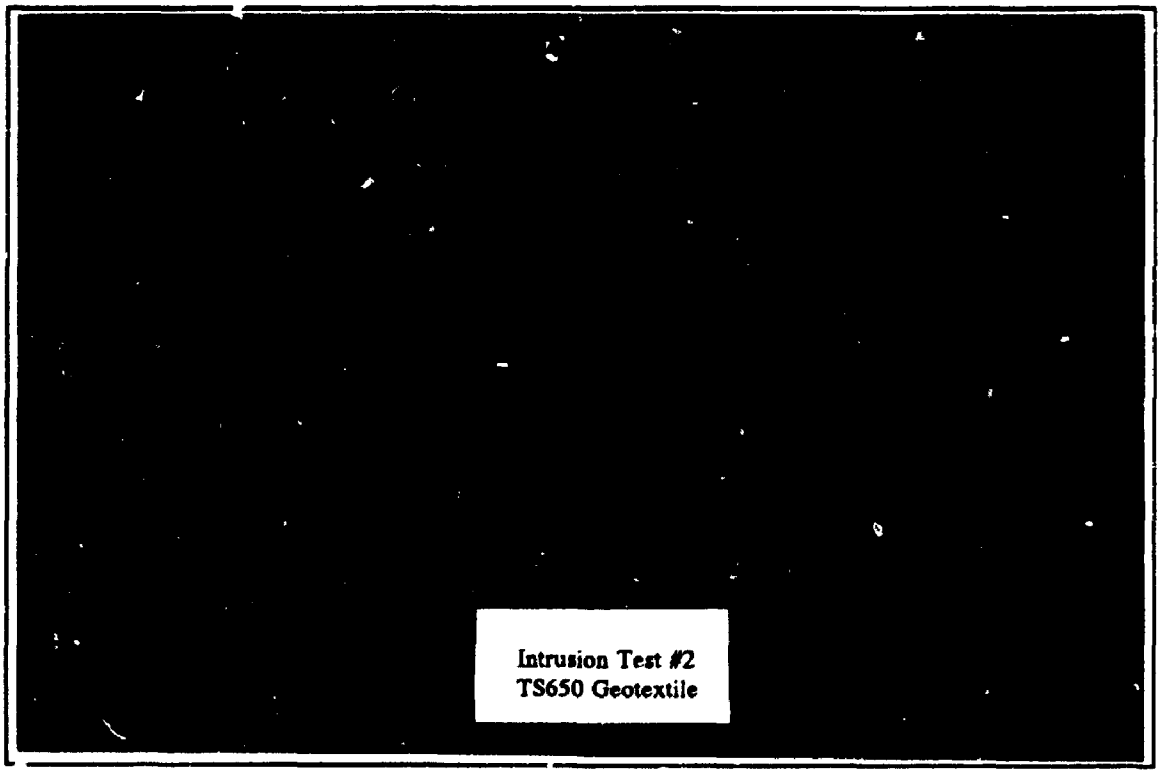

PHOTO 11.26 TS650 GEOTEXTILE PRIOR TO TEST #2

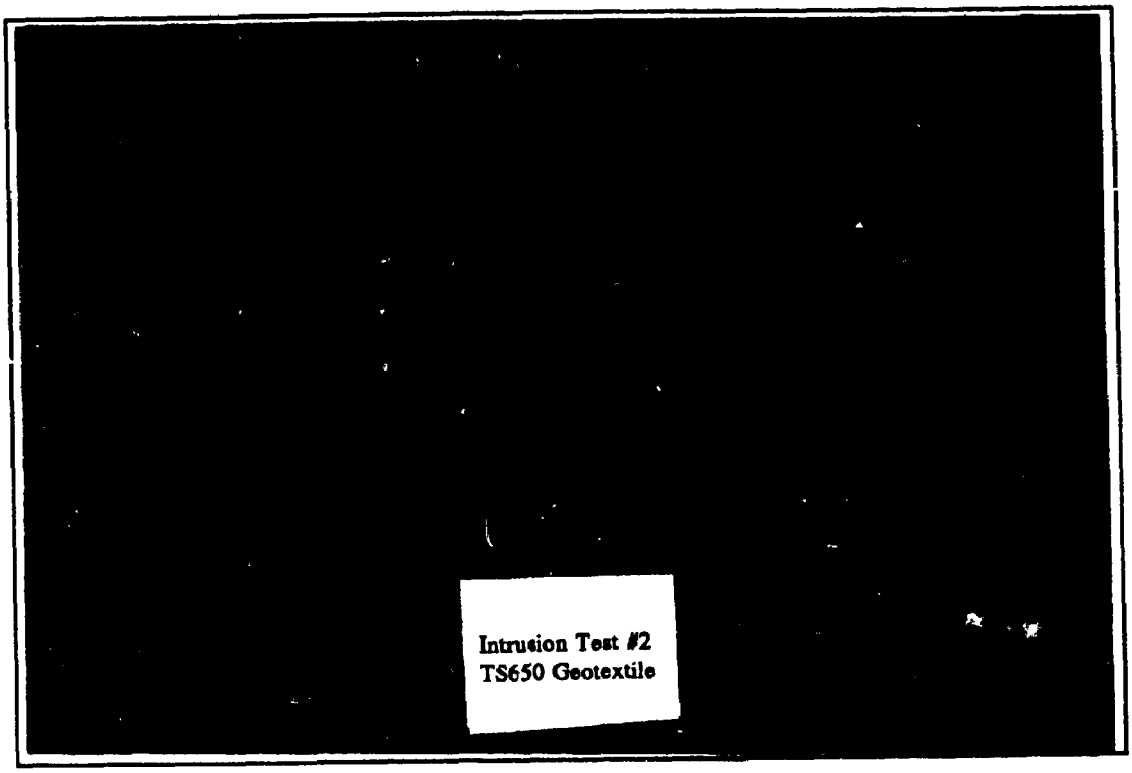

PHOTO 11.27 TS650 GEOTEXTILE AFTER COMPLETION OF TEST #2

PHOTO 11.28 TS650 GEOTEXTILE PRIOR TO TEST #3

PHOTO 11.29 TS650 GEOTEXTILE AFTER COMPLETION OF TEST #3

PHOTO 11.30 FIRST LAYER OF THE STONE WAS PLACED ON THE LOAD PLATE AND FLANGE (TESTS #4 AND #5)

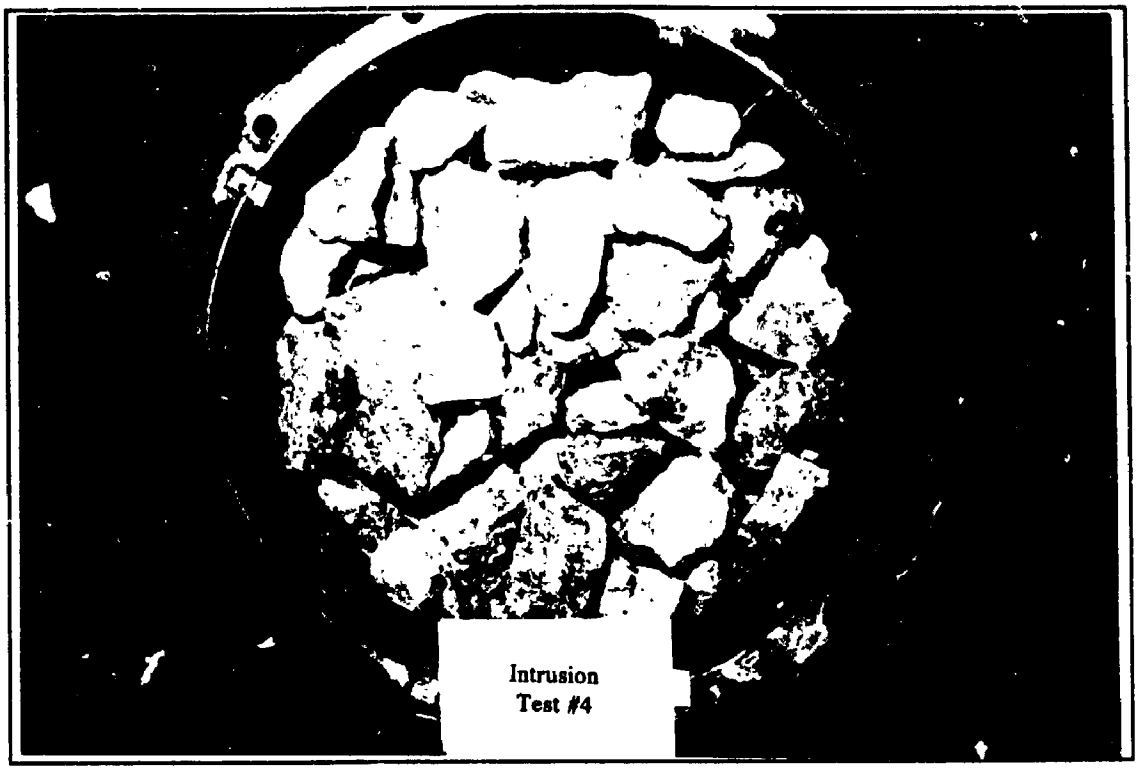

PHOTO 11.31 ADDITIONAL 50 mm STONE WAS PLACED TO FILL CYLINDER (TESTS #4 AND #5)

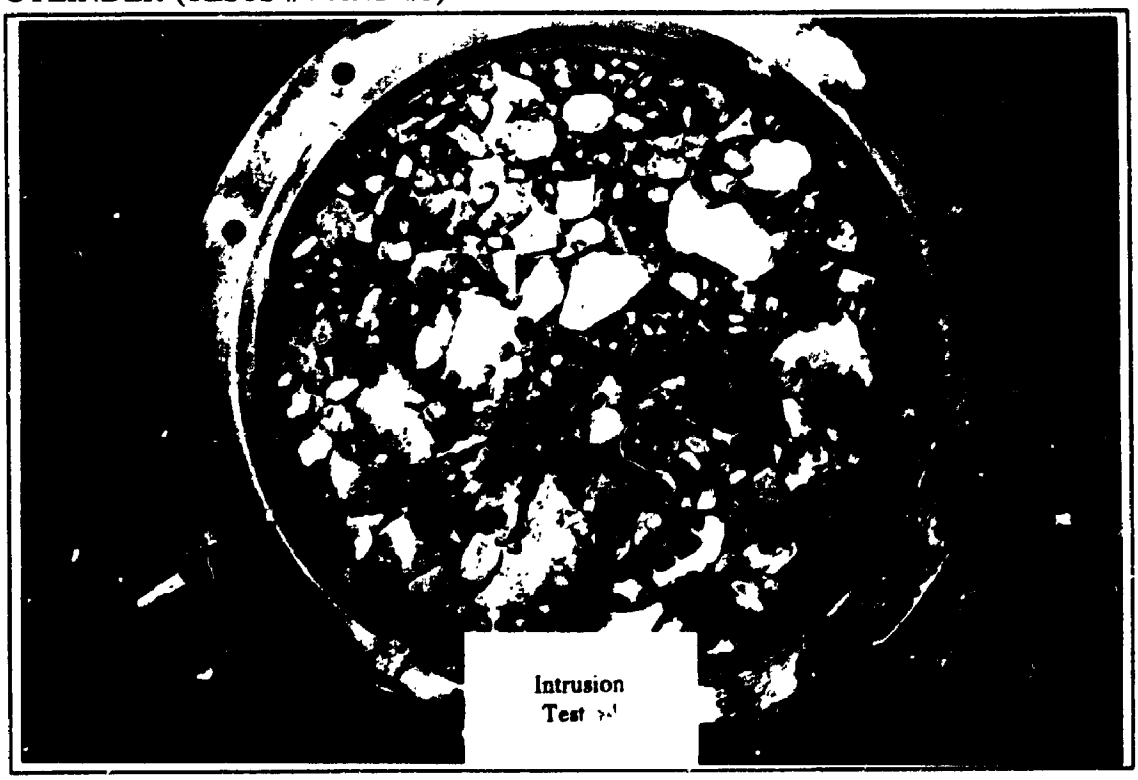

PHOTO 11.32 RIVER GRAVEL (20 mm) WAS PLACED OVER 50 mm STONE TO PROVIDE SMOOTH SURFACE FOR BASE PLATE

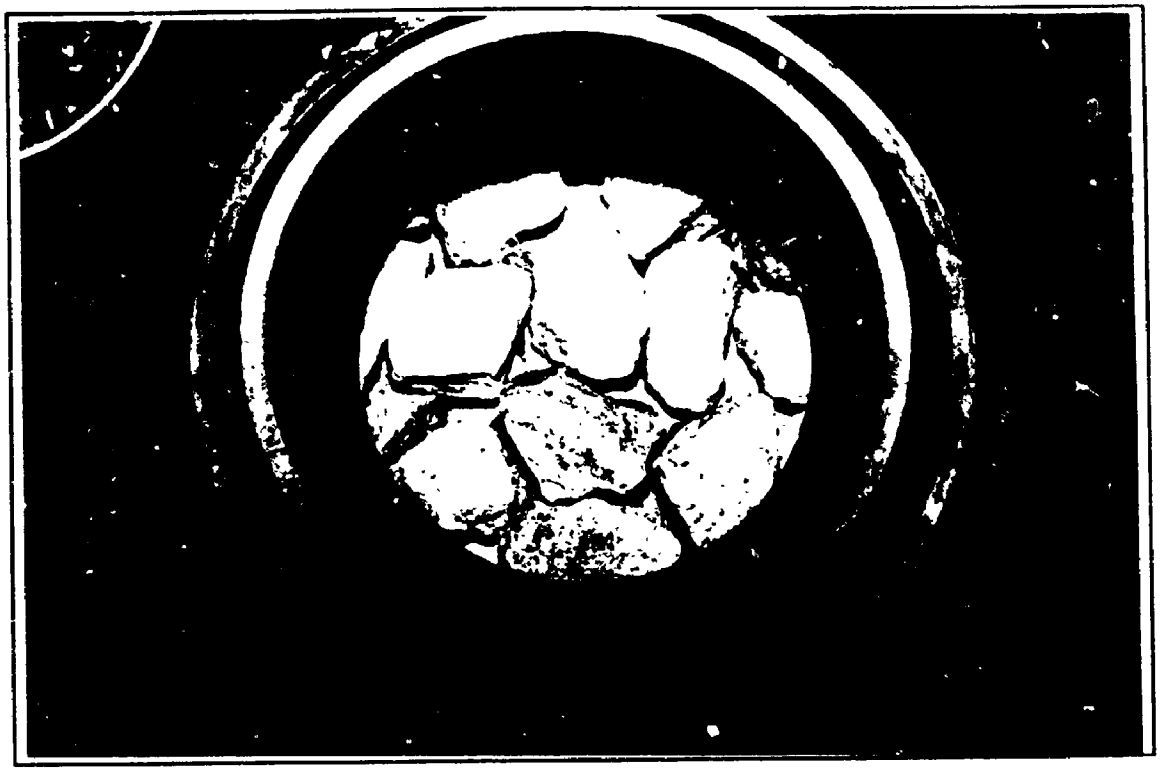

PHOTO 11.33 TEST CELL WAS INVERTED TO REVEAL THE TOP 50 mm STONE LAYER

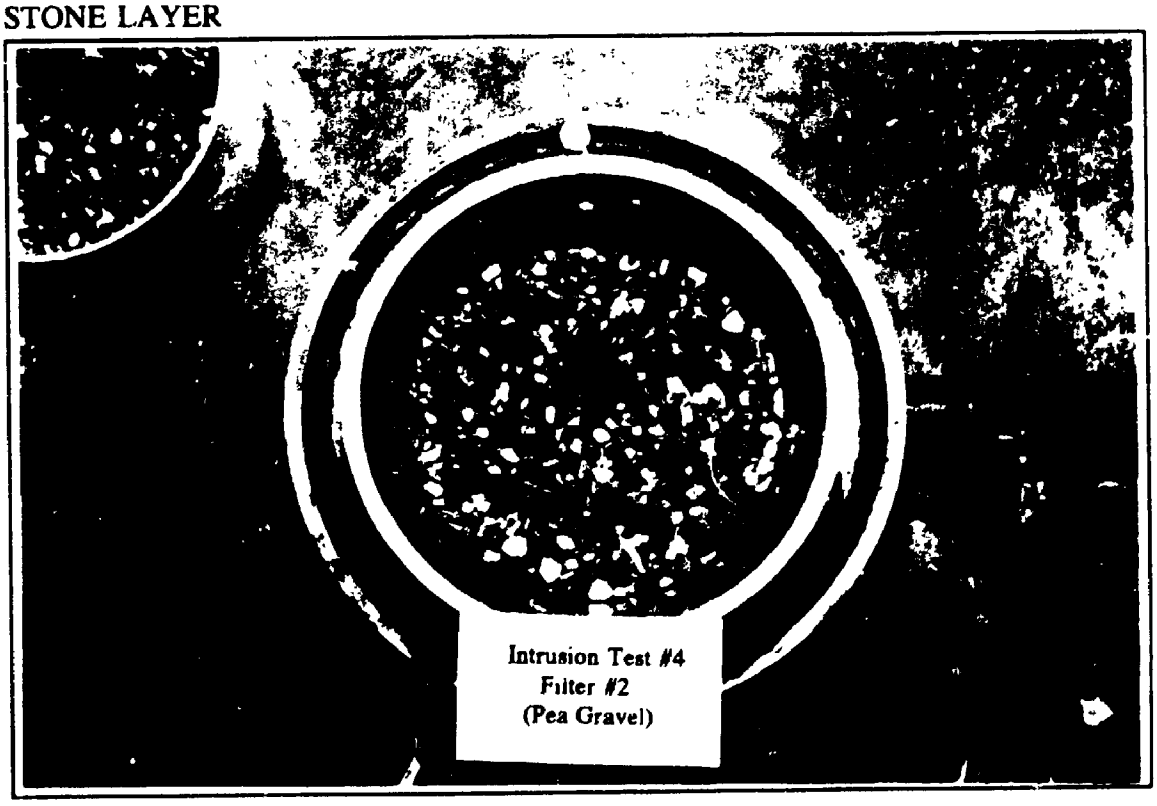

PHOTO 11.34 SECOND PEA GRAVEL FILTER LAYER WAS PLACED ON THE 50 mm STONE (TESTS #4 AND #5)

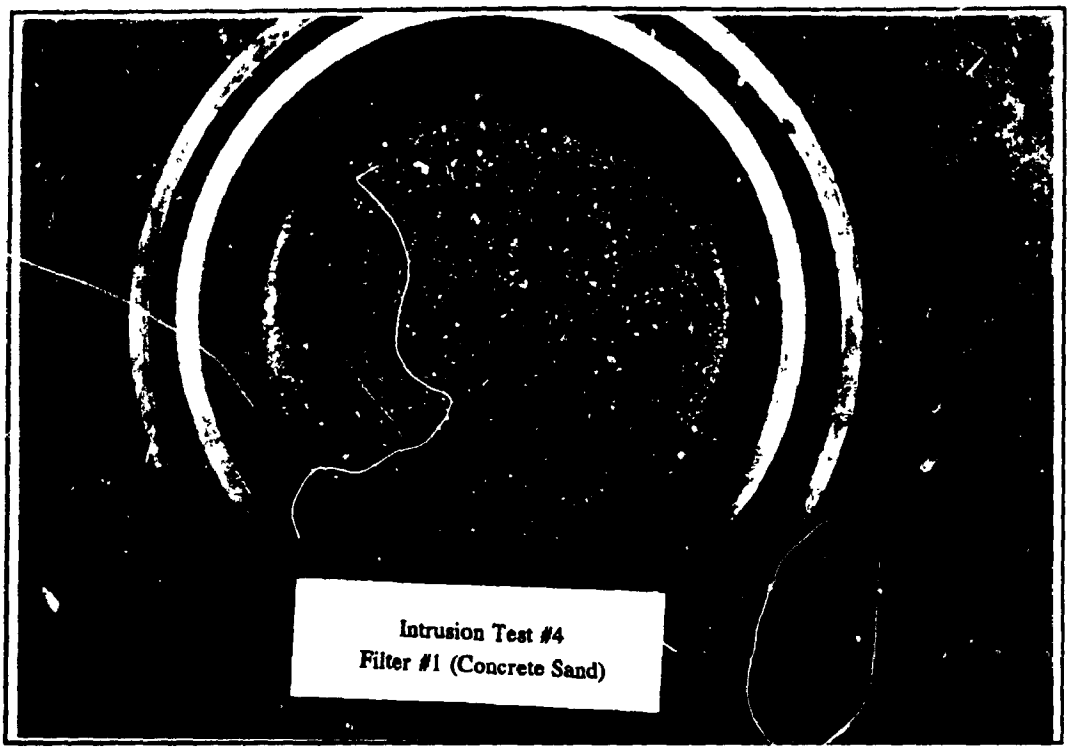

PHOTO 11.35 FIRST CONCRETE SAND FILTER LAYER WAS PLACED ON THE SECOND PEA GRAVEL FILTER LAYER (TESTS #4 AND #5)

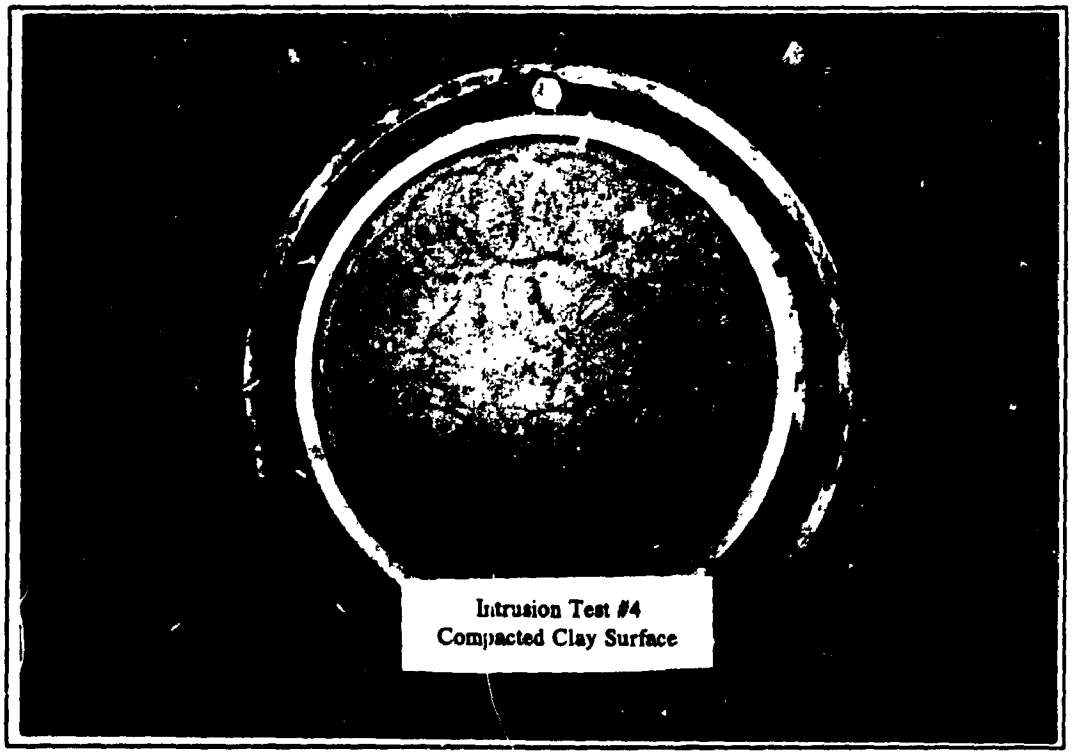

PHOTO 11.36 CLAYEY SOIL WAS COMPACTED ON THE FIRST FILTER LAYER AND FINAL SOIL SURFACE TAMPED TO PROVIDE SMOOTH SURFACE FOR LOAD PLATE

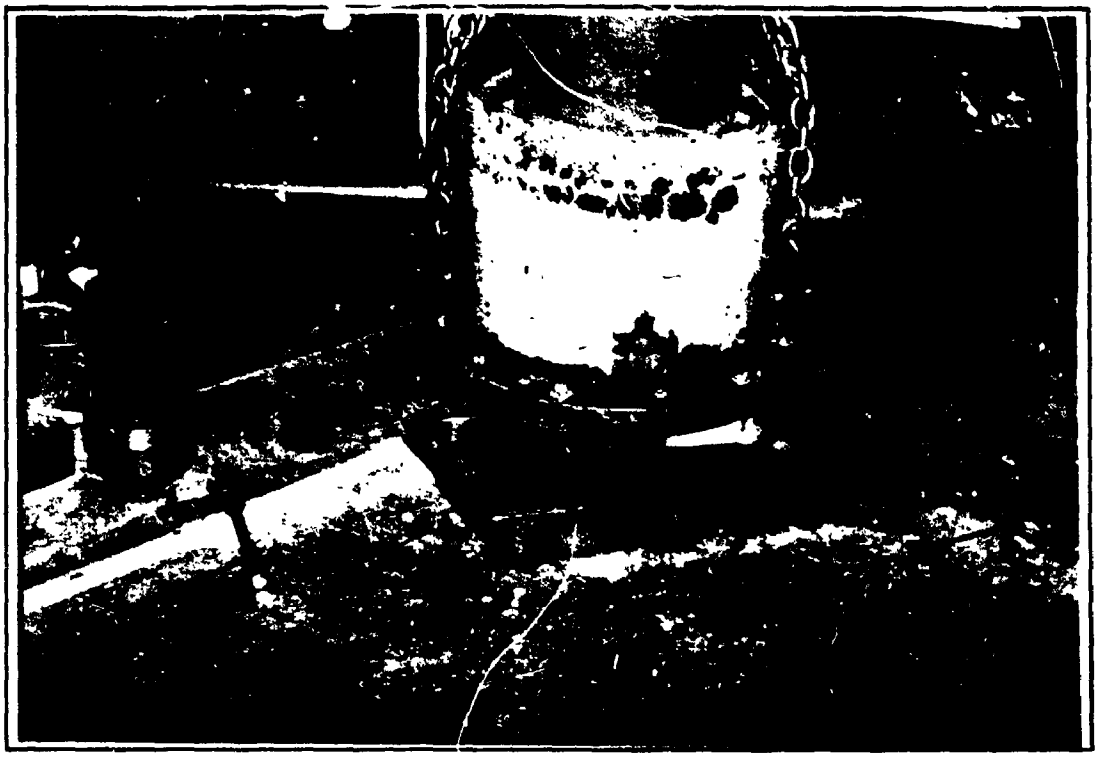

PHOTO 11.37 BOTTOM PLATE WAS LOOSENED AND REMAINING WATER IN THE CELL WAS DRAINED IN A TRAY (TESTS #4 AND #5)

PHOTO 11.38 EXPOSED SURFACE OF PEA GRAVEL FILTER LAYER AFTER REMOVAL OF ALL STONES (TESTS #4 AND #5)

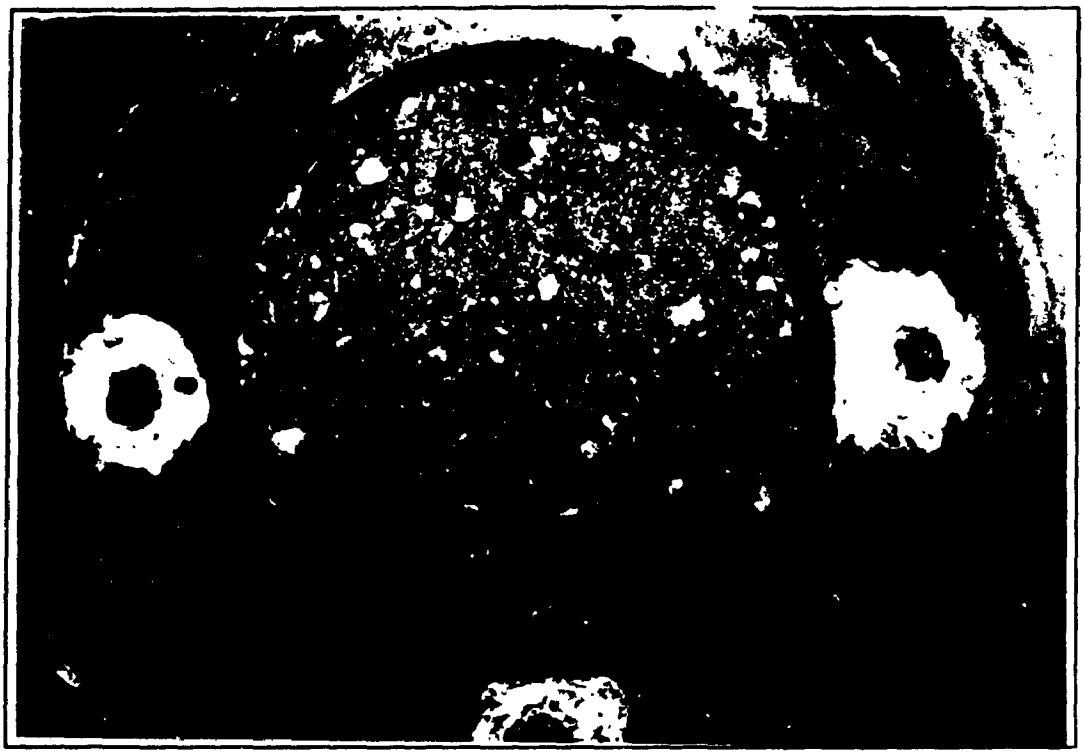

PHOTO 11.39 EXPOSED SURFACE OF CONCRETE SAND FILTER LAYER AFTER REMOVAL OF PEA GRAVEL (TESTS #4 AND #5)

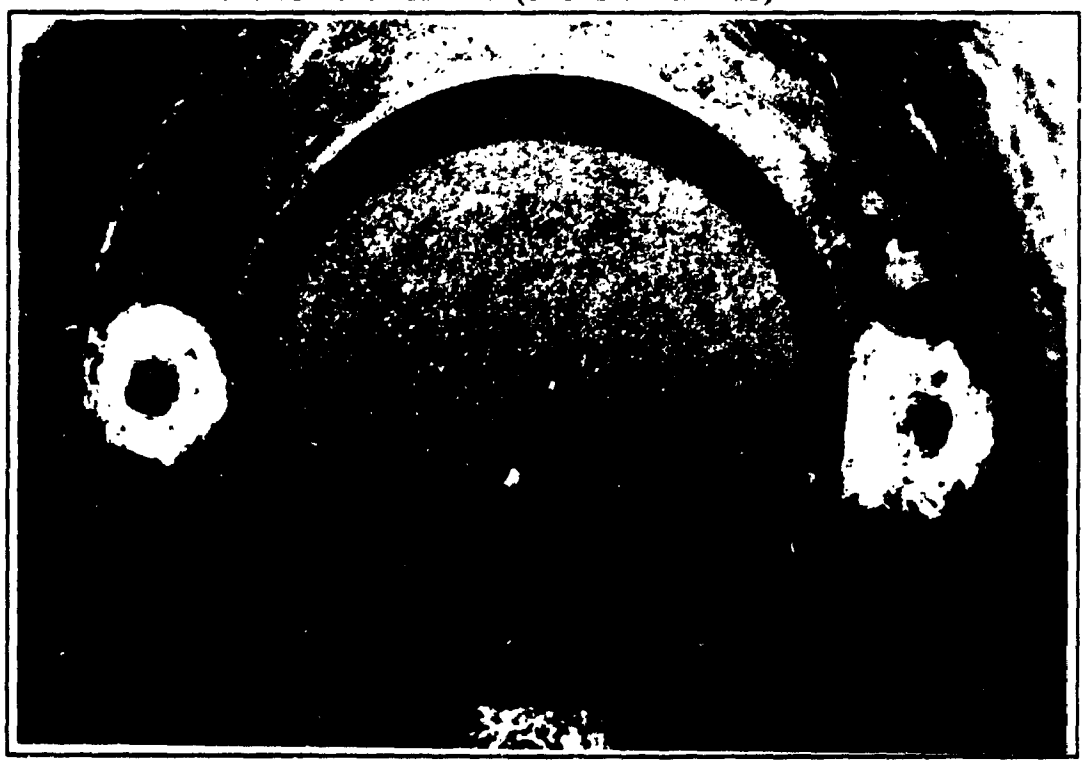

PHOTO 11.40 EXPOSED SURFACE OF SOIL AFTER REMOVAL OF FILTER MATERIAL (TESTS #4 AND #5)

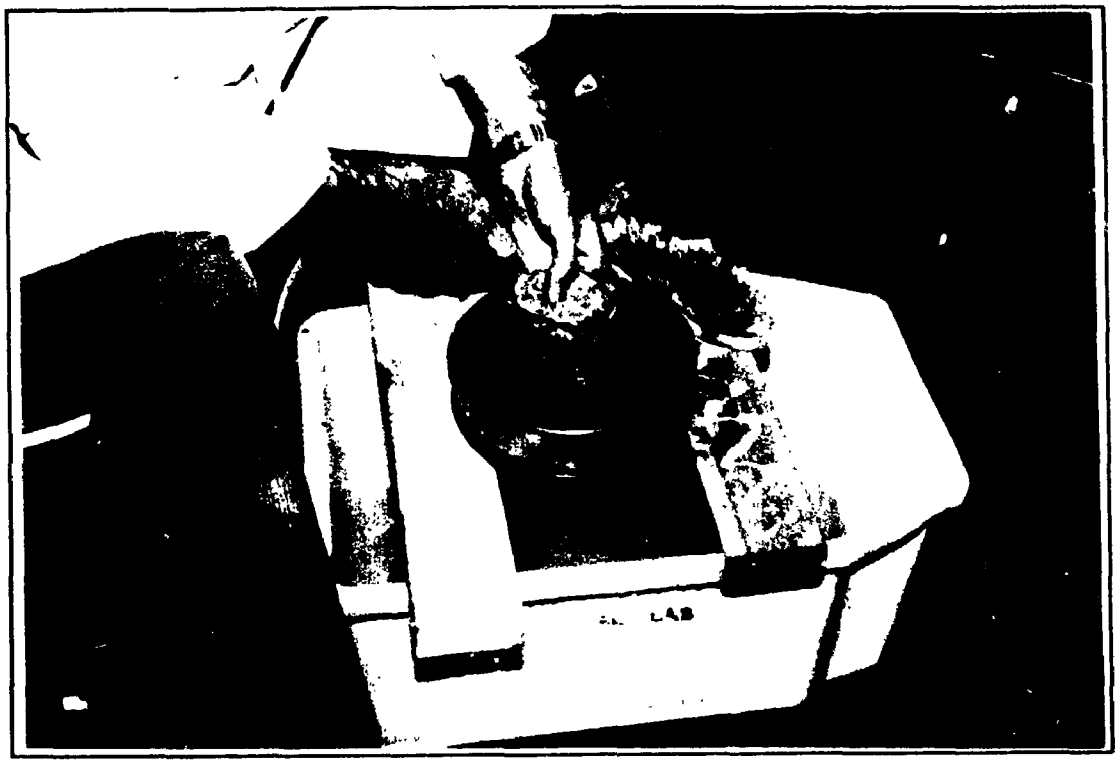

PHOTO 11.41 STONES WERE WASHED OVER SIEVE #200 AND WASH WATER COLLECTED IN A CONTAINER (TESTS #4 AND #5)

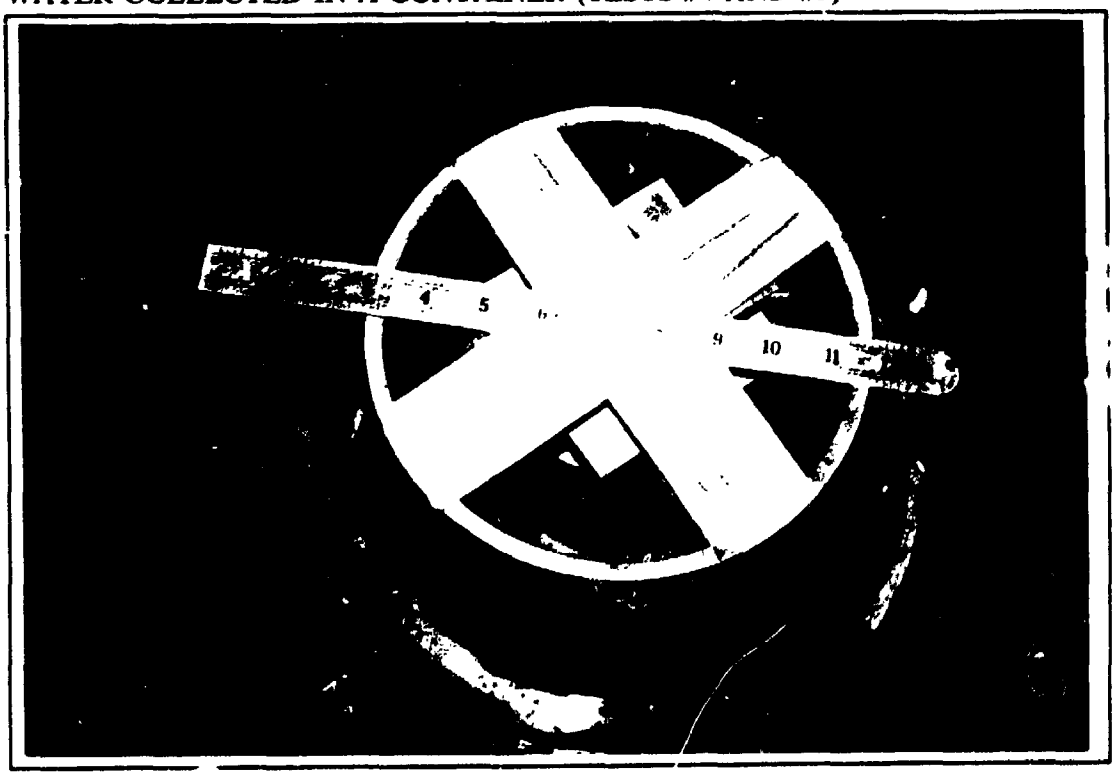

PHOTO 11.42 SPACERS WERE PLACED ON TOP OF THE LOAD PLATE AND FIXED TO THE SMALL CYLINDER USING A TAPE (TEST #6)

PHOTO 11.43 EXPOSED GEOTEXTILE SURFACE AFTER REMOVAL OF 50 mm STONES IN FIRST 100 kPa LOAD APPLICATION (TEST #6)

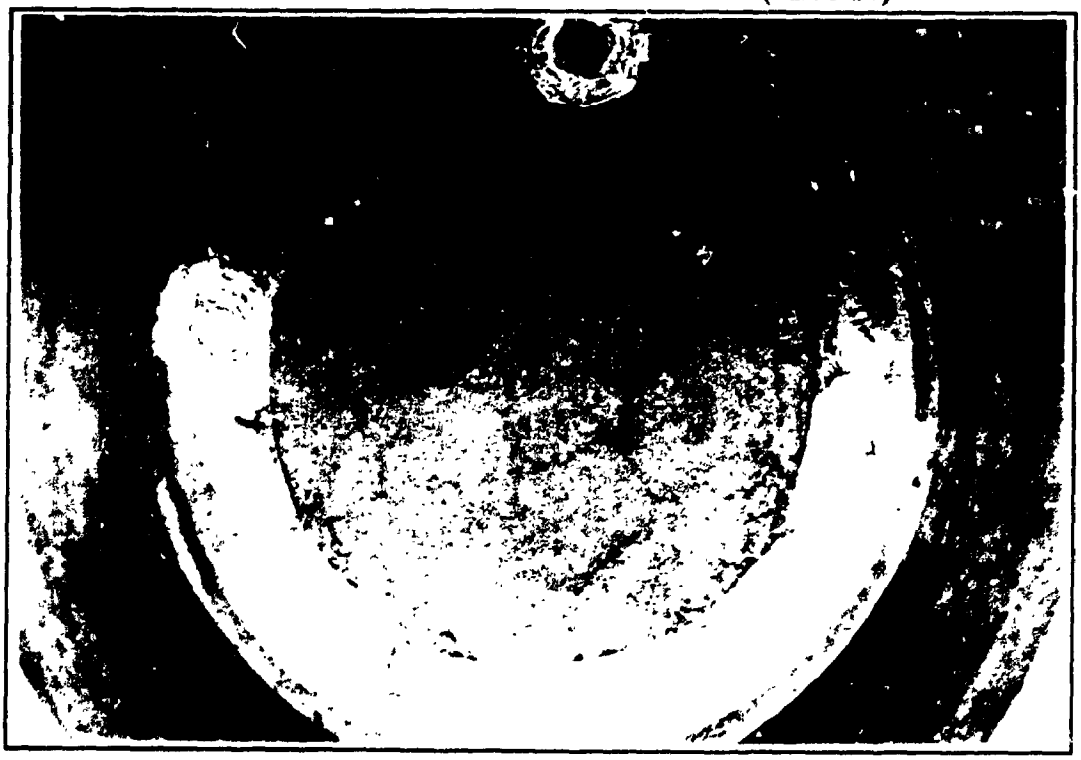

PHOTO 11.44 EXPOSED CLAYEY SOIL SURFACE AFTER REMOVAL OF THE GEOTEXTILE (TEST #6)

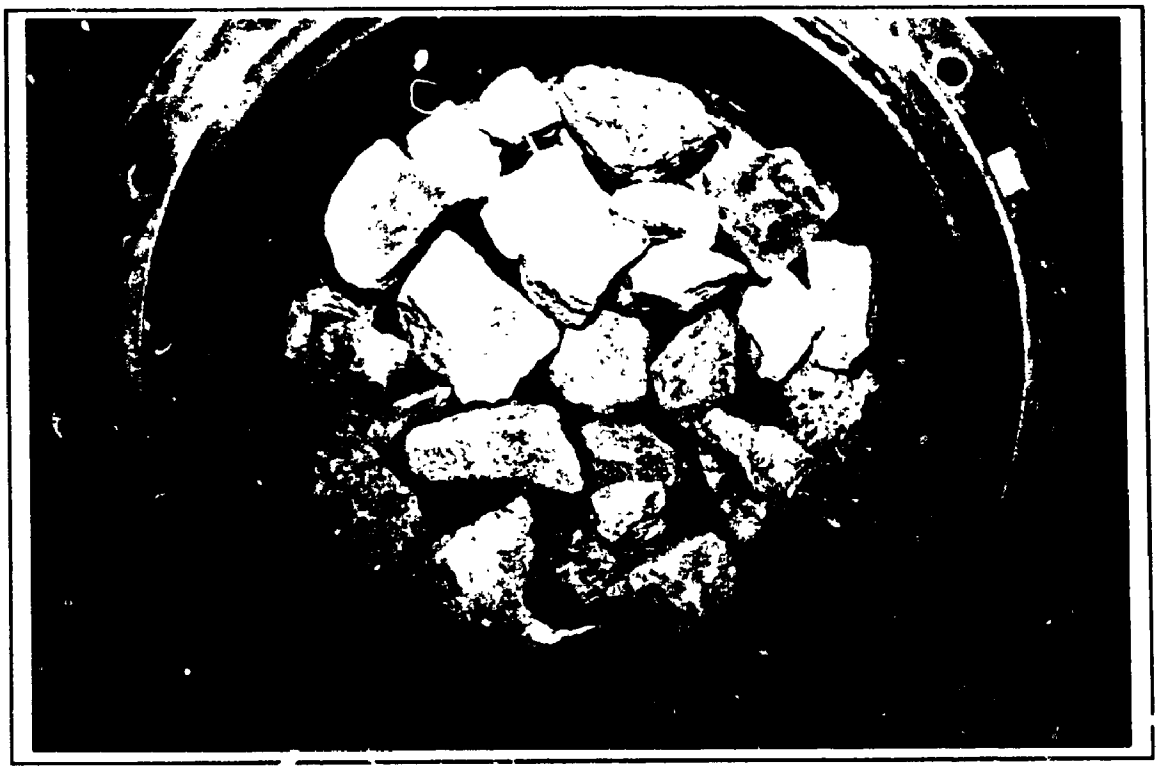

PHOTO 11.45 FIRST LAYER OF 50 mm STONE WAS PLACED ON THE CLAYEY SOIL SURFACE IN THE BIGGER CYLINDER

PHOTO 11.46 600 kPa VERTICALL PRESSURE AND 100 kPa CELL PRESSURE RELEASED AND SPACERS WERE PLACED ON TOP OF THE LOAD PLATE

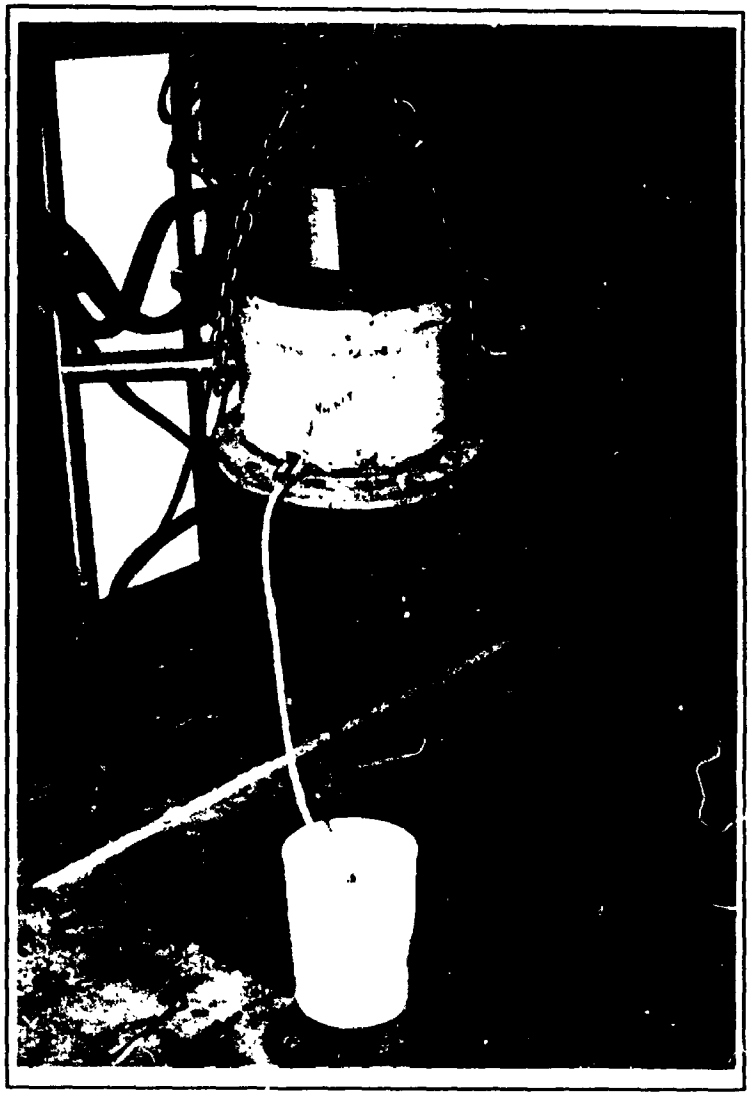

PHOTO 11.47 TEST CELL WAS LIFTED BY A CRANE AND CELL WATER WAS DRAINED INTO A CONTAINER

PHOTO 11.48 STONES WERE HAND EXCAVATED AND TRANSFERRED INTO A TRAY (TESTS #6 AND #7)

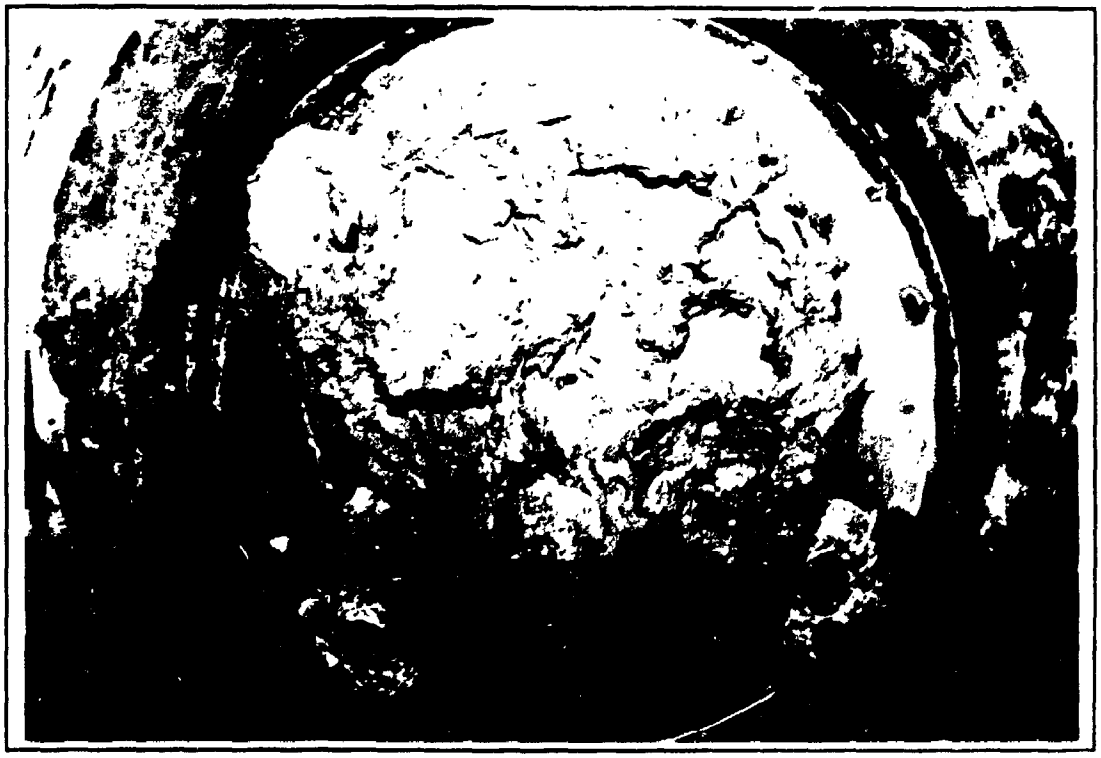

PHOTO 11.49 EXPOSED CLAYEY SOIL SURFACE AFTER TERMINATION OF THE TEST AND REMOVAL OF THE STONES (TEST #6)

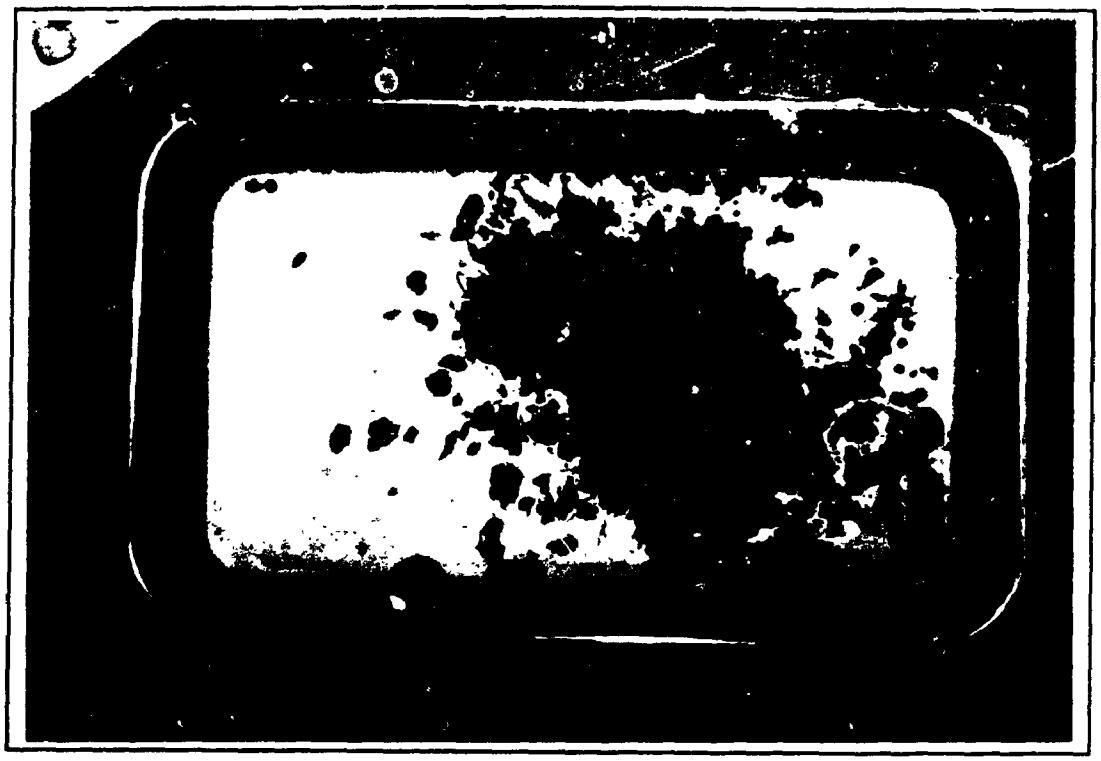

PHOTO 11.50 LOOSE CLAYEY SOIL WAS REMOVED FROM THE STONE SURFACES AND PLACED INTO A TRAY

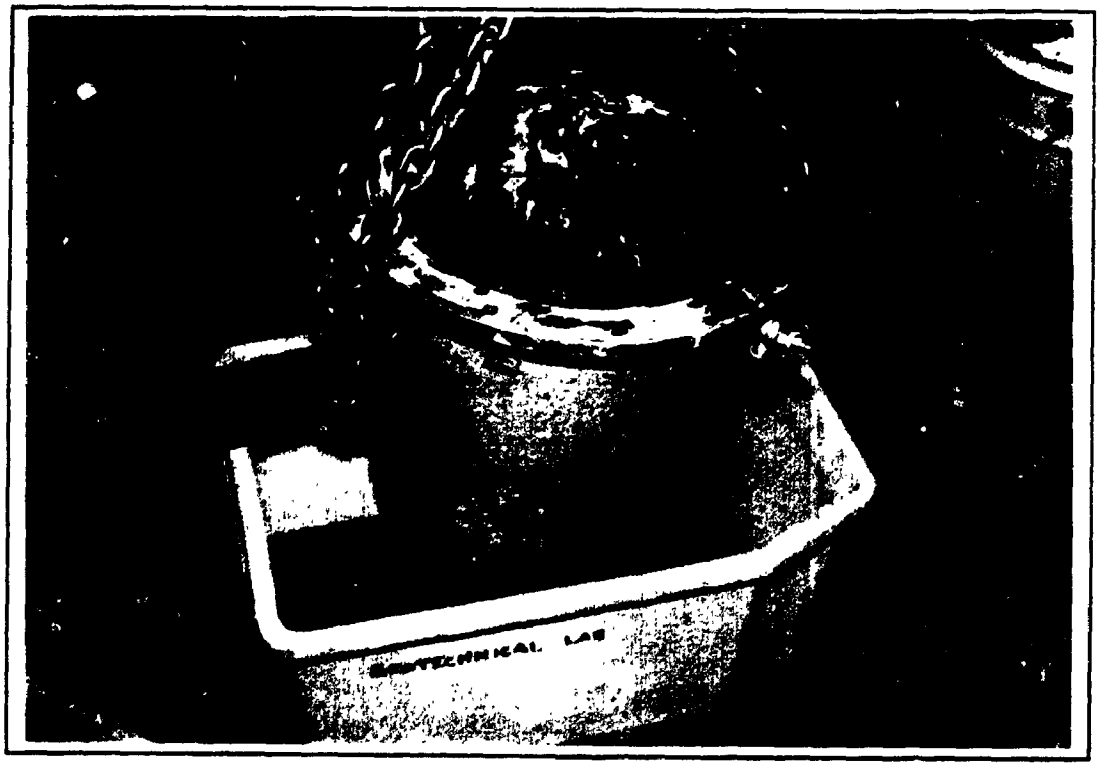

PHOTO 11.51 TEST CELL WAS WASHED INTO A CONTAINER

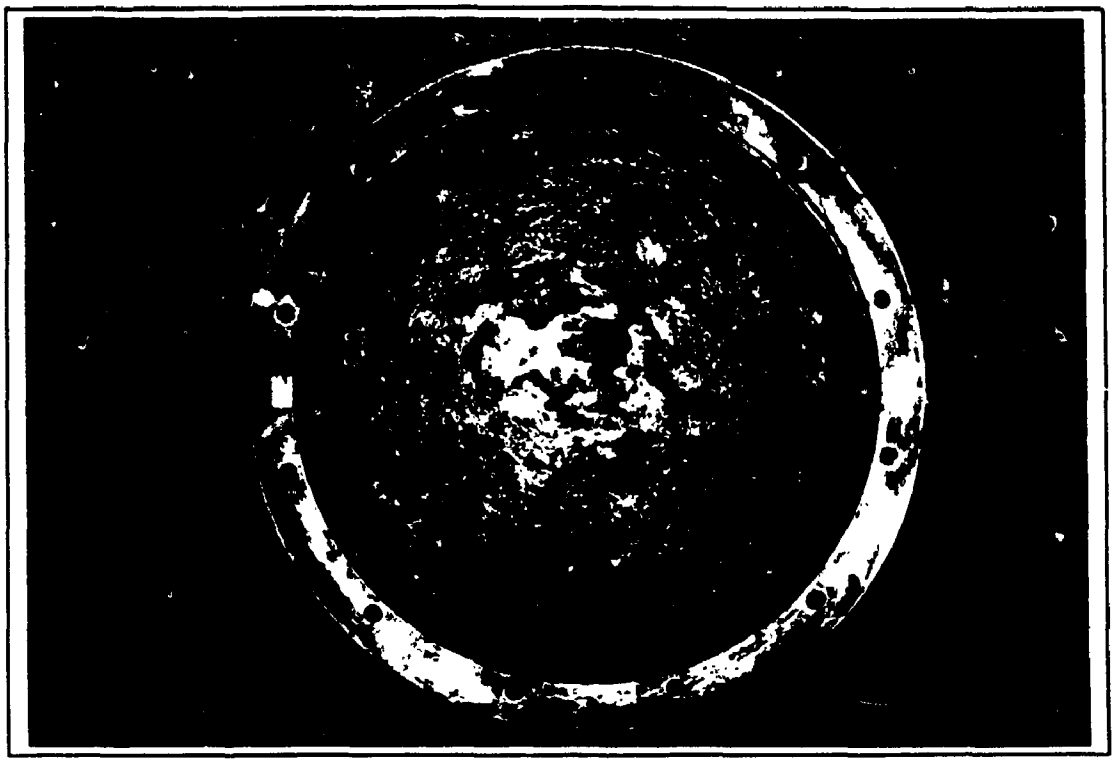

PHOTO 11.52 LOOSE CLAYEY SOIL ON THE SURFACE OF THE BASE PLATE AT THE END OF THE TEST (TESTS #6 AND #7)

PHOTO 11.53 INTRUDED VERY SOFT CLAYEY SOIL IN THE VOID SPACES AT THE BOTTOM OF THE STONE LAYER

PHOTO 11.54 INTRUDED VERY SOFT CLAYEY SOIL IN THE VOID SPACES OF THE STONE LAYER (TEST #6)

PHOTO 11.55 CLOSE VIEW OF THE INTRUDED SOIL IN THE VOID SPACES OF THE STONE LAYER (TEST #6)

PHOTO 11.56 INTRUDED VERY SOFT CLAYEY SOIL IN THE VOID SPACES OF THE FIRST STONE LAYER IN CONTACT WITH THE SOIL (TEST #5)

PHOTO 11.57 INTRUDED VERY SOFT CLAYEY SOIL IN THE VOID SPACES AT THE BOTTOM OF THE STONE LAYER (TEST #7)

PHOTO 11.58 INTRUDED VERY SOFT CLAYEY SOIL IN THE VOID SPACES OF THE STONE LAYER (TEST #7)

PHOTO 11.59 INTRUDED VERY SOFT CLAYEY SOIL IN THE VOID SPACES OF THE FIRST STONE LAYER IN CONTACT WITH THE SOIL (TEST #7)

PHOTO 11.60 EXPOSED CLAYEY SOIL SURFACE AT THE END OF THE TEST AND REMOVAL OF THE STONES (TEST #7)

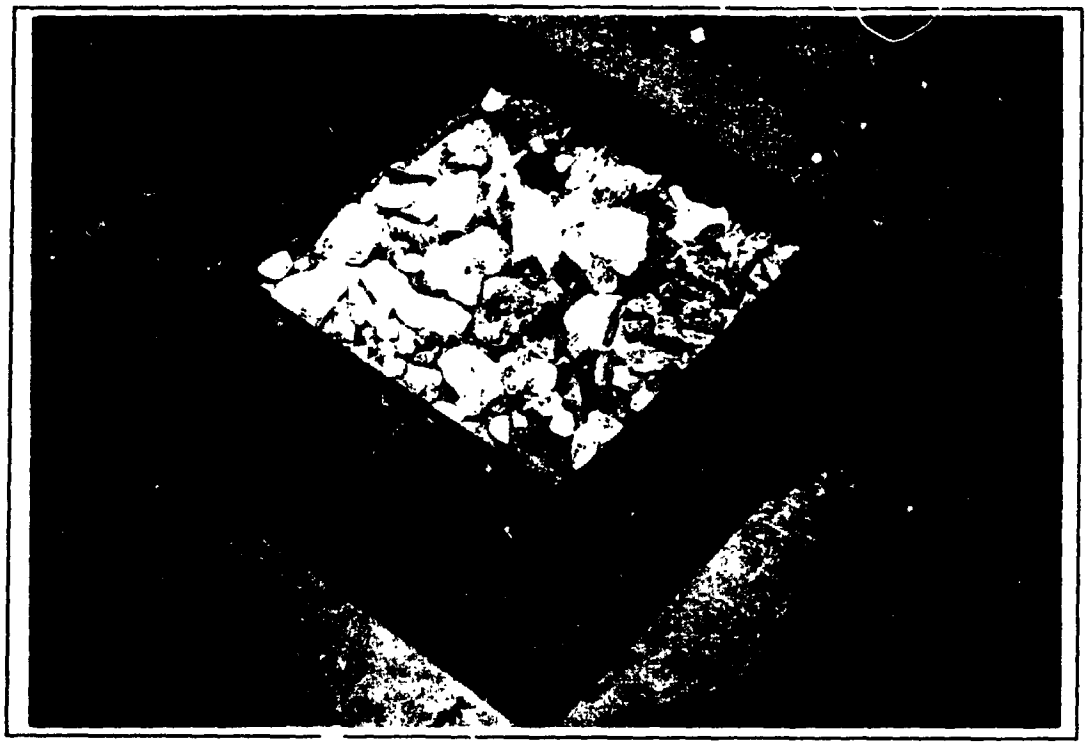

PHOTO 11.61 POROSITY MEASUREMENT OF THE STONE: A CUBIC CONTAINER WAS RANDOMLY FILLED WITH STONES AND RIVER GRAVEL ON TOP

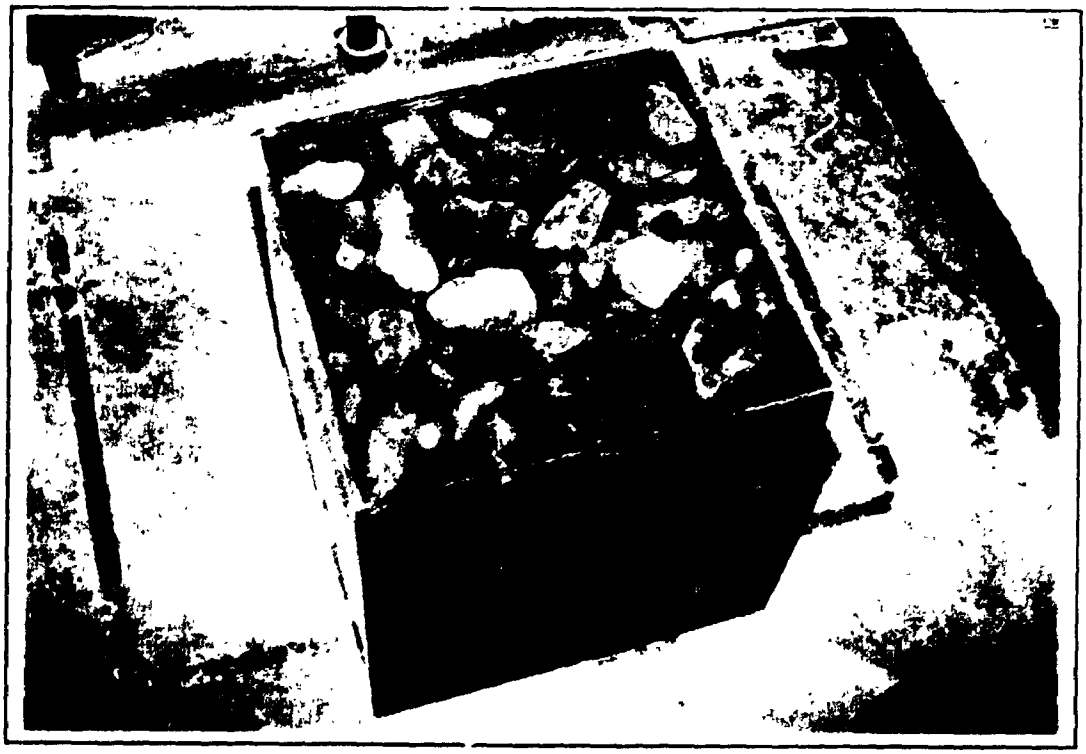

PHOTO 11.62 STONES WERE SATURATED WITH DEAIRED WATER

CHAPTER 12

SUMMARY, CONCLUSIONS AND RECOMMENDATIONS

In this chapter objectives, specific and general conclusions of the study made in individual chapters (Chapters 3 to 11) are summarized and recommendations for further research are presented.

This research described a series of laboratory experiments together with the theoretical analysis of contaminant migration through single and double layer soil systems with wide range of physical and chemical characteristics under both saturated and unsaturated conditions. The tracer used in all experiments was NaCl salt with specific attention being devoted to the Cl^- ion as a conservative species. The effective diffusion coefficients obtained for Cl^- and Na^+ ions are summarized in Tables 12.1 and 12.2 for quick reference.

The format of this chapter comprises :

(a) objectives and findings (specific conclusions) from individual chapters,

(b) general conclusions, and

(c) recommendations for further research.

12.1 SPECIFIC CONCLUSIONS

Chapter 3

At the beginning of this research program, preliminary study was done on the (1)

selection of the materials to be tested, (2) selection of the appropriate methods for materials pore water extraction and concentration measurement and (3) apparatus design for "diffusion" and "advection-diffusion" testing.

A "wash method" was successfully tested on fine and medium sand and fine gravel and was selected as the appropriate method for concentration measurement in these materials. This method was also successfully tested and used for concentration measurement in coarse stone (as will be discussed later).

The apparatus design for diffusion testing of a single layer granular material (i.e. fine and coarse sand and fine gravel) involved the following design considerations:

(1) Placement of the source solution beneath the soil to prevent from advective flow induced by gravity.

(2) Installation, saturation and desaturation (for some samples) of the soil in the test cell.

(3) Replacement of the distilled water in the source reservoir chamber with a source solution using a "flushing technique".

(4) Selection of the appropriate technique to mix the source solution during the test.

(5) Selection of the appropriate porous disk as an interface between the soil and source solution with the focus being made on the diffusion characteristics of the porous disk.

(6) Appropriate source solution sampling during the test by proper replacement of the sampled volume with the same volume of distilled water without dislocating the soil pore water.

(7) Using appropriate technique to minimize evaporation of the sample pore water during the test.

(8) In place sectioning of the sample at the end of the test without dislocating the pore water.

The apparatus designed for "small scale" advection-diffusion testing of a two-layer soil system involved the following design considerations:

(1) Using the same apparatus to be used for diffusion testing with slight modifications.
(2) Installation, saturation and gravity drainage of the granular soil in the test cell.
(3) Compaction and installation of the fine grained soil in a separate cylinder.
(4) Placement of the compacted fine grained soil on top of the granular soil with attention being made to appropriate contact between the two materials.
(5) Application of the source solution on top of the compacted fine grained soil and using the reservoir chamber of the test cell as a receptor reservoir.
(6) Selection of the appropriate techniques to mix the source and receptor reservoir solutions during the test.
(7) Source and receptor reservoirs sampling with proper replacement of the sampled volume with the same volume of distilled water (a) to maintain a constant water level in the source reservoir and (b) to prevent dislocation of the sample pore water due to the receptor reservoir sampling.
(8) Slicing the soil samples at the end of the test without dislocating the samples pore water.

Chapter 4

Four diffusion tests were conducted on fine sand (D1, D2, D3 & D4) under the condition of gravity drainage, and two tests were conducted on the compacted clayey silt. These tests were repeated (with essentially the same configurations but different test durations) for better verification of the results. The objectives of these experiments were as follows:

(1) Testing the design and methodology developed in Chapter 3.

(2) Diffusion coefficient determination of the fine sand and compacted clayey silt, using a theoretical model (program POLLUTE).

The following conclusions were made at the end of these experiments:

(1) The moisture content profiles in the tested fine sand showed that the samples remained essentially saturated (99%-100%) after gravity drainage. This was due to the fact that the matric suction in the samples was in equilibrium with the forces of gravity and the expected capillary rise in the fine sand was higher than the height of the samples tested.

(3) The average Cl^- diffusion coefficient of 9.8×10^{-10} m^2/s (Table 12.1) was found for the fine sand by fitting a theoretical curves to the experimental profiles of (a) concentration versus soil depth and (b) concentration versus elapsed time (in the source reservoir).

(4) The average tortuosity factor (D_e/D_o) of 0.53 (Table 12.1) was found for Cl^- in the fine sand by dividing the average effective diffusion coefficient of the fine sand (D_e) to the diffusion coefficient for Cl^- in aqueous solution (D_o) when diffusing together with Na^+ at the same test temperature. This value was consistent with the published value for glass beads of similar size.

(5) The calculated degree of saturation of the compacted clayey silt samples showed that both samples were tested in an almost saturated condition (S=96%) with the average porosity of 0.275.

(6) The diffusion coefficient for Cl^- giving the best fit was essentially the same for clayey silt samples with the average of 5.7×10^{-10} m^2/s (Table 12.1). The diffusion and distribution coefficients obtained for Na^+ was also essentially the same with the

average of $5.0x10^{-10}$ m^2/s and 0.15 mL/g respectively (Table 12.2). The diffusion coefficients obtained for Cl^- and Na^+ ions in this clayey soil was in the range of the reported values for clayey soils from different locations (e.g. Rowe et al., 1988).

Chapter 5

This chapter involved the "advective-diffusive" migration of NaCl salt in a two-layer soil system of fine sand over a compacted clayey silt. The materials used for this study were from the same source as used for diffusion testing in Chapter 4. A total of three tests were conducted (AD1, AD2 & AD3) with essentially the same configuration except that the fine sand sample in Test AD3 was saturated by capillary action while the other two in the duplicated Tests AD1 & AD2 were saturated by flowing water through the samples and then draining the samples by gravity. The objectives of this part of study were as follows :

(1) To develop a technique for advection-diffusion testing of a two-layer soil system of compacted fine grained soil underlain by a gravity drained granular material.
(2) To simulate a hydrogeological situation of a landfill site consisting of a compacted clayey liner underlain by a natural deposit of saturated or nearly saturated granular material such as fine sand.
(3) To predict the advective-diffusive migration of Cl^- in a two-layer soil system, using the diffusion coefficients found for Cl^- in the isolated diffusion tests conducted on the same material.

The following conclusions were made at the end of this part of study :

(1) The clayey soil and fine sand samples remained nearly saturated during the tests

and gravity drainage was not able to drain pore water due to a matric suction existing in the soils pore water.

(2) Application of two different wetting procedures resulted in slightly lower moisture content in the sand sample being saturated by capillary action (wetting) compared to those saturated by flowing water through the samples and then draining by gravity (drying). The difference in the average moisture contents was found to be 7.6 %.

(3) The duplicated drying Tests AD1 & AD2 gave essentially identical results with negligible differences which mainly arise from the slight differences between the tests.

(4) The concentration gradient in the clayey soil was greater than the underlying sand in all tests, qualitatively indicating that the migration process in clayey soil is slower than in the fine sand.

(5) Test AD3 with wetting fine sand had lower Darcy velocity compared to the duplicated Tests AD1 & AD2 with drying sand. This was likely due to the lower degree of saturation of the sand sample in wetting test (90 %) compared to those in drying tests (97.3 % & 96.0 %).

(6) The tests were analyzed using a method to predict effective diffusion coefficient of the samples knowing their volumetric moisture content and the "reference" values of the effective diffusion coefficient and porosity or volumetric moisture content of the same soils (Eq. 5.1, $D_e = D_{e(ref)}\theta/\theta_{ref}$). The diffusion coefficients for Cl^- determined from diffusion tests on isolated samples of clayey soil and fine sand (Chapter 4), along with the volumetric moisture content of each soil, was taken as the "reference" values to predict the Cl^- diffusion coefficients for clayey silt and fine sand in layered system, assuming a linear relationship to exist between the diffusion coefficient and volumetric water content of the soils. This procedure proved to give

good predictions of the concentration profiles in all advection-diffusion tests. The fact that the resulting analytical profiles fit the experimental data quite well, confirmed the applicability of the diffusion coefficient obtained from diffusion tests on isolated samples for prediction of the migration through the layered system.

(7) A comparison of the predicted profiles with the profiles obtained assuming "zero Darcy velocity" through the tests system, showed that the tests which involve Darcy velocities similar to that observed in many field situations, the velocity is sufficiently small not to significantly effect the transport of contaminants. This effect was not the case for systems including unsaturated granular material under the clayey liner (as will be discussed later).

(8) The analytical prediction using average values of the volumetric moisture content and diffusion coefficient across the soil sub-layers in wetting Test AD3 gave essentially the same results as that using slightly non-uniform values, indicating that for samples having essentially "uniform" moisture content across the soil layer, the "average" values of the volumetric moisture content and effective diffusion coefficients could be used in the analysis. This method was "not applicable" for the test systems including "unsaturated" soil with highly "non-uniform" moisture content (as will be discussed later).

(9) The tortuosity (0.515) and effective diffusion coefficient (9.5×10^{-10} m^2/s) through nearly saturated sand (the average values in Tests AD1 & AD2) was found to be 62 % greater than the saturated or nearly saturated clayey silt (0.32 & 5.9×10^{-10} m^2/s, the average values in AD1 & AD2).

(10) The tortuosity (0.515) and diffusion coefficient (9.5×10^{-10} m^2/s) of the fine sand samples in drying Tests AD1 & AD2 was found to be 9 % greater than the fine sand sample in wetting Test AD3 (0.473 & 8.8×10^{-10} m^2/s). This may be due to the hysteresis effect on the moisture content of the samples and consequently, on the tortuosity and effective diffusion coefficient.

Chapter 6

In this chapter the results of two advection-diffusion tests conducted on a two-layer soil system of compacted clayey soil underlain by (1) a wetting silt or (2) a drying silt, were described. This part of the study was in continuation of the work of Chapter 5 on contaminant migration in a two-layer system of saturated or nearly saturated soils. The objectives of this study were as follows :

(1) Further examination of the experimental and theoretical techniques developed in Chapter 5, for the prediction of the advective-diffusive migration in two-layer soil system using silt instead of fine sand as the underlying layer.
(3) Simulation of a hydrogeological system in a landfill site consisting of a clayey liner underlain by a natural deposit of nearly saturated silt.
(4) Examination of the tests systems in longer period of time (56 and 58 days) to include receptor reservoir concentration versus time data in the analysis.

The following conclusions were made at the end of these experiments :

(1) Clayey soil and silt samples remained nearly saturated during the tests due to the higher capillary rise compared to the height of the samples. This behaviour was similar to that observed in clayey soil and fine sand samples in Tests AD1, AD2 & AD3 (Chapter 5).

(2) As observed in fine sand sample in wetting Test AD3 (Chapter 5), two different wetting procedures resulted in slightly lower moisture content in the silt sample being saturated by capillary action (wetting) compared to that saturated by flowing water through the sample and then draining by gravity (drying). The difference in the moisture contents was 7.5 %. The average degree of saturation of the silt sample

(about 90 %) in wetting test was essentially the same as that observed in fine sand sample in wetting Test AD3.

(3) The shape of the concentration profiles across the soil layers in both drying and wetting tests was similar to those observed in Chapter 5, with the concentration gradient in the clayey soil being greater than the underlying silt in both tests, qualitatively indicating that the migration process in the clayey soil is slower than in the silt.

(4) Somewhat lower Darcy velocity was observed through the combined clayey silt-silt systems in both tests compared to that observed in clayey silt-fine sand systems. This might be due to the expected lower hydraulic conductivity of the silt compared to that in the fine sand.

(5) Using the method developed in Chapter 5, the effective diffusion coefficients of Cl^- in the clayey silt sublayers in both tests were predicted. Knowing the clayey silt and silt physical and geometrical characteristics and clayey silt sublayers predicted diffusion coefficients, theoretical analysis was performed using different series of effective diffusion coefficients for silt sublayers. The set of values resulting in the best fit to the experimental data was chosen as the representative effective diffusion coefficients (Table 6.3a). The resulting values (7.8×10^{-10} to 9.0×10^{-10} m^2/s) were slightly lower than the fine sand diffusion coefficient (9.8×10^{-10} m^2/s) and higher than the clayey silt diffusion coefficient (5.7×10^{-10} m^2/s). The result of the theoretical analysis using the average values of the volumetric moisture content and diffusion coefficient of the soils showed that this method also results in good fit to the experimental data with slightly better fit using the first method.

(6) The average values of the normalized diffusion coefficient or tortuosity (D_e/D_o) of the clayey soil sublayers in Tests AD4 & AD5 were 0.317 and 0.325 respectively (Table 6.3a). These values were very close to those values obtained in Tests AD1, AD2 & AD3 (Table 5.2). The average tortuosity factors in silt layers in Test AD4

& AD5 were 0.466 and 0.438 respectively. Compared to the clayey silt-fine sand drying Tests AD1 & AD2, the tortuosity and diffusion coefficient in saturated or nearly saturated fine sand was 10 % greater than nearly saturated silt in Test AD4. Similarly, the tortuosity and diffusion coefficient in 90 % saturated fine sand in wetting Test AD3 was 8 % greater than the 90 % saturated silt (Test AD5). The tortuosity and diffusion coefficient through nearly saturated silt was found to be 47 % greater than the nearly saturated clayey silt (Test AD4).

Chapter 7

The fine sand and silt samples used in previous experiments (Chapters 4, 5 & 6) did not yield any pore water under the condition of gravity drainage. This was due to the capillary tensions in these samples being greater than the force of gravity. The degree of saturation in these samples was greater than 90 % in all cases. Desaturation could be obtained using a coarser granular material which yields substantial pore water under low applied suction, leaving the significant part of the soil profile unsaturated.

The effect of unsaturated porous media on solute transport was studied in Chapter 2 and it was indicated that the natural deposits in the vadose zone or artificially created unsaturated layer or layers of soil attenuate the transport of solute and provide a form of barrier to diffusion.

Diffusion characteristics of the unsaturated porous media was studied in Chapter 7 using coarse sand and fine gravel as a porous media and Cl^- and Na^+ as a diffusing species. First, both materials were tested under saturated conditions to provide the "reference values" of the effective diffusion coefficients and porosity for further predictions of the diffusion coefficients in unsaturated case. Then the materials were tested under conditions of gravity drainage by maintaining the atmospheric pressure level

at the bottom of the samples. In summary, the objectives of these experiments were as follows:

(1) To obtain the diffusion coefficient and tortuosity of the diffusing ions in "saturated" coarse sand and fine gravel.
(2) To obtain the diffusion coefficient and tortuosity of the diffusing ions in the "unsaturated" coarse sand and fine gravel.
(3) To predict the diffusive migration of NaCl through the unsaturated materials using the method developed in Chapter 5 for prediction of the unsaturated porous medium diffusion coefficient using its volumetric moisture content along with the reference values of the diffusion coefficient and porosity in the saturated material.
(4) To examine the effectiveness of the unsaturated porous medium as a "diffusion barrier".

The following conclusions were made at the end of this study :

(1) Both coarse sand and fine gravel gave essentially the same diffusion coefficients for Cl^- and Na^+ under saturated condition. More likely, this is attributed to the equal porosity that these materials had during the test.

(2) After gravity drainage, both materials yielded a great amount of pore water leaving a significant portion of the soil profile unsaturated. Due to the smaller effective grain size of the coarse sand than the fine gravel, the capillary fringe was higher. The observed capillary rise in both materials was consistent with the values calculated by two different theoretical methods suggested in the literature.

(3) Observed concentration profiles in six diffusion tests conducted on both materials showed that the Cl^- and Na^+ ions have diffused much slower in the unsaturated zone

compared to the capillary saturated zone. This behaviour was manifested by a sharp decrease in the slope of the concentration profiles just above the capillary fringe.

(4) Theoretical analysis using the assumption of linear proportionality between the volumetric moisture content and the effective diffusion coefficient of the unsaturated soil (Eq. 5.1) resulted in a good fit to the experimental data. These results confirmed the applicability of the developed method in the unsaturated soils examined.

(5) Results of the theoretical analysis showed that for the soils having highly non-uniform water contents, the method using the volumetric moisture content and diffusion coefficients averaged for the entire soil profile "can not" be adopted. This method is only applicable for soils having relatively uniform water content (as discussed in Chapters 5 & 6).

(6) Comparison of the experimental and predicted concentration profiles of two selected tests conducted on the unsaturated coarse sand and fine gravel (D8 and D10) with the theoretical concentration profile of a compacted clayey layer having the same thickness showed that for the time of migration considered, the concentration front in clayey soil is higher than that in the unsaturated soils, indicating that the movement of chloride ion in clayey silt is faster than in the unsaturated coarse sand and fine gravel.

Chapter 8

This chapter involved the advective-diffusive migration of NaCl in a two-layer soil system of nearly saturated clayey soil over the unsaturated fine gravel (Tests AD6 & AD7). Geometrical characteristics of the tests were similar to the tests involved two-layer soil system including a compacted clayey soil over a nearly saturated fine sand (Chapter 5) and silt (Chapter 6) with the difference being that the underlying material

was unsaturated. The objectives of these experiments were as follows :

(1) To examine the applicability of the experimental technique developed in Chapters 5 and 6 for advection-diffusion testing on a two-layer soil system including unsaturated soil instead of a nearly saturated soil as the underlying layer.

(2) To simulate a hydrogeological or engineered situation in a landfill site comprising a compacted clayey liner underlain by a natural or artificial deposit of an unsaturated granular material such as fine gravel.

(3) To predict the advective-diffusive behaviour of Cl^- and Na^+ ions in the two-layer soil system based on the transport parameters obtained from diffusion tests conducted on the isolated soils of the same type.

(4) To study the effectiveness of the underlying unsaturated porous media as a "diffusion barrier" for contaminants.

The following conclusions were made at the end of these experiments :

(1) The results showed that the experimental methodology developed in Chapters 5 and 6 worked well for the case involving unsaturated granular layer underlying the clayey layer.

(2) The migration process in the unsaturated zone of the fine gravel layer was very slow and the concentration of ions in this zone had dropped to very low values when it migrated downward through the soil profile. This was due to existing of a very tortuous path in the unsaturated pore space which created a longer path to be travelled by the diffusing ion.

(3) Theoretical prediction of the concentration profiles which were based on parameters from the pure diffusion tests gave good agreement with the observed behaviour.

(4) The effect of the Darcy velocity on the migration through the unsaturated zone of the fine gravel was found to be significant. This behaviour was in contrast with the finding in Chapter 5 which involved nearly saturated fine sand as the underlying soil. This was due to the fact that at low levels of saturation in the soil, the flow paths become much narrower and hence water and contaminant moves faster in a zone where flow is limited to a small portion of the soil pores cross-section.

Chapters 9 and 10

Chapters 9 and 10 include the experimental and theoretical results of four large scale advection-diffusion tests conducted under "high" (8.1×10^{-8} m/s), "moderate" (3.9×10^{-9} m/s) and "low" (5.5×10^{-10} m/s) Darcy velocities. Three "large scale" apparatus were designed and used in these experiments. The apparatus design involved the following design considerations:

(1) Installation, saturation and gravity drainage of the clear stone in the test cell.
(2) Selection of the appropriate material as a filter/separator between the fine grained soil and clear stone.
(3) In place compaction of the fine grained soil on top of the clear stone.
(4) Selection of the appropriate techniques to mix the source and receptor reservoir solutions during the test.
(5) Source and receptor reservoirs sampling by proper replacement of the sampled volume with the same volume of distilled water.
(6) Adopting the appropriate technique for sampling from the compacted fine grained soil at the end of the test.
(7) Adopting the appropriate technique for sectioning the clear stone layer at the end of the test.

The geometrical configuration of the tests were similar to the small scale tests described in the previous chapters (e.g. Chapter 8) and involved a 12-13 cm thick compacted silt (Tests AD8 & AD9) or clayey silt (Tests AD10 & AD11) over a 38 cm thick unsaturated clear stone. The source solution was placed on top of the compacted soil layer and the receptor solution were collected in a receptor reservoir beneath the unsaturated stone. The methodology for tests set up, monitoring, sampling and experimental analysis was somewhat different than the small scale tests. The objectives of this part of research program were as follows:

(1) To simulate an engineered situation in a landfill site comprising a compacted liner over an unsaturated secondary leachate collection system.
(2) To examine the respond of the test systems under "high", "moderate" and "low" flow rates with the special attention being made to the behaviour of the underlying unsaturated stone layer.
(3) To predict the behaviour of the migrating ions (a) during the tests and (b) at the end of the tests using the information obtained from small scale tests.

The following conclusions were made at the end of this study :

(1) The experimental methodology for tests "set up" which was examined in a preliminary test prior to the actual tests and also methodology adopted for monitoring, sampling and experimental analysis showed to work well for all tests.

(2) The test with "high" flow rate (AD8) showed a very rapid migration so that after only 15 days of migration concentration in the receptor was about 1/3 of the initial source concentration. Test with "moderate" flow rate showed moderate migration,

and concentration in the receptor after about 160 days of migration was about 1/7 of the initial concentration Test with "low" flow rate showed significantly low migration rate with concentration in the receptor being 1/28 of the initial concentration after a longer period of migration (480 days) compared to the two other tests of AD8 & AD9. This behaviour was directly attributed to the effect of overlying compacted liner as an advection control layer.

(3) In all tests concentrations across the compacted soil layers were quite consistent. There was some scatter of the data in the stone layers which may be partly attributed to experimental error but is also likely partly due to statistical variations in stone size, shape and arrangement which would effect the preferential flow and also mechanical dispersion in the stone layer at the range of the velocities examined.

The observed Cl^- concentrations in the stone layers were quite high and relatively uniform with depth. This was likely due to the limited pore water available for migration in the stone and the fact that the ground water velocity along the wetted surface of the stones was quite high and hence there was rapid and relatively uniform migration through the stone at the Darcy velocities examined.

(4) Theoretical analysis using predicted effective diffusion coefficient for soil and unsaturated stone layers resulted in a good fit to the compacted silt and clayey silt data in all tests but predictions were not quite as good in the unsaturated stone layers. The analysis using slightly higher values as the "hydrodynamic dispersion coefficient" of the unsaturated stone layers gave better predictions with essentially no effect on the predictions in silt (Tests AD8 & AD9) and clayey silt (Test AD10) and also source and receptor reservoirs data. This indicated the effect of some dispersion in the unsaturated stone layers with slightly higher effect in Test AD8 with high flow rate. The effect of dispersion in tests with moderate (AD9) and low (AD10) flow rate was negligible and results showed that for stone similar to that examined here and typical cases where the advective velocity is likely to be of the order of 0.12 m/a or less, the effect of dispersion can be neglected without any significant loss of accuracy. Comparison of the calculated dispersivity values from the three tests

(AD8, AD9 & AD10) showed that for the range of the flow rates examined, dispersivity (α) is approximately a linear function of groundwater velocity (v) rather than a constant (as normally assumed).

(5) Verification of the results of the test with low permeability compacted clayey silt (AD10) showed that both advection and diffusion play comparative role in the migration process although the Darcy velocity was quite low (5.5×10^{-10} m/s or 0.017 m/a) and the effect of dispersion is negligible.

(6) Based on the available data, prediction of the theory for duplicated Test AD11 (in progress) is reasonably accurate.

Chapter 11

Chapter 11 involved the study of potential intrusion of compacted clayey till into the coarse stone when (1) a geotextile (Polyfelt TS650) or a granular material was used as a filter/separator between the soil and stone, and (2) when no filter/separator exists between the soil and stone. Tests were performed under large vertical pressures (up to 600 kPa) and 100 kPa pore pressure inside the stone to simulate the severe field conditions. The geotextile used in this study was the same geotextile used as a separator between the soil and the unsaturated stone in Tests AD8, AD9, AD10 & AD11.

The following conclusions were made at the end of this study :

(1) The geotextile efficiently minimized the intrusion of the soil into the stone void space and the actual quantity of fines which passed through the geotextile was insignificant with respect to the occupancy of void space in the stone. It is

considered that most of the fines passed through the geotextile due to compaction during installation of the clayey soil in the test cell and not due to the applied vertical pressure and water pressure.

(2) The granular filter/separator between the clayey soil and stone worked well and the amount of intruded fines was also insignificant with respect to occupancy of void space in the stone. The intrusion of the granular filter into the stone was limited to the upper 2.6-3.0 cm of the stone.

(3) In tests when no filter/separator was used in the final loading phase of the test, a significant amount of soil was observed to be intruded into the void spaces in the stone layer. The voids in the upper 3.5-4.0 cm of stone were almost completely filled with clayey soil. Conservatively considering the total intruded mass to be localized directly below the clayey silt plug, the void space occupied by the clayey soil was equivalent to that of a thickness of about 7 cm of stone. Although there was significant intrusion of clayey soil into the stone when there was no filter/separator between the clayey soil and stone, even with the worst case interpretation of the data most of the void space in the stone remained open.

12.2 GENERAL CONCLUSIONS

General conclusions representing the most important contribution of this thesis to the present knowledge of contaminant migration in saturated and unsaturated soils and stone are as follows :

(1) Diffusion coefficients for the selected chemical species in "saturated or nearly saturated" granular material can be determined directly by means of the 1-dimensional laboratory tests described in this thesis.

(2) Diffusion coefficients for the selected chemical species in the "unsaturated" granular material can be determined by means of the 1-dimensional laboratory diffusion tests described in this thesis, using the saturated diffusion coefficients obtained from the diffusion test on the saturated material. Predictions then can be made assuming a linear relationship to exist between the volumetric moisture content and the effective diffusion coefficient of the unsaturated material.

(3) Diffusion coefficients determined from diffusion tests on isolated clayey or granular material can be used with 1-dimensional advective-diffusive theory to predict the contaminant migration in a two-layer soil system including a compacted clayey soil underlain by (1) a nearly saturated or (2) an unsaturated granular material.

(4) A relatively high and uniform concentrations were observed in the unsaturated stone layer simulating the secondary leachate collection system of a landfill site in the large scale laboratory models developed. This behaviour was accurately modeled by the 1-dimensional advective-diffusive theory using the transport parameters obtained from the previous experiments. The effect of the groundwater velocity was found to be significant in migration through the stone, even in low flow rate system.

(5) The geotextile and granular filter/separators efficiently prevented from the intrusion of a compacted clayey soil into a pressurized coarse stone layer under high applied pressures. These materials were recommended for engineering practice to be used in landfill applications with more confidence.

12.3 RECOMMENDATIONS FOR FURTHER RESEARCH

(1) Unsaturated fine gravel in diffusion and advection-diffusion tests showed that this material can be used effectively as a "diffusion barrier". Diffusion and advection-diffusion tests could be carried out using the intermediate grain size material such as pea gravel (or coarser) to examine the effect of grain size on migration process.

(2) Diffusion tests could be carried out on "saturated" clear stone by some modification to the test cell, to more accurately determine the saturated diffusion coefficient of the stone. This parameter then can be used as the "reference" value to more accurately predict the diffusion coefficient of the unsaturated clear stone.

(3) Laboratory diffusion and advection diffusion tests could be carried out on the same material examined in this thesis but with different chemical species to examine the bahaviour of other chemicals in saturated and unsaturated granular material.

(4) Using the experimental methodology developed for advection-diffusion testing of two-layer systems, laboratory models could be set up to simulate more complicated landfill situations consisting of saturated-unsaturated layered systems.

(5) Diffusion and advection diffusion tests could be carried out at various temperatures (e.g. from 5 °C up to 30 °C), in order to examine the effect of temperature on the back-figured diffusion coefficient. This work would be important since landfill leachate temperatures are known to vary throughout the life of the landfill.

TABLE 12.1 SUMMARY OF THE EFFECTIVE DIFFUSION COEFFICIENTS (D_e) AND NORMALIZED DIFFUSION COEFFICIENTS OR TORTUOSITY (D_e/D_o OR τ) FOR [Cl^-] IN THE CLAYEY SILT, SILT TRACE CLAY, SILT SOME CLAY, SILT, FINE SAND, COARSE SAND, FINE GRAVEL AND CLEAR STONE

	D_e (m^2/s)		D_e/D_o	
	Saturated (Reference Values)	Unsaturated	Saturated	Unsaturated
Clayey silt	5.7×10^{-10} (0.28)[1]	--	0.31	--
Silt, trace clay	8.9×10^{-10} (0.43)	6.9×10^{-10} (0.33)	0.48	0.37
Silt, some clay	8.2×10^{-10} (0.40)	6.2×10^{-10} (0.30)	0.44	0.34
Silt	9.0×10^{-10} (0.40)	7.8×10^{-10} (0.343)	0.49	0.42
Fine Sand	9.8×10^{-10} (0.37)	8.1×10^{-10} (0.30)	0.53	0.44
Coarse sand[2]	10.4×10^{-10} (0.38)	9.7×10^{-11} (0.036)	0.56	0.05
	--	2.0×10^{-10} (0.072)	--	0.11
	--	6.0×10^{-10} (0.221)	--	0.32
Fine gravel[2]	10.4×10^{-10} (0.38)	8.5×10^{-11} (0.031)	0.56	0.05
	--	1.8×10^{-10} (0.064)	--	0.10
Clear stone[3]	--	3.0×10^{-10} (0.035)	--	--
	--	2.4×10^{-9} (0.031)	--	--
	--	3.6×10^{-7} (0.027)	--	--

1 - Listed values in the parentheses are the porosity values for the saturated samples and volumetric moisture content values for the unsaturated samples

2 - Listed values for the unsaturated coarse sand and fine gravel are the average values (see tables in the inserts of Figs. 7.23a & 7.23b)

3 - Listed values for the clear stone are the hydrodynamic dispersion coefficients obtained in Tests AD8, AD9 & AD10 under Darcy velocities of 0.017 m/a, 0.12 m/a and 2.6 m/a respectively.

TABLE 12.2 SUMMARY OF THE EFFECTIVE DIFFUSION COEFFICIENTS (D_e) AND NORMALIZED DIFFUSION COEFFICIENTS OR TORTUOSITY (D_e/D_o OR τ) FOR [Na^+] IN THE CLAYEY SILT, SILT SOME CLAY, COARSE SAND, FINE GRAVEL AND CLEAR STONE

	D_e (m^2/s)		D_e/D_o		K_d (mL/g)
	Saturated (Reference Values)	Unsaturated	Saturated	Unsaturated	
Clayey silt	5.1×10^{-10} (0.28)[1]	--	0.41	--	0.15
Silt, some clay	7.3×10^{-10} (0.40)	5.5×10^{-10} (0.30)	0.58	0.44	0.28
Coarse sand[2]	6.9×10^{-10} (0.38)	6.0×10^{-11} (0.036)	0.56	0.05	0.0
	--	1.3×10^{-10} (0.072)	--	0.11	0.0
	--	3.9×10^{-10} (0.221)	--	0.32	0.0
Fine gravel[2]	6.9×10^{-10} (0.38)	5.6×10^{-11} (0.031)	0.56	0.05	0.0
	--	1.1×10^{-10} (0.064)	--	0.09	0.0
Clear stone[3]	--	2.5×10^{-10} (0.035)	--	--	0.0
	--	2.0×10^{-9} (0.031)	--	--	0.0

1 - Listed values in the parentheses are the porosity values for the saturated samples and volumetric moisture content values for the unsaturated samples

2 - Listed values for the unsaturated coarse sand and fine gravel are the average values obtained from Table 7.8

3 - Listed values for the clear stone are the hydrodynamic dispersion coefficients obtained in Tests AD9 & AD10 under Darcy velocities of 0.017 m/a and 0.12 m/a respectively.

APPENDIX A

[Cl^-] MASS BALANCE CALCULATIONS FOR STAINLESS STEEL POROUS DISK DIFFUSION TEST

Calculation of the available volume :

volume of the source reservoir = 251.4 cm^3

volume of the upper reservoir = 1.92x45.604 = 87.6 cm^3

volume of the pores in disk = 24.93x0.53 = 13.21 cm^3

---

total available volume = 352.14 cm^3

Initial mass available :

[1.125(mg/mL) x [(251.4(cm^3)+13.21(cm^3)] = 297.7 mg

Observed equilibrium concentration = 815 mg/L

Final mass = mass recovered at the end of the test + mass removed during sampling

= 0.815 x 352.14 + 2.0 x 9.14 = 287.0 + 18.28 = 305.3 mg

Percent mass recovery = Final mass / Initial mass = (305.3 / 297.7) x 100 = 102.6 %

Input data for POLLUTE :

Using program POLLUTE to calculate the diffusion coefficient of the disk, two layers were modelled. The first layer is the layer of water in upper reservoir with the thickness of 1.92 cm measured at the beginning of the test and porosity of 1 and a very high diffusion coefficient. This high diffusion coefficient simulates the effect of mixing in upper reservoir to maintain uniform concentration throughout the upper reservoir at any time during the test. Second layer is the porous disk having the thickness of 0.3075 cm.

Layers data for this test is shown in table below:

Layer No.	Diffusion Coefficient (m^2/s)	Matrix Porosity (cm^3/cm^3)	Distribution Coefficient (cm^3/g)	Dry Density (g/cm^3)	Layer Thickness (cm)
1	0.011	1	0	1.0	1.92
2	8.68×10^{-10}	0.53	0	3.475	0.3075

To take into account the effect of dilution due to replacing of solution with distilled water in sampling processes, the option of "fixed outflow velocity" was chosen as the bottom boundary condition in POLLUTE. Fixed outflow velocity at the base is defined by:

Landfill length = 7.938 cm

Landfill width = 6.234 cm

Base thickness = 5.08 cm

Base porosity = 1.0

Outflow velocity = 0.0673 cm/s

Removed mass due to sampling is taken into account by introducing the base landfill dimensions and also base outflow velocity which is calculated as follows:

Base outflow velocity = (volume of sample x sampling times) / (base width x base thickness x duration of the test)

As the shape of the base (source reservoir) is cylindrical, a rectangular prism having the length equal to the diameter of the source reservoir and the width selected to give an equivalent volume in the source reservoir.

APPENDIX B

DESCRIPTION OF CHEMICAL TESTS USED FOR QUANTITATIVE MINERALOGICAL ANALYSIS

TABLE B1 DESCRIPTION OF CHEMICAL TESTS USED FOR QUANTITATIVE MINERALOGICAL ANALYSIS

Chemical Test	Method	Reference
Total Carbonate Analysis	Soil carbonates are dissolved in 6 N HCl using the Chittick apparatus. The volume of CO_2 gas evolved is measured and then used to calculate the total percentage of carbonates (air dried soil is used).	Dreimanis (1962)
Total Potassium Analysis	The soil sample is oven dried and completely digested with hydrofluoric and perchloric acids. The solution is then analyzed for K^+ concentration by atomic absorption spectrophotometry.	Pratt (1965)
Cation Exchange Capacity	Carbonate free soil exchange sites are sodium saturated by washing air dried soil with a 1.0 M sodium acetate solution. The adsorbed sodium is then replaced with magnesium by washing the soil with a 0.5 M magnesium acetate solution. The mass of sodium released from the clay is measured using an atomic absorption spectrophotometer, and the CEC calculated. For natural soil, subtraction of the pore water cations from the total cations displaced by combined silver thiourea and KCl washing yielded the adsorbed cation regime. The sum of these adsorbed species yielded an approximate value of CEC.	Bower et al.(1952)

TABLE B1 (CONT.)

Chemical Test	Method	Reference
Quartz Content	Air dried pulverized soil (< 74 μm) is mixed with potassium periodate KIO_4 and the mixture is analyzed by X-ray diffraction. The ratio of the quartz 4.26Å peak height to the KIO_4 5.22Å peak height is then used to calculate the percentage quartz.	Foscal-Mella (1976)
Organic Matter and Total Organic Carbon Content	Oven dried (< 0.106 mm) soil is digested with a maximum of an oxidizing agent (potassium dichromate) and a strong acid (sulphuric acid). The entire soil mixture is then titrated with an ammonium ferrous sulphate solution until the colour changes from green to black. The amount of ammonium ferrous sulphate added is used to calculate the % organic matter and % total organic carbon content.	Walkley and Black (1934)

APPENDIX C

[NaCl] SOLUTION PREPARATION AND ANALYSIS

1. NaCl SOLUTION PREPARATION

The NaCl solution is prepared by pouring 3.294 g NaCl mass into a 2000 mL flask and adding de-ionized distilled water up to the mark. The resulting solution will have 1000 mg/L Cl^- concentration. To prepare a solution with 2000 mg/L Cl^- concentration, the amount of NaCl mass should be doubled.

2. ANALYSIS OF CHLORIDE SOLUTIONS

Solutions were analyzed for their chloride content by using a multipurpose potentiometer (701A digital pH/mV meter). Using a series of standard solutions with chloride concentrations ranging from 0.25 mg/L to 1500 mg/L, a calibration curve is constructed on semi-logarithmic paper. Electrode potentials of standard solutions are measured and plotted on the linear axis against their concentrations on the log axis. More than 3 points is normally needed to accurately construct a calibration curve. Calibration must be checked in every 3 to 5 sample readings. To prepare samples for measurements, 25 mL diluted sample is transferred into a 100 mL beaker and 0.5 mL ISA solution (ionic strengthening) is added. The electrodes then rinsed and dried and placed in the sample. The sample stirred and millivolt reading was recorded when it was stable. The concentration was then determined from calibration curve. If during a reading it was noticed that the calibration had changed, a new calibration (as described above) should be established and used.

APPENDIX D

A SAMPLE OF CHLORIDE MASS BALANCE CALCULATIONS IN DIFFUSION TESTS

TEST # D2

Soil properties

Porosity = 0.364

Thickness = 13.1 cm

[Cl^-] background concentration = 0.005 mg/mL

Initial mass

a - In soil pore water :

Mass = soil porosity x soil thickness (cm) x 1 (unit area, cm^2) x soil background concentration (mg/mL)

Mass = 0.364 x 13.1 x 1 x 0.005 = 0.0238 mg

b - In source reservoir :

c_o = 1.275 mg/mL

Mass = reservoir normalized height (cm) x 1 (unit area, cm^2) x initial source concentration (mg/mL)

Mass = [251.37(reservoir volume)/45.604(soil cross-section)]x1.0x1.275 = 7.03 mg

INITIAL MASS = a + b = 0.0238 + 7.03 = 7.0538 mg

Final mass

a - In soil pore water :

Σ mass = Σ [slice thickness (cm) x porosity x 1 (unit area, cm^3) x slice pore water concentration (mg/mL)]

slice #	Slice Thickness (cm)	Porosity (cm^3/cm^3)	Pore Water Concn. (mg/mL)	Pore Water Mass (mg)
1	1.55	0.364	0.0035	0.00019
2	1.60	0.364	0.0047	0.00027
3	1.60	0.364	0.0021	0.00119
4	1.60	0.364	0.0149	0.00870
5	1.60	0.364	0.0610	0.03550
6	1.60	0.364	0.1858	0 10820
7	1.60	0.364	0.4201	0.24470
8	1.95	0.364	0.6180	0.43900
9 (disk)	0.3075	0.53	0.792	0.129

				Σ mass = 0.9664mg

b - In source reservoir

Mass = final source reservoir concentration (mg/mL) x normalized solution height (cm) x 1 (unit area, cm^2)

Mass = 0.9625 x 5.51 x 1.0 = 5.303 mg

c - Mass removed due to sampling:

Mass = (volume removed / soil cross-section) x 1 (unit area, cm^3) x average source reservoir concentration for the period of the test (mg/mL)

Mass = [(12 x 2.15) / 45.604] x 1.0 x 1.119 = 0.633 mg

TOTAL FINAL MASS = a + b + c = 0.9664 + 5.303 + 0.633 = 6.902 mg

PERCENT MASS RECOVERY = TOTAL FINAL MASS / TOTAL INITIAL MASS

= 6.902 / 7.054 = 0.978 OR 97.8 %

APPENDIX E

A SAMPLE OF CHLORIDE MASS BALANCE CALCULATIONS IN ADVECTION-DIFFUSION TESTS

TEST # AD3

Soil properties

a - Clayey silt :

Volumetric moisture content = 0.28-0.314 cm^3/cm^3

Thickness = 5.1 cm

$[Cl^-]$ background concentration = 0.123 mg/mL

b - Fine sand :

Volumetric moisture content = 0.303-0.363 cm^3/cm^3

Thickness = 10.1 cm

$[Cl^-]$ background concentration = 0.005 mg/mL

Initial mass

a - In clayey silt pore water :

Mass = soil porosity x soil thickness (cm) x 1 (unit area, cm^2) x soil background concentration (mg/mL)

Mass = 0.305 x 4.93 x 1 x 0.123 = 0.185 mg

b - In fine sand pore water :

Mass = 0.328 x 10.1 x 1.0 x 0.005 = 0.0166 mg

c - In source reservoir :

c_o = 1.66 mg/mL

Mass = reservoir height (cm) x 1 (unit area, cm^2) x initial source

concentration (mg/mL)

Mass = 2.9 x 1.0 x 1.66 = 4.814 mg

d - In receptor reservoir :

Mass = 5.51 x 0.00075 = 0.0041 mg

TOTAL INITIAL MASS = a + b + c + d = 0.185 + 0.0166 + 4.814 + 0.00413

= 5.01 mg

Final mass

a - In clayey silt pore water :

$\sum$ mass = $\sum$ [slice thickness (cm) x volumetric moisture content x 1 (unit area, cm^2)

x slice pore water concentration (mg/mL)]

slice #	Slice Thickness (cm)	Porosity (cm^3/cm^3)	Pore Water Concn. (mg/mL)	Pore Water Mass (mg)
1	1.27	0.314	0.836	0.333
2	1.27	0.303	0.748	0.287
3	1.26	0.295	0.666	0.247
4	1.30	0.280	0.564	0.205
				$\sum$ mass = 1.073 mg

b - In fine sand pore water :

slice #	Slice Thickness (cm)	Porosity (cm^3/cm^3)	Pore Water Concn. (mg/mL)	Pore Water Mass (mg)
1	1.60	0.303	0.399	0.193
2	1.65	0.318	0.317	0.166
3	1.65	0.330	0.282	0.153
4	1.60	0.326	0.195	0.102
5	1.55	0.330	0.134	0.068
6	2.05	0.363	0.074	0.055
7(disk)	0.3075	0.530	0.057	0.009

				Σmass = 0.747 mg

c - In source reservoir :

Mass = final source reservoir concentration (mg/mL) x solution height (cm) x 1 (unit area, cm^2)

Mass = 0.794 x 2.7 x 1.0 = 2.14 mg

d - In receptor reservoir :

Mass = final receptor reservoir concentration (mg/mL) x normalized solution height (cm) x 1 (unit area, cm^2)

Mass = 0.0406 x 5.51 x 1.0 = 0.224 mg

e - Mass removed due to sampling :

e.1 From source reservoir :

Mass = (volume removed / soil cross-section) x 1 (unit area, cm^2) x average source reservoir concentration for the period of the test (mg/mL)

Mass = [(15 x 2.25) / 45.604] x 1.0 x 1.11 = 0.82 mg

e.2 From receptor reservoir :

Mass = (volume removed / soil cross-section) x 1 (unit area, cm^2) x average receptor

reservoir concentration for the period of the test (mg/mL)

Mass = [(13 x 2.25) / 45.604] x 1.0 x 0.01325 = 0.0085 mg

Total mass removed = e = e.1 + e.2 = 0.82 + 0.0085 = 0.8285 mg

TOTAL FINAL MASS = a + b + c + d + e = 1.073 + 0.747 + 2.14 + 0.224 + 0.8285 = 5.01

PERCENT MASS RECOVERY = TOTAL FINAL MASS / TOTAL INITIAL MASS

= 5.01 / 5.01 = 1.0 or 100 %

APPENDIX F

INCREMENTAL ANALYSIS FOR TESTS AD10 AND AD11

Incremental analysis for Tests AD10 and AD11

The analysis was performed by using the "Variable Properties" option in POLLUTEv6. The analysis started by selecting one time period and using the initial source concentration (c_o) and source solution height ($H_f(t=0)$). After performing the analysis for one time period (say $\Delta t=25$ days) the following hand calculations were made to calculate the new source solution height ($H_f(t=25)$) and the concentration ($c'(t=25)$) based on conservation of mass, and recognising that POLLUTE assumes that the advective flow out of the reservoir is being replaced by distilled water:

Initial source solution height at time zero : $H_f(t=0)$ = 12.0 cm

Initial source solution concentration at time zero : c_o = 1930 mg/L

Calculated source concentration at 25 days (by POLLUTE) : $c(t=25)$ = 1764 mg/L

Calculated change in source solution height at 25 days : $\Delta H_f(t=25) = \Delta t.v_a$ = 25(days) x 0.0048(cm/day) = 0.12 cm

New source solution height at 25 days : $H_f(t=25) = H_f(t=0) - \Delta H_f(t=25)$ = 12.0 - 0.12 = 11.88 cm

Adjusting factor to calculate the expected source solution concentration at 25 days : $A = H_f(t=0)/H_f(t=25)$ = 12/11.88 = 1.01

The expected source solution concentration at 25 days = $c'(t=25) = c(t=25)$ x A = 1764 x 1.01 = 1782 mg/L. It should be noted that this adjustment is made to correct for the dilution that POLLUTE had assumed had occurred over this time period which, in fact had not occurred.

The second run was performed using two time periods in POLLUTE (i.e., 0-25, 25-50 days) and using $c'(t=25)$=1782 mg/L and $H_f(t=25)=11.88$ cm for predicting the concentration between 25 and 50 days. The value of H_f and $c(t=50)$ were then adjusted

as described above. The analysis was repeated in an incremental manner by increasing the time periods in each run until the time of the first dilution in the source reservoir (i.e, 177 days). At this time the water level in the source reservoir was increased to almost the original water level. This change in the water level was added to the last calculated H_f value and the volume of the source solution after first dilution was calculated. The available contaminant mass in the source reservoir before dilution was calculated knowing the concentration and the volume of the source solution before dilution and hence could be used to find the new source concentration after the dilution. The analysis proceeded in an incremental manner using the newly calculated H_f and concentration, up to the next dilution time at which the entire process described above was repeated. This cycle continued until the end of the test.

It is noted that if the loss of fluid due to flow into the soil had been continuously replaced by distilled water, the height of leachate, H_f, would have remained constant and the test could have been easily modelled using the "Finite Mass" option in POLLUTE. In fact if this procedure is adopted one gets a good "average" estimate of the change in concentration with time as shown in Figs. F1 and F2. However to more accurately model the actual experimental procedure it is necessary to adopt the incremental procedure described above. When this is done, the agreement between POLLUTE and the experimental data is excellent as is a'so evident from Figs. F1 and F2.

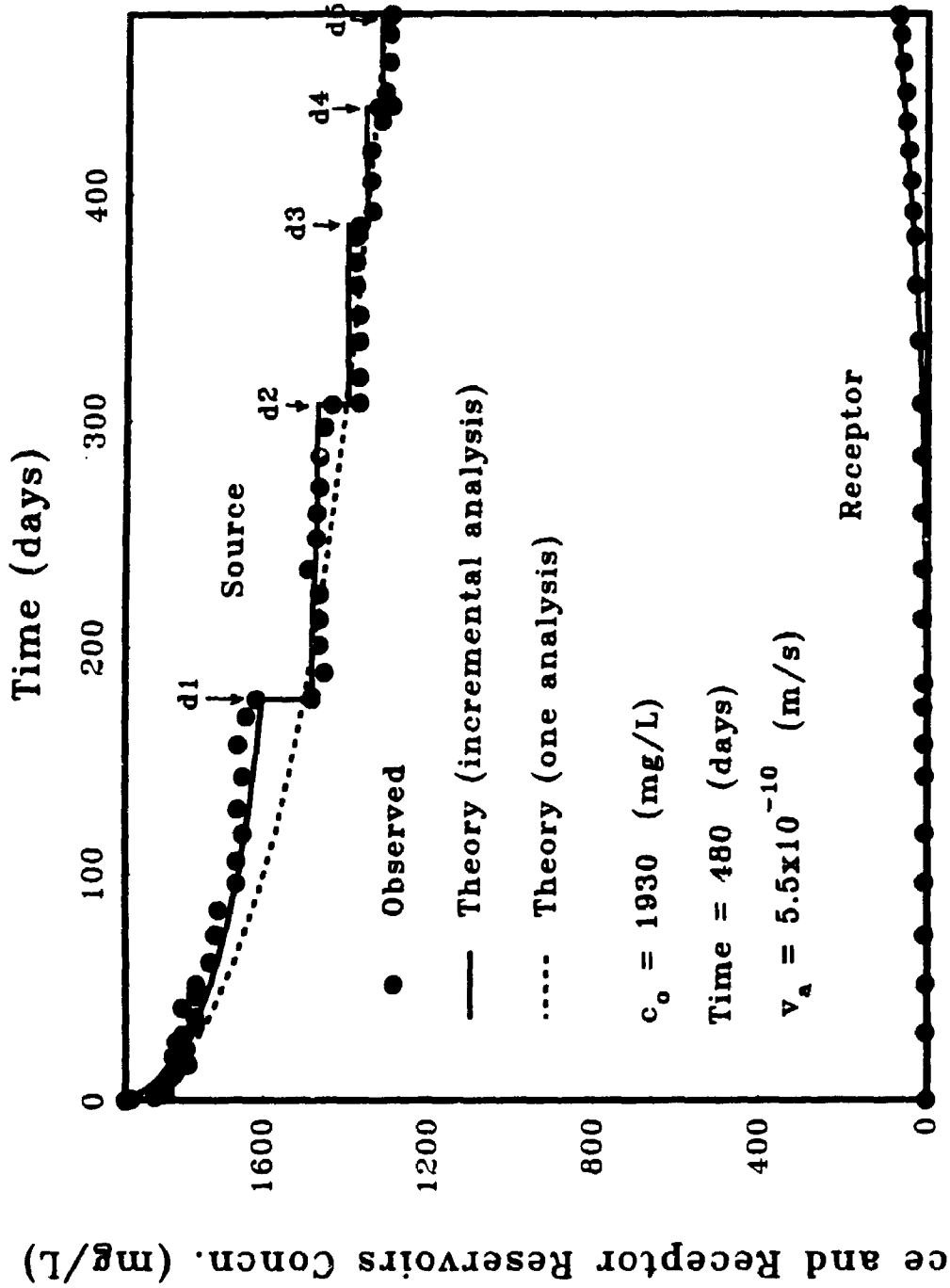

FIG. F1 OBSERVED AND CALCULATED $[Cl^-]$ CONCENTRATIONS VERSUS ELAPSED TIME IN SOURCE AND RECEPTOR RESERVOIRS OF TEST #AD10, BASED ON TWO DIFFERENT ANALYSIS

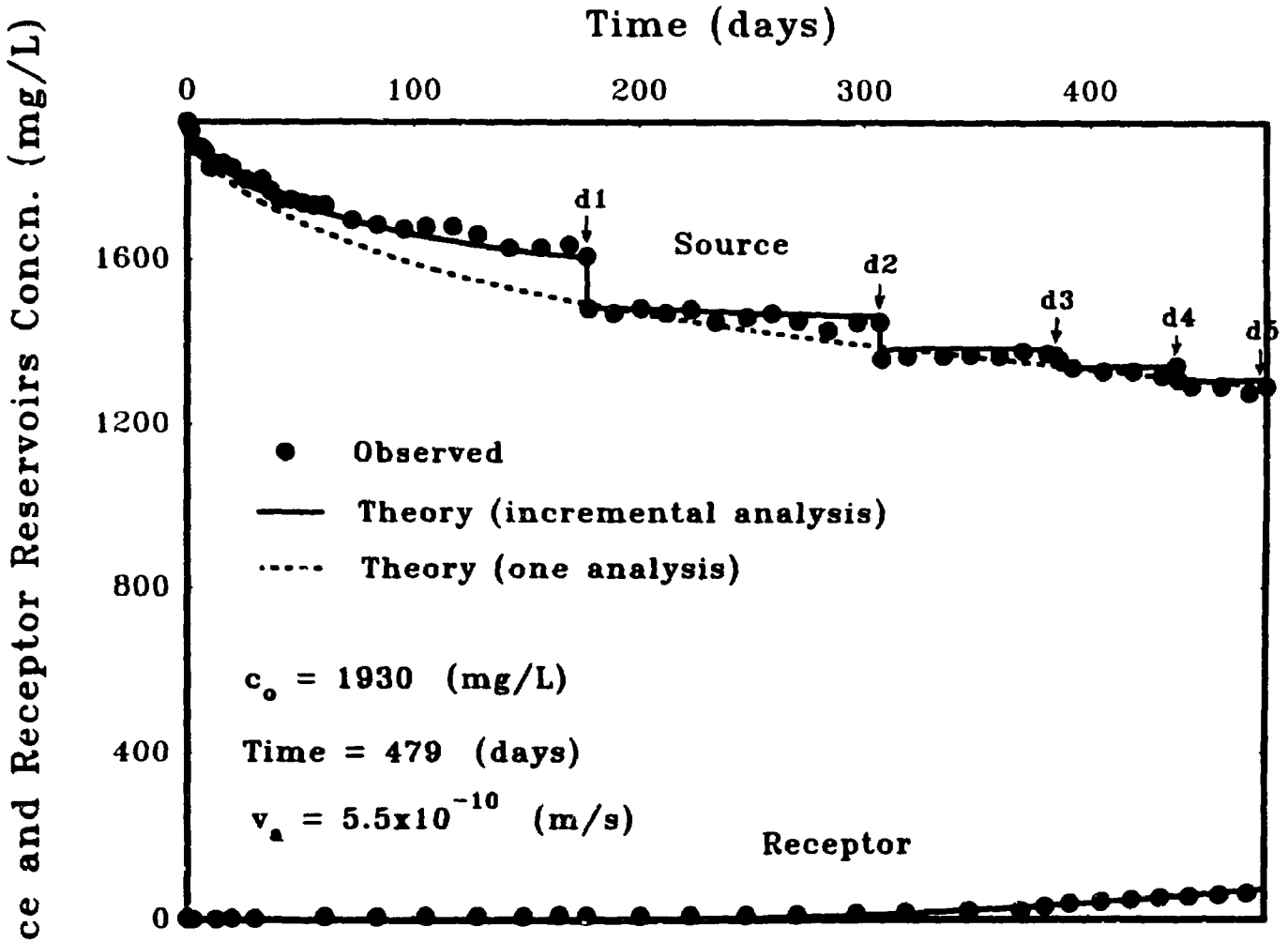

FIG. F2 OBSERVED AND CALCULATED [Cl^-] CONCENTRATIONS VERSUS ELAPSED TIME IN SOURCE AND RECEPTOR RESERVOIRS OF TEST #AD11, BASED ON TWO DIFFERENT ANALYSIS

APPENDIX G

CALCULATION OF THE THICKNESS OF THE STONE WITH VOID SPACE EQUIVALENT TO THE VOLUME OF THE INTRUDED SOIL IN INTRUSION TESTS # 6 & 7

A - Test Number 6 :

Dry weight of the intruded soil = 1600 g

Water content of the intruded soil = 23.6 %

Porosity of the stone = 0.449

Specific gravity of the soil solids = 2.77

Porosity of the intruded soil : $n = wG_s / (1 + wG_s)$

$n = 0.236 \times 2.77 / (1 + 0.236 \times 2.77) = 0.395$

Void ratio of the intruded soil : $e = n / (1 - n) = 0.395 / (1 - 0.395) = 0.653$

Dry density of the intruded soil : $\rho_d = G_s.\rho_w / (1 + e)$

$\rho_d = 2.77 \times 1 / (1 + 0.653) = 1.68$ g/cm^3

Surface area beneath the smaller cylinder : $A_s = 320.5$

Volume of the intruded soil : $V_{int} = M_s / \rho_d = 1600 / 1.68 = 955$ cm^3

Thickness (T_k) of stone with void space equivalent to the volume of intruded soil considering only stone directly beneath the smaller cylinder :

$T_k = V_{int} / (nA_s) = 955 / (0.449 \times 320.5) = 6.64$ cm

B - Test Number 7 :

Dry weight of the intruded soil = 1630 g

Water content of the intruded soil = 24.8 %

Porosity of the stone = 0.449

Specific gravity of the soil solids = 2.77

Porosity of the intruded soil : $n = wG_s / (1 + wG_s)$

$n = 0.248 \times 2.77 / (1 + 0.248 \times 2.77) = 0.407$

Void ratio of the intruded soil : $e = n / (1 - n) = 0.687$

Dry density of the intruded soil : $\rho_d = G_s.\rho_w / (1 + e)$

$\rho_d = 2.77 \times 1 / (1 + 0.687) = 1.64$ g/cm^3

Volume of the intruded soil : $V_{int} = M_s / \rho_d = 1630 / 1.64 = 993$ cm^3

Thickness (T_t) of stone with void space equivalent to the volume of intruded soil considering only stone directly beneath the smaller cylinder :

$T_t = V_{int} / (nA_s) = 993 / (0.449 \times 320.5) = 6.9$ cm

REFERENCES

Aitchison, G.D., Ed. (1965a). "Moisture equilibria and moisture changes in soils beneath covered areas." A Symposium in Print, G.D. Aitchison, Ed., Australia: Buttherworths, 278pp.

Akindunni, F.F., Gilham, R.W., and Nicholson, R.V. (1991). "Numerical simulations to investigate moisture retension characteristics in the design of oxygen-limiting covers for reactive mine tailings." *Canadian Geotechnical Journal*, 28: 446-451.

Appelt, H., Holtzclaw, K. and Pratt, D.F. (1975). "Effect of anion exclusion on the movement of chloride through soils." *Soil Science Society of America Proceedings*, 39: 264-267.

Bagchi, A. (1987). "Natural attenuation mechanisms of landfill leachate and effects of various factors on the mechanisms." *Waste Management and Research*, 5: 453-464.

Barbour, S.L., and Yanful, E.K. (1994). "Acolumn study of static nonequilibrium fluid pressures in sand during prolonged drainage." *Canadian Geotechnical Journal*, 31: 299-303.

Barbour, S.L. (1990). "Reduction of acid generation in mine tailings through the use of moisture-retaining cover layers as oxygen barriers: Discussion." *Canadian Geotechnical Journal*, 27: 398-401.

Barone, F.S. (1990). "Determination of diffusion and adsorption coefficient for some contaminants in clayey soil and rock: Laboratory determination and field evaluation." *P.hD. thesis, Department of Civil Engineering, The University of Western Ontario, London, Ontario, pp 326.*

Barone, F.S., Yanful, E.K., Quigley,R.M. and Rowe, R.K. (1989). "Effect of multiple contaminant migration on diffusion and adsorption of some domestic waste contaminants in a natural clayey soil." *Canadian Geotechnical Journal, 26: 189-198.*

Bear, J. (1972). *Dynamics of Fluids in Porous Media*, American Elsevier Publishing Company, Inc., Amsterdam, Holland.

Bear, J. (1979). *Hydraulics of Groundwater*, McGraw-Hill, New York.

Bear, J. and A. Verruijt (1987). Modelling Flow and Pollution. D. Reidel Publishing Company, Dordrecht, Holland.

Benedek, G.B. and Purcell, E.M. (1954). "Nuclear magnetic resonance in liquids under high pressure." *The Journal of Chemical Physics*, 22: 2003-2012.

Biggar, J.W. and Nielson, D.R. (1963). "Miscible displacement: V. Exchange processes." *Soil Science Society of America Proceedings*, 27: 623-627.

Biggar, J.W. and Nielson, D.R. (1960). "Diffusion effects in miscible displacement occurring in saturated and unsaturated porous materials." *Journal of Geophysical Research*, 65(9): 2887-2895.

Bond, W.J., Gardiner, B.N. and Smiles, D.E. (1982). "Constant-flux absorbtion of a tritiated calcium chloride solution by a clay soil with anion exclusion". *Soil Science Society of America Journal* 46: 1133-1137.

Bower, C.A., Reitemeier, R.F., and Fireman, M. (1952). "Exchangeable cation analysis of saline and alkali soils." *Soil Science*, 73: 251-261.

Brenner, H. (1962). "The diffusion model of longitudinal mixing in beds of finite length: Numerical values." *Chemical Engineering Science*, 17: 229-243.

Bresler, E. (1973). "Simultaneous transport of solutes and water under transient unsaturated flow conditions." *Water Resources* research, 9(4): 975-986.

Bresler, E. (1973). "Anion exclusion and coupling effects in nonsteady transport through unsaturated soils, I. Theory." *Soil Science Society of America Proceedings*, 37(5): 663-669.

Bresler, E. and Laufer A. (1974). "Anion exclusion and coupling effects in nonsteady transport through unsaturated soils, II. Laboratory and numerical experiments." *Soil Science Society of America Proceedings*, 38: 213-218.

Brutsaert, W. (1976). "The concise formulation of diffusive sorption of water in a dry soil." *Water Resources research*, 12(6): 1118-1124.

Buckingham, E. (1907). "Use of models for the study of mining problems." *American Institute of Mining and Metallurgical Engineering Technical Publication*, 425, 28pp.

Campbell, D.J.V., Parker, A., Rees, J.F. and Ross, C.A.M. (1983). "Attenuation of potential pollutants in landfill leachate by lower greensand." *Waste Management and Research*, 1: 31-52.

Carman, P.C. (1937). "Permeability of saturated sands, soils, and clays." *Journal of Agricultural Science*, 29, 262.

Cassel, D.K., Van Genuchten, M.Th. and Wierenga, P.J. (1975). "Predicting anion movement in disturbed and undisturbed soils." *Soil Science Society of America Proceedings*, 39: 1015-1019.

Childs, E.C. (1967). "Soil moisture theory" *Advances in Hydroscience*, 4: 73-117.

Childs, E.C. and Collis-George, N. (1950). "The permeability of porous materials." *Proceedings of the Royal Society of London*, A201: 392-405.

Chong, S.K. and Green, R.E. (1983). "Sorptivity measurement and its application." *Proceedings of the National Conference on Advances in Infiltration*, Chicago, 82-91.

Coats, K.H. and Smith, B.D. (1964). "dead-end pore volume and dispersion in porous media." *Society of Petroleum Engineering Journal*, 4: 73-84.

Cooke, A.B., (1991). "Centrifuge modelling of flow and contaminant transport through partially saturated soils." *P.hD. Thesis, Queen's University, Kingston, Ontario*, pp 232.

Cooke, A.B. and Mitchell, R.J. (991). "Physical modelling of a dissolved contaminant in an unsaturated sand." *Canadian Geotechnical Journal*, 28: 829-833.

Cooke, A.B. and Mitchell, R.J. (1991). "Evaluation of contaminant transport in partially saturated soils." *Centrifuge*, 91: 503-508.

Corey, A.T. (1977). "Mechanics of heterogeneous fluids in porous media." *Water Resources Publications*, Fort Collins, Co, pp 259.

Corey, J.C., Nielsen, D.R. and Biggar, J.W. (1963). "Miscible displacement in saturated and unsaturated sandstone." *Soil Science Society of America Proceedings*, 27: 258-262.

Darcy, H.P.G. (1986). "Les fontanies publiques de la ville de Dijon." Dolmont, Paris.

Day, P.R., and Luthin, J.N. (1956). "A numerical solution of the differential equation of flow for a vertical drainage problem." *Soil Science Society of America Proceedings*, 20: 443-447.

Desaulniers, D.D., Cherry, J.A. and Fritz, P. (1981). "Origin, age and movement of pore water in argillaceous quaternary deposits at four sites in southwestern Ontario." *Journal of Hydrology*, 50: 231-257.

De Smedt, F. (1981). "Theoretical and experimental study of solute movement through porous media with mobile and immobile water." *P.hD. thesis*, Vrije University, Brussels, Belgium, pp. 219.

De Smedt, F. (1981). "Solute transfer through unsaturated porous media." *Quality of Ground Water - Studies in Environmental Science*, 17: 1011-1016.

De Smedt, F. and Wierenga P.J. (1984). "Solute transfer through columns of glass beads." *Water Resources Research*, 20(2): 225-232.

De Smedt, F. and Wierenga P.J. (1979). "Mass transfer in porous media with immobile

water." *Journal of Hydrology*, 41: 59-67.

De Smedt, F. and Wierenga P.J. (1978). "Solute transport through soil with nonuniform water content." *Soil Science Society of America Journal*, 42: 7-10.

De Smedt, F. Wauters, F. and Sevilla, J. (1986). "Study of tracer movement through unsaturated sand." *Journal of Hydrology*, 85: 169-181.

DeWiest, R.J.M. (1965). *Geohydrology*. Wiley, New York, N.Y.

Dreimanis, A. (1962). "Quantitative gasometric determination of calcilte and dolomite by using chittick apparatus." *Journal of Sedimentary Petrology*, 32: 520-529.

Drysdale, C.V., and others (1923). *The Mechanical Properties of Fluids.*, Glasgow, Blackie and Son, 362p.

Edlefsen, N.E. and Anderson, A.B.C. (1943). "Thermodynamics of soil moisture." *Hilgardia*, 15: 31-298.

El-Kadi, A.I. (1986). "On estimating the hydraulic properties of soil, III: Parameters of the Philip infiltration equation." *Advances in Water Resources*, 9: 16-23.

Elzeftawy, A. and Cartwright, K. (1981). "Evaluating the saturated and unsaturated hydraulic conductivity of soils. Permeability and groundwater contaminant transport." *ASTM STP 746. T.F. Zimmie and C.D. Riggs. Eds., American Society for Testing and Materials*, 168-181.

Fredlund, D.G., and Rahardjo, H. (1993). Soil Mechanics for Unsaturated Soils, John Wiley and Sons, Inc. New York. pp 517.

Freeze, R.A. and Cherry, J.A. (1979). *Groundwater*, Englewood Cliffs, New Jersy, Prentice-Hall Inc.

Gardner, W.R. (1958). "Some steady-state solutions of the unsaturated moisture flow equation with applications to evaporation from a water table." *Soil Science*, 85(4).

Gaudet, J.P., Jegat, H., Vachaud, G. and Wierenga, P.J. (1977). "Solute transfer with exchange between mobile and stagnant water, through unsaturated sand." *Soil Science Society of America Journal*, 41: 665-671.

Gerhardt, R.A. (1984). "Landfill leachate migration and attenuation in the unsaturated zone in layered and nonlayered coarse-grained soils." *Monitoring Review*, 4(2): 56-65.

Ghosh, K. (1980). "Modeling infiltration." *Soil Science*, 130(6): 297-302.

Gillham, R.W. and Cherry, J.A. (1982). "Contaminant migration in saturated

unconsolidated geologic deposits." *Geophysical Society of America*, Special Paper, 189: 31-62.

Goodall, D.C. and Quigley, R.M. (1977). "Pollutant migration from two sanitary landfill sites, Ontario." *Canadian Geotechnical Journal*, 14: 223-226.

Graham-Bryce, J.J. (1963). "Effect of moisture content and soil type on self diffusion of ^{86}Rb in soils." *Journal of Agricultural Science*, 60: 239-244.

Green, W.H. and Ampt, G.A. (1911). "Studies in soil physics. I. The flow of air and water through soils." *Journal of Agricultural Science*, 4: 1-24.

Hayduk, W. and Laudie, H. (1974). "Prediction of diffusion coefficients for non-electrolytes in dilute aqueous solutions." *American Institute of Chemical Engineering Journal*, 20: 611-615.

Heath, R.C. and Lehr, J.H. (1987). "A new approach to the disposal of solid waste on land." *Groundwater*, 25(3): 258-264.

Hildebrand, M.A. and Himmelbau, D.M. (1977). "Transport of nitrate ion in unsteady unsaturated flow in porous media." *American Institute of Chemical Engineering Journal*, 23: 326-335.

Hillel, D. (1982). "Introduction to soil physics." New York: Academic, pp 364.

Holtan, H.N. (1961). "A concept for infiltration estimates in watershed engineering." *ARS Publication*, 41-51, U.S. Department of Agriculture, Agricultural Resource Service.

Horton, R.E. (1940). "An approach toward a physical interpretation of infiltration capacity." *Soil Science Society of America Proceedings*, 5: 399-417.

Horvath, A.L. (1985). *Handbook of Aqueous Electrolyte Solutions*. John Willey & sons, New York.

Irmay, S. (1954). "On the hydraulic conductivity of unsaturated soils." *Transactions of the American Geophysical Union*, 35: 463-468.

James, R.V. and Rubin, J. (1986). "Transport of chloride ion in a water-unsaturated soil exhibiting anion exclusion." *Soil Science Society of America Journal* 50: 1142-1149.

Johson, A.I., Prill, R.C. and Morris, D.A. (1963). "Specific yield, column drainage, and centrifuge moisture content." *Geological Suevey Water Supply Paper*, 1662-A: A1-A60.

Kemper, W.D. and Van Schaik, J.C. (1966). "Diffusion of salts in clay-water systems." *Soil Science Society of America* Proceedings, 30: 534-540.

Kisch, M. (1959). "The theory of seepage from clay blanketed reservoirs." *Geotechnique*, 9: 9-21.

Kirda, C., Nielson, D.R. and Biggar, J.W. (1973). "Simultaneous transport of chloride and water during infiltration." *Soil Science Society of America Proceedings*, 37: 339-345.

Klute, A. (1952). "Some theoretical aspects of the flow of water in unsaturated soils." *Soil Science Society of America Proceedings*, 16: 144-148.

Klute, D. and Law, M. (1985). "Codisposal of industrial and municipal waste." *Proceedings MOE Technology Transfer Conference*, Toronto.

Klute, A. and Letey, J. (1958). "The dependence of ionic diffusion on the moisture content of nonadsorbing porous media." *Soil Science Society of America Proceedings*, 22: 213-215.

Kostiakov, A.N. (1932). "On the dynamics of the coefficient of water percolation in soils and on the necessity of studying it from a dynamic point of view for the purpose of amelioration." *Transactions of the Sixth Commission of the International Society of Soil Science*, Moscow, Part A, 17-21.

Krupp, H.K. and Elrick, D.E. (1968). "Miscible displacement in an unsaturated glass beads medium." *Water Resources Research*, 4: 809-815.

Lam, L. (1984). "KCAL - A computer program for calculating unsaturated permeability." Department of Civil Engineering, University of Saskatchewan, Saskatoon, Saskatchewan.

Lim, P.C., Barbour, S.L. and Fredlund, D.G. (1994). "Laboratory determination of diffusion and adsorbtion coefficients of inorganic chemicals for unsaturated soil." *The American Society for Testing and Materials*

Lim, P.C., Barbour, S.L. and Fredlund, D.G. (1994). "A new technique for diffusion testing of unsaturated soil." *The American Society for Testing and Materials*

Mansell, R.S., Selim, H.M., Kanchanasut, P. Davidson, J.M. and Fiskell, J.G.A. (1977). "Experimental and simulated transport of phosphorous through sandy soils." *Water Resources Research*, 13: 189-194.

Mavis, F.T. and Tsui, T.P. (1939). "Percolation and capillary movement of water through sand prisms." *Bull. 18, University of Iowa, Studies in Engineering*, Iowa City.

McMahon, M.A. and G.W. Thomas (1974). "Chloride and tritiated water flow in disturbed and undisturbed soil cores." *Soil Science Society of America Proceedings*, 38: 727-732.

Mitchell, R.J. (1992). "Physical modeling of solute transport by matrix suction." *45th Canadian Geotechnical Conference Paper*, No. 84: 1-9.

Nicholson, R.V., Gillham, R.W., Cherry, J.A., and Reardon, E.J. (1989). "Reduction of acid generation in mine tailings through the use of moisture retaining cover layers as oxygen barriers." *Canadian Geotechnical Journal*, 26: 1-8.

Nielsen, D.R., Van Genuchten, M.Th. and Jury, W.A. (1989). "Transport processes from surface to groundwater." *contamination*, IAHS Publication No. 185: 99-108.

Nielsen, D.R., Van Genuchten, M.Th. and Biggar, J.W. (1986). "Water flow and solute transport processes in the unsaturated zone." *Water Resources Research*, 22(9): 89S-108S.

Nielsen, D.R. and Biggar, J.W. (1961). "Miscible displacement in soils I: Experimental information." *Soil Science Society of America Proceedings*, 25: 1-5.

Nimmo, J.R., Rubin, J. and Hammermeister, D.P. (1987). "Unsaturated flow in a centrifugal field: Measurement of hydraulic conductivity and testing of Darcy's law." *Water Resources Research*, 23(1): 124-134.

Ornatsky, N.V. (1950). "Mechanika gruntov." *Izd. Moskow University*, Moscow.

Perkins, T.K. and Johnston, O.C. (1963). "A review of diffusion and dispersion in porous media." *Society of Petroleum Engineering Journal* 3(1): 70-83.

Philip, J.R. (1954). "An infiltration equation with physical significance." *Soil Science*, 77: 153-157.

Philip, J.R. (1969). "Theory of infiltration. Advances in hydroscience." 5: 215-296.

Pockells, F. (1908). "Kapillarität in winkelmann." *A., Handbuch der Physik*, Leipzig, Verlag von Johann Ambrosins Barth, 1119-1160.

Polubarinova-Kochina, P.Ya. (1962). "Theory of groundwater movement (in Russian), *Gostekhizdat*, Moscow, 1952; English translation by DeWiest, R.J.M., Princeton Univ. Press, Princeton, N.J.

Porter, L.K., Kemper, W.D., Jackson, R.J. and Stewart, B.A. (1960). "Chloride diffusion in soils as influenced by moisture content." *Soil Science Society of America Proceedings*, 24: 460-463.

Pratt, P.F. (1965). "Digestion with hydrofluoric perchloric acids for total potassium." *In Methods of Soil Analysis*, Published by American Society of Agronomy, Madison, Wisconsin, pp 1019-1021.

Reid, R.C., Prausnitz, J.M. and Poling, B.E. (1987). *The properties of gases and liquids*. 4th edition McGraw-Hill Co., New York.

Rethati, L. (1957). "Kapillaris jelensegek a talajban." Kandidatusi disszertacio. Kezirat. (Capillary phenomena in the soil. Thesis for the candidate degree. Manuscript.) Budapest.

Rethati, L. (1960a). "A talaj kapillaritasanak mernoki vonatkozasai." (Engineering relations of soil capillarity.), *Vizugyi Koziem.* No. 1.

Rethati, L. (1960b). "Capillary properties of soils." *Acta Technica, Tom.* XXIX., fasc. 1-2., Budapest.

Richards, L.A. (1931). "Capillary conduction of liquids through porous mediums." *Physics*, 1: 318-333.

Richardson, B.G. (1965). "Measurement of the free energy of soil moisture by the psychrometric technique using thermistors." In moisture equilibria and moisture changes in soils beneath covered areas, A Symposium in Print. Australia: Butherworths, pp. 39-46.

Rode, A.A. (1952). "Pochvennaya vlaga." *Izd. AN SSSR*, Moscow. Das Wasser im Boden. Akademie Verlag, Berlin.

Romkens, M.J.M. and Bruce, R.R. (1964). "Nitrate diffusivity in relation to moisture content of nonadsorbing porous media." *Soil Science*, 98: 332-337.

Ross, C.A.M. (1985). "The unsaturated zone as a barrier to groundwater pollution by hazardous wastes." *Hydrogeology in the Service of Man*, Memories of the 18th Congress of the International Association of Hydrogeologists, Cambridge.

Roth, K. Jury, W.A., Flühler, H. and Attinger, W. (1991). "Transport of chloride through an unsaturated field soil." *Water Resources Research*, 27(10): 2533-2541.

Rowe R.K. (1992). "Test liner construction and evaluation, Halton Waste Management Site." *Report submitted to the Proctor and Redfern Ltd., Consulting Engineers and Planners, Hamilton, Ontario.*

Rowe, R.K. (1987). "Pollutant transport through barriers." *Proceedings of ASCE Specialty Conference, Geotechnical Practice for Waste Disposal*, 87, Ann Arbor, June, pp. 159-181.

Rowe, R.K. (1989). "Movement of Pollutants through clayey soil." *Proceedings 37th Annual Geotechnical Conference, Minnesota Section* ASCE, St. Paul, U.S.A., 1-34.

Rowe, R.K., and Booker, J.R. (1994). "POLLUTE-v6 A program for modelling

pollutant migration through soil". Geotechnical Research Centre, The University of Western Ontario © 1983, 1990, 1994.

Rowe, R.K., and Booker, J.R. (1985). "1-D pollutant migration in soils of finite depth." *ASCE Journal of Geotechnical Engineering*, 111: 479-499.

Rowe, R.K., and Booker, J.R. (1987). "An efficient analysis of pollutant migration through soil." *In, numerical methods for transient and coupled systems*. Edited by R.W. Lewis, E. Hinton, P. Bettess and B.A. Schrefler. John Wiley and sons Ltd., New York, N.Y., chapter 2, pp. 13-42.

Rowe, R.K., Booker, J.R., and Quigley R.M. (994). Clayey barrier systems for waste disposal facilities. *E & FN Spon Chapman Hall Publishing Co., London (in press).*

Rowe, R.K., Caers, C.J. and Barone, F. (1988). "Laboratory determination of diffusion and distribution coefficient of contaminants using undisturbed soil." *Canadian Geotechnical Journal*, 25: 108-118.

Rowe R.K., Caers, C.J. and Chan, C. (1993). "Evaluation of a compacted till liner test pad constructed over a granular subliner contingency layer." *Canadian Geotechnical Journal*, 30: 667-689.

Rowell, D.L., Martin, M.W. and Nye, P.H. (1967). "The measurement and mechanism of ion diffusion in soils: III. The effect of moisture content and soil solution concentration on the self diffusion of ions in soils." *Journal of Soil Science*, 18: 204-222.

Sherard, J.L., Dunnigan, L.P. and Talbot, J.R. (1984). "Basic properties of sand and gravel filters." *ASCE - Journal of the Geotechnical Engineering Division* - 110(6): 684-700.

Sherard, J.L., Dunnigan, L.P. and Talbot, J.R. (1984). "Filters for silts and clays." ASCE - *Journal of the geotechnical Engineering Division* - 110(6): 701-718.

Smith, W.O. (1961). "Mechanism of gravity drainage and its relation to specific yield of uniform sands: Infiltration and drainage in uniform sands." *Geological Survey Professional Paper*, 402-A.

Smith, W.O. (1936). "Sorption in an ideal soil." *Soil Science*, 41(3): 209-230.

Smith, W.O. (1933). "Minimum capillary rise in an ideal uniform soil." *Physics*, 4: 184-193.

Smith, W.O. (1933). "The final distribution of retained liquid in an ideal uniform soil." *Physics*, 4: 425-439.

Smith, W.O., Foote, P.D. and Busang, P.F. (1931). "Capillary rise in sands of uniform spherical grains." *Physics*, 1(1): 18-26.

Terzaghi, K. (1943). *Theoretical Soil Mechanics*, J. Wiley, New York.

Thomas, G.W. and A.R. Swoboda (1970). "Anion exclusion effects on chloride movement in soils." *Soil Science*, 110: 163-166.

Topp, G.C. and Miller, E.E. (1966). "Hysteresis moisture characteristics and hydraulic conductivities for glass beads media." *Soil Science Society of America Proceedings*, 30: 156-162.

U.S. Bureau of Reclamation, (1974). *Earth Manual*, - 2nd edition, 810p.

Vachand, G. (1967). "Determination of hydraulic conductivity of unsaturated soils from an analysis of transient flow data." *Water Resources Research*, 3(3): 697-705.

Van Genuchten, M.Th. (1978). "Calculating the unsaturated hydraulic conductivity with a new closed form analytical model." *Research Report 78 - WR - 08*, Department of Civil Engineering, Princeton University, Princeton, New Jersey.

Versluys, J. (1917). "Die Kapillarität der boden." *Inst. Mitt. J. Bodenk*, 7: 117-140.

Walkley, A., and Black, I.A. (1934). "An examination of the degtjareff method for determination of soil organic matter and a proposed modification of the chromic acid titration method." *Soil Science*, 37: 29-38.

Warncke, D.D. and Barber, S.A. (1972). "Diffusion of zinc in soil: I. The influence of soil moisture." *Soil Science Society of America Proceedings*, 36: 39-42.

Warrick, A.W., Biggar, J.W. and Nielsen, D.R. (1971). "Simultaneous solute and water transfer for an unsaturated soil." *Water Resources Research*, 7(5): 1216-1225.

Weiland, H. (1933). "Die vorgänge im kupillarwasser des bondens bei veränderung der grundwasser spiegelhoenlage." *Der Kulturtechniker.*

Whisler, F.D. and Bouwer, H. (1970). "Comparison of methods for calculating vertical drainage and infiltration for soils." *Journal of Hydrology*, 10: 1-19.

Wierenga, P.J. and Van Genuchten, M.Th. (1989). "Solute transport through small and large unsaturated soil columns." *Groundwater*, 27(1): 35-42.

Wilke, C.R. and Chang, P. (1955). "Correlation of diffusion coefficients in dilute solutions." *American Institute of Chemical Engineering Journal*, 1(2): 264-270.

Wilson, L.G. (Winter 1982). "Monitoring in the vadose zone, Part II." *Groundwater*

Monitoring Review, 31-41.

Wilson, L.G. (Fall 1981). "Monitoring in the vadose zone, Part I: Storage changes." *Groundwater monitoring Review*, 31-41.

Youngs, E.G. (1969). "An estimation of sorptivity for infiltration studies from moisture movement considerations." *Soil Science*, 86: 202-207.

Yule, D.F. and Gardner, W.R. (1978). "Longidudinal and transverse dispersion coefficient in unsaturated and plainfiled sand." *Water Resources Research*, 14: 582-588.

Zunker, F. (1930). "Das verhalten des bodens zum wasser." *Handbuch der Bodenlehre*, Vol. VI.J. Springer, Berlin.

Zimmerman, B.G. (1936). "Determining entrapped air in capillary soils." *Engineering News Record.*